1990

An analysis of machining accuracies in CNC machining operations

Mohammad Nazrul Islam
University of Wollongong

AN ANALYSIS OF MACHINING ACCURACIES IN CNC MACHINING OPERATIONS

A thesis submitted in fulfilment of the

requirements for the award of the degree of

MASTER OF ENGINEERING (HONOURS)

from

THE UNIVERSITY OF WOLLONGONG

by

MOHAMMAD NAZRUL ISLAM

Department of Mechanical Engineering

1990

753454

This is to certify that this work has not been submitted for a degree to any other university or institution.

/ M. N. Islam /

To my parents

ABSTRACT

Dimensional repeatability and predictability of tolerance levels are two of the most fundamental requirements of today's automated manufacture leading towards unmanned manufacture. Regarding continuous batch production, when Computer Numerical Control (CNC) machines are utilized, the certainty of achieving these is rather poor, despite the high order of accuracies claimed by CNC machine manufacturers. The aim of the present thesis is to investigate the likely causes for the poor performances in CNC machining operations and to propose some control measures to eliminate or at least reduce the shortcomings.

The extensive literature survey reveals that, most researchers have applied some form of in-process error compensation techniques to improve "machining accuracy"; but this approach has not addressed the root of the problem. It is the author's firm belief that the likely sources of error can be eliminated at an early stage by adequate designing and process planning procedures which are a follow up from the old saying that "prevention is better than cure". On this basis, the geometric dimensioning and tolerancing approach was applied in the present work to assess machining accuracies, as the conventional plus/minus (co-ordinate) tolerancing does not take into account the geometric configurations, alignments of mating surfaces, etc.

The geometric tolerancing features such as the dimensional variations, positioning and shape variations of the holes, flatness, parallelism and perpendicularity of different planes, perpendicularity of the hole axes with a given datum, etc, were considered in the design of a simple component that was to be machined on a CNC machining centre. The preliminary work aimed at demonstrating the possible inaccuracies which may occur in typical CNC machining operations. The machined components' accuracy was measured using a general purpose co-ordinate measuring machine (CMM). Results from such tests

indicated the following clear tendencies: (i) the machined dimensions were always smaller than the designed dimensions in linear profile machining, (ii) holes were always oversized andtheir diameter increased to some peak value in the middle for through holes and then decreased (barreling effect), (iii) a flatness error of about 20 microns was observed in the end milled surfaces and the surface geometric error of the end milled surfaces showed the effect of end mill deflection on them.

Encouraging results from preliminary findings lead to further investigations, being conducted on some of the specific aspects influencing dimensional accuracies and surface finish, such as : inherent statistical variations in cutting tool dimensions, effect of surface finish on accuracy and repeatability of measurements, effect of tool deflection, and calculation of volumetric accuracy. An extensive analysis of experimental results revealed the following major findings: (i) large variations in cutting tool dimensions, sometimes beyond the acceptable limits, were observed, (ii) tool deflection was a major problem in end milling, which caused geometric inaccuracies in the machined component., (iii) surface finish on the machined component played a significant role on the dimensional accuracy and repeatability of measurements, (iv) it was shown that the machine tool geometric errors do not always form the major portion of machining errors, as claimed by some authors.

Concluding, this thesis highlights the inherent and controllable geometric errors in CNC machining operations and analyses how these errors can be reduced by adopting appropriate precautionary measures .

ACKNOWLEDGEMENTS

The author gratefully acknowledges the guidance, continuous support and encouragement of his supervisor Dr. I. S. Jawahir throughout the course of this work and Dr. E. Siores, for his guidance and assistance during the absence of Dr. Jawahir and reviewing the final script.

The author also sincerely acknowledges the assistance provided by the following individuals during the various stages of this work:

- Prof. J.E. Freckleton of Rochester Institute of Technology, USA, for his invaluable discussions about various geometric dimensioning and tolerancing related problems, during his short visit to our department.
- Mr. I.J. Kirby, who in spite of his busy schedule spared time to carry out the cutting tests and helped in arranging all experimental works.
- Mr. D. Jamieson, for his assistance and advice in computer programming.

Special thanks are due to my wife, Hosna and daughters Fifi and Fari, for their love, patience and understanding.

TABLE OF CONTENTS

LIST OF FIGURES

LIST OF TABLES

GLOSSARY OF TERMS

ACC	Adaptive Control with Constraints
ACO	Adaptive Control with Optimization
ACS	Adaptive Control System
AVG	Average
BUE	Built-Up Edge
CAD	Computer Aided Design
CAM	Computer Aided Manufacturing
CAPP	Computer Aided Process Planning
CIM	Computer Integrated Manufacturing
CMM	Co-ordinate Measuring Machine
CNC	Computer Numerical Control
DNC	Direct Numerical Control
FMS	Flexible Manufacturing System
GAC	Geometric Adaptive Control
GD & T	Geometric Dimensioning and Tolerancing
LCL	Lower Control Limit
LMC	Least Material Condition
LTL	Lower Tolerance Limit
MMC	Maximum Material Condition
MRR	Metal Removal Rate
NC	Numerical Control
PI	Performance Index
RFS	Regardless of Feature Size
TWR	Tool Wear Rate
UCL	Upper Control Limit
UTL	Upper Tolerance Limit

NOMENCLATURE

b	width of cut
d	depth of cut
C_e	end cutting edge angle
C_p	process capability
C_s	side cutting edge angle
D	cutter diameter
D_x	X - co-ordinate deviation
D_y	Y - co-ordinate deviation
E	modulus of elasticity
F	cutting force
F_a	axial cutting force
F_r	radial cutting force
F_t	tangential cutting force
h	chip thickness
H	relative lip height (drill)
I	moment of inertia
k	half point angle (drill)
K_t	number of teeth
N	spindle RPM
N_c	commanded spindle speed
N_p	programmed spindle speed
Q	metal removal rate
R	cutter radius
R_a	arithmetic mean roughness
R_{ma}	peak to valley roughness height
R_p	repeatability
R_z	ten point average roughness height

s	sample standard deviation
S	feed per revolution
S_m	feed rate
S_t	feed per tooth
t	time
t_c	tool change time
T	tool torque
T_p	position tolerance
U	cutting speed
V	volumetric error
w	tool wear
w_0	terminal allowable width of flank wear
X_d	desired value of measurement
X_m	measured value of measurement
δ_t	tool deflection
δ_x	error
Δ_a	absolute deviation
Δ_r	relative deviation
σ	population standard deviation

1.0 INTRODUCTION

1.1 General

The automation of machine tools has been the central theme of manufacturing engineering since the invention of the first Numerical Controlled (NC) machine, in 1947* by John T. Persons. In the late 1950s, the introduction of computers into manufacturing processes has revolutionized machine tool automation. During the last few decades, expansion of computer power has led to the development of Computer Numerical Control (CNC) and Direct Numerical Control (DNC) systems. It is to be noted that, day by day the cost of labour is rising, while the cost of computer power is falling significantly (Figure 1.1). Moreover, recent technological developments in computer science have increased the capabilities of computers tremendously to perform complex calculations quickly and to manage vast amount of data. Logical outcome of all these is the implementation of more and more computers in production processes. This is expected to lead towards unmanned manufacturing (automated factory) in the near future (Figure 1.2).

Today CNC systems are widely used in industry. The principal application of CNC systems has been in metal machining processes. The main idea behind the implementation of computer applications in machine tools is to produce faster and more accurate machining. Unfortunately, despite high order "machine accuracies" specified by the manufacturers of CNC machines, in practice we observe rather poor "machining accuracy" levels, sometimes even extending beyond the anticipated limits in CNC machining operations.

---

* Based on Persons concept, the first prototype NC milling machine was developed at Massachusettes Institute of Technology in 1952.

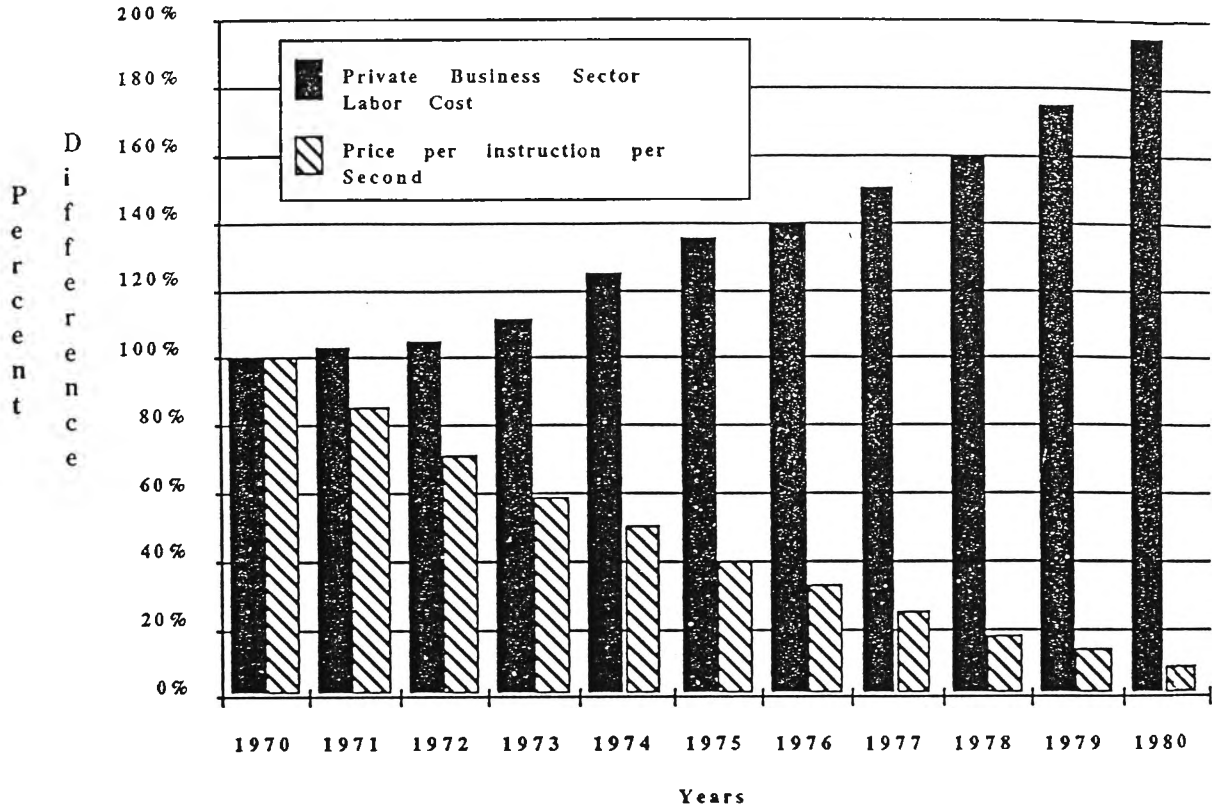

Figure 1.1 As Labour Costs Rise, the Cost of Computer Power Falls [1].

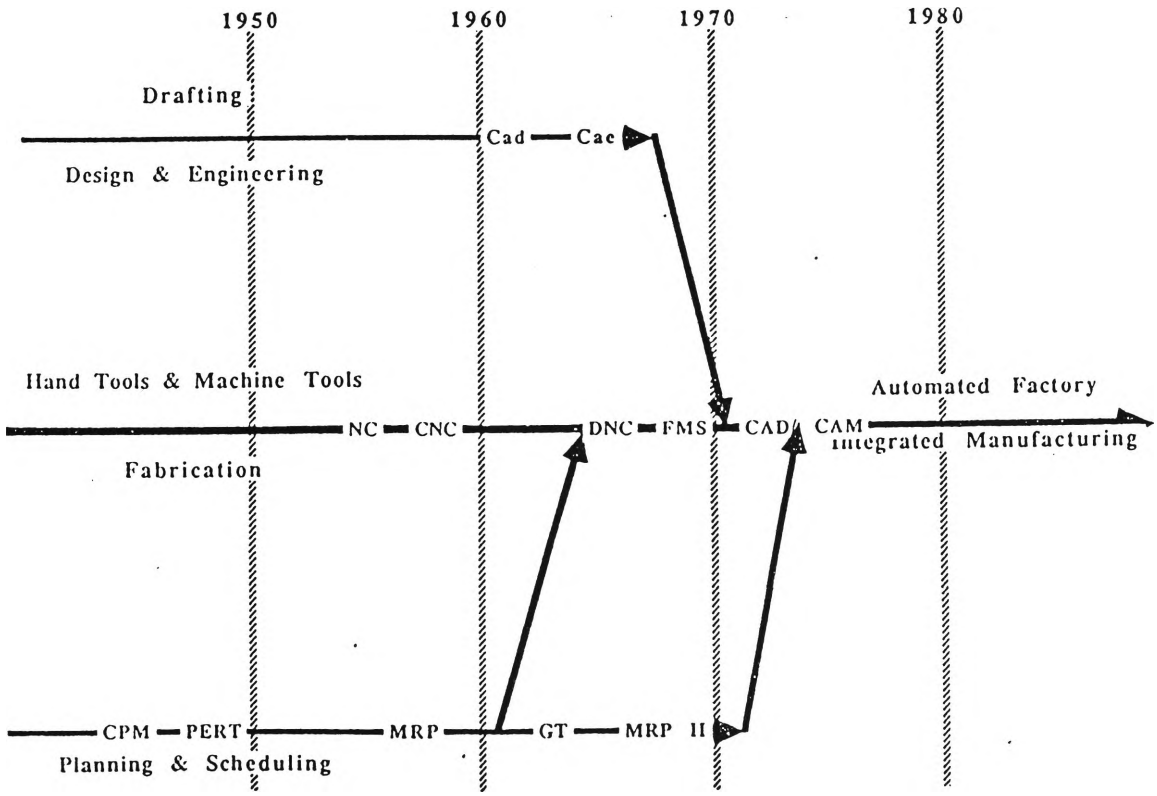

Figure 1.2 The Paths Towards the Automated Factory [1].

The concept of geometric dimensioning and tolerancing (GD & T) is a relatively recent development in the field of metrology. Day by day GD & T is becoming more and more popular and it is used successfully in all phases of manufacturing, including design, production and inspection. However, it seems clear that the full potential of GD & T has not yet been utilized. It has been realised that more attention must be paid to study the capability and the functional requirements of GD & T, as this can yield significant cost savings with little capital investment. In this thesis an attempt has been made to demonstrate the potential benefits relating to the quality enhancement and improved accuracy through the application of geometric dimensioning and tolerancing in CNC machining operations.

The introduction of co-ordinate measuring machines (CMM), is a milestone in today's manufacturing technology. Since its introduction in the early 1960's, CMMs are gaining popularity very fast because of a number of advantages: flexibility, reduced set up time, improved accuracy, reduced operator influence, improved productivity, etc. Now CMM is becoming a mandatory piece of equipment for all automated manufacturing plants. The reason is that, CMM provides digital information suitable for today's computer dominated manufacturing processes and eventually it will become a feedback link for Computer Integrated Manufacturing (CIM). The CMM is considered as a universal measuring machine and its introduction has changed the concept, strategy and techniques of dimensional and geometric measurements. An integrated system of CNC machines and CMMs can give high productivity as well as high accuracy levels. The correct use of GD & T techniques plays a major role in such an integrated system.

1.2 The Problem of Quality Requirements

The biggest challenge facing today's manufacturing industry is achieving better quality, higher productivity at the lowest cost. From an economic point of view, productivity is the most important parameter, as high productivity will reduce the cost; however, the

market is not only cost concerned but also quality conscious. Therefore, manufacturers are forced to adopt a parallel approach towards these three aspects (Figure 1.3).

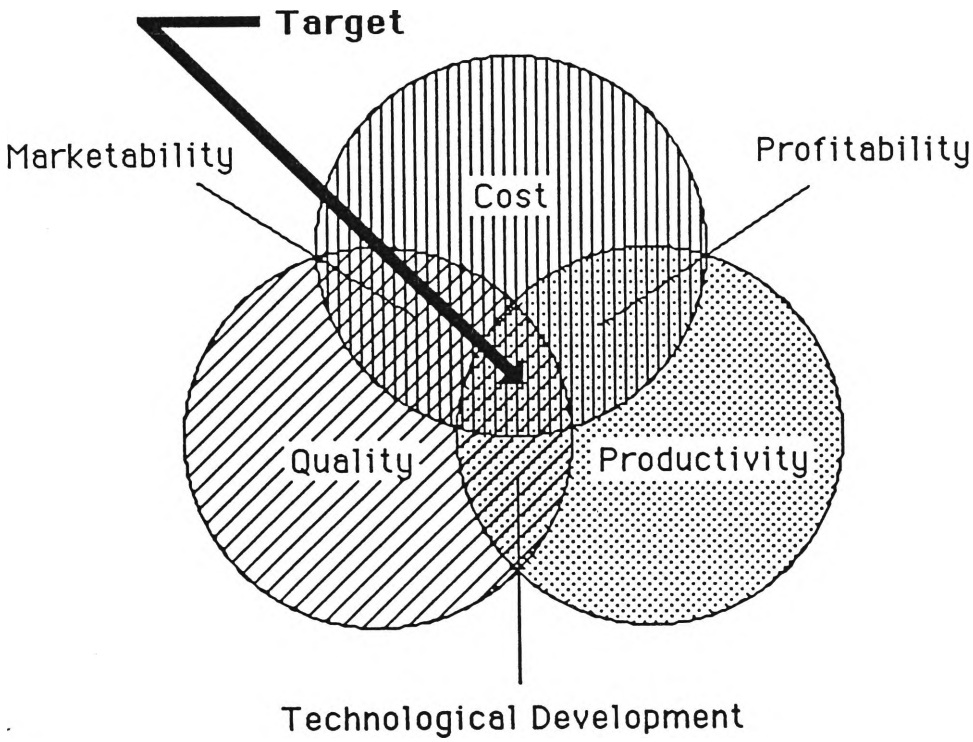

Figure 1.3 Modern Manufacturing Strategy.

1.2.1 What is Quality?

There are a number of definitions for quality. McKeown defines quality as "fully confirming to the agreed requirements of the customer" [2]. This definition considers requirements of the customer as the bottom line of achieving quality. Another school of thought states quality as "conformance to specification". Juran [3] emphasized the concept known as "fitness for use". Deming [4], the founder of modern quality control concepts, states that "Good quality does not mean high quality. It means a predictable degree of uniformity and dependability at low cost with a quality suited to the market".

1.2.2 Japanese Approach towards Quality Improvement

A fundamental difference can be noticed between the western approach and the Japanese approach towards quality improvement. The western approach is to inspect the product after it is manufactured and then carrying out any necessary correction before despatching to the customer. The idea is to achieve quality by "inspecting the quality-in". But this strategy has proved to be inadequate and wasteful. The Japanese approach is based on "in-process controls" from the designing of a product to the despatch to the customer, at all levels. This approach is aimed at quality being "built-in" rather than "inspected-in". The Japanese approach has demonstrated its effectiveness and it is believed that the western system is now beginning to follow a preventative approach to quality, having adapted the Japanese concept in appropriate proportions.

1.2.3 Why Increased Accuracy ?

In metal machining, the accuracy of a finished product is the best way to judge its quality. Peters et al [5] justifies the increased accuracy by the following considerations:

(a) BETTER PERFORMANCES AND RELIABILITY: Better performances and reliability of products especially in the case of miniaturized products or weight and space saving applications. Examples of this are numerous in computer and aerospace industries and also in classical products, even in raw materials.

(b) AUTOMATIC ASSEMBLY AND MATERIALS HANDLING: Increased accuracy and precision in positioning is required for automatic assembly and discrete materials handling.

(c) SIMPLIFICATION OF DESIGN: Manufacturing accuracy requirements also lead to simplification in design, ensuring simpler manufacturing techniques be employed retaining the functional requirements of the manufactured component.

(d) NOISE REDUCTION AND INCREASED LIFE: Increasing accuracy of gears, bearings or cams can reduce the noise in a machine, providing longer life.

(e) RAW PRODUCTS MUST BE ACCURATE: Raw products used today also require a greater accuracy, e.g. the straightness of bars for automatic lathes or the accuracy of castings to be clamped on pallets are significant time saving factors.

(f) INCREASED ACCURACY IN OTHER FIELDS: Manufacturing accuracy must respond to increased accuracy in other fields. Due to availability and continuing growth in electronics, computer science and various control systems, accuracy levels in other fields have reached a high level and so manufacturing accuracy is required to match those high accuracy levels.

Here it must be pointed out that a customer's satisfaction is paramount in the quality assessment of a product, sometimes it may happen that the product is within the limits of all specifications and standards; but the customer simply does not like it. Thus, while improving the accuracy of a product, the customer's satisfaction must also be taken into account.

It is well known that the cost of production increases exponentially as the dimensional tolerances are reduced (Figure 1.4). So as a rule, tolerances must always be kept as large as possible without risking the function. But if we have a closer look at Figure 1.4, we find that there is a zone where tolerances can be reduced without much increment of cost. Such a zone is related to the machine capabilities. El Maraghy et al [7] write, "... modern machine tools are capable of producing tight dimensional tolerances, and a range of

tolerances can be obtained for the same cost." When we use CNC machine tools, it is highly desirable that we machine the components with high accuracy enabling the machine's capability to be fully utilized, this way the benefit of capital investment (for CNC machine) can be justified. In the present thesis work the desire for higher accuracy did not aim at reduction of the tolerance band of the product without functional requirements. The primary interest was to see whether CNC machines can achieve the specified accuracy, when such high accuracy is asked by functional requirements.

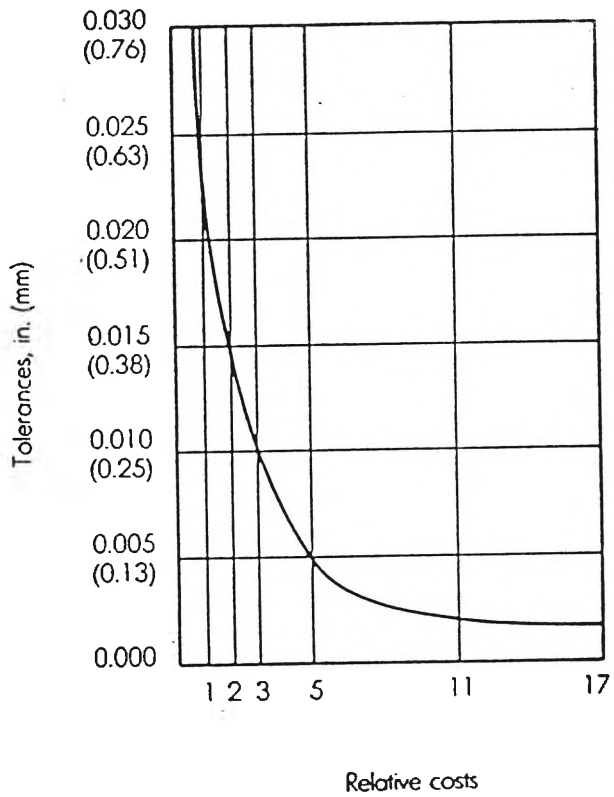

Figure 1.4 Relationship Between Tolerances and Production Costs [6].

1.3 Machine Accuracy Versus Machining Accuracy

1.3.1 Some Important Terms:

The terms accuracy, error, etc. are often used without much care and that may lead to various interpretations. The difference between the measured and the true value is generally known as **error**. There can be errors of size or quantity and errors of

measurement. When we are interested in the error of a machined component, basically this refers to the error of size. "An error of size or quantity is the difference between the desired or specified size or quantity without reference to any uncertainty in measurement" [8].

Uncertainty is the range in which the true value of the quantity measured is likely to lie at a given level of confidence. In the industry normally 95% confidence level is adopted. Unless otherwise stated, in this thesis the same level of confidence (i.e. 95%) is accepted, which means, the value of uncertainty leaves a 19 to 1 chance of being right.

Repeatability is an important property of a measuring instrument. British Standard 5233:1975 defines repeatability as: "The ability of a measuring instrument to give identical indications, or responses, for repeated applications of the same value of the measured quantity under the same conditions of use" [9].

Accuracy is the degree of conformity of a measured or calculated value to some recognized standard or specified value. Good repeatability is a necessary but not a sufficient condition to warrant a good accuracy.

1.3.2 Machine Accuracy

In CNC machining operations, NC programmes are written, giving command values to the machine and the workpiece is machined accordingly. In practice, it is found that the machined dimensions do not comply with the command values. Although it is impossible to produce any error-free component, using any type of machine, the errors in CNC machining can be higher than what is expected, despite high order of "machine accuracy" claimed by the CNC machines' manufacturers. In fact "machine accuracy" and "machining accuracy" are different, although, quite often mixed in understanding.

The **machine accuracy** of a CNC machine refers to the ability of the CNC machine to produce a component within a specified degree of accuracy. The machine accuracy of CNC machines depends on the structure of the machine as well as on the accuracy of the NC system. It is surprising to note that, the performance tests (and their allowable limits) are equivalent for NC machines and manually operated machines [10] although NC machines are generally claimed to be superior. In effect, NC machines and manually operated machines will be expected to have similar magnitudes of structural inaccuracies.

1.3.3 Machining Accuracy

Machining accuracy or working accuracy as called by some authors, is the accuracy achieved on the machined workpiece and clearly differs from the command value. It is obvious that "machining accuracy" will depend on the "machine accuracy"; but there are some other factors influencing the machining accuracy, investigation of which is the topic of the present thesis work. It is worth noting that machine accuracy, specified by the manufacturer of CNC machines, is generally set for working under "ideal" (non machining) conditions; but in actual machining operations these levels of accuracies are not achievable as practical machining conditions can not be non-productive and idle. In CNC machining operations a significant magnitude of accuracy is lost during interpolations and other related manipulative operations.

1.4 Application of GD & T

Prior to this century, only the basic dimensions were placed on engineering drawings. In those days everything machined was understood to be, 'exact' or 'perfect'. If some components did not fit, physical means, as necessary, were applied to fit them. The measuring instruments which could register the small variations responsible for such difficulty in assembly, were also not there in those days. With years of experience and innovative developments of very sensitive measuring instruments, it was found that, in

manufacturing processes such as turning, milling, drilling etc., it is not possible to consistently produce many parts with exact size or shape. Moreover, the practice showed that, parts need not be exact, and always a variation (within some limit) can be allowed. From this, the idea of plus/minus tolerancing (also known as coordinate tolerancing) came and is still in use. The plus/minus tolerancing is generally used to define the size and position variations. But it is not sufficient for today's industrial needs, because component assembly is dependent not only on size and position but also on the geometric configurations, alignments of mating surfaces, etc.

Geometric dimensioning and tolerancing (often referred in colloquial terms as "geometrics") is used to control form, profile, orientation, runout and location. GD&T is defined by ANSI Y14.5M-1982 [11] as a functional system of dimensioning that benefits both the design and manufacturing functions. In simple terms, GD&T can be described as a means of specifying the shape or geometry of a part on an engineering drawing. GD&T is rapidly becoming a universal engineering drawing language. If properly applied it also yields economic benefits. Different national and international standards have already accepted GD&T. Australian Standard AS1100.201 states "Geometric tolerances should be specified for all applications where assembly and interchangeability are mandatory requirements of design" [12].

The most common terms used in the language of GD&T in ANSI Y 14.5 are given in Appendix A. A comparison of symbols used in GD&T by different standards (ISO, AS1100 (Australia), ANSI Y14.5 (U.S.A.), BS 308(U.K.) and B78.2 (Canada)) are also given in Appendix B.

1.4.1 Advantages of GD & T:

The basic advantages of GD &T are as follows:

- It is the best available means to convert functional requirements into parts that can be produced at the lowest cost.

- It ensures a single interpretation of drawing and improves communication among the designer, manufacturer and the inspector. It is increasingly becoming the "spoken word" through industry, the military, and internationally, on engineering drawing documentations.

- It allows the design dimensional and tolerance requirements, as they relate to the actual function. All restrictions required can be given (if the designer decides), in the drawing and thus carried out accordingly.

- It ensures interchangeability of mating parts at assembly if properly applied.

1.4.2 Problems with Old Method

In the old method, holes are located with positioning tolerance that have plus and minus values; e.g. in Figure 1.5, position tolerance is ± 1.0 mm. This method of tolerancing creates a square tolerance zone, within which the axes of the holes must lie (see Figure 1.6). A Square tolerance zone allows the holes to be off location more in a diagonal direction than across the flats as shown in Figure 1.7. As it is not desirable the holes to be off location more in one direction, the tolerance zones should be round and not square (see Figure 1.8).

Another advantage of round tolerance zones over the square zones is that in some cases we may get additional tolerances [13], [14]. The reason is that in the plus/minus system, the axis of the hole can be anywhere in the square. If we located the axis of the hole in the corner of a 1.0 mm square zone, it is possible that the hole could be approximately 0.707 mm off the basic centre, if measured in a diagonal direction as shown in Figure 1.9. If

1.0 mm square zones were used, the diameter would be approximately 1.414 mm. Thus, it is possible to have an increase of 57% additional tolerance as shown in Figure 1.10. If 1.0 mm dia. zone is used 21.5% reduction of position tolerance could take place and if 1.0 mm dia. zone is changed to 1.414 mm dia. zone, 100% increase of position tolerance may be achieved.

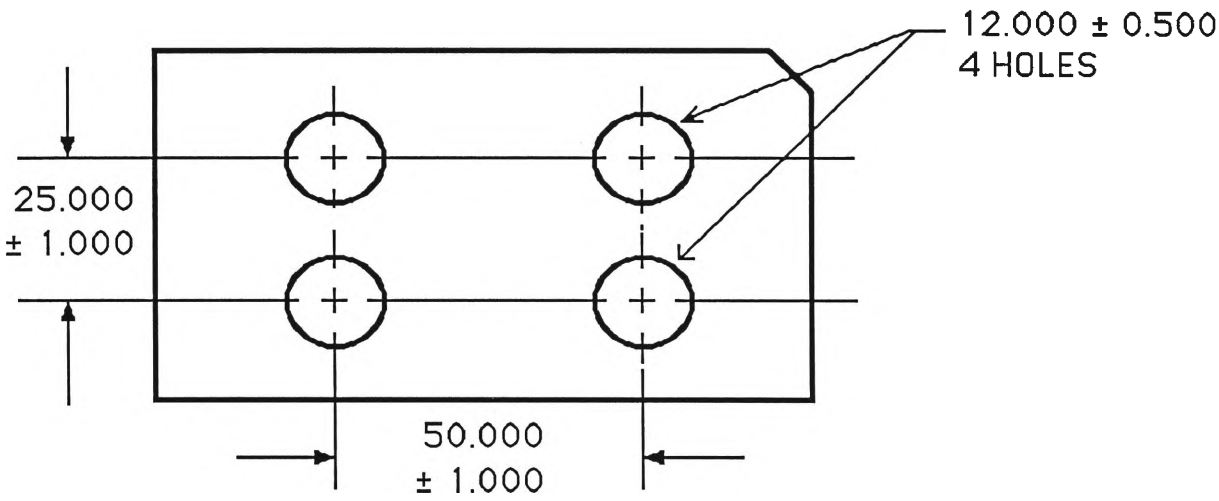

Figure 1.5 Part with Holes Located with Plus/Minus Type Dimensioning [13].

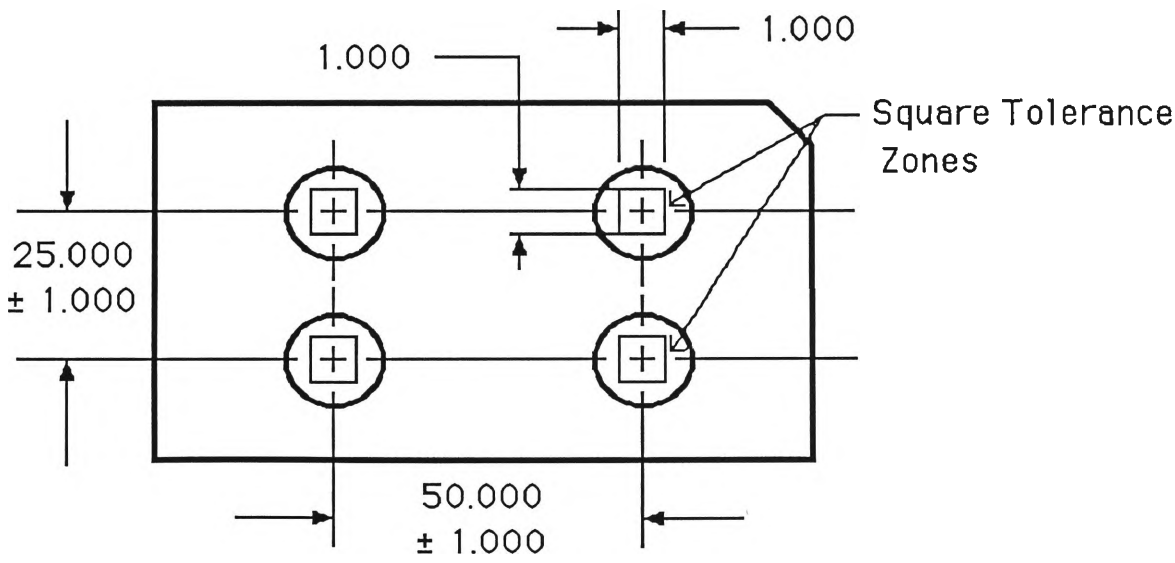

Figure 1.6 Square Tolerance Zone Created by Plus/Minus Type Dimensioning [13].

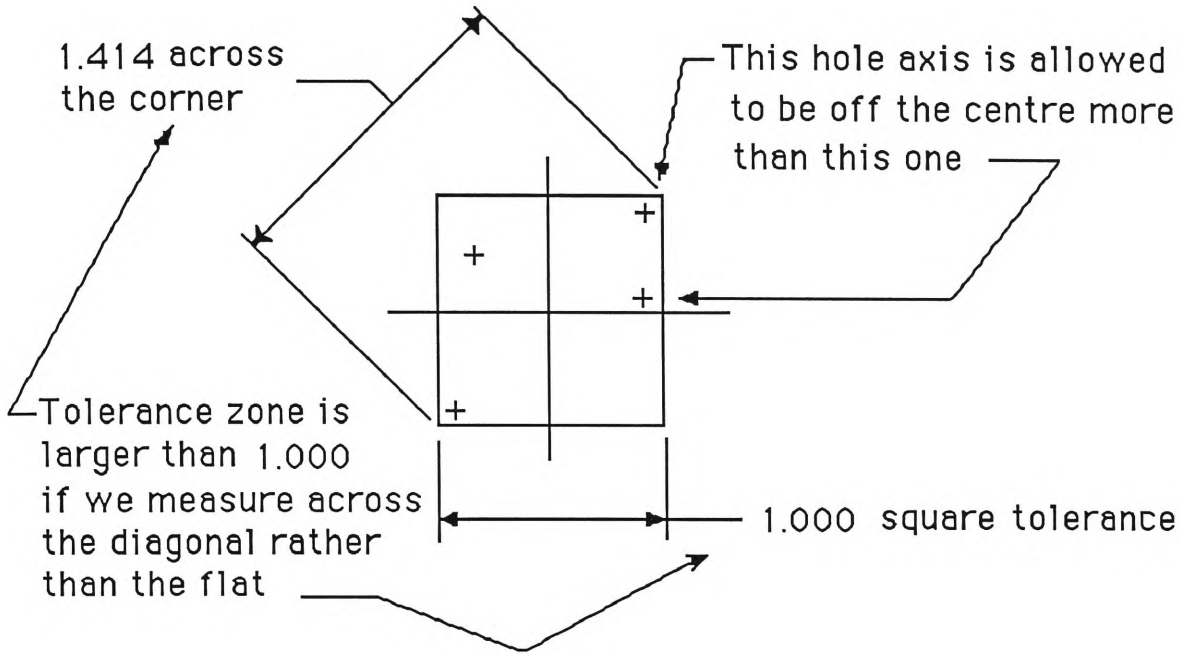

Figure 1.7 Square Tolerance Zone [13].

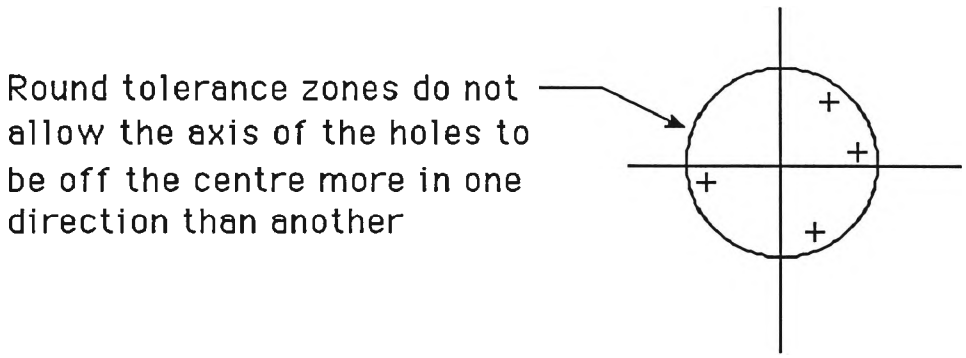

Figure 1.8 Round Tolerance Zone [13].

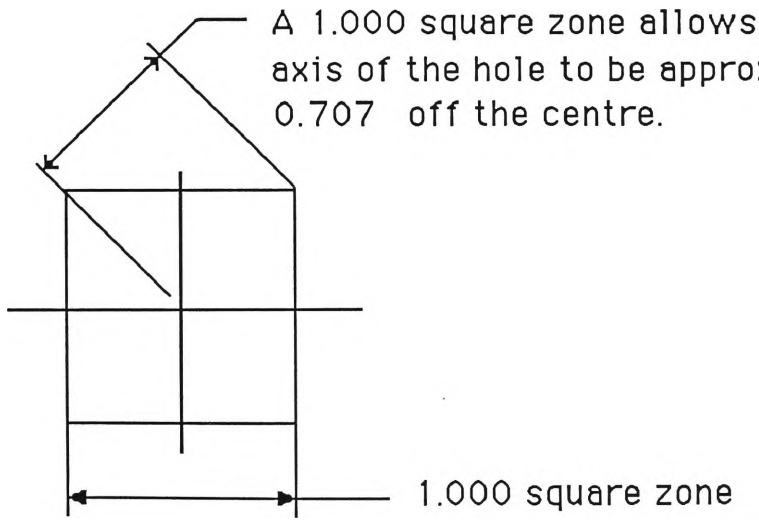

Figure 1.9 Square Tolerance Zone [13].

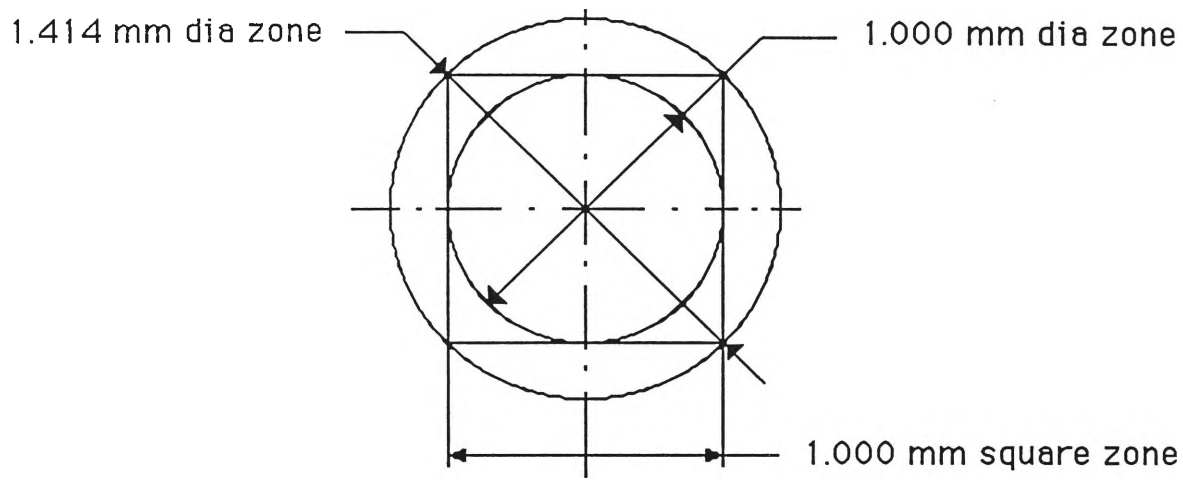

A_{sq} = Area of square s = side of the square

$A_{o.c.}$ = Area of outer circle d_o = outer diameter

$A_{i.c.}$ = Area of inner circle d_i = inner diameter

1.000 mm square zone = $A_{sq} = s^2 = 1.0^2 = 1.0$

1.414 mm dia zone = $A_{o.c.} = \pi d_o^2 / 4 = \pi (1.414)^2 / 4 = 1.57$

$$\% \text{ Increase} = \frac{A_{o.c.} - A_{sq}}{A_{sq}} \cdot 100 = \frac{1.57 - 1.0}{1.0} \cdot 100 = 57\ \%$$

1.000 mm dia zone = $A_{i.c.} = \pi d_i^2 / 4 = \pi (1.00)^2 / 4 = 0.785$

$$\% \text{ Increase} = \frac{A_{i.c.} - A_{sq}}{A_{sq}} \cdot 100 = \frac{0.785 - 1.0}{1.0} \cdot 100 = -21.5\ \%$$

% Increase of 1.414 mm dia zone with respect to 1.000 mm dia zone

$$= \frac{A_{o.c.} - A_{i.c.}}{A_{i.c.}} \cdot 100 = \frac{1.57 - 0.785}{0.785} 100 = 100\ \%$$

Figure 1.10 Comparison of Square and Round Tolerance Zones.

In addition to the above-mentioned additional tolerance, more position tolerance can be achieved by the application of GD&T without risking the function. If a position tolerance is specified at MMC, it would mean that the position tolerance is applicable only when the feature is manufactured at its MMC. If the feature departs from MMC size, the position tolerance increases (Figure 1.11). The amount that feature deviates from MMC size is added to the specified position tolerance. This extra tolerance is known as **bonus tolerance**. As a feature departs form its MMC size, gain of bonus tolerance will be more and it reaches its maximum value as the feature goes to LMC. Moreover, as position tolerance gains bonus tolerance on its departure from MMC size, the concept of "zero positional tolerancing" at MMC can be applied. In that case the position tolerance allowed will totally depend on the actual size of the feature; thus, one check can be eliminated.

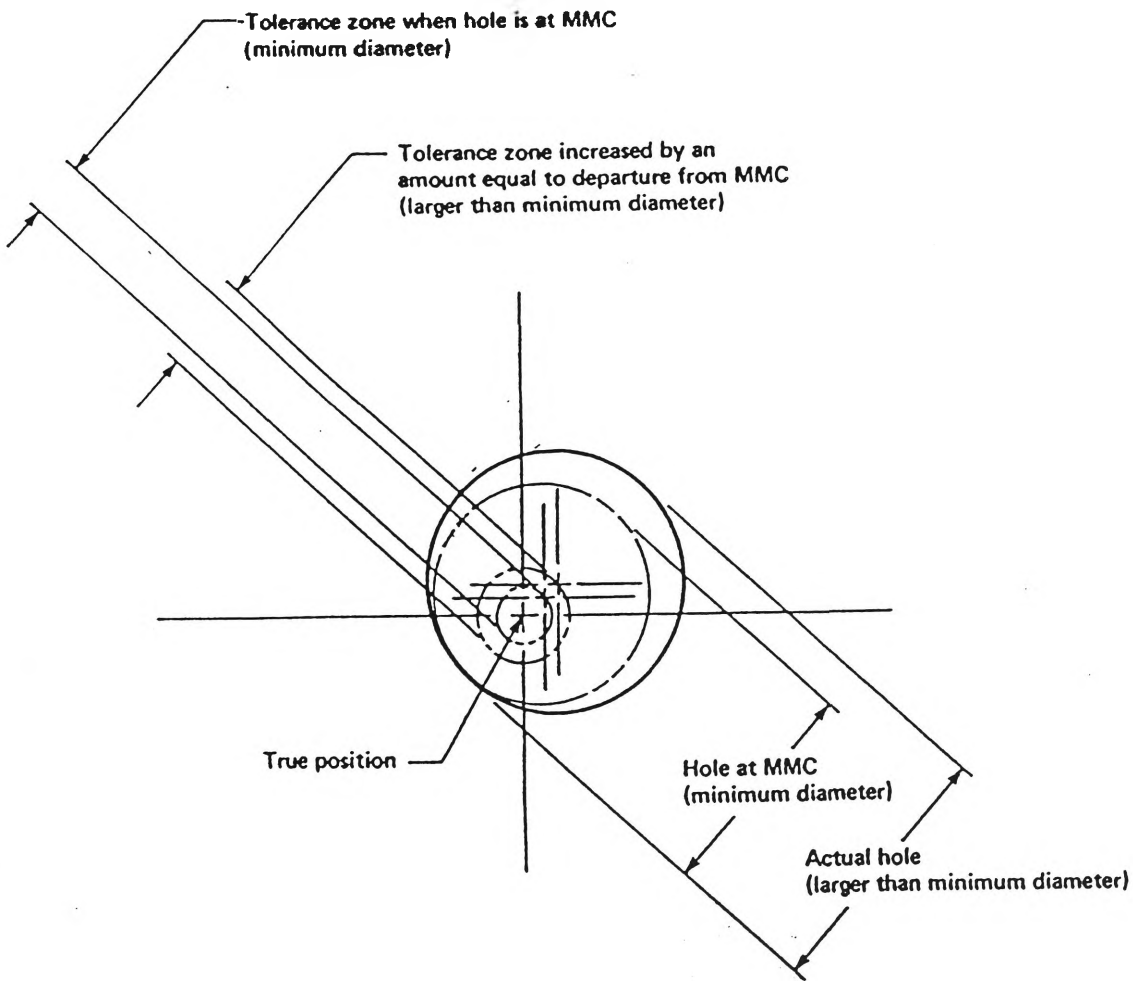

Figure 1.11 Increase in Position Tolerance where Hole is not at MMC [11].

1.5 Significance of CMM

Undoubtedly, the most significant advance in dimensional metrology is the Co-ordinate Measuring Machine (CMM). With the advent of NC machine tools, the demand has grown for means to support the equipment with faster and more accurate inspection. The concept of measuring the geometry of a workpiece is not new. This concept has led to the development of the first CMM in the early 1960s. As in the case of NC machine tools, industrial acceptance of CMMs came only after a long period of time from their first development. At present CMMs are widely used in the manufacturing industry in one of three ways [15].

The first approach is to place the CMM at the end of the production line or in an inspection area. With this approach, the CMM is used to check the set up of the first component. Once the set-up is verified, then the components are inspected randomly. In this setting the CMM can be placed outside the shop floor and then it will not have to work in the shop environment.

The second approach is to incorporate the CMM between two workcentres and then measure 100% of the parts produced by the first centre before any secondary work operations are performed at the second centre. When this approach is applied, the CMM indirectly controls the production process. In this setting the CMM should be capable of working in an industrial environment.

The third approach is to integrate the CMM into the production line. When applied this approach, CMM becomes an essential part of the Computer Integrated Manufacturing (CIM) system, and in this case, the production quality is directly controlled (on-line) by CMM.

1.6 Present Philosophy

The present study on accuracies has been undertaken from a CNC machine user's point of view. It has been mentioned in a previous section that the machining accuracy depends on machine accuracy. But as a user of CNC machines there is very little opportunity to alter the machine accuracy, hence the machine accuracy is taken as inherent in the present study.

The present study adopts "quality first" principle, i.e. where a decision was needed about quality, productivity and cost, the first preference chosen is quality. This approach may contradict general production practice, where cost effective manufacture in high productivity environment is aimed at. It is the strong belief of the author of this thesis that improved quality will eventually bring in a more favourable marketability increasing the productivity levels which leads to cost reduction in manufacture.

This thesis work also reflects the traditional belief that "prevention is better than the cure", which in terms of the modern quality management philosophies reasserts the concept that "the quality can not be inspected-in, but has to be built-in to the product right from the designing stage".

2.0 LITERATURE SURVEY

From the extensive literature survey that was carried out to identify the present knowledge on machining accuracy in CNC machining operations, it has been found that only a very limited number of published work* has been reported to date. It appears that this subject has somehow been overlooked by most of the authors, as rightly pointed out by Arai et al [16], "The authors have made various kinds of research on the turning of NC lathe for several years, but they have not yet tried the research of working accuracy". Due to the vastness of the problem, many of the researchers have concentrated on specific factors affecting the machining accuracy of CNC machining operations. These authors consider the problem only from their own point of view totally ignoring the combined effect of all factors that are likely to influence the process. In truth, the problem is far more complex.

The study of machining accuracy calls for wide understanding and greater knowledge in a number of fields. Over 100 publications that were reviewed with a view to establishing the present level and developments are classified into four major groups as shown in Table 2.1. A summary of the review is presented in four major subsections of this chapter.

2.1 Machine Accuracy

Researchers have been concerned about machine accuracy for a long time and several publications have been produced examining this problem. Pioneering work on machine tool accuracy was done by Schlesinger, who has been reported to have started his work on acceptance standards for machine tools in 1901. His famous book "Testing Machine Tools" [17] is still very widely used by machine tool manufacturers, users, inspectors

* It seems that, there is a great deal of unpublished industry-sponsored work done by different industrial organizations, which they do not want to share with their competitors.

and plant engineers. In this book 44 inspection charts, a discussion of the basic principles and an explanation of testing procedures are given. In its recent edition a chapter on NC machine tools written by Koenigsberger and Burdekin is included. This book is to be regarded as a reference book due to its diversity of contents. Schlesinger's machine tool accuracy tests include: flatness of tables, straightness of sideways, accuracy of spindle rotation, accuracy of linear motion, lead or pitch error of lead-screws, etc. In his book measurement procedures of these inaccuracies are explained in details. In the test charts tolerances of the inaccuracies are also given.

Group No	Research Area	References
1	Machine Accuracy	[17], [18], [19], [20], [21], [22], [23], [24], [25], [26], [27], [28], [29], [30], [31], [32], [33], [34], [35], [36], [37], [38], [39], [40], [41], [42], [43], [44]
2	Machining Accuracy	[16], [45], [47], [48], [49], [50], [51], [52], [53], [54], [55], [56], [57], [58], [59], [60], [61], [62],[63], [64], [65], [66]
3	On-line Monitoring and Adaptive Control Systems	[46], [67], [68], [69], [70], [71], [72], [73], [74], [75], [76], [77], [78], [79], [80], [81], [82], [83], [84], [85], [86], [87], [88], [89], [90], [91], [92], [93], [94]
4	Studies on Co-ordinate Measuring Machine	[95], [96], [97], [98], [99], [100], [101], [102], [103], [104], [105], [106], [107], [108], [109], [110], [111], [112], [113], [114], [115], [116], [117], [118]

Table 2.1 Summary of Literature Survey.

Tlusty and Koenigsberger [18] pointed out that the classic concept of geometric accuracy which was created by Schlesinger and later accepted by various national and international standards, does not take into account a number of functional effects, such as, weight deformation, deformation due to clamping forces, thermal effects, dynamic errors of displacement systems, etc. These inaccuracies are particularly important for CNC machines, because in CNC machining operations normally the operator who can take necessary actions to eliminate most of those effects is not present. Tlusty and Koenigsberger studied the geometric accuracy of machine tools using a "work zone concept" (where the error is calculated within the whole work zone) and a "master part trace test" (where a master part is used to find error components). Their study also includes spindle rotation accuracy, displacement accuracy, weight and clamping effects, thermal effects, forced vibration and cutting force deformations. Main findings of their study are:

- Weight and clamping effects may cause errors many times greater than the basic alignment errors.
- On average, the thermally induced error is of equal significance to the positioning error.
- Cutting force deformations may entirely be neglected for turning, boring and milling.*

Tlusty et al [18] must have been referring to Schlesinger's original work in which some functional effects were not included. But in the recent edition of Schlesinger's book [17] where a new Chapter is added titled "Recent Developments in Machine Tool Testing", the accuracy of positioning system, cutting tests for accuracy assessment using a standard test piece, weight deformations, indexing table errors, thermal deformations, spindle rotation accuracy, dynamic testing of machine tools, etc. are discussed.

---

* But findings of other researchers (which will be discussed later in Chapter 5) show that tool deflection in end mills is relatively high and thus cannot be neglected.

Tlusty has also elaborated the work zone concept for testing accuracy of NC machine tools in another work [19]. He used a simplified method called "the linear system of accuracy of NC machine tools". The system is called linear because, only linear (translative) and no angular deviations connected with the motions of the bodies of the machine are considered. In effect, only 9 error components of the total 21* error components representing the volumetric accuracy of a 3-axis machine tool were considered. Tlusty advocated avoiding the use of a machining test, because: (a) it is more expensive and time consuming; (b) the effects of tool wear and workpiece distortions cannot be separated from those of the machine inaccuracy. In his work Tlusty used a graphical template as master part for testing the accuracy of NC machine tools. He developed tolerances for accuracy tests and tolerances were expressed as linear functions of distances of points in the working zone (another reason for calling the system linear). The angular motions were avoided because these are very difficult to measure, and, there is no direct criterion for determining the tolerances for the the angular motions. But the effects of angular deviations were checked indirectly by increasing the number of measurements on the linear deviations. Finally, Tlusty showed how to determine the minimum necessary number of linear measurements which can, in a fully comprehensive way, express the effect of errors connected with the individual co-ordinate motions on the accuracy of relative tool-workpiece motions in the whole working zone of the machine.

Cowley and Hinduja [20] applied a finite element method for machine tool structural analysis. Computer programmes were developed for computation of the static deformation of the machine tool structures and structural elements. Machine tool structures were subdivided into different plate-like elements (rectangular, triangular, etc) and beam like elements. The deformations of each individual element was calculated and

* 21 components of the volumetric accuracy include 6 components for each axis (each axis having six degrees of freedom of movement) and 3 components coming from non-orthogonality of axes. (For details see Chapter 7).

were then combined to form resultant deformation of the overall structure. This type of approach is very helpful for designing machine tool structures and structural elements, as their deformation, which contributes to machine error significantly, can be minimized. But as pointed out by Cowley and Hinduja, their analysis was based on a very simple structure and detailed analysis of a complete machine tool using their techniques involves calculation of a large number of finite elements.

Schultschik [21] examined the "volumetric" errors in 3-axis machine tools having investigated the way of combining the error components in the work space of a given machine tool. A geometric model of the machine tool was developed and his analysis was based on vector diagrams. A typical machine tool and its vector diagram is shown in Figure 2.1.

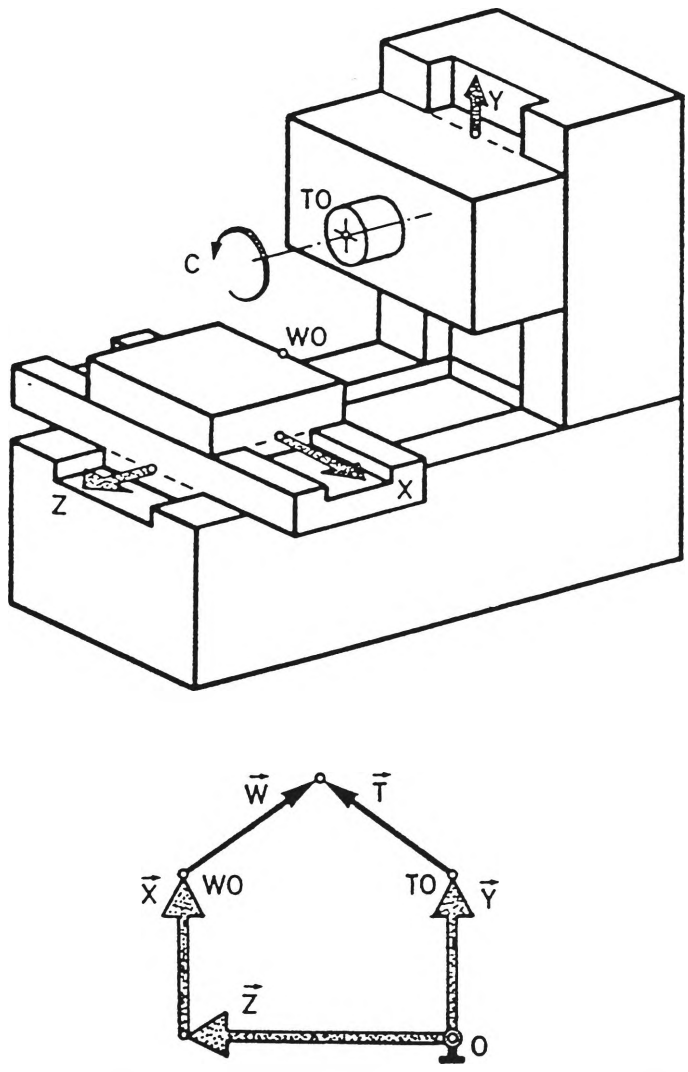

Figure 2.1 A Typical Machine Tool and it's Vector Diagram [21].

In general, the combined vectors have the following form:

$$\vec{Z} + \vec{EZ} + \begin{pmatrix} EAZ \\ EBZ \\ ECZ \end{pmatrix} . (\vec{X} + \vec{EX}) + \begin{pmatrix} EAX \\ EBX \\ ECX \end{pmatrix} . \begin{pmatrix} EAZ \\ EBZ \\ ECZ \end{pmatrix} (\vec{W} + \vec{EW}) = \vec{Y} + \vec{EY} + \begin{pmatrix} EAY \\ EBY \\ ECY \end{pmatrix} . \vec{T} \quad (2.1)$$

where

X,Y,Z	translatory axes
A,B,C	rotational axes
EAZ	is the rotation of Z axis along A etc.
E	error
$\vec{W}$	workpiece offset
$\vec{T}$	tool offset
$\vec{EW}$	workpiece error

In a later study Schultschik [22] added the effect of load conditions on the accuracy of machine tools. Under load conditions, additional effects, such as workpiece weight or thermal deflections take place, and this makes the problem more complicated. But it is found that, in practice, these loads cause typical effects on the machine tool. Thus while testing a machine under load conditions, it is possible to restrict the measurements to these types of errors. The method described by Schultschik is suitable to use for machine tool accuracy improvement.

Eman, Wu and De Vries [23] presented a methodology to build a generalized error model of an arbitrary multi-axis machine. They considered geometric errors of the machine and errors resulting from the relative motion between machine elements. Their error model is based on rigid-body kinematics and the spatial relationship between the machine's components was described by a set of homogeneous transform matrices. Equations for error components were derived, which can be useful for error estimation as well as for

identifying dominant contributors to the total error. The model could offer benefits in the design of new machines and in their real-time error-compensation.

Knapp [24] proposed a testing method called "circular test" to determine the geometric errors of machine tools and measuring machines. Compared to the other methods for measurement of geometric errors of machines, his method is simple and does not need expensive equipment (laser interferometers, electronic levels etc). For the circular test a cylindrical masterpiece with high precision (out of roundness less than 1 micron) is used. The masterpiece is placed on the machine table. A two-dimensional probe is mounted in place of the cutting tool. The machine is programmed to move on a circle in a way that the probe keeps in steady touch with the masterpiece. The path of the probe is plotted. In ideal conditions (i.e., if the machine is error-free), the probe should follow a circular path with a diameter equal to the diameter of the masterpiece. Any deviation from the nominal circular path indicates the presence of machine error. By analyzing the shape and size of the distorted circle the amount of different geometric error components can be determined (see Figure 2.2).

In recent years, a number of research projects on machine tool accuracy have been undertaken at Purdue University, USA by the precision engineering group, which includes studies by Donmez [25], Venugopal [26], Venugopal and Barash [27], Ferreia and Liu [28], [29], Lee and Barash [30] etc.

Donmez [25] developed a general methodology for machine tool accuracy enhancement. A general mathematical model was developed to determine the total error at the cutting tool tip by using homogeneous co-ordinate transformations for each element of the machine tool. A methodology for establishing a model for different machine tools was presented and applied to a two-axis turning centre. In his model, geometric and thermally-induced errors were considered. Unlike other studies of thermal errors, which used finite element methods to find thermal deformations, Donmez studied the end effect

of the thermal changes on the geometric behaviours of the machine elements, which makes all of the individual error components as functions of axis position and the temperatures of the selected locations on the machine tool structure. A modular, flexible and easily maintainable software system was developed for error compensation in real-time.

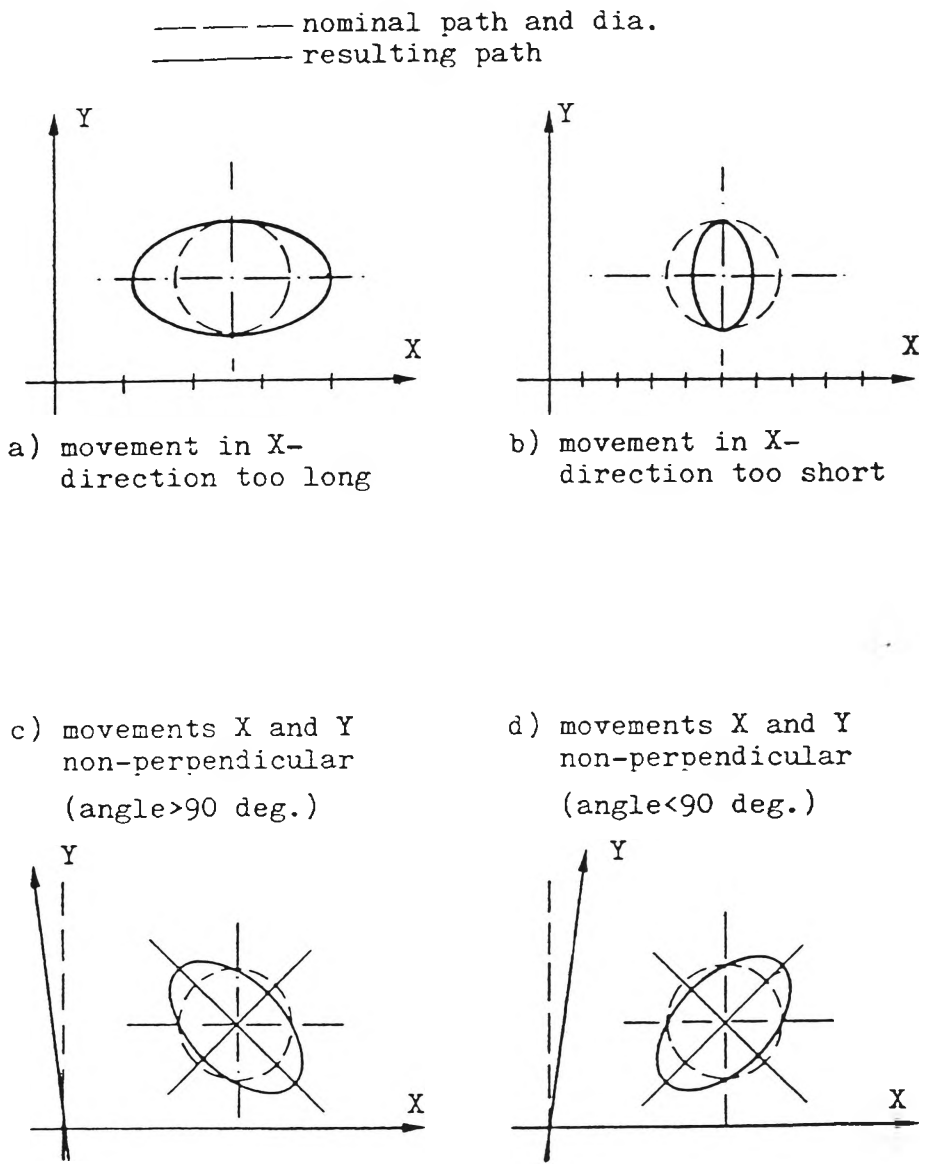

Figure 2.2 Effect of Principal Errors on a Circular Movement [24].

Venugopal [26] identified the thermal effects as the main source of machine error of NC machine tools. The thermal characteristics of a hypothetical machine were studied. Thermally induced errors were predicted using regression equations. Experimental results were compared with numerical work and it was found that the thermal influence on the

accuracy of machine tools was predictable. Experimental results showed that positioning errors are the largest of the six measured errors (viz. positioning error, horizontal straightness error, vertical straightness error, roll, yaw and pitch). It was found that the standard deviations of the positioning errors vary dramatically. This means positioning errors cannot be easily predicted with a simple regression technique. Venugopal [26] suggested the use of an external reference such as a magnetic scale for compensation of positioning error. Other errors are predictable as a function of the temperature of the machine tool.

Ferreira and Liu [28] presented an anatomical quadratic model for the geometric errors of a machine tool. They used rigid body kinematics to relate the error vector at a point in the machine tool workspace to the co-ordinates of that point by the dimensional and form errors of the individual links and joints of the machine's kinematic scheme. In previous works by other authors, it was assumed that the angular misalignments (pitch, yaw and roll) and the positioning error along any axis of the machine are constants, i.e., the axes of motion of the machine are straight, although no suitable justification of this assumption was given. Ferreira et al [28] considered linear relationships between the error components (positioning, pitch, roll and yaw) of a joint and displacement along the joint. Based on the linear variation of individual errors, an expression for the geometric error of a machine tool was developed, which is quadratic. A method for estimating the co-efficients of the model from the error obtained on a workpiece was also proposed.

Lee and Barash [30] used a touch probe and a metrology pallet for improvement of a CNC machining centre. A mathematical model was developed to obtain the position errors of the tool tip within the entire workspace under varying thermal conditions. The error map of the whole workspace was obtained using a touch probe and a master metrology pallet. The master pallet has several measurement points and was mounted on the machine table at certain intervals. After calibration of the master pallet in cold condition, the master pallet was recalibrated in warm condition and the difference

between these calibration measurements gave the "thermal growth" of the machine tool, which was later used in error compensation. A "dynamic" method of compensating the backlash was proposed using ANOVA (Analysis of Variance) analysis to determine the dominant factors affecting the backlash. The positioning error and the angular error were modeled by the General Method of Data Handling (GMDH) technique of the Russian engineer Ivakhenko. Machining tests were performed to check the acceptability of the model and an accuracy enhancement of around 50% was achieved.

2.2 Machining Accuracy

As machining accuracy is the accuracy achieved on the machined workpiece, it can only be verified by conducting machining tests. Some researchers [19], [21] have suggested avoiding machining tests, as in machining tests the results of different factors affecting machining accuracy and machine accuracy cannot be separated. But a machine is only a machine when it does the job. Thus without machining tests, performance of machine tools cannot be properly evaluated. Moreover from the users' point of view machining tests are essential, because the manufacturers of CNC machines usually make exaggerated claims.

Farmer [10] raised the question about accuracy of NC machine tools and showed that NC machine tools are not as accurate as generally thought to be. Due to various inaccuracies, dimensions of NC machined components vary significantly. From this Farmer concluded that in NC machining, dimensions of machined components still have to be inspected and tolerance limits should be specified on the product drawings. This shows the invalidity of the generally accepted notion that, "tolerances are no longer required on the dimensions of products that are to be produced on NC machines". He also emphasized the use of datums in dimensioning. Farmer and Harris [45] in an earlier work highlighted the need for further studies on change of datums, tolerances and their corresponding effects on the machining accuracies achievable in CNC operations.

2.2.1 Factors Affecting Machining Accuracy

There are a number of factors which can cause poor accuracy levels in CNC machining operations. One observation [46] shows that over thirty factors directly or indirectly influence milling operations. Lawrence Livermore laboratory, USA has established the following factors as causing poor machining accuracy [47]:

(a) geometric and kinematic errors of the machine tools;
(b) spindle errors of the machine tools;
(c) thermal effects on the machine tool and on the workpiece;
(d) static loading;
(e) dynamic loading;
(f) tool wear; and
(g) errors due to work holding.

Factors affecting machining accuracy listed by Tlusty et al [19], McKeown [48], and Koval and Igonin [49] are given in Figures 2.3, 2.4 and 2.5 respectively.

Koval and Igonin [49] made a comparative analysis of machining errors for a heavy NC machine tool. They listed the factors affecting machining accuracy (see Figure 2.5). All those error components for a heavy NC vertical milling machine were calculated analytically. As error components in point-to-point machining and contour machining differ, these two cases were considered separately. The results of their calculation of error components are given in Figures 2.6 and 2.7. The method of quadratic summation was used to find the resultant error and the error values obtained analytically showed close match with the experimental values.

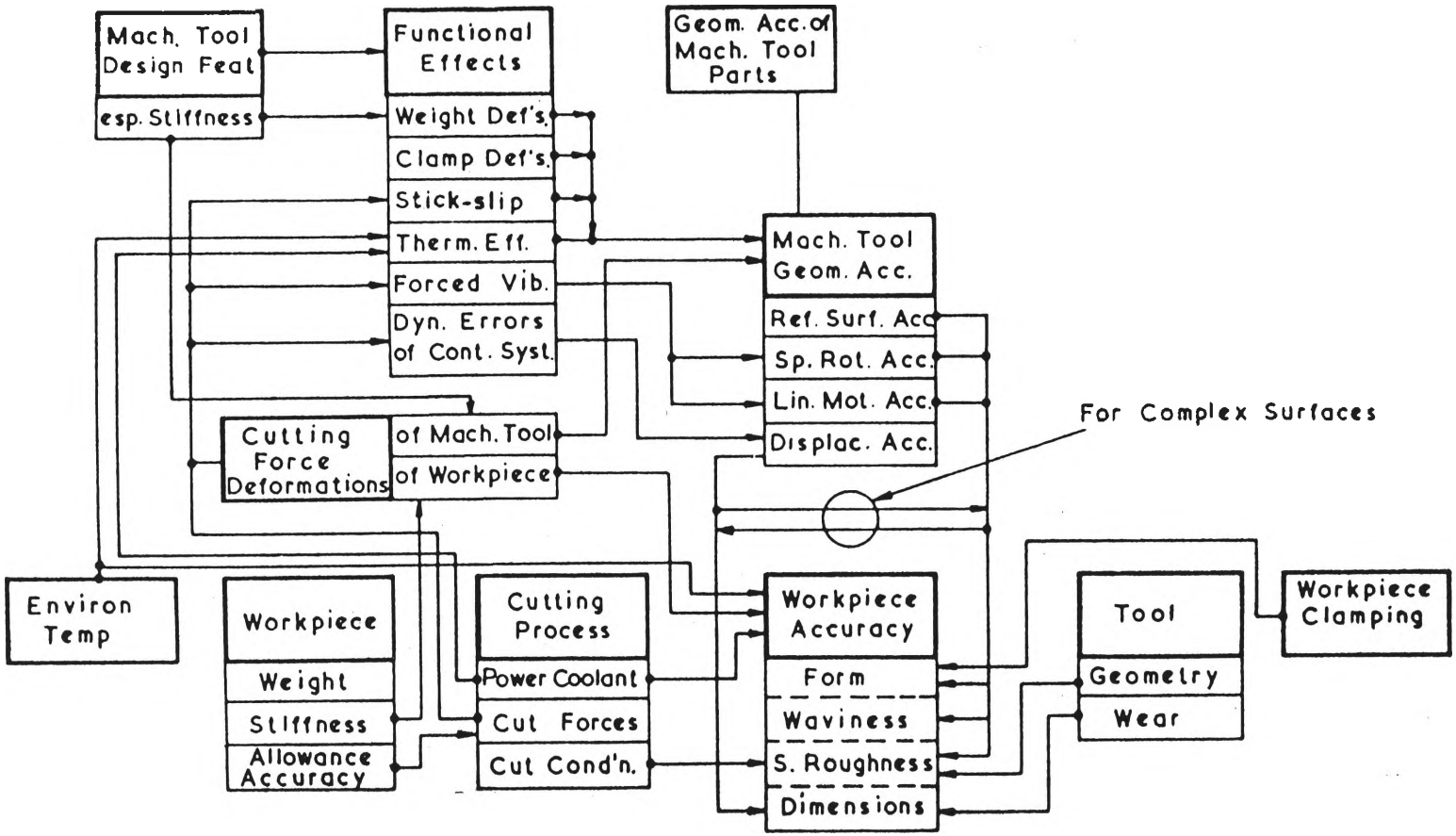

Figure 2.3 Factors Influencing Accuracy of the Workpiece [18].

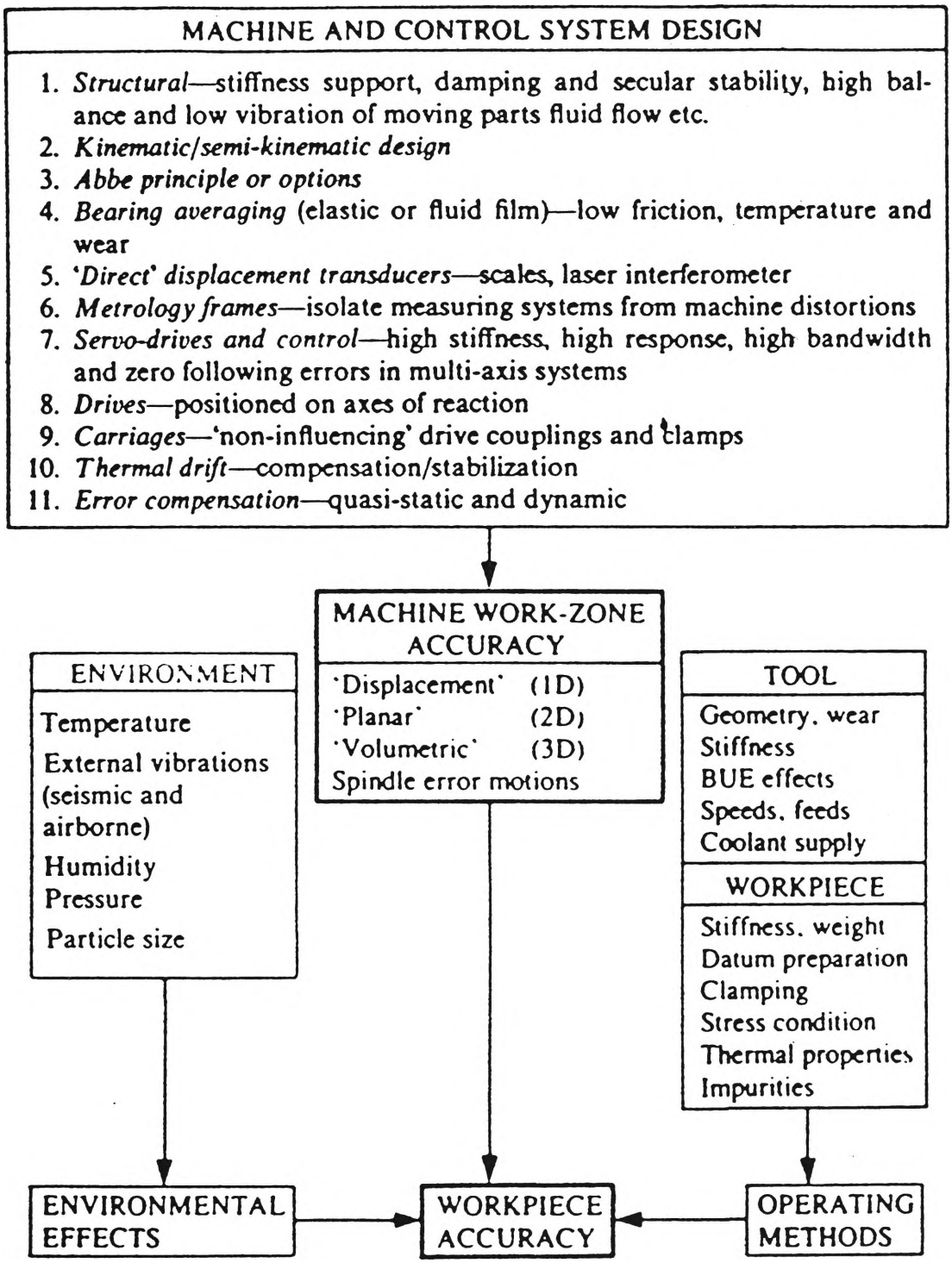

Figure 2.4 Factors Affecting and Controlling Workpiece Accuracy [48].

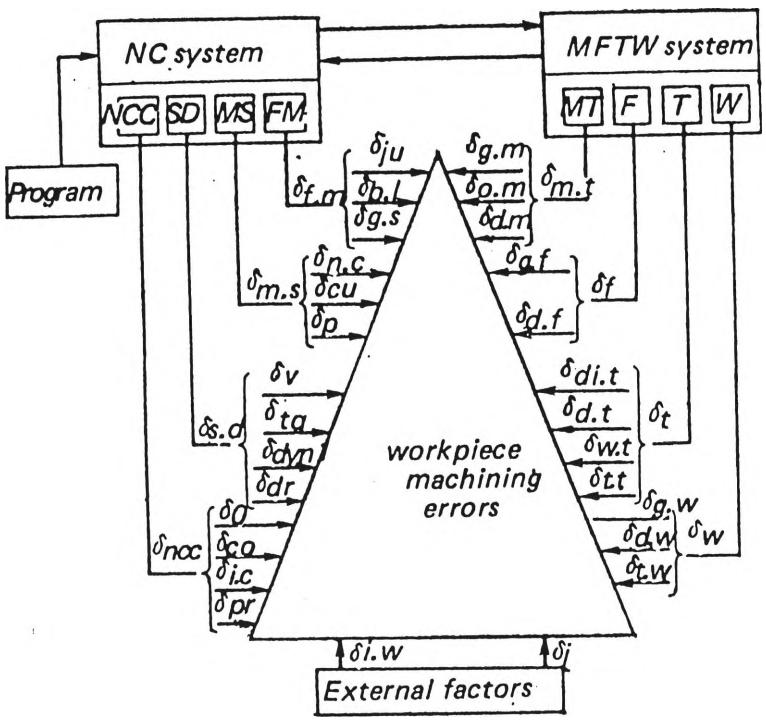

Machining error components and their sources in a machine tool with an NC contouring system: *NCC*—NC controller; *SD*—controlled drive (servodrive); *FM*—feed mechanism; *MS*—measuring system; *MT*—machine tool; *F*—fixture; *T*—tool; *W*—workpiece; δ_{ncc}, $\delta_{s.d}$, $\delta_{m.s}$, $\delta_{f.m}$, $\delta_{m.t}$, δ_f, δ_t, δ_w—machining error components caused by the respective elements of NC and MFTW systems; δ_{pr}—programming error; $\delta_{i.c}$—interpolator error (calculated); δ_{co}—error of interpolator correctors; δ_o—errors in forming the 'go to zero' instructions for the machine tool moving parts; δ_{dr}—drift error of servodrive unit characteristics; δ_{tq}—drive torque error; δ_{dyn}—dynamic error of the drive; δ_v—drive velocity error; δ_p—in-pitch transducer error; δ_{cu}—cumulative transducer error; $\delta_{n.c}$—norming converter error; $\delta_{g.s}$—geometric error of the leadscrew; $\delta_{b.l}$—backlash error of the ball bearing screw; δ_{ju}—error caused by the jump type (stick-slip) character of machine parts motion at low feed rates; $\delta_{g.m}$—geometric machine error; $\delta_{o.m}$—orientation change error of machine tool moving parts; $\delta_{d.m}$—machine parts deflection error; $\delta_{g.f}$—geometric error of the fixture; $\delta_{d.f}$—fixture deflection error; $\delta_{di.t}$—dimensional tool error; $\delta_{d.w}$—tool deflection error; $\delta_{w.t}$—tool wear error; $\delta_{t.t}$—tool thermal error; $\delta_{g.w}$—workpiece geometric error; $\delta_{d.w}$—workpiece deflection error; $\delta_{t.w}$—workpiece thermal error; $\delta_{i.w}$—workpiece inspection error; δ_j—errors caused by other external factors.

Figure 2.5 Machining Error Components and Their Sources in a Machine Tool with an NC Contouring System [49].

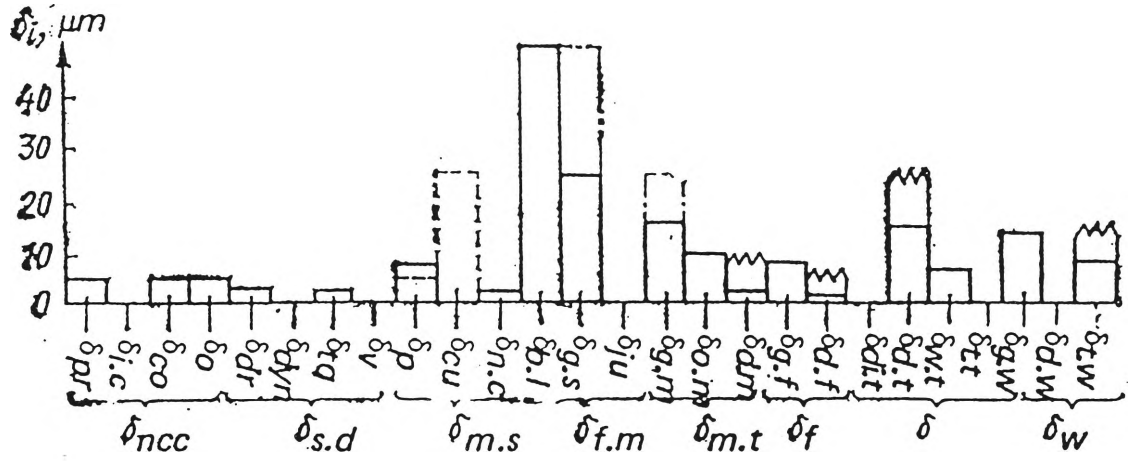

Figure 2.6 Diagram of Dimensional Error Components in Point-to-Point Machining[49].

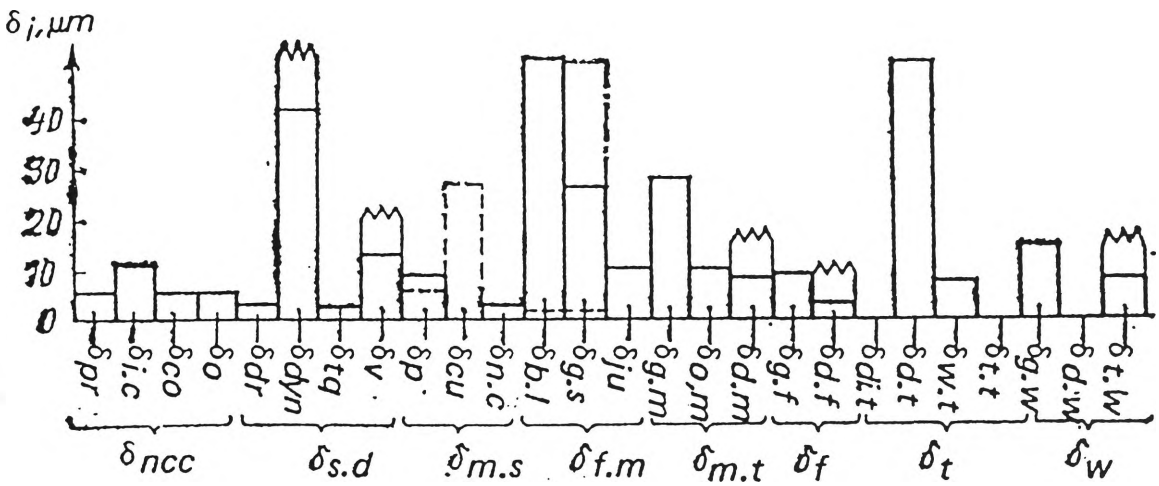

Figure 2.7 Diagram of Dimensional Error Components in Contour Machining [49].

Venugopal and Barash [27] claim that 60-70% of total error in machine tools come from thermal effects alone; while Arai et al [16], found that thermal displacement affects 40% and tool wear affects 20% of total errors. Takeuchi et al [50] found that 52% of the total cylindrical errors of the workpiece comes from thermal effects on the machine tool and workpiece. As such we find different opinions among the researchers about the likely causes of errors as the experimental set-ups were quite different from each other with significantly different cutting conditions, tool geometry and work materials being used.

It is to be noted that some of the factors affecting machining accuracy of CNC machining operations are common in conventional machining operations and these factors have been well known to researchers for a long time. Due to involvement of computers in CNC machines, it is "generally believed" that CNC machines are error-free. However, this is far from true in an actual machining operation, since the use of computers is for computation and decision making based on a preprogrammed logic and that it is an electronic device with high accuracy, whereas the actual work done is mechanical with lower accuracy, particularly when the operation is performed under a dynamic load.

2.2.2 Methods for Machining Accuracy Improvement

A systematic approach to improve the machining accuracy is shown in Figure 2.8. Two basic methods for the improvement of machining accuracy have been proposed [51]: (a) error avoidance and (b) error compensation (error reduction). Error avoidance calls for elimination of the source of the error through improved design and controlled manufacturing technology. Sometimes it is possible to improve machining accuracy of a machine by a series of thoughtful and conscientious design features and by optimizing machining process without any (or very little) extra cost. Thus, the error avoidance should be the first step of accuracy control. Error compensation is defined [47] as "a method of canceling the effect of the error by predicting it using a model built for the

purpose". There are two basic approaches to error compensation: (1) pre-calibrated error compensation and (2) active error compensation.

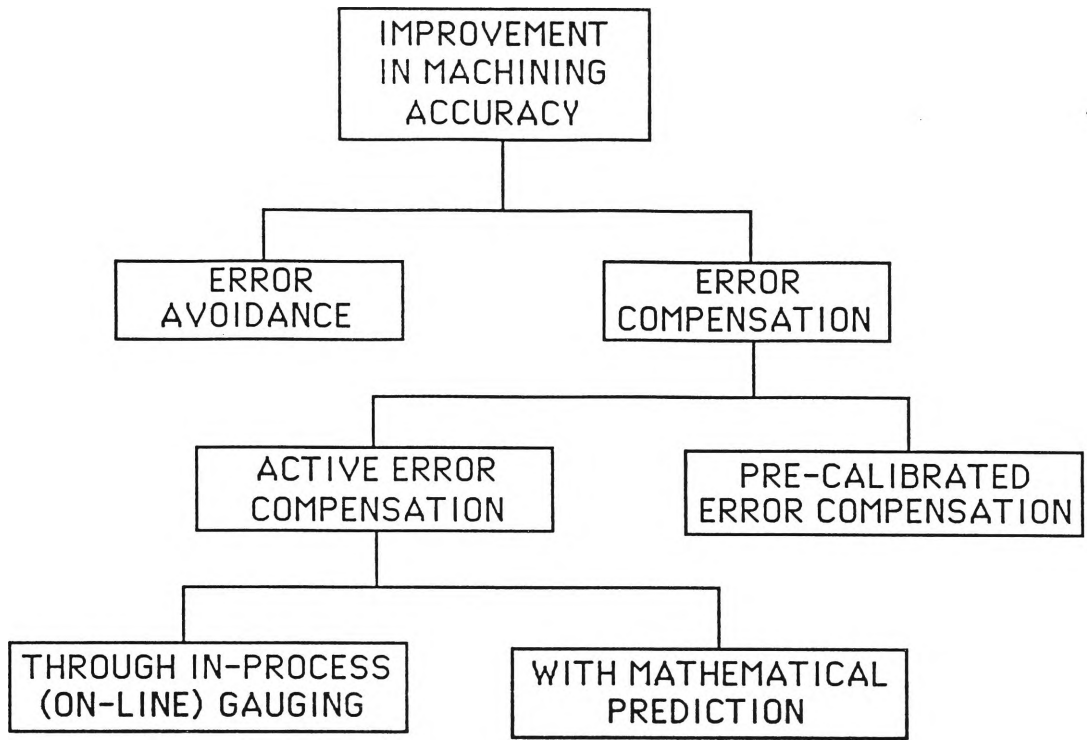

Figure 2.8 A Systematic Approach to Machining Accuracy Enhancement.

For pre-calibrated error compensation, errors are measured or identified first, either before or after the machining process (test cut). Once the errors are known, they are compensated for and corrected during the subsequent operations. Pre-calibrated error compensation technique is based on the assumption that the errors and the measurements are repeatable. In active error compensation, the identification of the error and its control are done simultaneously during machining. There are two general approaches to the identification of errors for active compensation: (i) through an in-process (on-line) gauging and (ii) with a mathematical prediction.

Active error compensation through in-process gauging is the most recent and complex technique of error reduction. This approach identifies the workpiece error directly and

there is no need to find the cause-and-effect relationship between errors and sources. This approach can sense and correct non-repeatable errors, which pre-calibrated error compensation cannot do, as pre-calibrated error compensation is based on the assumption that the errors are repeatable. Active error compensation through in-process gauging is difficult to implement, because it needs highly effective on-line sensors. At present, lack of such sensors is the main obstacle for the implementation of this type of error compensation in CNC machining operations.

In error compensation with mathematical prediction, the cause-and-effect relationship between the error and the source is established through a mathematical model. In recent years this type of error compensation has gained popularity and different computer software compensation techniques have come to market.

Sata, Takeuchi and Okubo [52] tried to improve the machining accuracy of a machining centre by implementing an error compensation method. They considered the general error as the summation of geometrical error and deformation error. The geometrical error was estimated by using a standard master part fixed on the table. The deformation error was evaluated by applying a simplified finite element model of the structure from temperature measurements taken of the machine tools. NC commands were modified to compensate the error. Experiments were performed to show improvements in machining accuracy of a machining centre by adopting the proposed method.

In another study Sata et al [53] found that in turning, machining error is dominated by thermal expansion of the tool and they produced improved machining accuracy on an NC lathe by predicting the thermal expansion of the single point tool using a finite element method. They used feed-forward strategy in error improvement and the NC control commands were regulated according to the thermal expansion of tool in advance of machining. The thermal expansion of the tool was calculated from the amount of heat

generation in machining, which is a function of cutting conditions. The tool offsets were changed according to the calculated amount of thermal expansion of the tool.

Rahman [54], [55], [56] examined the machining accuracy of a chucked workpiece. In a turning operation of a cylindrical workpiece with length to diameter ratio less than three, the workpiece is generally overhung clamped and machined with three jaw chucks. In this type of turning operation, a deviation in shape called "out of roundness" is commonly observed (see Figure 2.9). Rahman [54] shows the factors causing this type of machining error. His experimental results show that the directional orientation in a three-jaw chuck and jaw/workpiece contact chord length play major roles in the out of roundness error of the machined workpiece. It was also found that in the first cut the deviation in shape was larger and in the second cut the deviation in shape was different from that in the first cut. In his contemporary work [55], the effect of clamping conditions on chatter stability and machining accuracy are discussed. It was found that the chucking force, the chucking length of workpiece and the type of contact between the workpiece and jaw faces are the main causes for the variation of stiffness. In a more recent work [56] an attempt was made to optimize the error of roundness to achieve the maximum metal removal rate (MRR) with some specified accuracy satisfying all the constraints of clamping and cutting conditions and workpiece specification. An optimization programme was developed, which gives the lathe operator the optimum cutting conditions to achieve the desired machining error and maximum MRR.

Nevelson [57] determined the factors which have the greatest influence on machining accuracy and developed an optimum control algorithm to achieve the desired accuracy level. He considered the cutting force, the varying yield of the blank in a collet chuck, the tool wear, the clamping error and the positioning error as the main sources of machining error in a turret lathe. Values of all three error factors were recorded and, using a regression analysis, relationships were established between these factors and the resulting dimensional deviation. The equations obtained from these relationships were

used in error compensation of the workpiece. Thus the error compensation technique developed by Nevelson is error compensation with mathematical prediction.

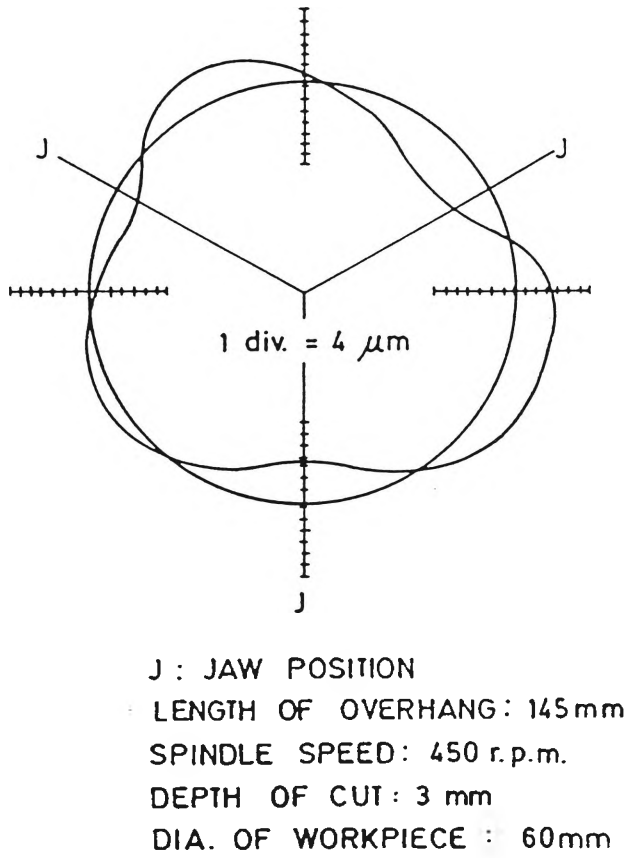

Figure 2.9 Deviation in Shape of a Workpiece Turned in a Three-Jaw Chuck [56].

2.3 On-line Monitoring and Adaptive Control Systems

In the previous section we have seen that many authors have applied different methods to eliminate or at least reduce the errors in CNC machining operations [50], [51], [56],[57]. The most popular among those methods is active error compensation through in-process gauging, or as commonly known, "adaptive control". A common drawback of most of the CNC systems is that operating parameters, such as speeds or feed rates (in metal machining), are prescribed by a part-programmer and consequently depend on his or her experience, knowledge or handbook data. The so-obtained values are conservative since they are determined by referring to the worst cutting conditions (which in reality will seldom occur) and do not take into account the variation of both the cross-section of the

metal removal along the tool path and the actual workpiece material characteristics with respect to the standard.This problem is especially important in CNC machining operations, because the part-programmer is unable to see the results of his choice of cutting conditions as would the machinist. In conventional machining, the machinist can readily change the cutting conditions if such change is needed. Therefore, the part-programmer tends to be conservative, in trying to be on the safe side. More often he is reasonably well satisfied just to get the part machined without worrying about productivity and accuracy levels unless specified. In CNC machining the productivity is of particular importance, as the high cost of the machine is involved. Therefore, significant savings of time and money can be attained by a control system which measures, while machining under actual conditions, automatically selecting and implementing the optimum parameters on the machine.

There are two types of automatic control systems that might be implemented for this purpose:

(i) Feedback control system

(ii) Adaptive control system

2.3.1 Feedback Control System

Unfortunately there appears to be no single, universally accepted, definition for either the feedback or the adaptive control system [46]. The common feedback control strategy is given in Figure 2.10. In feedback control systems it is desired that the output of the process Y (also known as **controlled variable**), be as close as possible at all times to an arbitrary given input X (also called **reference variable** or **command**) to the system. In other words, at all instants of time it is desired to keep the error $\delta_x = |X-Y|$ as small as possible.

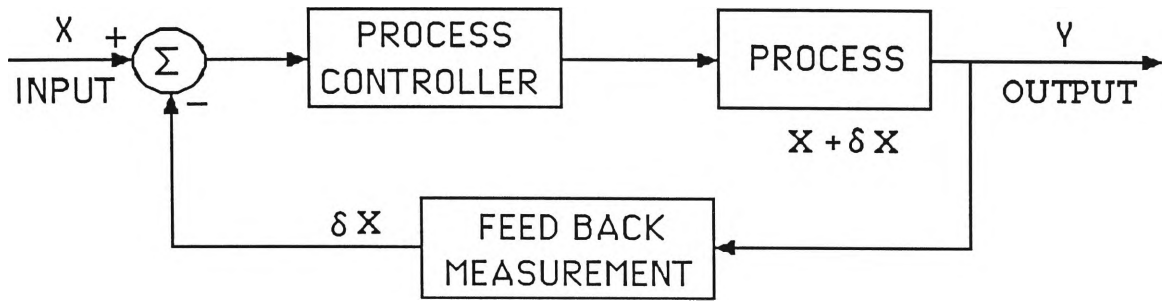

Figure 2.10 Feedback Strategy.

There are two basic requirements for effective design of a feedback system. First, the controlled variable must be measurable. Second, the properties and characteristics of the process or system to be controlled are known and constant; but in metal cutting, the second condition is not met, as the metal cutting process is not static. Moreover the feedback system only attempts to maintain a zero error signal, so the system output would not be optimal unless the command signals were optimal at all times. Unfortunately, the optimal input is not known for all situations in advance. Hence the feedback control system does not appear to be the means for keeping the system operating at the optimal conditions.

2.3.2 Adaptive Control System

An adaptive control system is more sophisticated than a feedback control system. "Adaptive Control Systems (ACS) are defined to be systems which automatically change their parameters in response to varying process conditions in such a way as to improve their operations with respect to a performance index" [67]. As applied to the metal removal process, adaptive controllers alter such parameters as feed rate, spindle speeds, etc. in response to the other varying cutting conditions (increase/decrease in width or depth of cut, changing workpiece hardness, rapid tool wear, etc). The performance index may be the production rate, the cost per part produced, the surface finish of the part

produced or many other measurable features. The universal example of adaptive control is the human being driving a car. The driver continually inputs small correctional signals on the steering wheel and accelerator in order to drive the car safely on the road. The driver continually measures the dynamics of the process to be controlled in order that he may be prepared to effect near-optimum control when an error condition arises.

There are three functions which characterize ACS (Figure 2.11) [68]:

1. Identification
2. Calculation and Decision
3. Modification

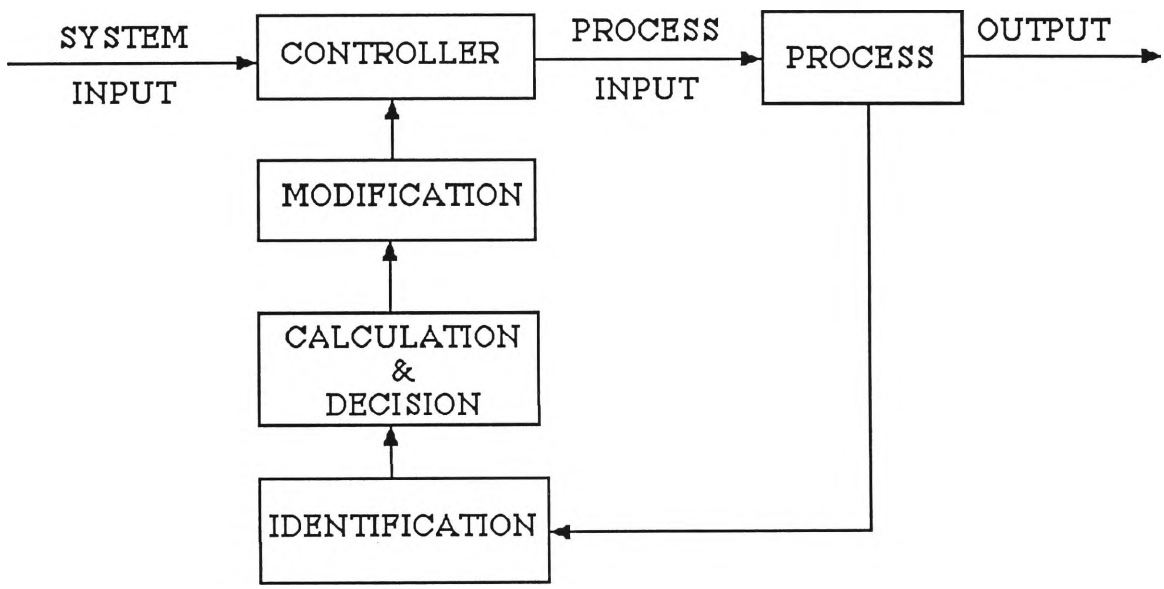

Figure 2.11 Structure of Adaptive Control System [68].

The identification measures the actual state of the process performance without taking its quality into consideration. Once the system performance is determined, the next function is to decide how the control mechanism should be adjusted to improve the process performance. The decision is taken on the basis of a preprogrammed logic provided by

the system designer. The third function is to implement the decision. The decision function is a logic function, whereas the modification function is concerned with the physical or mechanical change in the corrective action needed to adaptively control the process.

ACS for machine tools can be classified into two categories: (1) adaptive control with optimization (ACO) and (2) adaptive control with constraints (ACC). ACO refers to systems in which a given performance index (usually an economic function) is maximized subject to process and system constraints. With ACC the machining parameters are optimised within a prescribed region bounded by the process and system constraints, such as maximum torque or power. ACC systems however do not use a performance index.

Although there has been considerable research on ACO systems, only a few of these systems are used in practice [69]. The main difficulties encountered with such systems have been in defining realistic indices of performance and finding suitable sensors which can reliably measure on-line, the necessary parameters in a production environment within reasonable costs.

Some researchers have classified ACS in three categories. Besides ACO and ACC, they have also introduced a third term, geometric adaptive control (GAC) [71], [72]. GAC refers to the control technique for maintaining the stability of dimensional accuracy and improving the surface finish and shape accuracy.

2.3.3 Survey of Existing Adaptive Control Systems

Pioneering work in adaptive control in machining operations was conducted at Bendix Research Laboratories under the technical supervision of the U.S. Air Force during the years 1962 through to 1964 [73]. The system introduced by them is known as the Bendix

System. In this system feed rate and spindle speed are used as the controlled variables and cutting torque, tool temperature and machine vibration are used as the measured variables. In the Bendix System, the performance index PI is defined as follows:

$$PI = f(MRR/TWR) \tag{2.2}$$

where MRR = metal removal rate

TWR = tool wear rate

The objective in implementing an ACS is to continually maintain the value of PI as the highest possible within the constrains.The constraints in the Bendix system were maximum and minimum spindle speed, maximum torque, maximum feed, maximum temperature and maximum vibration amplitude. The optimization method used to find the maximum is based on gradient method. In the Bendix system, MRR and TWR and finally performance index (PI) are calculated by using the following formulae typically in a milling operation [73]:

$$MRR = b.d.S_m \tag{2.3}$$

where

b = milling width

d = depth of cut

S_m = feed rate

$$TWR = K_1 . (MRR) + K_2 . \theta + K_3 . \frac{dT}{dt} \tag{2.4}$$

where

θ = tool temperature

$\frac{dT}{dt}$ = time rate of change of the cutting torque

K_1, K_2, K_3 are constants which depend on tool and workpiece materials.

$$PI = \frac{MRR}{C_1 + (C_1 t_1 + C_2 \beta).(TWR) / w_0} \qquad (2.5)$$

where

C_1 = cost of machine and operator per unit time

C_2 = cost of tool and regrind per change

t_1 = tool changing time

w_0 = terminal allowable width of flank wear

β = adjustable parameter ($0<\beta<1$) which determines the type of performance index:

If $\beta = 1$, the performance index is the reciprocal cost per unit

If $\beta = 0$, the performance index is production rate

If $0 < \beta < 1$, the performance index takes into account both the cost per part and the production rate

From the above formulae, it seems that it is not difficult to calculate the performance index (PI) and to find its maximum using some optimization technique. The difficulty is that the TWR cannot be measured by on-line sensors available today. The Bendix researchers measured the TWR indirectly using Equation (2.4). However, in Equation (2.4) the constants K_1, K_2, K_3 depend on tool and workpiece materials and off-line experiments are needed to determine their values for every combination of tool and workpiece material, which is time consuming and may override the economic benefits of ACS.

The oldest known ACS still in use is offered by Macotech Corporation, Seattle, Washington, U.S.A. [75]. Mathias, Vice President of Macotech Corporation has reported the successful implementation of ACS in milling operations by his company

[75], [76]. The original system is called MAC I and several modifications are now available, such as MAC 22, MAC 40, MAC 42, etc. In MAC I system the feed is used as the controlled variable, and cutter force and horsepower are used as the measured variables. In this system, when the force increases due to increased workpiece hardness or depth or width of cut, the feed rate is reduced to compensate. When the force decreases, owing to decreases in the foregoing variables or airgaps in the part, feed rate is increased to maximize MRR. It provides protection against total breakage due to high side load and spindle motor overload. The MAC system has reduced operation time significantly, thus high productivity is achieved, but Mathias has not given any data about the machining accuracy, geometric tolerances and reliability.

The Cincinnati Milling Machine Company developed an ACS for milling operations [46]. Their system uses spindle speed and feed rate as controlled variables, and spindle torque, spindle deflection and spindle horse power as measured variables. Empirical equations, derived from the data gathered by the Physical Research Department of Cincinnati Milling Machine Co. were used in their ACS. The relationship which satisfied their analysis is as follows:

$$N_c = N_p \cdot \left\{ 1 - K. \left(\frac{\delta_t^2}{T} \right) \right\} \qquad (2.6)$$

where

Nc	=	commanded spindle speed
Np	=	programmed spindle speed
δ_t	=	tool deflection
T	=	tool torque
K	=	weight factor

In Equation (2.6) the weight factor takes into consideration the tool material used. The lower values of K, indicate strong tools, high rigidity, and mild material. High values indicate the other extremes of the above-mentioned parameters.

The feed rate equation used is:

$$S_m = S \,.\, N + S_{ge} - C_\delta - C_{hp} \qquad (2.7)$$

where

S_m = feed rate (command)

S = feed per revolution (programmed)

N = spindle RPM

S_{ge} = gap eliminator feed rate

C_δ = deflection constraint

C_{hp} = horsepower constraint

In Equation (2.7), the last three terms are zero when **normal** milling operation is performed. During machining, if some airgaps are met, the feed rate is required to be increased to reduce the machining time. The gap eliminator term is used to increase the feed rate. At the same time torque and deflection constraints are applied to avoid tool breakage. The latter two constraints act to decrease the feed rate upon violation of a constraint.

The system developed by Cincinnati is not an ACS in the true definition of ACS. In fact it is a group of feedback control loops using analog computation to implement the control equations within the control loops. The Cincinnati system showed reduction in machining time of 20 to 90% over non-adaptive time on the same machine. The primary limitations of this system are its dependency on empirical equations which cannot be relied upon for all cutting conditions, and, the need for off-line experiments to determine the optimal programmed values of feed and speed.

Abdulov [78] considers not only the productivity, but also increased accuracy and quality through ACS. A new Mechanical Adaptive Control System has been produced. It consists of a multi-loop elastic dissipative device which serves as an adaptive regulator. The functions of adaptive regulators are: to regulate the technological process and the machining operation; to increase machining accuracy and improve machined surface finish; to ensure a stable cutting process and stable tool-life. He made a mathematical model of the process and showed the increase in accuracy of a number of parts made of different materials.

Bedini et al [70] have conducted a series of experiments using an ACS in a milling machine. They considered only the technological part of the problem although a more general approach would be required for considering the geometrical and technological problem together. The performance index chosen by them is the maximum value of machining cost. Different constraints on values of the cutting speed and feed rate were applied. Initially they developed the mathematical model of the process, which was later optimised. The tests showed a good reliability of the proposed ACS, but results were only obtained for a prototype and it needs more studies for industrial applications.

Yen and Wright [79] have proposed a new concept to integrate traditional approaches of ACO and ACC. They criticized both ACO and ACC and in their words, "Apparently these two methods can be appropriate for certain classes of applications, but they are not a general solution". They chose plastic deformation, cratering, and fracture as the main causes of failure which set the limits on the speed and feed. The performance index chosen, was the maximum production rate, which they defined as the product of cutting speed and feed rate assuming that the depth of cut was fixed. The aim of their ACS was to maintain a smooth wear of the cutting tool by operating the machine within the specified constraints. In this method, most of the variables are physical properties of tool materials which are either invariant or a function of temperature. Some of them depend on

the cutting forces. Both the temperature and cutting force sensors are well developed and were used for on-line measurements. But some constants can only be determined by experiments. As we have seen in the Bendix system, the off-line experiments to determine the constant values are inconvenient and remain the principal disadvantage for that system. The performance index chosen is the maximum production rate, and this cannot improve the accuracy levels; on the contrary, the high production rate achieved by this ACS might decrease the accuracy levels.

Shirashi [72] has built a GAC model in an NC turning operation by a system which can continuously monitor the radius change of the workpiece in an on-line fashion. Laser beams were used as sensors to monitor the radius change of the workpiece. As the sensors use optical techniques, mechanical vibration, chips and cutting fluids will make the measurements difficult and inaccurate. Shirashi overcame those problems (with limited success) by using filter techniques and blast systems. The major problem with Shirashi's GAC system is to implement it in an industrial environment.

2.3.4 Sensors

Sensor technology is the key to advances of ACS. We have seen that the major problem with the Bendix system is the lack of on-line sensors to measure the TWR. In fact, the development of reliable and effective sensors is the main challenge facing today, for the unmanned manufacturing centres. High cost and questionable reliability of sensors are the obstacles most difficult to overcome. Considerable research and development work has been done with enormous time being devoted to the subject of sensors. At present different types of sensors are available in the market built by different manufacturers. But some important machining parameters such as tool wear and surface quality cannot be directly measured practically and accurately during cutting under production conditions with the current state of the art technology. A very good survey of commercially available

(in 1983) sensors have been done by Tlusty and Andrew sponsored by the CIRP Technical Scientific Committee on Machine Tools [74]. Their list of sensors includes:

(a) Dimensional Sensors
    (i) Touch Trigger Probe
    (ii) Proximity Sensors
(b) Sensors for Measuring the Preload in a Rolling Type Bearing
(c) Cutting Force Sensors
(d) Spindle Motor Power Sensors
    (i) Torque Control Monitor
    (ii) Power Monitor
(e) Acoustic Emission Sensors

Besides the sensors available in the market, there are many more at the research stage. A number of research programmes are undertaken to develop on-line tool wear sensors. There are two main categories of on-line tool wear sensing techniques: (a) direct tool wear sensing and (b) indirect tool wear sensing. Direct tool wear sensing is very difficult, indirect tool wear sensing is advisable. In indirect tool wear sensing technique, some other variable(s) (not tool wear) is (are) monitored in the process and being known the relationship between tool wear and that (those) variable(s) tool wear is calculated.

Yamazaki, Yamada and Sawai [81] proposed an ACS for an NC milling machine in which tool wear was measured on-line directly. They also established an ACS which can determine tool wear off-line indirectly. In the indirect method equations were derived using experimental parameters which relate cutting force components, cutting speed, feed rate, width of cut, depth of cut, cutter diameter and flank wear. Using these equations tool wear was estimated by measuring cutting force components. In the on-line measuring method, tool wear was determined by frequency analysis of the cutting sound, as it is known for years that cutting sound changes with progression of tool wear.

Control algorithm used in their ACS, selects cutting conditions based on tool wear. To verify the validity of the algorithm, simulation tests were performed and the results showed the feasibility of the control system.

Arsovski [82] developed a wear sensor on the measurement of the radioactivity of activated cutting elements of the tool during cutting. It is an indirect method of tool wear sensing and the basis for application of this method is the relationship between the radioactivity and the tool wear. Several cutting tests were performed and verified by using a tool maker's microscope. The results showed that this type of sensors can measure the tool wear with sufficient accuracy. But for application of this type of sensors, off-line experiments are necessary to determine the constants to relate the radioactivity and tool wear. Prior to experiment it is also necessary to know the initial background noise (cosmic radiation), distance, number of revolutions per minute, and the cutting temperature.

Suzuki and Weinmann [71] developed an on-line tool wear sensor for straight turning operations. They also measured tool wear by an indirect method. In their case, tool wear was detected by measuring the change in distance between tool holder and work surface using a stylus which is mounted on the tool holder. The sensor is composed of two main parts : (1) a displacement transducer, and (2) a stylus. Several cutting tests were performed. The results indicate that, this type of sensor is capable of measuring tool wear with reasonable accuracy. It is also capable of detecting the premature tool failure. When the stylus reaches a point where the tool failed, the stylus starts to vibrate due to the rough work surface. But the failure of the tool cannot be detected immediately since the stylus trails the cutting edge. This is regarded as one of the shortcomings of this sensor. The nature of its design restricts its use to straight cutting operations and it cannot be readily applied to contour cutting.

El Gomayel and Bregger [68] used the electromagnetic method to determine on-line tool wear in turning operations. The increase in the workpiece diameter was used as a tool wear criterion. The instrumentation used in their research were: a Bently electromagnetic proximotor, an oscillator and demodulator circuit connected to an 18 v d-c power supply generated the waves. The turning was performed by coupling the probe face with the workpiece surface. The voltage output varies with the change in distance between the probe and the workpiece because of the variation in the magnetic field. In order to compensate the deflection in the workpiece and the centres and the machine tool vibrations, the sensors were set up in a differential mode. They found that, the increase in workpiece diameter (decreasing the gap) results in a decrease of voltage at a linear rate. Later it was confirmed by a calibration procedure. Several experimental metal cutting were done with different cutting speeds, feed rates and some graphic representation of the relations with the accumulative flank wear were done. The results were in agreement with generally accepted trends, i.e.,an increase in cutting speed or the feed results in faster tool wear when all other properties are kept constant.

2.4 Studies on Co-ordinate Measuring Machine

Over the past few years, the CMMs have been in the centre of ever increasing importance for the comprehensive measurement of components used in today's production technology. A number of articles have been published in recent years describing its importance, construction, flexibility and other aspects [95], [96], [97], [98]. Since this is a measuring instrument, most of the authors are concerned about its accuracy and repeatability of measurements [99], [100], [102], [106]. Different methods of increasing accuracy levels have been discussed [104], [106], [107]. Kunzmann and Waldele [105] have pointed out , "The application of CMMs have changed the measurement principles in a lot of cases". We are still in the learning process of the CMM applications and considerable efforts are being made exploring new methods for the analysis of results. In the past, measurements and inspections of workpieces were done separately for

dimensions, forms, positions and surface characteristics. But CMMs have opened the door for measuring all these properties at the same time with the same instrument.

2.4.1 Accuracy of Co-ordinate Measuring Machine

The performance of CMMs can be estimated for different aspects. For a CMM, being a measuring instrument, the most significant aspects of its performance are accuracy and repeatability of measurements. Error sources causing inaccuracy in CMMs are generally divided into three groups [104]:

(a) Static errors caused by geometric inaccuracies or constant loads and constant accelerations;
(b) Software induced errors caused by software packages used in CMMs; and
(c) Dynamic errors caused by vibrations (fluctuating forces and accelerations).

To investigate the performance of any measuring instrument, definitive documents are needed. Although CMMs were introduced nearly 20 years ago, the definitive documents to clarify the performance evaluation of CMMs have become available only in recent years. Most commonly used standards for the evaluation of CMMs are listed below:

(i) Accuracy Specification of CMMs, CMM Manufacturers Association, 1982 [103]
(ii) British Standard, CMMs, Part 2, Methods for Verifying Performance, BSI, 1987 [107]
(iii) ANSI/ASME Standards B89.1.12, Method Performance Evaluation of CMMs, 1986 [108]

In the literature survey we find that a number of researchers have carried out work on the accuracy study of CMMs. Most of these workers have investigated the static geometric errors of CMMs. In some cases geometric errors were calculated by using mathematical

models and appropriate software compensation techniques were applied to eliminate these errors. For example, Thwaite [99] has studied the overall error of a 3-dimensional CMM by building a model which incorporates a series of errors forming a kinematic chain. This approach identifies 21 likely sources of errors. These errors can be reduced using software corrections, but as Thwaite pointed out, day-to-day users of CMM need corrections of the software.

Zhang et al [106] applied a software error compensation technique to compensate geometric positioning errors and some thermal errors of a 3-axis CMM. Their computation is based on a "rigid body" model of workpiece motion in the machine co-ordinate system. Rigid body model consists of choosing the minimum number of ideal co-ordinate systems necessary to represent a machine and to relate co-ordinates in these chosen co-ordinate systems using matrix transformations. The dominant thermal effects were removed by introducing the concept of "effective" nominal differential expansion co-efficient. A software was added to the control computer of the CMM as a single subroutine. The error compensation was tested by measuring a gauge block in different positions and the results showed that the errors were reduced considerably. But the successful application of this method requires a correct geometric model, a correct thermal model, and careful machine calibration. Zhang et al suggested that the method will yield more benefits if they were considered at the design stage of a CMM.

Hocken et al [110] studied the three dimensional measurement process using a classically designed measuring machine and attempted to update the performance of that machine. Machine behaviour was analysed using three separate techniques, viz. (1) rigid body kinematics, (2) methods of temporal modelling and production sampling and (3) technique of multiple redundancy. A laser interferometer was fitted with the measuring machine to achieve a machine independent co-ordinate system. All the error terms were calculated and stored as matrices and were used to correct the data during a measurement. Temperature and other external effects were eliminated using cross referenced

measurement algorithms. Errors that cannot be assessed by calibration, such as axis non-orthogonality, were obtained by measuring the object in different angular positions within the measurement values.

Oya, Hokari and Tamura [111] improved the accuracy of a 3-axis co-ordinate measuring machine by calculating and compensating its systematic errors, viz the geometrical error of the structure, the deformation caused by the movement of the carriage, and the error in the detecting scale of the co-ordinates. The authors used the ideas of a standard co-ordinate system and error vector, introduced by them in a previous paper. They determined the errors in discrete points in the measuring space by using some standard part(s) (They used a gauge block for distance measurement.). The discrete distribution of the error vector was interpolated to find the continuous distribution of the error vector. They divided the measuring space into a number (24) of cubic elements and the error vector at any position in the element was calculated by interpolation. They claimed the proposed method can reduce the measuring error of a CMM to less than 3 microns.

In the literature it is reported that the CMM software packages are not capable of handling many common geometric features [100], [109]. This problem was identified and discussed in the CIRP Scientific Technical Committee meeting on Dimensional Metrology and Quality Control and was published in their 1987 report. ".....because of the seriousness of the situation, the STC decided to ask Kunzmann to prepare a keynote paper on the subject for presentation at the 1988 meeting in Japan" [109]. In the keynote paper presented in that 1988 meeting, Kunzmann and Waldele [105] have studied the performance (accuracy and reliability of measurements) of different CMMs. Besides the mechanical (hardware) accuracy of the CMM, the accuracy of softwares was also included. Twelve packages from different CMM manufacturers and several institutes were tested using "black box testing" technique. In black box technique simulated measurement data are supplied to the software and the geometric parameters (such as length, diameter, angle, etc.) are evaluated by the different software packages. Later the

results are compared with the results obtained by using some reference software. Results of software test are given in Table 2.2.

geometric element	level of conformity 1	2	3	4	no information
line	60 %	13 %	5 %	5 %	17 %
plane	73 %	12 %	6 %	9 %	0 %
circle	76 %	7 %	9 %	0 %	8 %
circle in space	56 %	19 %	0 %	0 %	25 %
cylinder	52 %	1 %	5 %	9 %	33 %
cone	27 %	5 %	10 %	25 %	33 %

level	max. deviation from references
1	0.1 µm
2	0.5 µm
3	2 µm
4	2 µm

Table 2.2 Results of Software Test [105]† .

Peggs [112] of the National Physical Laboratory (NPL), UK also discussed the problem of CMM software. In [112] Peggs informed that in collaboration with the British Standards Institute (BSI), NPL was doing work on: (i) the formation of specification

† In [105] it is published that both levels 3 and 4 have maximum deviation of 2 µm from references; but it is likely to be read as max. deviation > 2 µm from references for level 4.

standards for performance verification of CMMs, (ii) the provision of calibration facilities for reference artefacts used in CMM acceptance testing, and (iii) developing various measurement sub-systems checking techniques including a software validation service. According to Peggs, at present the black box testing technique is the only **practical** method available for evaluating the CMM software performance. But in the UK the "software gauge" philosophy is becoming familiar and BSI is developing a Standard against which software could be checked for conformance.

Nijs et al [104] have studied the dynamic errors of CMMs. They used Lagrange energy equation together with Guyan reduction, to predict the dynamic behaviour of CMM construction. The theoretical results were verified by means of model analysis of an existing CMM and only little difference was reported. The authors suggested, their method could be used to optimize the CMM structure, which will reduce the causes of dynamic errors in CMMs.

Day-by-day we are becoming more and more familiar with the CMM measuring techniques and thus we are opening new doors for CMM implementation. Osanna and Durakbasa [113] have reported about the successful use of CMMs in testing the microgeometry of workpiece surface. They have developed a programme system on the basis of the software of a CMM, which can trace a workpiece surface with high resolution by means of a CMM. Different surface characteristics which indicate the levels of surface roughness can be calculated easily. Thus, with CMMs now being allowed to explore the surface topography of machined components, this has opened a new area for research of potential applications in future.

2.5 Problem Identification

In the literature very limited number of published work was found on machining accuracy. Those authors who have studied about machining accuracy, have concentrated

on specific aspect(s) of machining accuracy and factor(s) affecting these aspect(s). For example Arai et al [16], Sata et al [53] and Rahman [54], all have studied machining accuracy of an NC lathe. But in their respective accuracy analysis, Arai et al considered diameter variation of the workpiece, Sata et al monitored the length variation of the workpiece and Rahman examined out of roundness error of the workpiece. These studies are useful; but in reality all these errors occur simultaneously due to combined effect of all the error components. It seems that nobody has studied the combined effect of all* (at least the dominant ones) factors affecting machining accuracy considered from different accuracy aspects such as dimension, form, surface texture, etc. In this thesis an attempt will be made to study different aspects of accuracy of a typical component machined on a 3-axis machining centre and then to trace back the factors causing these errors with a view to presenting a more realistic and "total effect".

In section 2.1 we have noticed that, several studies have been reported on machine accuracy. Different models are also available to calculate the machine error, in particular the geometric errors of machine tools. We have seen in Figure 2.8 that there are two basic approaches for accuracy improvements, viz., error avoidance and error compensation. We also note from Figure 2.8 that where the error compensation method is divided into many branches and sub-branches, while the error avoidance method is untouched. Although error avoidance should be the first step of accuracy control, in the literature we find almost all researchers have used some form of error compensation technique for reducing both the machine and machining error. While discussing about their error model and its effectiveness, some of the authors like Eman et al [23], Nijs et al [104] suggested that their model could offer more benefits if it was considered at design stage of the machine invariably "touching on" the need for error avoidance.

---

* As a matter of fact it is even not possible to list **all** the factors affecting machining accuracy.

Researches have applied different compensation techniques for machine and machining accuracy enhancement. Most popular among those techniques is ACS (Adaptive Control Systems). Although ACO (Adaptive Control with Optimization) and ACC (Adaptive Control with Constraints) were tried, however, this area has been only an area of academic research with no significant industrial application being reported. The problem with ACO is that it needs a huge database, which is practically impossible to store in the computer for all types of work and tool materials and for different cutting conditions. The main problem associated with ACC is, how to justify its objective or criterion of control strategy. Performance index can be maximum productivity, minimum cost, higher accuracy, better surface finish, or a compromise-combination of some of these objectives. In ACS where maximum productivity is used as performance index PI, Equation (2.2) is used to calculate PI. But in Equation (2.2) it is assumed that all cutting tools wear out identically under nominally identical work conditions. This is not true and there arises a need for on-line tool wear monitoring. Lack of on-line tool wear sensors is another obstacle in developing industrial ACS for CNC machining operations. This does not necessarily mean that ACS cannot be implemented to solve industrial problems. ACS can be applied to solve the problem part by part, but would not give a universal solution for the "total problem".

In the literature survey "Studies on Co-ordinate Measuring Machine" is included; because, first, due to similarity in configuration of 3-axis machine tools and 3-axis co-ordinate measuring machines, some authors like Knapp [24], Belforte [102], etc have studied geometric accuracy of both of these machines together; second, perhaps more important is the fact that **measured** accuracy of the machined components depends on the accuracy of the measuring machine (CMM). In Figure 2.5 we have also noticed that Koval et al [49] in their list of components of machining accuracy, have included the workpiece inspection error.

We have seen that, many authors have studied machine accuracy and have developed different models for error calculations. But no one seems to have analysed the effect of machine accuracy on machining accuracy. Using existing mathematical models, volumetric accuracy of any point within the machine space, can be calculated. But actual inaccuracy of the machined component will depend not only on the accuracy of the machine tool, but also on the volume of the workpiece (in other words amount of inaccuracy will depend on dimensions of the workpiece).* In machining, only a small part of machine space is generally used and in that case the error component of machining accuracy inherited from machine accuracy may not be as large as thought to be. Further investigations on the effects of machine accuracy on machining accuracy is therefore deemed necessary.

It seems that hardly anyone has studied the "error avoidance" method for accuracy control of CNC machining operations, although many researchers felt the need for it. At this stage the potential benefits of this method need to be established to generate adequate research interest. In the literature we also find that some authors, while advocating the error compensation method, have criticized the error avoidance method. For example Lee and Barash [30] wrote, "While the former (error avoidance) has been by no means completely achievable, the latter (error compensation) has been preferred as a convenient means to reduce the error". It is apparent that no method is capable of producing error-free-machining. Sensor-based adaptive control methods appear to be providing a reasonable compromise for reducing the errors that are resulting from the process of manufacture.

Considering the need for "total quality" in manufacture, when viewed in its integral role, representing the entire process of converting the raw materials into finished products, it seems reasonable to assume that error avoidance must play a significant role in the whole

* This is so, because it is generally accepted that the error along any axis is proportional to the length of the axis.

process. Thus, the core of future work must be aimed at achieving a partial solution to quality enhancement in manufactured products, by a thorough investigation into the dimensional and geometric accuracy features of a typical machined component.

2.6 Concluding Remarks

From the summary of the literature survey presented in this section the following general remarks are drawn:

1. Very little research has been done on the machining accuracy of CNC machining operations.

2. The causes of the poor accuracy levels produced in CNC machining operations are not well established and there exist significantly large differences of opinions among the researchers about the likely causes of errors and their levels of influence.

3. Adaptive control systems have been developed and tested by many researchers; but most of these researchers were concerned more about the productivity and in many cases the accuracy was sacrificed to increase the productivity.

4. The potentials for research into error avoidance methods are still ripe and would play a major role in quality enhancement of the manufactured product in CIM environment. It is the firm opinion of the author of this thesis that "prevention" is always better than the "cure".

3.0 PRELIMINARY WORK UNDERTAKEN ON THE ACCURACY OF CNC MACHINING OPERATIONS

3.1 General

In the previous chapter it was found that only a very limited published work was available on machining accuracy in CNC machining operations. It was also noted that the combined effects of all of the factors affecting machining accuracy were not considered. But in practice all the factors act simultaneously; thus the study of "total effect" reflects the reality. In this thesis an attempt will be made to study the combined effect of different error components typically found in CNC machining operations.

Today's CNC machine tools are capable of performing a variety of machining operations and day by day the capabilities of CNC machine tools are increasing. It is understood that the machining accuracy in CNC machining operations among many factors will depend on the types of machine tool, machining operations, part configuration and dimensions, etc. The author must admit that a study of the "total effect" of all of these factors, using all types of CNC machine tools and CNC machining operations, is beyond the scope of this thesis. But it is believed that such a complex problem can be considered in a much simpler form, and then more complexity can be added to the problem, if required. Taking such an approach it was decided to design a simple component, manufacture this test component using the facilities available and then using the measuring instruments, to find out the machined dimensions and to compare these dimensions with the designed values. The prime objective of this preliminary study is to determine the types of inaccuracies which may appear in a very simple component, and the repeatability of these errors. After finding the basic types of error which may occur, the cause of the errors can be investigated.

3.2 Work Design

3.2.1 Facilities for Experimental Work

Before designing the work, it was necessary to consider the facilities available in the Manufacturing Systems Laboratory. The Manufacturing Systems Laboratory is equipped with a Zenford Ziegler Machining Centre (Figure 3.1). It is a 3-Axis CNC machining centre of vertical-spindle type. This machining centre provides X and Y axis motions with a traveling table and saddle. Z axis movements are provided by a quill-type spindle in a sliding head. In this thesis under the term "CNC machining operations", only those operations which can be performed on the Zenford Ziegler CNC Machining Centre* , e.g. milling, drilling, boring etc are considered. Position resolution of this machining centre is 1 micron and its calibrated positioning accuracy in its full travel is no more than $\pm$ 10 microns along each axis.

The Manufacturing Systems Laboratory is also equipped with a Ferranti - (Mercury) Co-ordinate Measuring Machine (Figure 3.2), complete with a MICRO 900 microprocessor and a set of Renishaw probes and calibrating specimens. It is a manually driven, 3-axis, fixed-table, cantilever type CMM. The basic frame of the machine is placed on a granite table and its cantilever construction allows easy access to the work area. The microprocessor, MICRO 900 is capable of calculating a number of geometric elements such as: point, circle, sphere, mid-point, line to line intersection, etc. It has 1 micron position resolution and can achieve guaranteed uncertainties at 95% confidence under normal working conditions; axial repeatability of measurement is $\pm$7 microns within its full travel area.

---

* The turning operation was excluded from our experiments due to lack of an accurate turning machine, at the time of experimentation.

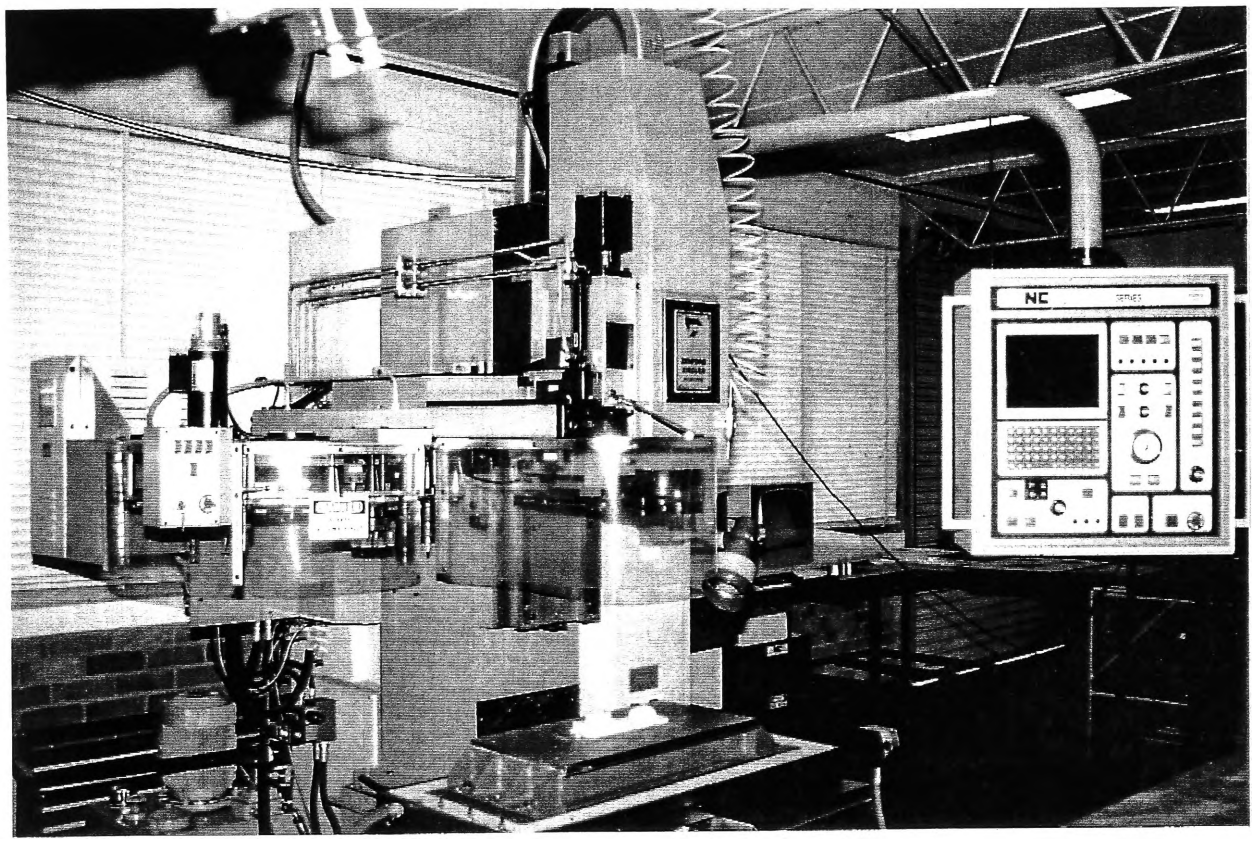

Figure 3.1 Zenford Ziegler CNC Machining Centre.

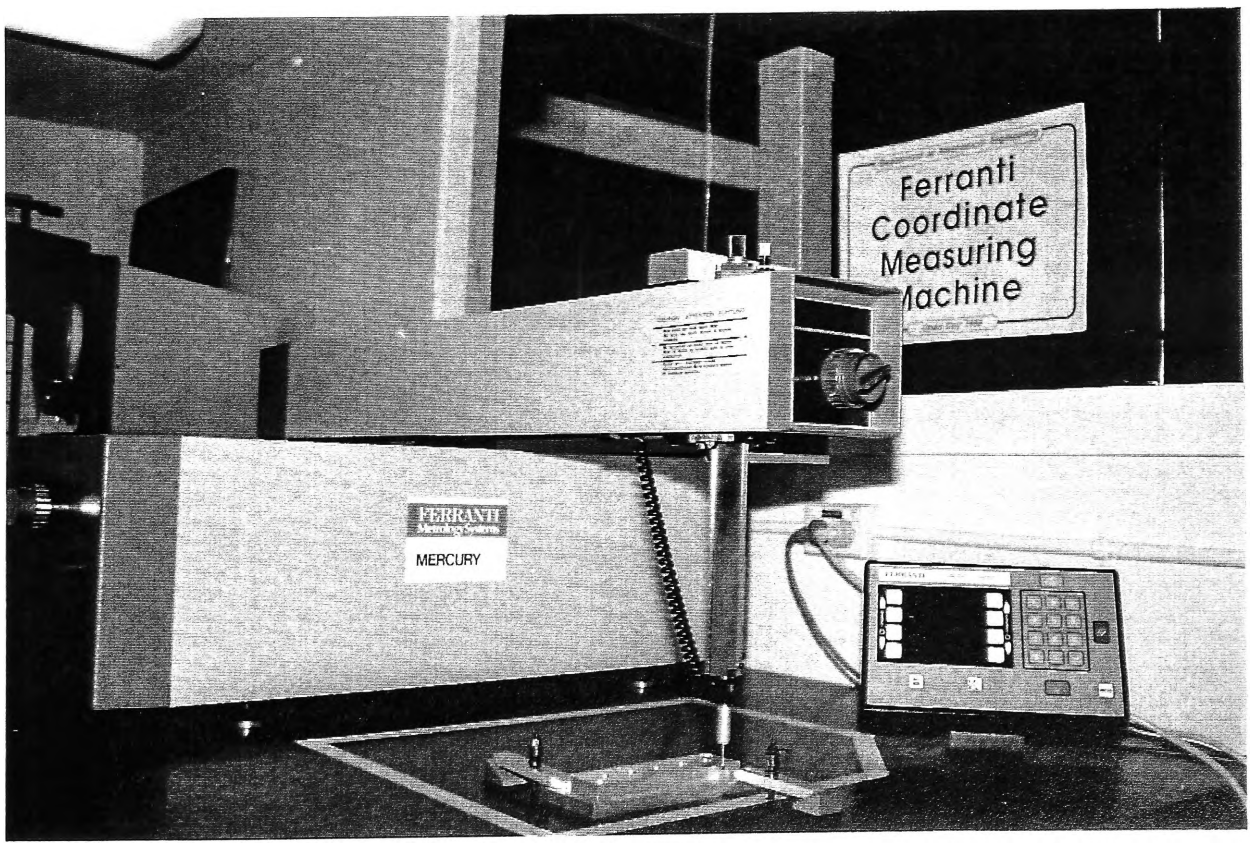

Figure 3.2 Ferranti (Mercury) Co-ordinate Measuring Machine.

The facilities at the Manufacturing Systems Laboratory also include a surface texture measuring instrument, Surfcom 550A (Figure 3.3). It is a Stylus tracing instrument and it digitally reads out eight roughness parameters and four waviness parameters. It has a built-in printer which prints out these parameters. Surfcom is connected with a chart recorder (E-RC-S01A) which can produce a hard copy of the surface profile precisely. Surfcom is also interfaced with a mini computer (through RS 232 connection) which can record the output data for further manipulations.

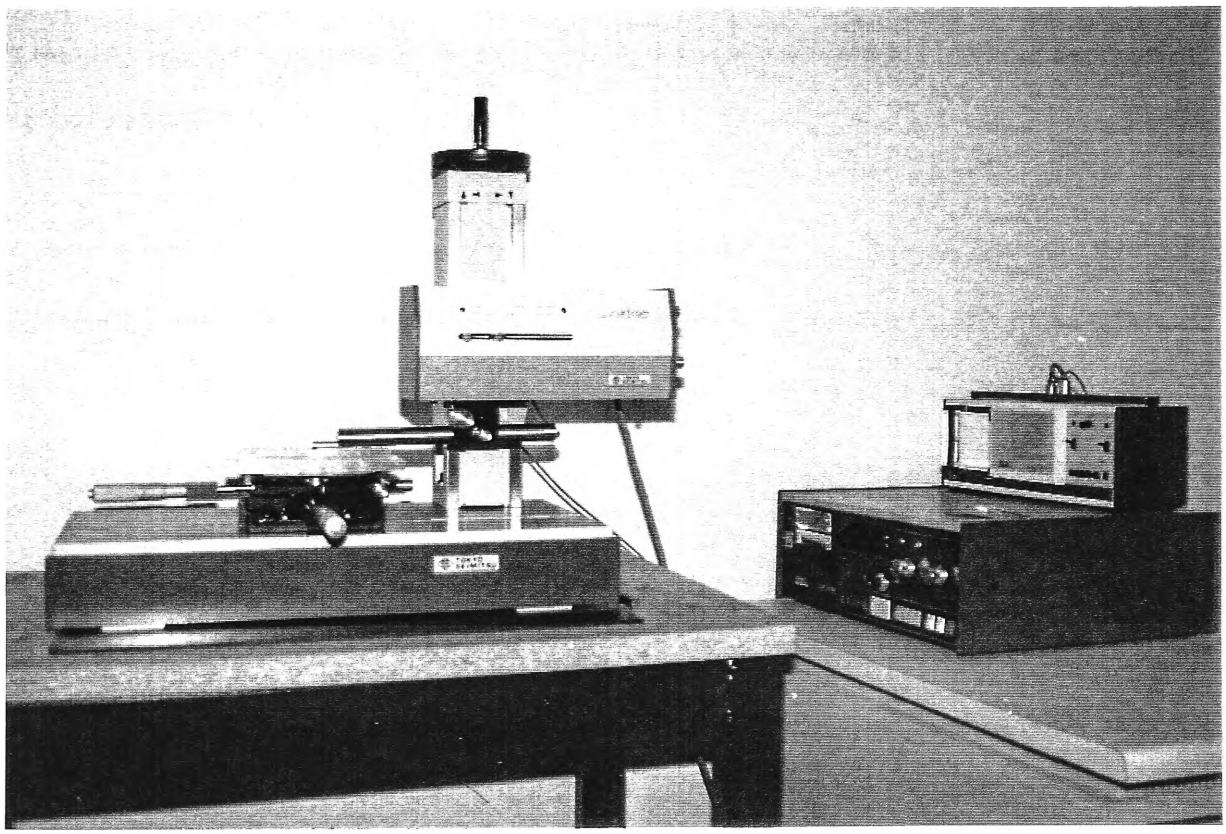

Figure 3.3 Surfcom Surface Texture Measuring Instrument.

3.2.2 Designing of Test Component

A simple component was designed for the experimental purpose (Figure 3.4). Oblique view of the test component with the nomenclature of surfaces adopted in this thesis is given in Figure 3.5. Attempts were made to include as many aspects of GD & T as

possible in the component within the basic features of the simple design chosen. This test component was designed so as to allow the study of dimensional variations, positioning and shape variations of the holes, flatness, parallelism and perpendicularity of different planes, perpendicularity of the hole axes with a given datum, etc. The test component was also designed to provide an independent analysis of each aspect of GD & T. In Figure 3.4, GD & T is used to restrict only positioning and shape variations of the holes. Any restriction on a part depends on the end application i.e., where it will be used or assembled. Figure 3.4 is only an example of the application of GD & T, and other restrictions should be shown if needed by assembly operations. All tolerance limits used in Figure 3.4 were chosen according to tolerance limits specified in [119] for economical machining operations.

An NC programme was written for the manufacture of this component on the CNC machining centre. A copy of this programme is given in Appendix C. The paths followed by different tools during machining, are illustrated in Appendix D.

3.2.3 Clamping of Workpiece

There were difficulties in clamping the workpiece on the machine saddle, as the workpiece required contour operation all along the workpiece. Attempts were made to machine the workpiece in one setting (to avoid any setting error). Different clamping methods were considered and the method of clamping as shown in Figure 3.6 was found to be the most effective method. In this case the workpiece was screwed to a special jig by two socket head cap screws placed diagonally on the workpiece. A jig was designed and considerable attention was paid to avoid any clamping error. Theoretically, the workpiece when attached to the jig, can move (translation or rotation) the distance equal to the clearances between the threads of the screws and the holes. But the workpiece was screwed also from the top by socket head cap screws with a view to reducing errors in such clamping. After placing the workpiece, it was checked physically, whether any

movement can be noticed. To be sure after machining the component rectangular corner angles were measured and only a small deviation (a few thousandth of a degree) was noticed.

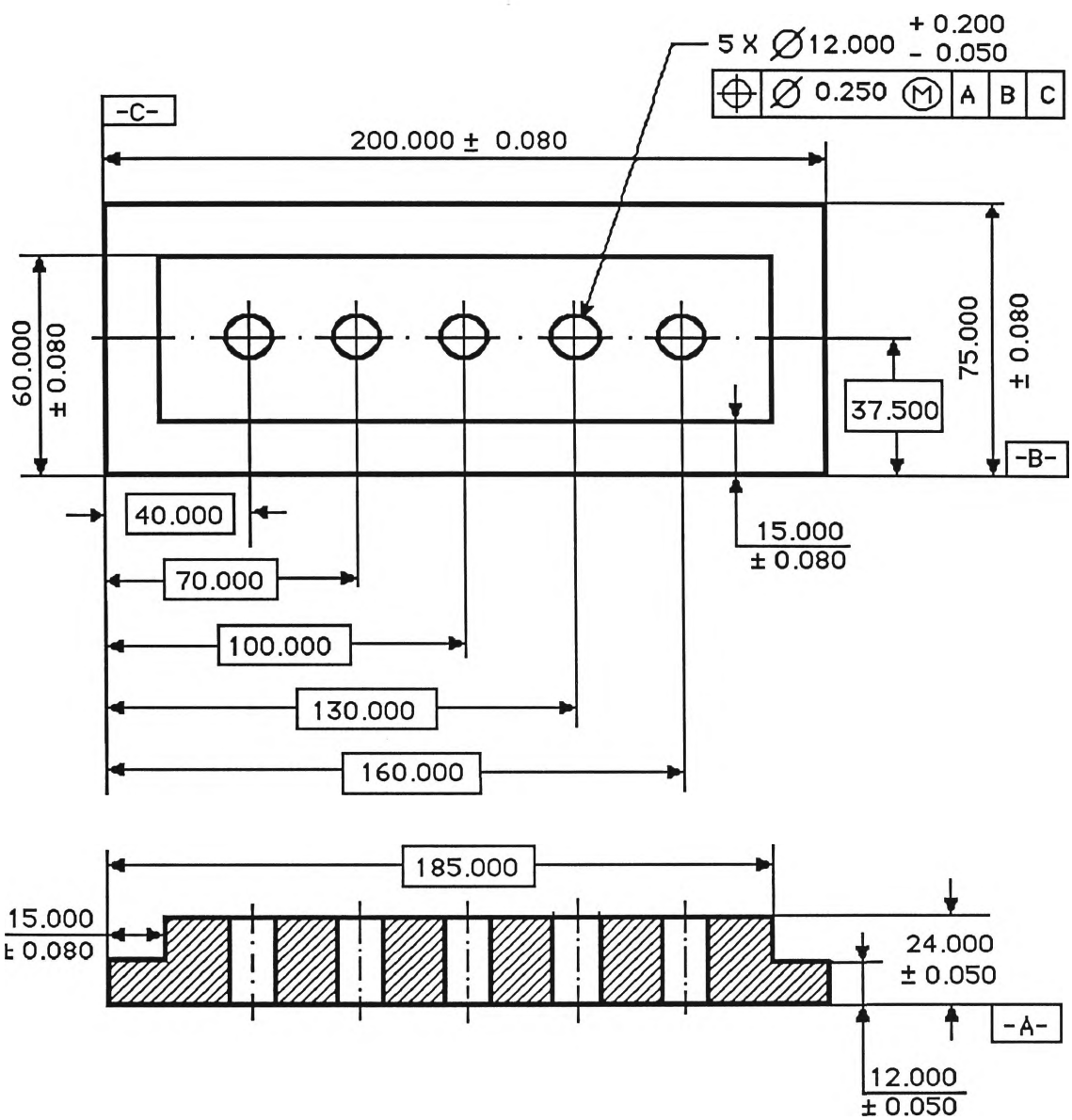

Figure 3.4. Test Component .

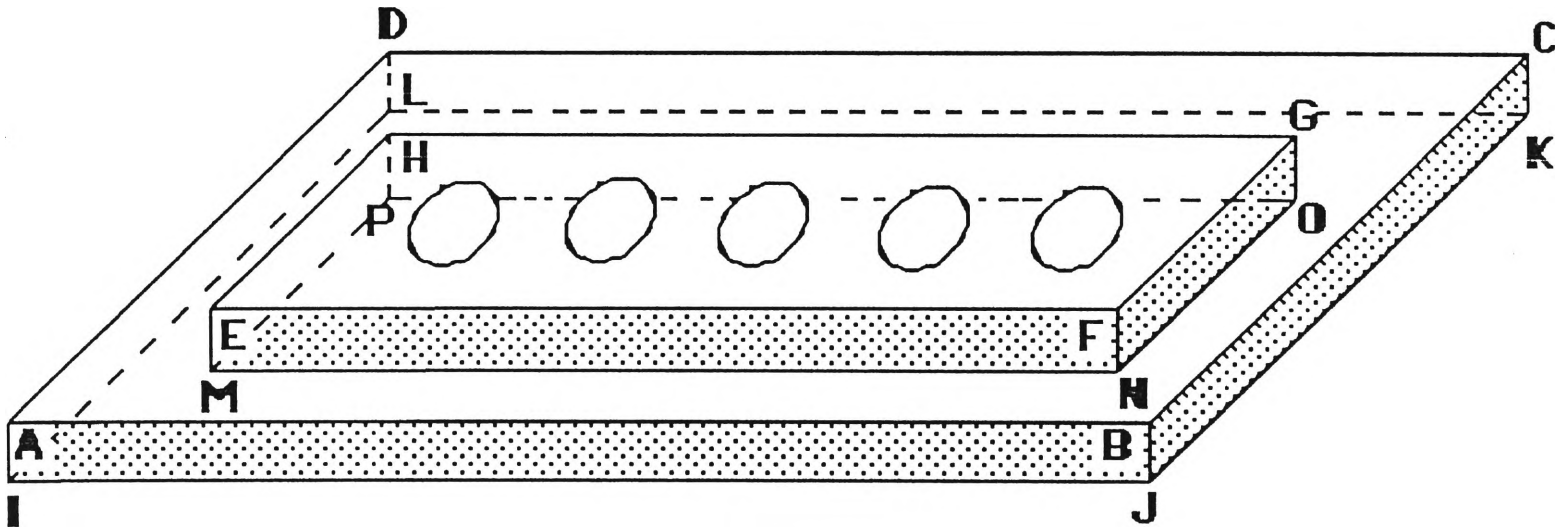

Figure 3.5 Oblique View Of Test Component.

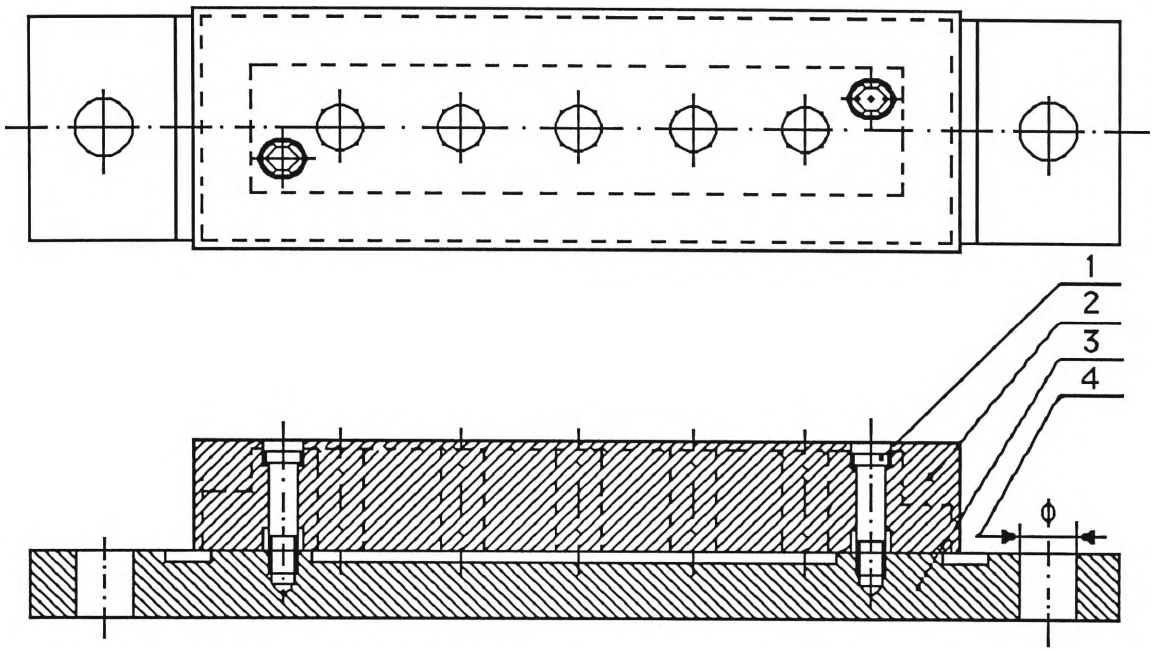

1 - Two Screws for Clamping Workpiece, 2 - Work piece, 3 - Jig Plate, 4 - Two Holes for Fixing the Jig on Machine Saddle.

Figure 3.6 Clamping of Workpiece.

3.2.4 Work Material

The material chosen for test components is Aluminium alloy, 6061. Chemical analysis of the work material in our Materials Laboratory showed the following chemical composition:

	Weight %	Atomic %
Aluminium	98.0159	98.3125
Copper	0.2395	0.1288
Iron	0.8364	0.1630

Magnesium	0.6522	0.7260
Manganese	0.0108	0.0053
Silicon	0.6950	0.6697

The reasons of choosing this Aluminium alloy are:

- It can be machined relatively easily (comparatively higher machinability rating) which improves tool life and reduces the tool wear effect.
- The anti-corrosive property of aluminium alloy keeps the dimension of the test components intact during a prolonged interval of time.
- The material used is easily available and widely used in industry.

3.2.5 Cutting Conditions and Cutting Tools

Cutting conditions and cutting tools chosen were as follows:

FACE MILLING CUTTER (ϕ 100mm)

Cutting speed, U = 314 m/min

Feed, S_m = 100 mm/min

Depth of cut, d = 1 mm

END MILL (ϕ 16mm)

		Rough Cut		Finish Cut
Cutting speed, U	(m/min)	126	126	126
Feed, S_m	(mm/min)	125	125	125
Depth of Cut, d	(mm)	7	7	1

DRILL (ϕ 12 mm)

Cutting speed, U = 75 m/min

Feed rate, S = 0.15 mm/rev

Selection of cutting conditions was also a problem, because improper cutting conditions can lead to inaccuracies in the test component. Cutting conditions were chosen according to handbook data. In an attempt to achieve better surface finish, at a later stage, some components were machined under improved cutting conditions. Cutting conditions for these components were chosen as follows:

FACE MILLING CUTTER (ϕ100mm)

Cutting speed, U = 314 m/min

Feed, S_m = 100 mm/min

Depth of cut, d = 1 mm

END MILL (ϕ16mm)

	Rough Cut			Finish Cut
Cutting speed, U (m/min)	126	126	151	202
Feed, S_m (mm/min)	125	125	125	125
Depth of cut, d (mm)	6	6	2.5	0.5

DRILL (ϕ 12 mm)

Cutting speed, U = 150 m/min

Feed rate, S = 0.1 mm/rev

3.3 Experimental Work

3.3.1 Machining of the Test Component

Forty test pieces were machined (see Figure 3.7) in the Zenford Ziegler CNC machining centre, of which ten selected components were marked TP1-TP10. All tools were new and new cutting edges were used for each set of experiments to avoid possible tool wear effect. Cutting fluid used was Castrol Hysol Ac (manufactured by Castrol Australia Pty Ltd.) which is a metal working lubricant and clear soluble type cutting fluid. During machining the machining centre required some manual operations such as, chip removal, directing the cutting fluid nozzle, etc. All deburring operations were also done manually with care.

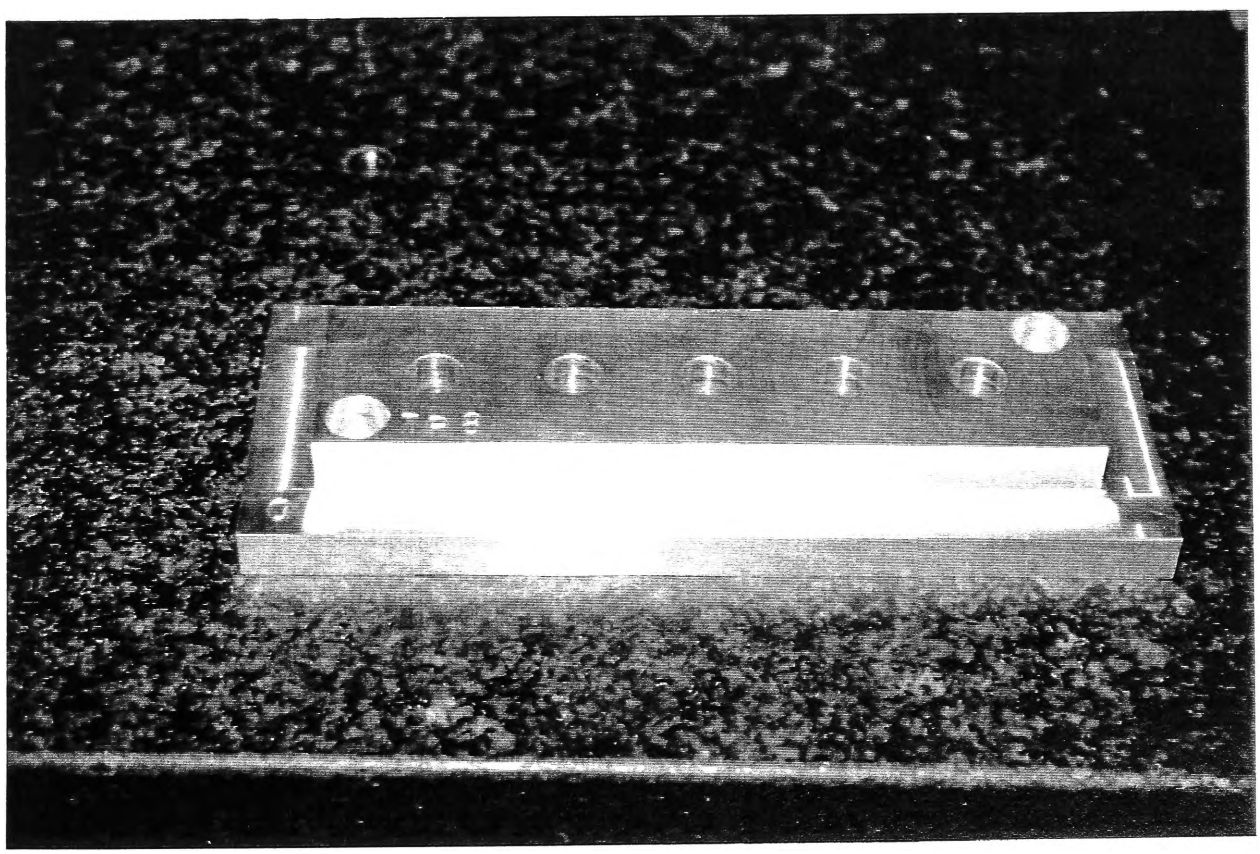

Figure 3.7 Machined Test Component.

3.3.2 Measurement Procedure

The test pieces were measured individually employing the CMM. The probe used was a Renishaw probe (manufactured by Renishaw Electrical Ltd.), which is a touch trigger probe and appears to be the most popular probe used in CMMs. A spherical probe of 4 mm diameter was used.The test components were secured on the granite table of the CMM. The primary datum plane A was established by the datum surface A contacting on the high points of the granite table of the CMM, which is considered to be a "perfect" (or at least "near perfect") plane (Figure 3.8).

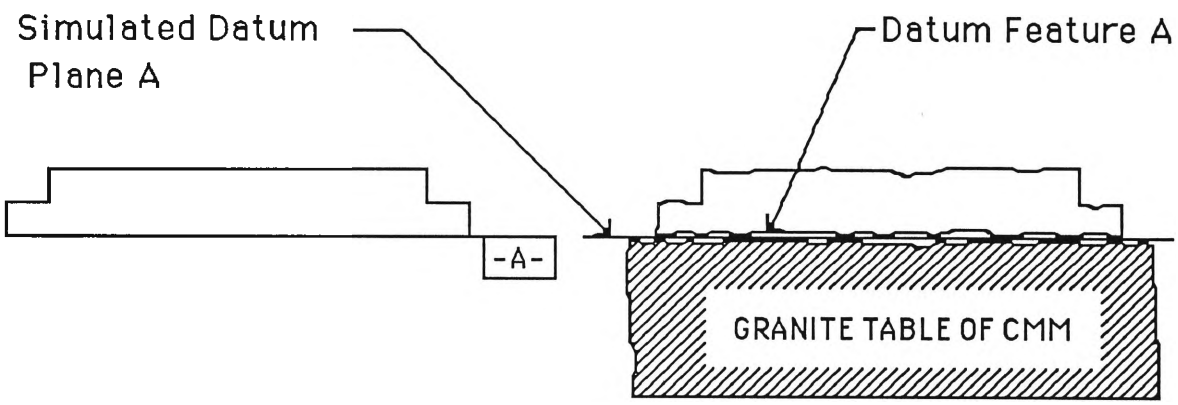

Figure 3.8 Datum Surface [13].

The datum reference frame adopted is shown in Figure 3.9. It is clear from Figure 3.9 that, by adopting such a datum reference frame, the bottom left hand corner of the test component (which is the intersection of the three datum planes) becomes the origin of a three axis co-ordinate system and any measurement taken is with respect to that origin. It is to be emphasized that datums are regarded as "perfect", whereas the parts are not. In agreement with the GD & T, primary, secondary and tertiary datum planes were selected by a minimum of three, two and one points of contact respectively. Built-in software

packages of the CMM were used to calculate different geometric elements. The effect of temperature variations was neglected, but efforts were made to conduct the experiments in an environment without much temperature difference.

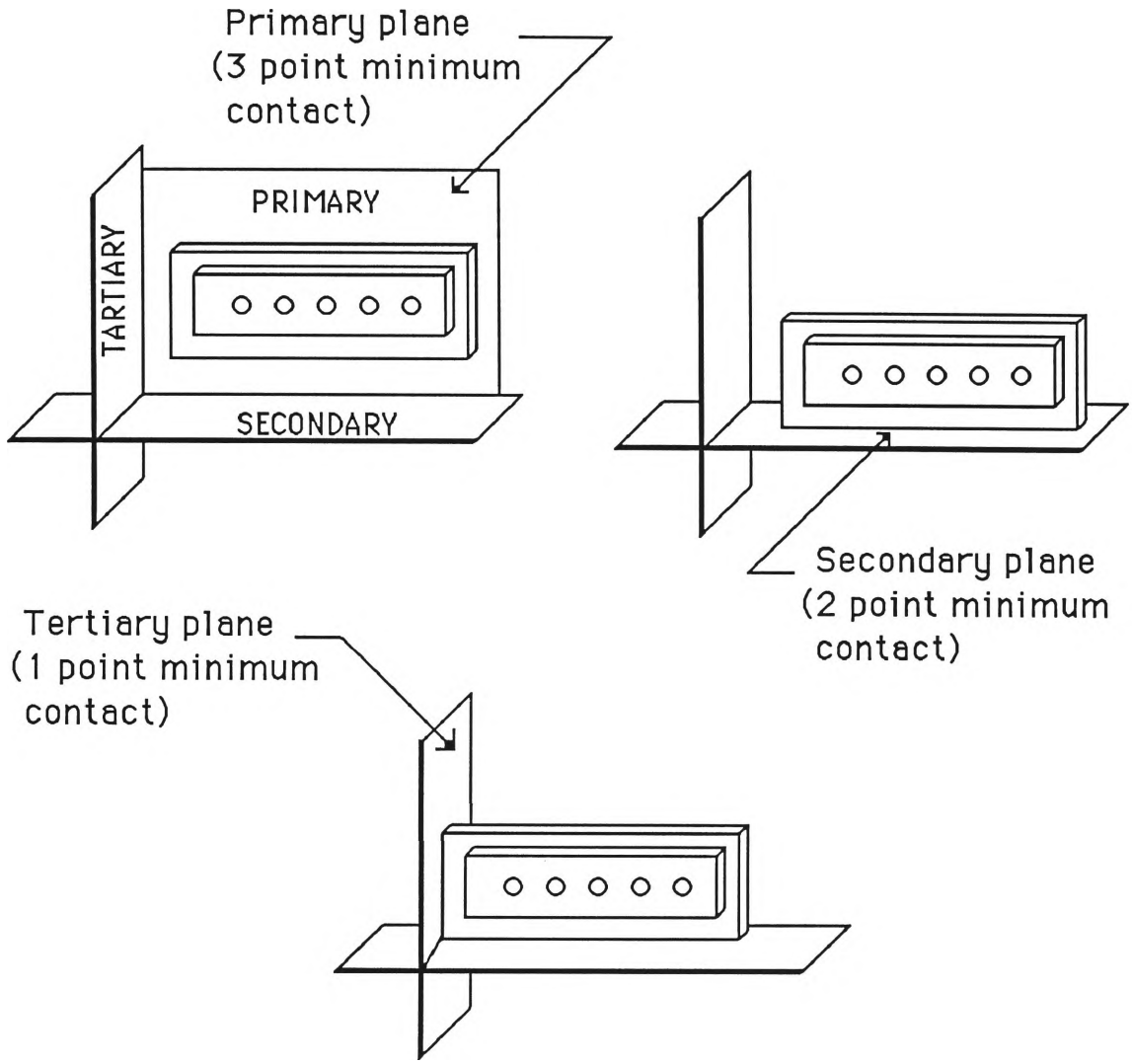

Figure 3.9 Datum Reference Frame [13].

3.3.3 Problems Associated with CMMs

Although most of the national and international standard organizations have adopted GD & T, there exist some difficulties in the use of methods by which the ideal geometric features are to be established [121], [122]. A number of methods have been proposed by different researchers, viz least square technique, Monte Carlo technique or simplex method, minimax approximation, median technique, etc. The advantages and disadvantages of different methods have been discussed in [121],[122]. However, no method has yet been universally accepted. Among the above-mentioned techniques the least square technique is found to be the most popular, due to its mathematical base and shorter computational time required. In most of today's CMMs, the least square method is used to define different geometric elements, such as circle, cylinder, plane, etc. A comparative study of the computation techniques is beyond the scope of our present research and we accepted the built-in software package in our CMM which is also based on least square technique.

The problem of software errors of CMMs has been discussed in the present the literature survey. In Table 2.2, it was shown that in some cases the CMM software showed a poor level of conformity. Sona [100] also pointed out this problem. The problem is more serious when the measured component is out of true form by a larger departure.

In the present experiments the CMM software package was used to find the diameter and the centre (co-ordinates) of the holes. Ferranti (mercury) CMM software package for this purpose has a 32 points (maximum number of points) programme and for a circle a minimum of 3 points is asked. It is obvious that the more points we take, the more accurate the results will be.

At this stage there was no indication about the accuracy levels achievable for a given number of points. Sona and Farmer [123] have investigated the influence of different

number of points taken on a circle and in some cases, as many as 60 points were taken. To select the number of points to be probed on a circle, ten readings were taken for each measurement with the number of points for each varying from 4 to 32. The repeatability of measurement was calculated from each of the ten readings using the following formulas given in British Standard for Co-ordinate Measuring Machines, BS 6808 : Part 2 [107]:

$$R_p = \pm 0.72.s \tag{3.1}$$

$$s = \left(\frac{1}{9} \sum_{i=1}^{10} (X_{mi} - \overline{X}_m)^2 \right)^{\frac{1}{2}}$$

$$\overline{X}_m = \frac{1}{10} \sum_{i=1}^{10} X_{mi}$$

where

R_p = repeatability

s = sample standard deviation

X_{mi} = measured values

$\overline{X}_m$ = mean measured value

The relationship was studied for three holes (Hole 1, 2, 3) of a test component. The results are illustrated in Figure 3.10. Polynomial Least Squares Fit was applied to smooth the curves.

Results shown in Figure 3.10 confirm that as the number of points taken on a circle (n) is increased the magnitude of the repeatability of measurement (R_p) is decreased, although the rate of decrease is different in different cases. It may be due to rough surface finish and/or the holes being out of form by large magnitude. As a whole the repeatability of measurement is good, as this is in all cases less than 8 microns. Considering the accuracy levels of all equipment used in this experiment, it was decided n = 8.

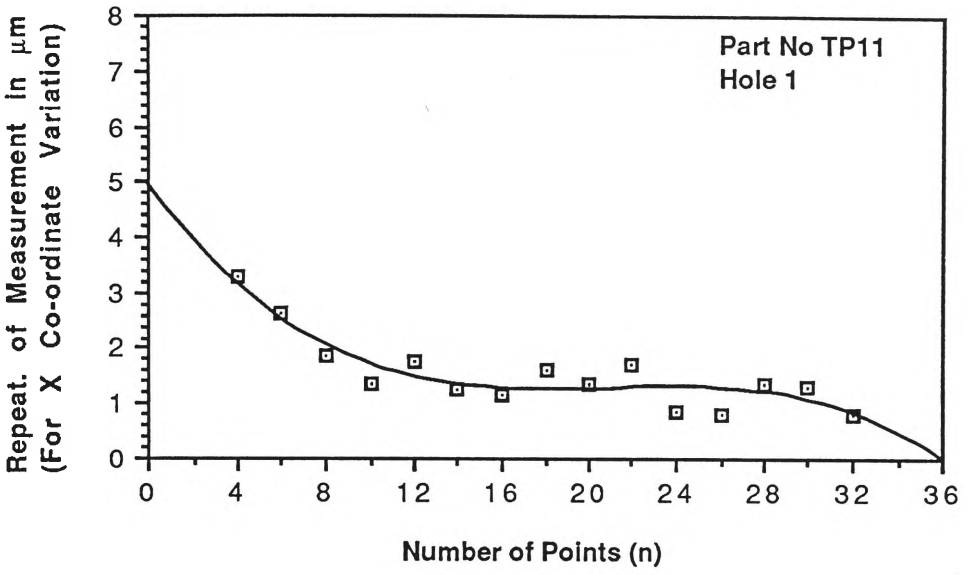

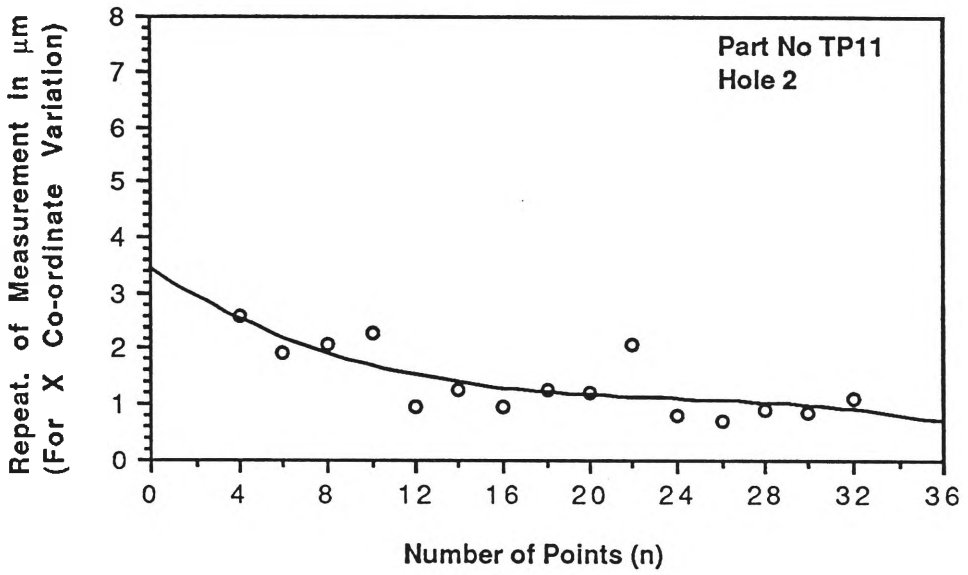

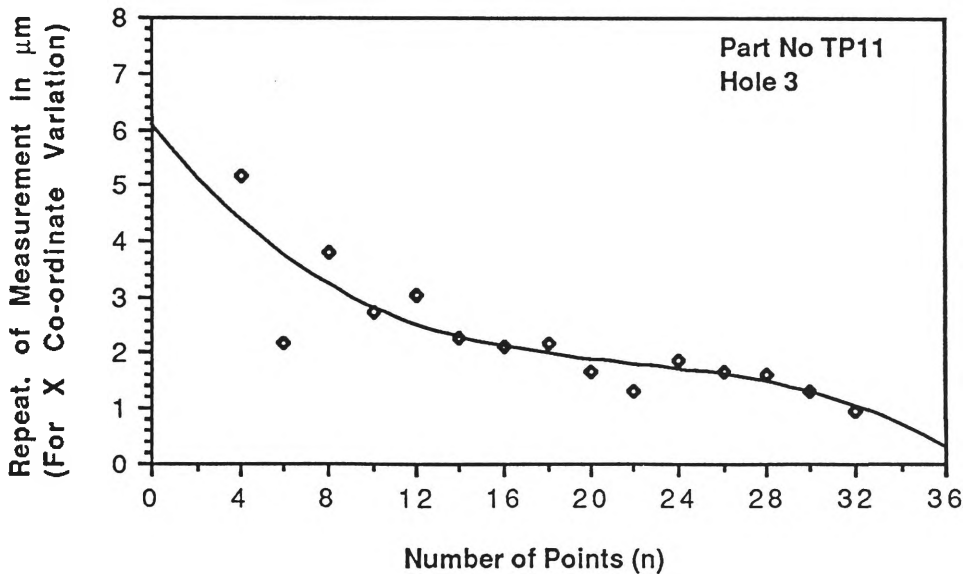

Figure 3.10.1 Repeatability of Measurements with CMM (For X co-ordinate Variation).

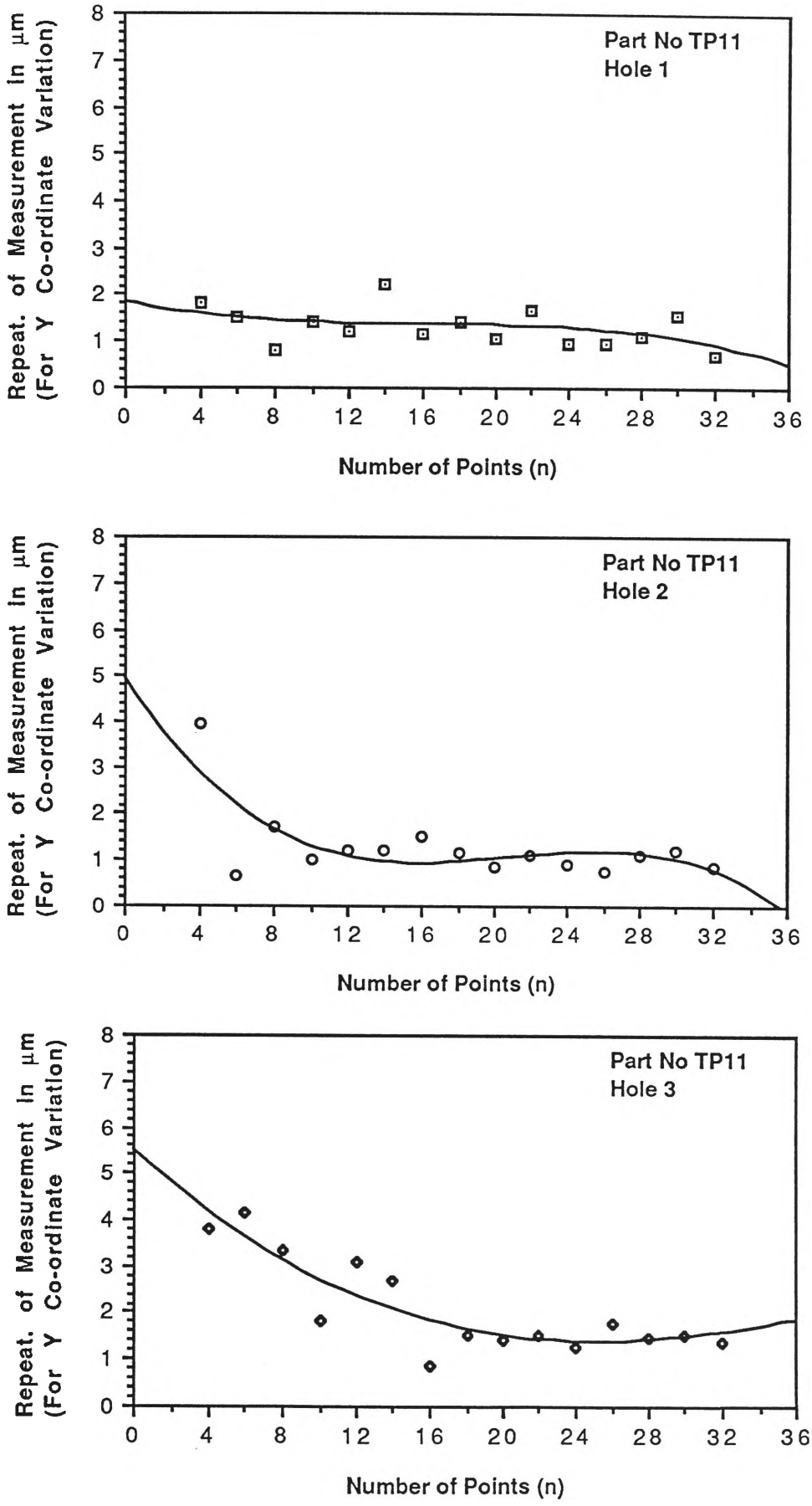

Figure 3.10.2 Repeatability of Measurements with CMM (For Y co-ordinate Variation).

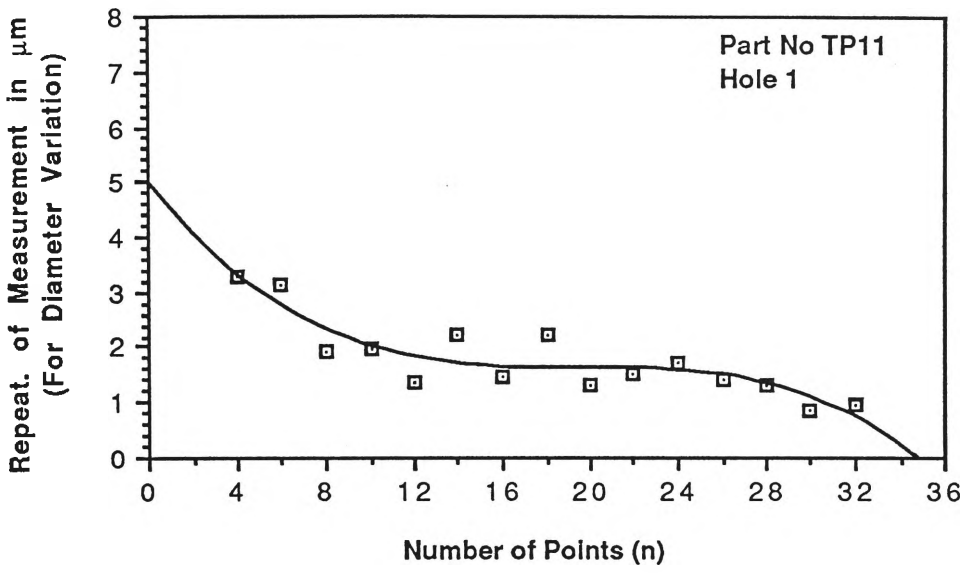

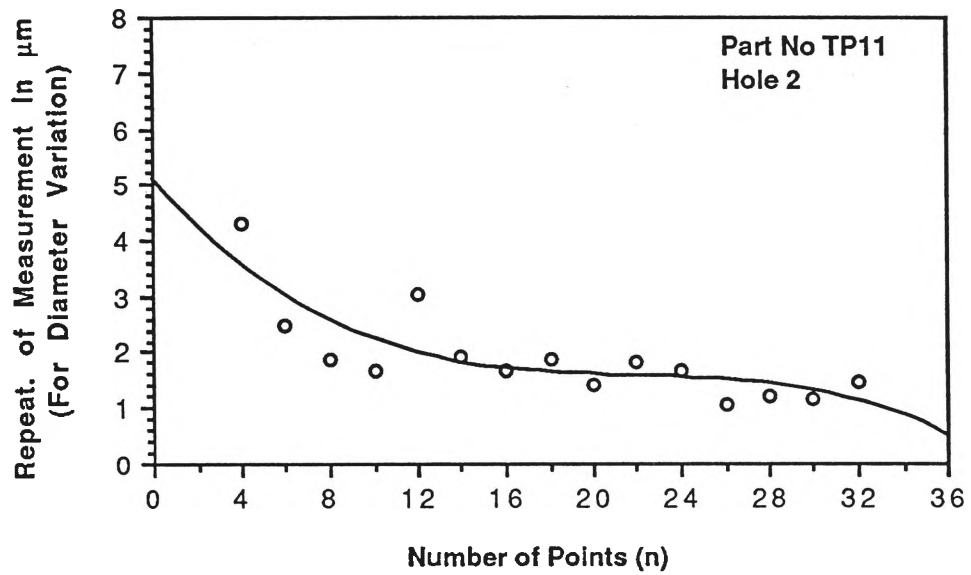

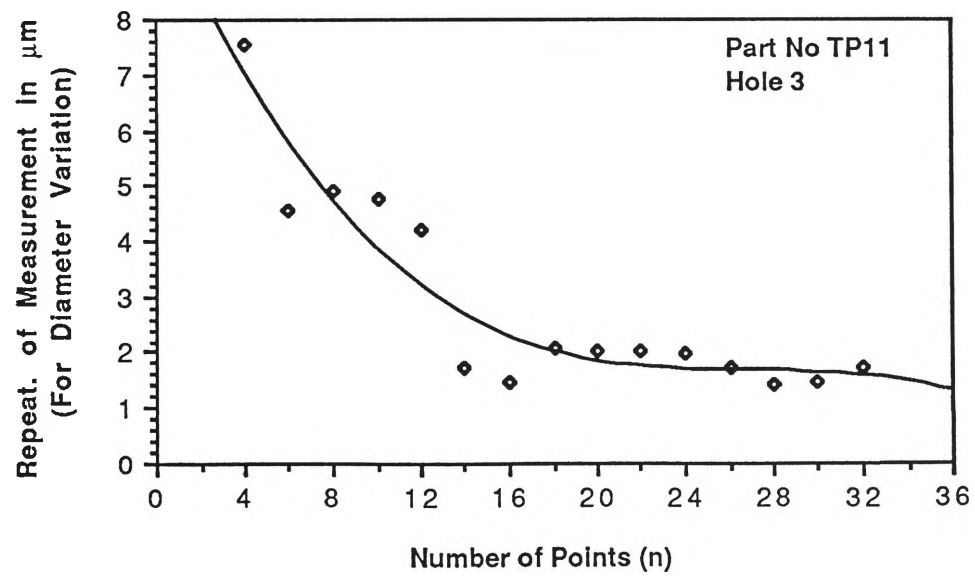

Figure 3.10.3 Repeatability of Measurements with CMM (For Diameter Variation).

3.3.4 Further Experimental Work

In CNC drilling, different ways of drilling are possible depending on the motion of the drill along feed direction (drill penetration). These operations are pre-programmed and known as **canned cycles** (For details see Appendix E)."Because aluminium alloys are easily machined, rates of drill penetration are rapid and chip disposal can be a problem; ...." [128]. Bearing this consideration in mind in our test component deep hole drilling canned cycle (G83) was used. To the best of author's knowledge no work on the effect of type of drilling canned cycle on hole accuracy has been reported in the literature. So we have decided to investigate the hole accuracy depending on the type of drilling canned cycle used. Three drilling canned cycles viz. chip break canned cycle (G73), spot drilling canned cycle (G81) and deep hole canned cycle (G83), were used for comparison. Three components were machined using each of those drilling canned cycles.

3.4 Analysis of Experimental Work

For each test component all measurements were recorded on a printer connected to the CMM and then fed into the computer creating individual data files. Various aspects of accuracy and GD & T have been studied separately. Computer programmes were developed to calculate and plot different relationships. All programmes were written in such a way, that by calling different data files (for different test components) the corresponding relationship can be plotted for a given test component. Relationships were plotted for every test component. Due to space constraints only a few are illustrated here, and the selection was made at random in most cases, and selectively (to justify some logic), in some cases.

3.4.1 Linear Dimensions

All linear dimensions were inspected thoroughly. For each test component about 400 points were probed. The procedure for determining linear dimensions is given in Appendix F. In further calculations mean values are used. In Table 3.1 results of the surface measurements are given. Absolute and relative errors of different linear dimensions are calculated using the following formulae:

$$\Delta_a = X_m - X_d \tag{3.2}$$

$$\Delta_r = \frac{X_m - X_d}{X_d} \cdot 100 \tag{3.3}$$

where X_d = designed value of dimension (mm)

X_m = measured value of dimension (mm)

Δ_a = absolute error (mm)

Δ_r = relative error (%)

Dimensions represented by L, B, H, etc. are given in Figure 3.11 and the results obtained for the ten test components are given in Table 3.2.

From Table 3.2, it can be seen that in all horizontal dimensions (such as L, B, D, A, etc) the deviation is negative, i.e. $X_m < X_d$. This means that the test components have been overcut. Many factors can be considered to be responsible for this deviation such as: positioning error of the tool, inaccuracy of the cutting tool, vibration, misalignment of the tool, non-optimum cutting conditions, etc. For the determination of the actual cause further investigations are required.

Surface*	Designed	PART No TP1			PART No TP2			PART No TP3		
	Value (mm)	$\overline{X}_m$ (mm)	s (μm)	Range (μm)	$\overline{X}_m$ (mm)	s (μm)	Range (μm)	$\overline{X}_m$ (mm)	s (μm)	Range (μm)
ABJI	$Y_d = 0.000$	- 0.002	5.085	21	- 0.005	2.768	11	0.001	4.375	15
DLCK	$Y_d = 75.000$	74.956	6.286	28	74.962	3.471	17	74.966	5.085	19
DAIL	$X_d = 0.000$	0.006	3.927	17	- 0.002	2.905	10	- 0.004	3.160	12
BCKJ	$X_d = 200.000$	199.965	5.546	27	199.964	2.872	11	199.963	3.435	15
EFNM	$Y_d = 15.000$	14.990	5.108	18	14.983	3.434	14	15.000	3.561	14
GOPH	$Y_d = 60.000$	59.963	5.662	24	59.957	4.385	18	59.980	6.480	19
HEMP	$X_d = 15.000$	15.003	4.845	19	14.993	7.156	38	14.990	3.884	13
FGON	$X_d = 185.000$	184.963	6.109	27	184.962	4.153	13	184.962	3.288	12
HEFG	$Z_d = 24.000$	24.368	4.136	16	24.347	5.798	22	24.412	3.869	16
ABCD	$Z_d = 12.000$	11.947	5.659	24	11.909	5.520	17	12.019	4.798	21

* For details see Figure 3.5.

Table 3.1 Measurement Results of Surfaces.

Surface*	Designed	PART No TP4			PART No TP5			PART No TP6		
	Value (mm)	$\overline{X}_m$ (mm)	s (μm)	Range (μm)	$\overline{X}_m$ (mm)	s (μm)	Range (μm)	$\overline{X}_m$ (mm)	s (μm)	Range (μm)
ABJI	$Y_d = 0.000$	- 0.002	4.506	17	0.001	5.236	19	0.001	3.839	17
DLCK	$Y_d = 75.000$	74.963	4.030	14	74.968	4.449	15	74.963	3.438	14
DAIL	$X_d = 0.000$	- 0.007	4.366	17	- 0.010	4.948	16	- 0.007	3.911	16
BCKJ	$X_d = 200.000$	199.967	4.173	14	199.953	5.844	24	199.962	5.930	22
EFNM	$Y_d = 15.000$	14.990	4.070	13	14.993	4.695	16	14.990	4.503	15
GOPH	$Y_d = 60.000$	59.970	4.403	18	59.969	4.320	15	59.974	4.811	15
HEMP	$X_d = 15.000$	14.999	3.095	10	14.989	4.514	18	14.998	4.880	14
FGON	$X_d = 185.000$	184.969	3.409	12	184.949	3.044	12	184.957	4.011	15
HEFG	$Z_d = 24.000$	24.353	5.196	17	24.366	3.553	13	24.382	7.833	27
ABCD	$Z_d = 12.000$	11.972	6.324	23	11.939	6.353	24	11.911	8.122	27

* For details see Figure 3.5.

Table 3.1 (Contd.) Measurement Results of Surfaces.

Surface*	Designed	PART No TP7			PART No TP8			PART No TP9		
	Value (mm)	$\overline{X}_m$ (mm)	s (μm)	Range (μm)	$\overline{X}_m$ (mm)	s (μm)	Range (μm)	$\overline{X}_m$ (mm)	s (μm)	Range (μm)
ABJI	$Y_d = 0.000$	- 0.007	4.675	17	- 0.005	4.857	17	0.001	3.492	15
DLCK	$Y_d = 75.000$	74.941	4.824	18	74.948	5.131	19	74.980	7.916	27
DAIL	$X_d = 0.000$	0.001	2.900	11	- 0.003	3.722	19	0.001	3.757	15
BCKJ	$X_d = 200.000$	199.959	5.190	21	199.962	8.569	29	199.967	5.564	20
EFNM	$Y_d = 15.000$	14.984	5.051	24	14.988	5.770	21	14.999	4.351	17
GOPH	$Y_d = 60.000$	59.959	4.368	17	59.963	4.945	18	59.989	4.394	19
HEMP	$X_d = 15.000$	15.001	4.930	17	15.005	4.793	18	14.998	3.779	16
FGON	$X_d = 185.000$	184.967	4.389	18	184.963	7.137	31	184.968	5.009	26
HEFG	$Z_d = 24.000$	24.389	5.912	17	24.393	5.889	24	24.365	3.366	14
ABCD	$Z_d = 12.000$	11.936	4.700	16	11.986	7.838	27	11.970	6.668	25

* For details see Figure 3.5.

Table 3.1 (Contd.) Measurement Results of Surfaces.

Surface*	Designed	TART No TP10		
	Value (mm)	$\overline{X}_m$ (mm)	s (μm)	Range (μm)
ABJI	$Y_d = 0.000$	0.000	3.480	16
DLCK	$Y_d = 75.000$	74.976	3.374	15
DAIL	$X_d = 0.000$	- 0.001	3.301	14
BCKJ	$X_d = 200.000$	199.971	4.346	17
EFNM	$Y_d = 15.000$	14.993	3.319	14
GOPH	$Y_d = 60.000$	59.985	3.468	15
HEMP	$X_d = 15.000$	14.996	6.182	25
FGON	$X_d = 185.000$	184.970	3.738	22
HEFG	$Z_d = 24.000$	24.393	4.567	20
ABCD	$Z_d = 12.000$	12.000	4.805	19

* For details see Figure 3.5.

Table 3.1 (Cont.) Measurement Results of Surfaces.

Feature*	Designed Val.	PART No TP1			PART No TP2			PART No TP3		
	X_d (mm)	$\overline{X}_m$ (mm)	Δ_a (mm)	Δ_r (%)	$\overline{X}_m$ (mm)	Δ_a (mm)	Δ_r (%)	$\overline{X}_m$ (mm)	Δ_a (mm)	Δ_r (%)
L	200.000	199.959	- 0.041	- 0.020	199.966	- 0.034	- 0.017	199.967	- 0.033	- 0.016
B	75.000	74.958	- 0.042	- 0.056	74.967	- 0.033	- 0.044	74.965	- 0.035	- 0.047
H	24.000	24.368	+ 0.368	+ 1.533	24.347	+ 0.347	+ 1.446	24.412	+ 0.412	+ 1.717
A	170.000	169.960	- 0.040	- 0.023	169.969	- 0.031	- 0.018	169.972	- 0.028	- 0.016
D	45.000	44.973	- 0.027	- 0.060	44.974	- 0.026	- 0.058	44.980	- 0.020	- 0.044
h	12.000	11.947	- 0.053	- 0.442	11.909	- 0.091	- 0.758	12.019	+ 0.019	+ 0.158
C	15.000	14.992	- 0.008	- 0.053	14.988	- 0.012	- 0.080	14.999	- 0.001	- 0.006
E	15.000	14.997	- 0.003	- 0.020	14.995	- 0.005	- 0.033	14.994	- 0.006	- 0.040
F	15.000	15.002	+ 0.002	+ 0.013	15.002	+ 0.002	+0.013	15.001	+ 0.001	+ 0.006
G	15.000	14.993	- 0.007	- 0.047	15.005	+ 0.005	+ 0.033	14.986	- 0.014	- 0.093

* For details see Figure 3.11.

Table 3.2 Linear Dimension Measurement Results.

Feature*	Designed Val.	PART No TP4			PART No TP5			PART No TP6		
	X_d (mm)	$\overline{X}_m$ (mm)	Δ_a (mm)	Δ_r (%)	$\overline{X}_m$ (mm)	Δ_a (mm)	Δ_r (%)	$\overline{X}_m$ (mm)	Δ_a (mm)	Δ_r (%)
L	200.000	199.974	- 0.026	- 0.013	199.963	- 0.037	- 0.018	199.969	- 0.031	- 0.015
B	75.000	74.965	- 0.035	- 0.047	74.967	- 0.033	- 0.044	74.962	- 0.038	- 0.051
H	24.000	24.353	+ 0.353	+ 1.471	24.366	+ 0.366	+ 1.525	24.382	+ 0.382	+ 1.592
A	170.000	169.970	- 0.030	- 0.018	169.960	- 0.040	- 0.023	169.959	- 0.041	- 0.024
D	45.000	44.980	- 0.020	- 0.044	44.976	- 0.024	- 0.053	44.981	- 0.019	- 0.042
h	12.000	11.972	- 0.028	- 0.233	11.939	- 0.061	- 0.508	11.911	- 0.089	- 0.742
C	15.000	14.992	- 0.008	- 0.053	14.992	- 0.008	- 0.053	14.989	- 0.011	- 0.073
E	15.000	15.006	+ 0.006	+ 0.040	14.999	- 0.001	- 0.006	15.005	+ 0.005	+ 0.033
F	15.000	14.998	- 0.002	- 0.013	15.004	+ 0.004	+ 0.027	15.005	+ 0.005	+ 0.033
G	15.000	14.993	- 0.007	- 0.047	14.999	- 0.001	- 0.006	14.992	- 0.008	- 0.053

* For details see Figure 3.11.

Table 3. 2 (Contd.) Linear Dimension Measurement Results.

Feature*	Designed Val.	PART No TP7			PART No TP8			PART No TP9		
	X_d (mm)	$\overline{X}_m$ (mm)	Δ_a (mm)	Δ_r (%)	$\overline{X}_m$ (mm)	Δ_a (mm)	Δ_r (%)	$\overline{X}_m$ (mm)	Δ_a (mm)	Δ_r (%)
L	200.000	199.958	- 0.042	- 0.021	199.965	- 0.035	- 0.017	199.966	- 0.034	- 0.017
B	75.000	74.948	- 0.052	- 0.069	74.953	- 0.047	- 0.063	74.979	- 0.021	- 0.028
H	24.000	24.389	+ 0.389	+ 1.621	24.393	+ 0.393	+ 1.637	24.365	+ 0.365	+ 1.521
A	170.000	169.966	- 0.034	- 0.020	169.958	- 0.042	- 0.025	169.970	- 0.030	- 0.018
D	45.000	44.975	- 0.025	- 0.055	44.975	- 0.025	- 0.055	44.990	- 0.010	- 0.022
h	12.000	11.936	- 0.064	- 0.533	11.986	- 0.014	- 0.116	11.970	- 0.030	- 0.250
C	15.000	14.991	- 0.009	- 0.060	14.993	- 0.007	- 0.047	14.998	- 0.002	- 0.013
E	15.000	15.000	0.000	0.000	15.008	+ 0.008	+ 0.053	14.997	- 0.003	- 0.020
F	15.000	14.998	- 0.002	- 0.013	14.999	- 0.001	- 0.006	14.999	- 0.001	- 0.006
G	15.000	14.982	- 0.018	- 0.120	14.985	- 0.015	- 0.100	14.991	- 0.009	- 0.060

* For details see Figure 3.11.

Table 3.2 (Contd.) Linear Dimension Measurement Results.

Feature*	Designed Val.	PART No10		
	X_d	$\overline{X}_m$	Δ_a	Δ_r
	(mm)	(mm)	(mm)	(%)
L	200.000	199.972	- 0.028	- 0.014
B	75.000	74.976	- 0.024	- 0.032
H	24.000	24.393	+ 0.393	+ 1.637
A	170.000	169.974	- 0.026	- 0.015
D	45.000	44.992	- 0.008	- 0.018
h	12.000	12.000	0.000	0.000
C	15.000	14.993	- 0.007	- 0.047
E	15.000	14.997	- 0.003	- 0.020
F	15.000	15.001	+ 0.001	+ 0.006
G	15.000	14.991	- 0.009	- 0.060

* For details see Figure 3.11.

Table 3.2 (Contd.) Linear Dimension Measurement Results.

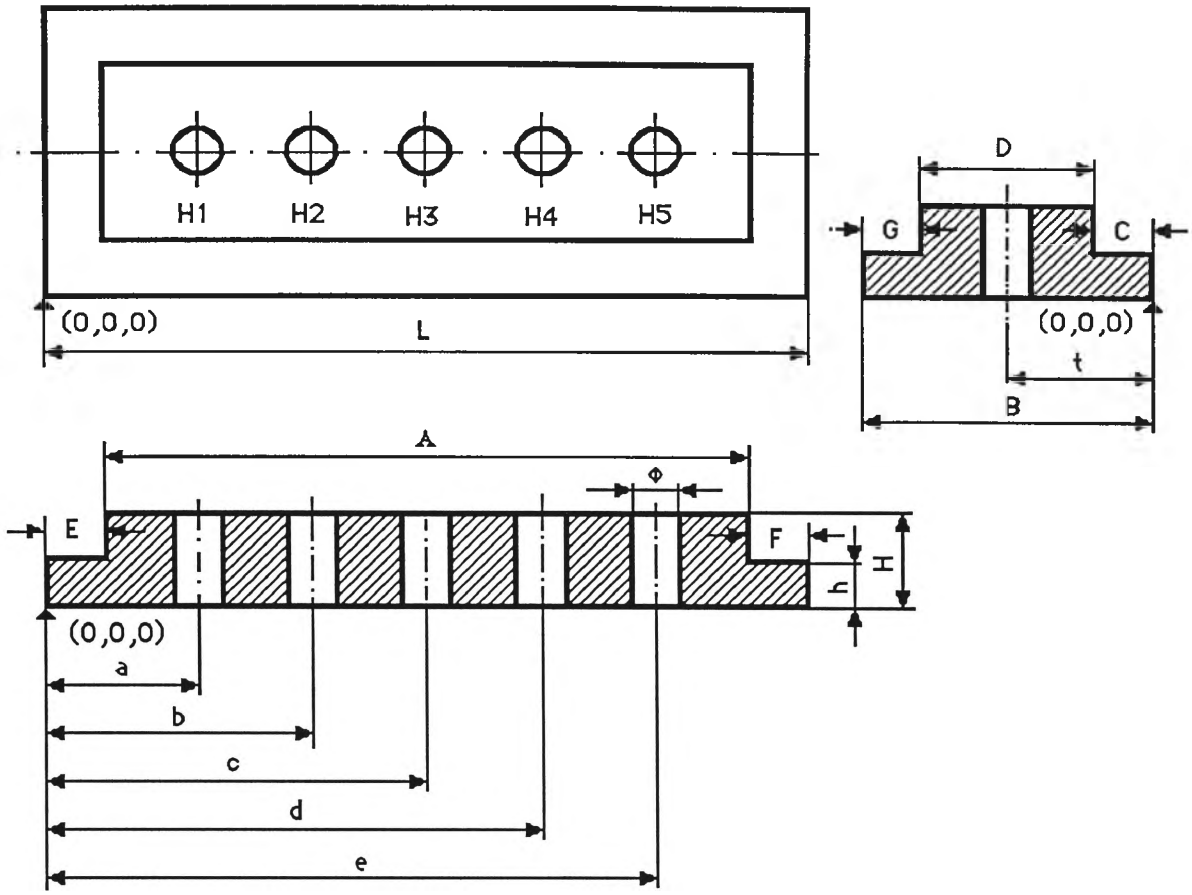

Figure 3.11. Linear Dimension Measurements.

On the basis of the measurement results given in Tables 3.1 and 3.2 a statistical analysis of the process has been done. X-bar and R charts for three major dimensions (L,B and H) are plotted and given in Figure 3.12. These charts show that for L and B dimensions are within the tolerance limits (as specified in Figure 3.4); but for H the dimension represented in X-bar chart is out of tolerance limits. The shift of average value in X-bar chart is normally related to systematic errors and can be compensated easily. The reason for this shift of the whole process out of the specified tolerance zones is incorrect identification of tool off-sets. In CNC machining at the beginning of the programme, tool off-sets are supplied which define the respective positions of the tool tips. In the present

work the tool off-sets were determined manually and there were some problems in identifying the correct tool off-sets. For L and B, a shift of respective average values towards lower tolerance limit can be noted, which is believed to be due to overcut of material and/or incorrect supply of radial compensation factors.

The quality of the product produced by a process with respect to the specifications (tolerance limits) can be quantified by a capability index. The larger the capability index, the better the quality. Capability index is generally estimated using the following formula [124]:

$$C_p = \frac{UCL - LCL}{6\,\sigma} \tag{3.4}$$

where C_p = capability index

σ = population standard deviation

UCL = upper control limit

LCL = lower control limit

$$\sigma = s' / C_4$$

$$s' = \sum \frac{s}{g}$$

where s = sample standard deviation

g = number of groups

C_4 = Const.

For our measurement results, the following process capability indices were calculated:

For L : $C_p = 1.474$

For B: $C_p = 1.436$

For H: $C_p = 1.610$

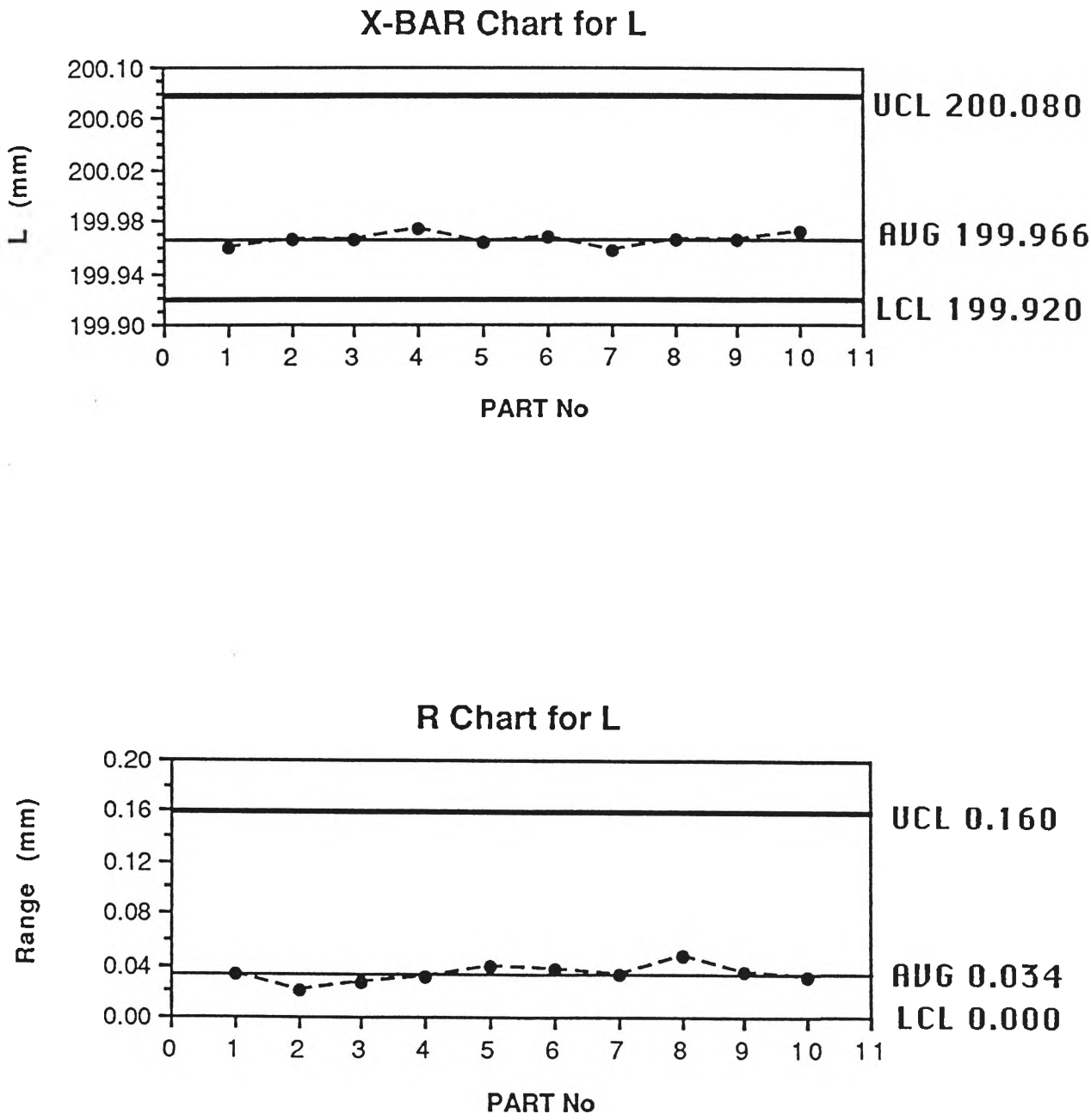

Figure 3.12.1 X-bar and R Chart for L.

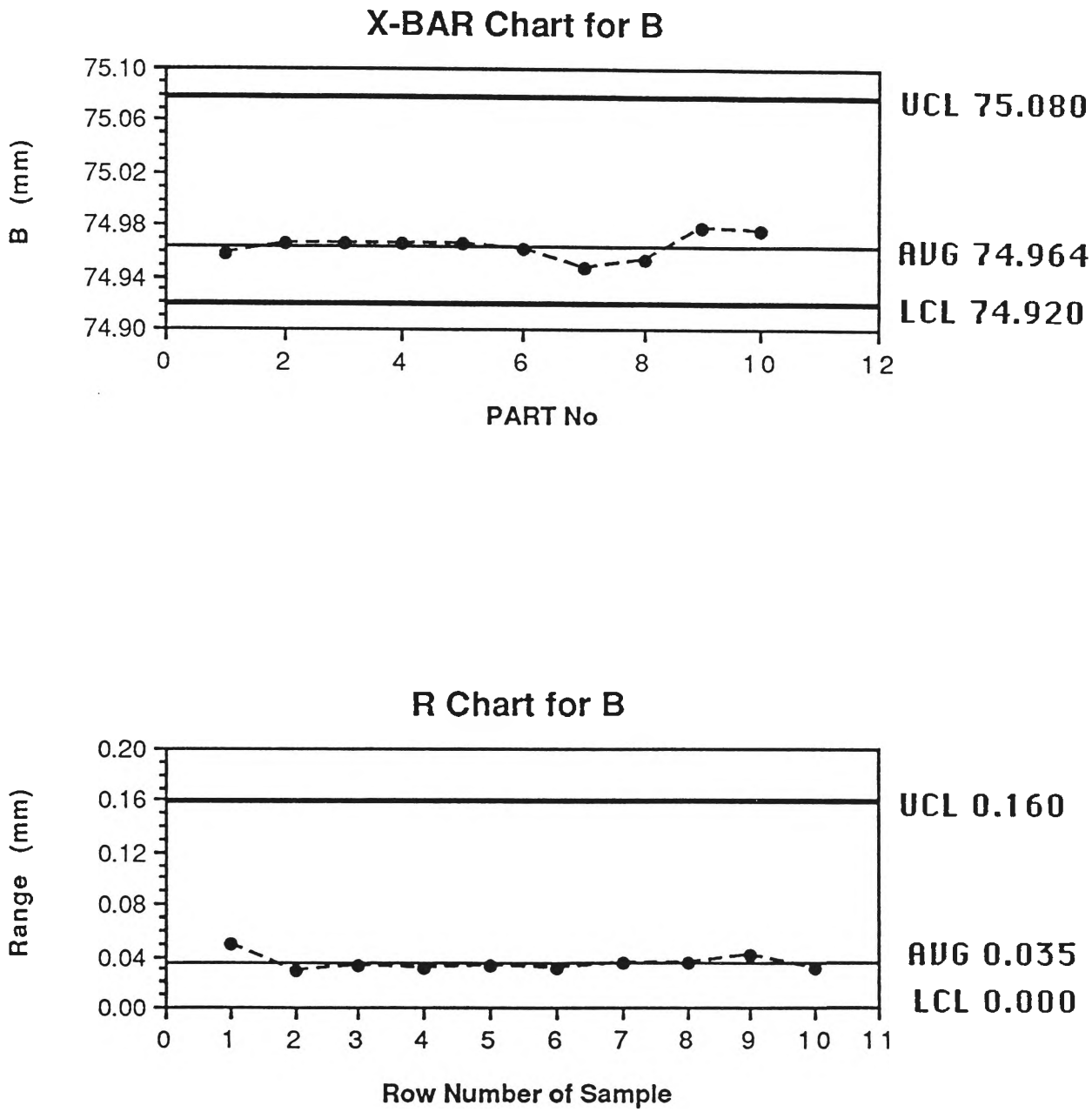

Figure 3.12.2 X-bar and R Chart for B.

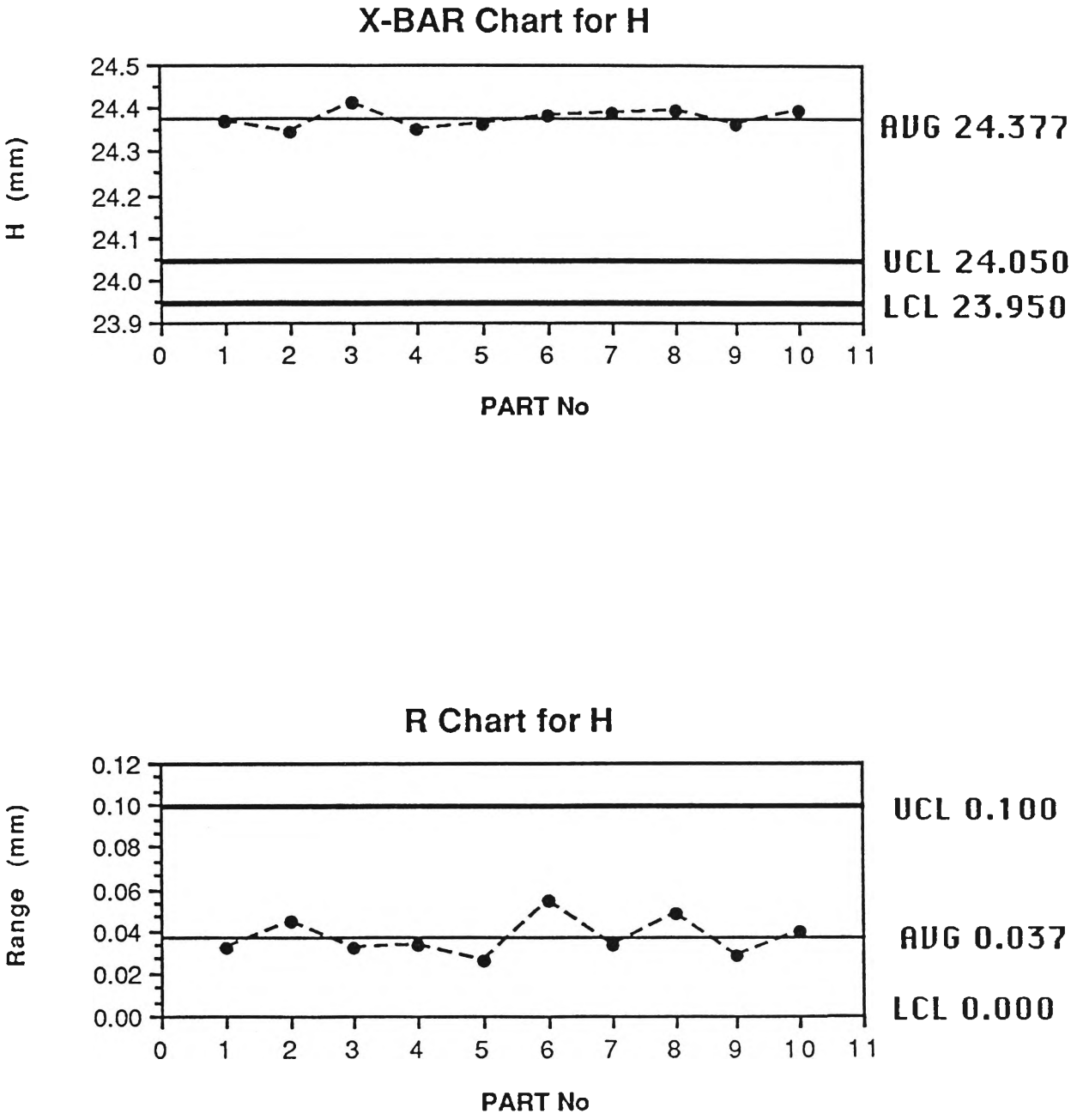

Figure 3.12.3 X-bar and R Chart for H.

The results show desirable capability indices. In normal production, the process capability index should be greater than 1.33 [124]. The capability indices for L, B and H show that L and B have similar capability indices and H has higher capability index. From this it can be concluded that face milling (H depends on face milling) gives better dimensional accuracy than end milling (L and B depend on end milling).

3.4.2 Flatness

Flatness is the condition of a surface having all elements in one plane [11]. A flatness tolerance specifies a tolerance zone defined by two parallel planes within which the entire surface must lie. This means that the range (R) given in Table 3.1 give the flatness error of each surface. Sometimes it may be very difficult to measure the flatness error (as in case of the top surface EFGH in the test component, illustrated in Figure 3.5). The measurement procedure adopted in fact checks parallelism of the surface with respect to the datum surface, rather than the flatness.

Depending on functional requirements, flatness tolerances must be specified. But while specifying flatness tolerances, the part programmer should take into account the surface texture, process capabilities, etc. When the surface is associated with a size dimension, the flatness tolerance must be less than the size tolerance.

Flatness tolerance gives the allowable range of variations and does not give any indication about the actual surface. For better understanding of the surfaces the surface topography of two surfaces EFGH and ABJI was produced. In Figures 3.13 and 3.14 surface topography of face milled surface EFGH and end milled surface ABJI are depicted. From Figure 3.13 no general tendency can be confirmed, although slight distortion of the surfaces at the entry and at the exit of the cutter is noted. From Figure 3.14 it can be seen that the surface generated is concave and that at the bottom of the test pieces there was some undercut of metal.

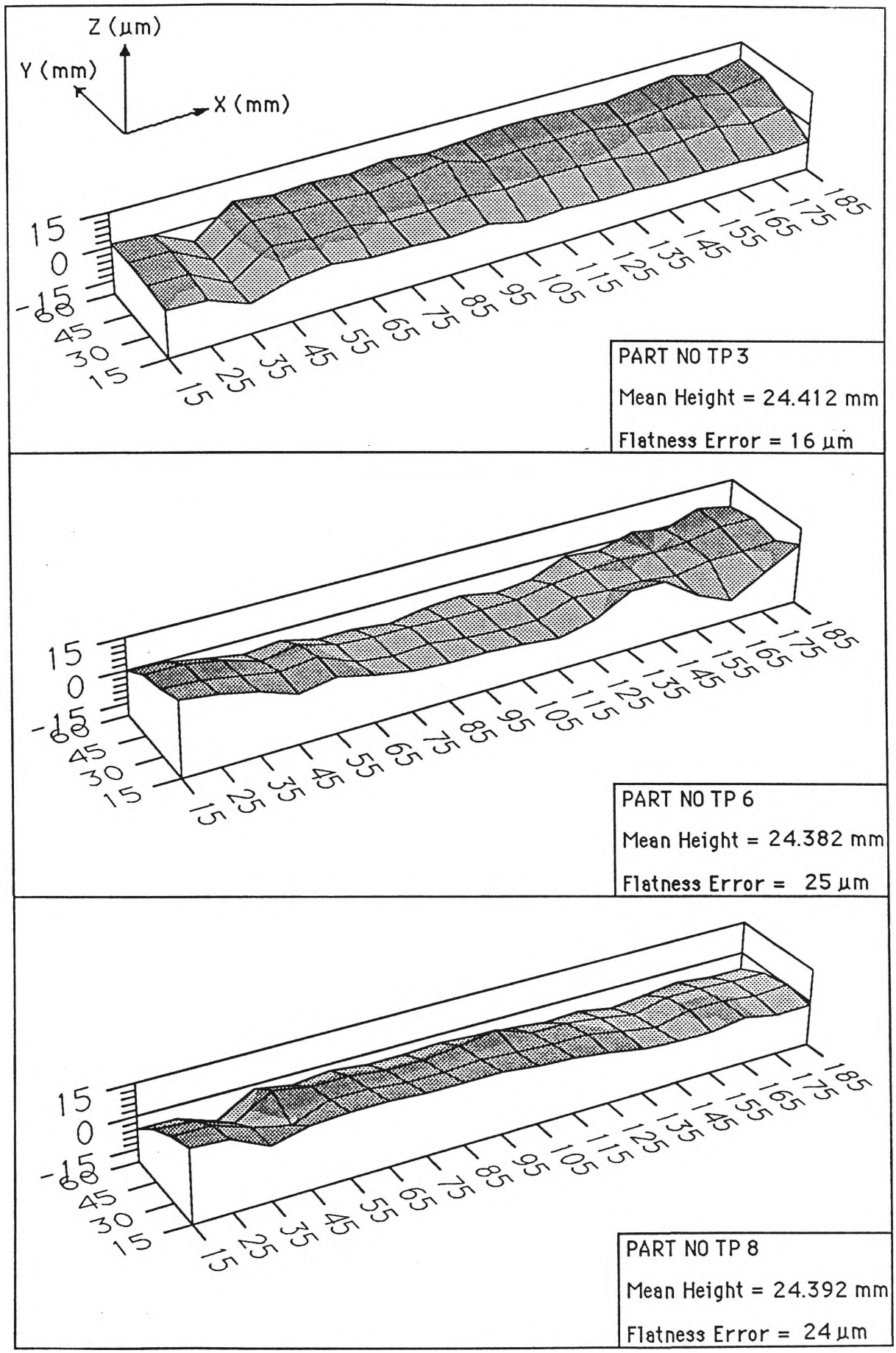

Figure 3.13 Surface Topography of Face Milled Surface (EFGH).

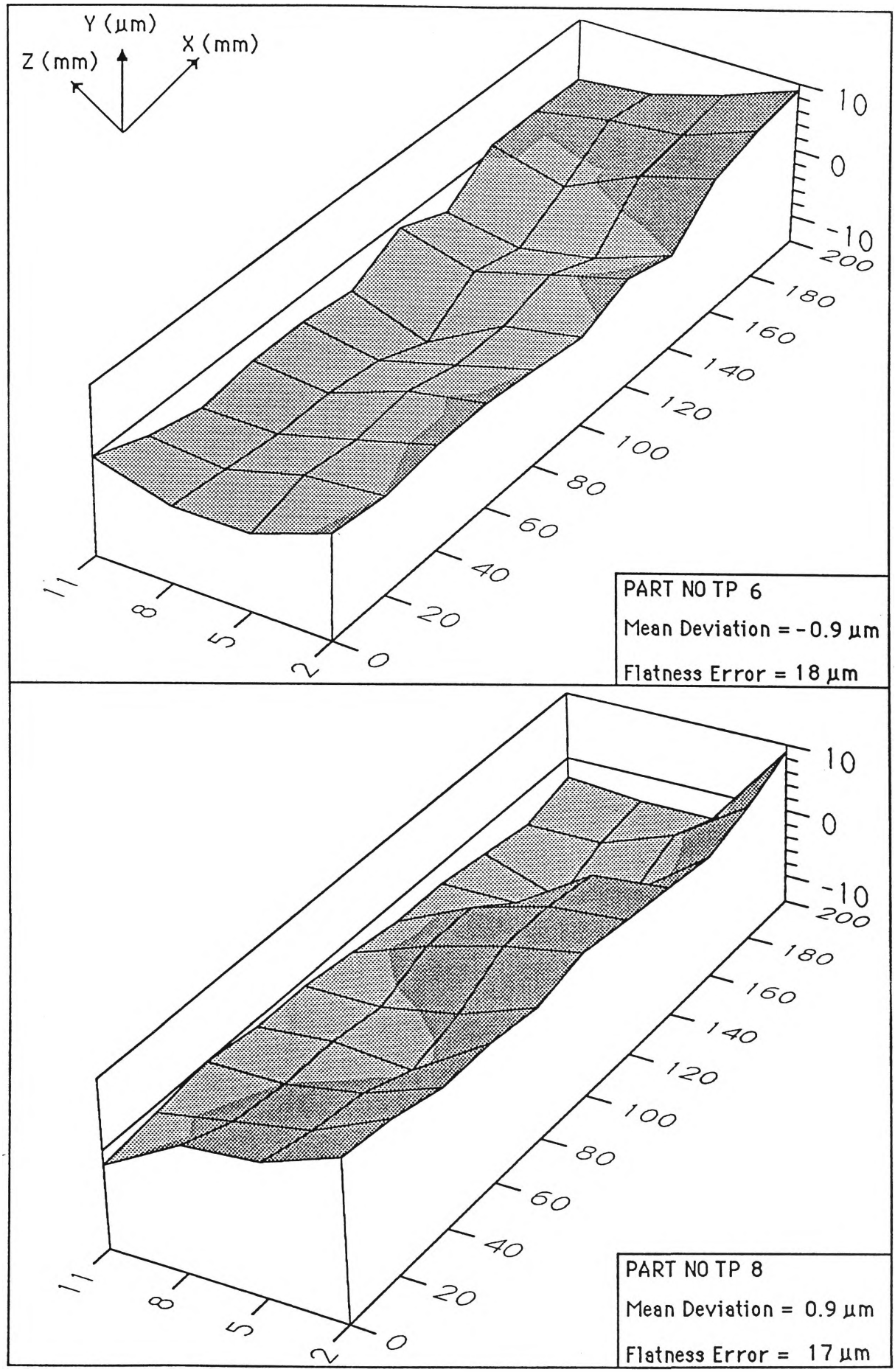

Figure 3.14 Surface Topography of End Milled Surface (ABJI).

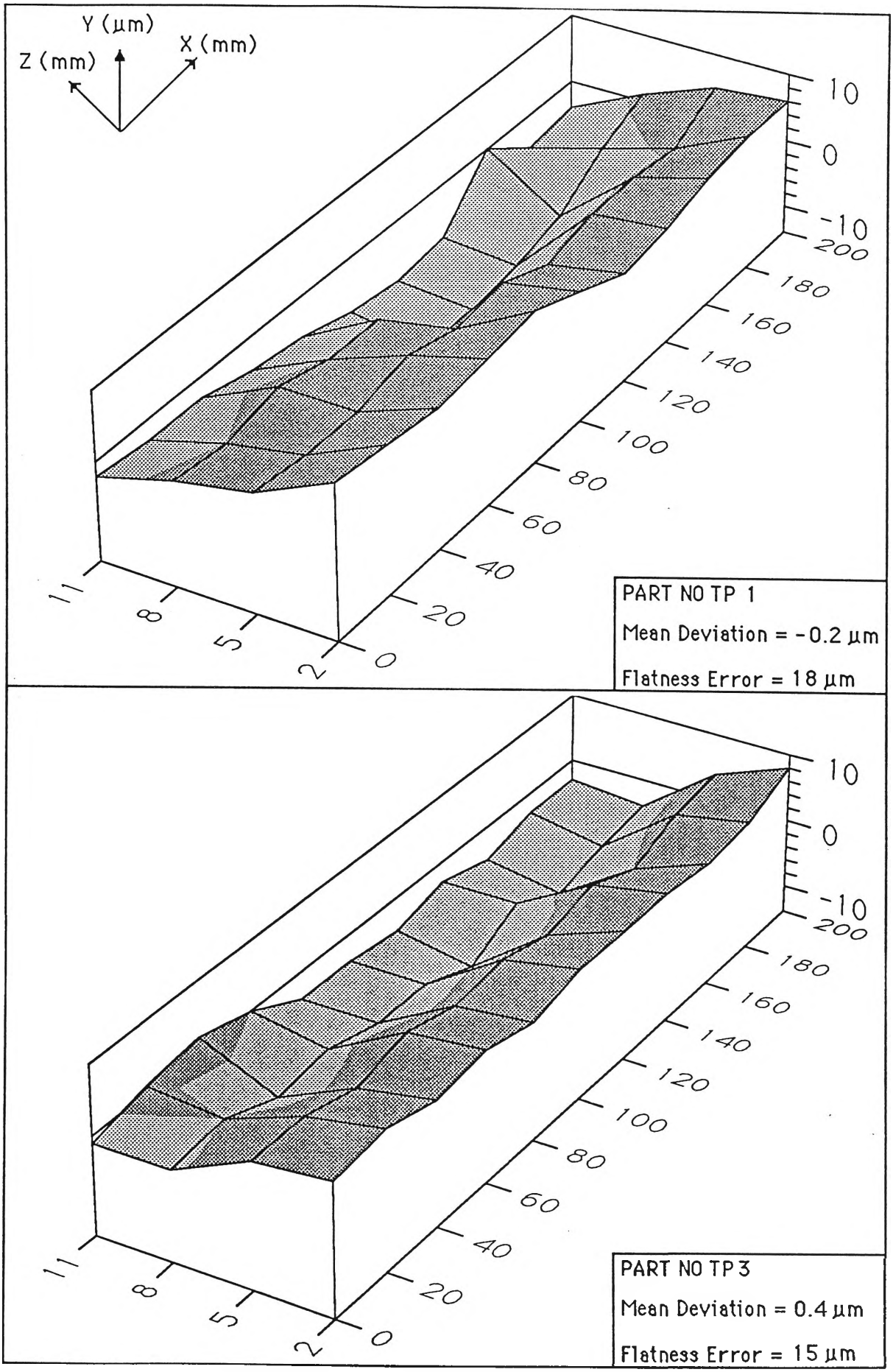

Figure 3.14 (Contd.) Surface Topography of End Milled Surface (ABJI).

3.4.3 Perpendicularity of Surfaces

Perpendicularity is the condition of a surface, median plane, or axis at a right angle to a datum plane on axis [11]. When perpendicularity conditions are applied to a surface, that surface must be between two parallel planes separated by the tolerance limit specified, which are perpendicular to the datum plane.It is interesting to note that perpendicular tolerance applied to a plane also controls the flatness of that plane.

The perpendicularity of the surfaces at each corner of test pieces was checked. Typical measurement results are given in Figure 3.15. In Figure 3.15 no significant deviation of the perpendicularity of the corner surfaces is noticed.

3.4.4 Diameter of the Holes

The diameter of the holes was calculated using the standard built-in software package of our CMM. 8 points were probed to determine each diameter taking Z = constant. Diameters of holes were recorded at different height intervals, taking Z = 0 at the primary datum surface. The change of diameters with the varying heights (with *fixed axis) for each hole was plotted. Some of the typical results plotted are given in Figure 3.16. From these figures it can be observed that in all cases the diameter variation is no more than 80 μm, which is regarded as good accuracy for drilling, which is a roughing operation. In these figures it is also noticeable that the diameter increases to some height and then decreases (some barreling effect). It is also significant that, in all cases the diameter variations were positive, i.e. the holes are oversized. Oversizing of holes is not a new problem in drilling operations. Galloway [125] discussed this common problem in 1957 and suggested the hole assymmetry as resulting from the relative lip height of the drill.

---

* In Figure 3.16 axes of the holes were considered as fixed; but in reality the positions of these axes may also vary.

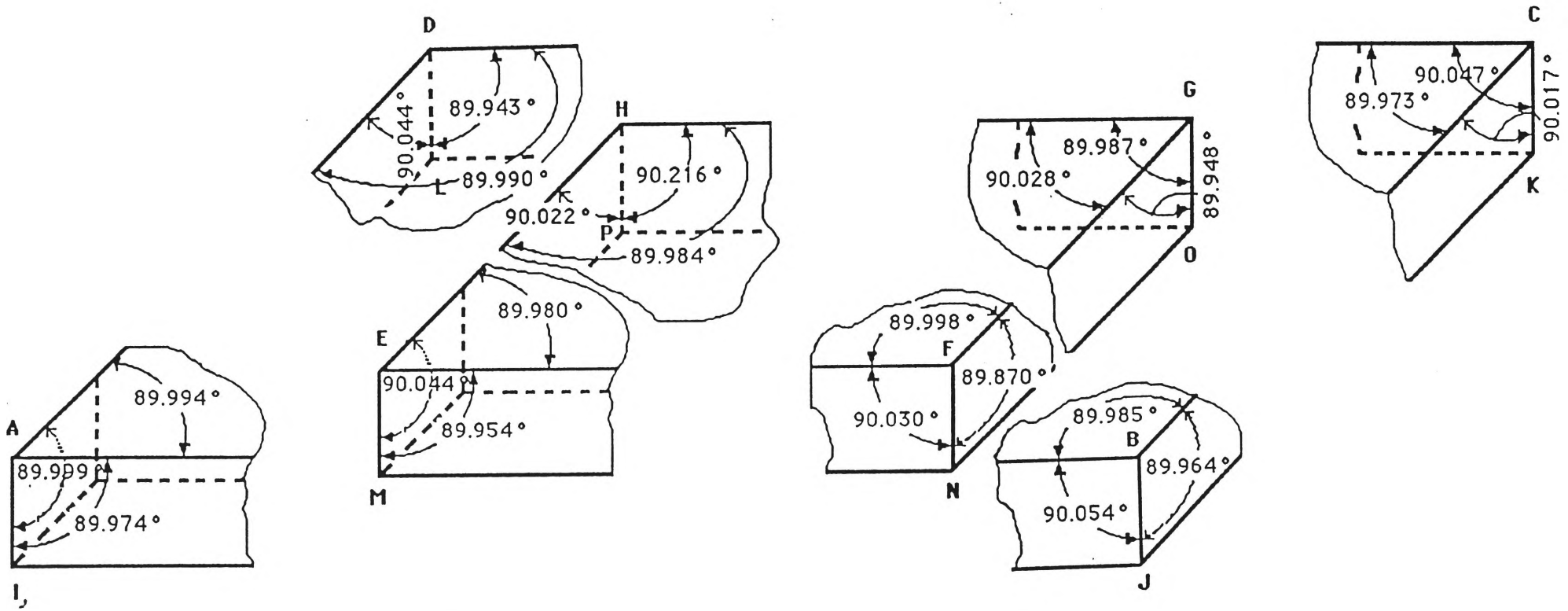

Figure 3.15 Verification of Perpendicularity of Surfaces.

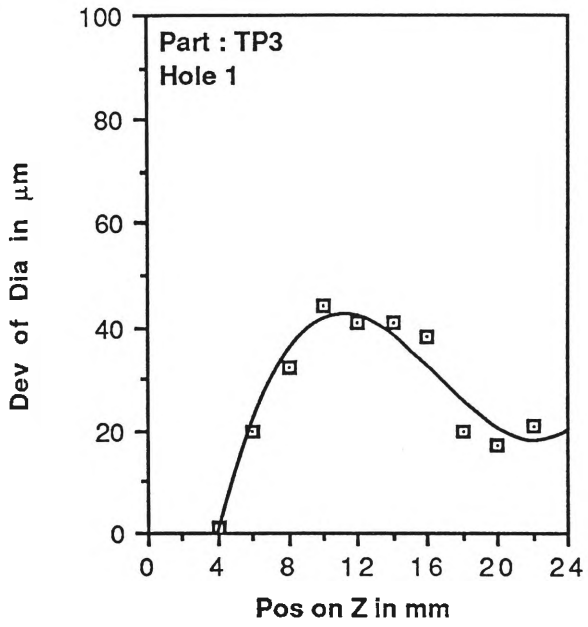

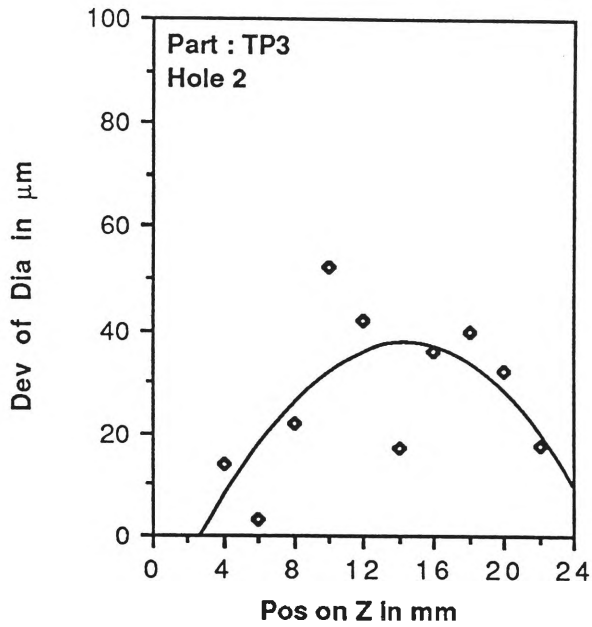

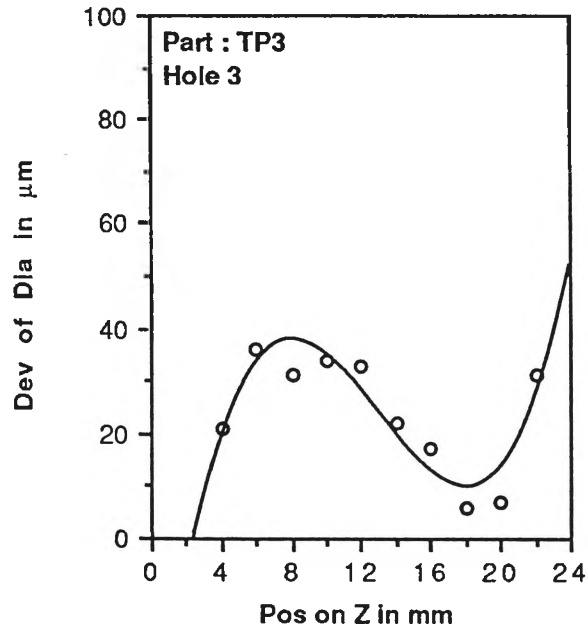

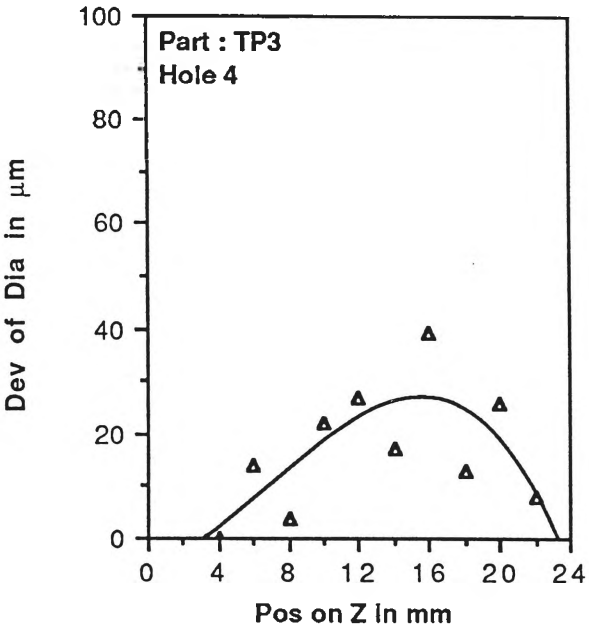

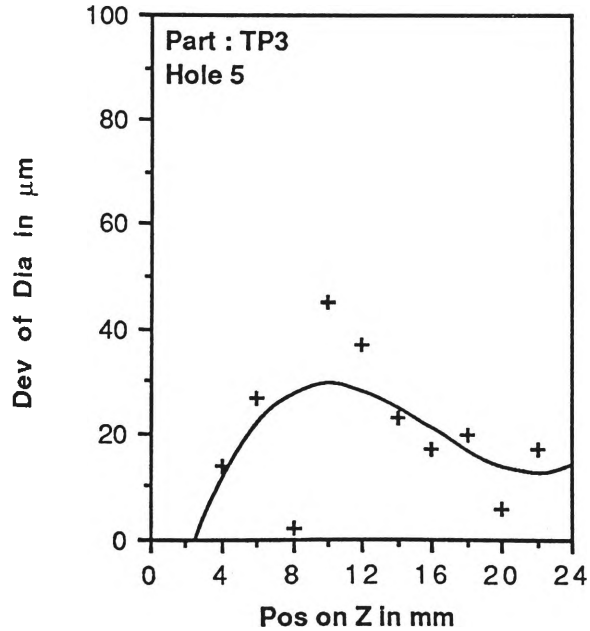

Figure 3.16.1 Variation of Diameter (Fixed Axis), Part No TP 3.

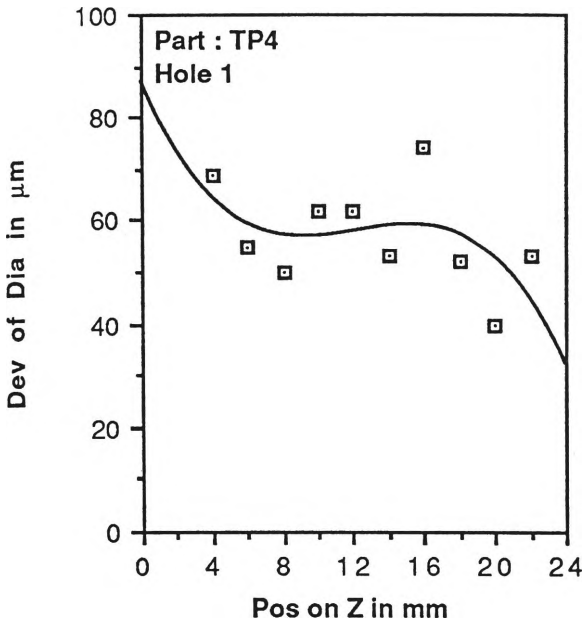

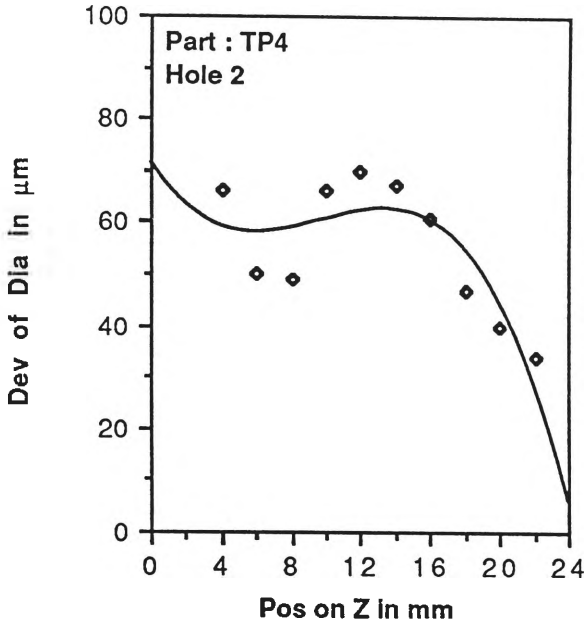

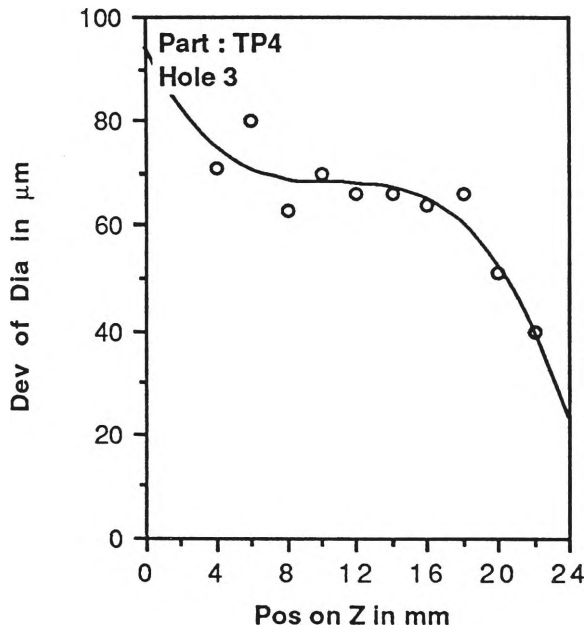

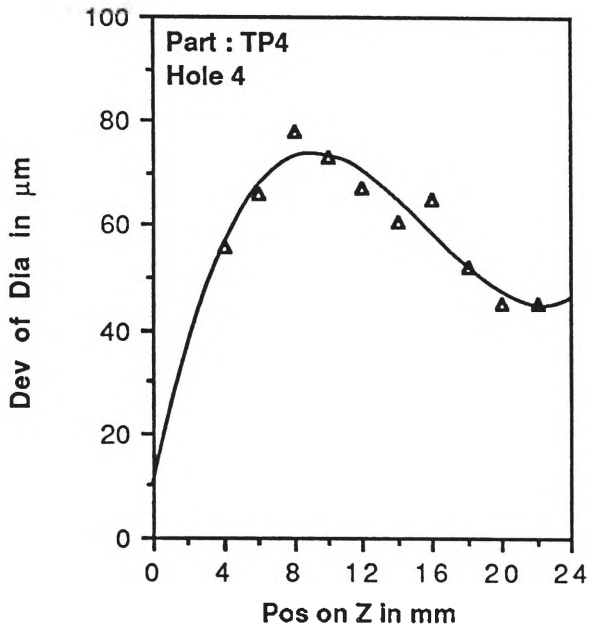

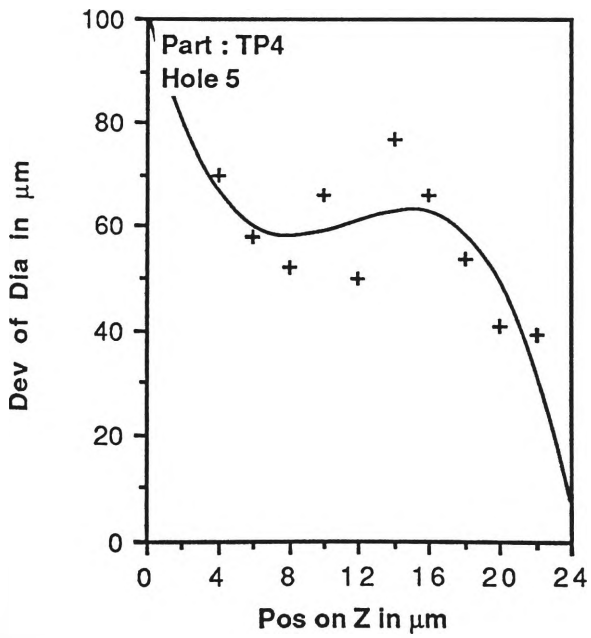

Figure 3.16.2 Variation of Diameter (Fixed Axis), Part No TP 4.

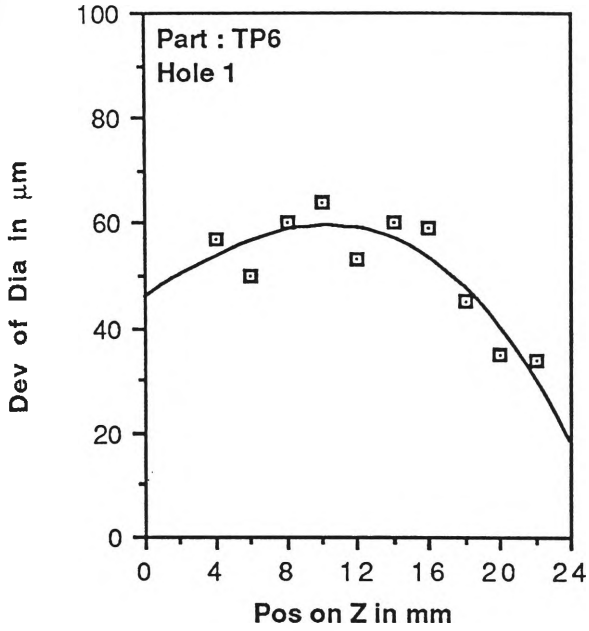

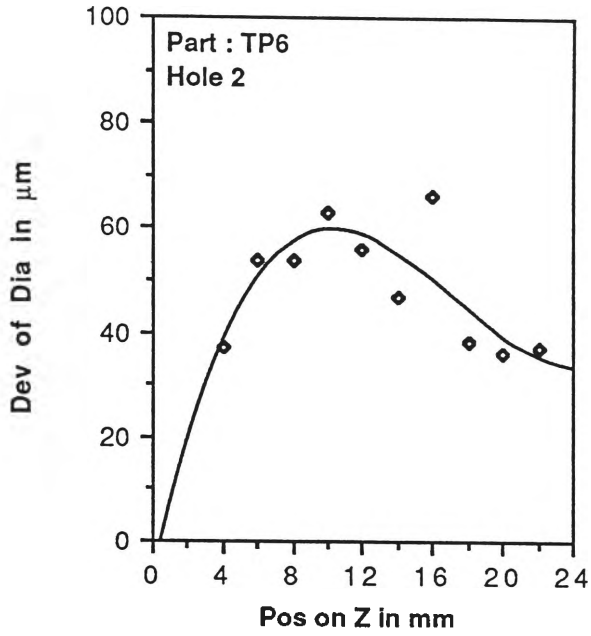

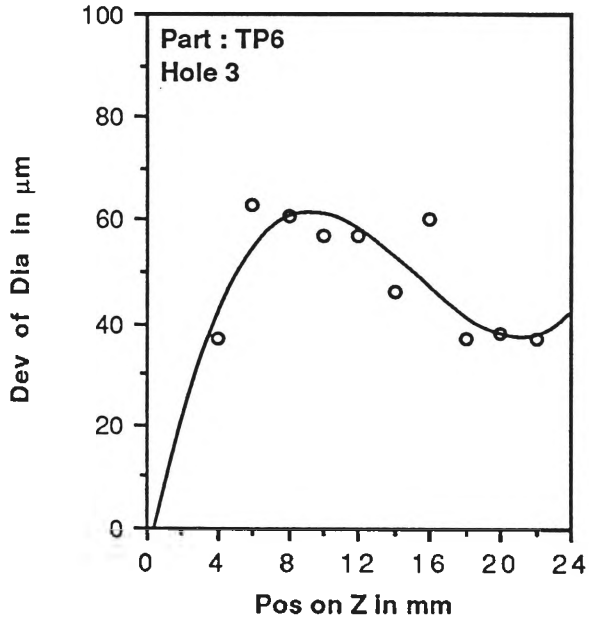

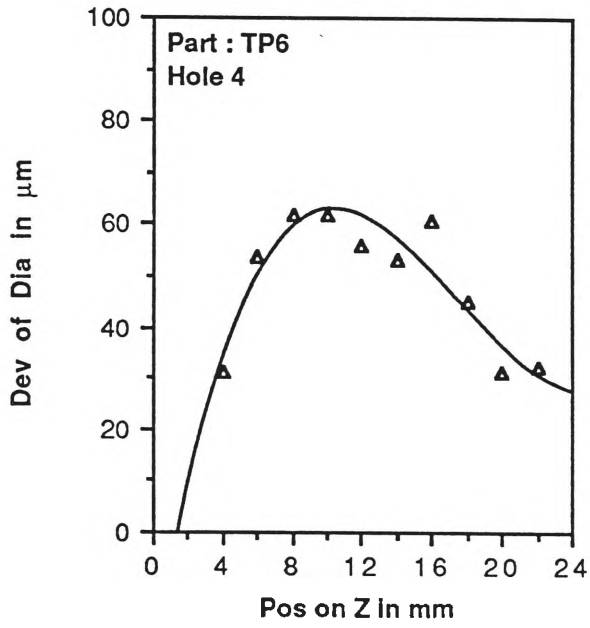

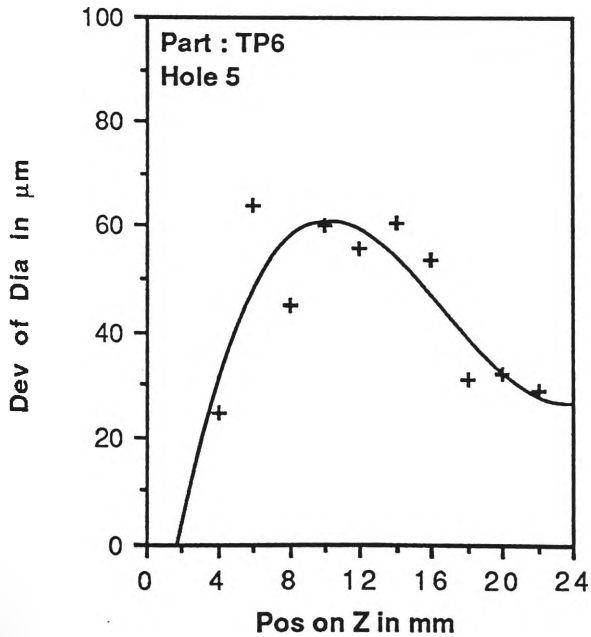

Figure 3.26.3 Variation of Diameter (Fixed Axis), Part No TP 6.

A statistical analysis of the hole dimensions (50 holes from all 10 test piece) each with ten readings was made. Results of this analysis for some of the components are given in Table 3.3. In Table 3.3 hole oversize is given in microns. Results are fairly consistent. The average hole oversize is 48.27 μm with an average sample standard deviation 14 μm. The process capability index for hole size is 2.89.

Foster, in his paper "Geometric Tolerancing" [126] has given an example of a part, a drawing of which is given in Figure 3.17. Measurement results by Foster, in comparison with some results of the present work are given in Table 3.5. In his results we also observe the general oversizing trend of the holes. The relative errors in the present work were less. The hole diameter deviations in experiments carried out during the course of this work was smaller which gives better consistency in machining operations.

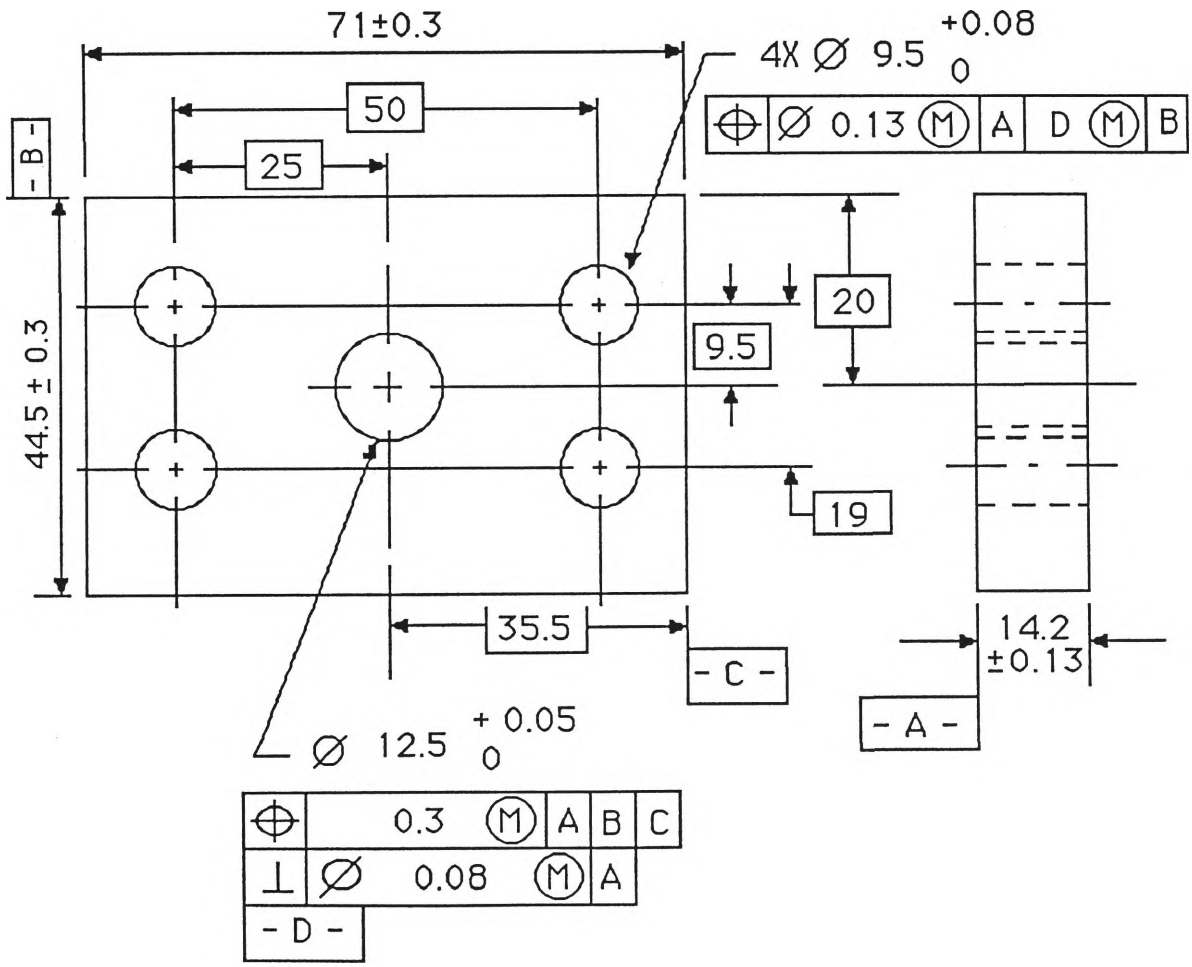

Figure 3.17 Part Drawing [126].

	TP5						TP7						TP9					
	H1	H2	H3	H4	H5	Av*	H1	H2	H3	H4	H5	Av*	H1	H2	H3	H4	H5	Av*
Average†	53	54	51	51	51	52	52	51	47	50	53	50	55	56	53	51	56	54
Standard Deviation	13	14	13	16	20	15	15	17	16	15	16	16	19	20	17	12	19	17
Range	40	41	40	50	52	45	44	47	50	49	47	47	69	68	49	34	64	57
Minimum	29	31	29	29	23	28	26	27	23	17	25	24	11	9	23	35	16	19
Maximum	69	72	69	79	75	73	70	74	73	66	72	71	80	77	72	69	80	76

† Average of ten readings frome one hole; * Average of five hole headings; All measurements are in microns.

Table 3.3 Variation in Hole Oversizing in Different Components.

	IN X	DIFFERENTIAL	IN Y	DIFFERENTIAL	HOLE SIZE	BONUS TOLERANCE	POSITION TOLERANCE
HOLE 1	25.064	(-)0.064	9.553	(-) 0.053	9.563	0.063	+ 0.13 = 0.193
HOLE 2	24.916	(+)0.084	9.462	(-)0.038	9.54	0.04	+ 0.13 = 0.17
HOLE 3	24.947	(-)0.053	9.469	(-)0.031	9.563	0.063	+ 0.13 = 0.193
HOLE 4	24.929	(-)0.071	9.518	(-)0.018	9.52	0.02	+ 0.13 = 0.15
DATUM *D*	0	—	0	—	12.538	0.038	—

Table 3.4. Measurement Results [126].

Measurement Result		Hole No.	X^D (mm)	X^M (mm)	Δ^A (mm)	Δ^R (%)
Foster [126]		Hole 1	9.500	9.563	0.063	0.663
		Hole 2	9.500	9.540	0.040	0.421
		Hole 3	9.500	9.563	0.063	0.663
		Hole 4	9.500	9.520	0.020	0.210
		Datum *D*	12.500	12.538	0.038	0.304
PRESENT WORK	TP3	Hole 1	12.000	12.026	0.026	0.217
		Hole 2	12.000	12.028	0.028	0.233
		Hole 3	12.000	12.024	0.024	0.200
		Hole 4	12.000	12.017	0.017	0.142
		Hole 5	12.000	12.021	0.021	0.175
	TP6	Hole 1	12.000	12.052	0.052	0.433
		Hole 2	12.000	12.049	0.049	0.408
		Hole 3	12.000	12.049	0.049	0.408
		Hole 4	12.000	12.049	0.049	0.408
		Hole 5	12.000	12.044	0.044	0.367
	TP8	Hole 1	12.000	12.046	0.046	0.383
		Hole 2	12.000	12.053	0.053	0.442
		Hole 3	12.000	12.053	0.053	0.442
		Hole 4	12.000	12.047	0.047	0.392
		Hole 5	12.000	12.045	0.045	0.375

Table 3.5 Measurement Results.

3.4.5 Positioning

The positioning of the tool at the desired location is a difficult task. Positioning errors are generally caused by geometric inaccuracies of the machine tool components. Calibration of the machine is the best way to reduce this kind of error. The centre of the holes were calculated by probing 8 points on each hole at fixed height. Deviations of the centre of the holes in X and Y axis for different heights are given in Figure 3.18 and Figure 3.19. In all cases the positioning errors in X and Y direction were negative. This would mean that, if a cartesian co-ordinate system is drawn on each designed centre of the holes, the real centre would lie in the third quadrant in all cases. Overcut of the sides could have been the most likely cause, since the overcut of sides would result in the shifting of the secondary and tertiary datum planes and hence the origin of the co-ordinate system. But the overcut of the sides may not alone be responsible for this inaccuracy, due to irregularities (or non constancy) of the shifting with respect to each measurement* . Moreover from Figures 3.18 and 3.19 it can be seen that with increase in hole numbers the positioning error along X axis increases whereas along Y axis no such trend is observed. The holes were drilled in such a way that initially the tool moves to Y 37.5 mm to reach the hole centre line and then moves only along X axis (see Figure D.4). The reason for increasing positioning errors along X axis is, the positioning error of the machine tool along any axis is proportional to the distance traveled. The author's view is that the likely cause for the shift of the centre of the holes is, a combination of both, positioning error of the tool, and the shifting of the datum planes due to overcut of the sides of the test component.

The change of the position error (position tolerance) vector with height (Z) was studied. The magnitude of position tolerance vector was calculated using the following formula [15]:

$$T_p = 2.\sqrt{D_x^2 + D_y^2} \tag{3.5}$$

* For details see Equation.(7.48) and subsequent explanation in Chapter 7.

where

T_p = position tolerance (mm)

D_x = X - co-ordinate deviation (mm)

D_y = Y - co-ordinate deviation (mm)

The position error (tolerance) variation with height measured is given in Figure 3.20. In general, among the holes machined on any workpiece a tendency of increasing position error is noticed for holes machined later (within same component). The angular deviation is given in Figure 3.21. Only a slight variation in angular deviation is noticed.

We can apply GD & T to verify our test components and to find whether they satisfy the position tolerances specified in the drawing. For assembly operations, the verification of position tolerances is of particular importance and requires careful considerations. The position tolerances are used to restrict the variations in the location of a feature about its exact true position, with respect to the datum surfaces. For holes, the position tolerance indicates the diameter of a cylinder within which the axis of the hole must lie. It is to be noted that at least two features, one of which is a size feature, are required for position tolerancing. In our drawing of the test component (see Figure 3.4), the MMC principle was applied. This facilitates the function or the interchangeability of mating parts. Foster [127] points out, "The use of the position concept in conjunction with the maximum material condition concept provides some of the major advantages of the geometric tolerancing system."

In practice three methods are generally used to verify the position tolerance. They are:

(i) Functional Gauge

(ii) Graphical Analysis

(iii) Mathematical Analysis

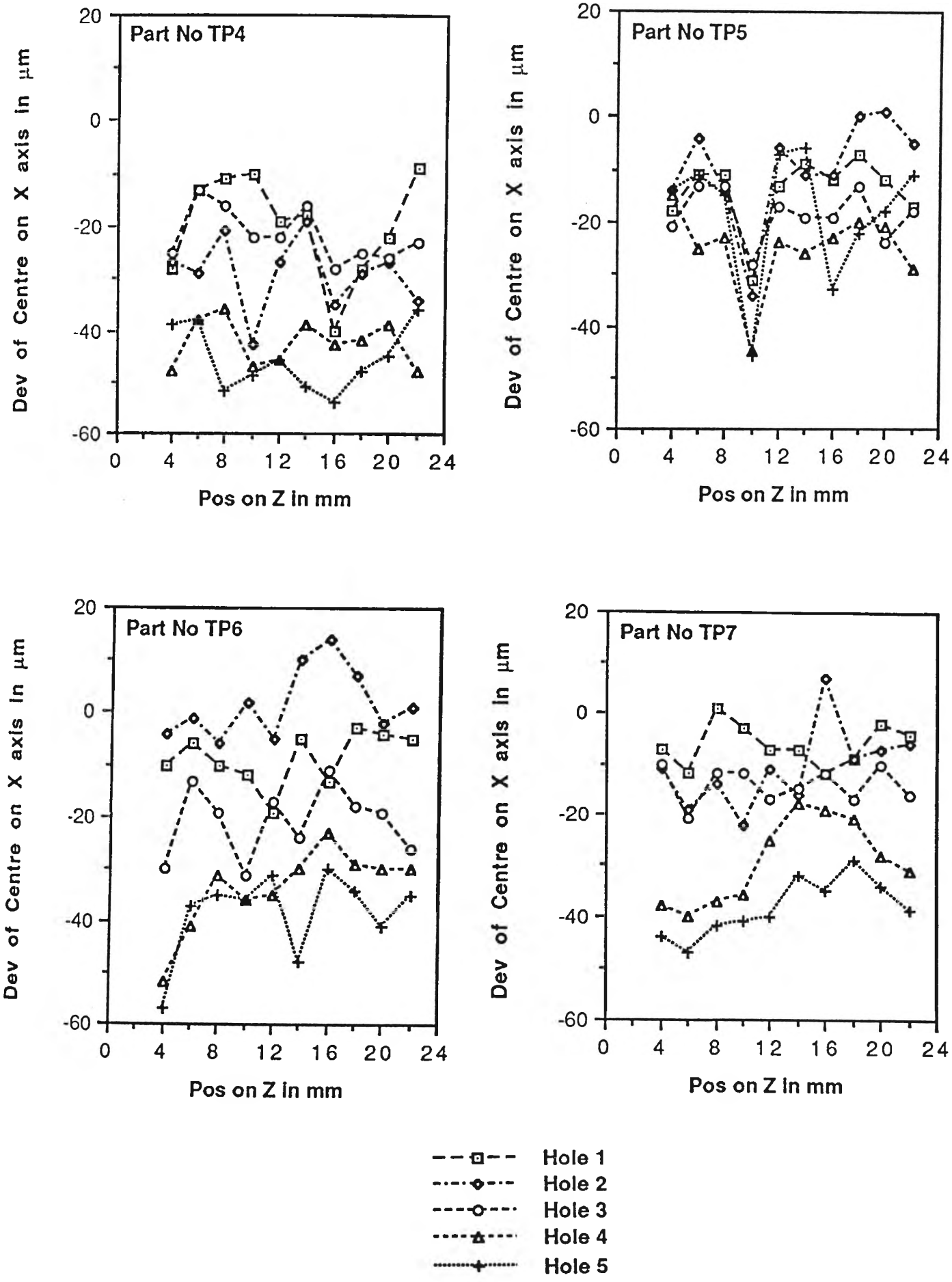

Figure 3.18 Deviation of Centre on X axis.

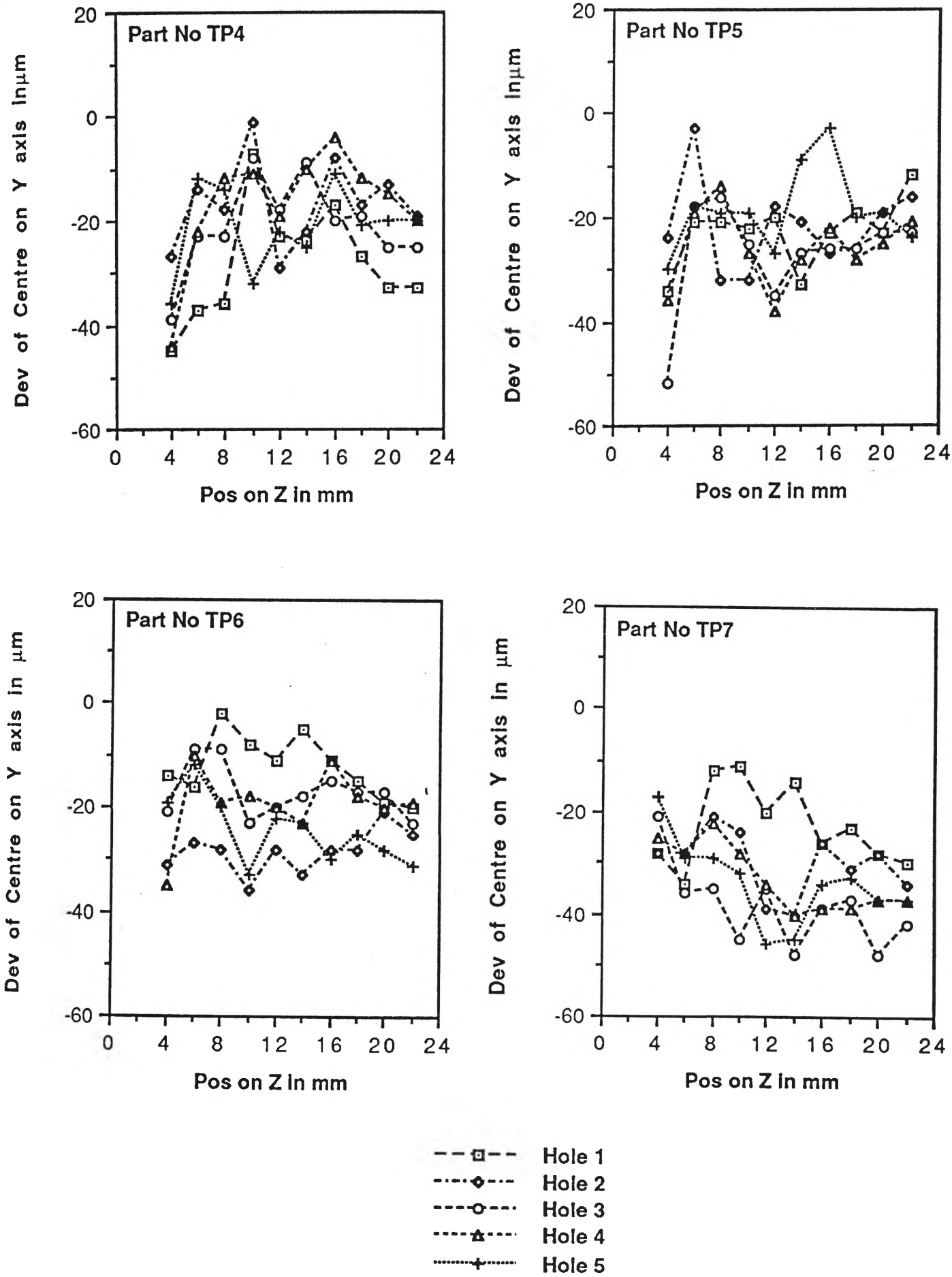

Figure 3.19 Deviation of Centre on Y axis.

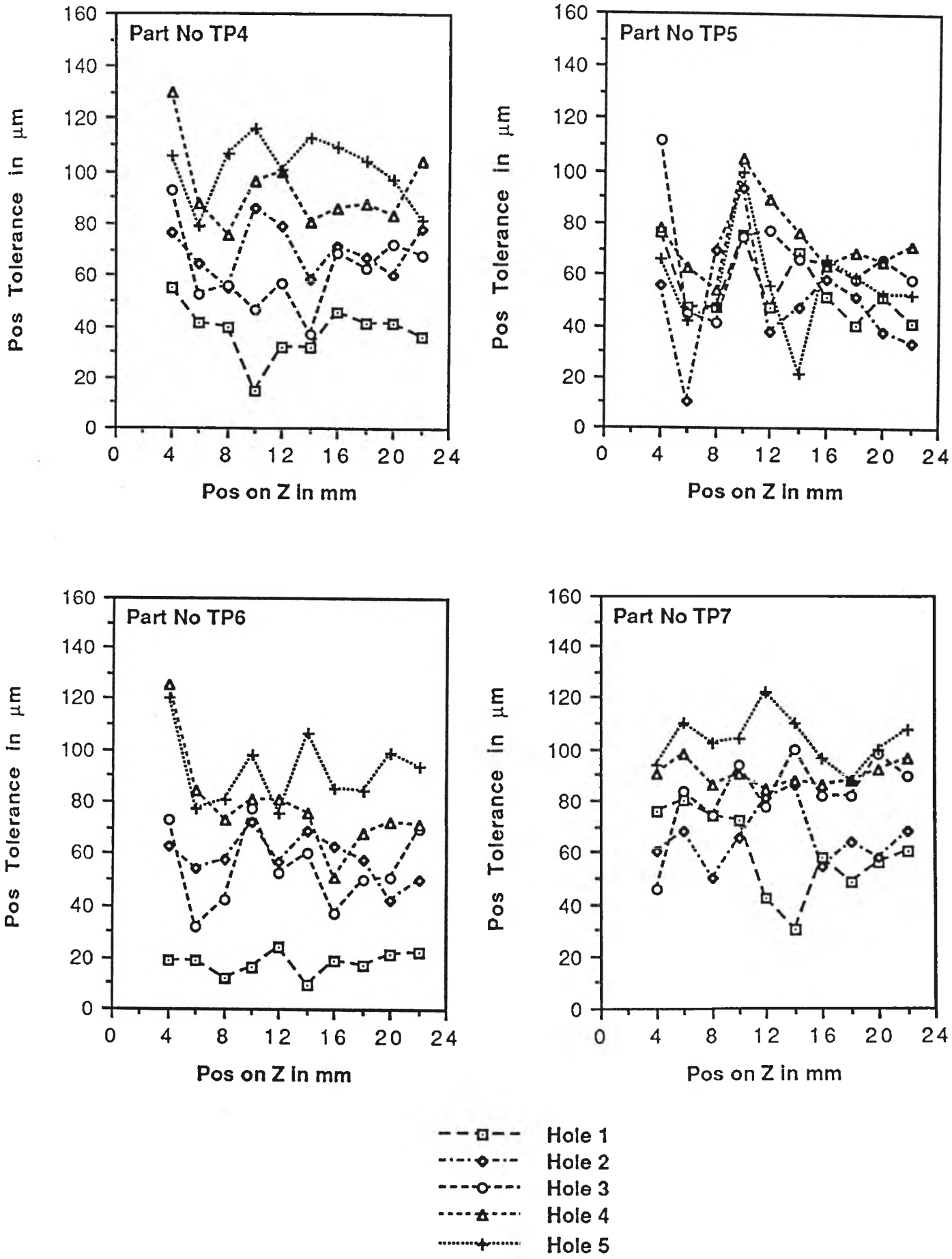

Figure 3.20 Verification of Position Tolerance.

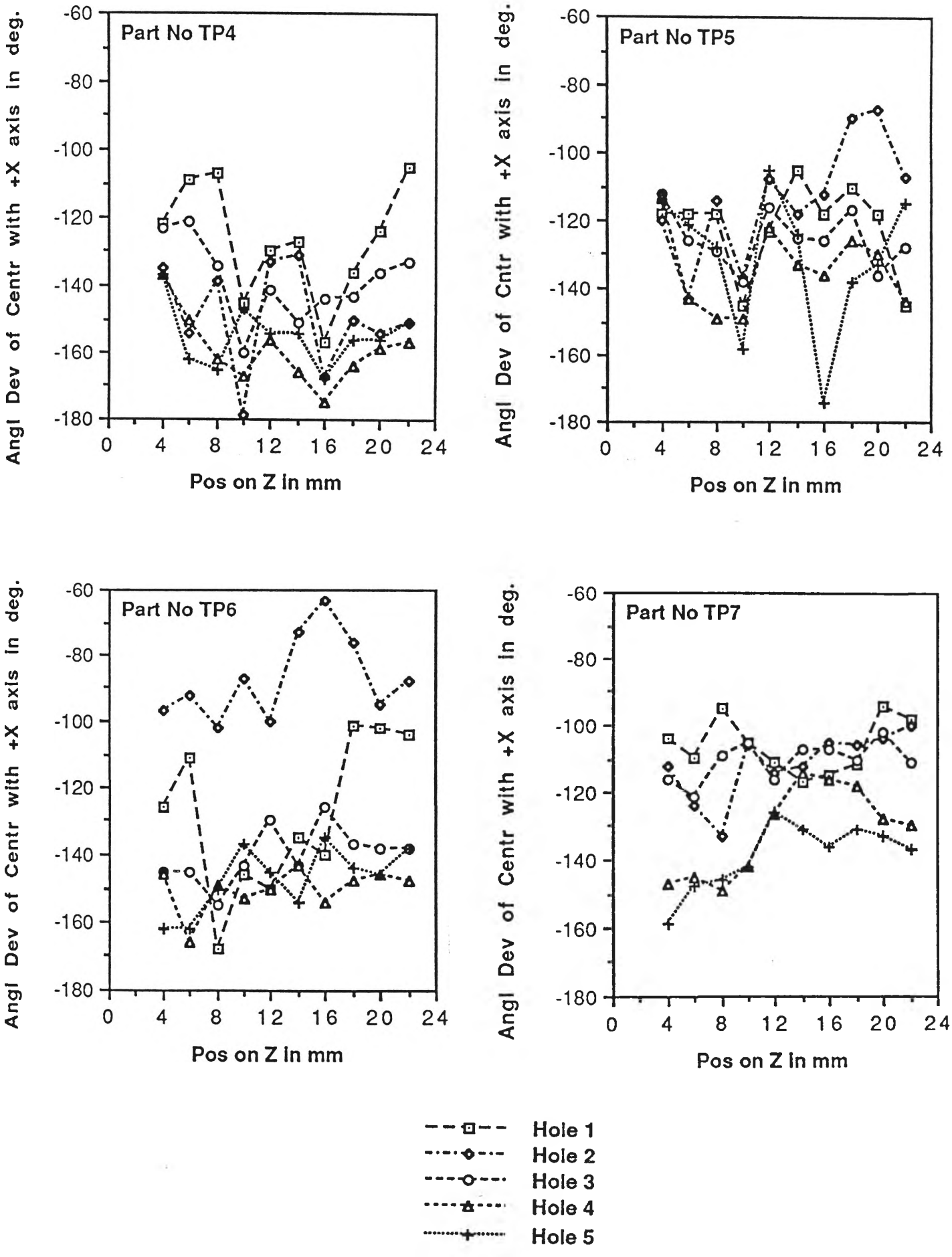

Figure 3.21 Angular Deviation of Centre of the Holes with + X axis.

(i) FUNCTIONAL GAUGE

Functional gauging techniques have been used in industry for many years. A functional gauge is a simulated master mating part at its worst condition. Simple GO or NOT-GO attributes are sufficient for verification. Although in the past, it was usually applied to measure a single dimension, this technique can be used for the verification of position tolerances also.

A functional gauge has the following advantages:

- Minimizes time and resources involved in verifying parts.
- Ensures the assembly operation, as it never accepts a 'bad' part.
- Provides a 'hard' tool which can be utilized by anyone with reasonable technical skills and does not require a highly skilled inspector.
- Represents functional interface of the concerned features.

Some of the disadvantages of a functional gauge are:

- Requires gauge-maker's tolerance taken from piece part tolerances (up to 10% usually).
- Could reject borderline parts.
- Does not quantify results (it is GO or NOT-GO).
- Must be reworked if the part is revised.

This method of verification is not used in this thesis work due to small numbers of parts involved and due to the availability of other more convenient methods.

(ii) GRAPHICAL ANALYSIS

Graphical inspection analysis (often called "paper gauging") permits the inspector to physically see what the tolerance zones look like. It provides the benefit of functional gauging without the expense and time required to design and manufacture a close-toleranced, hardened-metal functional gauge. Graphical inspection analysis is primarily suited for inspecting a small number of parts, but can also be used for large quantities. Graphical analysis simulates a physical functional gauge check, and it provides quantified results rather than the GO or NOT-GO attributes of a functional gauge.

Let us consider our test piece TP6 measurement, results of which are given in Table 3.6. For each hole, the deviations of the centre in X and Y axes are plotted on a graph (Figure 3.22). The basic dimensions of the point are assumed as zero in the co-ordinate system chosen. An overlay chart (gauge) of tracing paper or any other transparent material containing a series of graph-scale circles of desired increments (representing the tolerance zones) is placed over the graph to coincide with the hole's true position. If all the holes lie within the respective tolerance zones (including bonus tolerances), the part is graphically accepted. In our case all the holes lie within the respective tolerance zones, so the component is acceptable according to the tolerance zones specified in the drawing.

(iii) MATHEMATICAL ANALYSIS

Mathematical verification of the actual locations of the holes can be performed by using a calculator or computer programmes, as per Equation (3.5). The mathematical method can by-pass both the use of a functional gauge and the graphic analysis, due to its greater accuracy. In fact the accuracy of mathematicals method depends on the accuracy of the CMM measurements. Nowadays, many CMMs are equipped with standard computer programmes to perform such translations.

FEATURE NUMBER	FEATURE LOCATION						FEATURE SIZE (mm)			POSITION TOLERANCE (mm)			
	X AXIS (mm)			Y AXIS (mm)									
	Specified	Actual	Deviation	Specified	Actual	Deviation	Specified MMC size	Actual	Deviation	Material Condition	Specified	Bonus	Total
HOLE 1	40.000	39.995	-0.005	37.500	37.480	-0.020	11.950	12.034	0.084	MMC	0.250	0.084	0.334
HOLE 2	70.000	69.998	-0.002	37.500	37.479	-0.021	11.950	12.036	0.086	MMC	0.250	0.086	0.336
HOLE 3	100.000	99.974	-0.026	37.500	37.477	-0.023	11.950	12.037	0.087	MMC	0.250	0.087	0.337
HOLE 4	130.000	129.970	-0.030	37.500	37.480	-0.020	11.950	12.031	0.081	MMC	0.250	0.081	0.331
HOLE 5	160.000	159.966	-0.034	37.500	37.475	-0.025	11.950	12.031	0.081	MMC	0.250	0.081	0.331

Table 3.6 Inspection Data.

(Part No TP6)

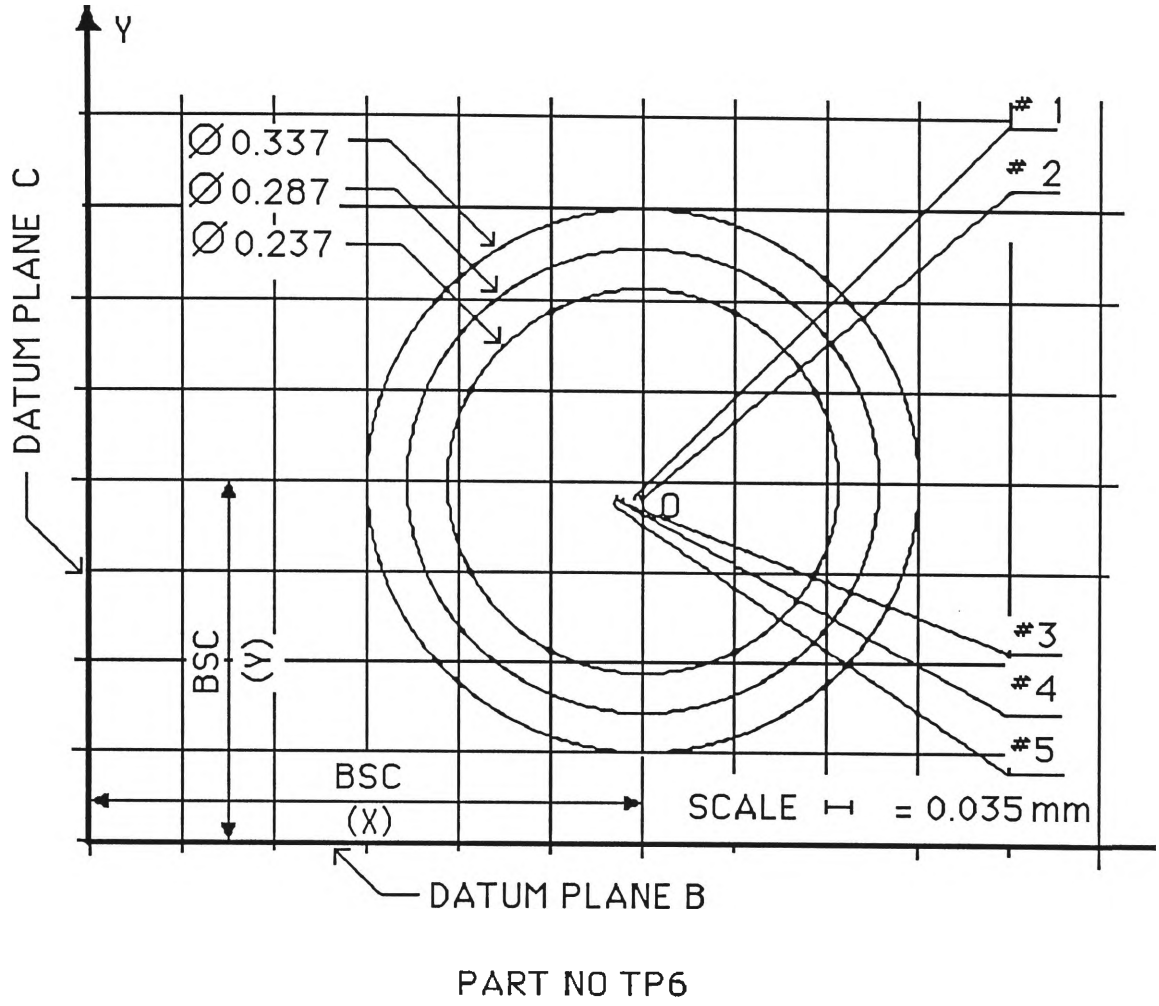

Figure 3.22 Graphical Analysis.

In our case, using Equation (3.5):

- Hole # 1 calculates to = ϕ 0.04123 mm. Hole # 1 is good (less than 0.250 mm).
- Hole # 2 calculates to = ϕ 0.04219 mm. Hole # 2 is good (less than 0.250 mm).
- Hole # 3 calculates to = ϕ 0.06943 mm. Hole # 3 is good (less than 0.250 mm).
- Hole # 4 calculates to = ϕ 0.07211 mm. Hole # 4 is good (less than 0.250 mm).
- Hole # 5 calculates to = ϕ 0.08440 mm. Hole # 5 is good (less than 0.250 mm).

It should be noted that when MMC is used and holes are oversized, bonus tolerance should be added to the specified tolerance and if necessary, a comparison should be made with the total tolerance, where total tolerance = specified tolerance + bonus tolerance.

3.4.6 Cylindricity Verification

(a) Circularity

For drilled holes, cylindricity is an important feature. The CMM software used is not capable of providing facilities for a complete cylindricity study. Therefore, the evaluation of cylindricity was done by tracing the circularity at different horizontal sections (i.e. at different heights) and relating these with the straightness (and perpendicularity) of the axis. The shape variations were studied with different holes keeping Z = constant. 60 points were probed for each hole. Taking the designed centre of the hole as origin, probed points were plotted in polar co-ordinates (Figure 3.23). Results show continuity of the points with the exception of a few. This may be due to poor surface finish. From the figure, the shift of the centre is clear. Results show good consistency of the drilling operation. No significant change of the shape is noted, but the oversize of the holes are confirmed.

(b) Perpendicularity of the Axis

Perpendicularity of the axis of each hole was studied separately. We have seen variations in diameter at different heights. We have also seen the change in positions of the centre of the holes for the same heights. Combining these two sets of results, the real shape of the hole in vertical planes (XZ and YZ) were plotted (Figure 3.24 and Figure 3.25). In Figure 3.24 deviation of centre and diameter of holes with same location in four different components are shown, and in Figure 3.25 deviation of centres and diameter of holes in same component are shown. From these figures the actual deviations from the originally intended shapes of the holes (drawn in dotted lines in Figure 3.24 and Figure 3.25), can be clearly seen.

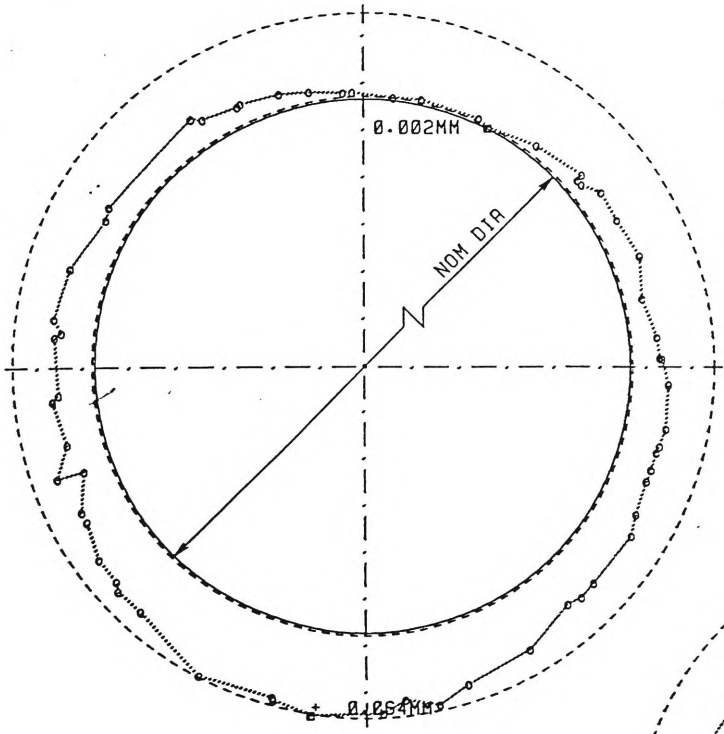

PART No : TP11

Hole 1

Z = 18 mm

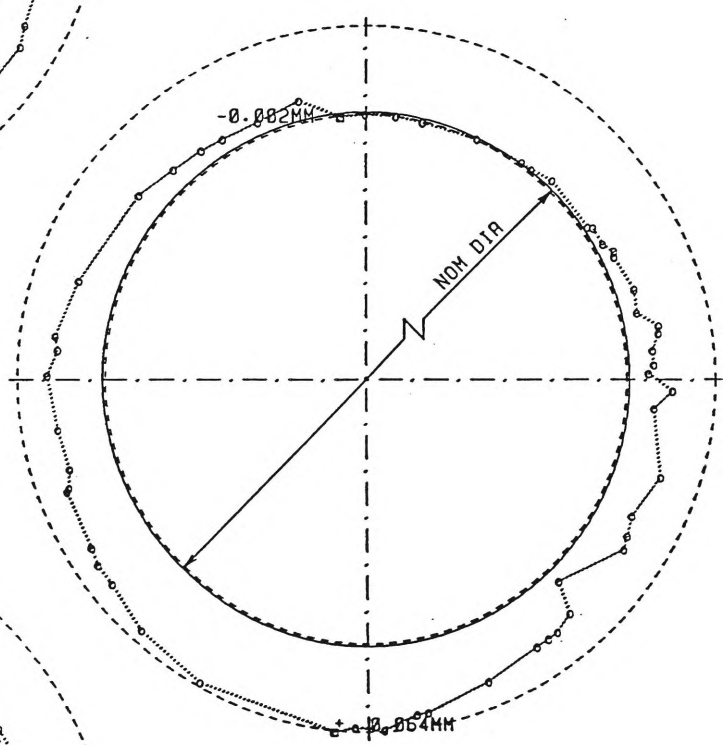

PART No : TP11

Hole 2

Z = 18 mm

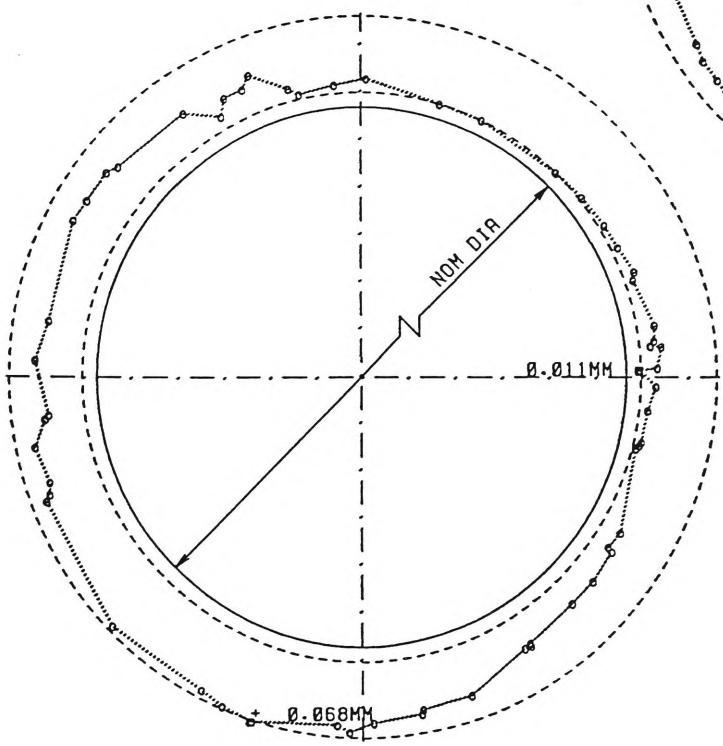

PART No : TP11

Hole 3

Z = 18 mm

Figure 3.23 Circularity Verification.

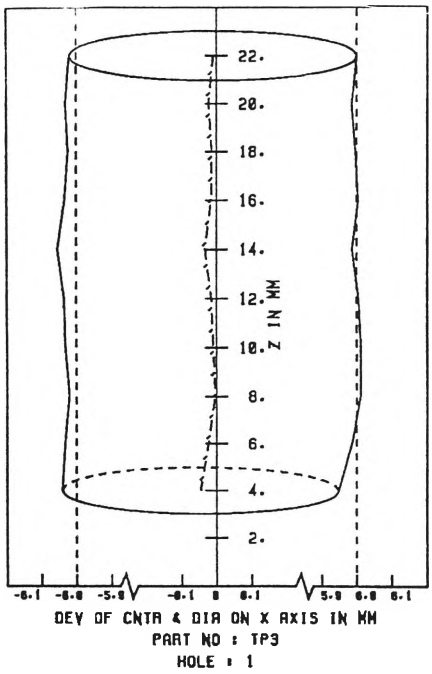

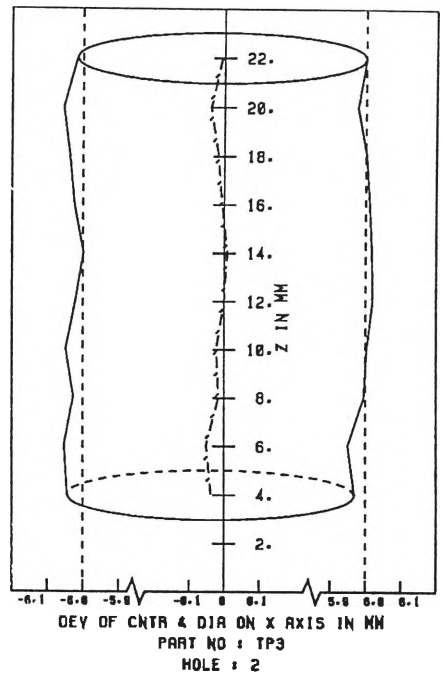

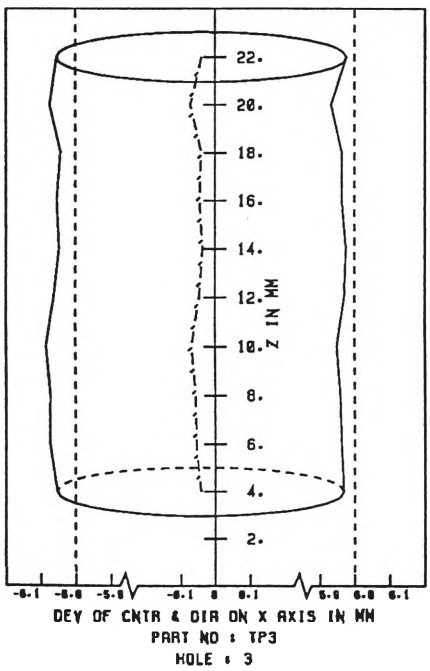

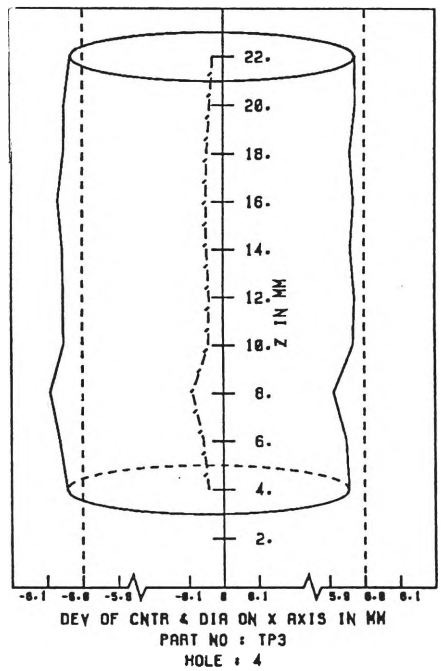

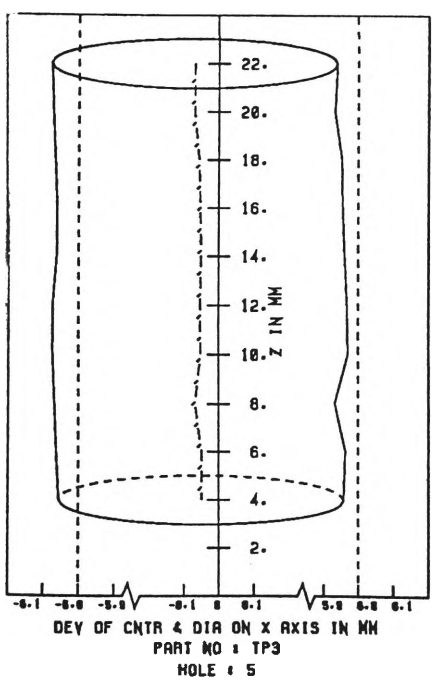

Figure 3.24.1 Deviation of Centre and Diameter (Floating Axis) for Different Holes in One Component on X axis.

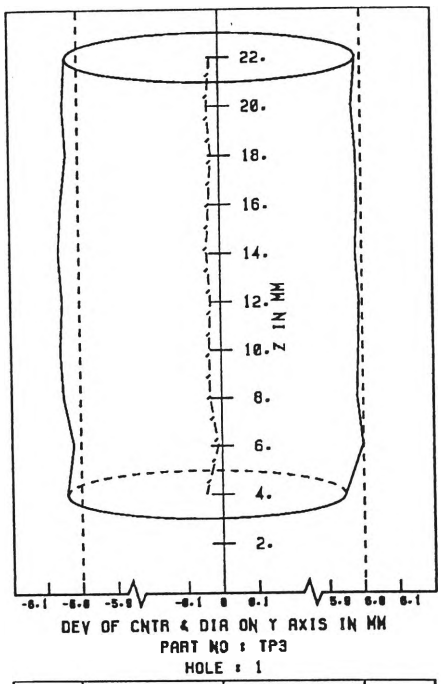

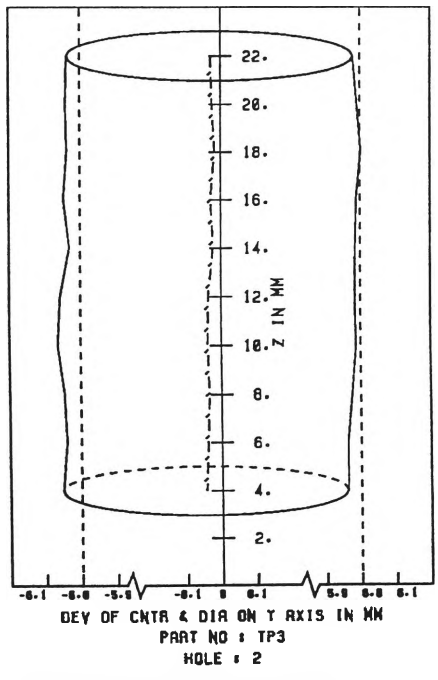

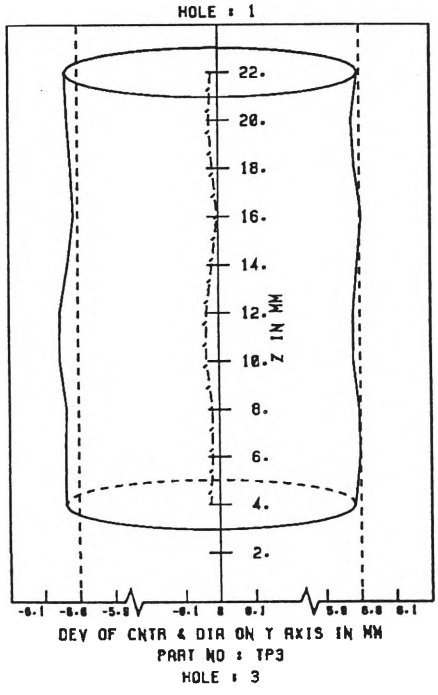

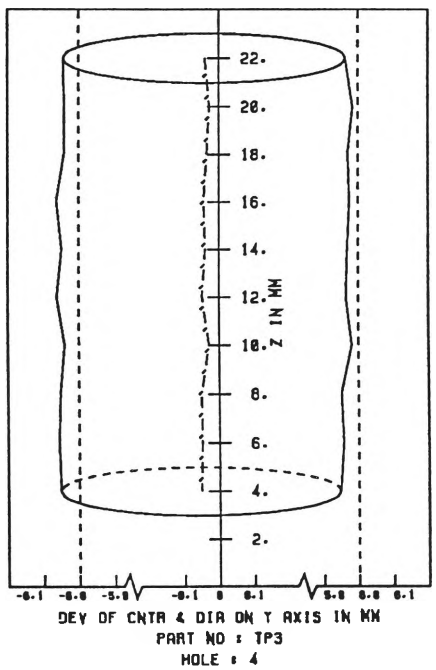

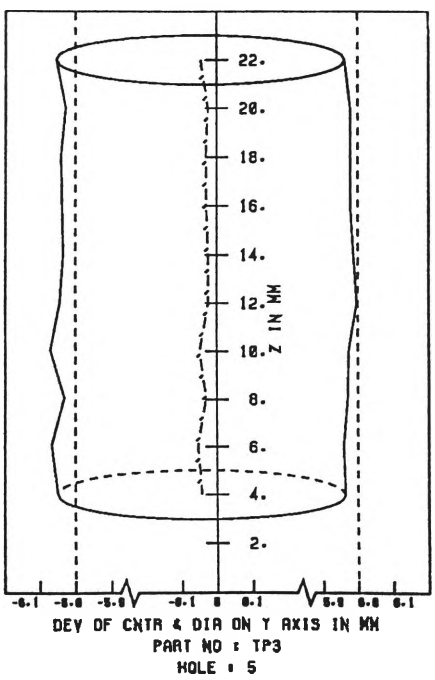

Figure 3.24.2 Deviation of Centre and Diameter (Floating Axis) for Different Holes in One Component on Y axis.

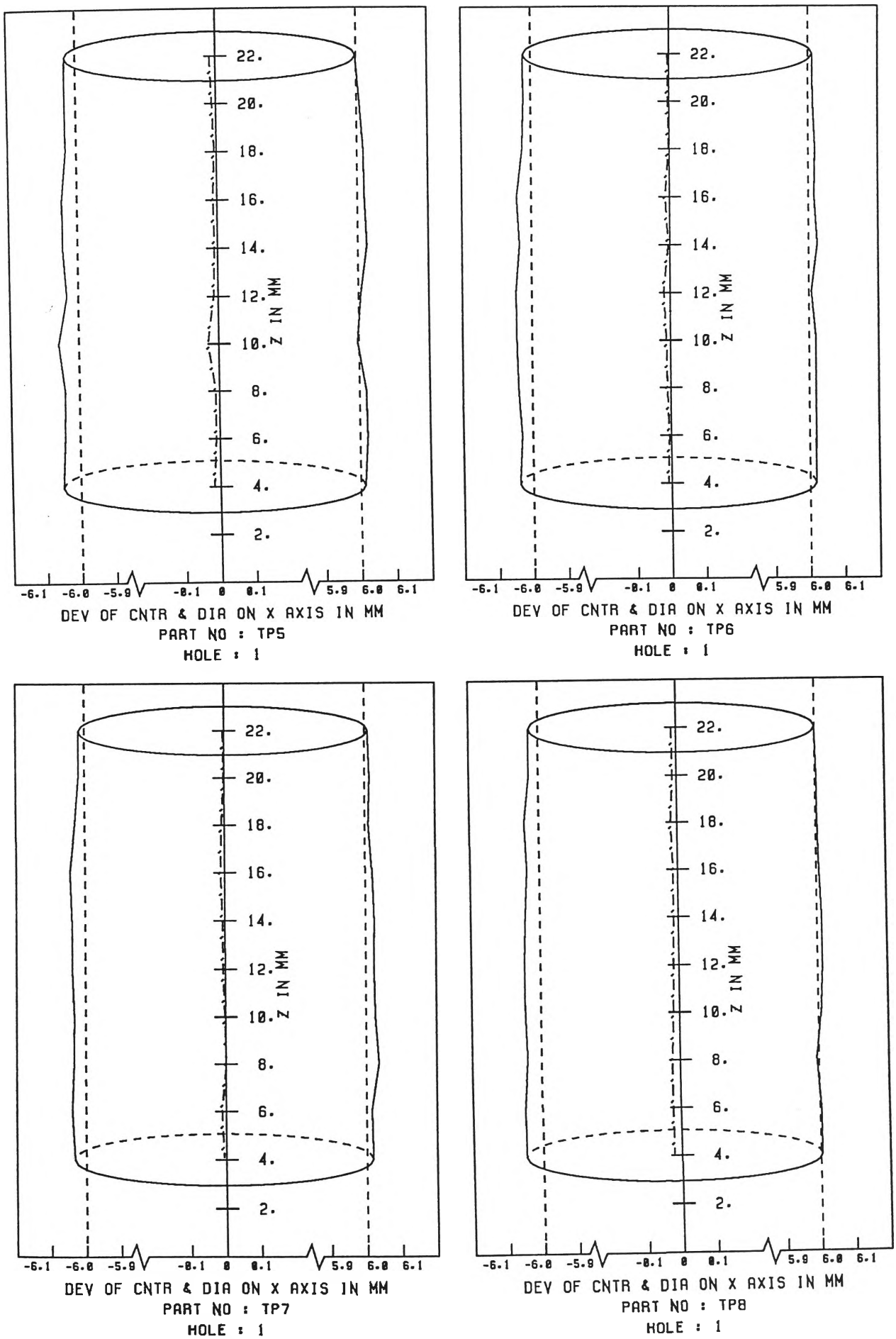

Figure 3.25.1 Deviation of Centre and Diameter (Floating Axis) for One Hole in Different Components on X axis

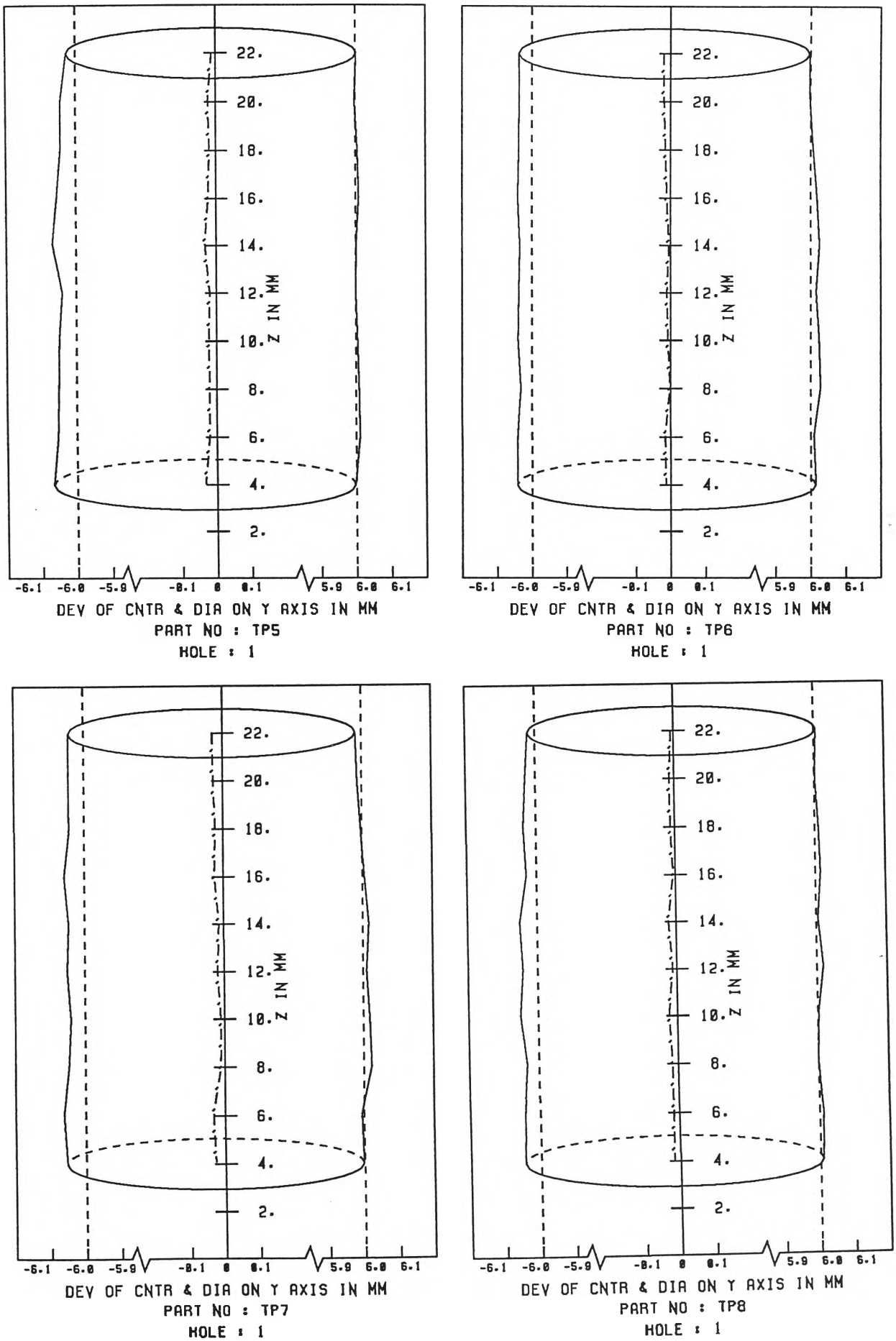

Figure 3.25.2 Deviation of Centre and Diameter (Floating Axis) for One Hole in different Components on Y axis.

3.4.7. Effect of Drilling Canned Cycle on Hole Accuracy

While considering the hole accuracy, all types of checking stated in previous sections can be applied. But due to the varied nature of the different drilling canned cycles the most likely difference expected is in hole size variation. So in this section results are analysed on the basis of this specific aspect only.

Measurement results for hole oversize are given in Table 3.7* and the changes of hole diameters at different heights are shown in Figure 3.26. No significant change in the shape of the holes is observed. This suggests that the oversize and barreling effect are caused during drill penetration (most probably due to drill deflection) and not during drill withdrawal. The average diameter of the holes drilled using G81 is considerably higher than those drilled using G83 and G73. This fact also supports the view that the drill deflection is responsible for hole oversize, because during spot drilling canned cycle drill deflection is expected to be highest. In Table 3.7 average values, minimum and maximum values of oversize are all included, because depending on material conditions used (i.e. MMC, LMC, etc), these values may be used as dimensions of the holes.

3.5 Discussions

In previous sections of this Chapter we have seen that even for a very simple component so many types of machining errors can occur. Needless to mention that with increasing complexity of the part these errors also increase. Here it should be mentioned that in practice all these described checks are not necessary and only those checks which are required by the function of the part should be done . Prior knowledge of the types of error which may occur in machining is useful for error reduction (either error avoidance or error compensation).

---

* Results given in Tables 3.3 and 3.7 should not be compared with each other, as in machining tests different tools were used.

	G73						G81						G83					
	H1	H2	H3	H4	H5	Av*	H1	H2	H3	H4	H5	Av*	H1	H2	H3	H4	H5	Av*
Average†	28	32	36	50	48	39	55	56	68	56	45	56	48	48	34	42	31	41
Standard Deviation	10	9	9	15	21	13	9	8	8	15	19	12	18	13	14	10	9	13
Range	33	32	31	48	55	40	28	26	26	50	54	37	57	41	42	30	29	40
Minimum	14	12	28	21	16	18	39	40	54	33	20	37	26	32	12	29	14	23
Maximum	47	44	59	69	71	58	67	66	80	83	74	74	83	73	54	59	43	62

† Average of ten readings frome one hole; * Average of five hole headings; All measurements are in microns.

Table 3.7 Variation in Hole Oversizing in Components Machined Using Different Canned Cycles.

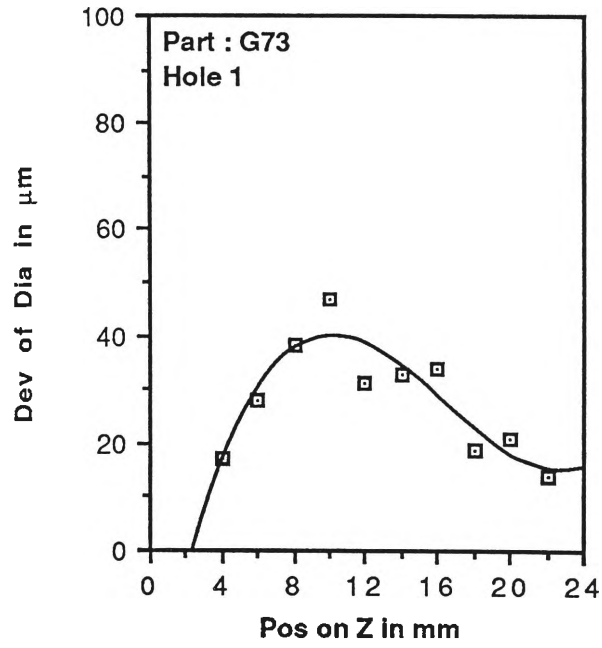

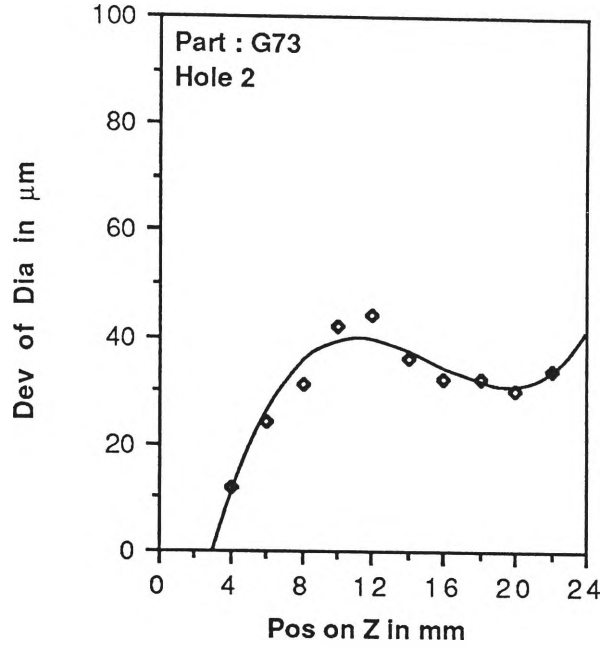

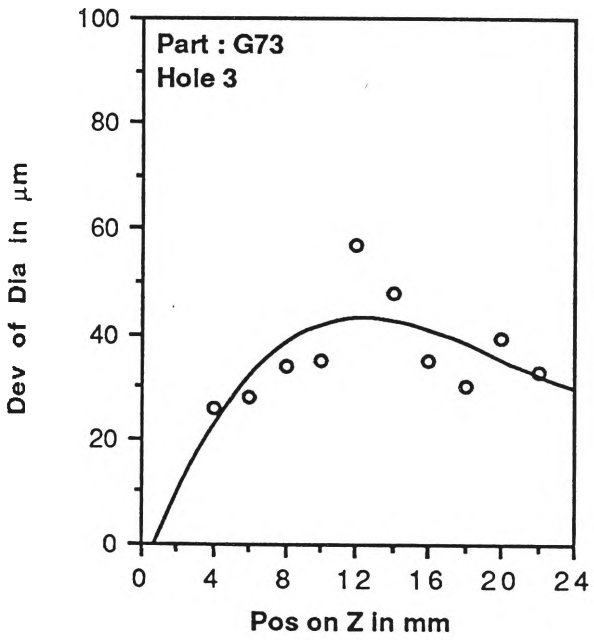

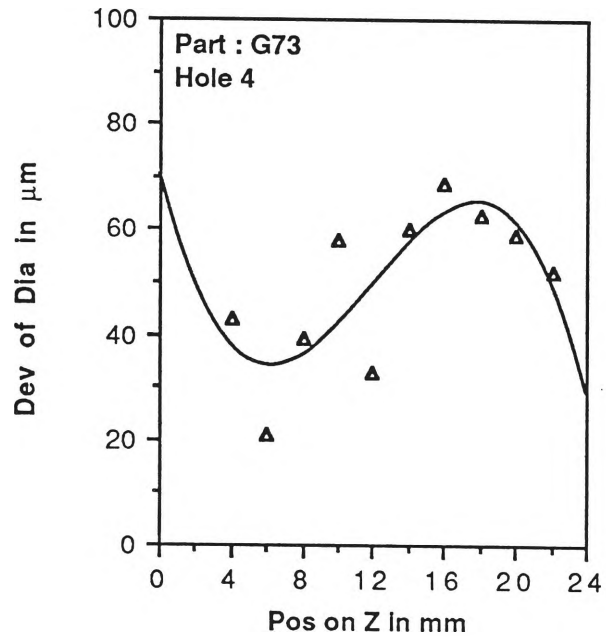

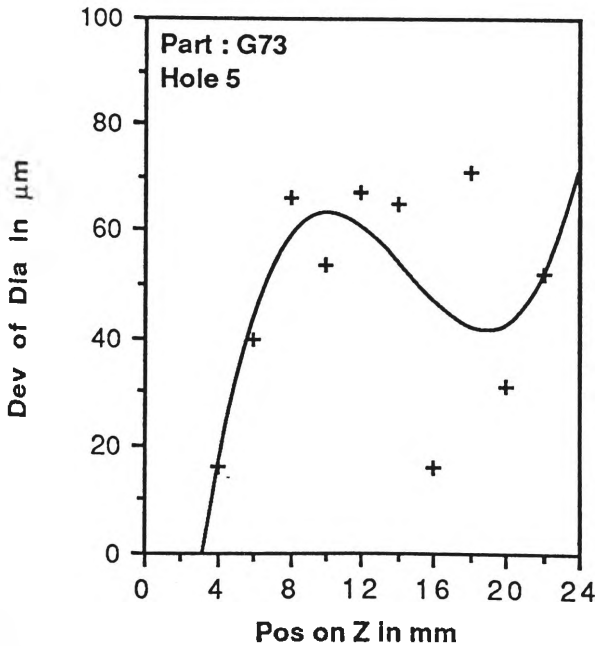

Figure 3.26.1 Variation of Diameter of Holes Drilled Using Chip Break Canned Cycle (G73).

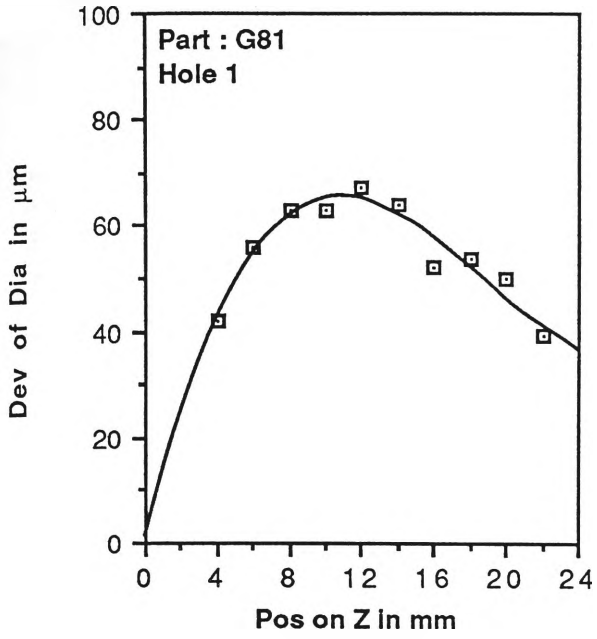

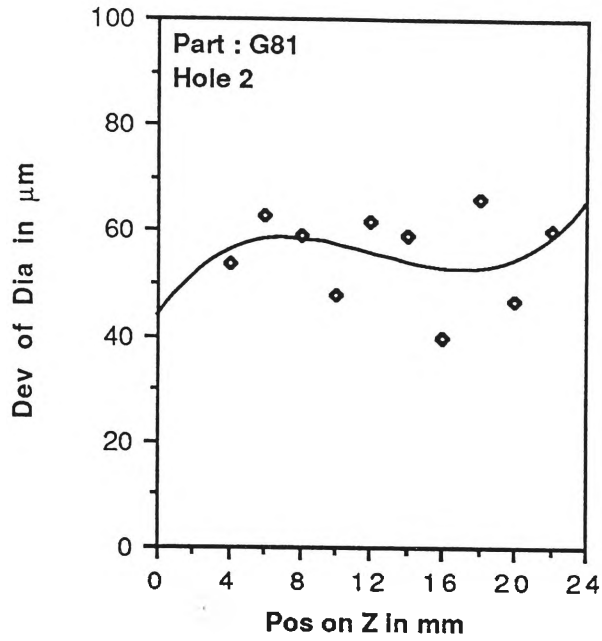

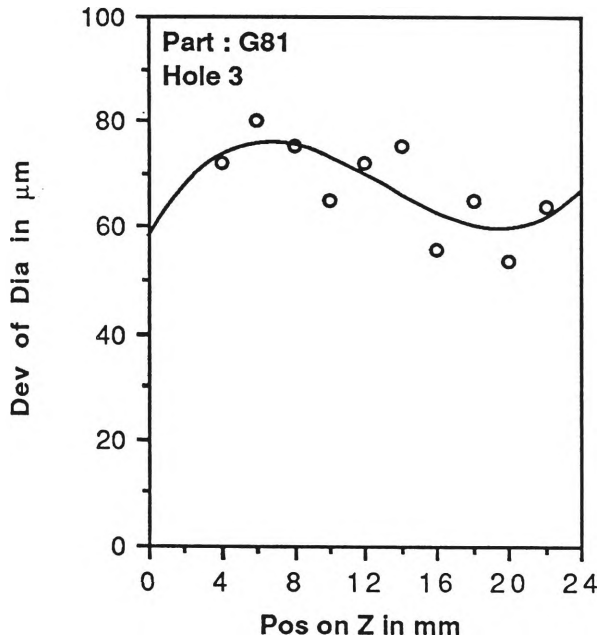

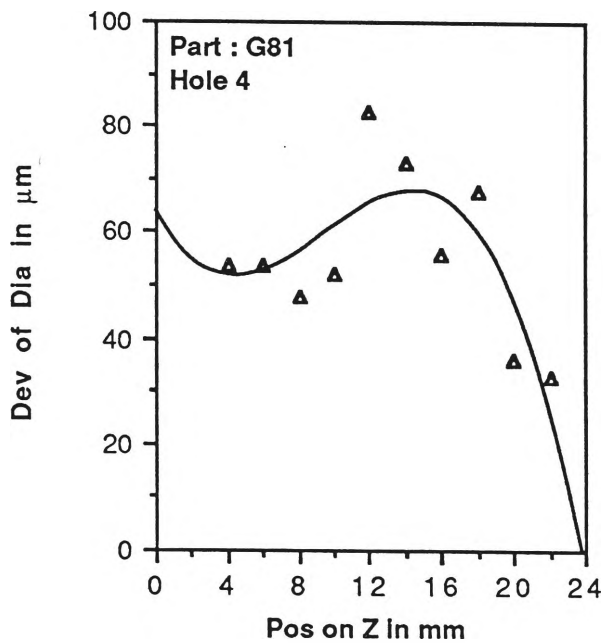

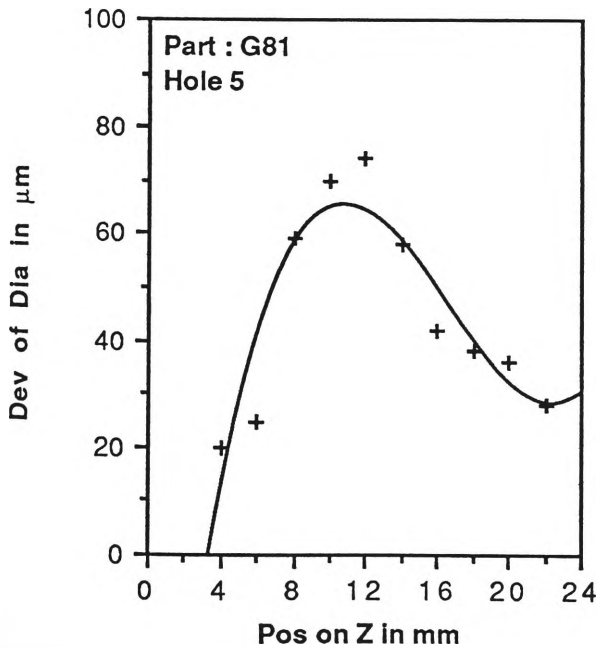

Figure 3.26.2 Variation of Diameter of Holes Drilled Using Spot Drilling Canned Cycle (G81).

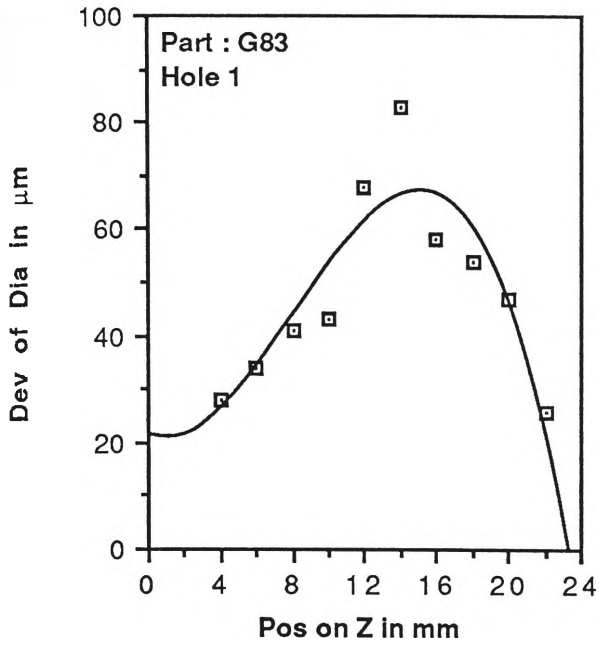

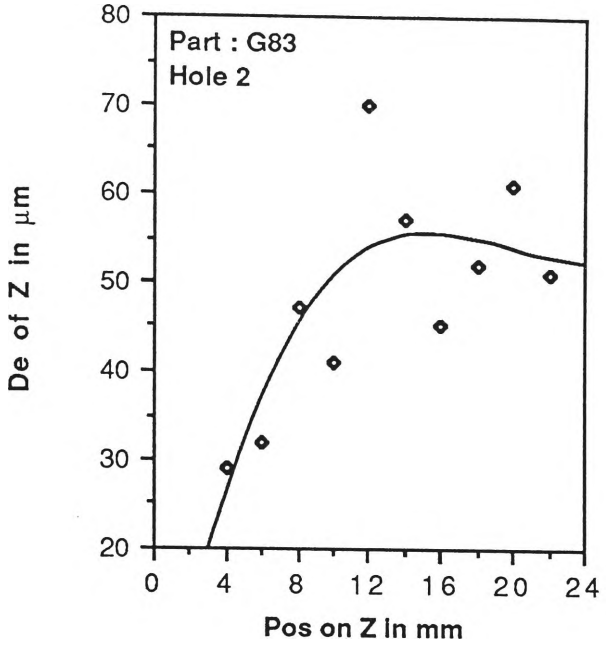

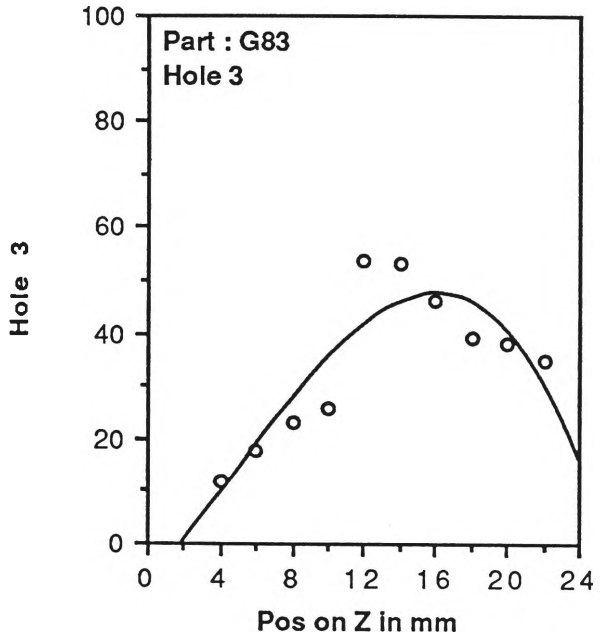

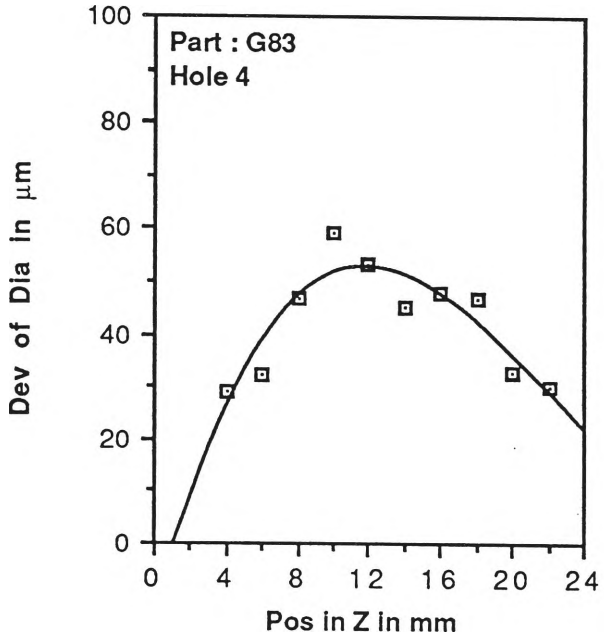

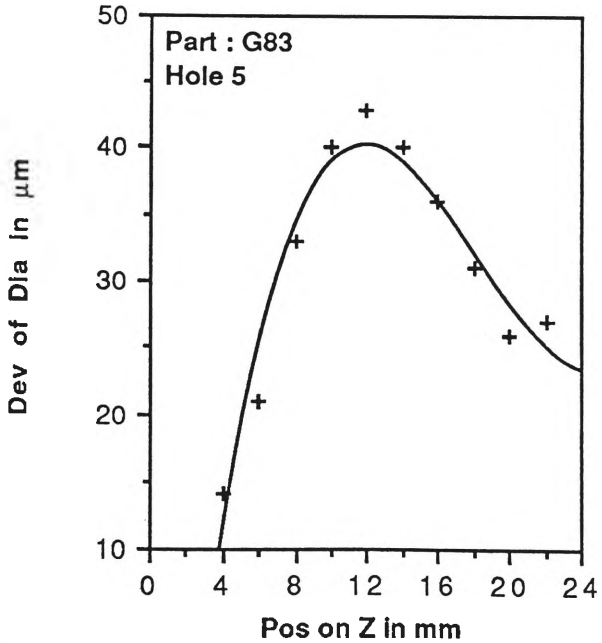

Figure 3.26.3 Variation of Diameter of Holes Drilled Using Deep Hole Canned Cycle (G83).

Tool dimensions play a major role in achieving the required machining accuracy, which is often ignored. While programming, we assume that the centre of the tool (i.e. drill, end mill, etc.) lies at a distance equal to half of the tool diameter from the edge, and accordingly, a radial compensation is made. For example, when a 16 mm end mill is used, we assume that the centre of the end mill lies 8.000 mm from the cutting surface. It would be interesting to investigate the validity of this assumption. The tool offsets and radial compensations supplied in the beginning of the programme have a great effect on machining accuracy as these figures identify the actual tool dimensions. Action should be taken to identify the actual parameters correctly. It would also be interesting to investigate the variation of tool dimensions and geometry (although these may be within the specified tolerance limits) and their effect on machining accuracy.

In end milling, tool deflection seems to be responsible for the inaccuracy of machined surfaces (flatness error). End mill deflection behaviour should be further investigated and proper action should be taken to reduce this error.

The surface finish of the machined component plays an important role in achieving high machining accuracy. While considering the machining accuracy, most authors did not look at this aspect. Surface finish aspect is not only important from the machining accuracy point of view but also from the measurement point of view (specially CMM measurement). In CMM measurements, the outcome depends on co-ordinates of the probed points, and when the surface finish is rough, there is a good chance of probing the peak points. From the pattern of measured values shown in Figure 3.23, it is clear that the if probed points were peaks, measurement results would be different. There are two ways of getting rid of this problem. One is to take more readings, which will make our measurement process lengthy, but still may not guarantee better results (only the probability of achieving better results will be higher). The other way is to improve the surface finish. The latter way seems reasonable and in future, efforts should be made to achieve better surface finish (possibly by using some finishing operations).

The use of proper cutting conditions is also significant in achieving higher accuracy. It is generally thought, higher cutting speeds will improve accuracy levels. But the idea may be proven incorrect, especially if some misalignment of the tool or vibration effect is present. Cutting fluid can also influence the accuracy of the machined components. In our CNC machining centre cutting fluid flow had to be directed manually and some problems in directing the flow were noticed when larger sized tools were used.

In the present experimental work, the centre of holes are calculated values and these values also might have been influenced by the surface finish. This means that the calculated centre may not be the point of positioning the tool. In future, some other methods should be applied to study the positioning errors. Comparisons of these results could be a new area for research.

In the experiments done so far some clear tendencies have been noticed. It is now necessary to investigate each influencing factor separately and then to combine these varying effects to reach at least a partial optimization.

3.6 Concluding Remarks

1. Tool dimensions and tool geometry play important roles in achieving high machining accuracy and a study into the variations of tool dimensions and tool geometry and their tolerances is necessary for improving machining accuracy.

2. For end milled surfaces, end mill deflection seems to be the major cause of machining error (flatness error). Therefore, action must be taken to reduce end mill deflection.

3. It has been identified that the surface finish on the machined component plays a significant role in the dimensional accuracy and the repeatability of measurements.

4. Selection of cutting conditions (i.e. cutting speed, feed and depth of cut) plays a major role in the quality of the finished products. Therefore, special care must be taken in using these parameters to optimize the outcome.

5. The quality of cutting fluids and the methods of their applications contribute to the quality of the product.

6. Tool positioning errors contribute to the poor accuracy of machined components and hence care must be taken to avoid or at least to reduce these errors.

7. Improved work clamping and tool setting will help to reduce the effects of work piece deflection, vibration, and poor rigidity of the "Tool - Work - Machine" system. This requires further study.

3.7 Further Work Undertaken

Based on the preliminary work presented in this chapter several findings have emerged. The work undertaken is therefore to further investigate the effects of these new findings. This encompasses:

(a) A statistical analysis of inherent variations in cutting tool dimensional features and their effects on machining accuracy. (Chapter 4)

(b) The effect of end mill deflection on machining accuracy. (Chapter 5)

(c) Identification of optimum cutting conditions to achieve dimensional accuracy and consistency in the surface finish of the machined component. (Chapter 6)

(d) Mathematical modeling for volumetric error analysis involving a 3 dimensional matrix solution and to analyse the effect of machine tool geometric accuracy on the accuracy of machined component. (Chapter 7)

Before proceeding with further experiments some changes in the experimental set up are felt necessary. The clamping was improved by introducing four screw clamping instead of two. Although no significant clamping error was noticed in the preliminary studies, due to large length to thickness ratio of the component, the distances between the clamping screws were also reduced to reduce the likely buckling effect of the component specially in drilling. Previously the two clamping screws were at the corners of a 154 mm x 30 mm rectangle and for further experiments four clamping screws were placed at four corners of a 96 mm x 26 mm rectangle.

Calibration of the machining centre was also necessary to find the actual state of the machining centre. The machining centre was calibrated for its positioning accuracy using a Hewlett Packard 5528A laser measurement system with auto compensation to 20 ° C. It was found that along X axis the positioning error was high (in some cases more than 80 microns). Necessary adjustments were done and the improved positioning accuracies are given in Figure 3.27.

The co-ordinate measuring machine was also subsequently calibrated for its full functional capabilities against the British Standard B.S. 6808 1987 and the American Standard ASME / ANSI B89.1.12.M 1985 and the findings of the calibration [130] will be taken into account in future work.

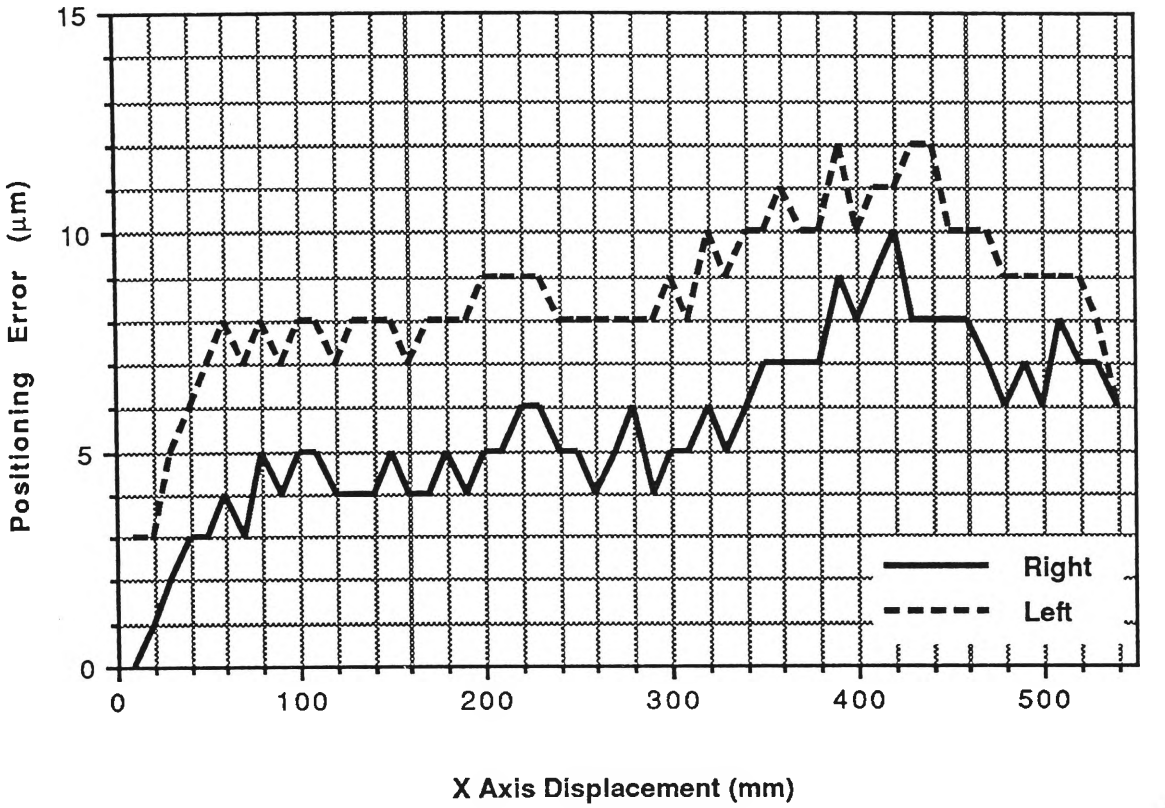

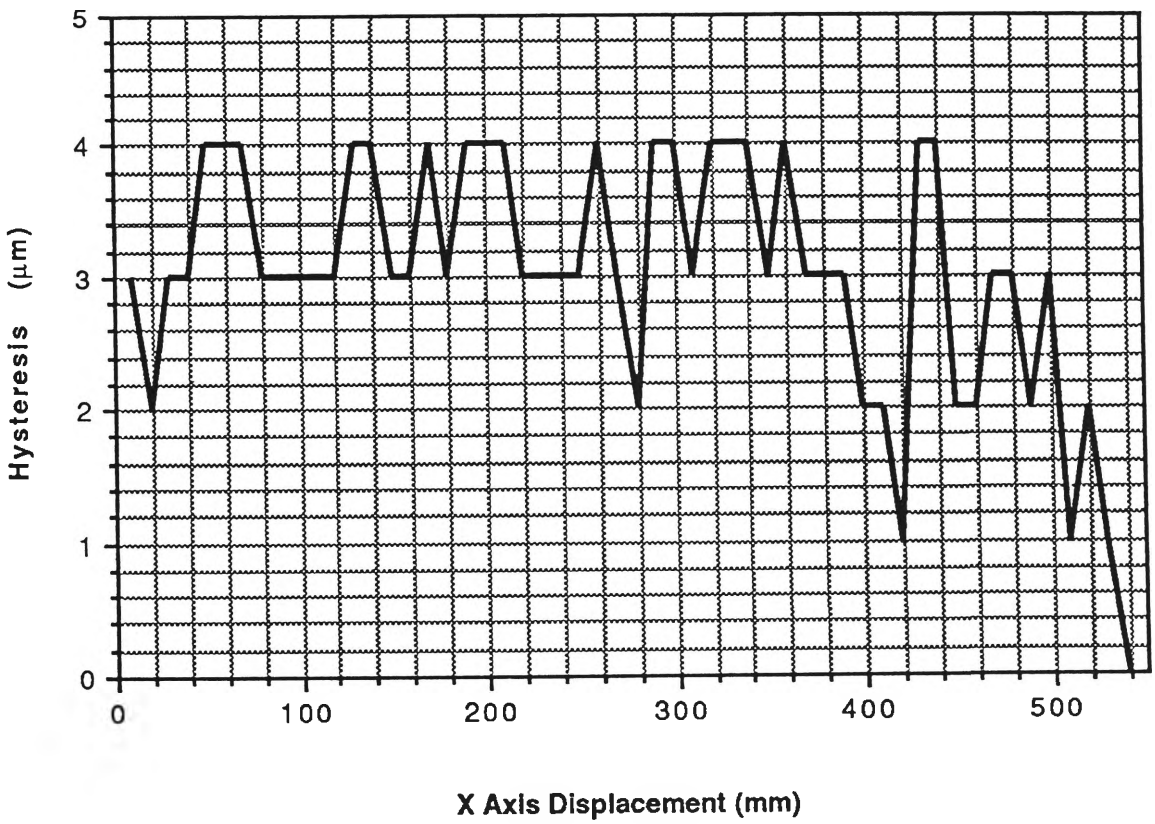

Figure 3.27.1 Calibration Results of Zenford Ziegler CNC Machining Centre along X-axis.

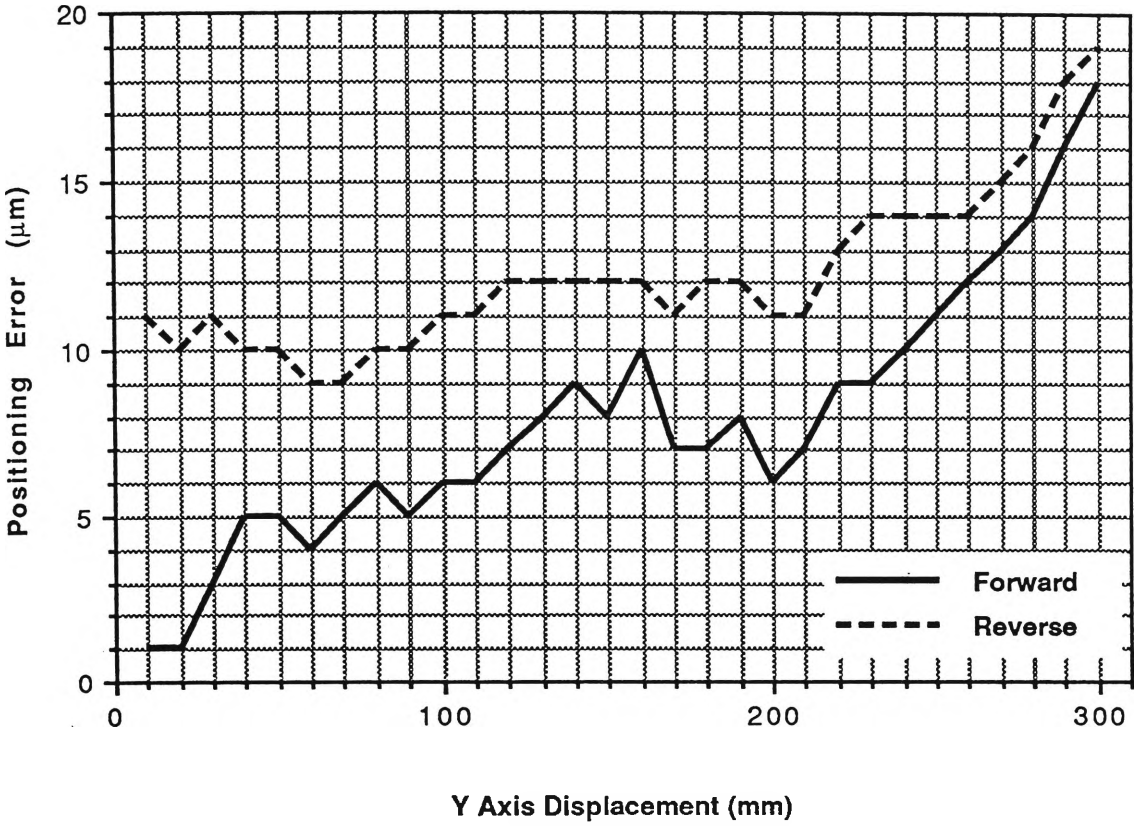

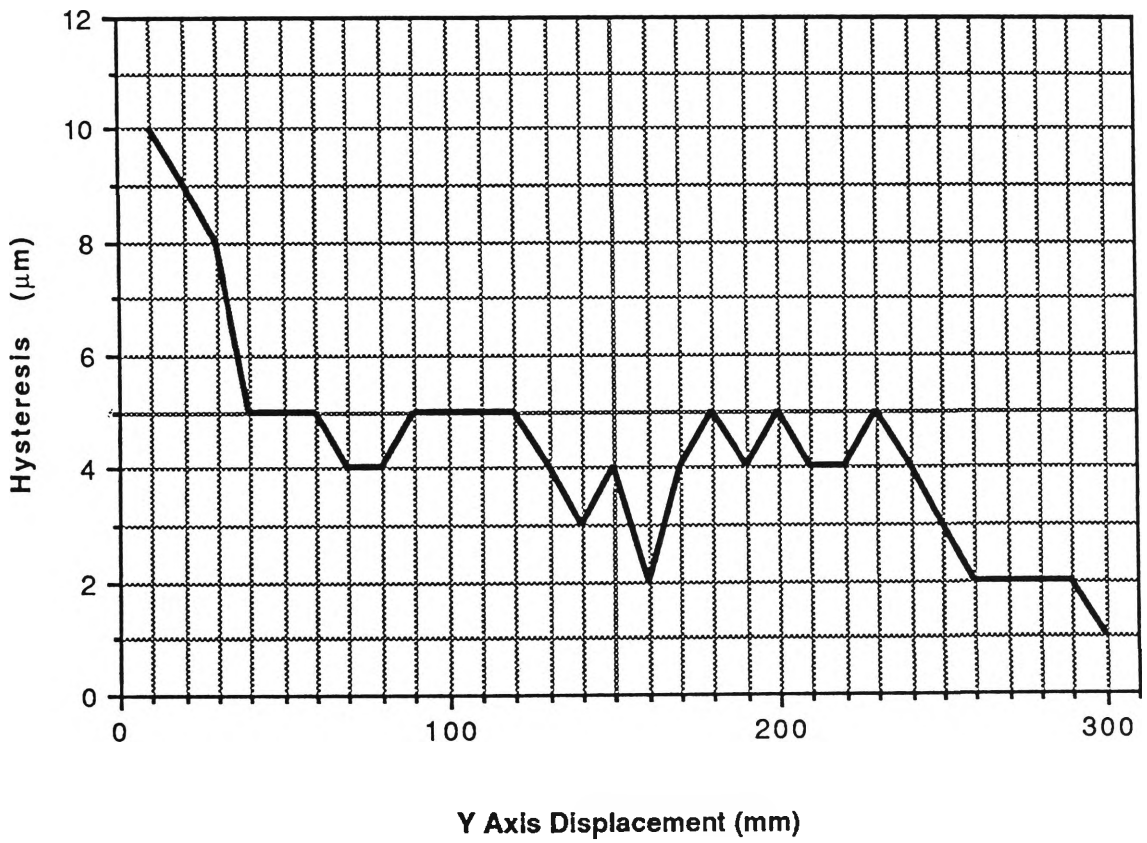

Figure 3.27.2 Calibration Results of Zenford Ziegler CNC Machining Centre along Y-axis.

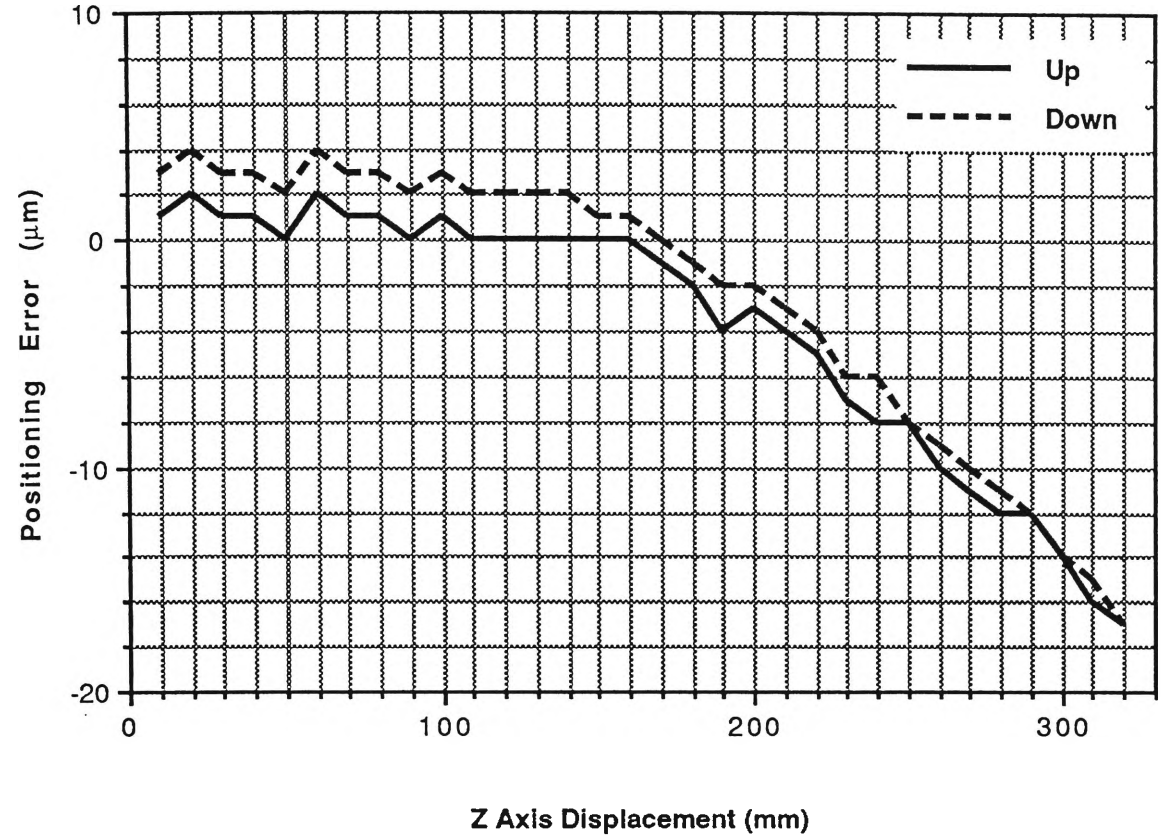

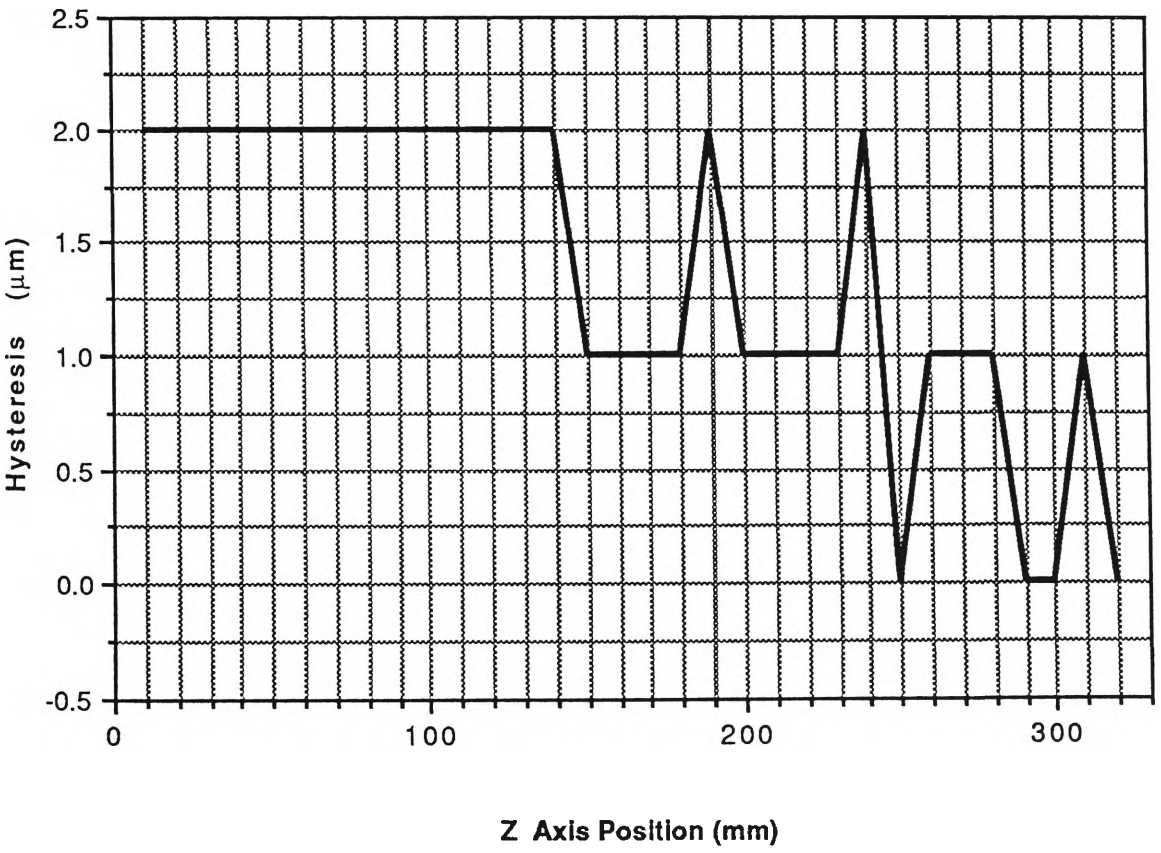

Figure 3.27.3 Calibration Results of Zenford Ziegler CNC Machining Centre along Z-axis.

4.0 A STATISTICAL ANALYSIS OF INHERENT VARIATIONS IN CUTTING TOOL DIMENSIONAL FEATURES AND THEIR EFFECTS ON MACHINING ACCURACY

4.1 Introduction

Perhaps the most overlooked aspect in CNC machining operations is the accuracy of the cutting tool. Many users of CNC machines are unaware of the fact that accuracy of the cutting tools directly influences the machining accuracy, as the actual machining is executed by cutting tools (which are in direct contact with the workpiece during machining). While discussing about the machining accuracy, many researchers also appear to have missed this point. The author, however, believes that more attention must be paid towards maintaining a consistent and high cutting tool accuracy for improving the overall machining accuracy.

Generally speaking, same types of cutting tools are used in CNC and conventional (manual) machining operations which produce similar magnitudes of machining inaccuracy in both operations. Moreover, the users (of CNC machine tools) do not take into account the wide tolerance band of the cutting tools used and they usually take nominal values of the dimensions of a cutting tool as its actual values, which in reality are most unlikely. It is acknowledged that like the inherent machine accuracy, the cutting tool accuracy also cannot be altered by the user and hence in the present study cutting tool accuracy is regarded as inherent. In this chapter an attempt has been made to demonstrate the variations in cutting tool dimensions and their effects on machining accuracy by a statistical analysis with a view to possibly using these results in error elimination, adopting any suitable method.

4.1.1 Cutting Tools Used

The cutting tools used in our machining operation are:

FACE MILLING CUTTER

Manufacturer: ISCAR Ltd, Israel

Nominal size: 100 mm

Type: Indexable insert (Triangular)

Number of inserts: 8

Insert No: TPKN 2204 PDR P25

END MILL

Manufacturer: Osborn Cutting Tools, Australia

Nominal size: 16 mm

Series: Normal

Shank: Straight shank (screwed)

Number of teeth: 4

Type: Right hand helix and square end

CENTRE DRILL

Manufacturer: Patience & Nicholson, UK

Nominal size: 8 mm (No. 4)

Type: Plain

TWIST DRILL

Manufacturer: Osborn Cutting Tools, Australia

Nominal size: 12 mm

Series: Jobbers

Shank: Parallel shank

Special requirement: None

4.1.2 Basic Tool Geometry and Effects of Its Individual Elements on Machining Accuracy

It has been decided to investigate the dimensional variations of twist drills and end mills accuracies of which affect the machining accuracy of our workpiece most. The basic tool geometry and the nomenclature adopted in this thesis are given below:

(a) TWIST DRILL

A typical twist drill geometry is shown in Figure 4.1. Apart from the simplification the basic specifications are generally in agreement with Australian Standard for Twist Drills (General Purpose) AS2438-1981 (Extract from AS2438-1981 is given in Appendix G).

The most significant drill features are:

Drill diameter

Overall length

Flute length

Point angle

Chisel edge angle

Web thickness

Relative lip height

Lip clearance angle

Helix angle

Rake angle

Shank diameter

Back taper, and

Shank runout

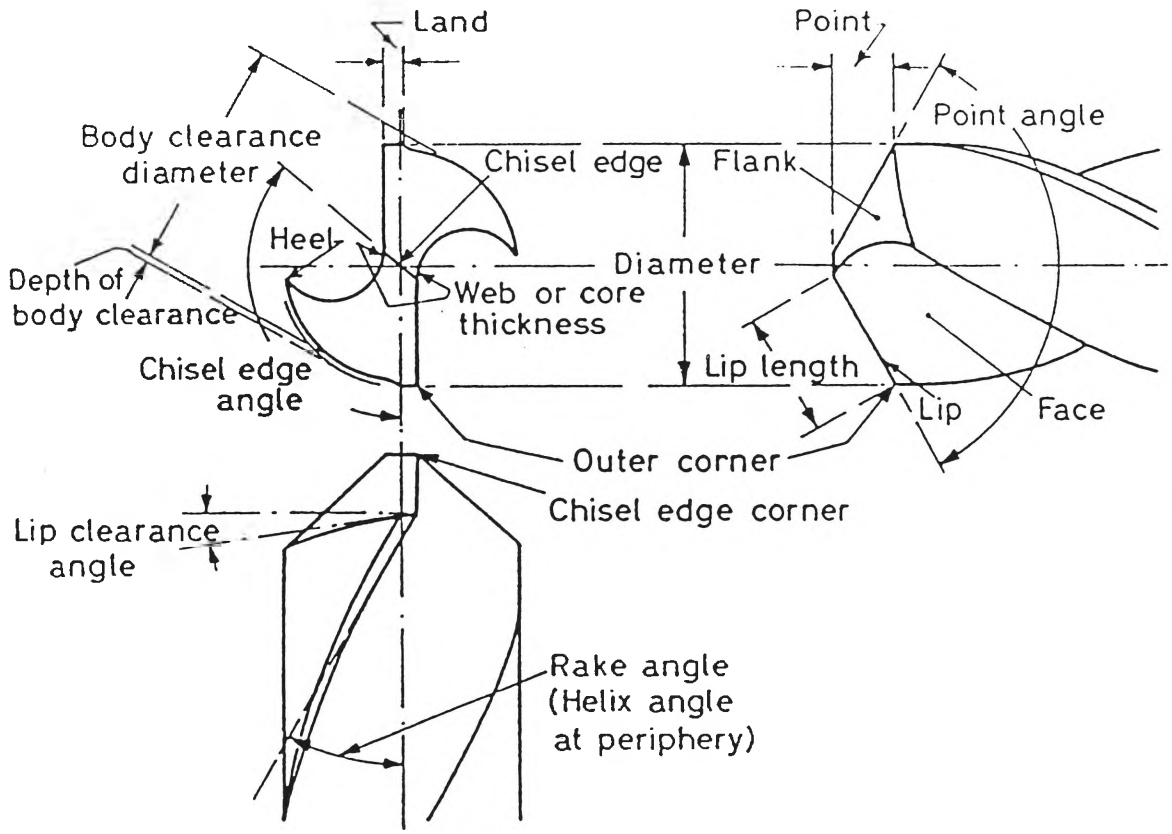

Figure 4.1 Nomenclature and Geometry for Twist Drills [131].

Drill diameter (also known as point diameter) is the most important geometric element of a drill. It is the diameter measured across the lands at the outer corners of the drill. In drilling, cutting occurs on the straight edges (lips) and on the chisel edge at the top of the drill. Except near the outer corners no cutting takes place at the drill periphery. Drill diameter is important for hole size accuracy as in ideal conditions* it is the size of the hole expected, using that drill.

---

* In real conditions, the machined hole size becomes larger due to a number of factors and the drill diameter is the smallest diameter of the hole that can be machined using that drill.

The distance between straight cutting edges (lips) is the **web thickness** and is usually specified and measured at the point end of the drill. The purpose of a web is to protect the drill point and stiffen the drill. To reduce drilling thrust, the web is gradually reduced towards the point (which is known as web thinning). Excessive web thinning weakens the point of the drill and slitting of the web can result. Uneven web thinning, i.e. more material removed from one side of the chisel edge than the other, could result in an unbalanced drill which will drill oversized holes and may even cause drill breakage.

Relative lip height is the axial displacement of the lips measured at a given radius and determined by the axial distance of the lips from a reference plane perpendicular to the drill axis (usually specified and measured at the outer corner of the drill). Galloway [125] found that the asymmetry of the drill point resulting from relative lip height causes the axis of rotation of the drill point to move to the centre of displaced chisel edge which results in the hole oversize. Galloway has also shown a relationship to predict the hole oversize as:

$$\Delta\Phi = H \tan k \qquad (4.1)$$

where

$\Delta\Phi$ = hole oversize

H = relative lip height

k = half point angle

However, the hole oversize appears to have been caused also by many other factors, such as spindle runout, rigidity of the setup, etc., thus in reality the actual oversize would be greater than those predicted by using Equation (4.1).

Point angle is the sum of the acute angles between the drill axis and the lines joining each outer corner to the corresponding corners of the chisel edge. The two acute angles

should be equal. The standard drills are ground with an included angle of 118° which has been established as the most suitable value for general purpose drilling. Galloway [125] assumed that these two angles which form the point angle are equal and, based on this, he formulated the hole oversize using half point angle. But in reality two cutting lips may not be at a similar angle to the drill axis, i.e. one angle may be larger than the other, even though the extreme point of the drill is central with the drill axis. It results in the shorter cutting lip doing most of the work and the drill being forced to the opposite side of the hole producing an oversize hole. Therefore, Galloway's formula for hole oversize should be extended to include the variation of these two angles.

Overall drill length is the distance between the two planes normal to the drill axis at the extreme ends of the point and shank respectively. Length of the drill influences drill deflection, which results in an inclined hole axis. Galloway [125] formulated the slope of the drilled hole (λ) as:

$$= \frac{3}{2l} \cdot \frac{R}{T} \left(l - \frac{1}{k} \tan k l \right) \qquad (4.2)$$

where

k = $\sqrt{\frac{T}{E I}}$

E = modulus of elasticity of drill material

I = moment of inertia

l = length of the drill (effective length)

R = transverse reaction at the drill point

T = thrust force

To avoid tool deflection it is always desirable to use a drill with a minimum length. In drilling operations, quite often the hole diameter is not uniform through the depth of the

hole. The magnitude of this error (shape error) depends primarily on the diameter and length-to-diameter ratio of the drill [6].

From the accuracy point of view, **shank runout** is another important parameter. In a production environment, spindle runout, tool holder errors and shank runout of the drill in combination may produce larger than expected drill runout, which results in size and shape variations of the hole.

Back taper is the reduction in diameter at the lands per unit length of the drill from the point towards the shank. Such reduction of diameter is intended to reduce frictional forces between the drill and the hole. Lack of proper back taper may also cause hole inaccuracy and bad surface finish.

In previous paragraphs important twist drill elements and their possible effects on machining accuracy have been discussed. The accuracy of holes produced with twist drills generally depends on many factors such as the type of drilling process, the workpiece material, cutting conditions, machine used, rigidity of the setup, tool material, tool geometry, etc. It is difficult to differentiate the effect of any individual factor. Here it must be pointed out that, twist drills are not considered as precision cutting tools; rather they are designed to produce holes rapidly and economically. If precision is required, a subsequent operation such as boring or reaming must be performed. To achieve better positioning accuracy, centre drill is often used. another solution is to use a step drill, which has two or more diameters ground into the lands of the drill. Step drills give better positioning accuracy and size accuracy (sometimes eliminating the need for subsequent reaming operations).

(b) END MILL

Milling cutter is a rotary cutting tool provided with one or more cutting edges called teeth, which intermittently engage the workpiece and remove material by the relative movement of the work piece and the cutter. Many different types of milling cutters are available in the market today. End mill is the most common and widely used type of milling cutter. A typical solid* end mill is shown in Figure 4.2. The most important end mill features are:

Cutter diameter
Cut length
Shank diameter
Overall length
Hand of cutter
Helix angle
Radial rake angle
Land
Clearance, and
Shank runout

Hand of cutter denotes the direction of the end mill while cutting. Cutters are classified as left and right-hand cutters. Right-hand cutter is a cutter with edges arranged to cut when the cutter rotates anti-clockwise when viewed facing the spindle nose. Left-hand cutter is a cutter with cutting edges arranged to cut when the cutter rotates clockwise when viewed facing the spindle nose. Hand of cutter is more important for using the cutter on horizontal-spindle machines, because the direction of rotation must be selected so that the

* End mills are available with solid, tipped a(brazed), insertable blade and indexable-insert constructions. We have used solid end mills in our experimental work.

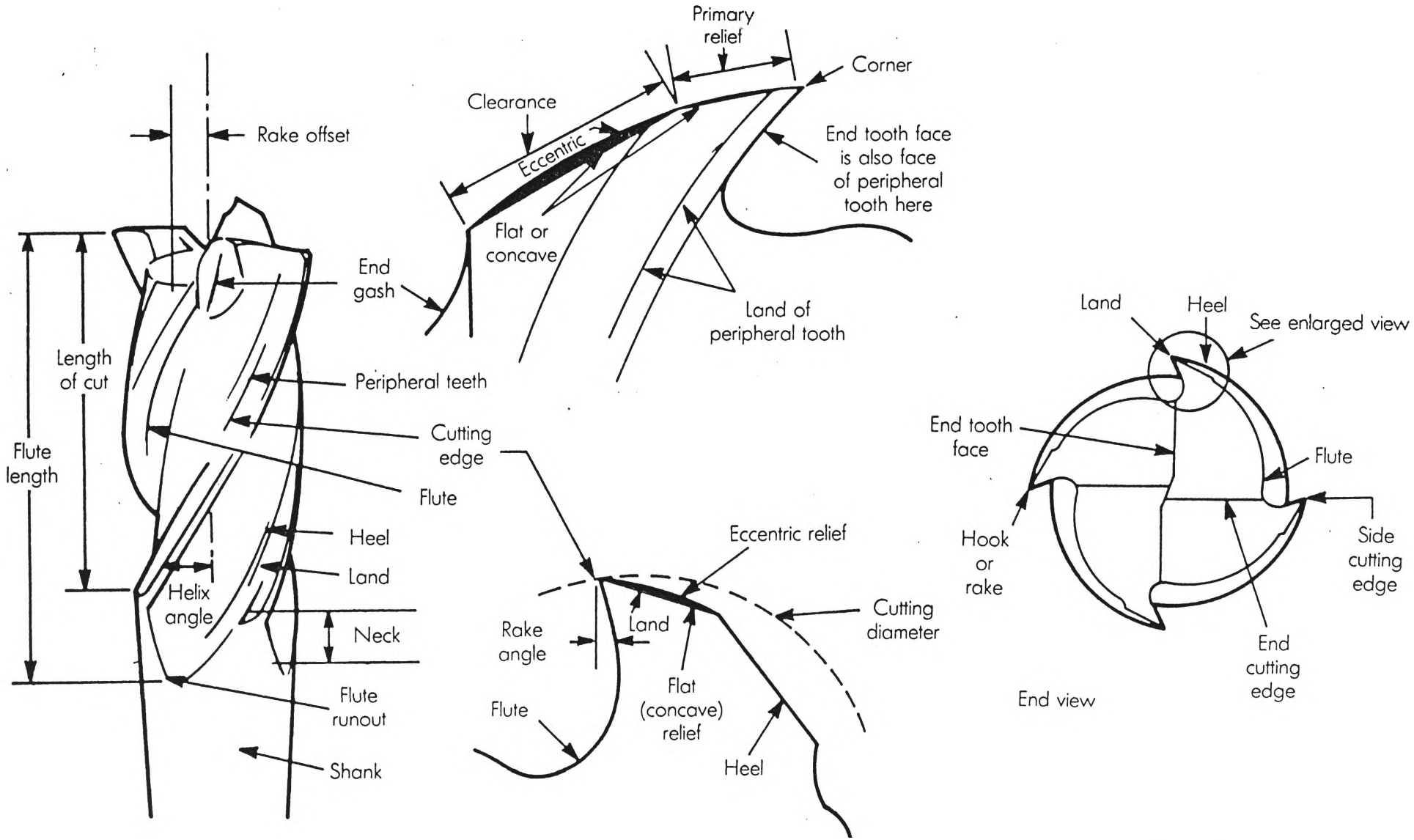

Figure 4.2 Nomenclature and Geometry for Solid End Mills [6].

tangential cutting forces press the workpiece down against the table. On vertical-spindle machines, the direction of the cutting force is less critical because the workpiece is normally equally supported on either side. In general, wrong selection of the hand of cutter may cause machining errors.

Helix angle is the acute angle between the tangent to the tooth cutting edge at a point on this edge, and the plane containing the cutter axis and the point on the edge in question. This angle lies in the plane normal to the cutter radius, at the point on the cutting edge considered. The helix angle is generally constant for every point on the tooth cutting edge and most end mills are made with helix angle 0° (straight-fluted tools) to 50° , and more often 27° to 30° . Cutters with helix angle give smooth force variations which reduce shock loads and vibrations. The effect of helix angle on force fluctuations is shown in Figure 4.3. Due to reduced force fluctuation helical cutters give better machining accuracy.

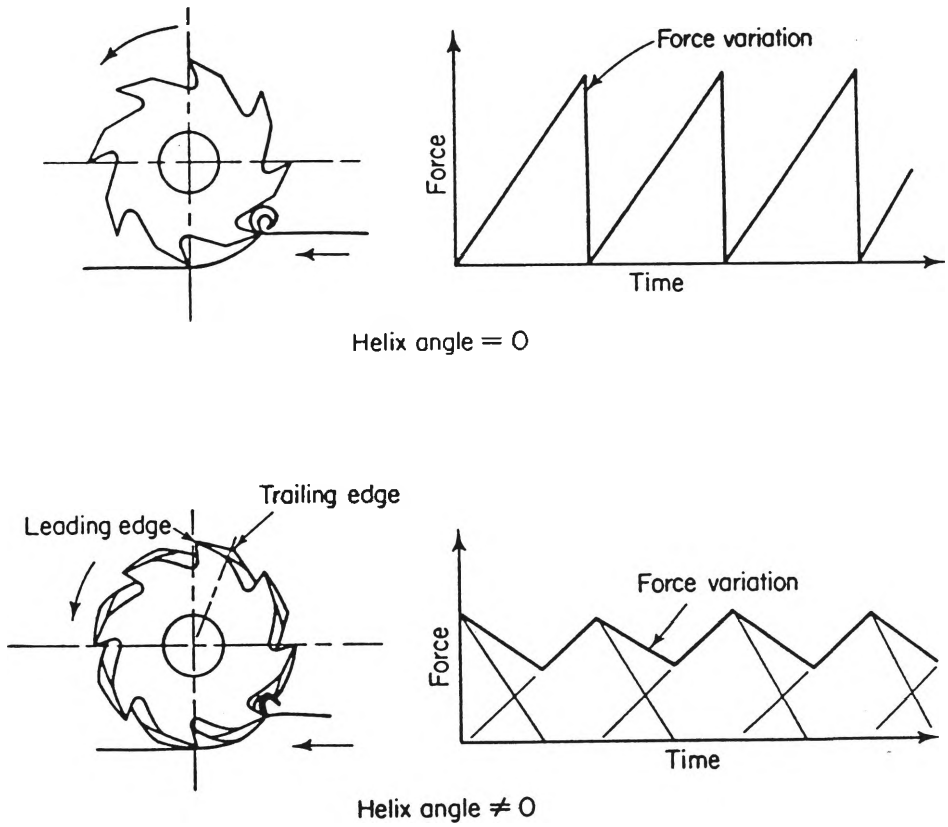

Figure 4.3 Effect of Helix Angle on the Force Fluctuations in Peripheral Milling [132]. (Force rise arbitrarily chosen to be linear for illustration purpose only)

Radial rake angle is the acute angle between the tooth face and a radial line passing through the cutting edge in a plane perpendicular to the cutter axis. The radial rake angle is generally constant for every point on the tooth cutting edge. The rake angle affects the type of chip produced, the pressure and temperature at the cutting edge and the power required in metal removal. It is found that with an increase in rake angle, a longer tool life, a better surface finish, and more efficient metal removal rate can be achieved [6].

Surface finish is an important aspect in milling, as almost every milling operation has some surface finish requirement. Martellotti [133] estimated peak to valley roughness height for peripheral operation using following formulae:

$$R_{ma} = \frac{S_t^2}{8\left(R \pm \frac{S_t . K_t}{\Pi}\right)} \tag{4.3}$$

where

R_{ma} = peak to valley roughness height

K_t = number of teeth in the cutter

S_t = feed per tooth

R = cutter radius

From Equation (4.3) it can be seen that the surface roughness in peripheral milling is affected by the cutter diameter, feed per tooth and the number of teeth. The larger the cutter diameter and/or less the feed, better is the surface finish. From the tool deflection point of view (which causes surface waviness), the use of larger cutter diameter and lower feed are desirable (Tool deflection and its effects on machining accuracy will be discussed in Chapter 5).

4.2 Previous Work on Cutting Tool Dimensional Variations

Some studies on dimensional variations of twist drills have been reported in the literature; but no such published work appears to be available on end mills. The reason for this may be that the twist drills are in use for a long time. The researchers have tried to improve the performance of twist drills within their conventional design, whereas although the end mills have been in use for a comparatively shorter time and their improvement has constantly changed their design. Moreover some researchers have shown interests in monitoring the grinding of twist drills, which also calls for a comparative study on twist drill (point) dimensions.

Galloway published his comprehensive investigation on drilling in 1957 [125]. Although the core of his study was an investigation of drill performance and factors affecting its performances, Galloway included a study of dimensional variations of drills as a preliminary investigation. Measurements were taken using s specially built apparatus which included a dial gauge (for large drill -points) and a microscope (for small drill-points). He found that there were considerable dimensional variations between drills supplied for the same purpose by different tool manufacturers. His measurement results (for nominally similar 5/8 inch diameter drills) are given in Table 4.1. Galloway however did not provide any data about the repeatability of measurements or sample size (except quoting "a large number of drills").

The repeatability of measurements is of particular importance, because when measuring very small dimensions such as relative lip height with an average value 0.0036 inch (0.09144 mm), without any information about its repeatability the measured results cannot be authenticated. Galloway considered drills of different manufacture which is one of the causes of the large variations of dimensions. Because in twist drills there are a

Element	Unit	Max.	Min.	Average	Range
Drill Point Dia.	inch	0.6254	0.6236	0.6246	0.0018
	mm	15.8852	15.8394	15.8648	0.0457
Web Thickness at Point	inch	0.122	0.070	0.0977	0.052
	mm	3.099	1.778	2.4816	1.321
Web Thickness near Shank	inch	0.160	0.113	0.1353	0.047
	mm	4.064	2.870	3.4366	1.194
Land Height	inch	0.040	0.012	0.0237	0.028
	mm	2.032	0.508	1.219	1.524
Land Width	inch	0.080	0.020	0.048	0.060
	mm	2.032	0.508	1.219	1.524
Longitudinal Relief	in./in.	0.0026	0.0008	0.0015	0.0018
	mm/mm	0.0660	0.0203	0.0381	0.0457
Relative Lip Height near	in./in.	0.008	0.0005	0.0036	0.0075
Chisel Edge	mm/mm	0.203	0.0127	0.0914	0.1905
Relative Lip Height near	inch	0.011	0.0000	0.0034	0.011
Outer Corner	mm	0.279	0.0000	0.0864	0.279
Point Angle	Degrees	127	115	119.6	12
Relief Angle near Chisel Edge	Degrees	35.5	16	23.65	19.5
Relief Angle near Outer Corner	Degrees	25	5	14.10	20
Chisel Edge Angle	Degrees	145	122	131.9	23
Helix Angle	Degrees	31	28	29.5	3
Lip Spacing Angle	Degrees	184	180	181.5	4
Hardness over Length of 4 inch	D.P.H.		0.070	0.0977	0.052
in. from Point	No	1,016	256	832	760

Table 4.1 Range of Variation of Drill Sizes and Hardness Observed in Nominally Similar 5/8 inch (15.875 mm) Dia. Drills [125].

number of elements which are not controlled by standard(s) and the manufacturers tend to differ in their choice of "target values". In our study drills of the same manufacturer are used, which would be expected to give lower dimensional variations.

Fugelso and Wu [134] measured drill point elements using a polar co-ordinate measuring machine which was designed and incorporated into a computer controlled twist drill grinder. The purpose of their measurement was to check the point shape after grinding and to feedback the measurement data to control the grinding process. Measurements were taken with a ball ended stylus (with 0.0625 inch or 1.587 mm radius) connected to an LVDT. The measurements were sent to a microprocessor via an A/D converter where drill dimensions and parameters were computed on-line. But the theoretical values of drill parameters were calculated off-line because of the memory limitation of the microprocessor. Their measurement results (the average and standard deviations) of twelve drills which were ground and measured with the same machine settings are given in Table 4.2. They also have not indicated any data about repeatability of their measurements;

Drill	Theoretical Values	Average	Standard Deviation
Relative Lip Height (mils)	0.0	1.708 (0.043 mm)	2.07 (0.053 mm)
Chisel Edge Angle (degrees)	135	137.2	4.12
Point Angle (degrees)	118	119.98	0.29
Clearance Difference (mils)	12.2 (0.309 mm)	12.11 (0.308 mm)	0.875 (0.0222 mm)
d Parameter (mils)	330 (8.38 mm)	351.36 (8.92 mm)	0.933 (0.0237 mm)
Optically Measured Chisel Edge Angle (degrees)	135	138.33	1.179

Table 4.2 The Average and Standard Deviation of Measured Dimensions of Twelve Drills Ground and Measured with the Same Machine Settings [134].

but data about dimensional repeatability of their grinding process were analysed. When using CMM in automatic mode, good repeatability of measurements for some drill point parameters is very unlikely. This problem will be discussed later in this chapter.

Tasi and Wu [135] developed an algorithm to check and control the drill point grinding operations. In normal production practice it very difficult to achieve and maintain the required accuracy of the drill point grinding. Tasi and Wu made a mathematical model of the drill point grinding operation and evaluated the performance of the grinding process by analysing the discrepancies of the drill point geometry estimated from the designed geometry and produced in practice. Their findings show that the accuracy of the drill point grinding operation is influenced by the systematic errors the in setting of the grinding parameters, the machine vibration and the bias of instrumentation,etc. as well as the random error associated with the nonlinear least-squares estimation. All these errors contribute to the geometrical variability of the drills.

A series of studies of the drill geometrical variability and their effects on the drilling process has been carried out at the University of Melbourne, Australia by Armarego and his Co-workers [136], [137], [138], and [139]. These studies have also confirmed large variation in dimensional features of twist drills. In a drill blank grinding process, for 7 mm blanks a shocking 40.6% defect has been reported in [139].

4.3 Present Work

Present study on the statistical variations in cutting tool dimensional features and their effects on machining accuracy was undertaken because, it is logical to believe that the cutting tool accuracy has a direct impact on the machining accuracy. In our literature survey it was found that virtually no work has been reported on the variation of cutting

tool dimensional features, in this context. But a few researchers who did study the cutting tool dimensional variations (although from different point of view) have generally found large variations in nominally similar tools.

The sample size of the present work was ten. The author must acknowledge that, a full statistical analysis requires a larger sample size. The aim of this study was to highlight the basic problem and to show how it can be handled using statistical tools. An increase in sample size will increase the confidence level; but the statistical evaluation procedure will remain the same.

Ten twist drills and ten end mills (details of which are given in Section 4.1.1) were bought. Each tool was numbered. Measurements were taken using the CMM with 1 mm diameter spherical probe. Tools were clamped on the CMM table using standard clamping devices. Positioning of tools was not a problem* because the CMM software was capable of aligning the tool along a desired axis and gives the measurement results on any desired plane. Each measurement was repeated twenty times to reduce measurement errors. Mean values of these twenty readings were taken as the actual values of particular dimensions considered. Using the twenty readings, the repeatability of measurements† was also estimated. The summaries of measurement results are given in Table 4.3 (for twist drills) and Table 4.4 (for end mills). For details of the actual readings please see Appendices I and J.

---

* Positioning of the tools is a major problem when instruments other than CMM are used. The CMM software is capable of aligning the tool with CMM axes.

† Repeatabilty was calculated using a standard repeatability formula [140]:
$R_p = t.s$, where R_p = repeatability, s = sample standard deviation and t = student's t, a constant depends on number of observations and confidence level.
When number of observations n = 20 and confidence level U = 95%, t = 2.09.

Measurement results were analysed following Australian Standard AS 2438 - 1981 (twist drills) and British Standard BS 122: Part 4 (end mills), as our contact with the manufacturer (Osborn Cutting Tools, Australia) revealed that, their tools were manufactured according to these standards. Details of the two standards considered are given in Appendices G and H.

Element	Max.	Min.	Average*	Range	Repeatab.†
Drill Diameter (mm)	11.997	11.962	11.987	0.035	0.018
Web Thickness at Point (mm)	2.163	1.611	1.956	0.552	0.327
Relative Lip Height (mm)	0.134	0.085	0.110	0.049	0.088
Point Angle (degrees)	119.137	116.291	118.119	2.846	0.656
Chisel Edge Angle (degrees)	137.381	132.914	135.251	4.467	3.689
Shank Diameter (mm)	11.948	11.903	11.930	0.045	0.008
Shank Radial Runout (mm)	0.015	0.005	0.009	0.010	0.008
Overall Length (mm)	152.176	150.897	151.736	1.279	0.059
Flute Length (mm)	112.317	110.326	111.215	1.991	0.324
Back Tapper (mm/mm)	0.00067	0.00037	0.00051	0.00030	calculated
Effective Diameter (mm)	12.055	12.011	12.033	0.044	0.030

* Average values are taken from 10 drills with 20 measured values each.

† Repeatability of measurements (worst case).

Table 4.3 Range of Variations of Drill Dimensions Measured in Nominally Similar 12 mm Diameter Twist Drills.

Element	Max.	Min.	Average*	Range	Repeatab.†
Cutter Diameter (mm)	16.019	15.978	15.995	0.041	0.055
Shank Diameter (mm)	15.990	15.983	15.986	0.007	0.008
Shank Radial Runout (mm)	0.017	0.005	0.010	0.012	0.008
Helix Angle (degrees)	30.586	28.962	29.834	1.425	2.926
Radial Rake Angle (degrees)	8.793	5.647	6.813	3.146	1.612
Effective Diameter (mm)	16.051	16.006	16.029	0.045	0.020

* Average values are taken from 10 end mills with 20 measured values each.
† Repeatability of measurements (worst case).

Table 4.4 Range of Variations of End Mill Dimensions Measured in Nominally Similar 16mm Diameter End Mills.

In effect AS 2438 - 1981 imposes the following tolerance limits on a 12 mm twist drill (parallel shank, jobber series): (see Table 4.5)

Element	Nominal	Tolerances	
	Values	LTL	UTL
Drill Diameter (mm)	12.000	- 0.027	0
Overall Length (mm)	150.000	- 3.000	+ 3.000
Flute Length (mm)	111.000	- 3.000	+ 3.000
Point Angle (Degrees)	≈ 118	No tol. limits specified	
Back Tapper (mm/mm)	---	0.0005	0.001
Hardness (HV) [HRC]	690 [60]	No upper limit	

Table 4.5 Tolerance Limits for 12 mm Twist Drills (Parallel Shank, Jobber Series) as Specified in AS 2438 - 1981.

BS 122: Part 4: 1980 imposes the following tolerance limits on a 16 mm end mill (screwed shank, normal series): (see Table 4.6)

Element	Nominal	Tolerances	
	Values	LTL	UTL
Cutter Diameter (mm)	16.000	- 0.013	+ 0.063
Shank Diameter (mm)	16.000	- 0.025	0
Thread on Shank (Tol. on Effect. Dia) (mm)	16.000	- 0.150	- 0.080

Table 4.6 Tolerance Limits for 16 mm End Mills (Screwed Shank, Normal Series) as Specified in BS 122: Part 4: 1980.

All measurement results are represented in graphical form in Figures 4.4 - 4.15 (for drills) and in Figures 4.16 - 4.22 (for end mills). Tools are regarded as non-acceptable if it is out of tolerance limits according to any of the specified tolerance limits. A summary of measurement results are given in Table 4.7 and 4.8. Among the tools measured a 40 % defects for the drills and 20 % defects for end mills were found.

Element	Drill No									
	1	2	3	4	5	6	7	8	9	10
Drill Diameter	O	X	O	O	O	O	O	O	O	O
Overall Length	O	O	O	O	O	O	O	O	O	O
Flute Length	O	O	O	O	O	O	O	O	O	O
Back Taper	X	O	O	X	O	O	X	O	O	O
Overall Results	Δ	Δ	◊	Δ	◊	◊	Δ	◊	◊	◊

O = within tolerance limits; X = out of tol. limits; ◊ = acceptable; Δ = non-acceptable

Table 4.7 Acceptance Results of Twist Drills.

Element	End Mill No									
	1	2	3	4	5	6	7	8	9	10
Cutter Diameter	O	O	O	X	O	O	O	O	X	O
Shank Diameter	O	O	O	O	O	O	O	O	O	O
Overall Results	◊	◊	◊	Δ	◊	◊	◊	◊	Δ	◊

O = within tolerance limits; X = out of tol. limits; ◊ = acceptable; Δ = non-acceptable

Table 4.8 Acceptance Results of End Mills.

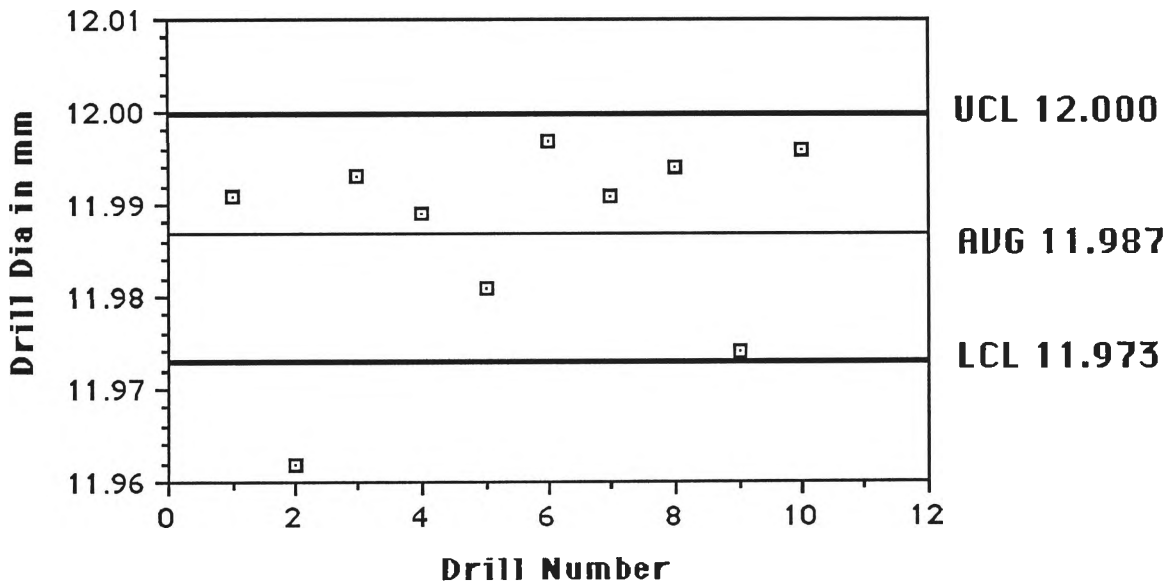

Figure 4.4 Variations of Drill Diameter Observed in 12 mm Twist Drills.

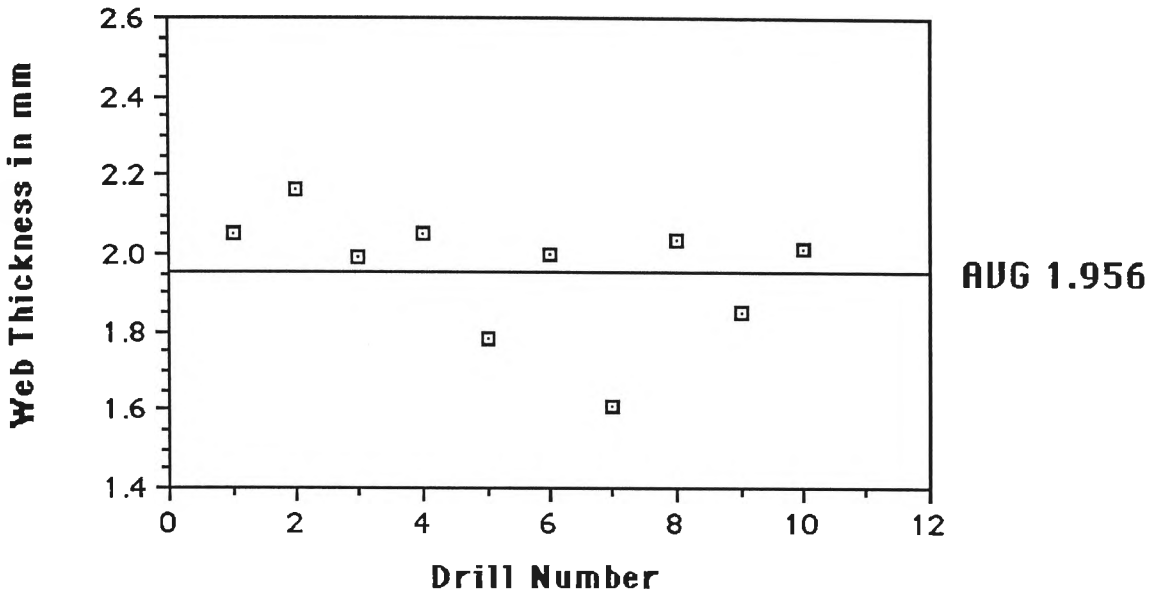

Figure 4.5 Variations of Web Thickness Observed in 12 mm Twist Drills.

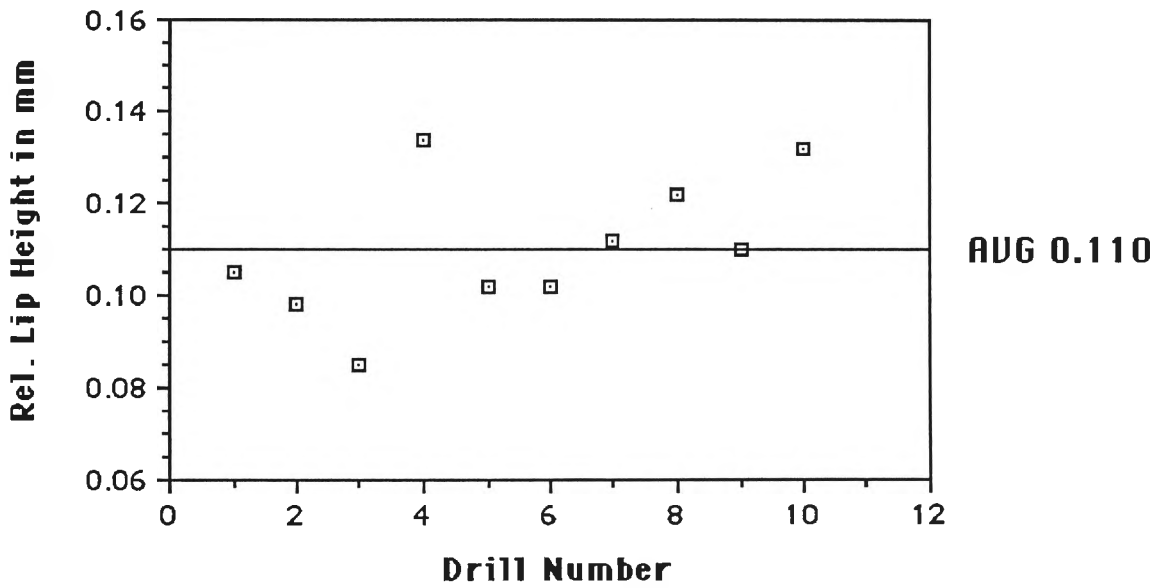

Figure 4.6 Variations of Relative Lip Height Observed in 12 mm Twist Drills.

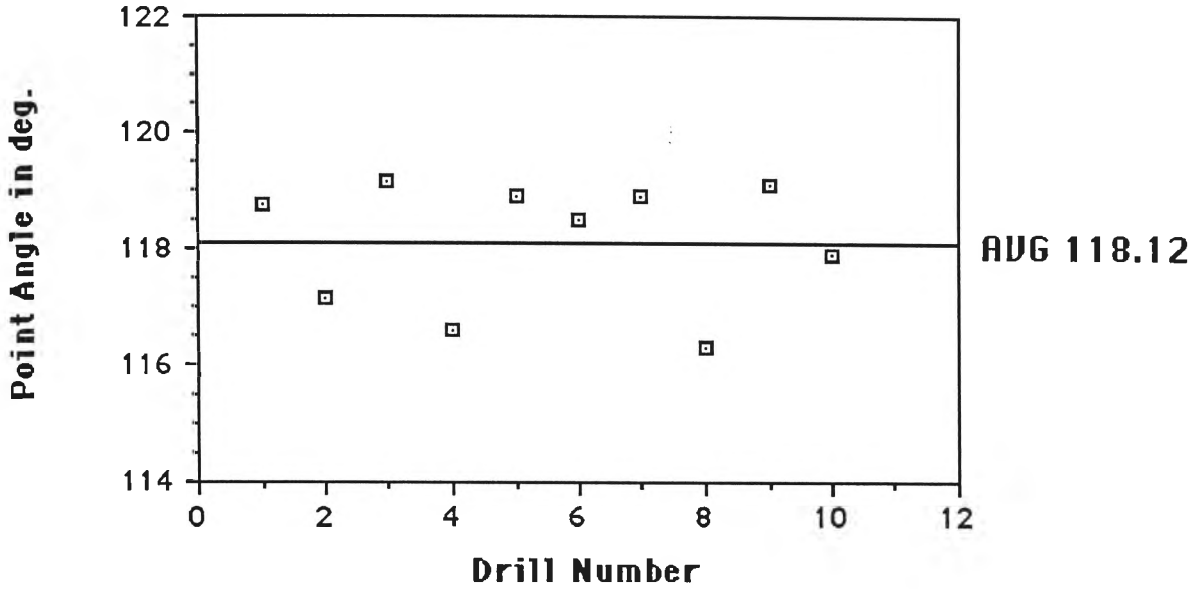

Figure 4.7 Variations of Point Angle Observed in 12 mm Twist Drills.

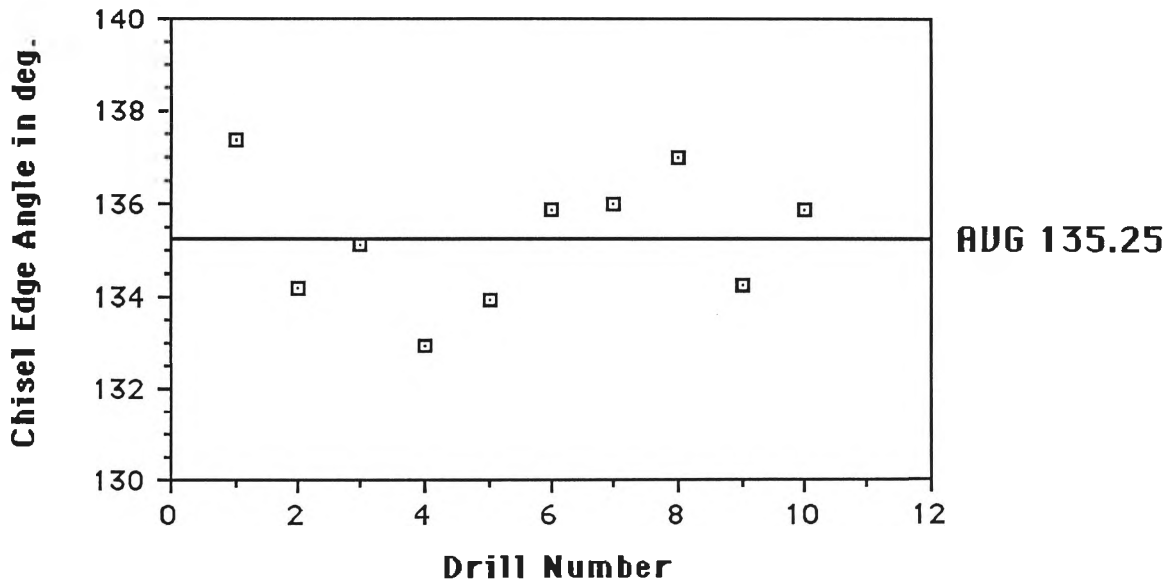

Figure 4.8 Variations of Chisel Edge Angle Observed in 12 mm Twist Drills.

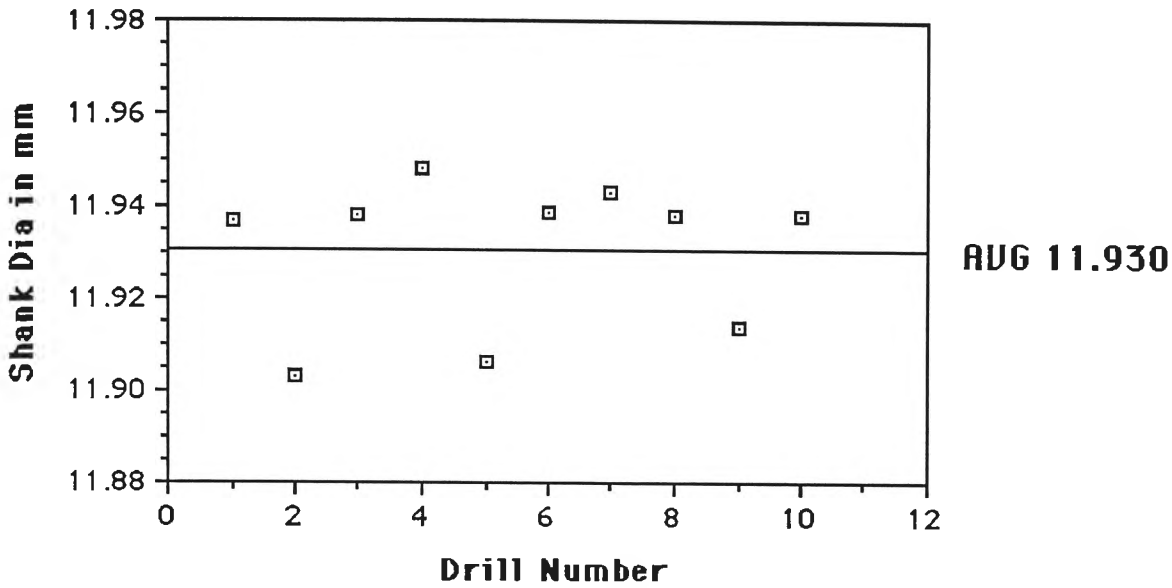

Figure 4.9 Variations of Shank Diameter Observed in 12 mm Twist Drills.

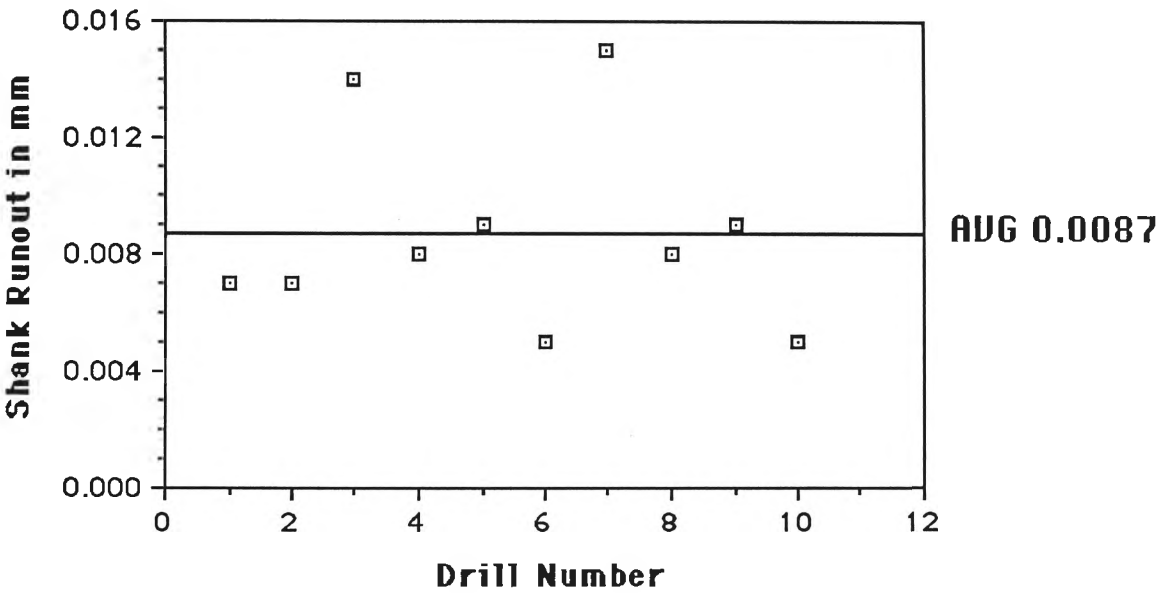

Figure 4.10 Variations of Shank Runout Observed in 12 mm Twist Drills.

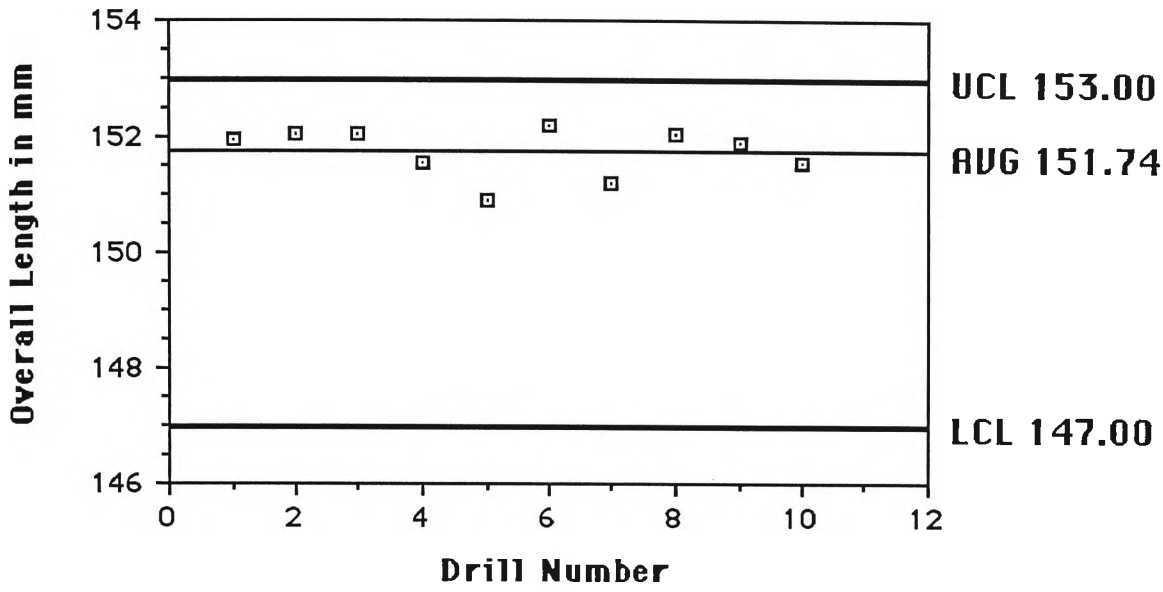

Figure 4.11 Variations of Overall Length Observed in 12 mm Twist Drills.

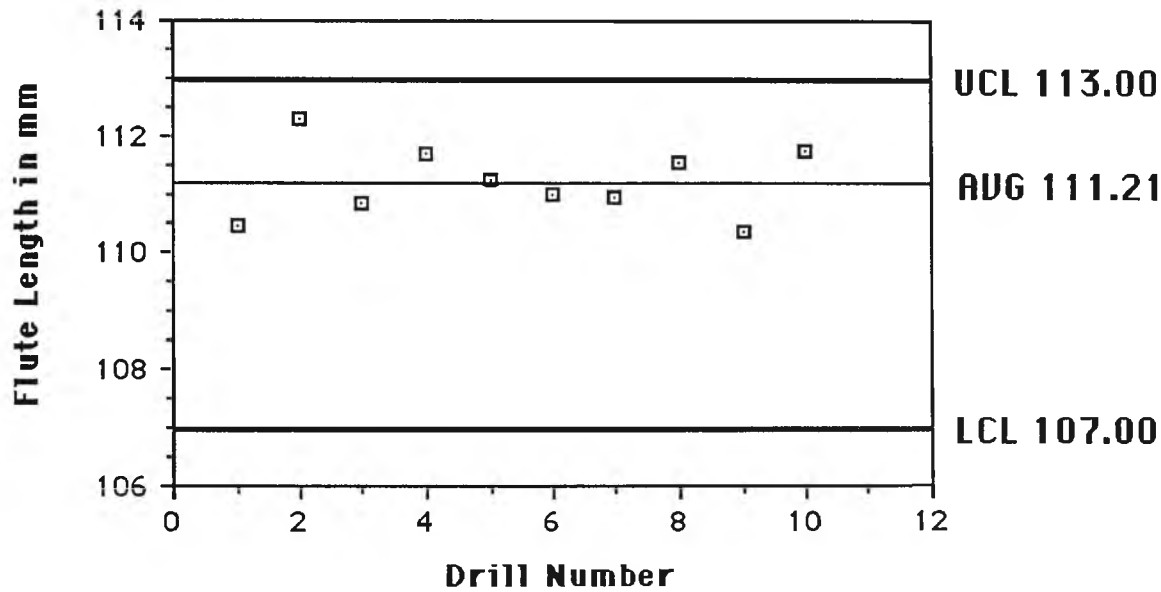

Figure 4.12 Variations of Flute Length Observed in 12 mm Twist Drills.

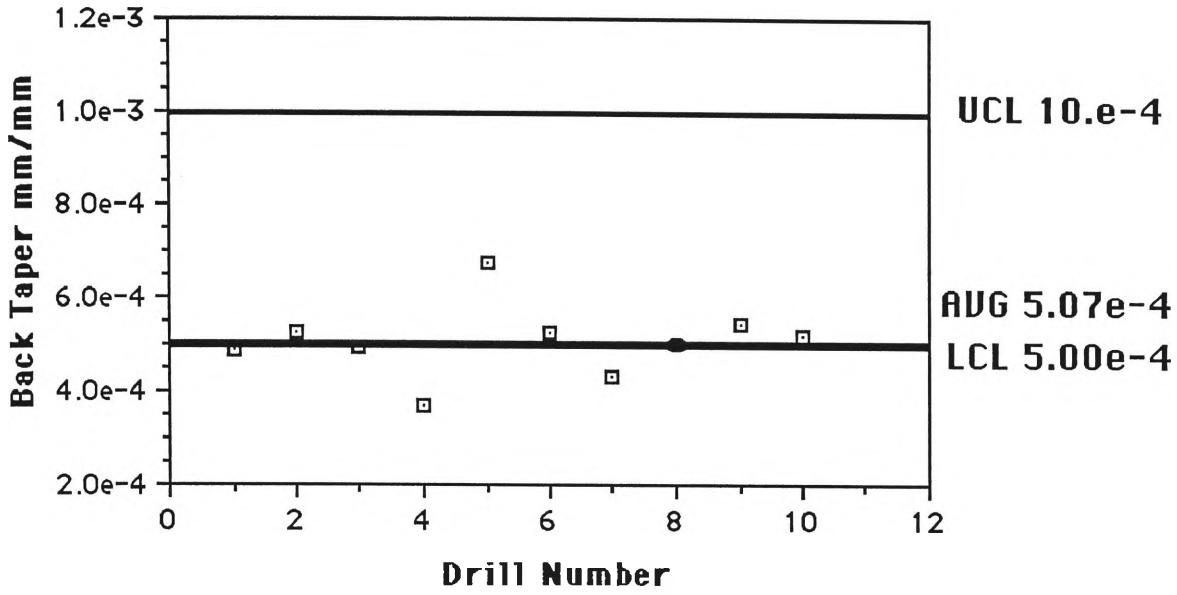

Figure 4.13 Variations of Back Taper Observed in 12 mm Twist Drills.

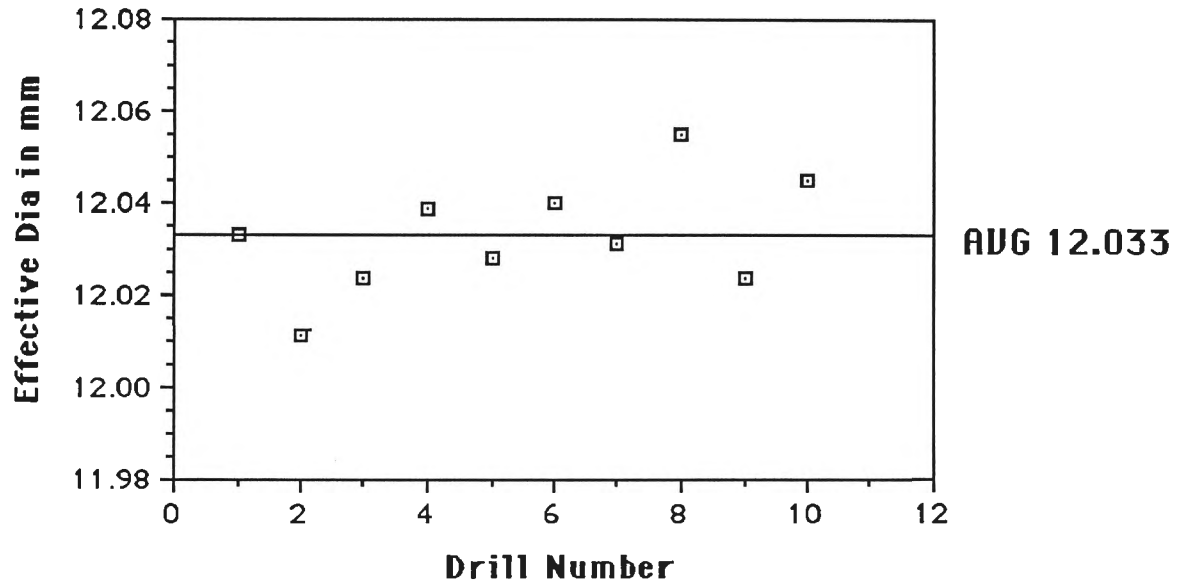

Figure 4.14 Variations of Effective Diameter Achieved Using 12 mm Twist Drills.

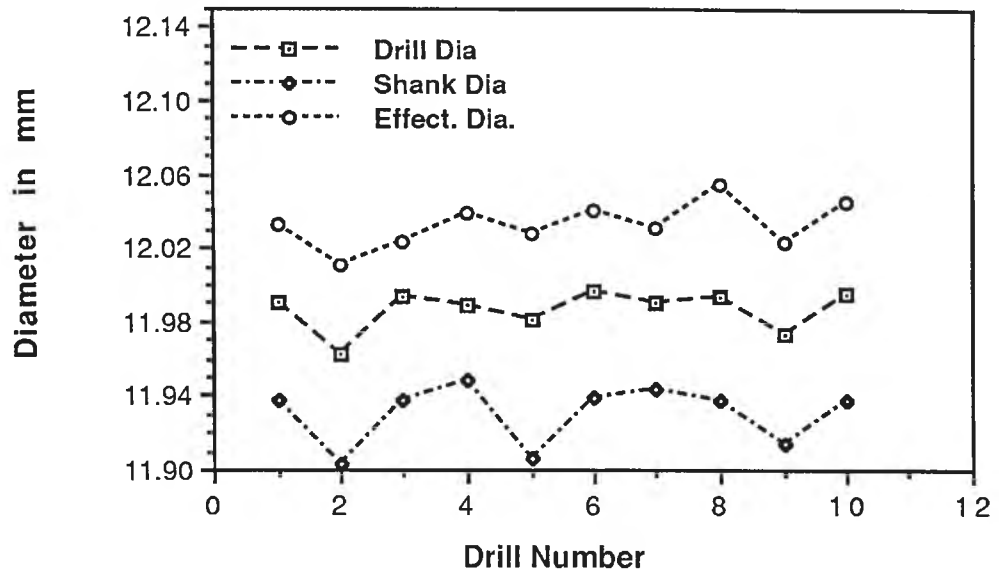

Figure 4.15 Variations of Point Dia, Shank Dia and Effective Dia Observed in 12 mm Twist Drills.

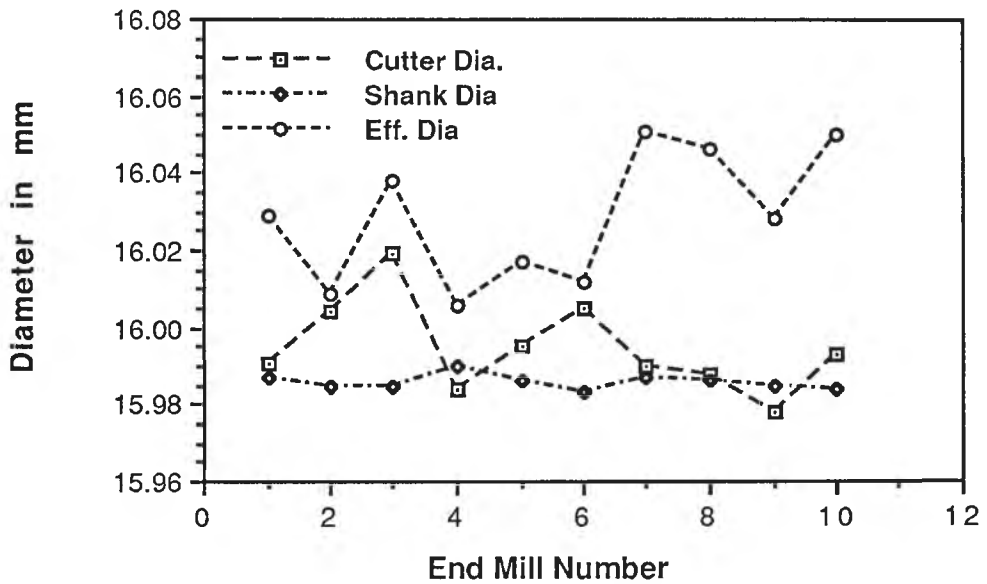

Figure 4.16 Variations of Cutter Dia, Shank Dia and effective Dia Observed in 16 mm End Mill.

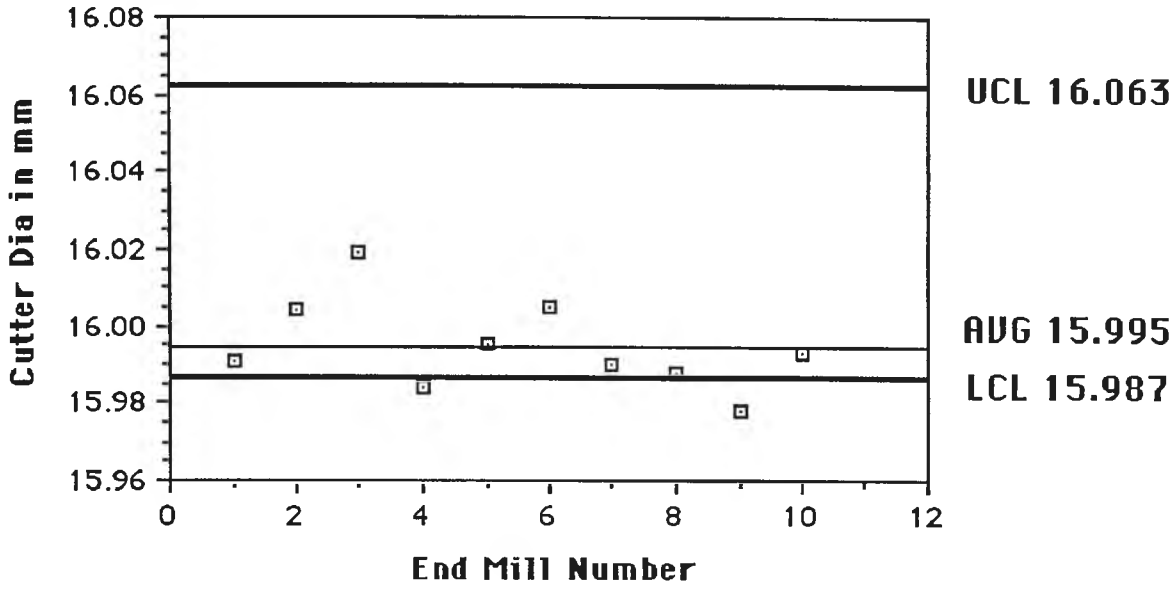

Figure 4.17 Variations of Cutter Diameter Observed in 16 mm End Mills.

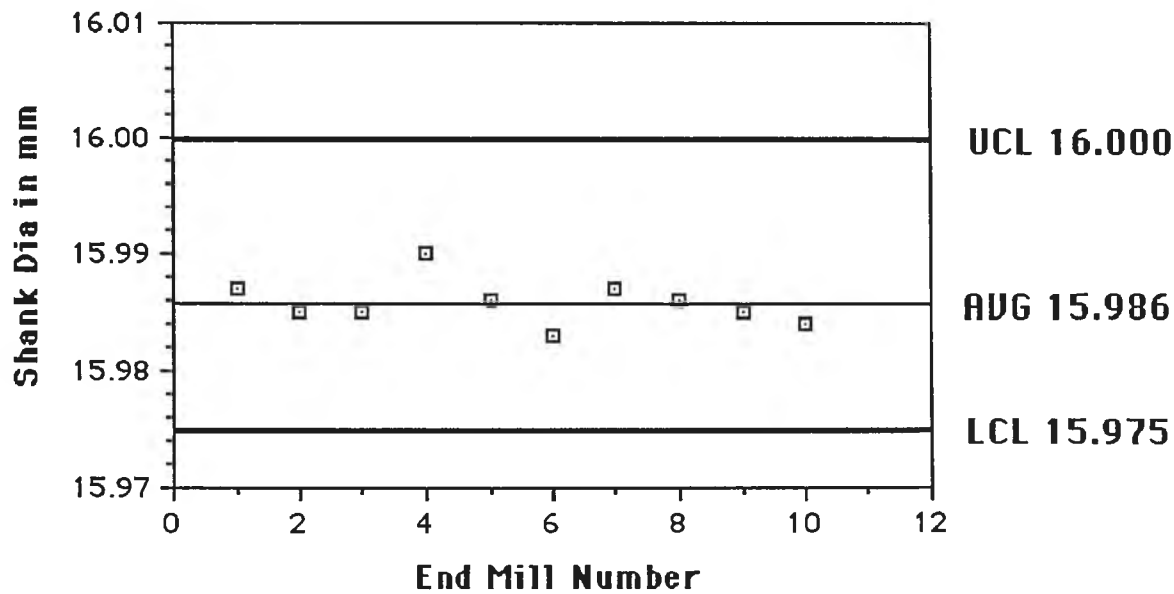

Figure 4.18 Variations of Shank Diameter Observed in 16 mm End Mills.

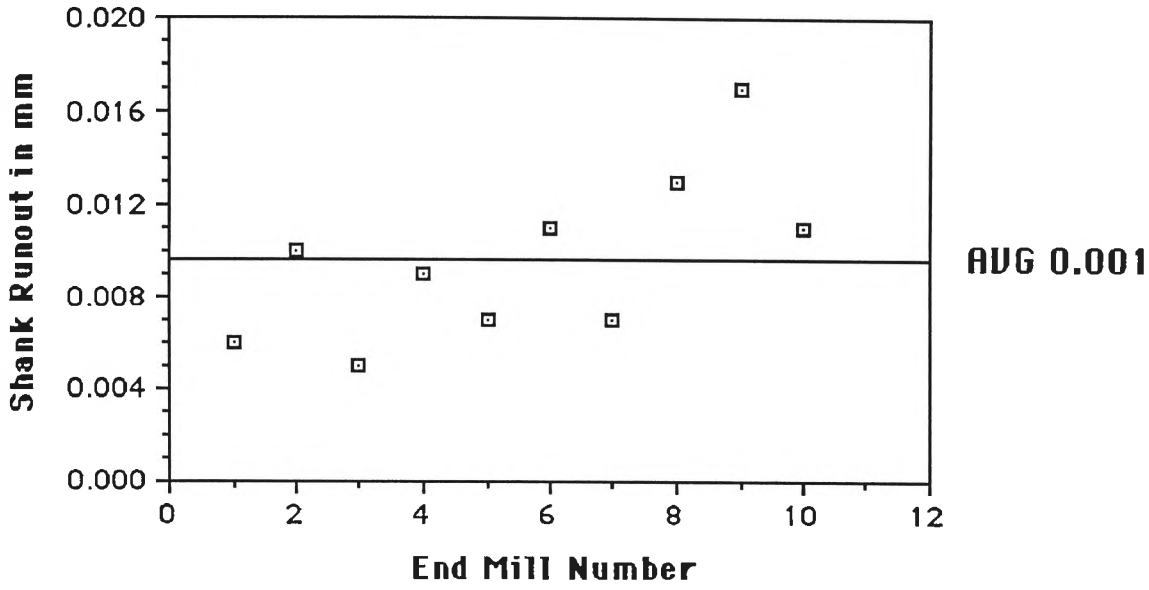

Figure 4.19 Variations of Shank Runout Observed in 16 mm End Mills.

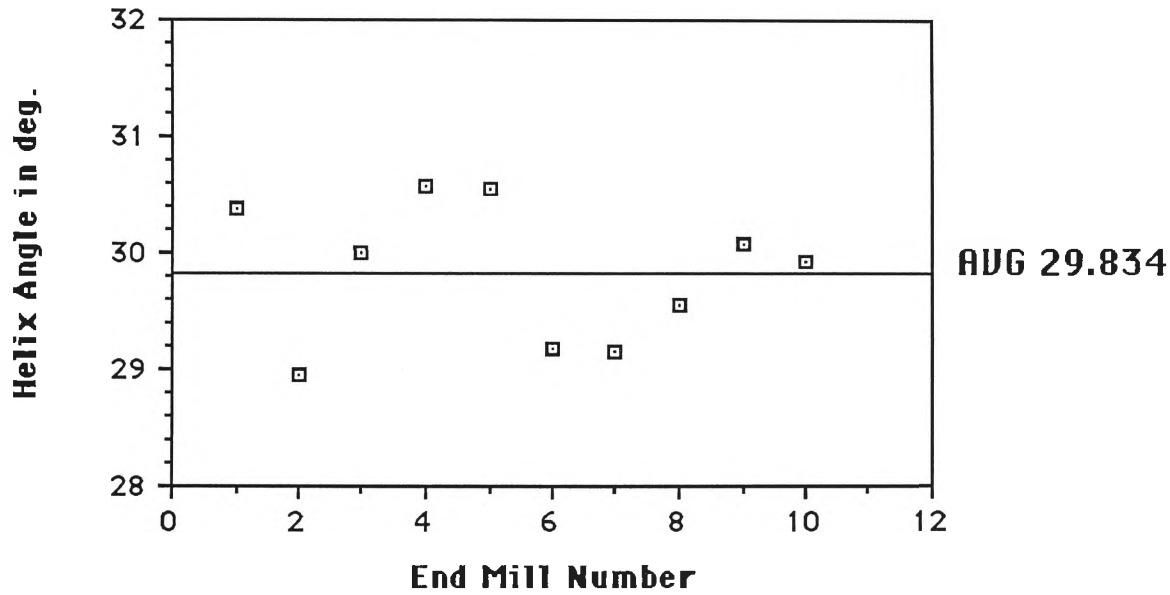

Figure 4.20 Variations of Helix Angle Observed in 16 mm End Mills.

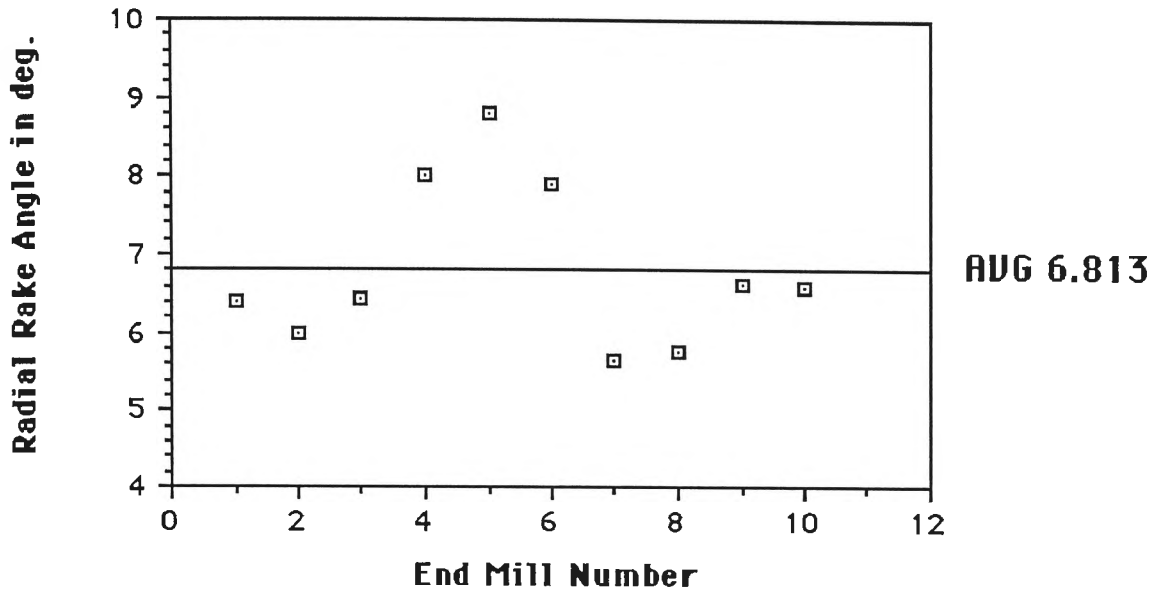

Figure 4.21 Variations of Radial Rake Angle Observed in 16 mm End Mills.

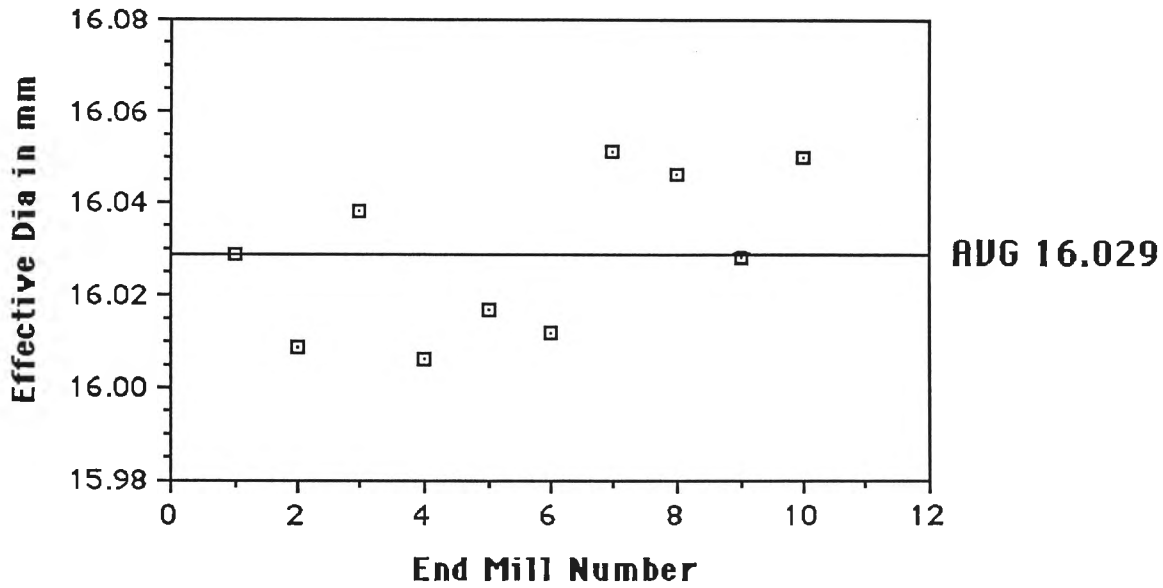

Figure 4.22 Variations of Effective Diameter Achieved Using 16 mm End Mills.

4.4 Comments and Discussions

Before commencing the discussion about the measurement results found in the present work, the author feels necessary to clarify the measurement procedure adopted in this work and its effectiveness. Present work was carried out using a general purpose co-ordinate measuring machine (CMM). In taking measurements of various tool elements using the CMM, different points on the tool are probed and the required feature (i.e. length, angle, etc.) is calculated either by using the CMM software or by using off-line calculations. Details of the CMM used in this work are given in Chapter 3. The repeatability of measurements of this CMM is ± 7 microns [130].

In Table 4.3 and 4.4, it can be seen that for some elements the repeatability of measurements (worst case) is fairly good, whereas for some other elements the repeatability of measurements is comparatively high (worse). For example in Table 4.3, for shank diameter the repeatability of measurements is ± 8 microns, whereas for drill diameter the repeatability of measurement is ± 18 microns. This is due to the very complex shape (geometry) of the drill point which was very difficult to probe with some points accurately using the CMM. The author found this as a major problem with the CMM measurement. For some elements where the values of repeatability of measurements are high compared with the element measured (such as web thickness, relative lip height, etc.), other method of measurement with better repeatability (e.g. optical comparator) must be applied.

Findings of present work can be now summarized under three headings:

(1) Tolerance Limits

(2) Variations in Cutting Tool Dimensional Features

(3) Effective Tool Diameter

4.4.1 Tolerance Limits

It is surprising to note that in some cases the tolerance bands specified in the standards are very wide (e.g. tolerance band of 0.076 mm for cutter diameter of 16 mm end mills). Tolerance band is important because of its direct effects on machining accuracy. It is also noted that substantial differences do exist among different national and international standards [141], [142], [143], [145] for the same cutting tool. Without going into much details, the differences between Australian Standard AS 2438 - 1981 and American Standard ANSI B94.11M-1979 for twist drills are listed in Table 4.9. It is also noted that some of the geometric elements of twist drills (e.g. relative lip height) are not controlled at all by the Australian Standard. But as explained before, the relative lip height is very important from the accuracy point of view. For general interests, diagrams for run-out tolerance and permissible relative lip height, specified in German Standard DIN 14412 [145] is given in Figure4.23. In this study the shank shapes were studied and plotting of the results are given in Figure 4.24 (for drills) and Figure 4.25 (for end mills). Shapes of two tools from each group were studied. Shank run-out is important , because together with the effect of the tool holding method it produces misalignment between the tool axis and the theoretical axis of the machine.

4.4.2 Variations in Cutting Tool Dimensional Features

Large variations in cutting tool dimensional features were observed in this study. As predicted before, the ranges of variations in different dimensional features found in this study were shorter than those observed by Galloway. (Because Galloway studied drills of different makes, whereas in this study tools of only one make were included).

Although in most cases the dimensional features were within the specified tolerance limits, a shift of average line towards the tolerance limits is found. The reason may be

Concentricity tolerance Tr

The concentricity tolerance Tr of the twist drills is calculated from the formula:

$$Tr = 0{,}03 + 0{,}01 \frac{l}{d}$$

where l is the overall length of the drill and d is the diameter.

Remark:
The test value of the diagram provide a statistical safety of 90%.

Test apparatus and test position according to instructions VDI 3331, sheet 1, paragraph 4.8, comma b-c.

Diagram for Run-out tolerance Tr

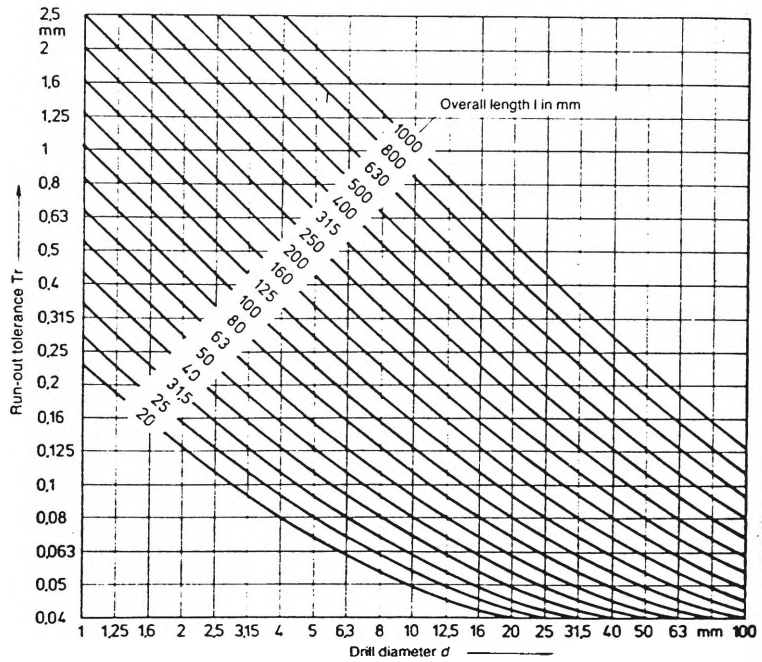

Permissible lip height difference $\Delta_{s\,zul}$ in mm

The values of the diagram provide a statistical safety of 90%. They are calculated from the formula:

$$\Delta_{s\,zul} = \pi\, d\, \frac{\delta}{360} \tan\alpha_x + 0{,}005$$

where d is the drill diameter in mm, δ is the max. deviation of the division in degrees and α_x is the side clearance angle in degrees.

It's accepted that:
for d = 1 mm $\delta = 3°$ $\alpha_x = 20°$
for d = 100 mm $\delta = 4°$ $\alpha_x = 8°$

Test apparatus and test position according to VDI instructions Nr. 3331, sheet 1, paragraph 4.3, comma c.

Diagram for permissible lip height difference $\Delta_{s\,zul}$

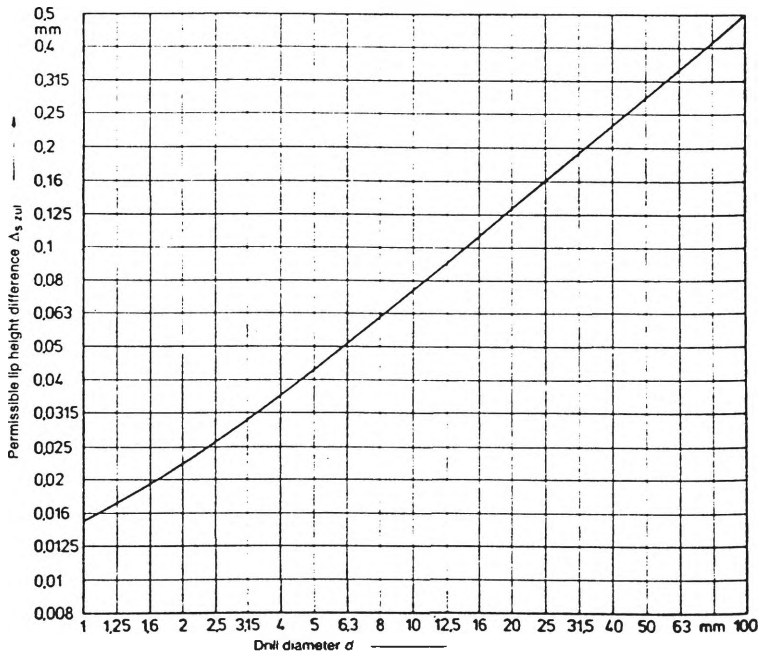

Figure 4.23 Diagrams for Runout Tolerance and Permissible Relative Lip Height Specified in DIN 1412 for Twist Drills [145].

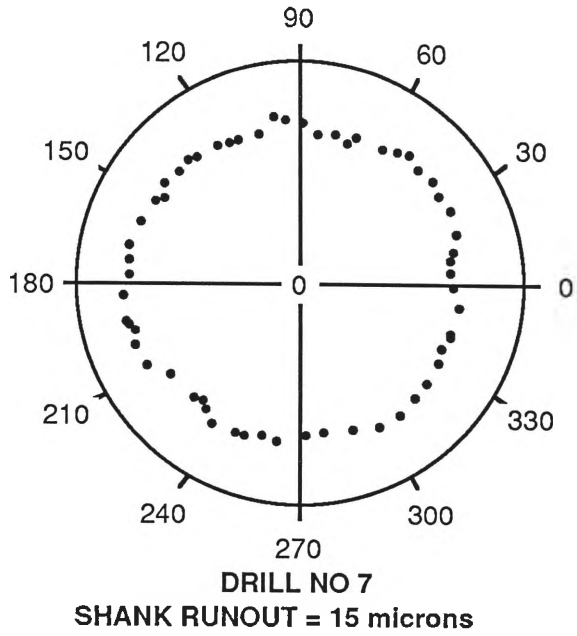

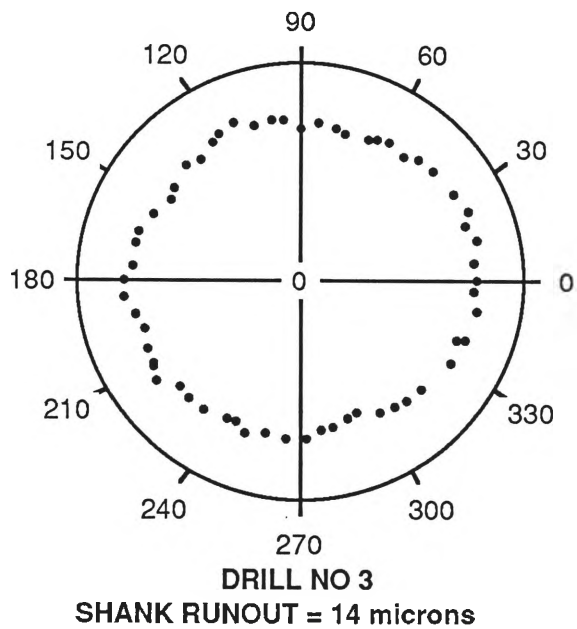

Figure 4.24 Shapes of Twist Drill Shank Cross-Sections.

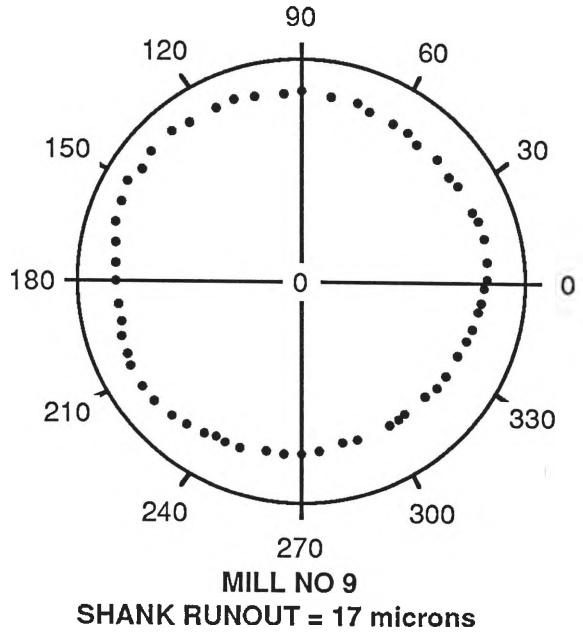

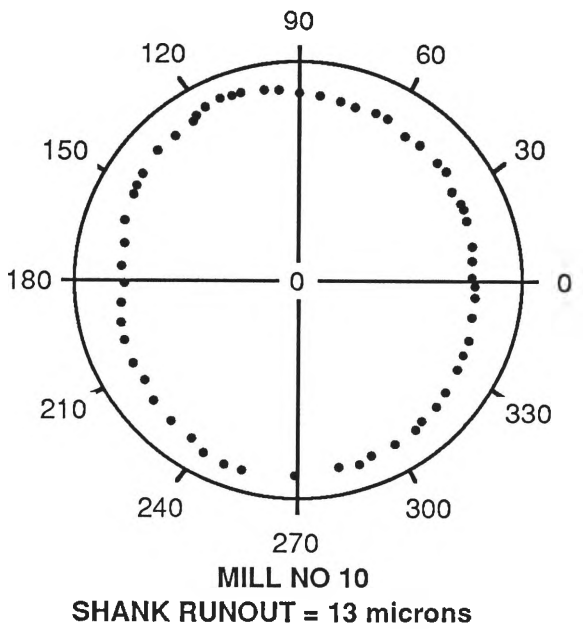

Figure 4.25 Shapes of End Mill Cross-Sections.

that, each manufacturer of the tools has his target value (or band) within the tolerance limits and generally tool manufacturers put an extra emphasis on tool stiffness and in doing so, they often choose values for general purpose tools same as for heavy duty tools. The variations of each element contributes to the overall variation, which is practically unpredictable; thus some method should be applied to find the effective tool diameter.

Element	AS 2438 - 1981		ANSI B94.11M - 1979	
	LTL	UTL	LTL	UTL
Drill Diameter (mm)	- 0.027	0	- 0.025	0
Shank Diameter (mm)	X	X	- 0.114	+ 0.013
Back Tapper (mm/mm)	0.0005	0.001	0.0002	0.0009
Overall Length (mm)	- 3.000	+ 3.000	- 3.200	+ 3.200
Flute Length (mm)	- 3.000	+ 3.000	- 3.200	+ 3.200
Point Angle (degrees)	X	X	- 5	+ 5
Relative Lip Height (T.I.V.)	X	X	0	0.012
Centrality of Web (T.I.V.)	X	X	0	0.127
Flute Spacing (T.I.V.)	X	X	0	0.254

X = no tolerance limit specified; T.I.V. = Total Indicator Variation

Table 4.9 A Comparison of Australian Standard And American Standard for 12 mm Twist Drill (Parallel Shank, Jobber Series).

4.4.3 Effective Tool Diameter

Effective tool diameter is the **actual** tool diameter during machining. As it very difficult to predict the effective tool diameter correctly and the author suggests to determine it by machining some holes or slots using the same tools to be used in machining, prior to actual machining operation. This technique is in use in the industry for conventional machining for long time. In CNC machining this method can be applied successfully. The knowledge of hole oversize should be applied in the design stage, as no comparison technique can be applied after machining.

5.0 THE EFFECT OF END MILL DEFLECTION ON MACHINING ACCURACY

5.1. Introduction

End milling is one of the most universal metal removal processes used in today's industry. With the advent of NC machine tools, the use of end mills has grown tremendously, particularly in the aerospace and turbomachine industries. Moreover, in recently adopted "near net shape"* manufacturing where the finishing operation is the only machining operation, the use of end mills has become quite significant. End mills have cutting edges on both their faces and their peripheries, which make them capable of performing face milling and peripheral milling either separately or simultaneously, as desired. Due to a number of different types of machining possible, end mills are often called as versatile tools.

As reported by some researchers [146], [147], [148], [149], the major problem in the use of end mills is its deflection which causes a geometric error on the machined surface. The preliminary results presented in Chapter 3 also showed some geometric errors associated with the variation in geometry of the work piece end milled surface. The resulting work surface configuration is consistent with the end mill deflection. A further study on end mill deflection was undertaken in the present thesis work to reduce it to its minimum possible value.

5.2 Factors Affecting End Mill Deflection

The end mill can be considered as a cantilever beam, rigidly gripped by the tool holder. As the cutting force is applied very near to the non-supported end, the end mill deflects

* In "near net shape" manufacturing, components are forged or cast to their possible near shape and then machined to their final shape in a minimum number of passes (most often in only one pass).

from its normal position. In its simplest form the end mill deflection is shown in Figure 5.1.

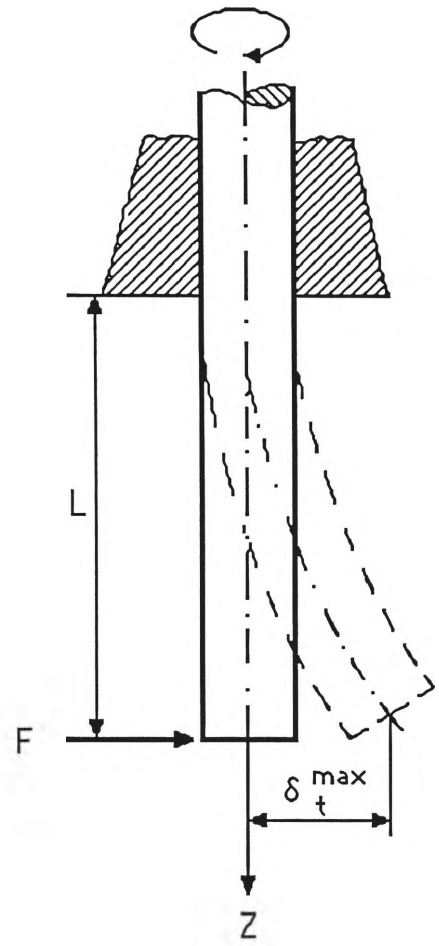

Figure 5.1 End Mill Deflection.

In this case, the equation of elastic curve and maximum tool deflection can be estimated using the following formulas:

$$\delta_t(z) = \frac{F}{6EI}(z^3 - 3Lz^2) \tag{5.1}$$

$$\delta_t^{max} = |\delta_t(L)| = \frac{FL^3}{3EI} \tag{5.2}$$

where

δ_t = tool deflection

F = cutting force

L = tool overhang

E = modulus of elasticity

I = moment of inertia of the end mill

The moment of inertia of the end mill is generally calculated using the following formula [146], [158]:

$$I = \frac{D^4}{48} \tag{5.3}$$

where

D = cutter diameter

Substituting Equation (5.3) in (5.2)

$$\delta_t^{max} = \frac{16FL^3}{ED^4} \tag{5.4}$$

From Equation (5.4) it can be seen that the tool deflection can be reduced by (a) increasing modulus of elasticity of the cutter; (b) reducing tool over hang; (c) increasing diameter of the cutter; and (d) reducing the cutting force.

5.2.1 Modulus of Elasticity of End Mills

The most important material property which influences the tool deflection is the modulus of elasticity of the tool. Modulus of elasticity of the tool should be increased to its highest possible level, as a higher modulus will result in a lower deflection. But like strength or hardness, elastic modulus can not be increased by heat treatment or by any other similar method, because the elastic modulus depends on the fundamental atomic structure of the material whereas strength or hardness are very dependent on small percentages of elements which do not affect the modulus. It is interesting to note that all steels,

regardless of their alloy contents, heat treatment or hardness, have approximately the same modulus of elasticity. So an increase in modulus of elasticity can be achieved only by using better materials such as tungsten carbide, which has approximately a three times higher modulus of elasticity than steel. (See Table 5.1)

MATERIAL	MODULUS OF ELASTICITY, E	
	(psi)	(GPa)
Aluminium	9,000,000	62
Cast iron	14,000,000*	96*
Steel	29,000,000	200
Tungsten Carbide	85,000,000	585

*varies widely

Table 5.1 Modulus of Elasticity of Some Common Materials [150].

Mannan [151] has done a comparative study of the end milling cutters of two different tool materials (cemented carbide and high speed steel) with an evaluation of these cutters' performance with respect to static deflection, vibration and surface finish. As expected, his results showed that solid cemented carbide end mills have superior performance compared to the high speed steel end mills with respect to static deflection and forced vibrations.

5.2.2 Tool Overhang

Tool deflection can be reduced by reducing tool overhang. So as a rule, to reduce end mill deflections tool overhang should be kept to a minimum. But for a user, besides selecting the tool type (short, normal, etc.), there is very little choice left, to achieve reduction of tool overhang.

5.2.3 Cutter Diameter

Cutter diameter has the greatest effect on tool deflection, as it appears with a power of four in Equation (5.4). In other words, if the cutter diameter is doubled, tool deflection is reduced sixteen times (if other parameters remain constant). But often an increase in diameter is restricted by the geometric configuration of the component to be machined. Moreover, the increase of diameter may be found to be uneconomical if the number of teeth remains the same, as it will increase machining time. This is because milling is an intermittent cutting process and each tooth cuts metal only a portion of the time when the cutter is engaged with the workpiece.

5.2.4 Cutting Force

The tool deflection can be reduced by reducing the cutting force. But as the cutting force is proportional to metal removal rate (see Equations (5.5) - (5.8) below, a reduction of cutting force will reduce metal removal rate, which is uneconomical.

$$HP_S = K\ U\ F \tag{5.5}$$

where

HP_S = power required at spindle

K = conversion factor

U = cutting speed

F = cutting force

Also $$HP_S = Q\ P\ C_{cf} \tag{5.6}$$

where

Q = metal removal rate

P = unit power factor

C_{cf} = correction factor

$$C_{cf} = C_{sp}\, C_t\, C_r\, C_{tw} \tag{5.7}$$

C_{sp} = cutting speed correction factor

C_t = chip thickness correction factor

C_r = rake angle correction factor

C_{tw} = tool wear correction factor

Combing Equations (5.5) and (5.6)

$$F = C\frac{Q}{U} \tag{5.8}$$

where

$$C = \frac{P\, C_{cf}}{K} = \text{Const.}$$

However, from the "quality first" point of view a reduction in metal removal rate may be justified in order to achieve better machining accuracy. For milling operations MRR is calculated using Equation (2.1) (which is described in Chapter 2).

$$Q = S_m\, b\, d \tag{2.1}$$

where

Q = metal removal rate

b = width of cut (axial depth of cut)

d = depth of cut (radial depth of cut)

$$S_m = S_t\, K_t\, N \tag{5.9}$$

$$U = \pi\, D\, N \tag{5.10}$$

where

S_t = feed per tooth

K_t = number of teeth

N = spindle speed

D = cutter diameter

Substituting Equations (5.9) and (5.10) into (2.1)

$$Q = \frac{S_t K_t U b d}{\Pi D} \tag{5.11}$$

Substituting Equation (5.11) into (5.8)

$$F = \frac{C S_t K_t b d}{\Pi D} \tag{5.12}$$

By further substituting (5.12) into (5.4), we obtain,

$$\delta_t^{max} = \frac{16 C S_t K_t b d L^3}{\Pi D E D^4} \tag{5.13}$$

After simplification

$$\delta_t^{max} = \frac{C_1 S_t K_t b d L^3}{E D^5} \tag{5.14}$$

where

$$C_1 = \frac{16 C}{\Pi} = \text{Const.}$$

Equations (5.12) and (5.14) give the mathematical expressions which can be used to calculate the cutting force and maximum tool deflection. It is interesting to note that in these equations the cutting speed does not appear, which means that the cutting force in

end milling operation is not influenced by the cutting speed* (see Figure 5.2). Even then, the selection of cutting speed require a careful consideration, as the cutting speed has greater effect on tool life than the depth of cut and feed rate. Equation (5.14) shows the importance of the cutter diameter, as a 15% increase in cutter diameter will reduce the tool deflection by 100%. From Equation (5.14) it also becomes clear that for in-process control systems, feed is the only variable which can be manipulated easily. For this reason a number of researchers [70], [75], [152] have used feed as the controlled variable in their ACS system for milling.

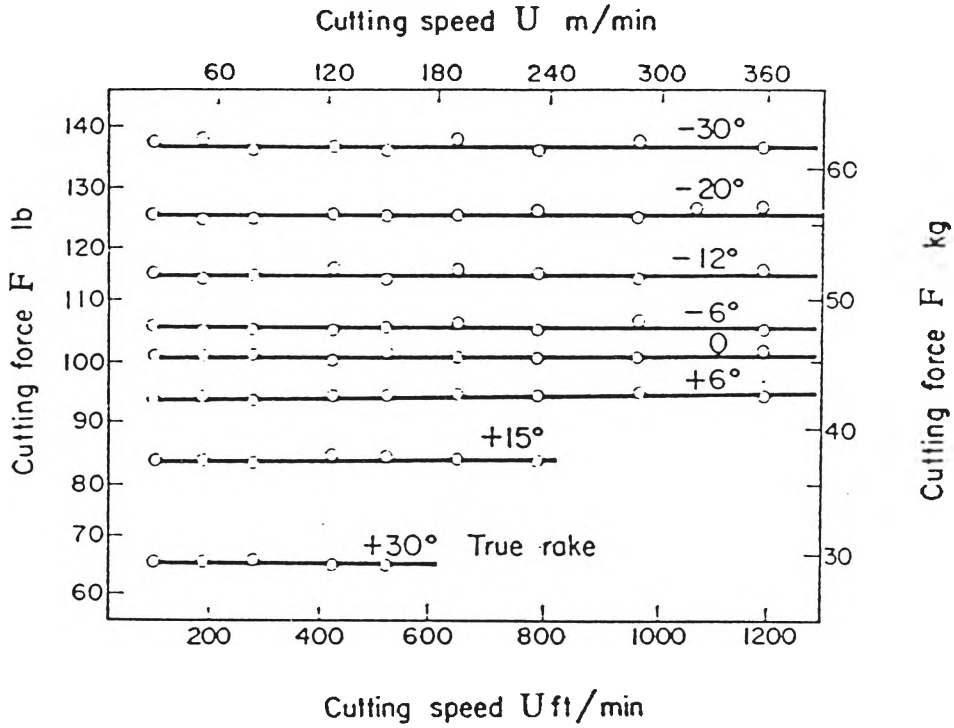

Figure 5.2 Independence of the Cutting Force F from Cutting Speed U in Milling [131].

The end mill deflection model illustrated in Figure 5.1, is a text book situation and in reality the problem is far more complex. This is because, in milling, the cutting force is continuously changed not only in magnitude (see Figure 4.3) but also in its direction and point of application.

---

* In reality cutting force may be slightly influenced by the cutting speed, as in Equation (5.13) the constant C_s (cutting speed correction factor) is a function of cutting speed. For most of the common machining materials, when the cutting speed is increased C_s is reduced slightly.

A number of researchers [153], [154], [155], [156], [157], [158], [159], [160] have studied the cutting force in end milling and they have developed different models to represent the cutting force and its components. Researchers showed much interest in cutting force calculation in milling because this is important not only from the deflection point of view, but also from the power consumption point of view. A study of cutting force is also necessary for the evaluation of cutter breakage.

There are three force components (of the cutting force) acting on the individual end mill tooth during cutting: tangential force (F_t), radial force (F_r) and axial force (F_a). It is customary to resolve those force components in X, Y and Z directions, where X is the direction parallel to feed, Y is the direction perpendicular to X (in the same plane) and Z is the direction perpendicular to both X and Y. The force situation is different depending on whether up or down milling* (see Figures 5.3 and 5.4) is being used.

In up milling:

$$F_x = F_t \cos\phi + F_r \sin\phi \tag{5.15}$$

$$F_y = F_r \cos\phi - F_t \sin\phi \tag{5.16}$$

$$F_z = F_a \tag{5.17}$$

In down milling:

$$F_x = F_r \sin\phi - F_t \cos\phi \tag{5.18}$$

$$F_y = F_r \cos\phi + F_t \sin\phi \tag{5.19}$$

$$F_z = F_a \tag{5.20}$$

---

* Depending on the relative motion of the cutter and feed, milling operations are classified as up or down milling. In **up milling** (also known as **conventional milling**), the peripheral velocity of cutter is in the opposite sense to the feed direction. In **down milling** (also known as **climb milling**), cutter velocity and the feed velocity are in the same sense.

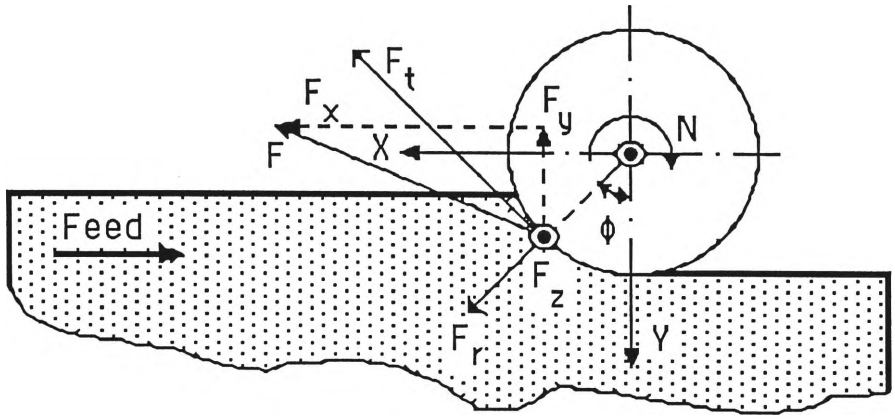

Figure 5.3 Forces in Up Milling.

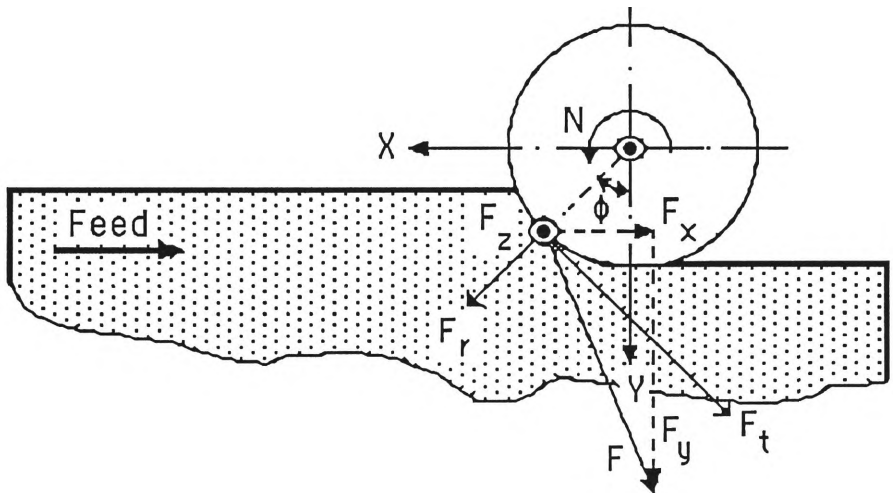

Figure 5.4 Forces in Down Milling.

Tangential force (F_t) can be calculated using the following relationship [153]:

$$F_t = K\,b\,h = K\,b\,S_t \sin\phi \tag{5.21}$$

where

b = width of cut

h = chip thickness

S_t = feed per tooth

ϕ = angular position of the cutting edge with respect to Y axis

K = "specific force", a constant which depends on the material of the workpiece and on the geometry of the tool as well as on the average chip thickness.

In normal operations tangential force is the highest of the three cutting force components. Radial and axial components are generally calculated as proportional to tangential force.

$$F_r = \eta_r\, F_t \tag{5.22}$$

$$F_a = \eta_a\, F_t \tag{5.23}$$

Values of η_r and η_a are taken up to 0.5, although there is no general agreement among the researchers about these constants. (see Table 5.2)

Author	η_r	η_a
Tlusty [153]	0.3	-
Yellowley [154]	0.2 - 0.5	-
Ber et al [155]	0.4	0.3

Table 5.2 Values of η_r and η_a as Suggested by Different Authors.

The reason may be that force components are influenced by a number of other factors, such as lead angle, rake angle, etc.

From the end mill deflection point of view, force component F_y is important, as this is the component responsible for producing the geometric error on end milled surface in the direction parallel to the cutter axis. The effect of end mill deflection in the feed direction is overridden by the movement of the cutter along the feed itself.

While cutting with a depth of cut d, the angle ϕ starts with $\phi = 0°$ and ends with an angle $\phi = \phi_2$. The angle ϕ_2 depends on the relative position of the cutter centre and workpiece, which is dependent on cutter diameter and radial depth of cut and its maximum possible value is 180°. But up and down milling exist in their pure form only when the cutter centre-line does not intersect the workpiece (i.e. cutter radius R is greater than depth of cut d) and in that case angle $\phi<90°$ and $\cos\phi>0$ and $\sin\phi>0$. From Equations (5.15) - (5.20) it can be noticed that in down milling, force components F_r and F_t are added to form F_y, whereas in up milling these force components are subtracted to form F_y. Depending on ϕ this force component may also become negative in up milling, whereas in down milling F_y is always positive. From this it can be deduced that in down milling the expected end mill deflection is more and the cutter always deflects away from the workpiece, which results in a positive error. In up milling the tool deflection is less and the cutter may deflect into the workpiece (depending on tool diameter, depth of cut etc), which may produce a negative error. The force component F_x has an opposite tendency, i.e., in up milling F_x is larger, as F_r and F_t are added to form it, and in down milling F_x is less. The force component F_x is important from the clamping point of view and in up milling attention must be paid to ensure proper clamping of the workpiece. This problem is more serious in horizontal spindle machines, as in up milling the cutting force tends to lift up the workpiece off the table* .

* The name up milling has come from this.

Based on the mechanics of cutting approach, Armarego and Despande [157] proposed a cutting force model which provides deeper understanding of the cutting action and average cutting force components in end milling. Their study showed that average cutting force components are directly proportional to the number of teeth, width of cut and feed per tooth. It has also shown that an increase in depth of cut, slightly increases all force component (F_x, F_y and F_z) and at lower depths of cut the values of the force component F_y shows a change in direction.

In our study of end mill deflection no attempt has been made to calculate the end mill deflection using an analytical method, because almost all of the cutting force models available use some empirical constants, and proper determination of them needs further experimental work. It is more convenient to trace the end milled surface using a co-ordinate measuring machine (CMM) and from there to determine the end mill deflection directly without calculating any force. On the basis of the initial deflection values, measures can be taken utilizing the existing knowledge about end mill deflection discussed in previous paragraphs.

5.3 Previous Work on End Mill Deflection

Although the phenomenon of end mill deflection has been known to researchers for some time, there is very little work reported in the literature on this topic. As end mills can be used in a number of machining processes (peripheral milling, face milling, slotting, and their various combinations), each end mill deflection model may be different and should be studied separately. Our study will be restricted to the two types of end milling used in machining of our test piece, viz peripheral milling and combined milling (combination of peripheral and face milling).

Tipnis [146] wrote about end mill deflection without going into much details. The dimensional accuracy of end milled surface depends on the amount of end mill deflection

and Tipnis gave the following figure (see Figure 5.5) to demonstrate it. In our case we have a rigid workpiece with small-diameter cutter (right most example in Figure 5.5). Tipnis suggested that the point of application of cutting force can be regarded as the middle of the width of cut (axial depth of cut).

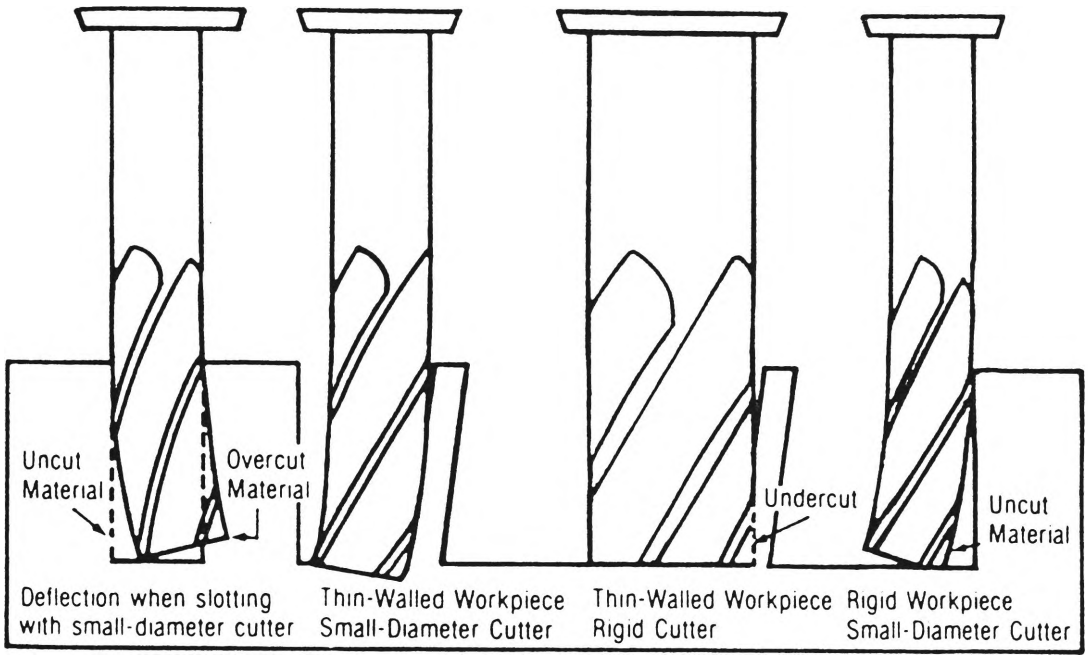

Figure 5.5 Modes of End Mill Deflections [146].

Kline et al [147] studied surface errors generated in end milling both analytically and experimentally. Their prediction of surface error was based on the prediction of cutting force, end mill deflection and workpiece deflection. The cutting force was predicted by using a "mechanistic model". End mill deflection was calculated assuming the end mill to be a cantilever beam. For the prediction of workpiece deflections a finite element method was used. To verify their predicted results a number of machining experiments were performed. Surface errors on machined work pieces were measured using a dial indicator. They did not supply any data about the accuracy of dial indicator used. But as it is common knowledge, dial indicators are not sensitive enough to trace surface errors of very small magnitudes. Their experiments included only down milling, so no comments could be made about the validity of surface predictions in up milling. In

general, the predicted surface error was shown to be in agreement with the experimental results. Effect of cutter runout on surface generation was also studied and reported.

De Vor [148] also examined the surface error caused by end mill deflection. The surface error was predicted by using similar methods to those used by Kline et al [147]. With high quality (i.e. less surface error), De Vor added high productivity (i.e. minimum machining time) in the objective function. It was suggested that surface errors in end milling can be eliminated in two passes. In the first pass entire amount of material is removed. The finish cut (so called "float cut") was applied to remove only the surface error produced by the roughing. To reduce the machining time a range of cutting parameters, cutter geometry, and workpiece geometry were also studied. It was found that the minimum time solution calls for the rough cut cutter radius to be as large as possible. The method suggested by De Vor can **only** remove positive surface errors, typical in down milling.

Fujii and Iwabe [161] used a dwell function of the controller of CNC machine to reduce the surface error caused by end mill deflection. The dwell function basically controls the feed and provides a short time stop of feed. They showed, by selecting proper dwell time, surface error generated by end mill deflection can be eliminated in one pass. (see Figure 5.6). The selection of proper dwell time is important in this method, because it is found to be effective only when proper dwell time is selected. This method is also capable of reducing positive surface errors found in down milling **only.**

5.4 Present Work

In the present work it is accepted that the geometric error on the machined workpiece in the axial direction of the end mill is caused by end mill deflection and the profile of the machined workpiece in that direction in some way represents the end mill deflection curve at that position. Profiles of the machined workpiece were traced using the Co-

ordinate Measuring Machine (CMM) at some fixed intervals* (40 mm in X direction and 25 mm in Y direction) along the feed direction. To trace the profile at a fixed position, the CMM axis was locked at that position and points were probed at some interval (1mm) in the Z direction (see Figure 5.7). The difference between the maximum and minimum of the value measured (value of Y as shown in Figure 5.7), is the geometric error. As all measurements are relative, the mean value of all points probed on the same surface was subtracted from the real values. This means, the values used for profile plotting are the deviations from the mean value. The mean value taken does not necessarily indicate the mean value of the points probed from the profile tracing. The mean value accepted is the mean value of randomly probed points on that surface. This type of probing is more realistic as it covers more area and the mean value determined in this way was accepted as the real value in dimensional analysis. (see Appendix F)

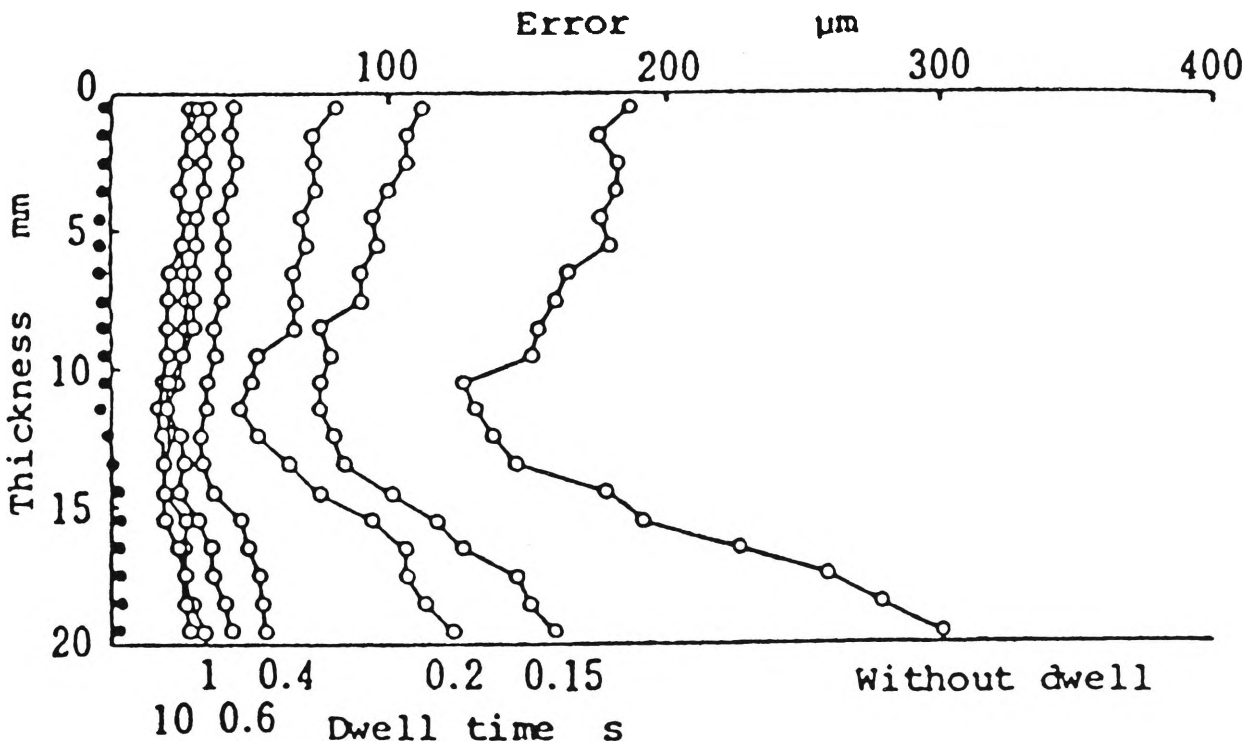

Figure 5.6 Influence of Dwell Time on Shape Error [161].

* Positions at the corners of the workpiece (i.e. x = 0 mm, x = 200 mm, y = 0 mm and y = 75 mm) were taken at the nearest possible close position (normally about 5 mm) apart from those theoretical values.

Measurement results of six components are considered for comparison. Details of cutting condition used in machining those six components are given in Table 5.3. As mentioned before, in the present work the end mill deflection was studied in two phases, viz peripheral milling and combined (peripheral and face) milling.

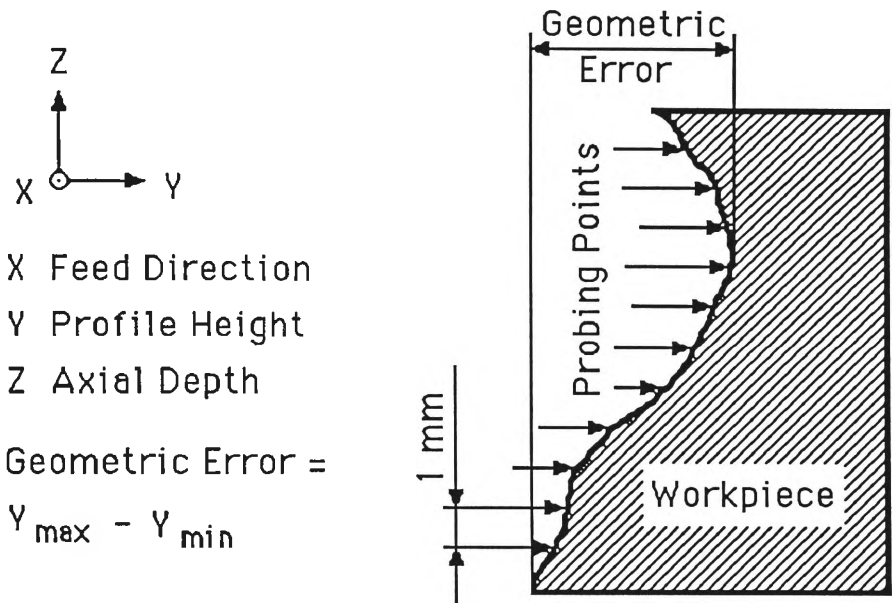

Figure 5.7 Surface Tracing of Workpiece Using CMM.

Part No	Type of Milling	Cutting Speed U (m/min)	Feed, S_m (mm/min)	Depth of Cut d (mm)
TP6	Down	126	125	1.0
TP11	Down	126	125	0.5
TP21	Down	126	62.5	1.0
TP22	Up	126	125	1.0
TP23	Up	126	62.5	1.0
TP24	Up	126	125	0.5

Table 5.3 Cutting Conditions Used in Finish Cut of Different Components.

5.4.1 Peripheral Milling

Peripheral milling was used to machine surfaces ABJI, CDLK, DAIL and BCJK of our test pieces (see Figure 3.5). A typical profile of the workpiece at a fixed position is given in Figure 5.8 and details of the profiles traced at different positions along the workpiece are given in Appendix K (Figure K.1). The profiles of the workpiece traced, closely resemble the expected end mill deflection curve. It is to be noted from Figure K.1 that, a pick (i.e. projection) is appearing at a fixed height (4 mm) all along the workpiece. It seems that those picks are not part of the end mill deflection curve and to verify this, all points probed for profile tracing, except the pick, are plotted in Figure 5.9. The curve of best fit of those points is in agreement with the expected end mill deflection curve, which justifies the assumption that the pick is not a part of the end mill deflection curve and is caused by some other factor such as the material nonhomogeniety.

In our study geometric errors are calculated at each position of profile tracing, which in some magnitude quantify the end mill deflection. But as explained in the previous paragraph, the pick value in profile tracing, which is not a part of the end mill deflection curve may change the waviness error data. So both situations are considered and the results are given in Tables 5.4 - 5.7. In these tables results in brackets represent the waviness error calculated by ignoring pick points, whereas results without brackets represent the real waviness error measured on machined components in the axial direction of the end mill. These geometric errors are illustrated in graphical form in Figures 5.10 - 5.17in comparison for several work specimen together. From these figures it can be seen that reduction of geometric errors in end milled surfaces is possible by reducing the feed and/or depth of cut.

The effects of feed, depth of cut and type of milling (i.e. up or down milling) were examined thoroughly. Typical examples of these effects are shown in Figures 5.18 - 5.22. (Full details are given in Appendix K).

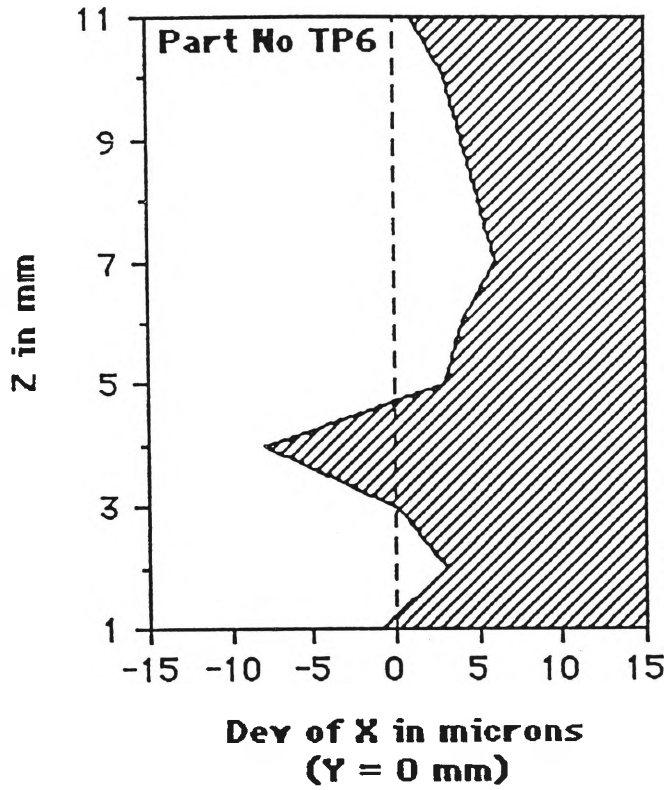

Figure 5.8 Effect of End Mill Deflection on the Profile of Machined Workpiece.

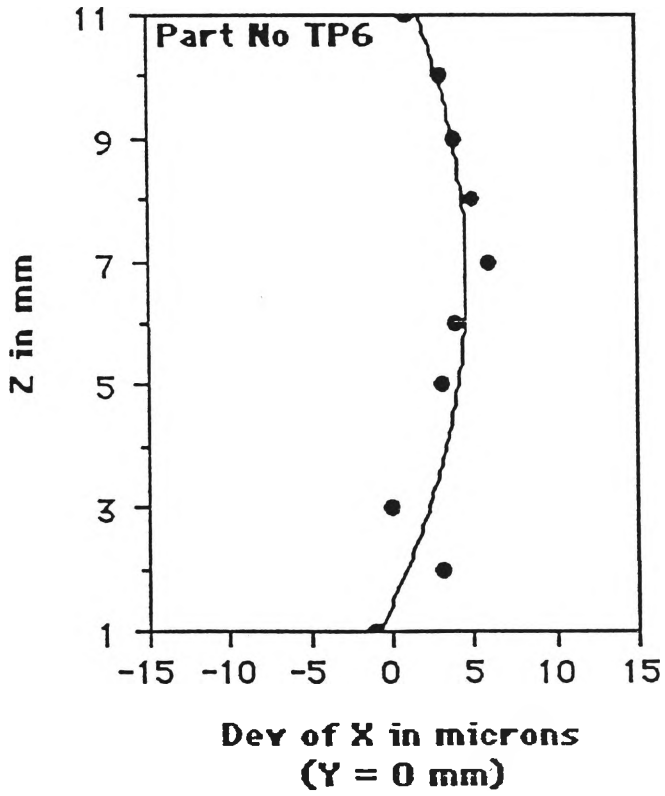

Figure 5.9 Curve of Best-Fit of the End Mill Deflection Curve.

Location	Surface ABJI: Geometric Error in microns					
X in mm	TP6	TP11	TP21	TP22	TP23	TP24
0	14 (12)	9 (7)	11 (6)	9	7	5
40	18 (16)	11 (9)	10 (6)	11	8	5
80	14 (14)	16 (10)	10 (9)	10	9	5
120	13 (12)	12 (6)	13 (12)	11	8	6
160	15 (15)	15 (9)	12 (9)	13	9	5
200	13 (11)	12 (7)	13 (7)	9	11	7

Table 5.4 Geometric Error Measured on Surface ABJI.

Location	Surface CDLK: Geometric Error in microns					
X in mm	TP6	TP11	TP21	TP22	TP23	TP24
0	17 (12)	8 (8)	8 (6)	9	10	7
40	18 (11)	14 (12)	10 (9)	13	9	8
80	15 (11)	11 (11)	9 (6)	12	9	9
120	16 (11)	11 (8)	10 (7)	12	9	6
160	13 (10)	14 (9)	8 (6)	15	12	10
200	13 (10)	8 (6)	12 (7)	13	13	7

Table 5.5 Geometric Error Measured on Surface CDLK.

Location	Surface DAIL: Geometric Error in microns					
Y in mm	TP6	TP11	TP21	TP22	TP23	TP24
0	14 (7)	9 (8)	9 (6)	11	12	7
25	13 (10)	8 (8)	9 (7)	13	9	8
50	17 (11)	7 (7)	11 (6)	16	8	6
75	14 (10)	8 (8)	9 (9)	15	8	7

Table 5.6 Geometric Error Measured on Surface DAIL.

Location	Surface BCJK: Geometric Error in microns					
Y in mm	TP6	TP11	TP21	TP22	TP23	TP24
0	10 (6)	11 (9)	12 (8)	11	8	7
25	9 (9)	8 (4)	10 (6)	10	10	7
50	17 (8)	13 (11)	9 (7)	9	6	5
75	16 (12)	12 (10)	11 (8)	11	8	7

Table 5.7 Geometric Error Measured on Surface BCJK.

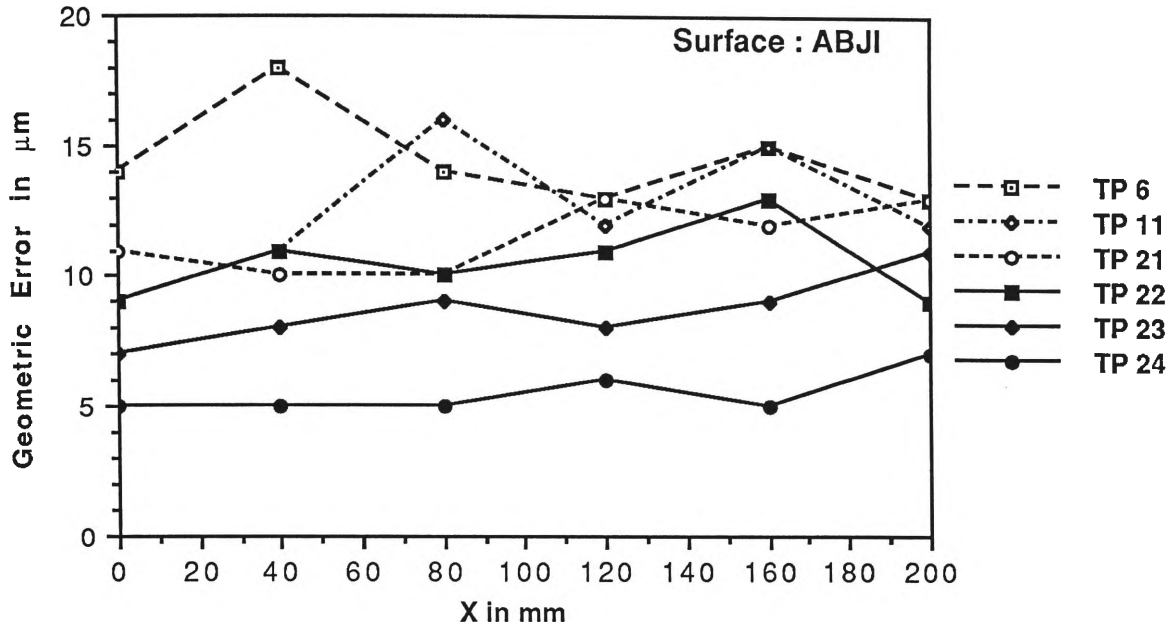

Figure 5.10 Geometric Error Measured on Surface ABJI.

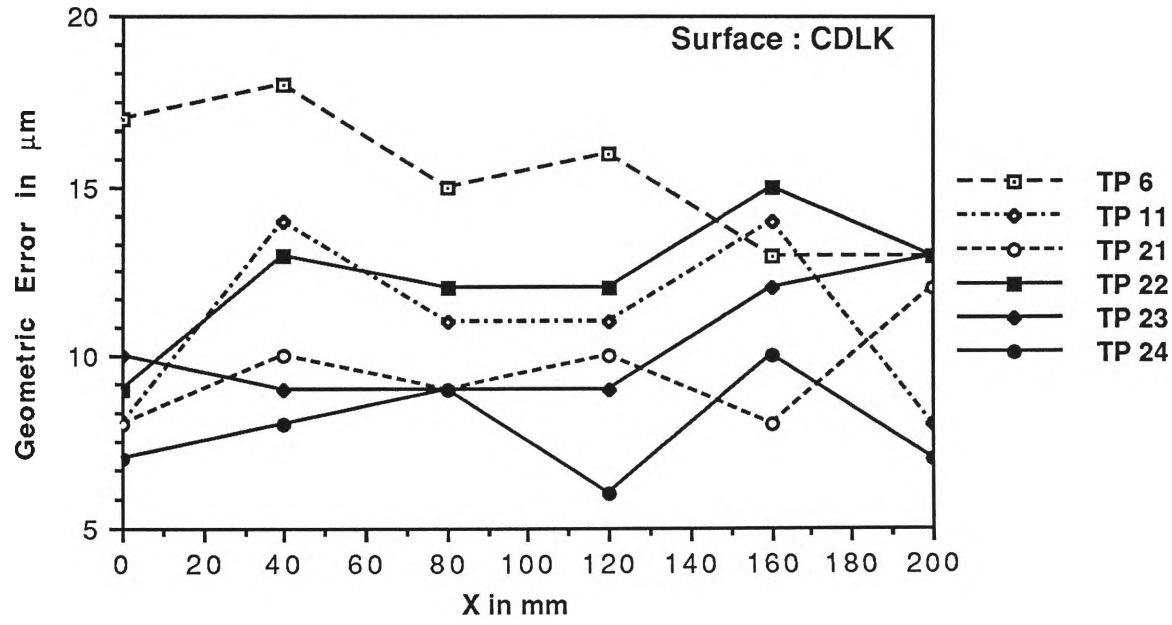

Figure 5.11 Geometric Error Measured on Surface CDLK.

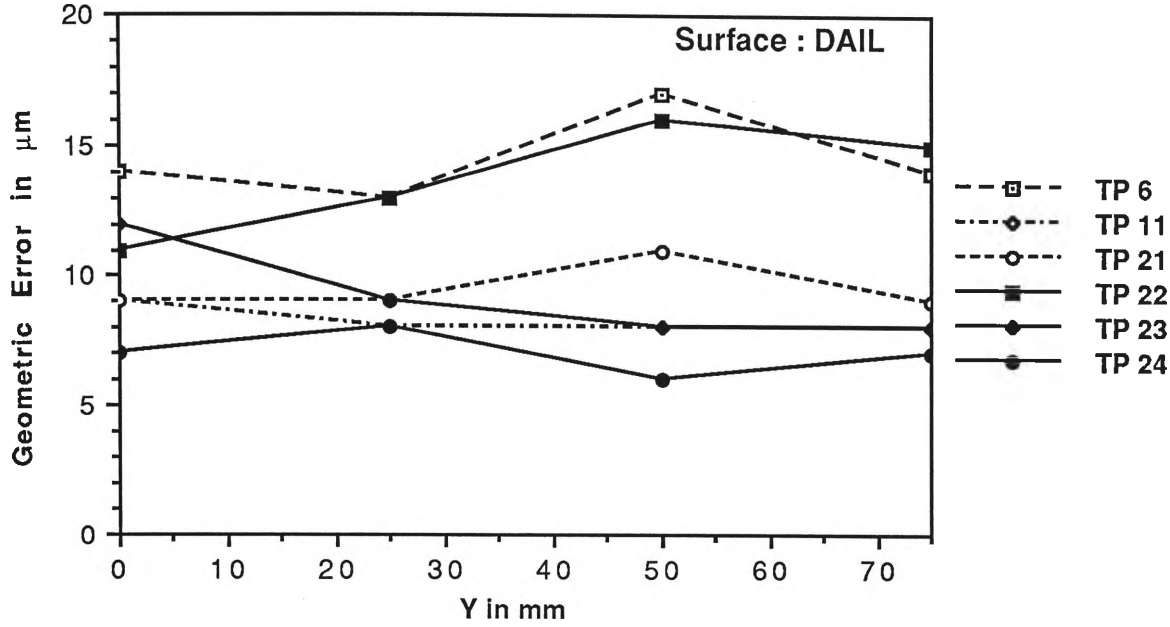

Figure 5.12 Geometric Error Measured on Surface DAIL.

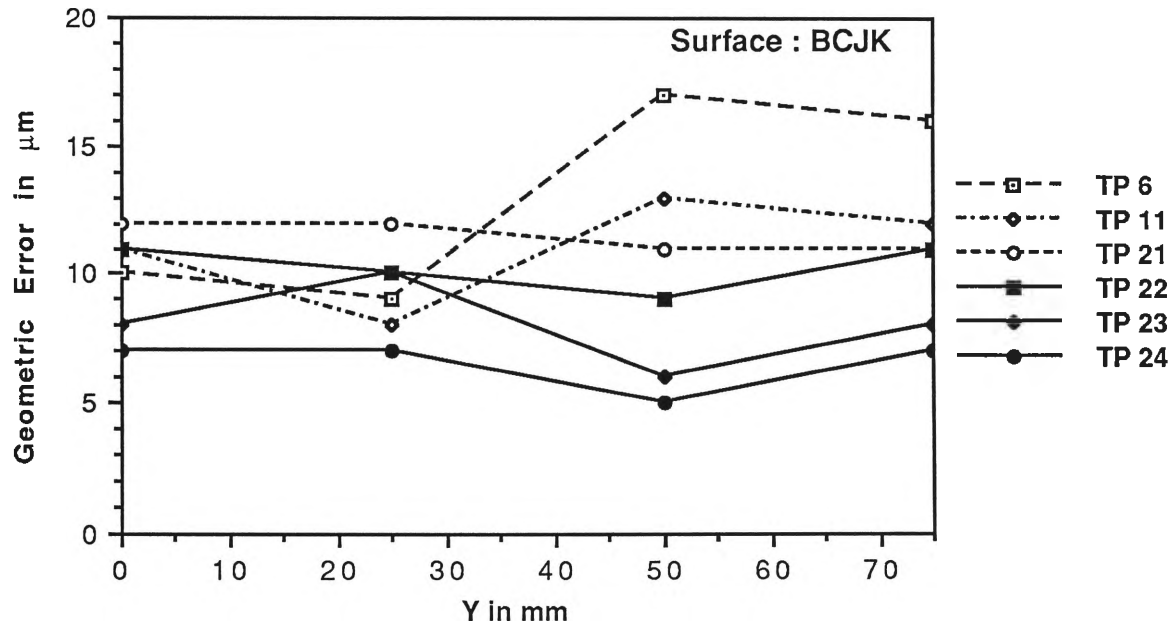

Figure 5.13 Geometric Error Measured on Surface BCJK.

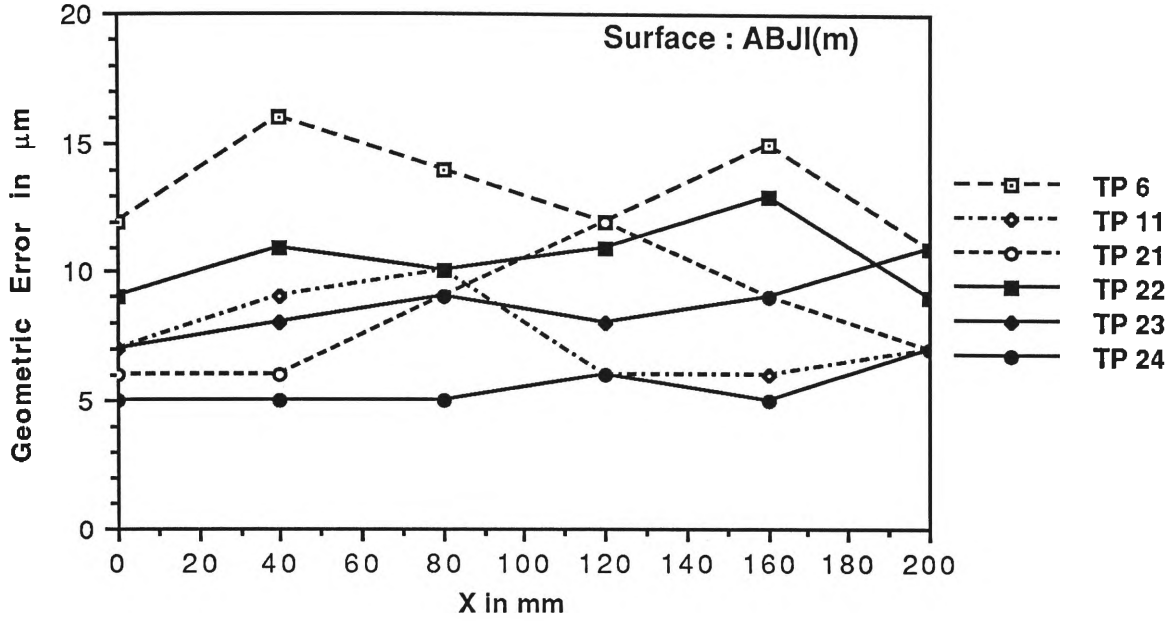

Figure 5.14 Geometric Error Measured on Surface ABJI (Modified).

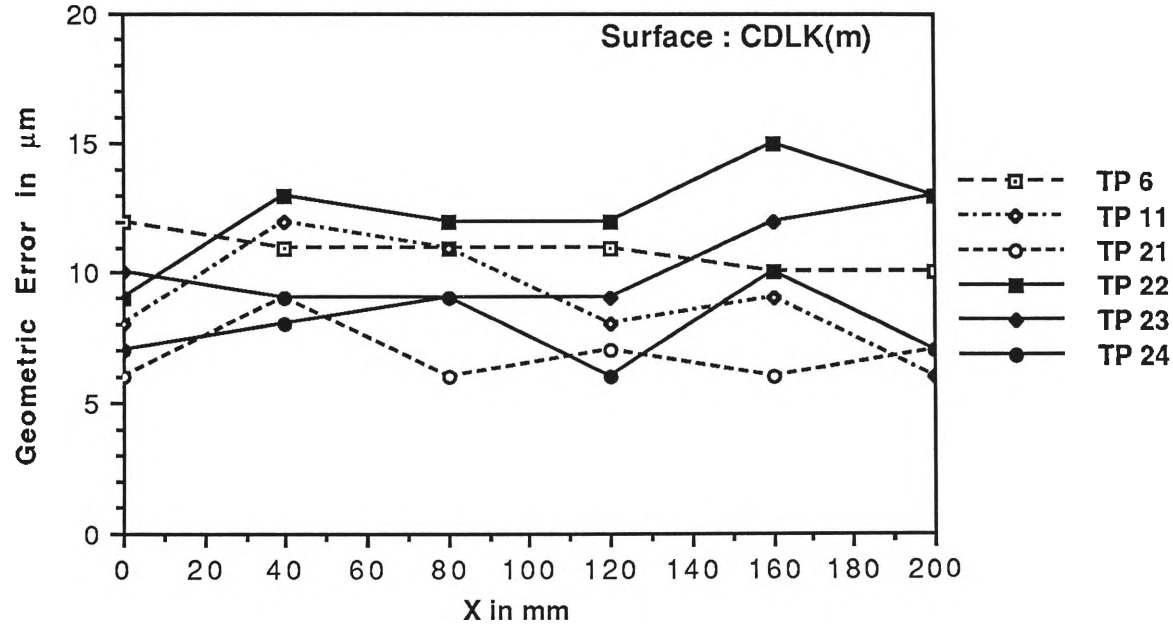

Figure 5.15 Geometric Error Measured on Surface CDLK (Modified).

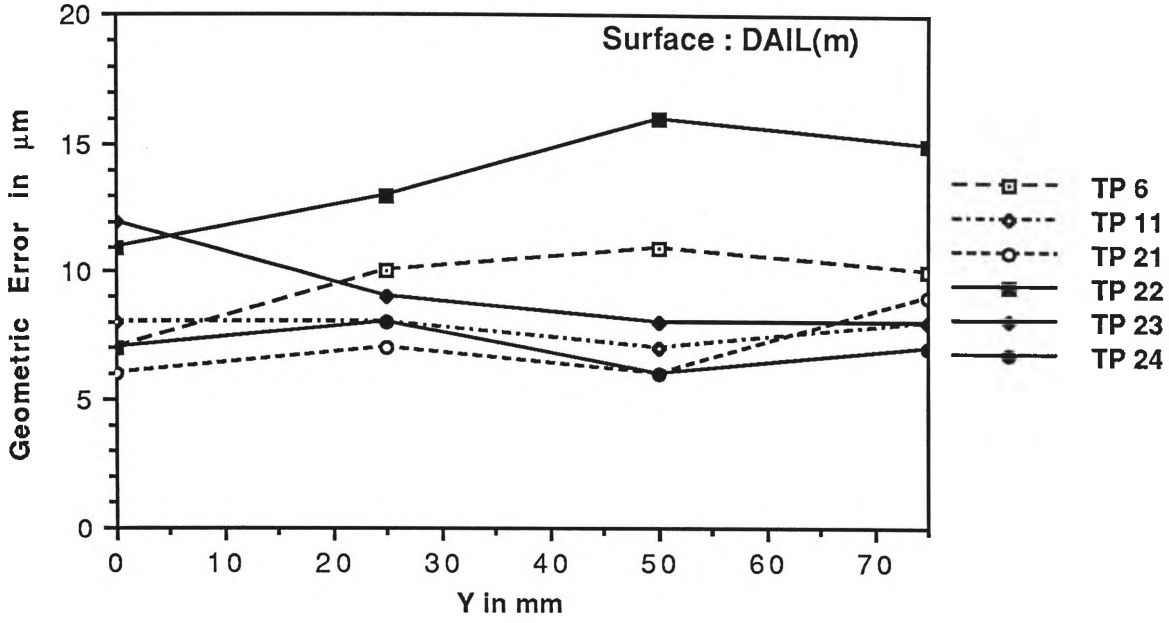

Figure 5.16 Geometric Error Measured on Surface DAIL (Modified).

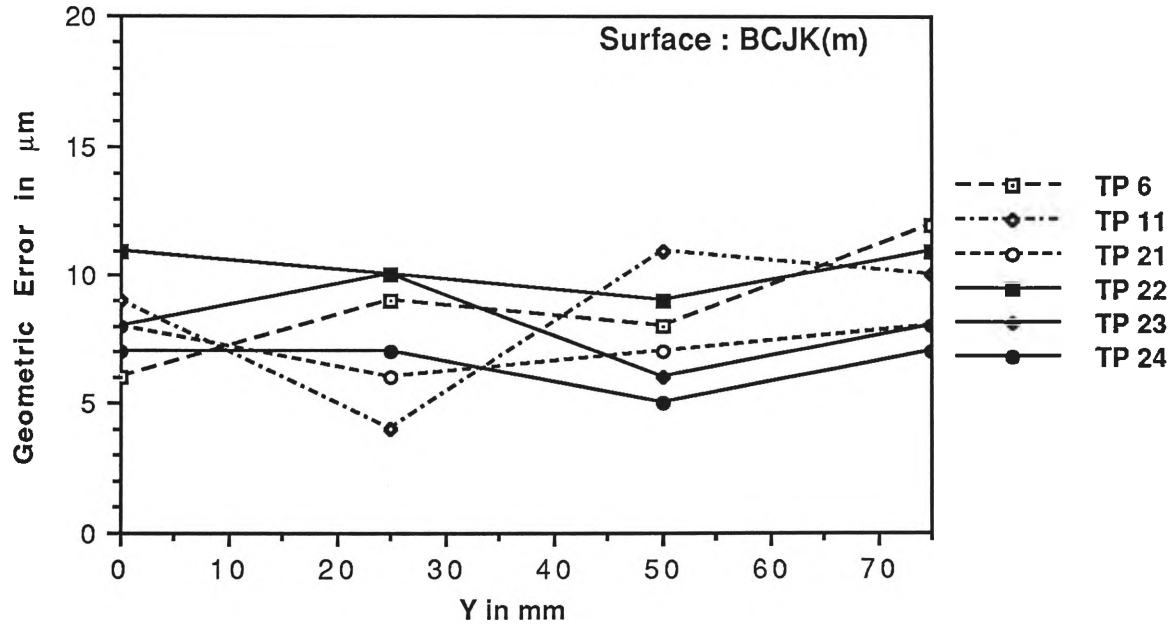

Figure 5.17 Geometric Error Measured on Surface CDLK (Modified).

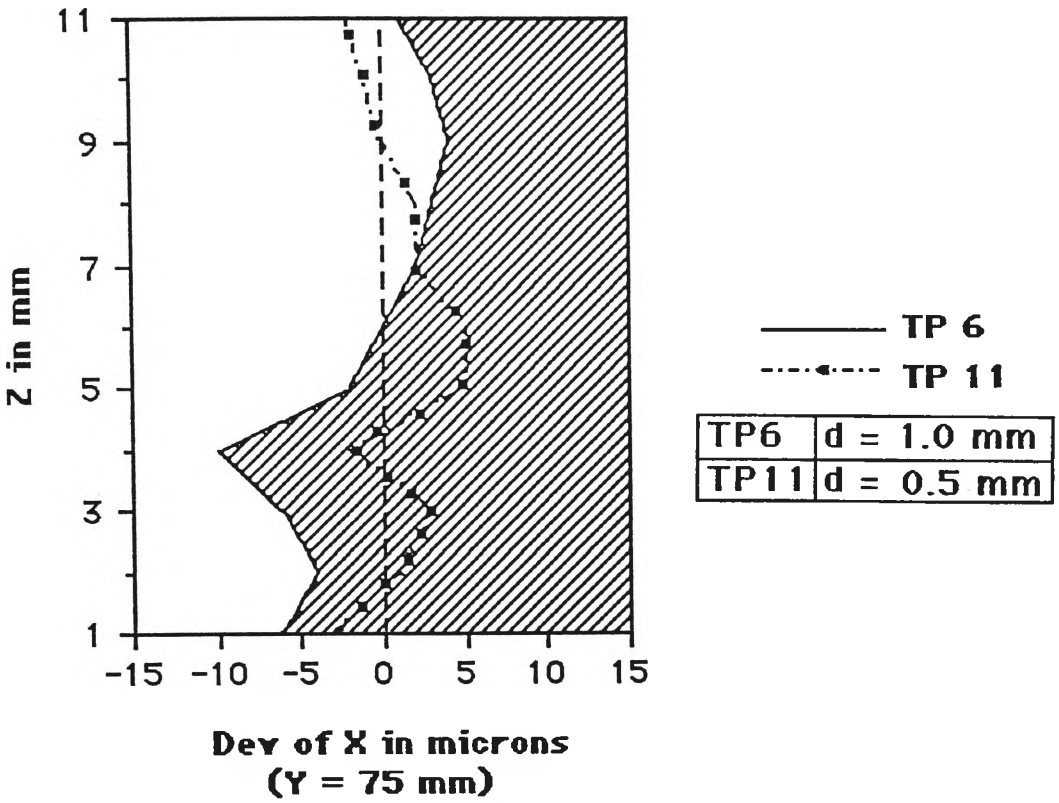

Figure 5.18 Effect of Depth of Cut on End Mill Deflection in Down Milling.

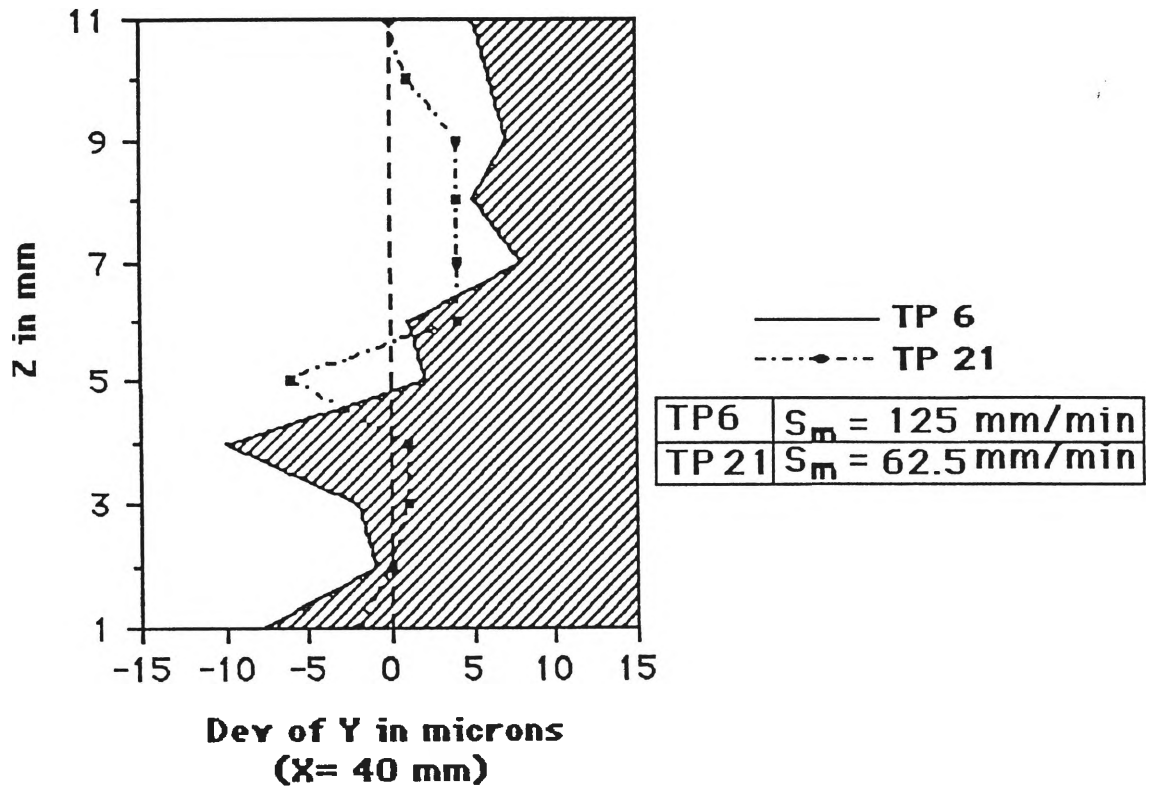

Figure 5.19 Effect of Feed on End Mill Deflection in Down Milling.

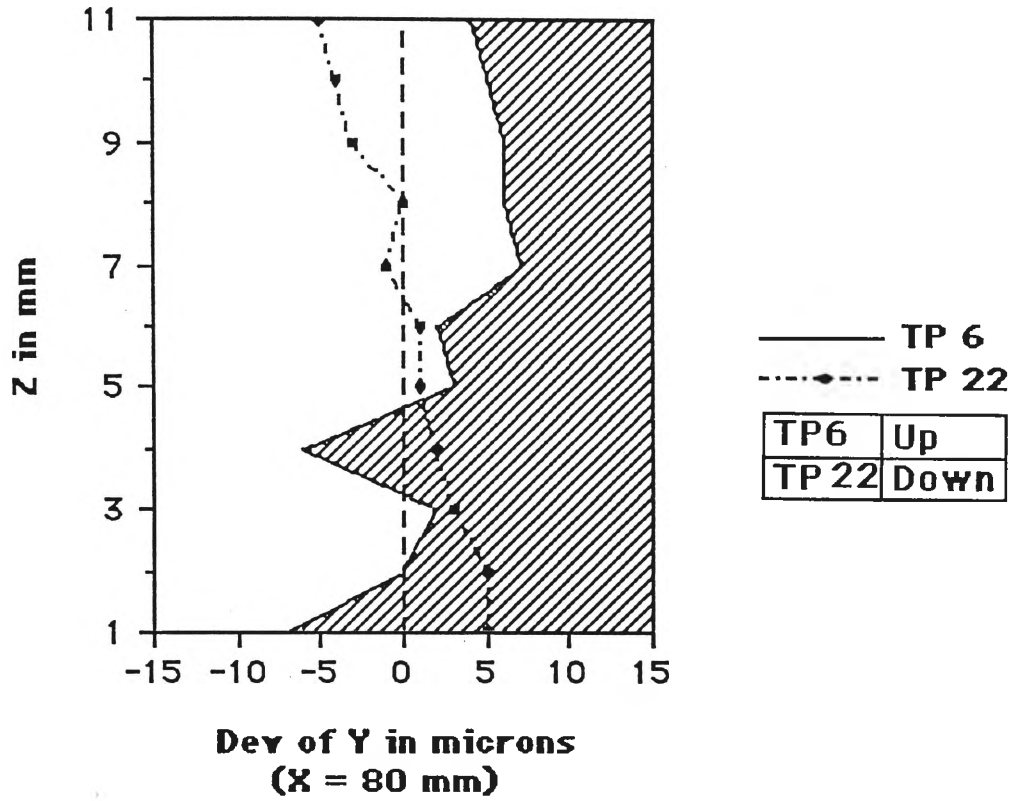

Figure 5.20 Effect of Up and Down Milling on End Mill Deflection.

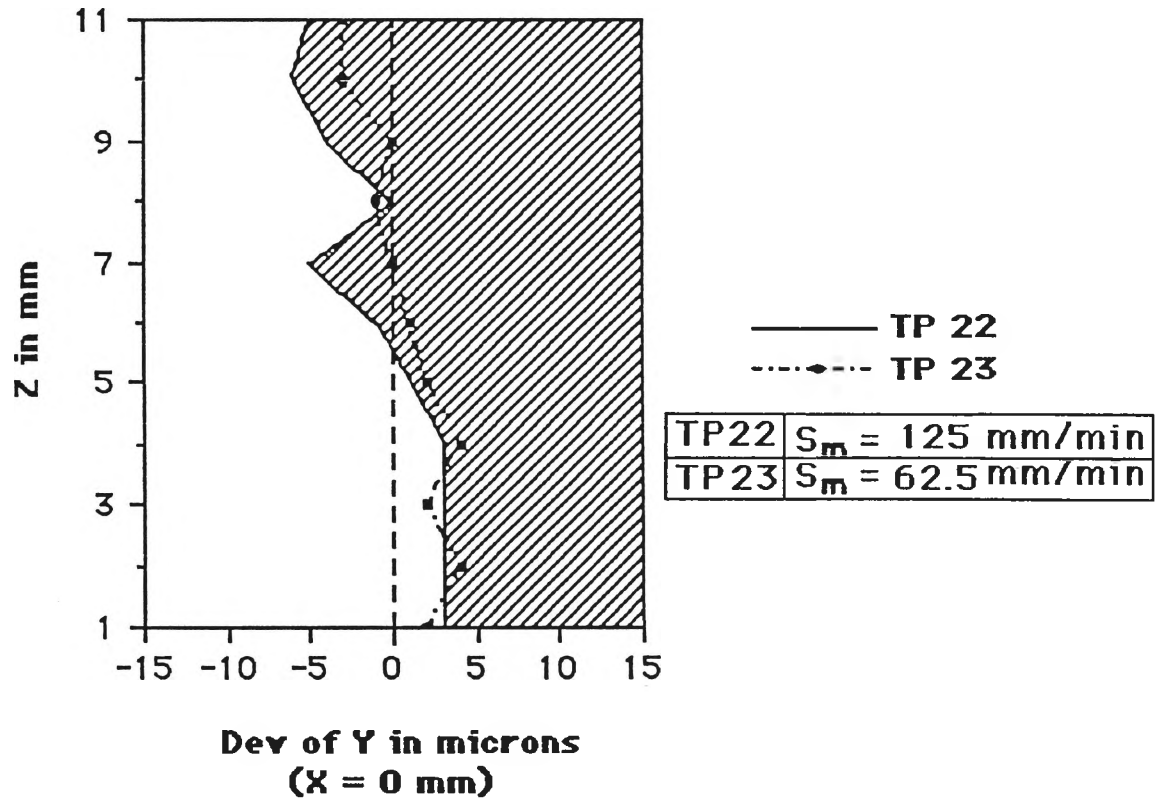

Figure 5.21 Effect of Feed on End Mill Deflection in Up Milling.

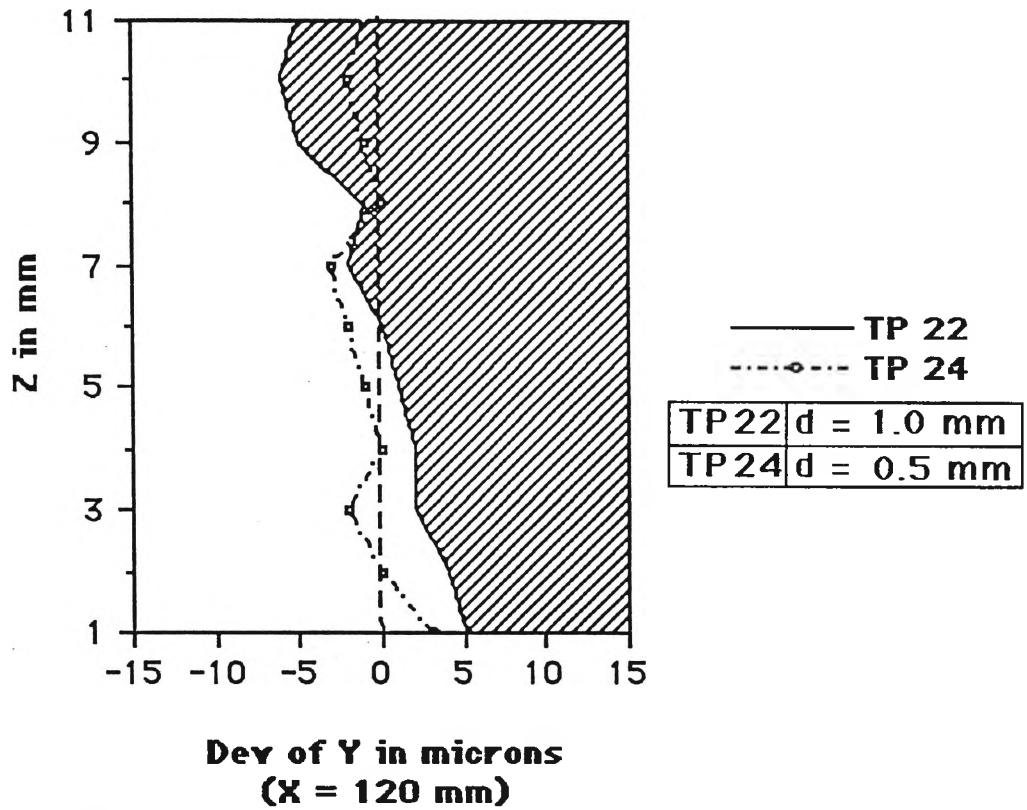

Figure 5.22 Effect of Depth of Cut on End Mill Deflection in Up Milling.

5.4.2 Combined (Peripheral and Face) Milling

Combined milling is a combination of peripheral and face milling performed simultaneously. In this type of milling two perpendicular surfaces are generated at the same pass. The deflection curve of an end mill in the axial direction is similar to that in simple peripheral milling; but due to constraints at the end, the deflection is expected to be less than that of in simple peripheral milling, where the end of the tool is free (i.e. unconstrained). A typical comparison of surfaces machined by simple peripheral milling and surfaces machined by combined milling is given in Figure 5.23. (A detailed study is shown in Figure K.7 in Appendix K)

Any end mill deflection may have effects on the face milled surface of combined milling also. While considering end mill deflection most authors overlooked this aspect. If we have a closer look at Figure 5.5 (right-most example), we find that due to end mill deflection there will be under cut not only at the periphery but also at the bottom where

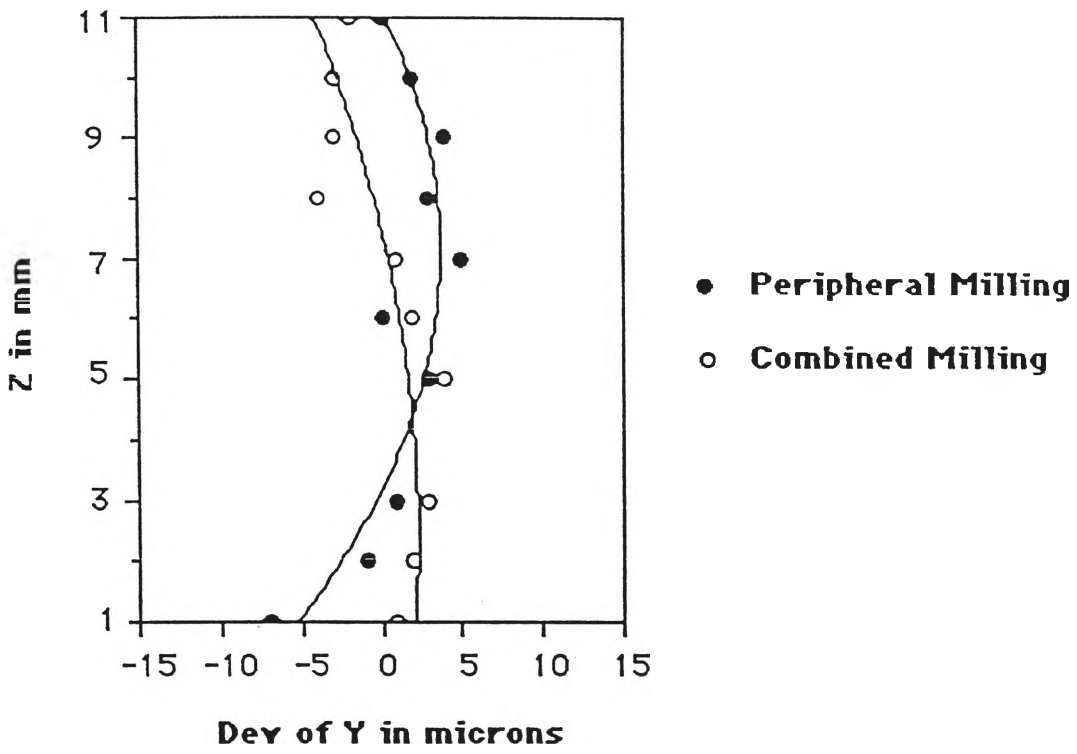

Figure 5.23 Curves of Best-Fit for Peripheral Milling and Combined (Peripheral) Milling Showing More Deflection in Peripheral Milling.

face milling is performed. This is so, because end mill deflection changes the perpendicularity of the tool and the bottom of the end mill makes an angle with the horizontal plane. This angle is the same as the angle of the slope of end mill deflection curve. As we know the slope* of end mill deflection curve is proportional to cutting force, which among other variables is proportional to the depth of cut. Normally in end milling a number of passes with different depth of cuts are used to produce the finished surface, which produces superimposed surface waviness. But as the final cut is generally with a smaller depth of cut, the slope produced at the bottom of the end mill is less than the slope produced in previous cuts, which makes the finished surface smoother although still with some inclination. If the diameter of the end mill used is smaller than the combined depth of cuts the face milled surface may show differences in heights on the

* Slope of the end mill deflection model shown in Figure 5.1 can be calculated using following formula: $\theta_t{}^{max} = |\theta_t(L)| = \frac{FL^2}{2EI}$

surface caused by different passes. This problem is explained in Figure 5.24 where a 15 mm cut is performed with an end mill of 12 mm diameter in three passes (7 + 7 + 1). Figure 5.24 shows how the surface flatness is affected by end mill deflection. If the diameter of the cutter is larger than the total cut, such flatness error is unlikely, but still an inclined surface is expected. We have examined this aspect of surface flatness error of the surface produced by combined milling. A typical example of surface flatness error is shown in Figure 5.25 (For details see Figure K.8 in Appendix K).

5.5 Comments and Discussion

As expected a reduction of end mill deflection was achieved by reducing the feed and/or depth of cut. The magnitudes of end mill deflection attributed to reducing feed and depth of cut are approximately the same (see Tables 5.4 - 5.7 and Figures 5.10 - 5.17). But reduction of feed considerably increases machining time; whereas the same goal can be achieved by reducing the depth of cut in finishing (which can be adjusted with rough cuts) without increasing machining time. From this point of view, reducing the depth of cut is more suitable.

In general, geometric errors in down milling were greater than those in up milling. This is so because in down milling end mill deflection in Y direction (direction perpendicular to feed) is more, as F_r and F_t are added to form F_y, whereas in up milling those force components are subtracted to form F_y. The nature of the curves suggested that in down milling the cutter always deflects away from the job whereas in up milling the cutter tends to dig into the job (see Figure K.4). Existence of distinct marks on end mill surface in down milling made flatness errors of the surface worse. Initially it was suspected that some inaccuracy of the tool is responsible for those marks. But after a close examination of the tool no such irregularities were found. Moreover, the same tool when used in up milling did not produce such marks and new tools used in down milling produced the same type of marks. These were noticed by Martellotti and he wrote, "Under certain

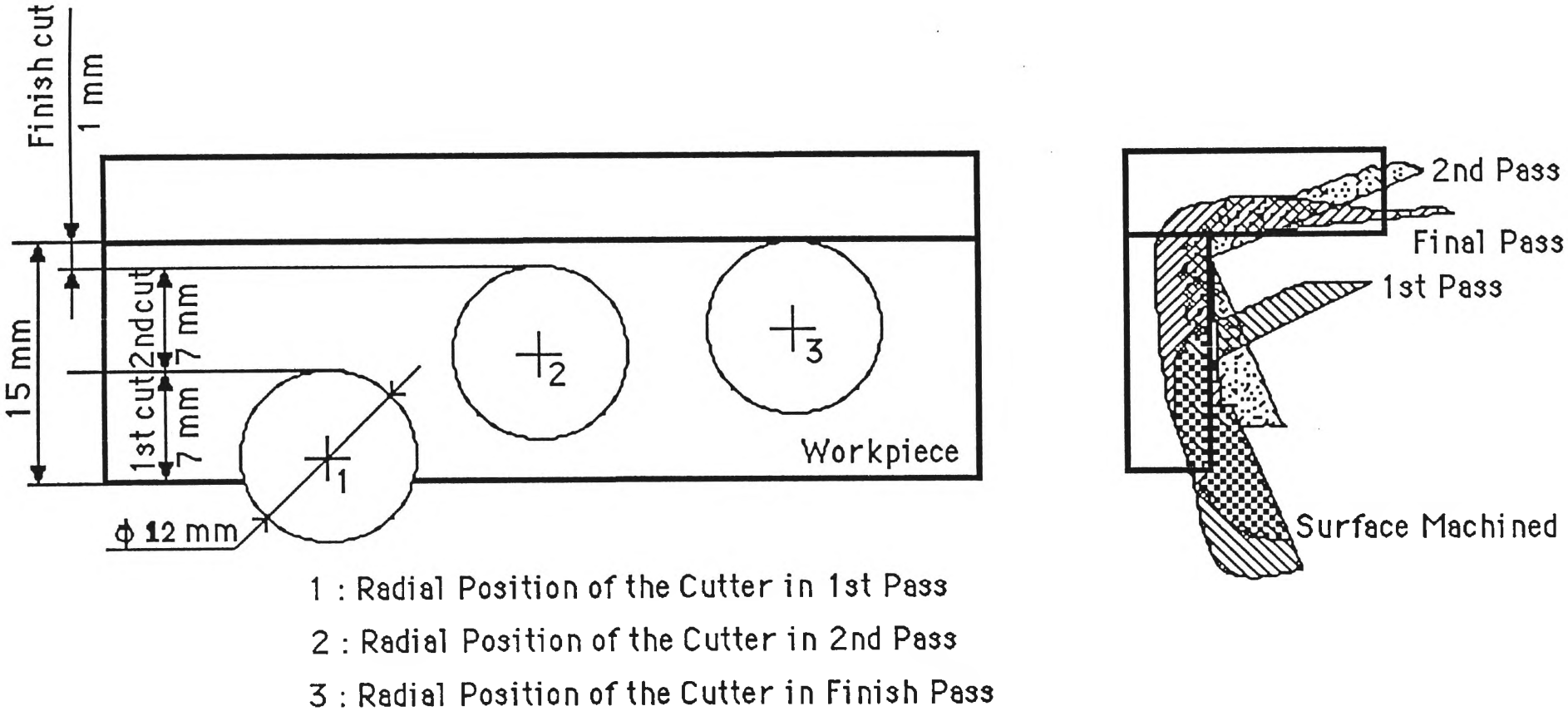

Figure 5.24 Surface Error Generated in Combined (Face) Milling due to End Mill Deflection.

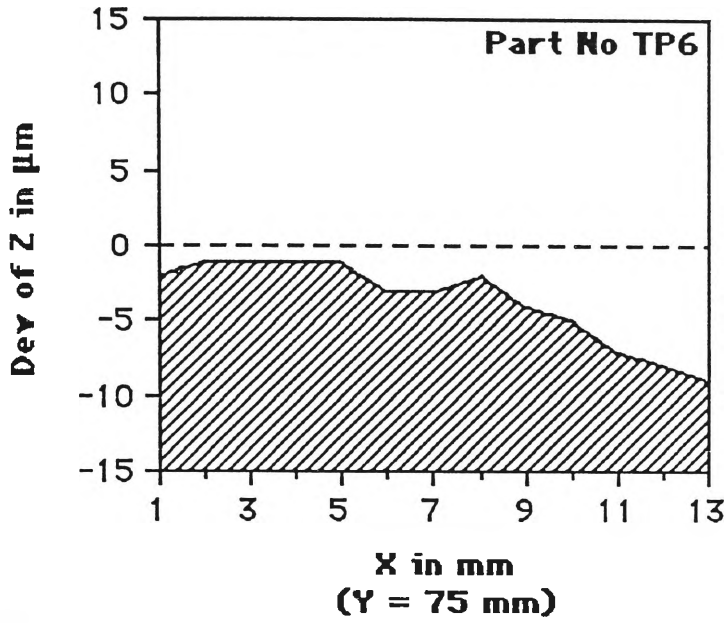

Figure 5.25 Inclined Surface Generated by Combined (Face) Milling Due to End Mill Deflection.

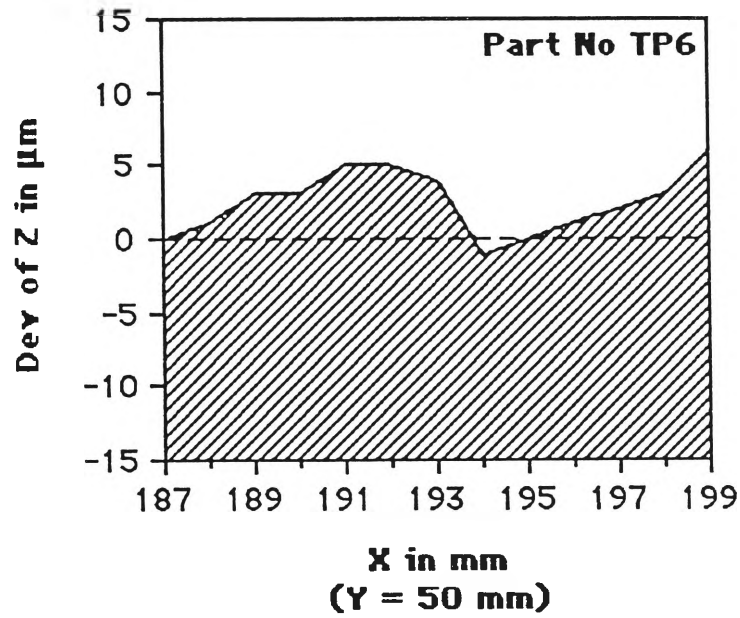

Figure 5.26 Surface Error Occurred in Different Passes in Combined (Face) Milling.

conditions, however, definite marks are produced on a surface generated in down milling"[162]. In up milling some stains were found on the surface which in some cases changed the shape deflection curves unexpectedly.

In combined milling the end mill deflection is less than that in peripheral milling (see Figure 5.23) The surface produced in combined milling at the bottom of the cutter showed a slope due to end mill deflection (see Figure 5.25) In Figure 5.26 it can be seen that a sudden change of height occurs at some point. That point is the position of the cutter in first cut. Due to end mill deflection in each cut the end mill generates a sloped surface. But normally in the final cut, which is less than the rough cuts, end mill deflection is less and all previous irregularities are eliminated in that cut if the diameter of the cutter is larger than the total cuts. If, for some reason, end mill deflection is larger in the finish cut than in rough cuts, previous irregularities cannot be eliminated in the finish cut. It is interesting to monitor the flatness error of the surface at the corners where the cutter changes its direction.

It is found that the geometric error of the finished surface in the axial direction can be reduced by adopting up milling and reducing feed and/or depth of cut. But in three dimensional machining, surface accuracy is represented by flatness error of the surface produced. In Table 5.8 overall flatness errors of surfaces generated by peripheral milling are listed.

Surface	Flatness Error in microns					
	TP6	TP11	TP21	TP22	TP23	TP24
ABJI	18	18	16	15	12	11
CDLK	19	16	13	17	18	16
DAIL	19	10	11	20	14	10
BCJK	18	15	14	14	12	8

Table 5.8 Study of Flatness Error of End Milled Surface.

From Table 5.8 it can be concluded that the overall flatness error of the surfaces cannot be reduced much by decreasing end mill deflection when length of the surface is large (surfaces ABJI and CDLK have length 200 mm each, whereas surfaces DAIL and BCJK have length 75 mm each). This is because the overall surface flatness **also** depends on the straightness error of the guideways, which is generally proportional to the length. When the length increases to some extent, the straightness error of guideway becomes the most dominant factor in the overall flatness errors and necessary action should be taken to reduce straightness error of the guideway, which will ultimately reduce the overall flatness error.

6.0 SURFACE TEXTURE AS AN ASPECT OF MACHINING ACCURACY IN CNC MACHINING OPERATIONS

6.1 Introduction

It appears that the surface texture aspect has not been considered by most researchers when analysing the machining accuracies. But surface texture of the machined component has been found to have a direct impact on measurements (specially on CMM measurements); thus surface texture influences all other aspects of machining accuracy, viz dimensional, positioning and form (shape) accuracy.

The surfaces generated by machining (both CNC and conventional) are generally irregular and complex. But extended research indicates that, the surface texture produced by different metal removal processes is characteristic for that particular process. There are several factors which directly or indirectly influence the surface texture of a machined component, such as: cutting conditions, tool geometry, machine accuracy, chatter or vibration of the machine tool, cutting fluid, chip formation, work material homogeneity, etc.

In general machining practice, near nominal dimension* and shape of the component are achieved by some primary machining operation(s) called **rough cut(s)** and then some secondary operation(s), called **finish cut(s)** is (are) performed with relatively small depth(s) of cut (normally less than 1.5 mm) and light feed(s) (normally less than 0.15 mm/rev). The purpose of the finish cut(s) is to ensure dimensional accuracy with enhanced surface quality of the component. But it is found that, each machining process has its limitations and the surface quality cannot be improved beyond certain limits (see Figure 6.1)

---

* leaving some margins for finish cuts.

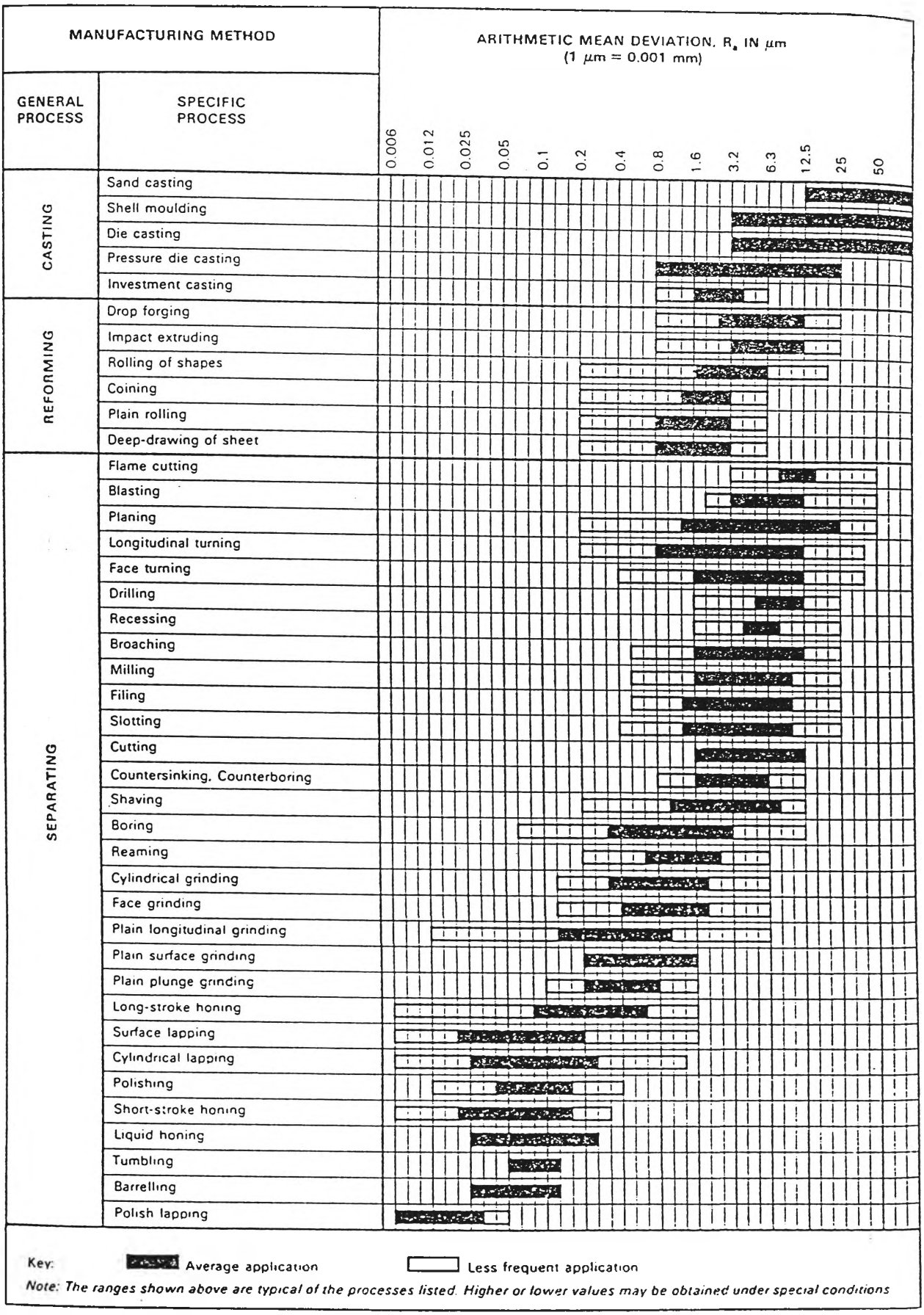

Figure 6.1 Typical Roughness Values Obtained with Ordinary Materials and Common Production Processes [163].

6.1.1 Surface Texture Defined

Although in previous chapters of this thesis, the term **surface finish** has been used to denote the general quality of a surface, it is not a technically accepted term. In fact, surface finish is a colloquial term widely used for qualitative assessment of a surface and generally is not quantified.

Surface texture is the technically accepted term which is used to describe the repetitive or random deviations from the nominal surface which forms the three-dimensional surface topography. A variety of techniques is available today for examining surfaces, e.g. stylus tracing, optical microscopy, light scattering, electron microscopy, laser scanning, etc.

According to Australian Standard for Surface Texture, AS2536-1982 [164], surface texture includes four elements - roughness, waviness, lay and flaws (see Figure 6.2) and these elements are defined as follows:

Surface roughness - the topography of a surface which consists of short wavelengths only. It comprises surface irregularities with relatively small spacings and usually incorporates irregularities resulting from the method of manufacture.

Waviness - the topography of a surface which consists of wavelengths of intermediate length. Waviness may result from such factors as machine or work deflection, vibration and chatter or heat treatment.

Lay - the direction of the predominant surface pattern ordinarily determined by the production method used.

Flaws - unintentional irregularities which occur at one place or at relatively infrequent or widely varying intervals on the surface. Flaws include such defects as cracks, inclusions, ridges and scratches.

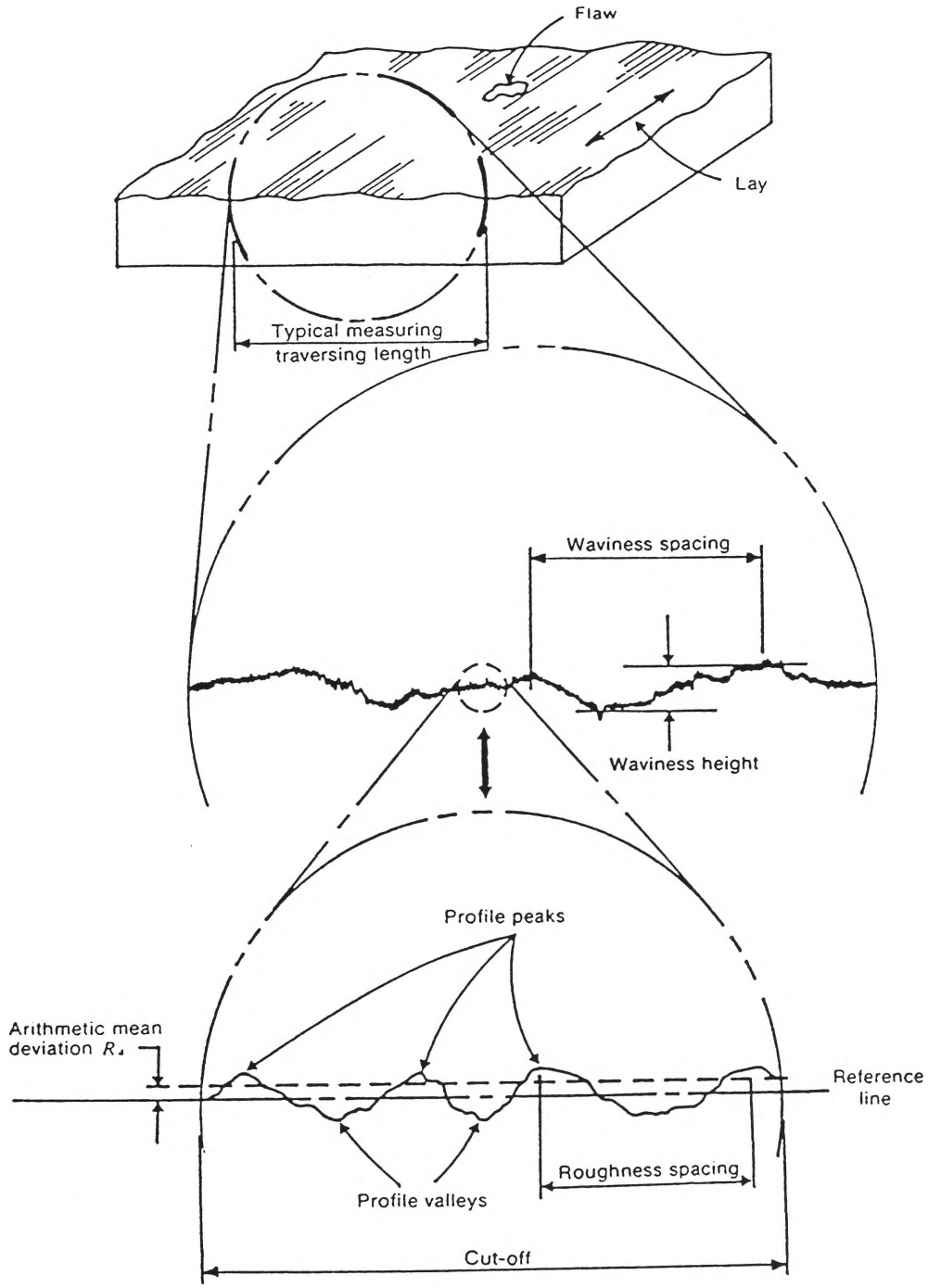

Figure 6.2 Surface Characteristics [164].

Surface texture is described by various parameters. At present more than 50 parameters exist to quantify surface conditions [15]. The most widely used and internationally accepted parameter is arithmetic mean deviation $(R_a)^*$. Details of the 30 most frequently used parameters for describing surface quality are given in Appendix L. Unfortunately no single parameter appears to be capable of describing the surface texture adequately. For example two different surfaces may have same R_a values (see Figure 6.3) while having totaling different surface topography. To reduce this ambiguity, often more than one parameter is used. Nowicki [165] has done a comparative analysis of various surface texture parameters and established a subset of four uncorrelated parameters of which at least two parameters should be used to represent the surface texture property. The measured values of surface roughness parameters generally depend on the direction of surface measurement. A surface measured along different directions could give completely different R_a values. It is accepted that the direction of surface roughness measurement should be chosen in such a way that, the "worst case" values are likely to be registered.

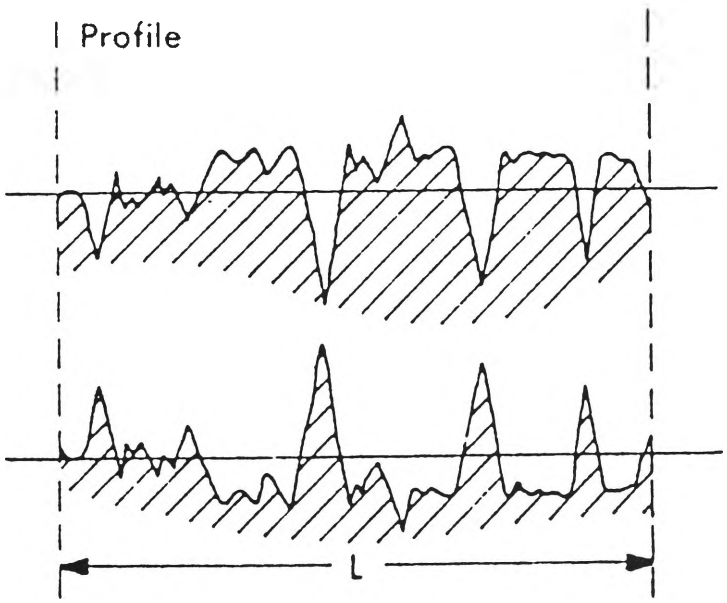

Figure 6.3 Profile Traces of Two Different Surfaces Having the Same Roughness Average [15].

* nomenclature adopted in this thesis is in accordance with AS2536-1982.

6.1.2 Effects of Surface Texture on Quality of a Product

Surface texture has the following effects on the quality of a product:

(a) Effect of Surface Texture on Functioning

In many cases the surfaces texture dominates the functional requirements of the component. So while considering the surface texture of a component the part designer must give first priority to the functional requirements. Good surface finish is necessary to prevent premature fatigue failure, to improve corrosion resistance, to reduce friction, wear and noise, to improve product life, etc. But good surface finish is not always useful and in some cases some definite range of roughness values should be maintained; an example of this is when a gasket is to be used for sealing. An extremely smooth surface is as difficult to seal as a very rough one. So part designers should be careful in choosing the appropriate surface texture for the designed component.

(b) Effect of Surface Texture on Measurement

Surface texture of a component directly influences the measurement results. With deterioration of the surface quality the uncertainty of measurement rises. This problem is more prominent in CMM measurements where the measurement results are based on the co-ordinates of the probed points. In GD&T the dimensional relationships of a part are established with reference to datum surfaces. In GD&T it is accepted that the datum surfaces are perfect, although it is simply not possible to manufacture any perfect part. So from the datum features (which are the features of a real part), datum planes are simulated. For a primary datum plane, a minimum of three points, for a secondary plane, a minimum of two points of contact, and for a tertiary plane, a minimum of one point contract are required. But this way of simulation can lead to a change of co-ordinate system and subsequently all measurement results will differ. In Figure 6.4 it is shown (in two dimensions) how a change (translation and rotation) can occur when a secondary

datum surface is established by two point contacts (M and D). (In the figure the variations are exaggerated for clarity.) In reality (i.e. in three dimensions), different types of rotational errors (roll, pitch and yaw) may occur. To get rid of this problem, generally flatness tolerances are imposed on the datum surfaces. But unfortunately in normal measurement practice, effects of flatness errors of the datum surfaces are considered in linear translations **only**, ignoring the rotational changes of the axes.

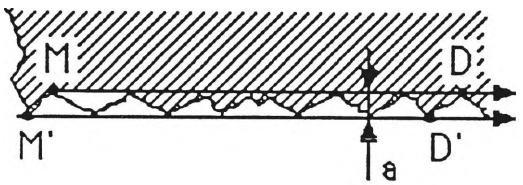

(a) Translation

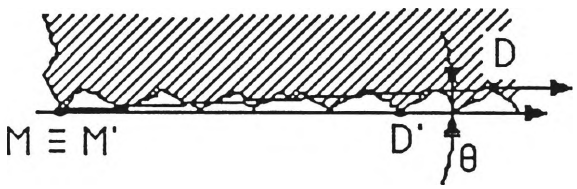

(b) Rotation

Figure 6.4 Change of Co-ordinate System.

There is a direct relationship between the dimensional tolerance of a part and its surface texture; thus while choosing dimensional tolerance the part designer should take into account the surface texture of the part. For example, the roughness parameter arithmetic mean deviation (R_a) defines the average linear deviation of the actual surface from the nominal surface defined by the dimension. If the deviations induced by the surface roughness exceed those permitted by the dimensional tolerance, the dimension will be subject to an uncertainty beyond the tolerance, as shown in Figure 6.5. In turning the maximum peak-to-valley roughness height (R_{ma}) is approximately four times the arithmetic mean deviation (R_a). On a diameter measurement of a part, this value would

be doubled. So the R_a value on a diameter should not exceed one-eighth the dimensional tolerance on the diameter to ensure useful dimensional controls.

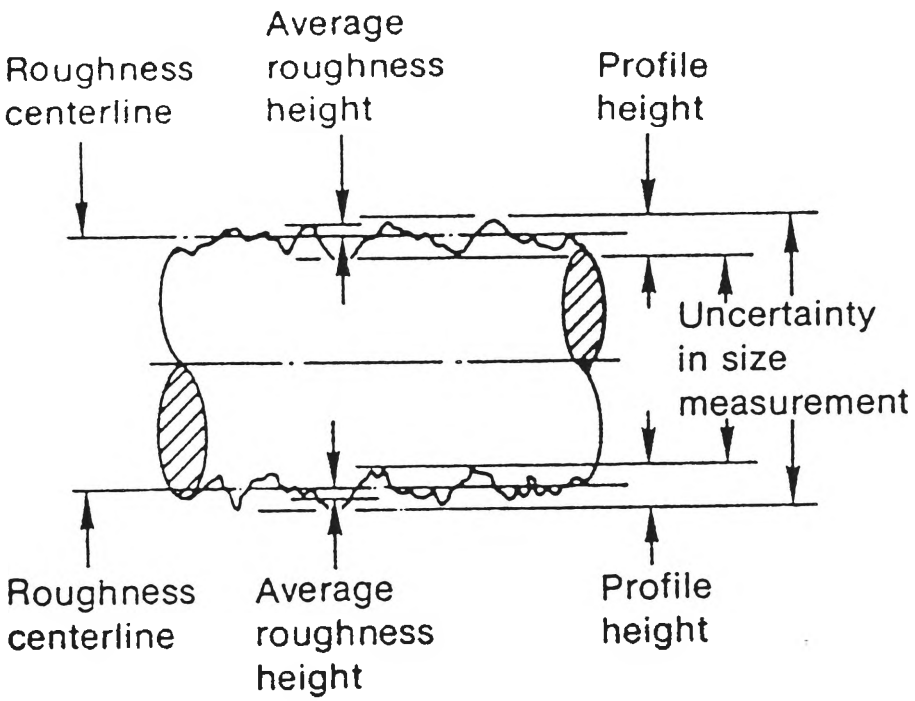

Figure 6.5 Uncertainty in Size Measurement in Relation to Surface Roughness Parameters for a Cylindrical Surface [166].

(c) Effect of Surface Texture on Overall Aesthetics

Surface texture influences the overall apearance of the product and it is important from a cosmetic point of view. Customers are often influenced by the outlook of a product without considering its technical specifications. As customers' satisfaction is the bottom line in product quality assessment, part designers should consider the cosmetic (or aesthetic) aspect of that product. Sometimes it is found that the designer has to impose more restrictions on surface quality than is required by the function.

6.2 A Summary of the Present Knowledge on Surface Texture in Machining Operations

Basically all metal machining operations are aimed at achieving the desired size and shape of the workpiece by removing the surface layer of it. Removal of surface layer is caused by the relative motions of the cutting tool and workpiece and is facilitated by the special shape of the tool. The surface produced by machining operations consists of the marks left after the desired amount of metal is removed. There are a number of factors which may influence the surface texture of the machined surface; but in ideal conditions the surface produced consists of marks (feed marks) similar to the tool nose geometry (contour). Apart from tool nose geometry, feed is the other dominating factor affecting the surface texture of a machined surface, as the feed regulates the contact frequency between workpiece and the tool nose.

Based on the above assumptions, the surface roughness achievable by different machining operations can be calculated. These roughness values are known as "ideal" surface roughness, as they are based on ideal conditions (i.e. without built-up edge, chatter, inaccuracies in NC tool movement, etc). Although it is practically impossible to achieve ideal surface roughness, the values are estimated by using ideal surface roughness formulas, which are useful as they indicate the best possible finish which may be obtained for a given tool shape and feed. For simple geometrical profiles, the two most commonly used roughness parameters, arithmetic mean roughness (R_a) and maximum peak-to-valley height (R_{ma}) can be readily related. But in practical machining such relationship is difficult to establish. However as the surface texture produced by different machining operations is characteristic for that particular operation, some relationship between these two parameters (R_a and R_{ma}) can be suggested.

For example in turning [132], [166]

$$R_a = 0.25\ R_{ma} \tag{6.1}$$

In face milling [167]

$$R_a = 0.318\, R_{ma} \tag{6.2}$$

The "ideal" effect of tool geometry on surface texture in turning is illustrated in Figure 6.6. Chisholm [168] showed that for a lathe tool with a perfectly sharp corner (i.e. with zero nose radius) (see Figure 6.6(a)) the maximum peak-to-valley height (R_{ma}) can be determined using following formula:

$$R_{ma} = \frac{S}{\tan C_s + \cot C_e} \tag{6.3}$$

where

S = feed per revolution

C_s = side cutting edge angle

C_e = end cutting edge angle

Substituting Equation (6.1) into Equation (6.3), we obtain:

$$R_a = \frac{S}{4(\tan C_s + \cot C_e)} \tag{6.4}$$

For a corner radiused tool (see Figure 6.6(b)), the maximum peak-to-valley height can be estimated using following expression [132]

$$R_{ma} = (1 - \cos C_e)\, R + S \sin C_e \cos C_e - \sqrt{(2SR\sin^3 C_e - S^2 \sin^4 C_e)} \tag{6.5}$$

When the nose radius is large and the feed is comparatively small, the surface is generated by the nose radius alone (see Figure 6.6(c)), then

$$S \leq 2R \sin C_e$$

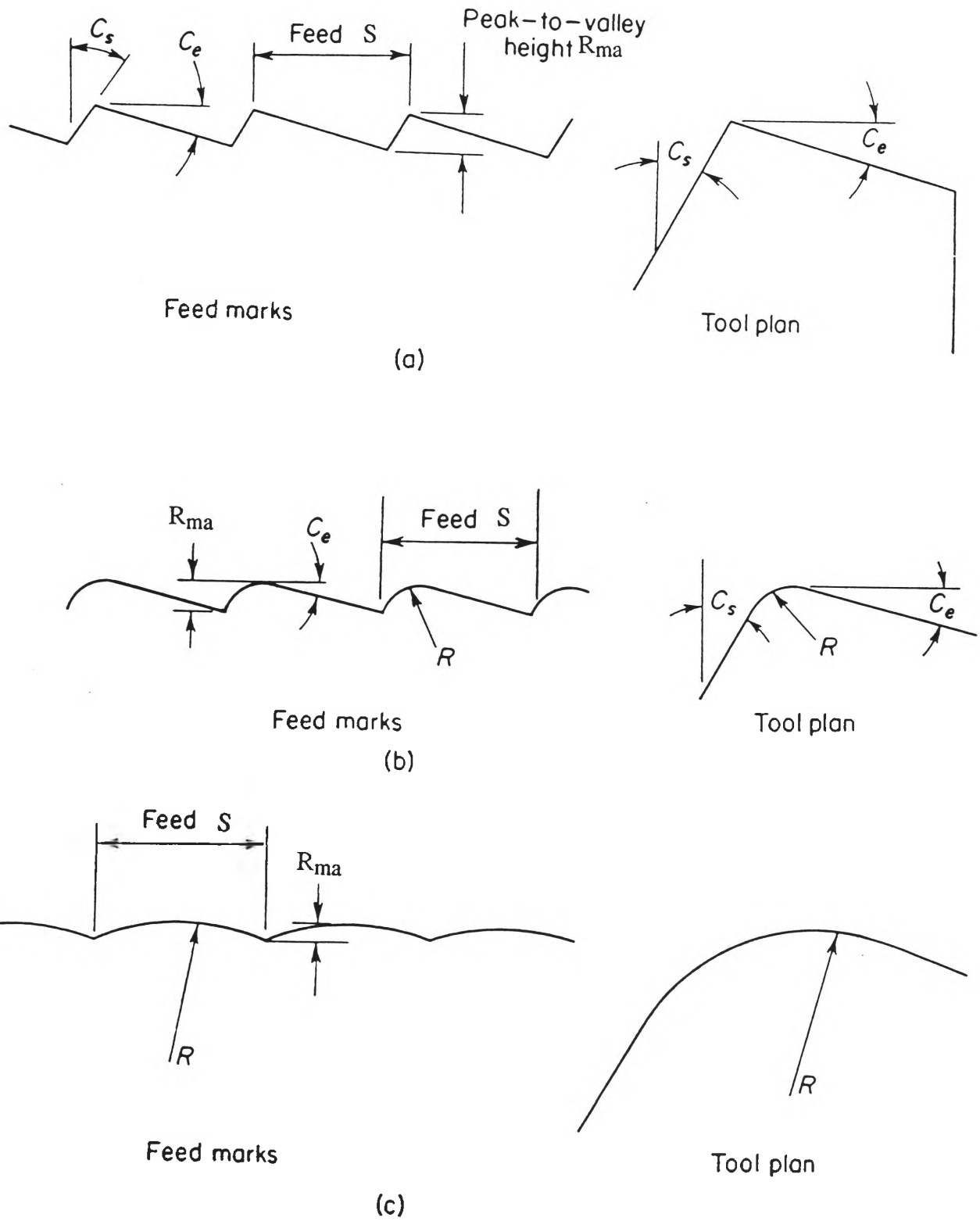

Figure 6.6 Effect of Tool Geometry on the Surface Finish in Turning [132].

and $$R_{ma} = R - \frac{1}{2}\sqrt{4R^2 - S^2} \cong \frac{S^2}{8R} \quad (6.6)$$

$$R_a \cong \frac{S^2}{18\sqrt{3}R} = \frac{0.0321\ S^2}{R} \quad (6.7)$$

The tool geometry of face milling cutters is similar to lathe tools and the maximum peak-to-valley height (R_{ma}) in face milling can be determined by using Equation (6.3).

For peripheral milling if the tool path is considered as a circular arc, then

$$R_{ma} = \frac{S_t^2}{8R} \quad (6.8)$$

where

R = cutter radius

S_t = feed per tooth

Martellotti [133] showed that the path of a milling cutter is trochodial and in that case

$$R_{ma} = \frac{S_t^2}{8\left(R \pm \frac{S_t.K_t}{\Pi}\right)} \quad (6.9)$$

where

K_t = number of teeth in the cutter

S_t = feed per tooth

R = cutter radius

The plus sign is for up milling and the minus sign is for down milling, which means that theoretically, up milling will produce better surface finish, than down milling.

For conventional drilling the following formula can be applied to calculate the ideal value of maximum peak-to-valley height (R_{ma}) [169]:

$$R_{ma} = \frac{(S/2) \,.\, \tan k \,.\, \tan \psi}{\tan k + \tan \psi} \qquad (6.10)$$

where

S = feed per revolution

k = half point angle

ψ = back taper of drill

It is interesting to note that the ideal roughness values of surfaces generated by turning, milling and drilling, depend only on tool geometry and feed. As the tool geometry remains constant during machining, feed is the only parameter which can be manipulated during machining. From the above-mentioned formulas for ideal surface roughness, it is clear that to achieve better surface finish, feed must be kept as low as possible.

As mentioned earlier, the ideal roughness parameters are never achievable. The following factors are responsible for variations from the ideal roughness values [170]:

(a) Built-up edge deposits on the machined surface.

(b) Side flow (i.e. the flow of metal perpendicular to the direction of cutting),

(c) Tool wear.

(d) Tearing of the machined surface.

(e) Relative vibration between the tool and the workpiece.

The phenomenon of built-up edge (BUE) has been known to researchers for quite a long time; but still controversy remains about the mechanism of its formation. The most accepted theory is, as the cutting speed is increased from low level , the friction between chip and tool will increase and when the friction force becomes large enough to cause a shear fracture in the vicinity of the tool face, a BUE is formed. The other theory assumes that the BUE is initiated by the bluntness of the tool edge rather than by the high friction

force. There are many publications about BUE and we are not going into much details, but it is well established that the formation of BUE has a direct relationship with the roughness parameters of the machined surface.

Nakayama et al [171] studied the relationship between cutting forces, temperatures, built-up edge and surface finish in turning operations. They highlighted the importance of cutting speed on surface finish, by showing the cutting speed to have the greatest influence on cutting temperature. At very low cutting speeds no BUE is formed, as the temperature on the face of the chip is then not sufficient to cause the chip surface to behave in a ductile manner. With an increase in cutting speed the chip metal in contact with the tool face becomes ductile and the resulting plastic flow causes strong welds to form between the chip and tool, which has the effect of changing the effective geometry of cutting. At high speeds BUE disappears, as the high temperature does not allow the metal to stick on the tool. Nakayama et al [171] showed that surface finish improves with increased speed not only due to loss of BUE, but also due to the loss of extruded wedge-shaped bodies which form at asperities on the tool flank, called "microchips". The microchips play the same role on the tool flank as the BUE does on the tool face; for that reason the best surface finish is not obtained immediately after BUE is lost. The microchips disappear only at very high speeds, where tool flank temperature approaches the α-γ transformation temperature.

Selvam and Radhakrishnan [172] examined the influence of side-flow and BUE on the roughness and hardness of the machined surface with a single point tool. Their experimental results show that direct correlation (correlation co-efficient 0.955) exists between the side flow and surface roughness. The BUE affects surface roughness in the direction transverse to the direction of cut. When cutting speed and rake angles are increased the size of the BUE and side flow decreases, which results in a smoother surface.

Shaw and Crowell [170] have reviewed the state of knowledge in finish machining. Their study indicates contributing factors to surface roughness such as sub-surface fracture, vibration, the lower limit of undeformed chip thickness for a tool having a given edge radius (sharpness), plastic side flow at the tool tip and concentrated wear that occurs on the secondary cutting edge. It is found that at very low speeds the surface roughness is dominated by sub-surface fracture, which causes cracks on the machined surface. Their experimental results suggest that the depth of cut has a negligible effect on surface roughness.

From previous paragraphs it is clear that BUE plays an important role in the actual surface roughness production. To compare the actual surface roughness with ideal surface roughness, often a parameter called "cutting efficiency" (CE) is used:

$$CE = \frac{R_{ma}^{A}}{R_{ma}^{I}} \tag{6.11}$$

where R_{ma}^{A} = Actual peak to valley height

R_{ma}^{I} = Ideal peak to valley height

This parameter (CE) may be considered as a measure of the closeness of approach to ideal finish machining and ideal finish machining will correspond to CE = 1.0.

In normal machining practice regardless of the metal removal process adopted, the following tips are recommended to improve the surface roughness of a machined surface.

(a) Reduced feed.

(b) Increased tool nose radius.

(c) Increased cutting speed (to avoid BUE).

(d) Improved rigidity and stability of tool-work-machine system (reduce vibration) by altering the,

(i) cutting conditions.

(ii) workpiece size.

(iii) method of clamping.

(iv) cutting tool rigidity.

(e) Effective chip breaking and chip removal.

(f) Use a cutter with a high rake angle.

(g) Application of "correct" cutting fluid.

Bearing in mind the above recommendations, we can proceed towards the experimental work.

6.3 Experimental Work

Our experiments started with the measurement of surface texture parameters* of the test pieces machined for preliminary studies (TP1-TP10). Later more test pieces were manufactured under different cutting conditions, to monitor the effect of cutting conditions on the surface texture parameters and to identify optimum cutting conditions to generate consistent and required surface texture. Measurements were performed on surface texture measuring instrument, Surfcom 550. Our experimental work on surface texture can be divided into three sections according to different types of cutting operations used, viz (i) Face Milling, (ii) End Milling and (iii) Drilling.

6.3.1 Face Milling

Face milling was performed to machine two surfaces (top and bottom) of the test components. The roughness parameters of the top surface of ten components (TP1-TP10) were measured. Measurement results (obtained from Surfcom) of a typical face milled surface are given in Figure 6.7. It was found that the roughness parameters

*In the present study three surface texture components, namely arithmetic average (R_a), maximum peak to valley height (R_{ma}) and ten point average (R_z) were considered, as no single parameter is capable of producing a clear picture.

change along the feed direction. Roughness parameters R_a, R_{ma} and R_z were monitored continuously along feed direction and their values were recorded for each 10 mm traversing length. In Figures 6.8 - 6.10* these roughness parameters are plotted against the length of the workpiece. The average value of these 17 readings are taken to beactual values† of roughness parameters of those surfaces and are plotted for different components in Figure 6.11.

Effects of cutting speed and feed on roughness parameters in face milling were studied. A number of surfaces were generated with constant depth of cut, d = 0.5 mm, using face milling with different cutting speeds and feeds. Variation of roughness parameters versus cutting speed for face milling at different values of feed is given in Figure 6.12. Same data were plotted against feed with constant cutting speeds in Figure 6.13. The effect of cutting speed and feed on surface profile are illustrated in Figures 6.14 and 6.15.

6.3.2 End Milling

End milling operations were performed to make the prismatic shape of the test components. Both peripheral and combined (face and peripheral) milling were performed. The surface roughness parameters of the surface ABJI (which is the secondary datum surface) were measured. Measurement data of a typical peripheral milled surface are given in Figure 6.16. Five measurements were taken for each surface. The average values of roughness parameters in peripheral milling for ten test components are given in Figure 6.17. The average values of roughness parameters of ten components in face milling as part of combined milling are given in Figure 6.18.

---

* For plotting different relationships Cricket Graph Package (Version 1.2) software is extensively used. Unfortunately Cricket Graph package is unable to write subscripts in lebels. Therefore, R_a,R_{ma} and R_z are represented by Ra, Rma and Rz recpectively in subsequent figures.

† In general magnitude of any parameter means it's average value. Thus for roughness parameters we have taken the average values as their actual values, although in a number of cases some tendency of changes were noticed.

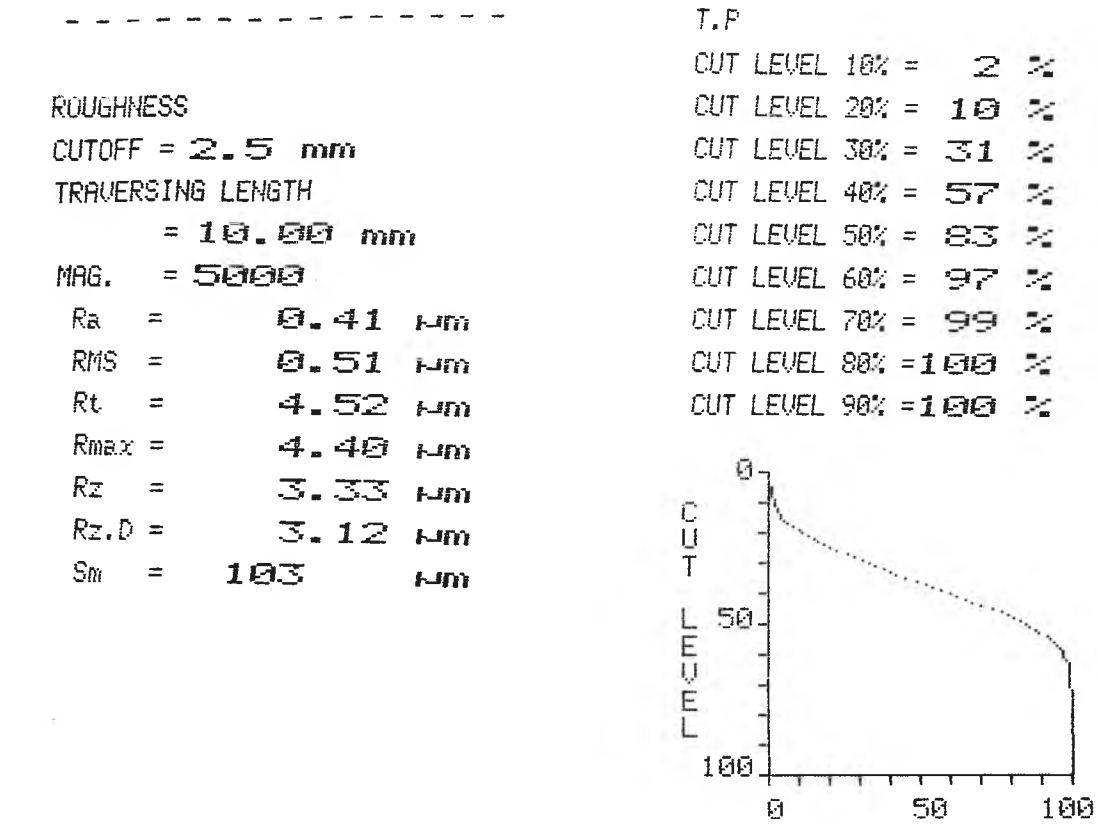

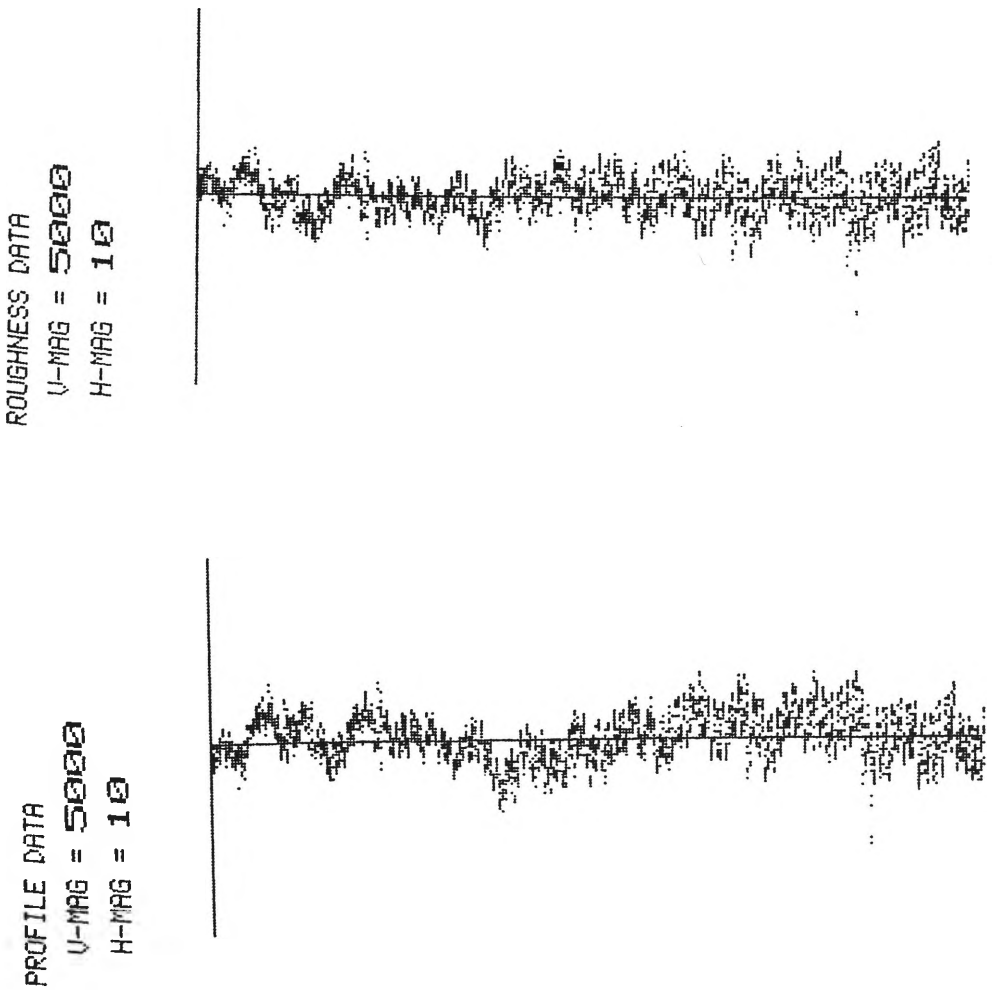

Figure 6.7 Roughness Parameters of a Typical Face Milled Surface.

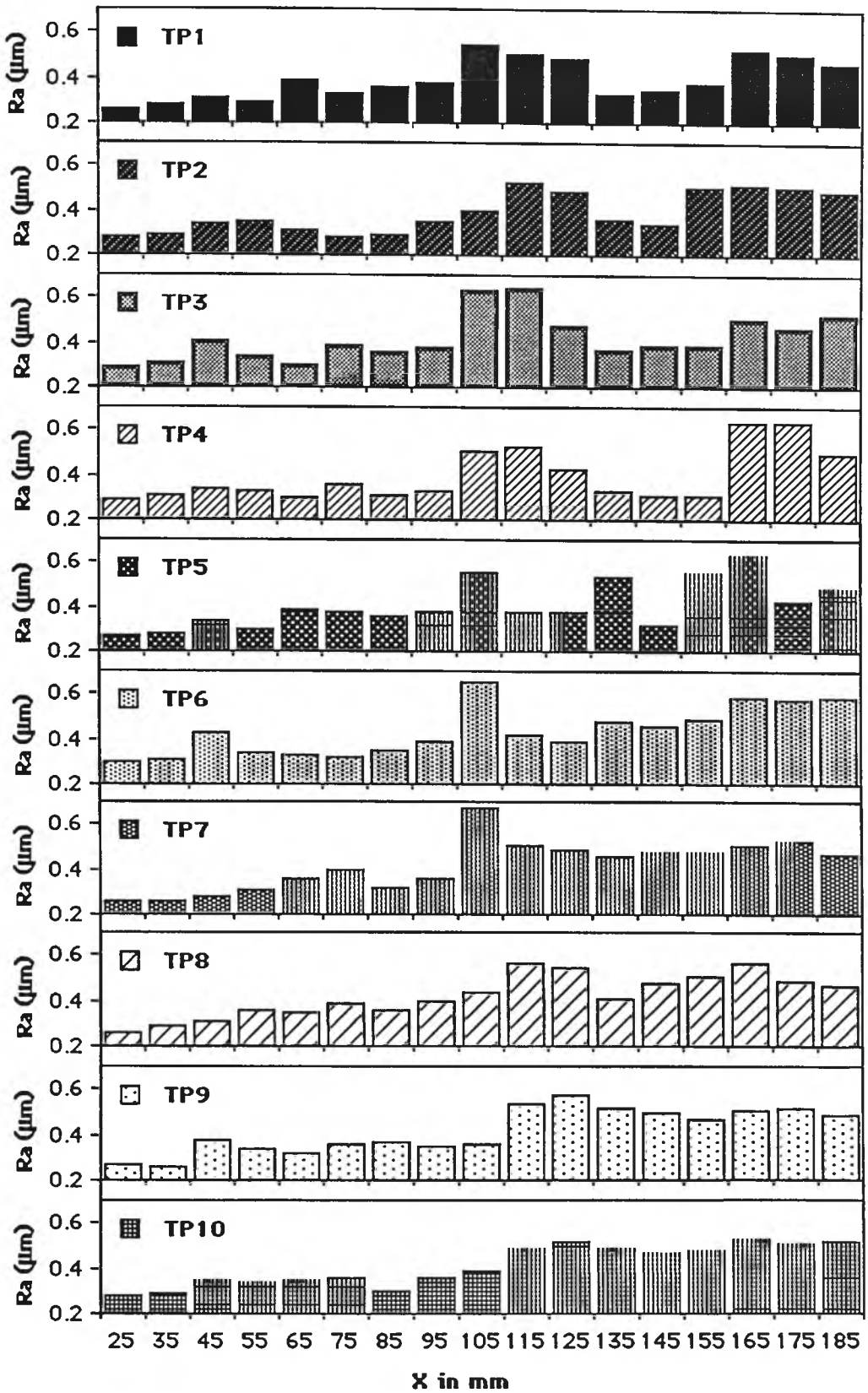

Figure 6.8 Variation of Arithmetic Average (R_a) along Feed Direction in Different Components in face Milling.

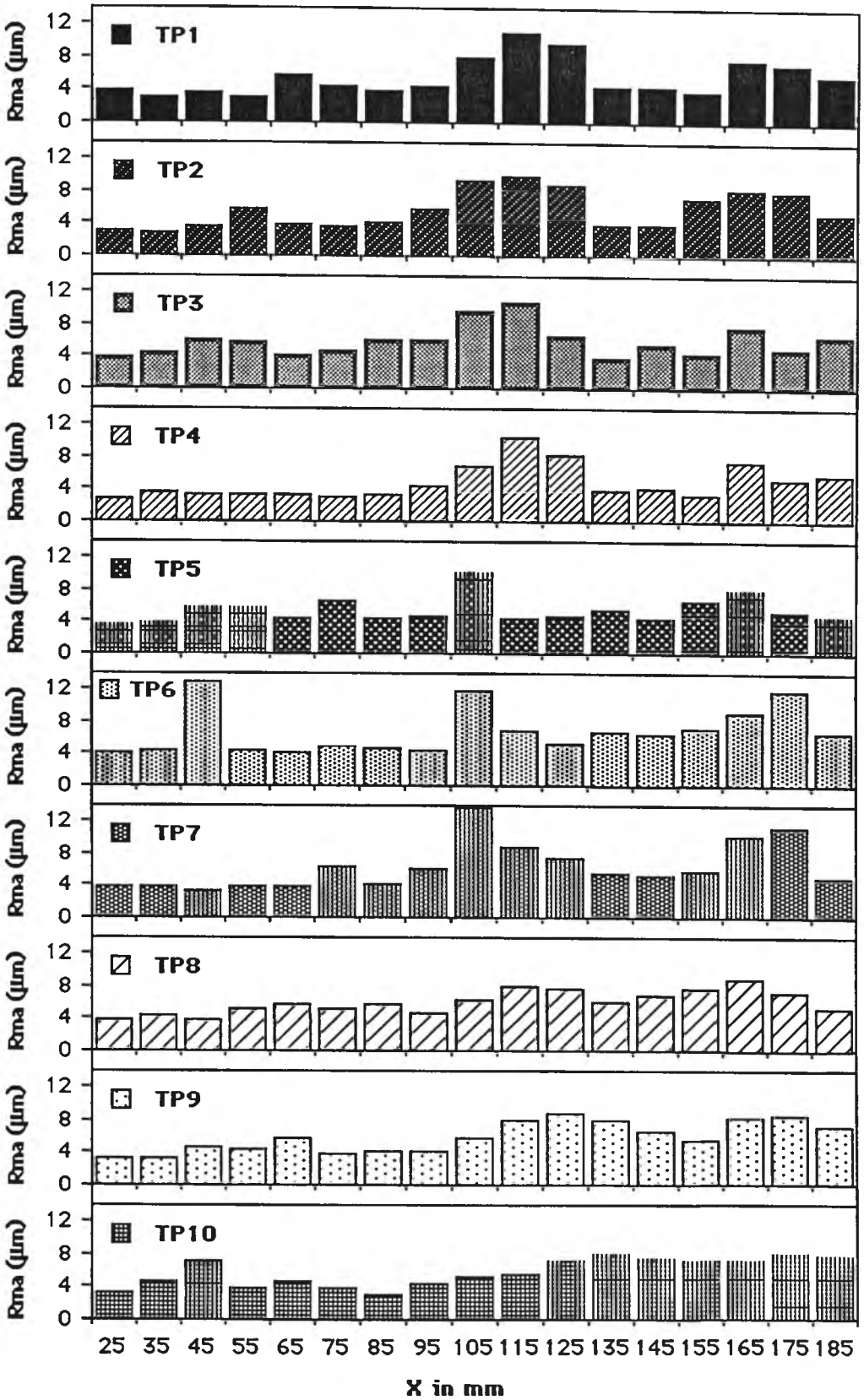

Figure 6.9 Variation of Peak to Valley Height (R_{ma}) along Feed Direction in Different Components in face Milling.

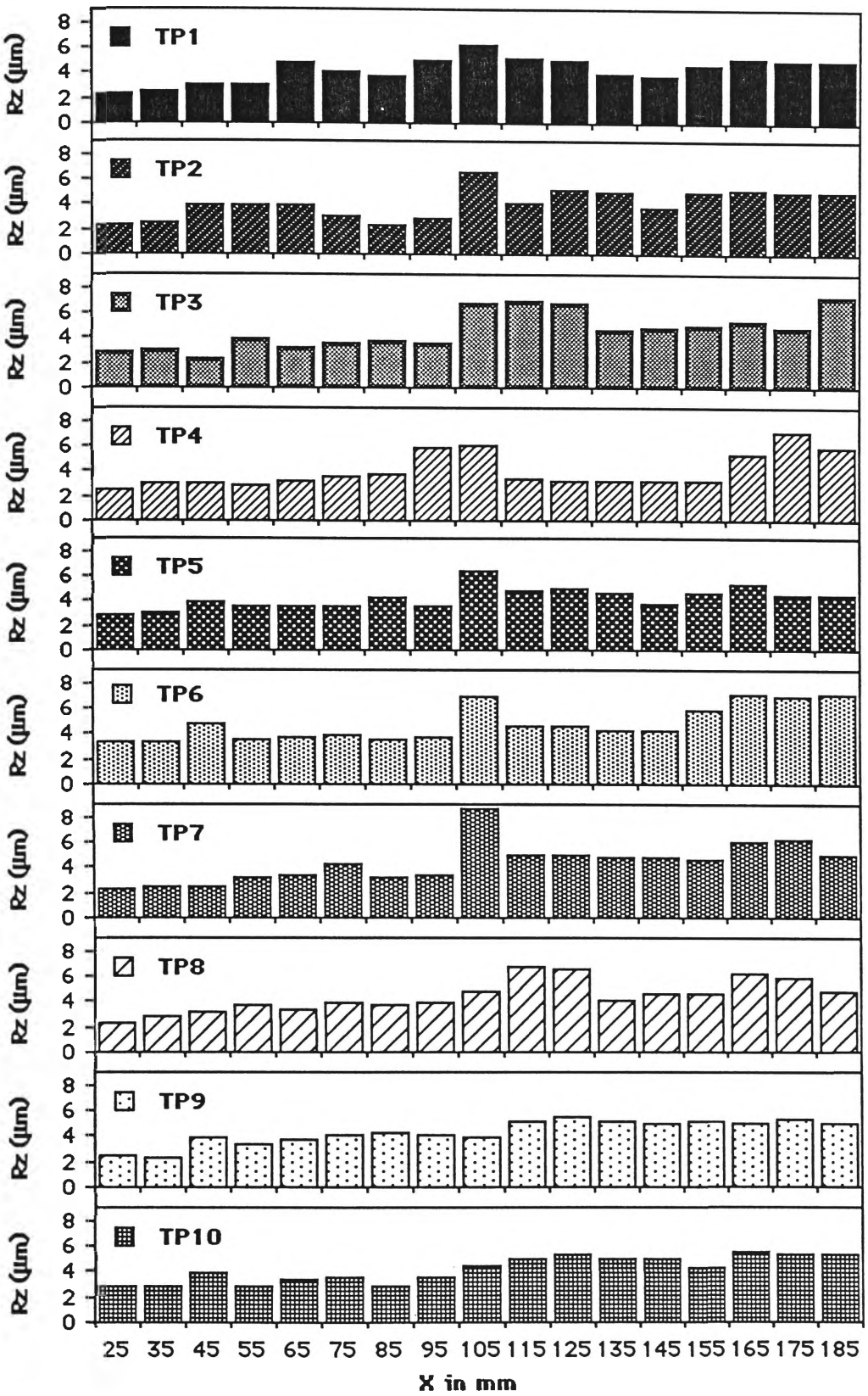

Figure 6.10 Variation of Ten Point Average (R_z) along Feed Direction in Different Components in face Milling.

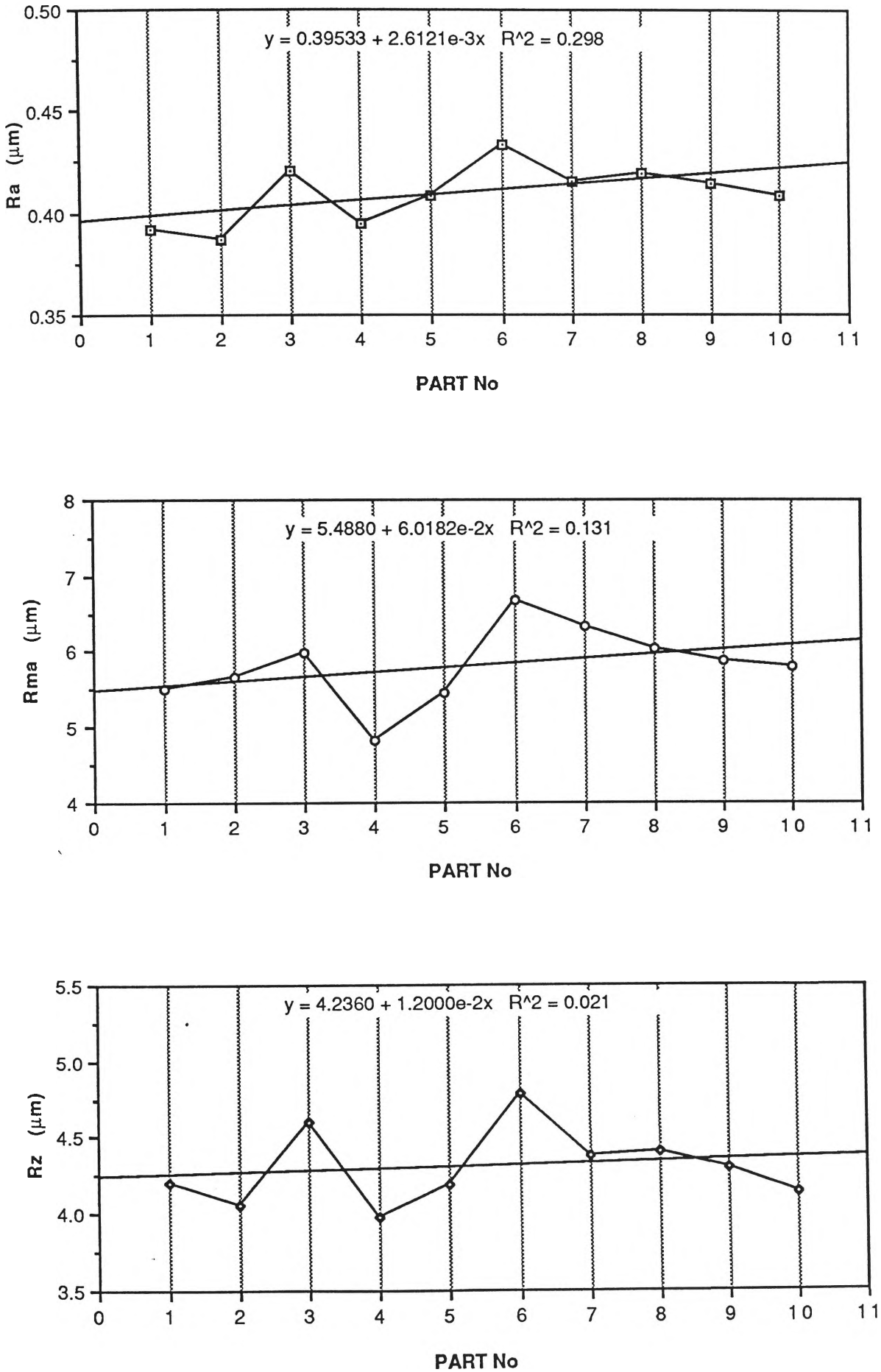

Figure 6.11 Variation of Roughness Parameters (R_a, R_{ma} and R_z) in Different Components in Face Milling.

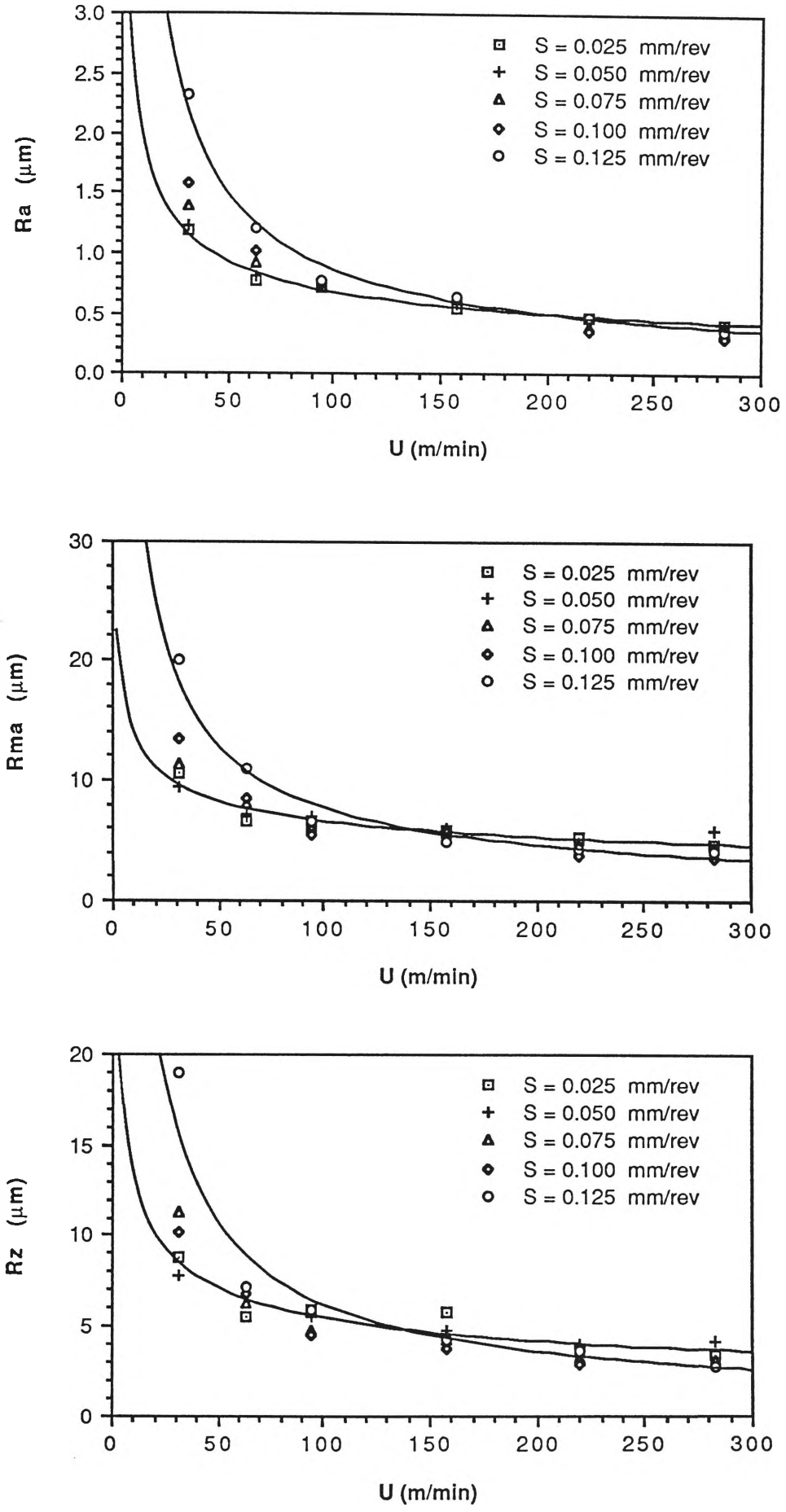

Figure6.12 Variation of Roughness Parameters (R_a, R_{ma} and R_z) versus Cutting. Speed (U) for Face Milling at Different Values of Feed (S).

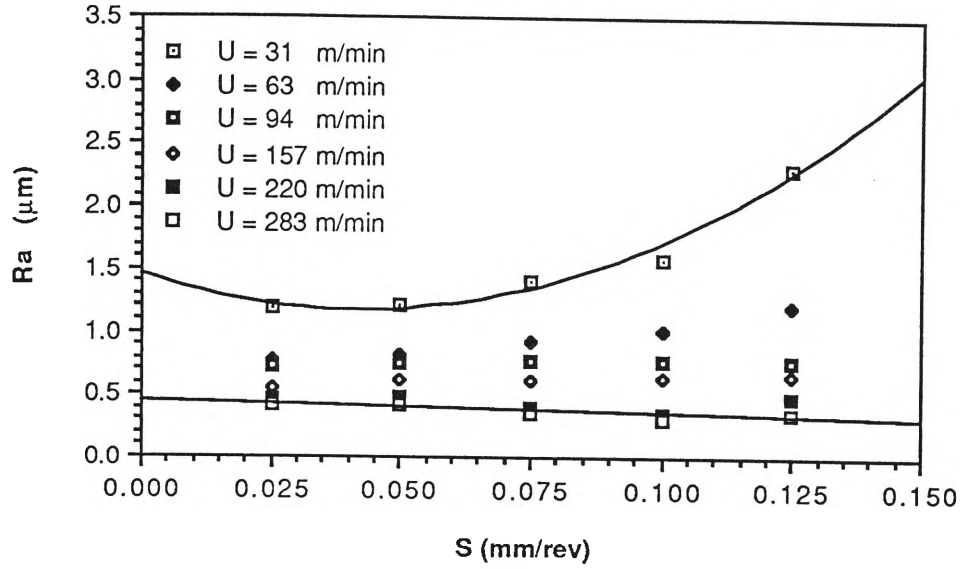

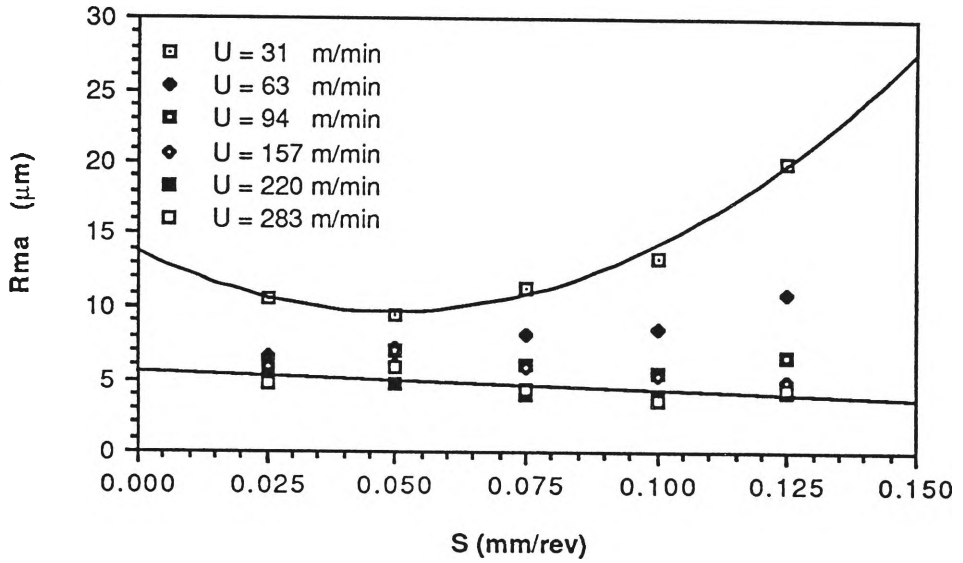

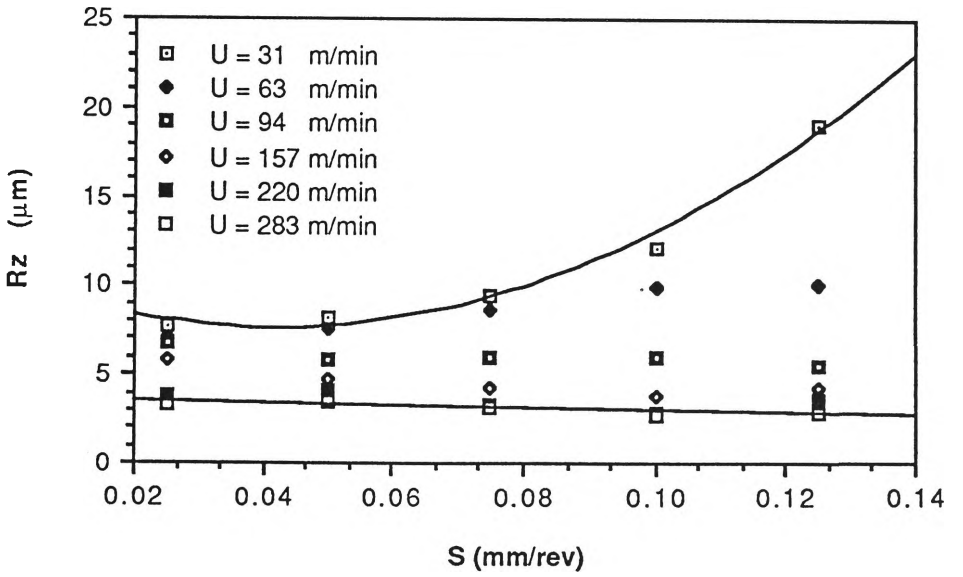

Figure 6.13 Variation of Roughness Parameters (R_a, R_{ma} and R_z) versus Feed (S) for Face Milling at Different Values of Cutting Speed (U).

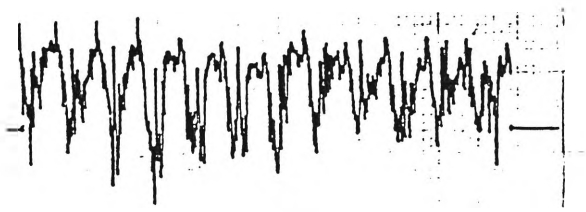

U = 31 m/min

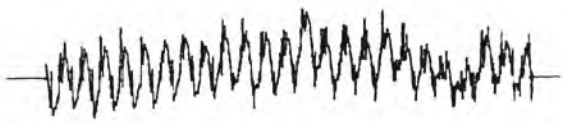

U = 94 m/min

U = 157 m/min

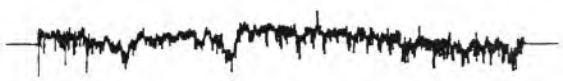

U = 220 m/min

Figure 6.14 Effect of Cutting Speed (U) on Surface Profile in Face Milling.

(S = 0.100 mm/rev)

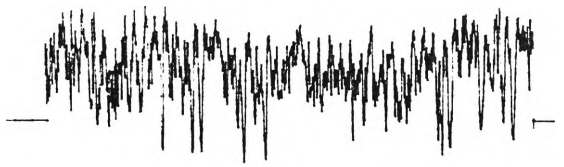

S = 0.025 mm/rev

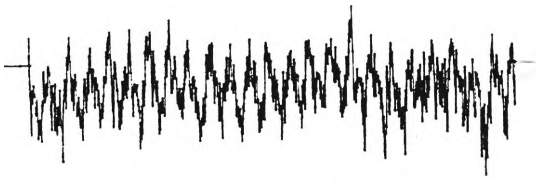

S = 0.050 mm/rev

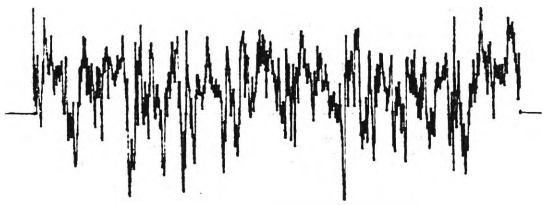

S = 0.075 mm/rev

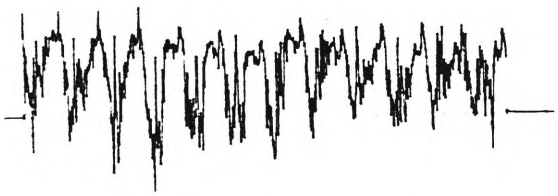

S = 0.100 mm/rev

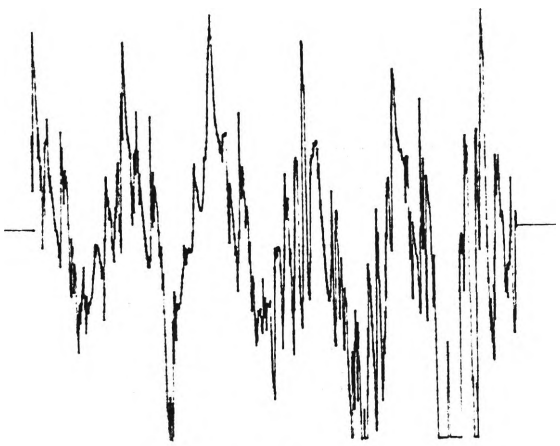

S = 0.125 mm/rev

Figure 6.15 Effect of Feed (S) on Surface Profile in Face Milling.

(U = 31.4 m/min)

The effect of cutting speed, feed and type of milling on surface roughness parameters in peripheral milling were investigated. Measured values of a number of surfaces under different cutting speeds and feeds are given in Figures 6.19 and 6.20.

The surface profile of end milled surfaces showed shape similar to the tool deflection (see Figure 6.16). The surface profiles of end milled surface showed clear difference in shapes of surfaces generated by up and down milling (see Figure 6.21), which confirms the findings of the previous chapter about end mill deflection.

6.3.3 Drilling

Drilling was performed to make holes on the test components. For the initial positioning, a centre drill was used. Drilling normally produces rough surfaces (with R_a values 12.5 - 5.1 mm, see Figure 6.1) and the feed marks are visible. We measured the roughness parameters of the hole peripheries (along the axial direction). Measurement data of a typical drilled surface are given in Figure 6.22. Five measurements were taken for each hole. The roughness parameters with their trends for ten test components (each with five holes) are given in Figure 6.23.

The effect of cutting speed and feed on surface roughness parameters in drilling were examined. A number of holes were drilled with varying cutting speeds (37.5 - 150 m/min) and feed rates (0.05 - 2.5 mm/rev). Variations of roughness parameters versus cutting speeds at different feed rates is given in Figure 6.24.

In modern NC programming, different types of canned cycles can be chosen, e.g. deep hole drilling canned cycle (G83), chip break canned cycle (G73),* etc. But no information is available about the effect that different types of drilling canned cycle may be on the surface finish of the holes. We have done some experiments to monitor this

*For details, please see Appendix F.

effect. Three drilling canned cycles (G73, G81 and G83) were chosen for comparison. For this purpose 60 holes were drilled (20 holes using each canned cycle). The results of the surface roughness parameters of these holes are given in Figure 6.25. As Figure 6.25 does not show any clear tendency, a statistical analysis of those data was done. Results of the Statistical analysis are given in Table 6.1.

Most of the surface profiles of the holes showed, the diameter increases to some peak value in the middle of the holes (a barreling effect) and then decreased, most probably caused by drill deflection. Three typical examples of surface profiles are given in Figure 6.26. In Figure 6.26 as large as 20 mm deviation can be noticed. The findings of the preliminary studies (see Chapter 3) about barreling effect of the holes thus can be confirmed.

Surface Rough-ness Paramet. (μm)	G73			G81			G83		
Statist. Paramet.	R_a	R_{ma}	R_z	R_a	R_{ma}	R_z	R_a	R_{ma}	R_z
Average	5.92	52.37	44.59	5.94	52.47	44.61	6.22	49.91	44.29
Stand. Dev.	0.64	10.96	5.52	0.98	12.77	8.78	0.84	7.35	4.33
Variance	0.41	120.09	30.45	0.96	163.11	77.13	0.71	54.02	18.75
Skewness	0.23	0.74	0.29	-0.09	0.54	0.13	0.64	0.85	0.49
Kurtosis	3.21	2.39	2.38	1.84	2.16	2.27	2.96	2.94	2.37
Range	2.90	36.30	22.30	3.34	43.4	34.10	3.30	26.60	17.40
Median	5.90	47.40	44.00	5.90	47.8	44.70	6.20	48.70	42.00

Table 6.1 Statistical Analysis of Roughness Parameters of Holes, Drilled Using Different Canned Cycles.

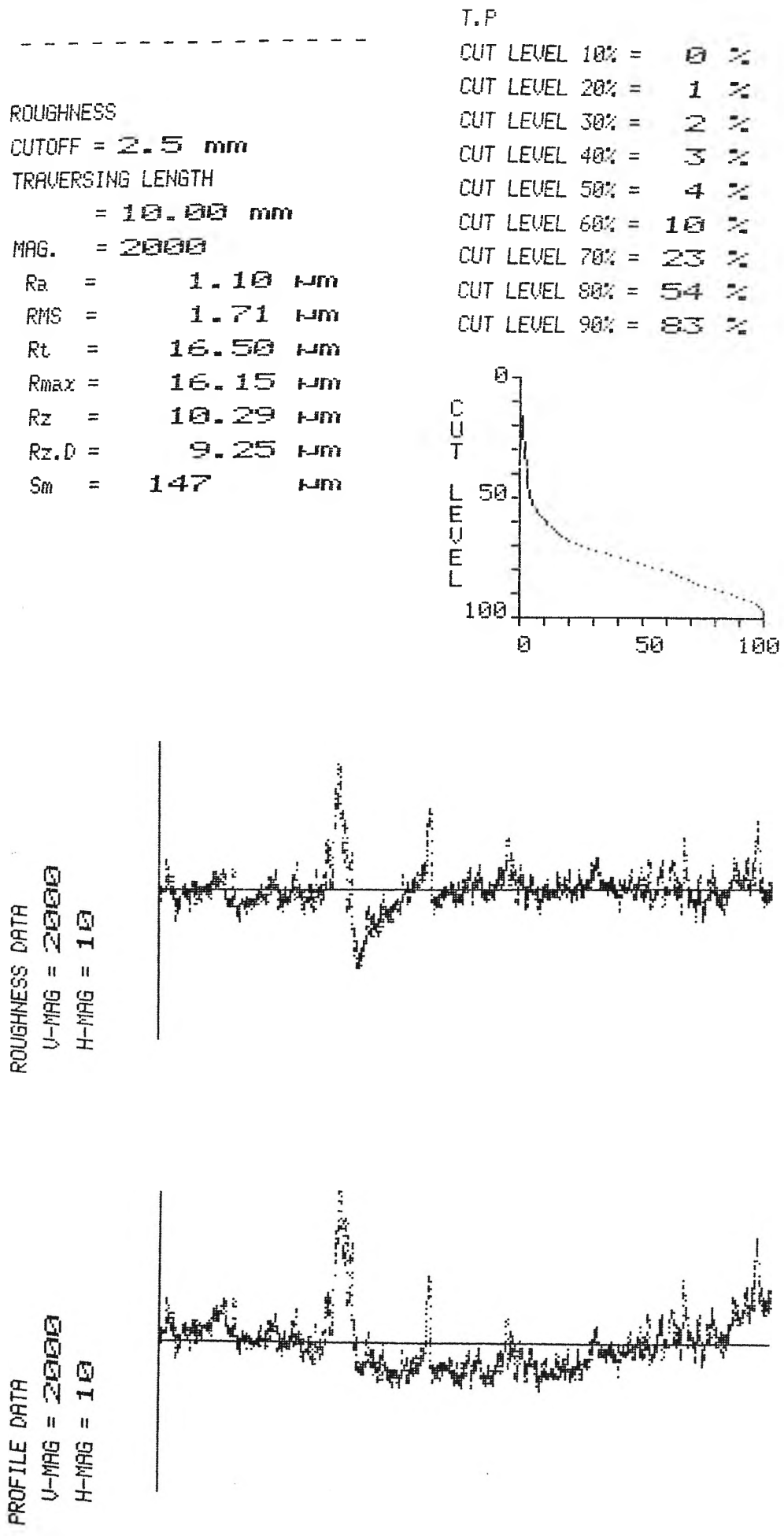

Figure 6.16 Roughness Parameters of a Typical End Milled Surface.

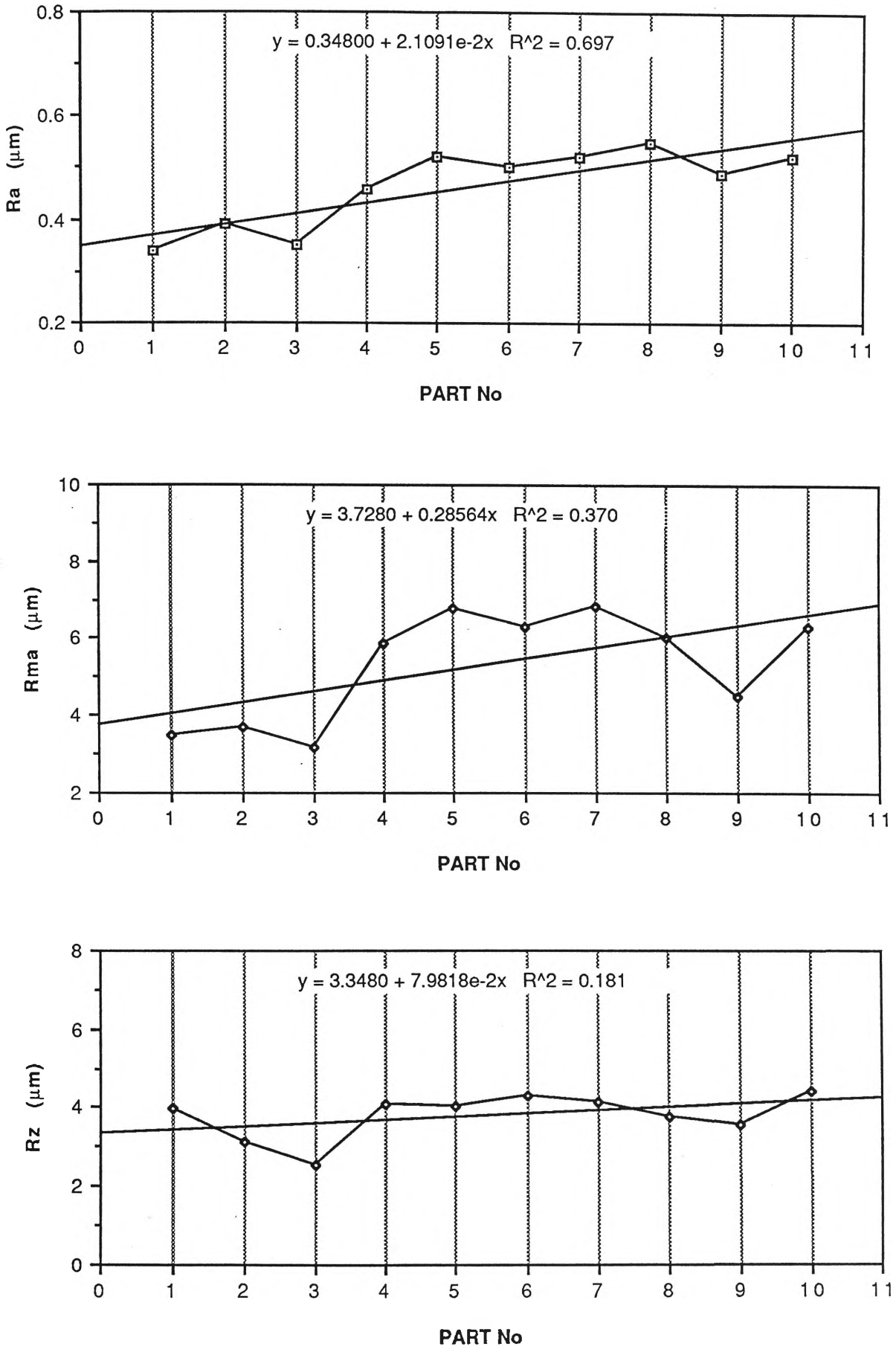

Figure 6.17 Variation of Roughness Parameters (R_a, R_{ma} and R_z) in Different Components in Peripheral Milling.

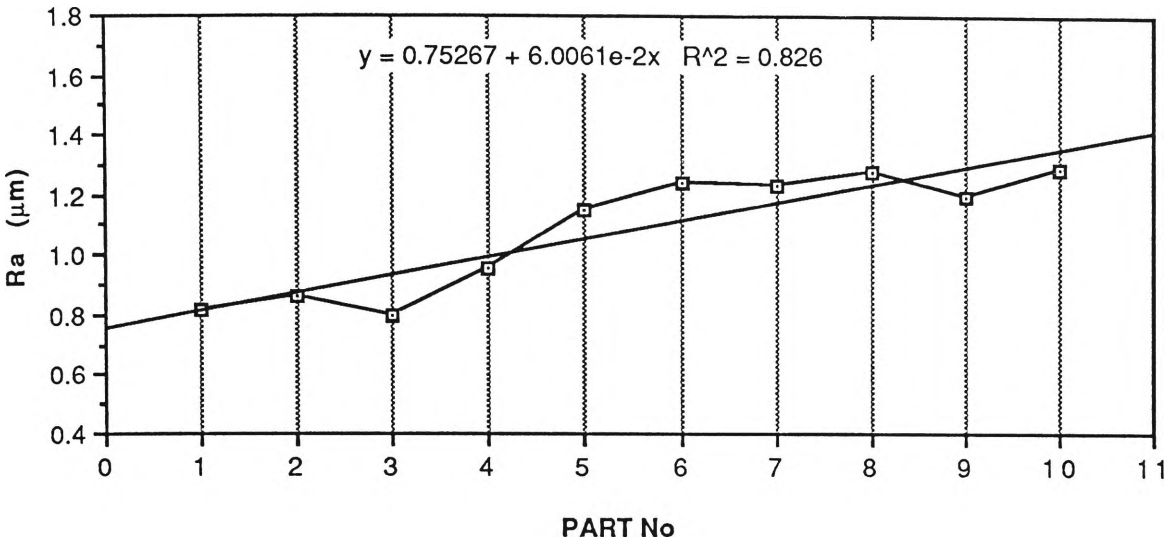

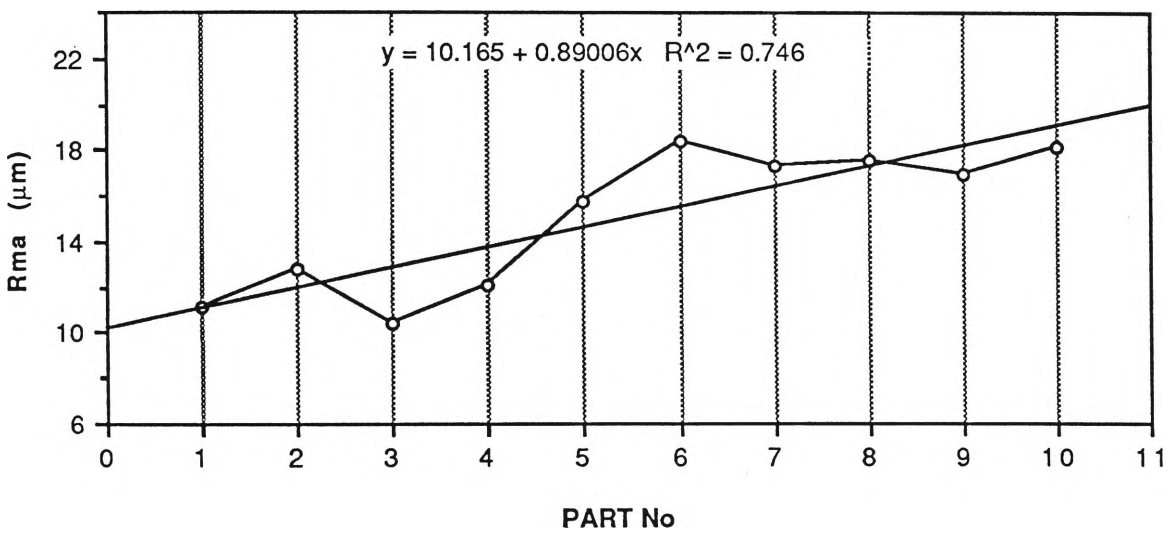

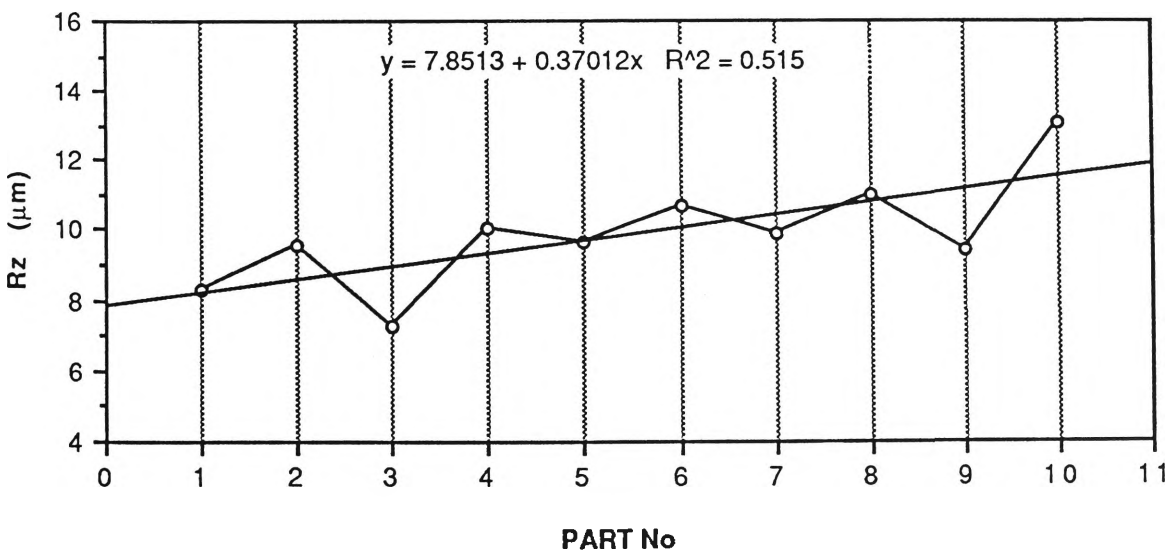

Figure 6.18 Variation of Roughness Parameters (R_a, R_{ma} and R_z) in Different Components in Face Milling as a part of Combined Milling.

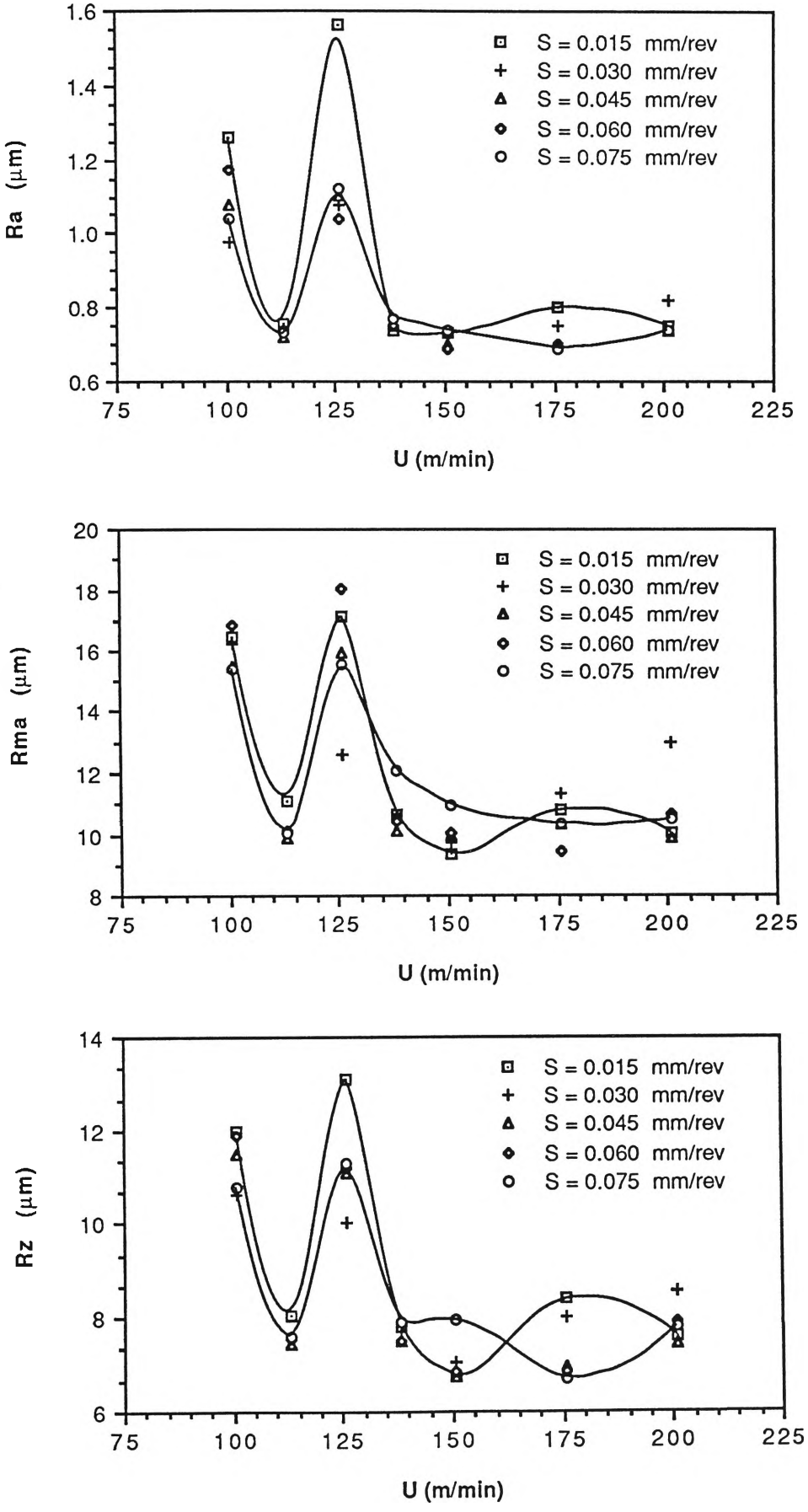

Figure 6.19 Variation of Roughness Parameters (R_a, R_{ma} and R_z) versus Cutting Speed (U) for Peripheral Milling (Up) at Different Values of Feed (S).

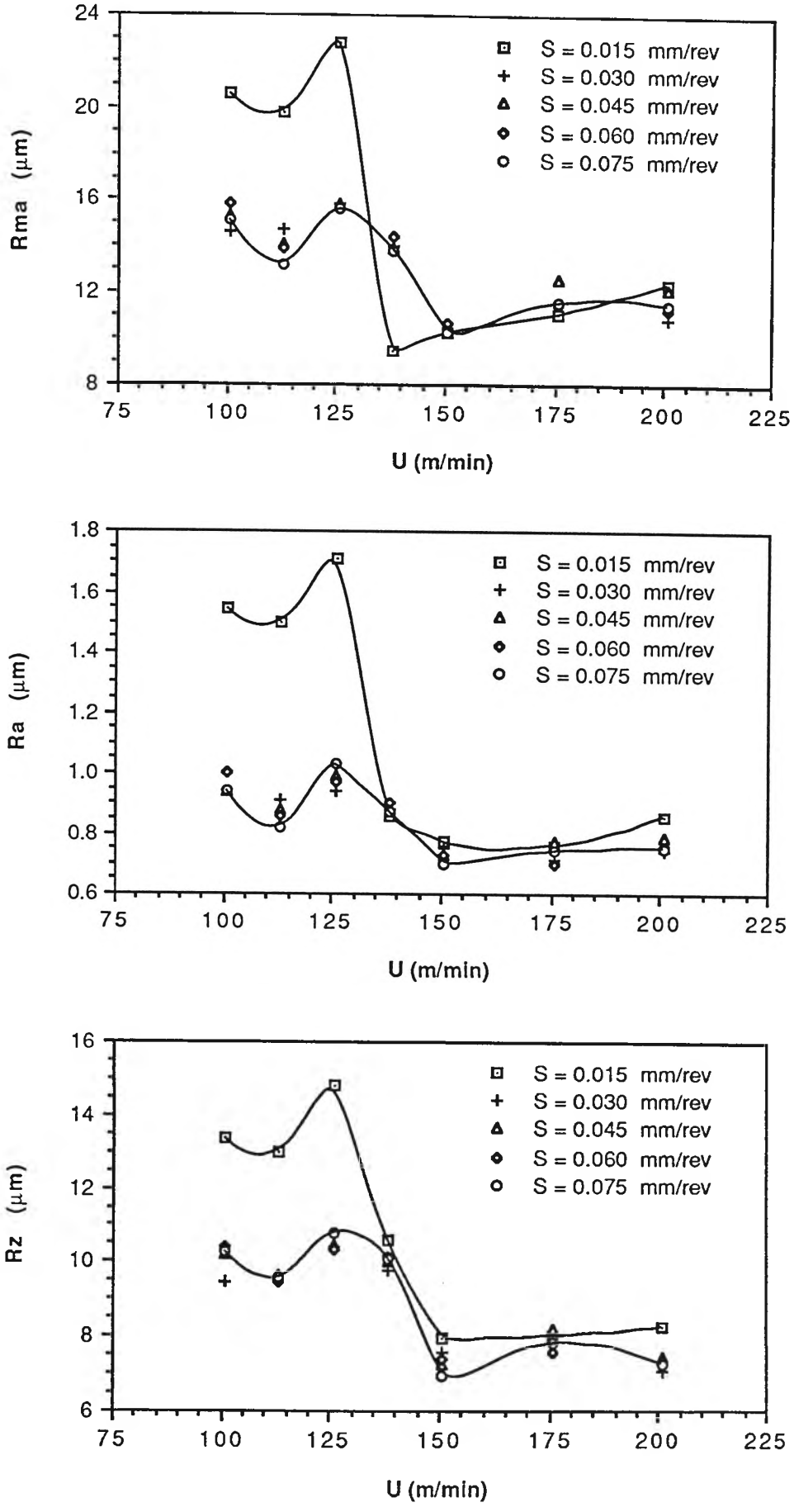

Figure 6.20 Variation of Roughness Parameters (R_a, R_{ma} and R_z) versus Cutting Speed (U) for Peripheral Milling (Down) at Different Values of Feed (S).

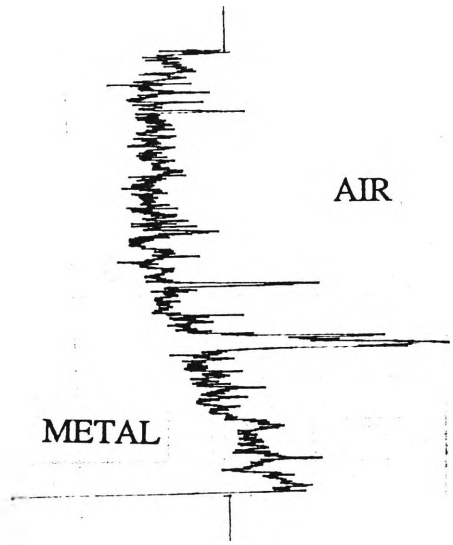

Down Milling

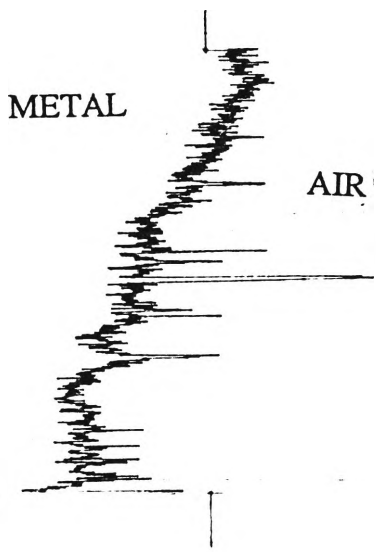

Up Milling

Figure 6.21 Surface Profile of End Milled Surfaces Show the Different Shapes of Surfaces Generated by Up and Down Milling.

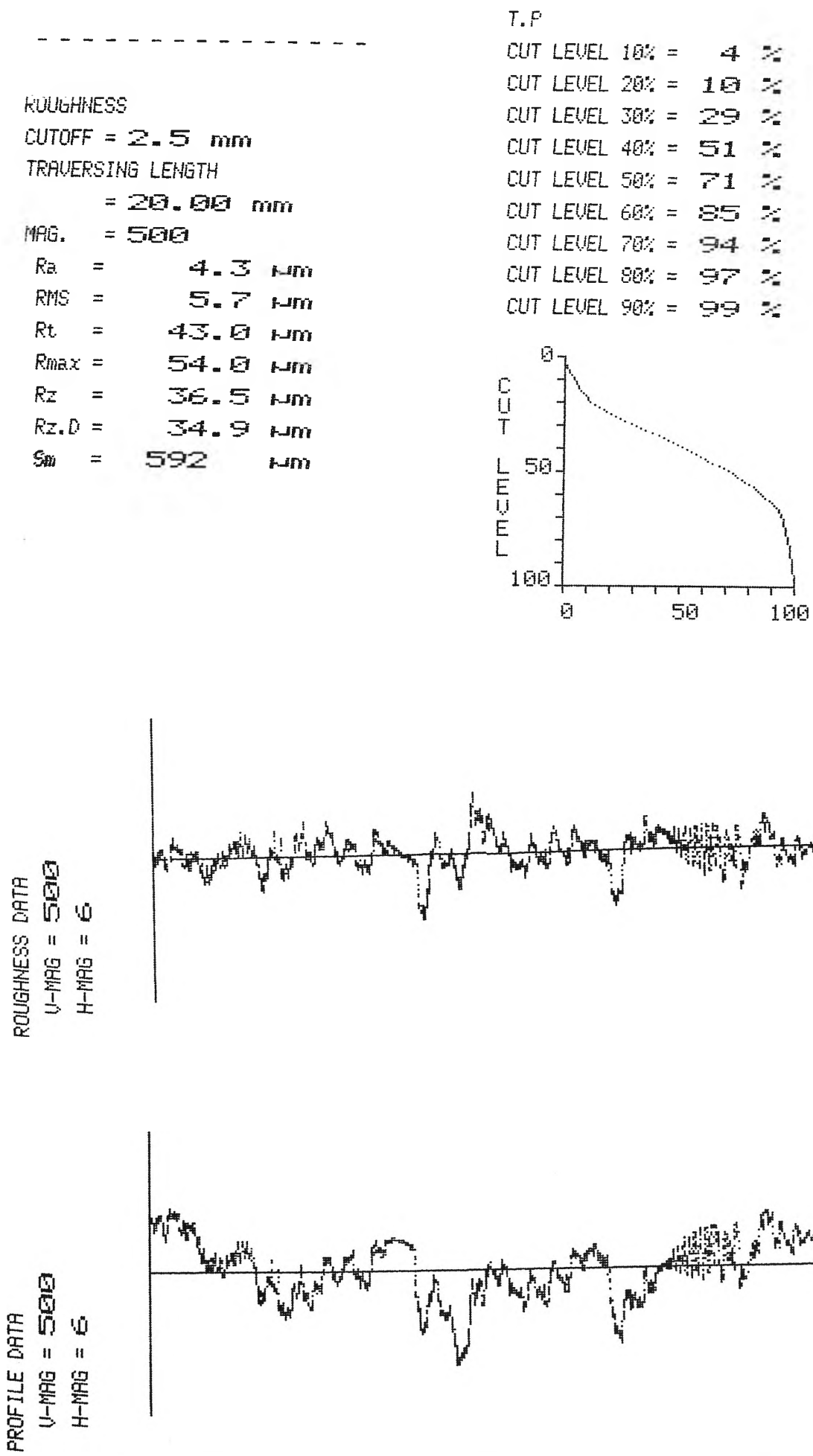

Figure 6.22 Roughness Parameters of a Typical Drilled Surface.

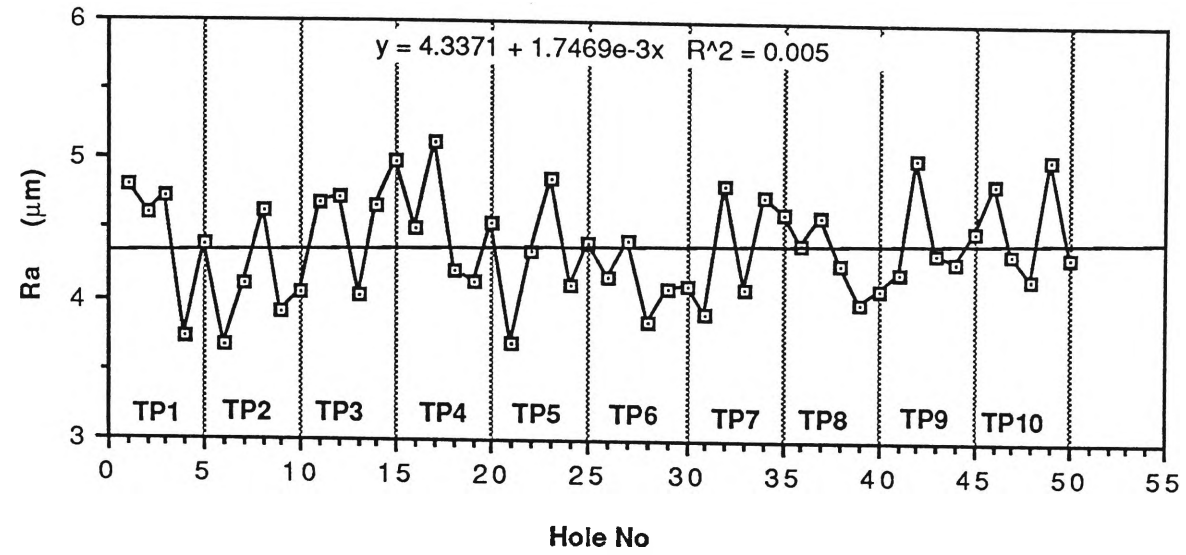

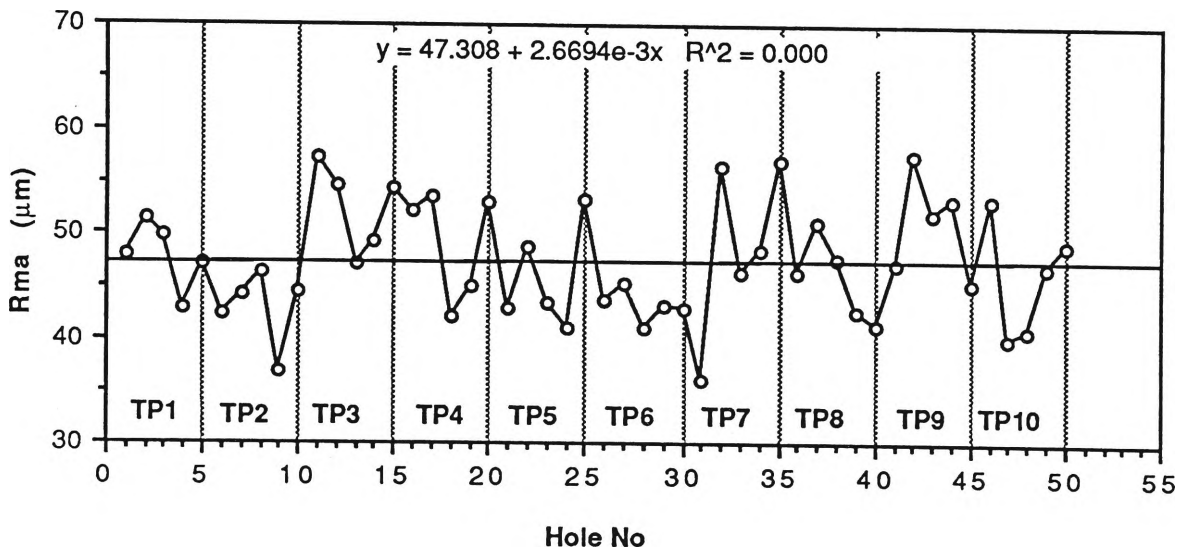

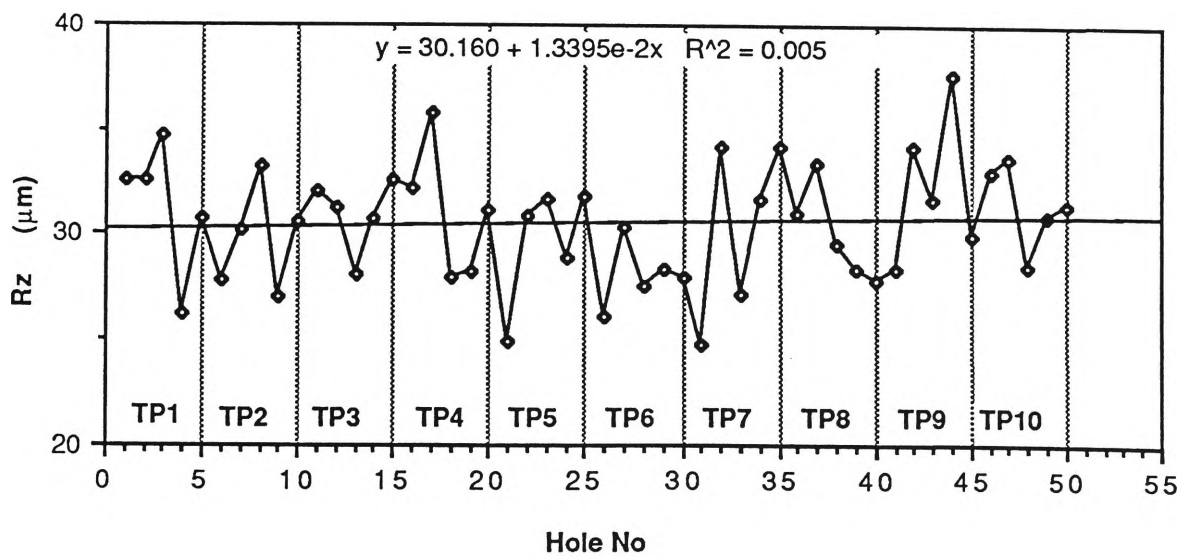

Figure 6.23 Variation of Roughness Parameters (R_a, R_{ma} and R_z) in Different Holes in Drilling.

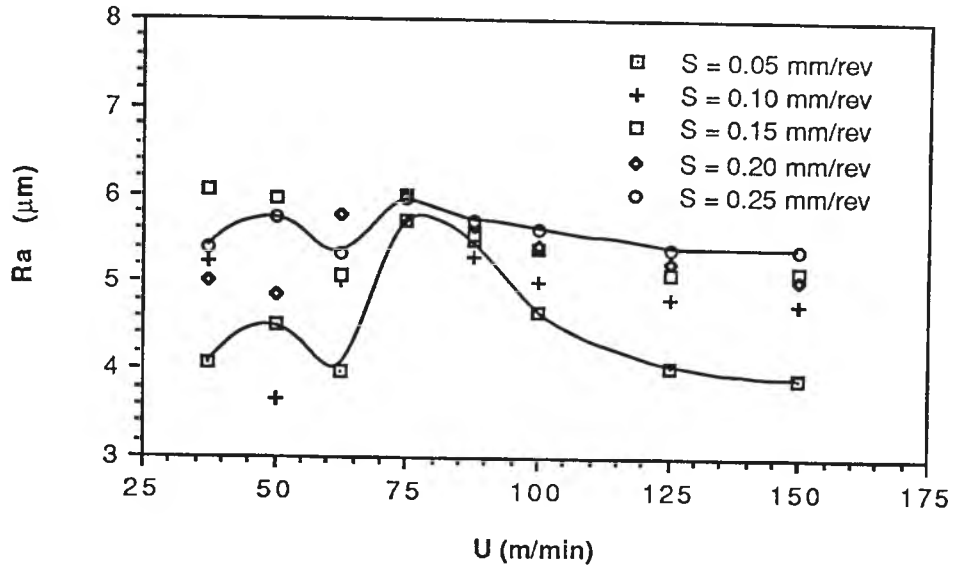

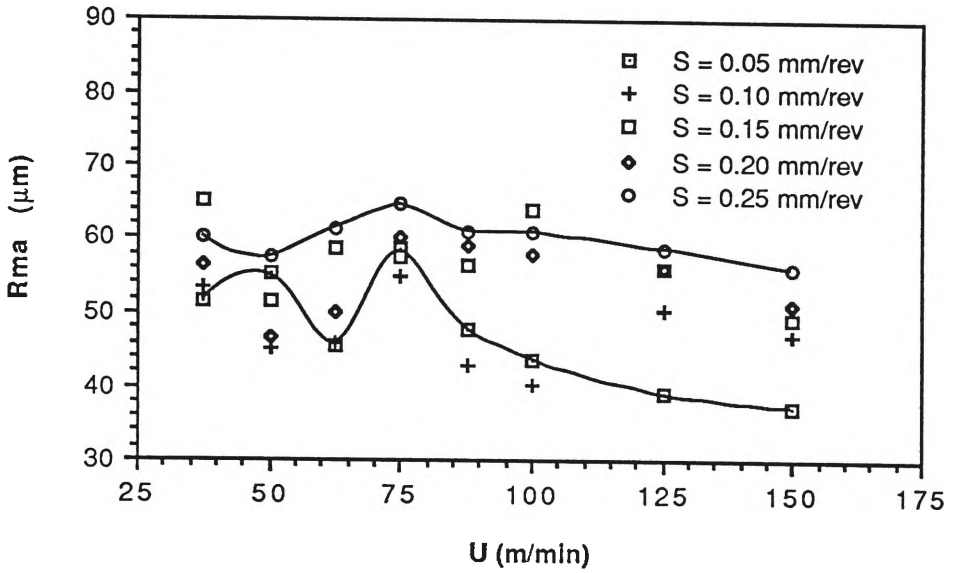

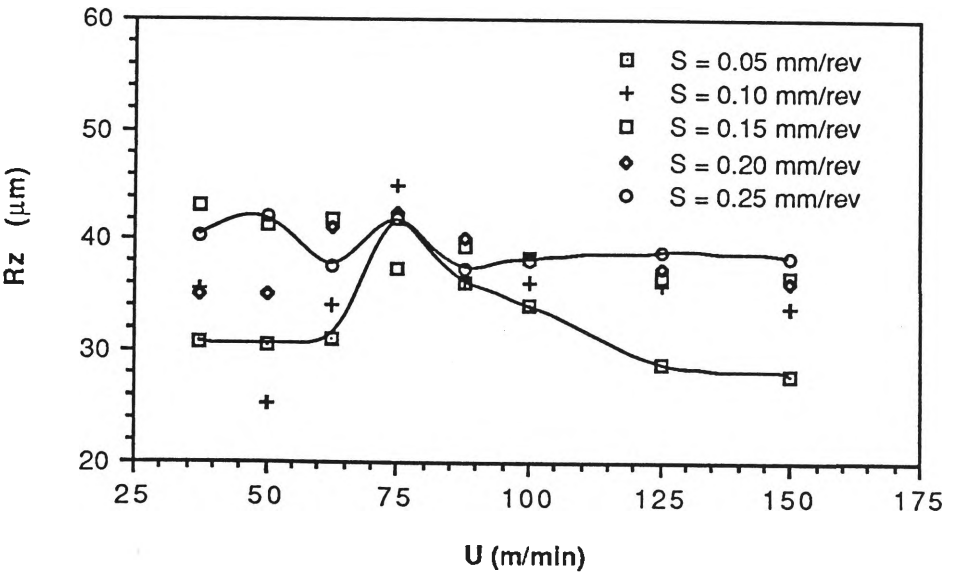

Figure 6.24 Variation of Roughness Parameters (R_a, R_{ma} and R_z) versus Cutting Speed (U) for Drilling at Different Values of Feed (S).

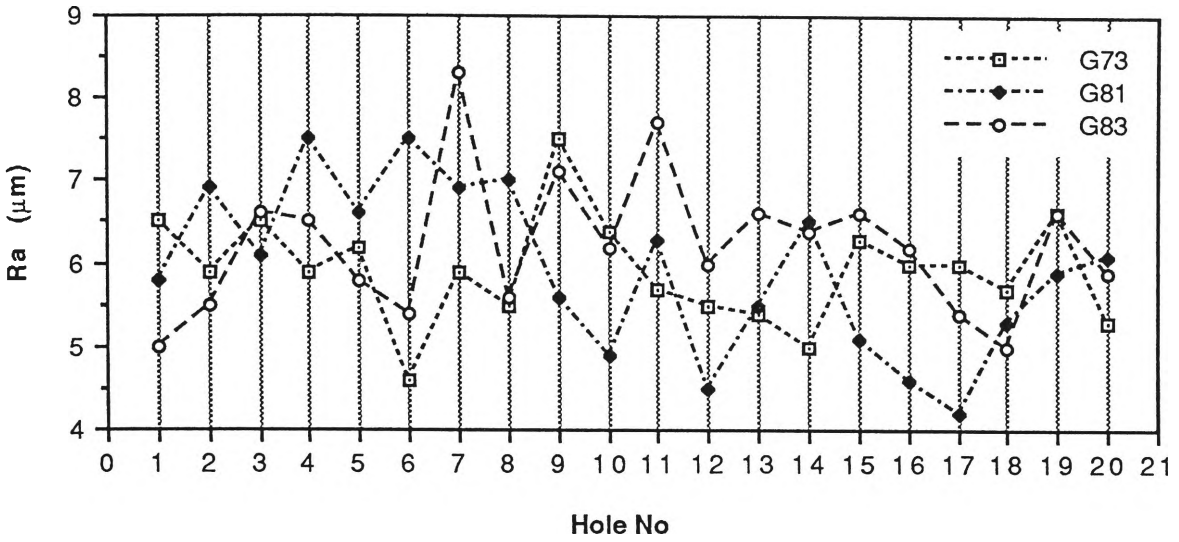

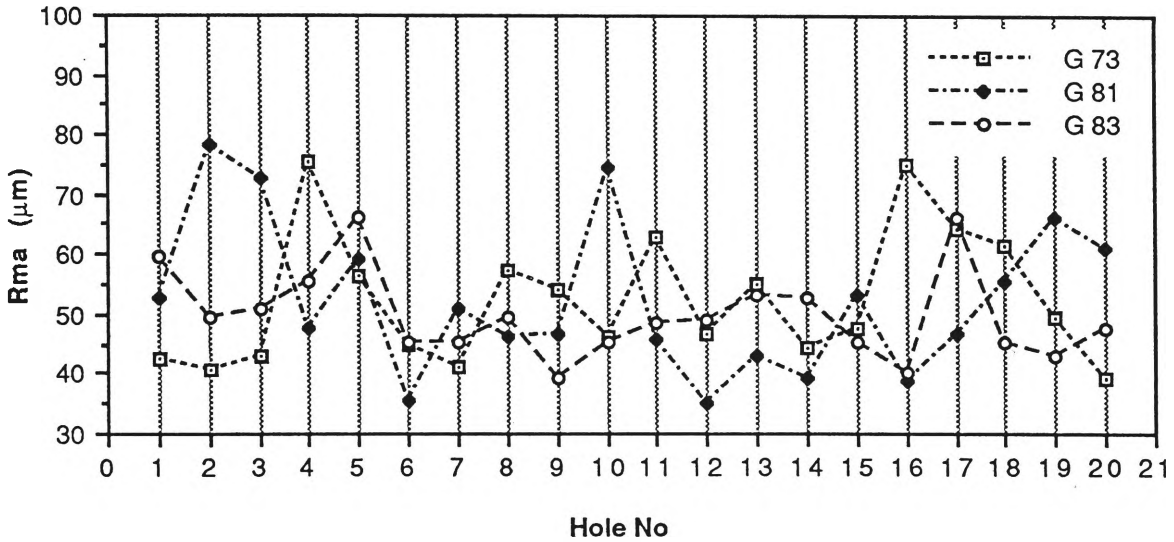

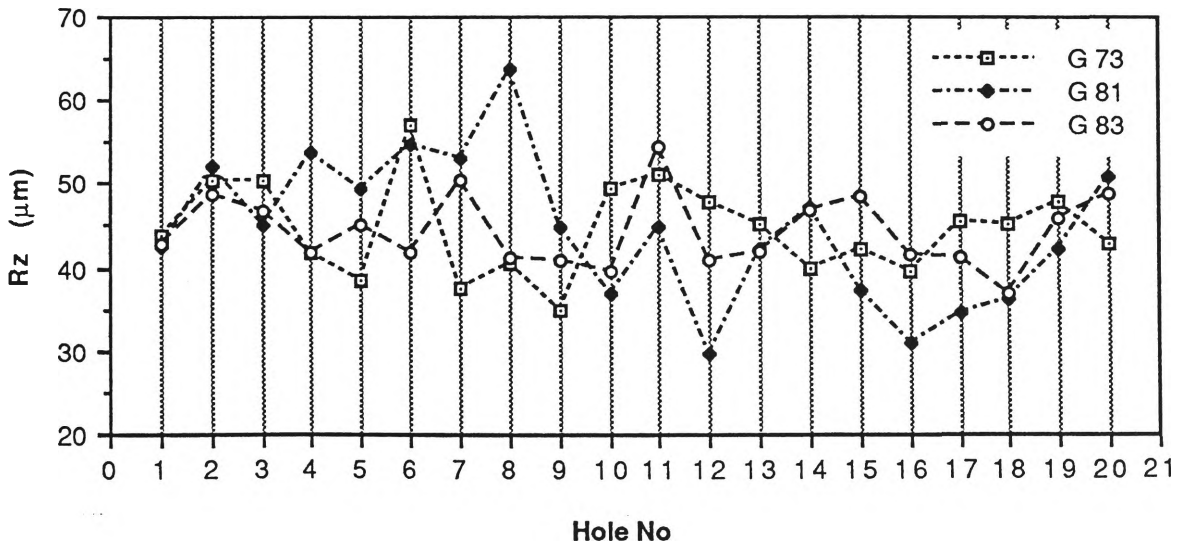

Figure6.25 Comparison of Roughness Parameters of Drilled Surfaces Using Different Canned Cycles.

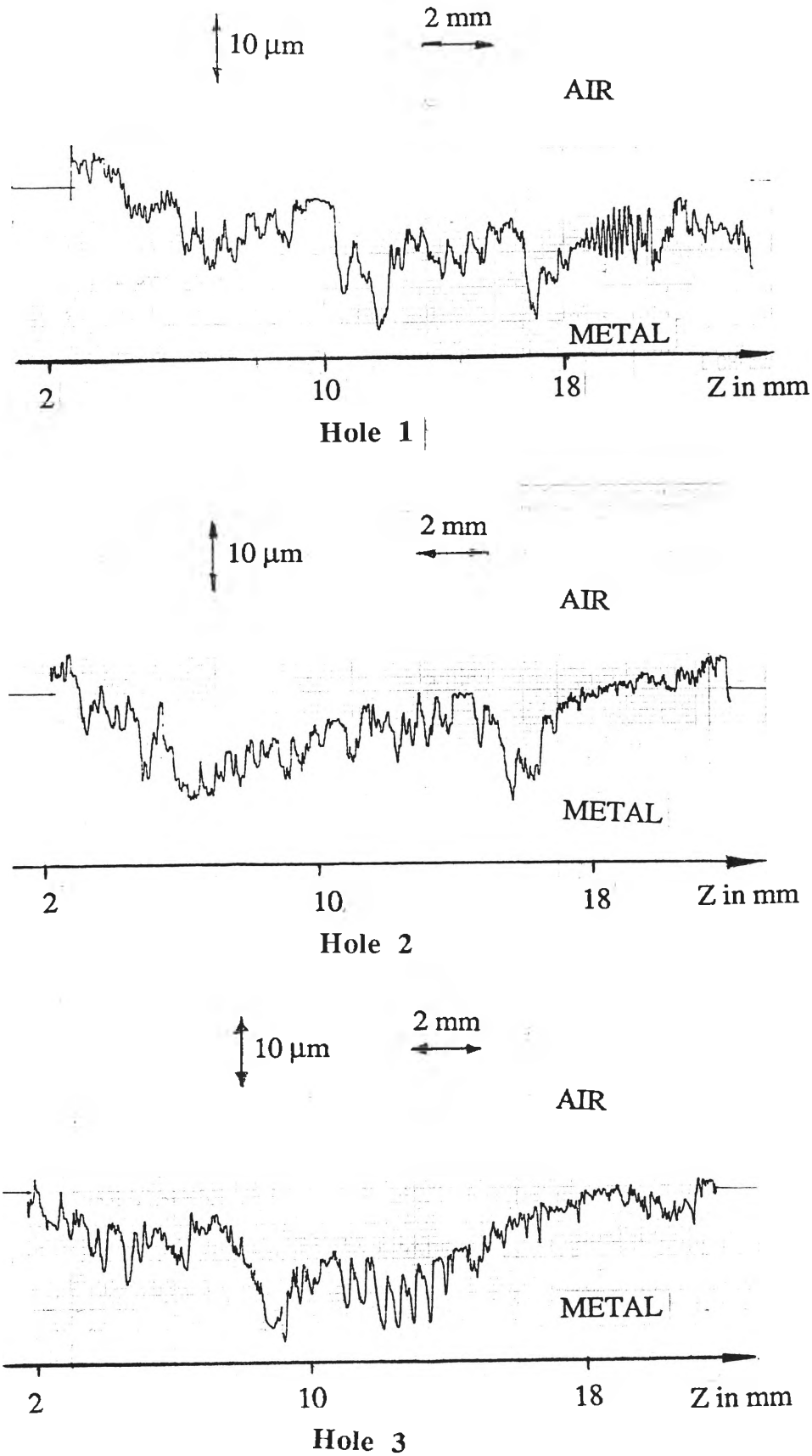

Figure 6.26 Surface Profile of the Holes Showing the "Barreling Effect".

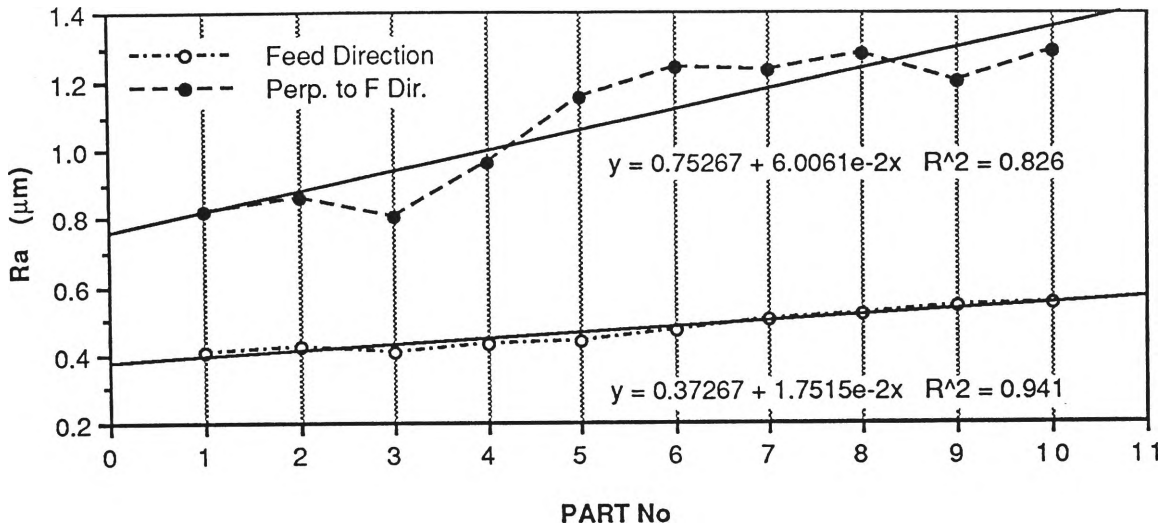

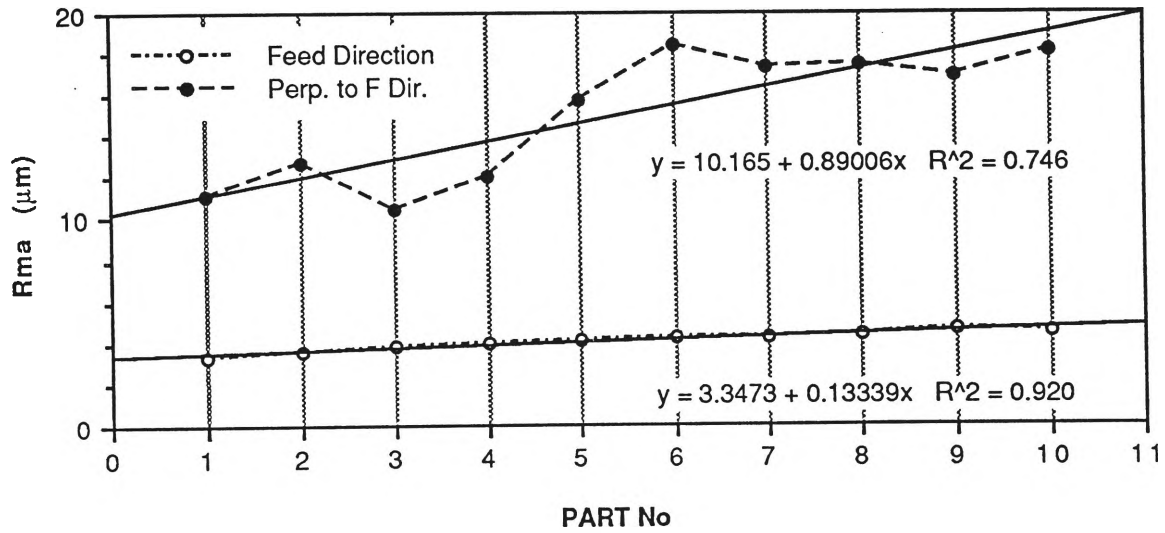

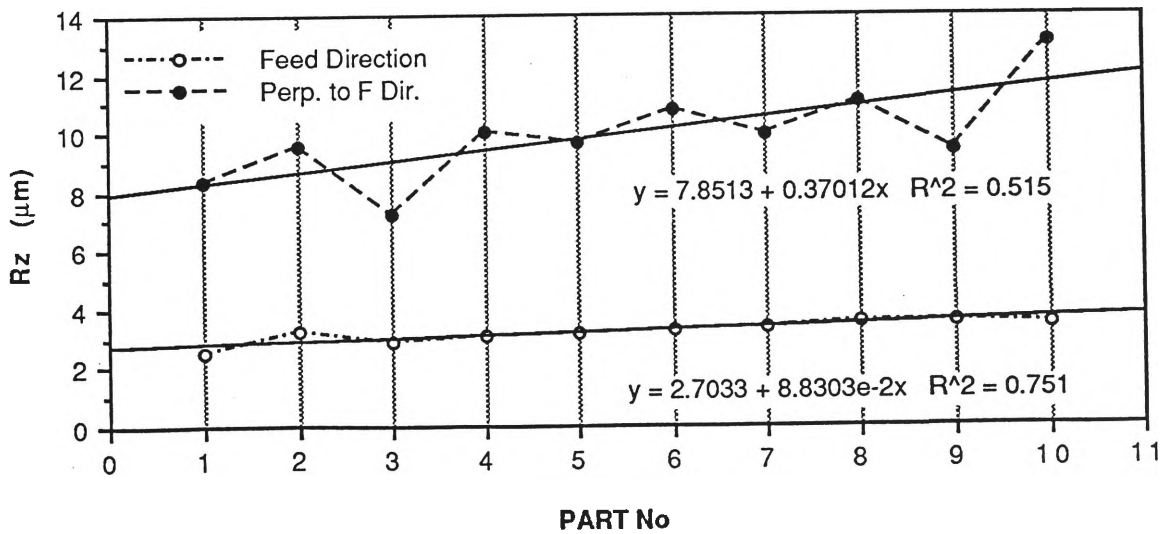

Figure 6.27 Comparison of Surface Roughness Parameters (R_a, R_{ma} and R_z) of Same Surface Measured in Two Directions (Feed Direction and Direction Perpendicular to Feed). (in Peripheral Milling)

6.3.4 Further Experimental Work

As mentioned earlier, no single parameter of surface texture is capable of describing comprehensively the topographical features of a surface. In fact, all the surface roughness parameters used today (for details see Appendix L) are based on two dimensional measurements. For total understanding of a surface, a three dimensional surface topography is felt to benecessary. In Chapter 3 an attempt has been made to plot three dimensional surface topography of machined surfaces using data from CMM (see Figures 3.13 and 3.14). However the data obtained from CMM was discrete in nature and with the size of the probe being large, it does not allow high-sensitivity of measurement (as far as surface topography is concerned). In this section surface topography of a machined surface was traced using a stylus-based surface measuring machine, Surfcom.

A face milled surface (machined by end mill) was taken as a specimen. On a 14 mm x 14 mm surface 70 parallel traces were taken at a tracing speed of 0.3 mm / sec. The output data were fed to a personal computer and a three dimensional plotting package was used to plot the surface topography (see figure 6.28). A contour plot of the same surface is given in Figure 6.29. These figures provide general information about the surface topography such as tool travel marks.

6.4 Comments and Discussions

We have seen in section 6.2 that the **actual** surface roughness values are greatly influenced by the BUE. On the other hand, the formation of BUE is very dependant on the material properties of the workpiece. So all the experimental results on surface texture stated in this chapter are valid **only** for the material used (aluminium alloy, 6000 Grade, marine quality). Moreover, aluminium being a ductile material is normally more adhesive and has a tendency to form a BUE. Due to this fact some of the results may appear to be paradoxical. We are also sceptical about the repeatability of the experiments.

Gladman [173] reported that in recent years research workers found large variability in measurements of surface finish. Greater variability is expected from machine to machine and from factory to factory in industry.

In the experimental work, it was found that in some cases the roughness values of the same surface may vary considerably. For plotting the relationships between roughness values against different variables, mean values of the surface roughness were used. To reduce the uncertainty of measurement, the number of measurements were increased.

In general, for all of the metal removal processes considered (i.e. face milling, end milling and drilling), the roughness values decrease with an increase in cutting speed at the high speed range (see Figures 6.12, 6.19, 620 and 6.24). At the initial stage, with the increase in cutting speed roughness values decrease sharply and after sometime the roughness values tend to stabilize at high speed. According to some researchers [168], the roughness values stabilize at ideal roughness values. Unfortunately due to spindle speed constraints (maximum spindle speed 4000 RPM) we could not extend our experiments to higher speed.

From Figures 6.8 - 6.10, it can be seen that in face milling the roughness parameters change considerably in feed direction and at some stage ($x \approx 100$ mm), the roughness parameters suddenly rise. This is the stage when the cutter starts to exit from the job. In face milling, the surface texture of the machined surface is dominated by the marks produced by the tracking teeth. This is known as **heel drag**. When the cutter starts to exit from the job, in fact no cutting takes place; but the cutter has to travel at a feed rate to allow the cutter to disengage its whole body from the job. This length is known as **over travel.** During this over travel period the cutting forces change, compared to the cutting period. Due to this fact the lay pattern of the face milled surface changes during over travel and sometimes crisscrossing of the lays are observed.

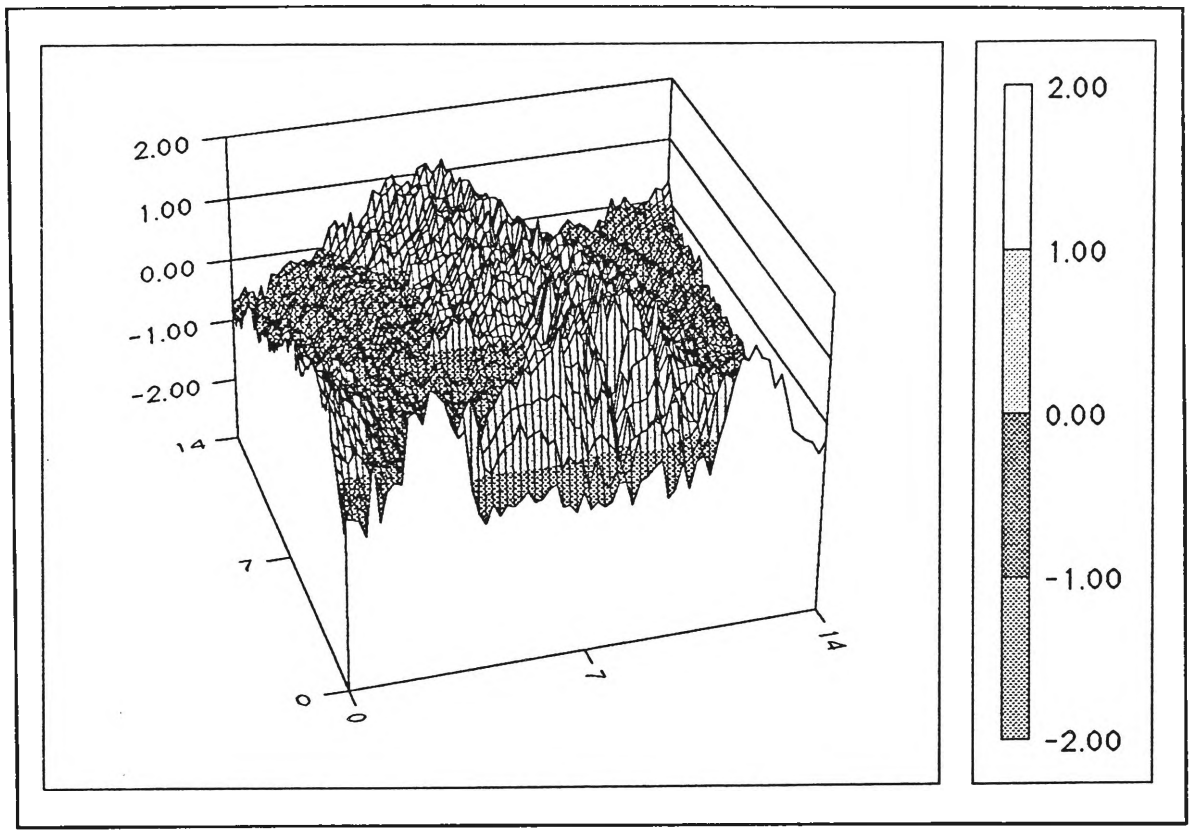

Figure 6.28 Surface Topography of a Face Milled Surface Plotted Using Data from Surfcom.

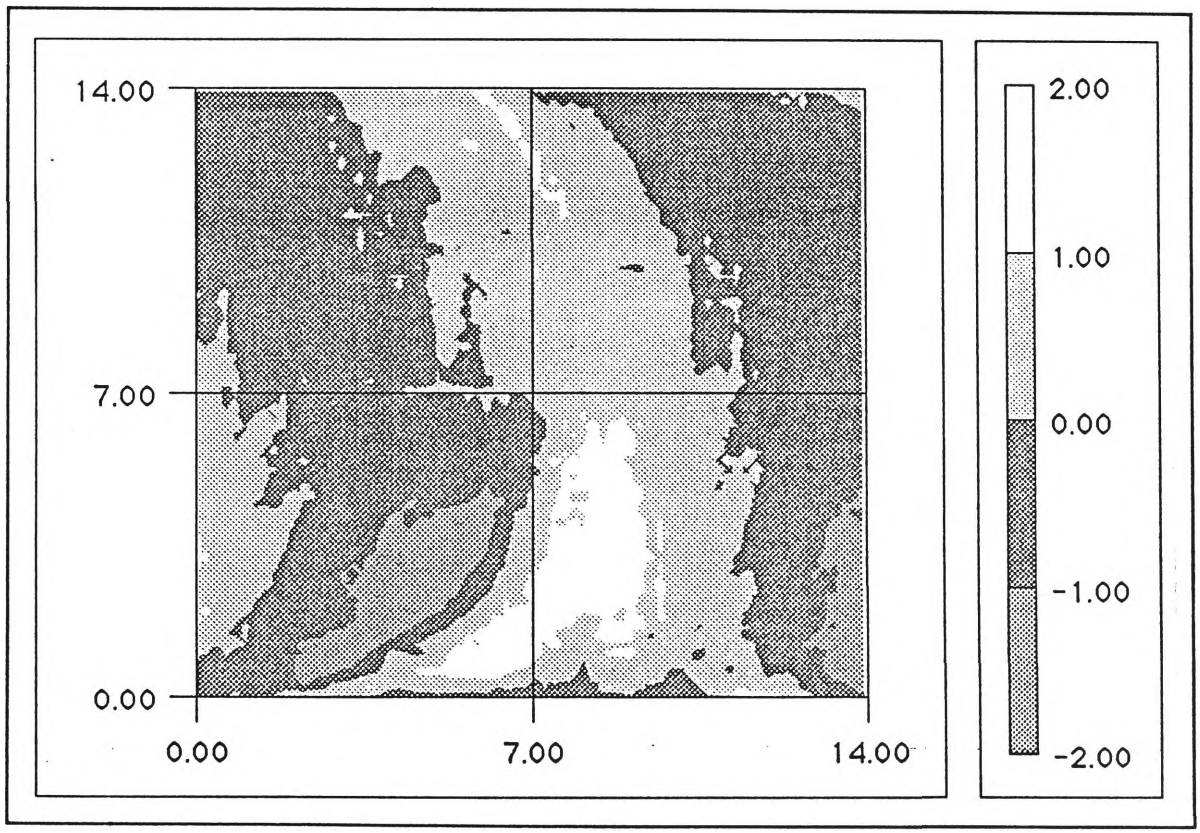

Figure 6.29 Contour Plot of a Face Milled Surface Plotted Using Data from Surfcom.

Heel dragging seems to be a common problem in face milling. Some researchers [174], [6] suggested the use of a very slight spindle tilt in the direction of feed (see Figure 6.30) to assure that the cutter does not recut the job by the back side of it. But the CNC machining centre used in our machining, has a flat spindle (in order to mill in any direction) and no provision for spindle tilt is available. However same effect can be achieved with thevariable height of inserts. In recent years with the availability of different types of inserts, this method has become popular. Often parallel-land corner chamber inserts or wiper inserts are used in in this case the surface is formed by only one insert - the insert that is placed highest (or furthest from the back of the cutter).

In Figure 6.11 the variation of roughness parameters in different components in face milling is shown. The line of best fit for each roughness parameter shows slight upward trend which reflects the effect of tool wear.

The graphs presented in Figure 6.12 are in agreement with the normally expected relationship between surface roughness and cutting speed, i.e. with the increase in cutting speed, surface finish improves and with the increase in feed, the surface finish deteriorates. It is also interesting to note that at low speed, feed has much effect on surface roughness parameter but at high speed the effect of feed is negligible (see Figure 6.13). Figures 6.14 and 6.15 are self explanatory.

Before commencing discussions on surface quality of end milled surface, the author feels necessary to clarify the following point. In face milling, drilling and turning the lay patterns of the surfaces are such that the worst cases of surface roughness parameters are measured when the measurements are taken along the feed direction; whereas in end milling (peripheral) the lay patterns of the surface are oriented in such a way that the direction perpendicular to the feed direction will register worst case of measurement. For that reason normally for face milled, turned or drilled surface the roughness parameters are measured along feed direction and for end milled (peripheral) those parameters are

measured along a direction perpendicular to the feed. As the ideal roughness values are measured along the feed direction, in effect for peripheral milling ideal, roughness values have no real significance. Comparisons of surface parameters of the same peripheral milled surface, measured in feed direction and direction perpendicular to feed are given in Figure 6.27. From those graphs the differences between surface roughness parameters caused by direction of measurement is clear. In Figure 6.27 a very slow and steady upward tendency of the process is also noticed.

In Figure 6.16, the profile data showed the effect of end mill deflection. Surface profiles of end milled surfaces illustrated in Figure 6.21 confirms the findings of Chapter 5 i.e. in down milling cthe utter deflects away from the job, whereas in up milling (depending on the cutting conditions and cutter geometry) cutter may dig into the job.

In Figure 6.17, variations of roughness parameters in different components in peripheral milling are shown. The lines of best fit have also show upward tendencies which are believed to be due to tool wear. If we compare Figures 6.17 (peripheral milling), 6.11 (face milling) and 6.23 (drilling), we find the slope† of the line of best fit for peripheral milling is considerably larger than the slope of the line representing face milling and drilling. One of the reasons may be, the end mill was used more extensively for machining (about 980 mm per part along feed direction) than the face cutter (about 200 mm per part along feed direction) and drill (about 120 mm per part along feed direction). This excessive use of the end mill caused faster tool wear per part. In Figure 6.18 variation of roughness parameters in different components in face milling as a part of combined milling is given. Surprisingly similarity was found between two figures (Figure 6.17 and 6.18) although two different faces of the same tool were used. This is perhaps due to the fact that both operations were performed with same cutting speed and cutting speed has greater influence on tool wear.

---

† See the equations of lines of best fits given in Figures 6.17, 6.11 and 6.23.

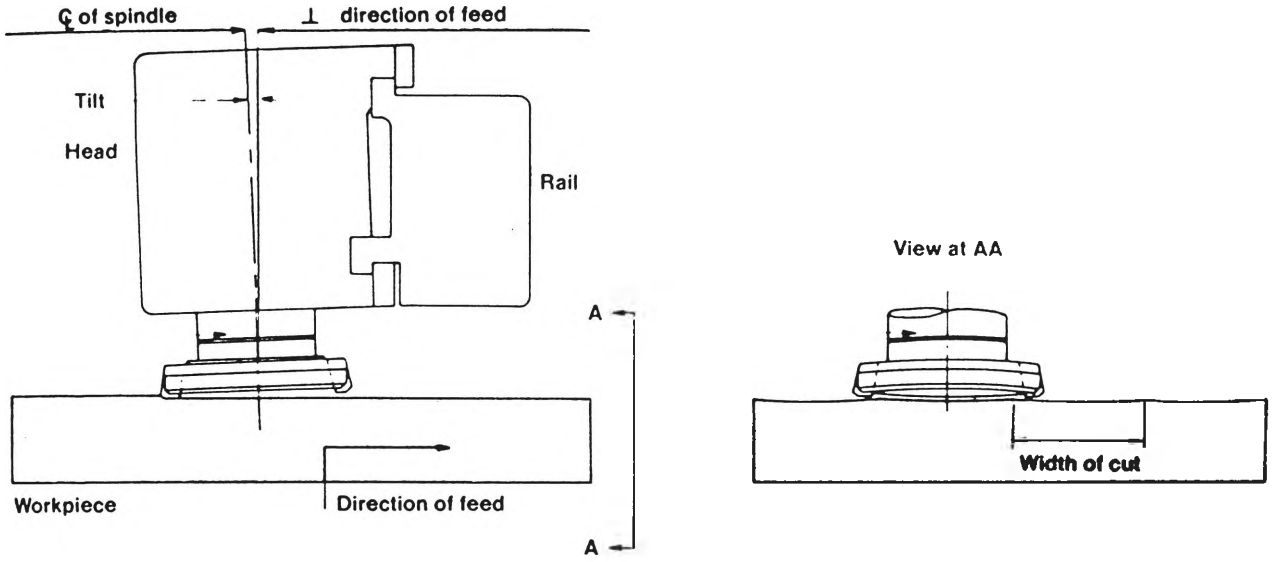

Figure 6.30 Spindle Tilt for Good Finish in Face Milling [174].

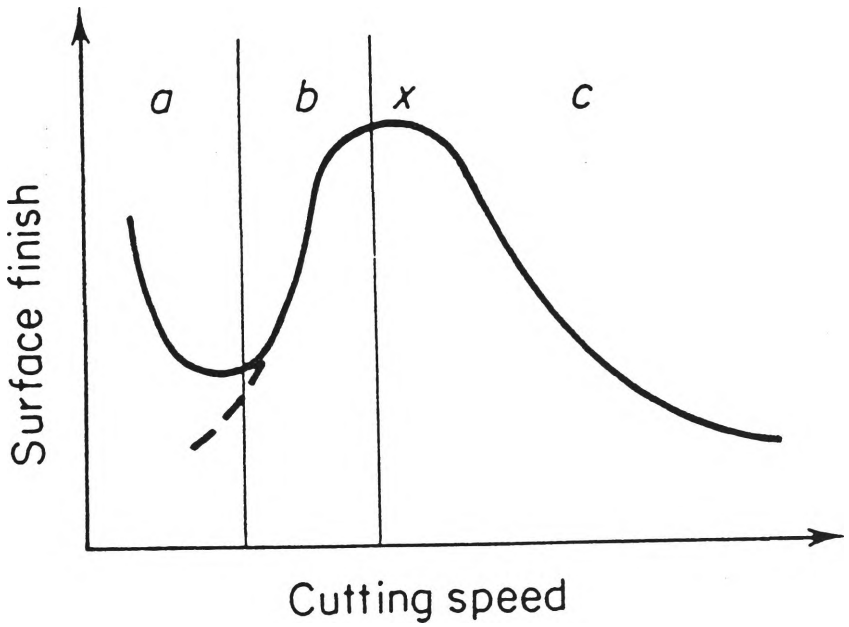

Figure 6.31 Effect of Cutting Speed (U) on Surface Finish [132].

In Figures 6.19 and 6.20, variation of roughness parameters in peripheral milling against cutting speed are given. The shape of the graphs resembles the shape of the graph of surface finish-speed curve for a single edge orthogonal cutting tool, given by Cook and Chandermani (see Figure 6.31). At slow speeds surface finish is poor due to discontinuous chip formation. As the speed increased the chip becomes continuous (zone a) which improves the surface finish. But with a further increase of speed BUE forms which deteriorates the surface finish (zone b). As the speed is increased further the BUE decreases and the surface finish is improved (zone c). The author has a feeling that the surface finish-speed curve given in Figure 6.31 is valid not only for turning but also for milling and drilling. The experimental results given in Figures 6.12, 6.19, 6.20 and 6.24 support such an assumption. In Figures 6.19 and 6.20 we notice that at very low speeds the surface finish is worse. This may be due to the fact that, in choosing the direction of measurement perpendicular to the feed direction, we measured variations of tool marks (and not the feed marks as it would be if measured along feed direction). At very low feed maybe the tool marks become larger.

Although theoretically, up milling should give better surface finish (see Equation 6.9) but our experimental results show that it is not always true. In Figure 6.32 a comparison between roughness values produced by up and down milling is given, where DRa is the difference between roughness values generated by up and down milling. So negative value of DRa indicates up milling is better and positive value indicates down milling is better. It appears that at low feeds up milling gives better surface finish.

Very little work on surface finishes produced by conventional drilling is reported in the literature; however some articles on special types of drilling have been published [169], [120]. The reason may be that drilling operations are not regarded as precision machining due to subsequent requirements of finishing operations to improve the accuracy levels. However, prior knowledge of the type and magnitude of the machining accuracies (including surface texture) inherited from drilling operations is necessary and

useful for improvement of machining accuracies. Moreover it is reported that when some other tool are used for improvement of surface finish of drilled holes, the position accuracy of the holes worsens. So such finishing operations should be avoided. The present study examines the scope and limitation of drilling operation to achieve better surface finish of the drilled holes.

The variation of roughness parameters for different holes illustrated in Figure 6.23 show very slight upward trends, believed to be due to tool wear.

Figure 6.24 is in agreement with the conventional roughness-cutting speed curve. From these graphs is appears that at high feeds the cutting speed has less effect on the surface roughness parameters. It is also significant that after U = 75 m/min the graphs show more obedience to the generally accepted rule - the larger the feed, rougher the surface. When U < 75 m/min this rule is not followed in general. In face milling (see Figure 6.12) and peripheral milling (see Figures 6.19 and 6.20) we have seen that at high speed the roughness values have approximately similar magnitudes regardless of feed. Whereas in drilling we notice that even at high cutting speeds the stabilized values of roughness parameters differ significantly.

Comparison of roughness parameters of holes drilled using different canned cycles was not conclusive. As the roughness parameters R_a, R_{ma} and R_z have different significance (depending on their application) the evaluation of the canned cycles should be done separately. From the statistical results given in Table 6.1 different comparisons can be made. A simple evaluation based on the process capability is given in Table 6.2.

The surface profile of the holes showed the clear tendency to a barreling effect (see Figure 6.26), which confirms the results found in preliminary studies. This fact can be conveniently used to determine the axial position of the hole for taking hole measurements depending on the material modifier used (i.e. MMC, LMC, etc).

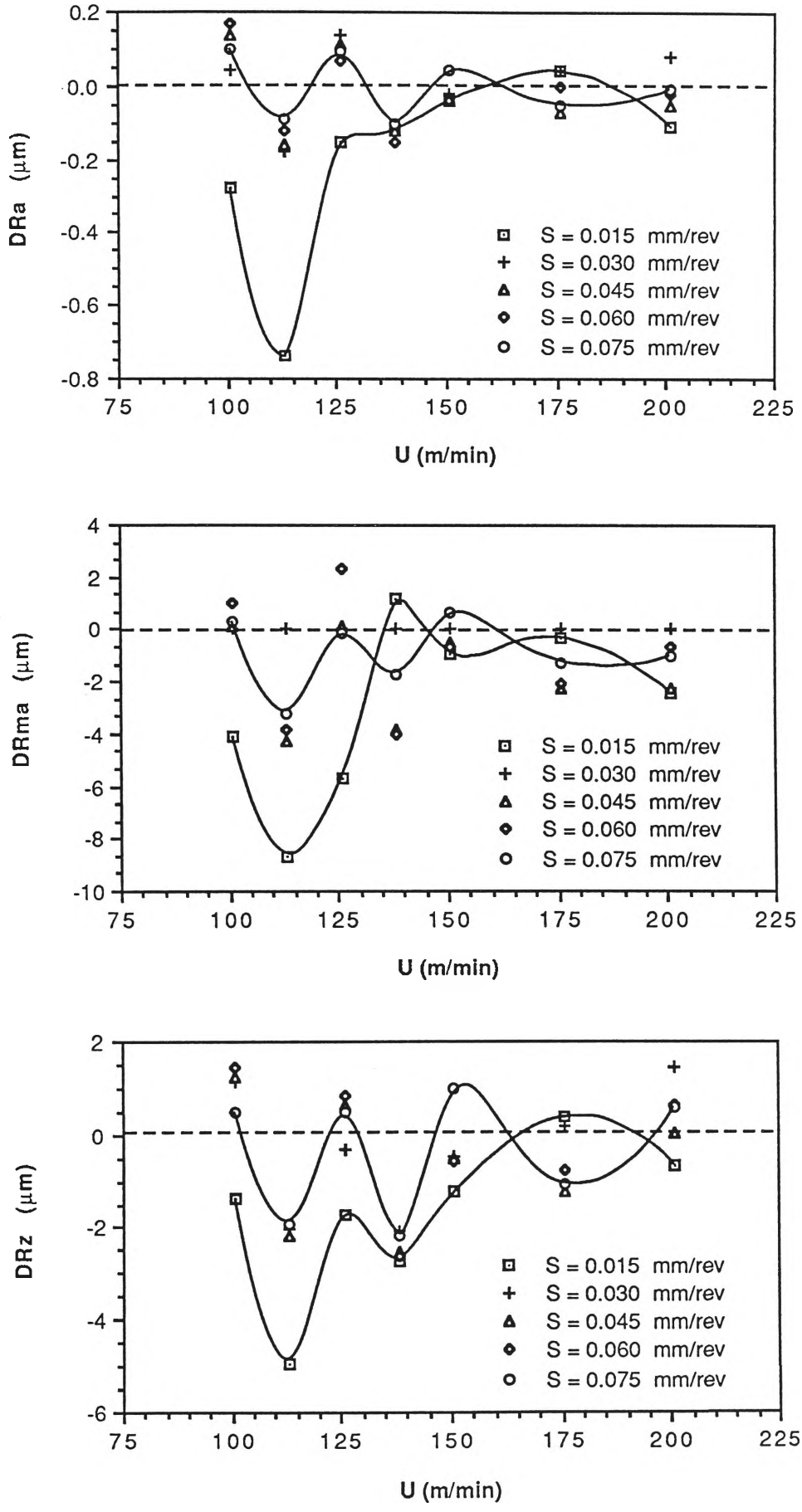

Figure 6.32 Comparison of roughness Parameters Generated by Up and Down Milling at Different Feed and Cutting Speed.

Process Capability	G73		G81		G83		Remarks*
Roughness Paramet.	UCL	LCL	UCL	LCL	UCL	LCL	
Ra (μm)	**7.84**	4.00	8.88	3.00	8.74	3.70	G73 is best
Rma (μm)	85.25	19.49	90.78	14.16	**71.96**	27.86	G83 is best
Rz (μm)	61.15	28.03	70.95	18.27	**57.28**	31.30	G83 is best

* "best" means the process which is most likely to produce lower values of capability index of roughness parameters for the worst case.

Table 6.2 Comparison of Process Capabilities of Canned Cycles G73, G81 and G83.

7.0 THE EFFECT OF MACHINE TOOL GEOMETRIC ACCURACY ON MACHINING ACCURACY

7.1 Introduction

It is obvious that machine tool geometric accuracy has a direct effect on machining accuracy. But, it appears that no effort has so far been made to quantify this effect although it has been claimed by a number of researchers [28], [30], [37] that the machine tool geometric error forms the major portion of machining error. Such assertion cannot be made readily because the effect of machine tool geometric accuracy on machining accuracy depends on the dimensions and geometric configurations of the workpiece also. In Chapter 5 (see Table 5.8) it was found that, for an end milled surface parallel to one of the machine axes, the effect of machine tool geometric accuracy (straightness error of the guideways) dominated the machining accuracy (flatness of the machined surface) when length of the surface is long. But when the length of the surface is short, end mill deflection dominated the machining accuracy. In this chapter an attempt has been made to study the effect of machine tool geometric accuracy on machine accuracy analytically.

7.2 Geometric Accuracy of CNC Machine Tools

The positioning of the workpiece with respect to the tool for metal removal, in CNC machine tools are performed by moving carriages. At present various configurations of CNC machine tools are available. But regardless of the configuration, the positioning devices are designed to move only in one direction (either linear or rotary). With one of the positioning axes spindle is attached and it is customary to denote that axis by Z. In fact, the positioning facilities in CNC machine tools are the most significant difference between NC machine tools and conventional machine tools. A typical linear carriage is shown in Figure 7.1. This carriage is designed to move only in X direction. But due to a number of factors, such error free movement is not possible and in the carriage having six

degrees of freedom of movement, in general, six error components can occur. The positioning error, δ_X (x) reflects the positioning repeatability of the machine tool along that axis and depends on the error in the pitch of the ball screw, the error of the positioning measurement unit, the characteristics of the control system, the error in the electromechanical transmission system, etc. Horizontal straightness error and vertical straightness error are represented by δ_Y (x) and δ_Z (x) respectively. The angular deviations during carriage motion (commonly known as roll, pitch and yaw) are represented by ε_X (x), ε_Y (x) and ε_Z (x). For a 3-axis machine tool, 18 error components can be classified. Beside these errors, the tool position can be influenced by the non-perpendicularity of the X, Y and Z axes. For a 3-axis machine tool 3 such errors can occur which lead to identification of 21 error components. These 21 error components includes, three positioning errors, six straightness errors, nine angular error and three orthogonality errors.

In the present analysis, above mentioned 21 error components of machine tool geometric error are considered* and following assumptions are made:

- The system is regarded as a rigid body system.
- All the geometric errors are concentrated in the guideways.
- Values of those 21 error components are known, from acceptance testing or calibration results.
- Error components considered, are static in nature and cause systematic errors only.

*Other machine tool geometric errors, e.g. spindle rotation errors, are not considered since those errors are difficult to evaluate and cannot be corrected.

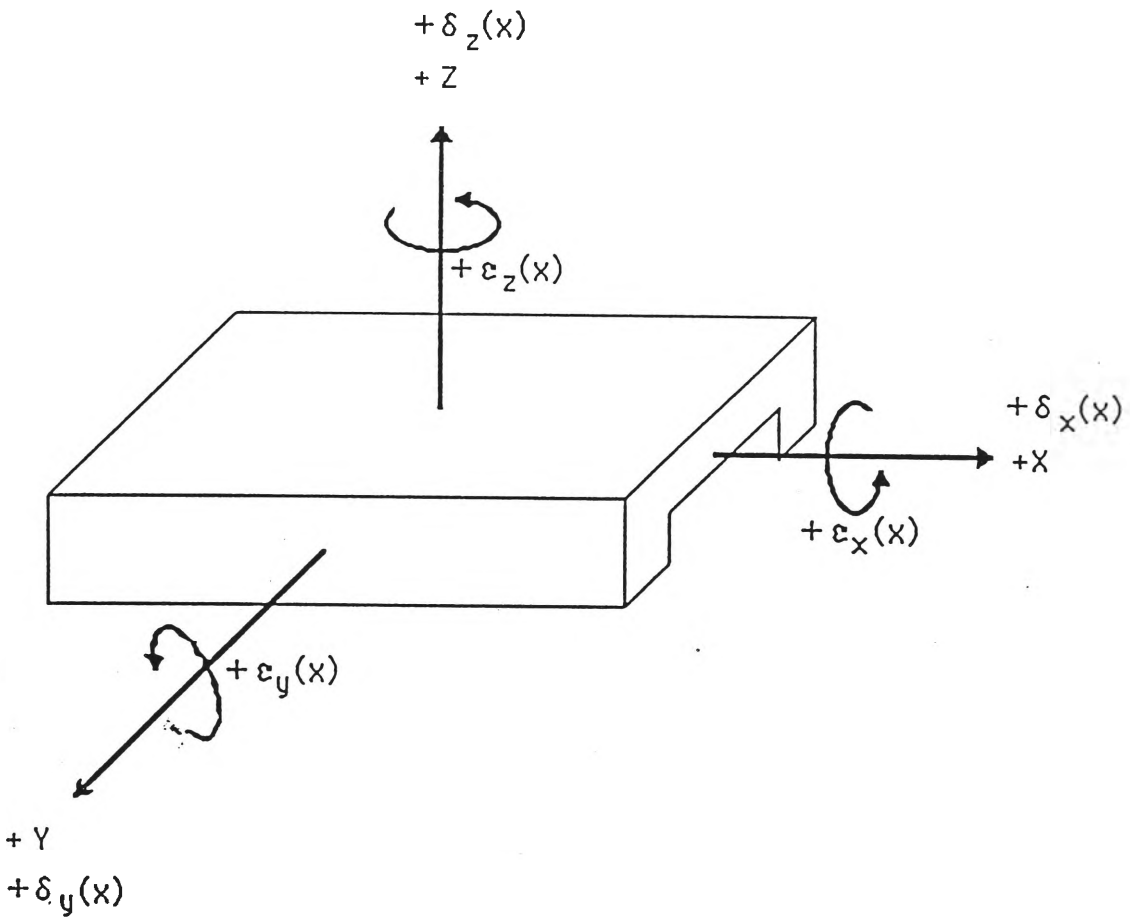

$+\delta_x(x)$: positioning error

$+\delta_y(x)$: horizontal straightness error

$+\delta_z(x)$: vertical straightness error

$+\varepsilon_x(x)$: roll error

$+\varepsilon_y(x)$: pitch error

$+\varepsilon_z(x)$: yaw error

Figure 7.1 A Typical Linear Carriage with Six Degrees of Freedom.

7.3 Calculation of Volumetric Error

The error vector of all combined errors in the work volume (space) is defined as volumetric error. In literature a number of techniques are reported for calculating the volumetric errors of machine tools. These methods include rigid body kinematics, measurement modeling, multiple redundancy, trigonometric analysis, error matrix representation, etc. Of these techniques, rigid body kinematics has been used extensively [34], [37], [106], [110]. In the present study rigid body kinematics principle is applied.

Let us consider an ideal co-ordinate system called space co-ordinate system attached very near to the machine co-ordinate system. All initial co-ordinates will refer to the space co-ordinate system, which is regarded as perfect. Designed position of any point within the machining space is represented by vector $\vec{P_d}$ (X_d, Y_d, Z_d). Due to geometric errors of the machine tool, carriage movements do not follow the space co-ordinate system, which results in the change of position of the point from its designed position. The new position is represented by vector $\vec{P_m}$ (X_m, Y_m, Z_m). As the space co-ordinate system and machine coordinate system may have translation and/or rotation, vector $\vec{P_m}$ (X_m, Y_m, Z_m) can be expressed using a homogeneous transformation of the space T as:

$$\vec{P_m} = T \cdot \vec{P_d} \tag{7.1}$$

where T is the transformation matrix capable of translational and rotational transformations.

Rotation of any vector about the axis of rotation A (a_x, a_y, a_z) through an angle θ can be represented by:

Rot (A, θ) =

$$\begin{bmatrix} a_x a_x \text{vers}\,\theta + \cos\theta & a_y a_x \text{vers}\,\theta - a_z \sin\theta & a_z a_x \text{vers}\,\theta + a_y \sin\theta & 0 \\ a_x a_y \text{vers}\,\theta + a_z \sin\theta & a_y a_y \text{vers}\,\theta + \cos\theta & a_z a_y \text{vers}\,\theta - a_x \sin\theta & 0 \\ a_x a_z \text{vers}\,\theta - a_y \sin\theta & a_y a_z \text{vers}\,\theta - a_x \sin\theta & a_z a_z \text{vers}\,\theta + \cos\theta & 0 \\ 0 & 0 & 0 & 1 \end{bmatrix} \quad (7.2)$$

where vers $\theta = 1 - \cos\theta$.

From Figure 7.1, the roll error which is caused by rotation of X axis by an angle ε_x can be expressed by:

$$\text{Roll error} = \text{Rot}(x, \varepsilon_x) = \begin{bmatrix} 1 & 0 & 0 & 0 \\ 0 & \cos\varepsilon_x & -\sin\varepsilon_x & 0 \\ 0 & \sin\varepsilon_x & \cos\varepsilon_x & 0 \\ 0 & 0 & 0 & 1 \end{bmatrix} \quad (7.3)$$

For very small angles $\cos\varepsilon_x = 1$ and $\sin\varepsilon_x = \varepsilon_x$. Then Equation. (7.3) can be written as

$$\text{Roll error} = \text{Rot}(x, \varepsilon_x) = \begin{bmatrix} 1 & 0 & 0 & 0 \\ 0 & 1 & -\varepsilon_x & 0 \\ 0 & \varepsilon_x & 1 & 0 \\ 0 & 0 & 0 & 1 \end{bmatrix} \quad (7.4)$$

Similarly pitch and yaw errors can be represented by following equations:

$$\text{Pitch error} = \text{Rot}(y, \varepsilon_y) = \begin{bmatrix} 1 & 0 & \varepsilon_y & 0 \\ 0 & 1 & 0 & 0 \\ -\varepsilon_y & 0 & 1 & 0 \\ 0 & 0 & 0 & 1 \end{bmatrix} \tag{7.5}$$

$$\text{Yaw error} = \text{Rot}(z, \varepsilon_z) = \begin{bmatrix} 1 & -\varepsilon_z & 0 & 0 \\ \varepsilon_z & 1 & 0 & 0 \\ 0 & 0 & 1 & 0 \\ 0 & 0 & 0 & 1 \end{bmatrix} \tag{7.6}$$

Translational transformation due to positioning error δ_x, horizontal straightness error δ_y and vertical straightness error δ_z, is given by

$$\text{Trans}\left(\delta_x, \delta_y, \delta_z\right) = \begin{bmatrix} 1 & 0 & 0 & \delta_x \\ 0 & 1 & 0 & \delta_y \\ 0 & 0 & 1 & \delta_z \\ 0 & 0 & 0 & 1 \end{bmatrix} \tag{7.7}$$

The homogeneous transformation of space T_x can be represented by matrix multiplication of rotational and translational matrices given in Equations (7.4) - (7.7).

$$T_x = \text{Rot}(x, \varepsilon_x) \bullet \text{Rot}(y, \varepsilon_y) \bullet \text{Rot}(z, \varepsilon_z) \bullet \text{Trans}(\delta_x, \delta_y, \delta_z) \tag{7.8}$$

Neglecting second order terms

$$T_x = \begin{bmatrix} 1 & -\varepsilon_z & \varepsilon_y & \delta_x \\ \varepsilon_z & 1 & -\varepsilon_x & \delta_y \\ -\varepsilon_y & \varepsilon_x & 1 & \delta_z \\ 0 & 0 & 0 & 1 \end{bmatrix} \tag{7.9}$$

Transformation matrix T_x takes into account of six error components along X axis only. But in a 3 axis machine tool, position of the tool within the machine space in general will depend on movement along the three axes. Then

$$T = T_x \cdot T_y \cdot T_z \tag{7.10}$$

where

$$T_x = \begin{bmatrix} 1 & -\varepsilon_z(x) & \varepsilon_y(x) & \delta_x(x) \\ \varepsilon_z(x) & 1 & -\varepsilon_x(x) & \delta_y(x) \\ -\varepsilon_y(x) & \varepsilon_x(x) & 1 & \delta_z(x) \\ 0 & 0 & 0 & 1 \end{bmatrix} \tag{7.11}$$

$$T_y = \begin{bmatrix} 1 & -\varepsilon_z(y) & \varepsilon_y(y) & \delta_x(y) \\ \varepsilon_z(y) & 1 & -\varepsilon_x(y) & \delta_y(y) \\ -\varepsilon_y(y) & \varepsilon_x(y) & 1 & \delta_z(y) \\ 0 & 0 & 0 & 1 \end{bmatrix} \tag{7.12}$$

$$T_z = \begin{bmatrix} 1 & -\varepsilon_z(z) & \varepsilon_y(z) & \delta_x(z) \\ \varepsilon_z(z) & 1 & -\varepsilon_x(z) & \delta_y(z) \\ -\varepsilon_y(z) & \varepsilon_x(z) & 1 & \delta_z(z) \\ 0 & 0 & 0 & 1 \end{bmatrix} \tag{7.13}$$

Substituting Equations (7.10) - (7.13) in Equation (7.1) and neglecting second order terms and denoting following variables

$$\begin{aligned}
\sum x &= \varepsilon_x(x) + \varepsilon_x(y) + \varepsilon_x(z) \\
\sum y &= \varepsilon_y(x) + \varepsilon_y(y) + \varepsilon_y(z) \\
\sum z &= \varepsilon_z(x) + \varepsilon_z(y) + \varepsilon_z(z) \\
\Delta x &= \delta_x(x) + \delta_x(y) + \delta_x(z) \\
\Delta y &= \delta_y(x) + \delta_y(y) + \delta_y(z) \\
\Delta z &= \delta_z(x) + \delta_z(y) + \delta_z(z)
\end{aligned} \tag{7.14}$$

we can write

$$\begin{bmatrix} X_m \\ Y_m \\ Z_m \\ 1 \end{bmatrix} = \begin{bmatrix} 1 & -\sum z & \sum y & \Delta x \\ \sum z & 1 & -\sum x & \Delta y \\ -\sum y & \sum x & 1 & \Delta z \\ 0 & 0 & 0 & 1 \end{bmatrix} \cdot \begin{bmatrix} X_d \\ Y_d \\ Z_d \\ 1 \end{bmatrix} \tag{7.15}$$

Where transformation matrix

$$T = \begin{bmatrix} 1 & -\sum z & \sum y & \Delta x \\ \sum z & 1 & -\sum x & \Delta y \\ -\sum y & \sum x & 1 & \Delta z \\ 0 & 0 & 0 & 1 \end{bmatrix} \tag{7.16}$$

The difference between the designed position and machined (actual) position is defined as error. Then volumetric error V can then be expressed by

$$[V] = [P_m] - [P_d] = [T] \cdot [P_d] - [P_d] \qquad (7.17)$$

or

$$[V] = \begin{bmatrix} V_x \\ V_y \\ V_z \\ 1 \end{bmatrix} = \begin{bmatrix} X_m - X_d \\ Y_m - Y_d \\ Z_m - Z_d \\ 1 \end{bmatrix} = \begin{bmatrix} -Y_d \cdot \sum z + Z_d \cdot \sum y + \Delta x \\ -Z_d \cdot \sum x + X_d \cdot \sum z + \Delta y \\ -X_d \cdot \sum y + Y_d \cdot \sum x + \Delta z \\ 1 \end{bmatrix} \qquad (7.18)$$

Equation (7.16) gives the transformation matrix T, which can be used to find the actual position of any point P_m, within the machine space, if the designed position of that point P_d and 21 geometric error components of the machine tool are known. Consequently it is possible to determine the volumetric error of all points in the machine space (a process known error mapping).

It is interesting to note that (from Equation 7.18), volumetric error component (V_x) of a point along any of the three axes (e.g. X) is the sum of the error due to rotation of that point about other two axes ($Z_d \cdot \sum y$ and $- Y_d \cdot \sum z$) and those from displacement errors along that axis (Δx).

In the above-stated evaluation of volumetric error, it was assumed that the machine axes are orthogonal (i.e. perpendicular to each other). But in reality these axes may not be perpendicular to each other, which will obviously contribute to the volumetric error. In Figure 7.2, the non-orthogonality error components are shown. For convenience it is assumed that X axis of the machine tool coincides with the X axis of the space system. Considering effect of non-orthogonality errors, Equation (7.16) becomes

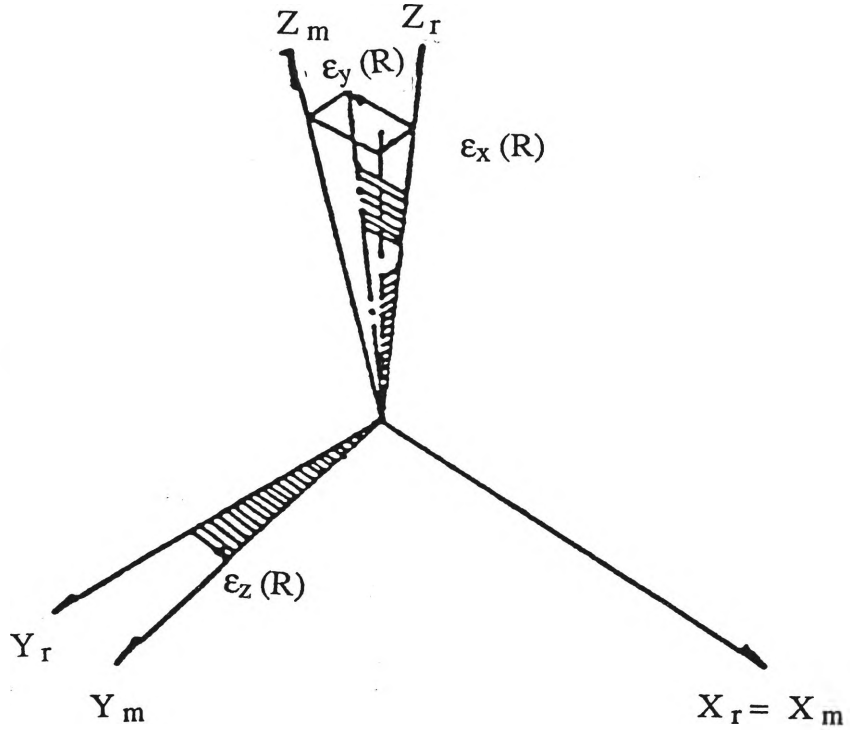

Figure 7.2 Non-orthogonality Errors [21].

$$T = \begin{bmatrix} 1 & -\sum z & \sum y & \Delta x \\ \sum z & 1 & -\sum x & \Delta y \\ -\sum y & \sum x & 1 & \Delta z \\ 0 & 0 & 0 & 1 \end{bmatrix} \cdot \begin{bmatrix} 1 & -\varepsilon_z(R) & \varepsilon_y(R) & 0 \\ \varepsilon_z(R) & 1 & -\varepsilon_x(R) & 0 \\ -\varepsilon_y(R) & \varepsilon_x(R) & 1 & 0 \\ 0 & 0 & 0 & 1 \end{bmatrix} \tag{7.19}$$

Neglecting second order terms,

$$T = \begin{bmatrix} 1 & -\sum z - \varepsilon_z(R) & \sum y + \varepsilon_y(R) & \Delta x \\ \sum z + \varepsilon_z(R) & 1 & -\sum x - \varepsilon_x(R) & \Delta y \\ -\sum y - \varepsilon_y(R) & \sum x + \varepsilon_x(R) & 1 & \Delta z \\ 0 & 0 & 0 & 1 \end{bmatrix} \tag{7.20}$$

Equation (7.18) for volumetric accuracy could be written as

$$[V] = \begin{bmatrix} V_x \\ V_y \\ V_z \\ 1 \end{bmatrix} = \begin{bmatrix} -Y_d \cdot \left[\sum z + \varepsilon_z(R)\right] + Z_d \cdot \left[\sum y + \varepsilon_y(R)\right] + \Delta x \\ -Z_d \cdot \left[\sum x + \varepsilon_x(R)\right] + X_d \cdot \left[\sum z + \varepsilon_z(R)\right] + \Delta y \\ -X_d \cdot \left[\sum y + \varepsilon_y(R)\right] + Y_d \cdot \left[\sum x + \varepsilon_x(R)\right] + \Delta z \\ 1 \end{bmatrix} \quad (7.21)$$

Equation (7.21) gives the complete expression for volumetric error components and can be used to find the actual position of a point within the machine space when the designed position and components of geometric error are known.

The 21 components of machine tool geometric accuracy are considered as a function of position along each axis and depending on their relationship with position. They can be divided into three groups:

(i) when the error component is constant along the axis (E = c);

(ii) when the error component is a linear function of position along axis (E = bx + c);

(iii) when the error component is a quadratic function of position along axis ($E = ax^2 + bx + c$).

The regression equations adopted in [30], which are based on measurement results given in [21], are listed in Table 7.1. It is understood that the relation ships between error components and position will depend on the behaviour of the individual machine tool. But experience showed that in general, positioning errors are quadratic, rotation errors have linear and straightness errors and orthogonal errors have constant relationship with position. In the present study, the following relationships (see Table 7.2) are accepted.

GROUP 1	GROUP 2	GROUP 3
$E = c$	$E = b\,x + c$	$E = a\,x^2 + b\,x + c$
$\varepsilon_x(x)$	$\varepsilon_y(x)$	$\delta_x(x)$
$\delta_y(x)$	$\varepsilon_z(x)$	$\delta_y(y)$
$\delta_z(x)$	$\varepsilon_x(y)$	$\delta_z(z)$
$\varepsilon_y(y)$	$\varepsilon_z(y)$	
$\delta_x(y)$	$\varepsilon_x(z)$	
$\delta_z(y)$	$\varepsilon_y(z)$	
$\delta_x(z)$	$\varepsilon_z(z)$	
$\delta_y(z)$		
$\varepsilon_x(R)$		
$\varepsilon_y(R)$		
$\varepsilon_z(R)$		

Table 7.1 Three Groups of Machine Tool Geometric Errors [30] .

GROUP 1	GROUP 2	GROUP 3
$E = c$	$E = b\,x + c$	$E = a\,x^2 + b\,x + c$
$\delta_y(x) = c_1$	$\varepsilon_x(x) = b_1 x + c_{10}$	$\delta_x(x) = a_1 x^2 + b_{10} x + c_{19}$
	$\delta_z(x) = c_2$	$\varepsilon_y(x) = b_2 x + c_{11}$
$\delta_y(y) = a_2 x^2 + b_{11} x + c_{20}$		$\delta_x(y) = c_3$ $\varepsilon_z(x)$
$= b_3 x + c_{12}\delta_z(z) = a_3 x^2 + b_{12} x + c_{21}$		
$\delta_z(y) = c_4$	$\varepsilon_x(y) = b_4 x + c_{13}$	
$\delta_x(z) = c_5$	$\varepsilon_y(y) = b_5 x + c_{14}$	
$\delta_y(z) = c_6$	$\varepsilon_z(y) = b_6 x + c_{15}$	
$\varepsilon_x(R) = c_7$	$\varepsilon_x(z) = b_7 x + c_{16}$	
$\varepsilon_y(R) = c_8$	$\varepsilon_y(z) = b_8 x + c_{17}$	
$\varepsilon_z(R) = c_9$	$\varepsilon_z(z) = b_9 x + c_{18}$	

Table 7.2 Regression Equations Adopted in the Present Work.

Substituting the regression equations (given in Table 7.1) into Equation (7.21),

$$V_x = X_m - X_d = - Y_d \bullet [\sum z + \varepsilon_z (R)] + Z_d \bullet [\sum y + \varepsilon_y (R)] + \Delta x$$

$$= - Y_d \bullet [\varepsilon_z (x) + \varepsilon_z (y) + \varepsilon_z (z) + \varepsilon_z (R)] + Z_d \bullet [\varepsilon_y (x) + \varepsilon_y (y) + \varepsilon_y (z) + \varepsilon_y (R)] + \delta_x (x) + \delta_x (y) + \delta_x (z)$$

$$= - Y_d \bullet [(b_3 X_d + c_{12}) + (b_6 Y_d + c_{15}) + (b_9 Z_d + c_{18}) + c_9] + Z_d \bullet [(b_2 X_d + c_{11}) + (b_5 Y_d + c_{14}) + (b_8 Z_d + c_{17}) + c_8] + a_1 X_d^2 + b_{10} X_d + c_{19} + c_3 + c_5$$

$$= (c_{19} + c_3 + c_5) + b_{10} X_d + (- c_{12} - c_{15} - c_{18} - c_9) Y_d + (c_{11} + c_{14} + c_{17} + c_8) Z_d + (- b_3) X_d Y_d + (- b_9 + b_5) Y_d Z_d + b_2 Z_d X_d + a_1 X_d^2 + (- b_6) Y_d^2 + b_8 Z_d^2$$

$$= A_1 + A_2 X_d + A_3 Y_d + A_4 Z_d + A_5 X_d Y_d + A_6 Y_d Z_d + A_7 Z_d X_d + A_8 X_d^2 + A_9 Y_d^2 + A_{10} Z_d^2 \qquad (7.22)$$

Similarly

$$V_y = Y_m - Y_d = - Z_d \bullet [\sum x + \varepsilon_x (R)] + X_d \bullet [\sum z + \varepsilon_z (R)] + \Delta y$$

$$= (c_{20} + c_1 + c_4) + (c_{12} + c_{15} + c_{18} + c_9) X_d + b_{11} Y_d + (-c_{10} - c_{13} - c_{16} - c_7) Z_d + b_6 X_d Y_d + (- b_4) Y_d Z_d + (- b_1 + b_9) Z_d X_d + b_3 X_d^2 + a_2 Y_d^2 + (- b_7) Z_d^2$$

$$= A_{11} + A_{12} X_d + A_{13} Y_d + A_{14} Z_d + A_{15} X_d Y_d + A_{16} Y_d Z_d + A_{17} Z_d X_d + A_{18} X_d^2 + A_{19} Y_d^2 + A_{20} Z_d^2 \qquad (7.23)$$

$$V_z = Z_m - Z_d = -X_d \cdot [\sum y + \varepsilon_y(R)] + Y_d \cdot [\sum x + \varepsilon_x(R)] + \Delta z$$

$$= (c_{21} + c_2 + c_4) + (-c_{11} - c_{14} - c_{17} - c_8) X_d + (c_{10} + c_{13} + c_{16} + c_9) Y_d + b_{12} Z_d + (-b_5 + b_1) X_d Y_d + b_7 Y_d Z_d + (-b_8) Z_d X_d + (-b_2) X_d^2 + b_4 Y_d^2 + a_3 Z_d^2$$

$$= A_{21} + A_{22} X_d + A_{23} Y_d + A_{24} Z_d + A_{25} X_d Y_d + A_{26} Y_d Z_d + A_{27} Z_d X_d + A_{28} X_d^2 + A_{29} Y_d^2 + A_{30} Z_d^2 \quad (7.24)$$

Expressions given in Equations (7.22) - (7.24) can be used to calculate volumetric error components of any point within the machining space. The constants appearing in those equations are generally determined by comparing the command values given to the CNC machine tool with the real values. Real values are obtained using precision measuring instruments (e.g. laser interferometer) or using precision part of known dimensions (known as master part).

7.4 An Assessment of the Effect of Machine Tool Geometric Accuracy on Machining Accuracy

In the previous section it was shown, how the various components of volumetric error can be determined for any point within the machining space, if the geometric error components of the machine tools are known. In the literature it was found that a number of researchers have used similar methods to calculate volumetric errors. These researchers have considered the problem from "machine accuracy" point of view and tried to compensate volumetric errors of each extreme point of the component. In other words their aim was to reduce the absolute volumetric error of extreme points. But in reality absolute errors of position by themselves have no practical significance. Because for a machined component, dimensions, positioning of some elements (e.g. hole),

perpendicularity, etc all are relative and are determined with respect to the datum, which is a part of that machined component. So when considering "machining accuracy", attention should be paid to the relative errors between the datum and other extreme points of the component, which define different dimensions of the part. The difference between these two approaches will be clear from the following example.

Let us consider machining of a rectangular block with dimensions L X B X H. Let $I_d J_d K_d L_d$ represents the base of the block in primary datum plane XOY (see Figure 7.3). Due to machine tool geometric errors block machined deviates from the designed block and $I_m J_m K_m L_m$ is the base of the machined block. So according to definition, $\overrightarrow{I_d I_m}$, $\overrightarrow{J_d J_m}$, $\overrightarrow{K_d K_m}$ and $\overrightarrow{L_d L_m}$ represent volumetric error of the points I_d, J_d, K_d and L_d respectively. The views expressed by those researchers who studied "machine accuracy" were to reduce the magnitudes of $\overrightarrow{I_d I_m}$, $\overrightarrow{J_d J_m}$, $\overrightarrow{K_d K_m}$ and $\overrightarrow{L_d L_m}$. But when machining accuracy is considered, we are interested about the dimensions of the block and while considering L we are interested about the magnitude of $\overrightarrow{I_m J_m}$.

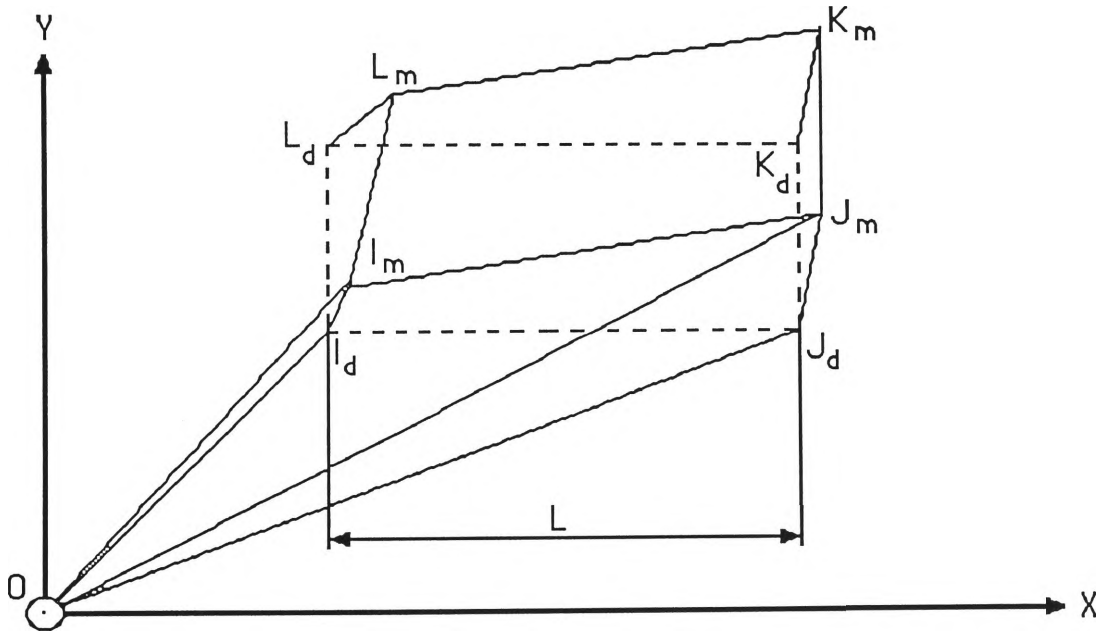

Figure 7.3 Position of Designed and Machined Component.

From $\Delta I_m O J_m$

$$\overrightarrow{I_m J_m} = \overrightarrow{O J_m} - \overrightarrow{O I_m} \tag{7.25}$$

From $\Delta J_m O J_d$

$$\overrightarrow{O J_m} = \overrightarrow{O J_d} + \overrightarrow{J_d J_m} \tag{7.26}$$

From $\Delta I_m O I_d$

$$\overrightarrow{O I_m} = \overrightarrow{O I_d} + \overrightarrow{I_d I_m} \tag{7.27}$$

Substituting Equations (7.26) and (7.27) into Equation (7.25)

$$\overrightarrow{I_m J_m} = \overrightarrow{O J_d} + \overrightarrow{J_d J_m} - \overrightarrow{O I_d} - \overrightarrow{I_d I_m}$$

or $$\overrightarrow{I_m J_m} = (\overrightarrow{O J_d} - \overrightarrow{O I_d}) + \overrightarrow{J_d J_m} - \overrightarrow{I_d I_m}$$

or $$\overrightarrow{I_m J_m} = \overrightarrow{I_d J_d} + \overrightarrow{J_d J_m} - \overrightarrow{I_d I_m}$$

or $$\overrightarrow{I_m J_m} - \overrightarrow{I_d J_d} = \vec{V}_J - \vec{V}_I \tag{7.28}$$

where $\vec{V}_J$ and $\vec{V}_I$ are volumetric errors of the points J_d and I_d respectively. From Equation (7.28) it can be seen that the change of length of the component (expression given in the right hand side of the equation) is equal to the change of volumetric errors of the points defining the length (expression given in the left hand side of the equation). Present strategy is, to reduce this difference of volumetric errors, and not the error it-self. It is interesting to note that if volumetric errors of the points I_d, J_d, K_d and L_d are all

equal in (magnitude and direction), the machined component will not have any dimensional variations (from designed dimensions), although the position of the component will be shifted. When considering machining accuracy, volumetric error of the datum is subtracted from the volumetric error of other points, which define that component. The volumetric error of the datum point, depends on the positioning of the job on machine table. Far the job is placed from the machine origin, more the volumetric error will be†. Thus placing of the job has a significant effect on the volumetric error specially when absolute errors are considered. Due to non-linearity of the volumetric accuracy, even when relative errors are considered, the positioning of the job has considerable effect (see Figure 7.4).

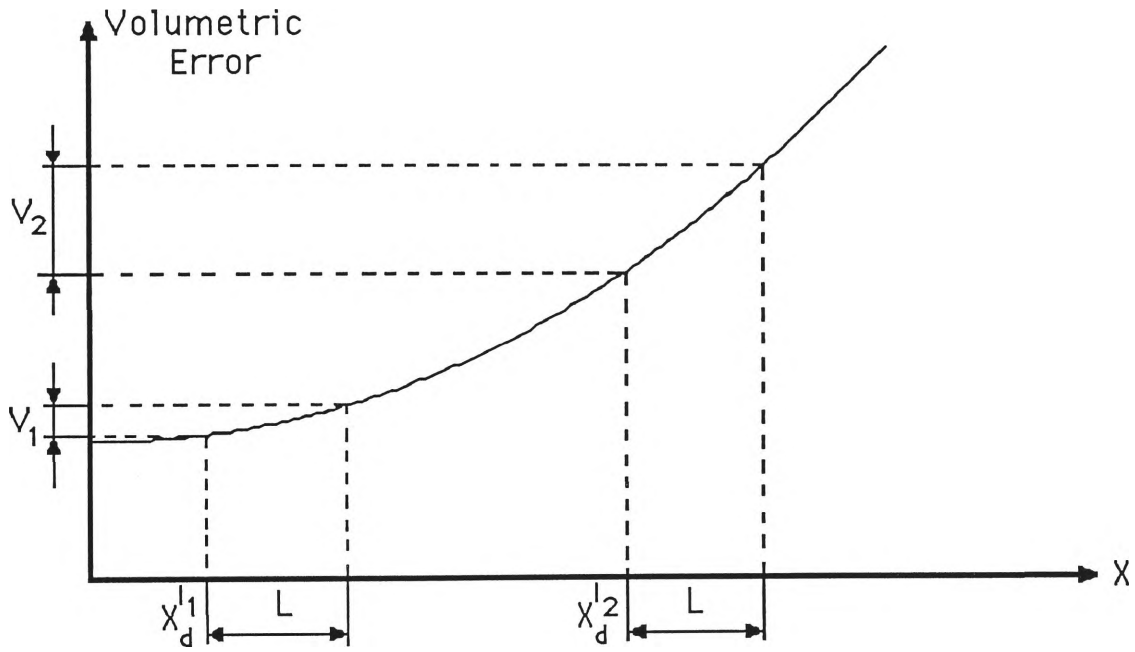

Figure 7.4 Effect of Non-linearity on Volumetric Error.

Machine tool geometric accuracy affects differently on the machined component depending on the dimensions and the geometric configuration of the workpiece. Even the orientation of the workpiece plays an important role in transferring machine tool geometric

† Because volumetric error components are either constant or function of distance traveled (see Table 7.2)

accuracy into machining accuracy. For example same rectangular block (shown in Figure 7.3) if machined in such a way that while machining the cutter does not move parallel to any of the axis, the machining error will be more. Because when the cutter is moved not parallel to any axis, the cutter movement is controlled by more than one axis and an operation called **interpolation** is performed by NC controller. Much accuracy is lost during interpolation.

In subsequent sections an attempt has been made to see analytically, the effect of machine tool geometric accuracy on different aspects of machining accuracy. However, as these effects depend on a number of factors (mentioned before), it is not possible to analyse all the cases. So it was decided to take the test component given in Figure 3.4 as an example and find the effect of machine tool geometric accuracy on different aspects of machining accuracy of that component. Similar methods can be applied to other parts also.

7.4.1 Linear Dimension

The following notations for co-ordinates of points will be used in this study. Any point O which has a designed position O_d has co-ordinates (X_d^O, Y_d^O, Z_d^O) and machined position O_m has co-ordinates (X_m^O, Y_m^O, Z_m^O), all in space co-ordinate system.

Then the designed length L can be calculated using following formula:

$$L = \left|\overrightarrow{I_d J_d}\right| = \sqrt{(X_d^J - X_d^I)^2 + (Y_d^J - Y_d^I)^2 + (Z_d^J - Z_d^I)^2} \quad (7.29)$$

But $$Y_d^J = Y_d^I \quad (7.30)$$

and $$Z_d^J = Z_d^I \quad (7.31)$$

Then $$L = X_d^J - X_d^I \quad (7.32)$$

Machined length (L + Δ L) can be calculated using following formula:

$$L + \Delta L = \left|\overrightarrow{I_m J_m}\right| = \sqrt{(X_m^J - X_m^I)^2 + (Y_m^J - Y_m^I)^2 + (Z_m^J - Z_m^I)^2} \tag{7.33}$$

Using Equation (7.23)

$$X_m^I = A_1 + A_2 X_d^I + A_3 Y_d^I + A_4 Z_d^I + A_5 X_d^I Y_d^I + A_6 Y_d^I Z_d^I + A_7 Z_d^I X_d^I + A_8 (X_d^I)^2 + A_9 (Y_d^I)^2 + A_{10} (Z_d^I)^2 + X_d^I$$

$$X_m^J = A_1 + A_2 X_d^J + A_3 Y_d^I + A_4 Z_d^J + A_5 X_d^J Y_d^J + A_6 Y_d^J Z_d^J + A_7 Z_d^J X_d^J + A_8 (X_d^J)^2 + A_9 (Y_d^J)^2 + A_{10} (Z_d^J)^2 + X_d^J$$

Then

$$X_m^J - X_m^I = A_2\left(X_d^J - X_d^I\right) + A_3\left(Y_d^J - Y_d^I\right) + A_4\left(Z_d^J - Z_d^I\right) + A_5\left(X_d^J Y_d^J - X_d^I Y_d^I\right) + A_6\left(Y_d^J Z_d^J - Y_d^I Z_d^I\right) + A_7\left(Z_d^J X_d^J - Z_d^I X_d^I\right) + A_8\left[\left(X_d^J\right)^2 - \left(X_d^I\right)^2\right] + A_9\left[\left(Y_d^J\right)^2 - \left(Y_d^I\right)^2\right] + A_{10}\left[\left(Z_d^J\right)^2 - \left(Z_d^I\right)^2\right] + \left(X_d^J - X_d^I\right) \tag{7.34}$$

Substituting relationship given in Equations (7.30) - (7.32) into Equation (7.34)

$$X_m^J - X_m^I = A_2 L + A_5 Y_d^I L + A_7 Z_d^I L + A_8\left(X_d^J + X_d^I\right) L + L$$

or $$X_m^J - X_m^I = L\left(C_d^x + A_8 L\right) \tag{7.35}$$

where $$C_d^x = 1 + A_2 + A_5 Y_d^I + A_7 Z_d^I + 2 A_8 X_d^I$$

C_d^x is a constant which depends on the machine tool geometric errors and the positioning of the datum point of the workpiece on the machine table.

Similarly

$$Y_m^J - Y_m^I = L\left(C_d^y + A_{18} L\right) \tag{7.36}$$

where $$C_d^y = A_{12} + A_{15} Y_d^I + A_{17} Z_d^I + 2 A_{18} X_d^I$$

$$Z_m^J - Z_m^I = L\left(C_d^z + A_{28} L\right) \tag{7.37}$$

$$C_d^z = A_{22} + A_{255} Y_d^I + A_{27} Z_d^I + 2 A_{28} X_d^I$$

where

Then $$L + \Delta L = L\sqrt{\left(C_d^x + A_8 L\right)^2 + \left(C_d^y + A_{18} L\right)^2 + \left(C_d^z + A_{28} L\right)^2}$$

or $$\Delta L = L\left(\sqrt{\left(C_d^x + A_8 L\right)^2 + \left(C_d^y + A_{18} L\right)^2 + \left(C_d^z + A_{28} L\right)^2} - 1\right) \tag{7.38}$$

Equation (7.38) shows that the deviation of length (ΔL) is a function of machine tool geometric error (A_i), position of the datum points (X_d^I, Y_d^I Z_d^I) and the designed length (L) of the workpiece. If all these parameters are known, the expected deviation of the length can be calculated before hand and these results can be used for error reduction. Similarly it can also be shown that, deviations of other dimensions (ΔB and ΔH) are also functions of machine tool geometric errors, position of the datum point and their respective dimensions (B and H).

7.4.2 Positioning

Let us consider the positioning of the hole centres after machining. The problem will be considered in two dimensions, as positioning of hole centres in its practical sense has two dimensions. In Figure 7.5 designed component is shown by $I_d\ J_d\ K_d\ L_d$ with designed positions of the centre of the holes P_d, Q_d, R_d, S_d and T_d . The machined component is shown by $I_m\ J_m\ K_m\ L_m$ with machined position of centre of the holes P_m, Q_m, R_m, S_m and T_m.

For assessing positioning accuracy another co-ordinate system known as CMM co-ordinate system is introduced. This is necessary because positioning accuracy depends on the co-ordinate system in which it is concisered, whereas dimensional variations are same in any orthogonal co-ordinate system. In practice while measuring the machined component, datum surface is aligned with the principal axis of the CMM. So we have introduced the CMM system where X_{cmm} lies along I_mJ_m and Y_{cmm} is perpendicular to X_{cmm} . Using the formulas for volumetric accuracy, new positions of the hole centres P_m, Q_m, R_m, S_m and T_m can be calculated. These results are in the space co-ordinate system and need to transform into CMM co-ordinate system. In general CMM Co-ordinate system and space co-ordinate system may have translation and rotation. It is known that transformation of co-ordinate system to another orthogonal co-ordinate system can be achieved by using following formulas:

$$X_2 = (X_1 + a)\cos\theta + (Y_1 + b)\sin\theta$$

$$Y_2 = (Y_1 + b)\cos\theta - (X_1 + a)\sin\theta \qquad (7.39)$$

where $X_1\ O_1\ Y_1$ original co-ordinate system and $X_2\ O_2\ Y_2$ is the secondary co-ordinate system. These co-ordinate systems have translation **a** along X and **b** along Y axis and angle θ is rotation between the principle axis of two systems, $O_1\ X_1$ and $O_2\ X_2$.

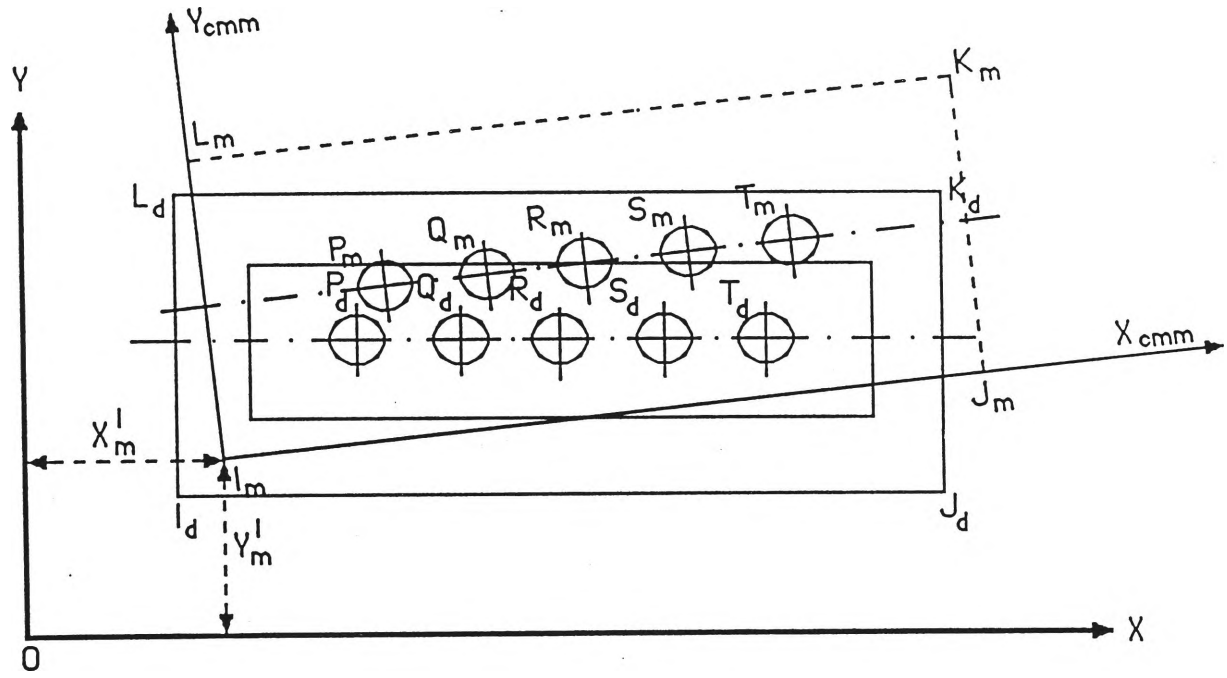

Figure 7.5 Positioning Accuracy of the Hole Centres.

In this case

$$a = -X_m^I = -(X_d^I + V_x^I)$$

$$b = -Y_m^I = -(Y_d^I + V_y^I) \qquad (7.40)$$

$$\theta = \tan^{-1}\left(\frac{Y_m^J - Y_m^I}{X_m^J - X_m^I}\right) = C_\theta$$

Substituting V_x^I and V_y^I from Equations (7.23) and (7.24) into Equation (7.40)

$$a = -X_d^I - \left(A_1 + A_2X_d^I + A_3Y_d^I + A_5X_d^IY_d^I + A_8\left(X_d^I\right)^2 + A_9\left(Y_d^I\right)^2\right) = C_d^{xa}$$

(7.41)

$$b = -Y_d^I - \left(A_{11} + A_{12}X_d^I + A_{13}Y_d^I + A_{15}X_d^IY_d^I + A_{18}\left(X_d^I\right)^2 + A_{19}\left(Y_d^I\right)^2\right) = C_d^{yb} \tag{7.42}$$

$$\theta = \tan^{-1}\left(\frac{Y_m^J - Y_m^I}{X_m^J - X_m^I}\right) = \tan^{-1}\left(\frac{L(C_d^Y + A_{18}L)}{L(C_d^X + A_8 L)}\right) = \tan^{-1}\left(\frac{C_d^Y + A_{18}L}{C_d^X + A_8 L}\right) \tag{7.43}$$

Above expression show that translation of the co-ordinate system are constants and depend on machine tool geometric errors and positioning of datum point, whereas rotation transformation is a function of designed length also.

Then

$$\begin{aligned}\left(X_m^P\right)_{cmm} &= \left(X_m^P + C_d^{xa}\right)\cos C_\theta + \left(Y_m^P + C_d^{yb}\right)\sin C_\theta \\ \left(Y_m^P\right)_{cmm} &= \left(Y_m^P + C_d^{yb}\right)\cos C_\theta - \left(X_m^P + C_d^{xa}\right)\sin C_\theta\end{aligned} \tag{7.44}$$

where $\left(X_m^P\right)_{cmm}$ and $\left(Y_m^P\right)_{cmm}$ are co-ordinates of P_m in CMM co-ordinate system; and X_m^P and Y_m^P co-ordinates of same points in space co-ordinate system.

From Equations (7.23) and (7.24)

$$\begin{aligned}\Delta X^P &= \left(X_m^P\right)_{cmm} - X_d^P = \left(V_x^P + C_d^{xa}\right)\cos C_\theta + \left(V_y^P + C_d^{yb}\right)\sin C_\theta \\ \Delta Y^P &= \left(Y_m^P\right)_{cmm} - Y_d^P = \left(V_y^P + C_d^{yb}\right)\cos C_\theta - \left(V_x^P + C_d^{xa}\right)\sin C_\theta\end{aligned} \tag{7.45}$$

In Equation (7.45) except V_x^P and V_y^P all are constants. So deviation of co-ordinates of the hole centres depends on components of volumetric error of that point.

From Equation (7.45) we can write

$$\Delta X^Q - \Delta X^P = \left(V_x^Q - V_x^P\right)\cos C_\theta + \left(V_y^Q - V_y^P\right)\sin C_\theta$$

$$\Delta Y^Q - \Delta Y^P = \left(V_y^Q - V_y^P\right)\cos C_\theta - \left(V_x^Q - V_x^P\right)\sin C_\theta \qquad (7.46)$$

Using Equations (7.23) and (7.24)

$$V_x^Q - V_x^P = A_2\left(X_d^Q - X_d^P\right) + A_3\left(Y_d^Q - Y_d^P\right) + A_5\left(X_d^Q Y_d^Q - X_d^P Y_d^P\right) + A_8\left[\left(X_d^Q\right)^2 - \left(X_d^P\right)^2\right]$$

$$+ A_9\left[\left(Y_d^Q\right)^2 - \left(Y_d^P\right)^2\right]$$

But $X_d^Q - X_d^P = X_d^R - X_d^Q = \ldots\ldots\ldots\ldots = X_d^T - X_d^S = u$

$$Y_d^Q = Y_d^P = \ldots\ldots\ldots\ldots = Y_d^T = v$$

Then $V_x^Q - V_x^P = u\left(C_1 + C_2 u\right)$

$$V_y^Q - V_y^P = u\left(C_3 + C_4 u\right) \qquad (7.47)$$

Substituting Equation (7.47) into Equation (7.46)

$$\Delta X^Q - \Delta X^P = u\left[\overline{C_1} + \overline{C_2}u + \overline{C_3} + \overline{C_4}u\right] = u\left(C_5 + C_6 u\right)$$

$$\Delta Y^Q - \Delta Y^P = u\left[\overline{C_3} + \overline{C_4}u - \overline{C_1} - \overline{C_2}u\right] = u\left(C_7 + C_8 u\right) \qquad (7.48)$$

From Equation (7.48) it can be seen that for the test component (given in Figure 3.4) the change of the deviation of co-ordinates of subsequent holes are proportional to the distance in between these holes (if it was due to machine tool geometric errors only). But the experimental results show that variations of deviations for positioning is not proportional to the distance in between those hole centres, which indicates that the machine tool geometric errors are not the only cause of shift of the centre of the holes.

7.5 Comments and Discussions

In the previous section it was shown that the errors which inherit from the machine tool geometric errors to the machined component are proportional to the dimensions of the component. This is due to the fact that the positioning error (which is the major portion of machine tool geometric error) is cumulative error and so it is proportional to the distance traveled by the spindle head. This means that when the specified positioning accuracy is ± 10 μm (for example), this does not necessarily mean that it will produce ± 10 μm machining inaccuracy along the axes, as for machining only a part of the axes travel is used. The importance of positioning and orientation of workpiece on the machine table was also highlighted.

Following the methodology given in this Chapter, volumetric error of any point within the machining space can be calculated, if the components of machine tool geometric errors are known. But in practice it is difficult and time consuming to gather data for all of those 21 components of machine tool geometric errors. Results given in [26], [30] show that positioning errors are most prominent error components among those 21 errors. So the author suggests that, if at least positioning error calibration results are available, the analytical expressions can be applied to calculate volumetric errors, taking other error components as zero. If more error components are known, it always possible to add those to the formula for volumetric error. The calculated values can give a rough idea of machining inaccuracy coming from machine tool geometric errors which can be used not

only for error compensation, but also for determining the process capabilities and tolerance limits.

Although it is easy to predict the effect of machine tool geometric error on machining accuracy of a component, it is very difficult to compensate these errors. Due to the fixed position of the spindle in a 3 axis vertical machining centre, compensation of errors in three axes simultaneously, is very difficult (in author's view practically impossible). Lee and Barash [30] have developed a 3 dimensional model for error prediction; but failed to implement the model in 3 dimensional error compensation. Venugopal [26] concluded, "The most important problem is, having modeled the machine, how does one implement the process of correcting errors?" These findings show the importance of adopting error avoidance method for error reduction.

8.0 CONCLUSIONS AND RECOMMENDATIONS

8.1 Conclusions

From the experimental work conducted, and the subsequent analysis, several conclusions can be drawn, which are summarized as follows:

1. Large variations in cutting tool dimensions, sometimes beyond the acceptable limits, were found. Also large tolerance bands, specified by the various standards, of the tool dimensions were noticed. It is therefore deemed essential to measure and determine the effective diameter of each tool before machining and to use these data in determining tool settings.

2. Tool deflection is a major problem in end milling, which causes geometric inaccuracies in machined components. Measures should be taken to reduce the end mill deflection. The comparisons of up and down milling operations showed distinct shape variations of the surfaces machined, due to different directions of force component F_y.

3. Surface finish on the machined component plays a significant role on the dimensional accuracy and repeatability of measurements. Attention must be paid to achieve consistent and acceptable levels of surface finish using the best possible cutting conditions, tool geometry and work materials.

4. In normal production and quality control practice, usually the linear accuracy is monitored, which is found to be insufficient and the recent developments in advanced manufacturing technology involving automated assembly and its quality control calls for a need for a volumetric accuracy assessment.

The findings of this thesis can be applied to eliminate the sources of various errors at an early stage such as design (for manufacture), process planning, etc. The variations of cutting tool dimensions generally produce systematic errors which generate dimensional errors of the machined components. In milling dimensional errors of the machined component can be eliminated by supplying the correct tool dimensions (effective tool diameter) to the CNC controller, which can easily compensate those errors. Unfortunately in drilling operations such compensation is not possible, specially when the holes are oversized. However, the knowledge of the hole oversize can be applied in the designing of the component. If the designer knows that a drill always produce oversized holes (and that oversize is predictable, say 80 μm for a 12 mm drill) and the drills are manufactured in 1 mm step (i.e.11, 12, 13 mm etc), then it is wise to put dimension on the hole as 12.080 mm instead of 12.000 mm on the drawing and the dimension of the mating part can be adjusted. If there is no scope of adjusting the mating part then, an alternative solution may be to use drill of smaller size and then use some finishing operation (e.g. reaming).

The effect of end mill deflection also can be reduced by selecting appropriate tool and cutting conditions. In the literature survey it was found that almost all of the researchers have considered the effect of end mill defection for down milling, which produces positive errors. The idea behind their error compensation is, first to allow some positive errors and then use another pass to eliminate it. But we have seen that in up milling both positive and negative error can occur depending on the cutting conditions and tool dimensions. So there is a situation where the force component F_y changes it's sign and it has zero magnitude (at least theoretically). That condition can be calculated before hand and applied to reduce geometric errors caused by end mill deflection.

8.2 Suggestions for Further Work

It was mentioned before that it is not possible for us to investigate the combined effects of all the factors on machining accuracy. But for a comprehensive study, further investigations on following aspects are felt necessary to :

1. The quality of cutting fluids and the methods of their applications will contribute to the quality of the finished product.

2. Improved work clamping and tool setting will help to reduce the effects of vibration, improving rigidity of the "Tool - Work - Machine" system.

3. The thermal effect of machine tool on machining accuracy needs further investigation.

4. Different materials behave differently during machining; thus the effect of work materials on machining accuracy also should be considered. This may possibly involve a more detailed study on the deformation patterns of materials including the work hardening effects on machining accuracy.

5. In batch production progressive tool wear plays an important role on machining and this requires a further study as the on-line techniques currently used do not provide a "prevention" (or even reduction in errors), but merely a "cure", costing high expenditure, in the long run.

REFERENCES:

[1] Gould L.S., Factory Automation - A Key to Survival, Grame Publ. Corp., Wilbraham, 1986.

[2] McKeown P., "Implementing Quality Improvement Programmes", Annals of the CIRP, Vol. 34/2/1985, pp. 527 - 529.

[3] Juran J.E., Quality Control Handbook, Third Edition, Mc Graw-Hill, New York, 1974.

[4] Sprouster J., TQC - Total Quality Control, The Australian Experience, Horwitz Grahame Pty Ltd, Second Revised Edition, 1987.

[5] Peters J., Leuven, K.U. and Heverless B., "Metrology in Design and Manufacturing - Facts and Trends", Annals of the CIRP, Vol 26/2/1977, pp. 415-421.

[6] Tool and Manufacturing Engineers Handbook, Vol. 1, Machining, SME, 1983.

[7] El Maraghy W.H., Knoll L. and El Maraghy H.A., "Limits of Repeatability and Dimensional Tolerances for Robotic Assembly", Proc. Int. Conf. ASME (MI'88, Atlanta, Georgia, USA), April 1988, pp. 9-13.

[8] Collett C.V. and Hope A.D., Engineering Measurements, Second Edition, Longman Scientific and Technical, Singapore, 1986.

[9] British Standard BS 5233: 1975, British Standard Inst., 1975.

[10] Farmer L.E., "Datums, Tolerances and NC Machine Tools", Automach Australia '85, Conf. Proc. (July 2 -5, 1985, Melbourne, Australia), pp. 5-62 - 5-71.

[11] American National Standard, ANSI Y 14.5M - 1982 - Dimensioning and Tolerance, ASME, 1982.

[12] Australian Standard, AS1100, Technical Drawing, Part 201-1984, Mechanical Drawing, The Standards Association of Australia, 1984.

[13] Neumann A.G., "Geometric Dimensioning and Tolerancing: Training Program", Al Neumann & Associates, Michigan, 1986.

[14] Freckleton J.E. "Production Advantages of GD & T", J. of Mech. Working Tech.,Vol. 17, (Proc. of the Int. Seminar on New Manufacturing Technology, Singapore, August 1988), pp. 237 - 246.

[15] Tool and Manufacturing Engineers Hand Book, Vol. 4, Quality Control and Assembly, SME, 1984.

[16] Arai N., Fujii N., Aoyama E. and Kitaguchi Y., "A Research of Factors Affecting Working Accuracy in NC Lathe Turning", The Science and Engineering Review of Doshisha University, Vol 24, No 2, July 1983, pp. 94-109 (in Japanese).

[17] Schlesinger G., Testing Machine Tools, Pergamon Press Ltd., Eighth Edition,1978.

[18] Tlusty J. and Koenigsberger F., "New Concepts of Machine Tool Accuracy", Annals of the CIRP, Vol. 19, 1971, pp. 261 - 273.

[19] Tlusty J., "Techniques for Testing Accuracy of NC Machine Tools", Proc. of 12th Int. MTDR Conf., 1972, pp. 333 - 345.

[20] Cowley A. and Hinduja S., "The Finite Element Method for Machine Tool Structural Analysis", Annals of the CIRP, Vol. 19, 1971, pp. 171 - 181.

[21] Schultschick R., "The Components of the Volumetric Accuracy", Annals of the CIRP, Vol. 25/1/1977, pp. 223 - 228.

[22] Schultschik R., "The Accuracy of Machine Tools under Load Conditions", Annals of the CIRP, Vol. 28/1/1979, pp. 339 - 344 , (in German).

[23] Eman K.F., Wu B.T. and De Vries M.F., "A Generalized Geometric Error Model for Multi-Axis Machines", Annals of the CIRP, Vol. 36/1/1987, pp. 253 - 256.

[24] Knapp W., "Test of the Three - Dimensional Uncertainty of Machine Tools and Measuring Machines and its Relation of the Machine Error", Annals of the CIRP, Vol. 32/1/1983, pp. 459 -464.

[25] Donmez M.A., "A General Methodology for Machine Tool Accuracy Enhancement: Theory, Application and Implementation", Ph.D. Thesis, Purdue University, USA, 1985.

[26] Venugopal R., "Thermal Effects on the Accuracy of Numerically Controlled Machine Tools", Ph.D. Thesis, Purdue University, USA, 1985.

[27] Venugopal R. and Barash M., "Thermal Effects on the Accuracy of Numerically Controlled Machine Tools", Annals of the CIRP, Vol. 35/1/1986, pp. 255 - 258.

[28] Ferreira P.M. and Liu R., "An Analytical Quadratic Model for the Geometric Error of a Machine Tool", J. of Manufacturing Systems, Vol. 5, No 1, 1986, pp. 51 - 63.

[29] Ferreira P.M. and Liu C.R., "A Contribution to the Analysis and Compensation of Geometric Error of a Machining Centre", Annals of the CIRP, Vol. 35/1/1986, pp. 259 - 262.

[30] Lee S.K. and Barash M.M., "Accuracy Improvement of a CNC Machining Centre by Using a Touch Probe and a Metrology Pallet", Final Report, Vol 6, Purdue University, USA, 1986.

[31] Lunsford J.S., "Automatic Inspection and Compensation Generation System for Machine Tools", Proc. Int. Conf. ASME (MI'88, Atlanta, Georgia, USA), April 1988, pp. 373 - 377.

[32] Chang C.H., "Automatic Monitoring NC Machine Tool Errors with Electronic Surface Sensing Probe", Proc. Int. Conf. ASME (MI'88, Atlanta, Georgia, USA), April 1988, pp. 333 - 344.

[33] Duffie N.A., and Malmberg S.J., "Error Diagnosis and Compensation Using Kinematic Models and Position Error Data", Annals of the CIRP, Vol. 36/1/1987, pp. 355 -358.

[34] Zhang G., et al, "A Displacement Method for Machine Geometry Calibration", Annals of the CIRP, Vol. 37/1/1988, pp.515 - 518.

[35] El-Sayed A.A. and El-Hakeem H.M., "Uncertainties of Two Analytical Methods Used for the Determination of Straightness Error", Int. J. Prod. Res., Vol. 24, No 5, 1986, pp. 1193 - 1202.

[36] Chen Z.X., Zhu Z.N. and Wu S.M., "Guideway's Geometrical Error Measurement and Forecasting Control", XII NAMRC Proc., 1984, pp. 386 - 393.

[37] Treib T., "Error Budgeting - Applied to the Calculation and Optimization of the Volumetric Error Field of Multiaxis Systems", Annals of the CIRP, Vol. 36/1/1987, pp. 365 - 367.

[38] Romanov V.L. and Philimonovskaya O.P., "Checking the Accuracy of the Co-ordinate Displacement of NC Machine Tools", Machines and Tooling, Vol. 48, No 3, pp. 12 -13.

[39] Portman V.T., "Error Summation in the Analytical Calculation of Lathe Accuracy", Machine and Tooling, Vol. 51, No 1, 1980, pp. 7 - 10.

[40] Weck M. and Schmit M., "An Optical Measurement Procedure for Determination of the Geometric Accuracy of Machine Tools", Annals of the CIRP, Vol. 33/1/1984, pp. 387 - 392, (in German).

[41] Duffie N.A. and Yang S.M., "Generation of Parametric Kinematic Error-Correction Functions from Volumetric Error Measurements", Annals of the CIRP, Vol. 34/1/1985, pp 435 -438.

[42] Takada K. and Takeyama H., "Accuracy Control of Machine-Tool by Means of Independent Optical Axes", Annals of the CIRP, Vol. 27/1/1978, pp. 271 - 276.

[43] Dimitriev B.N. and Shuneiko I.A., "Estimating the Capability of a Machine Tool to Ensure Geometric Accuracy", Machines and Tooling, Vol. 49, No 5, 1978, pp. 6 -8.

[44] Kakino Y., Yamamoto Y. and Ishi N.,"New Measuring Method of Rotating Accuracy of Spindle", Annals of the CIRP, Vol. 25/1/1977, pp. 241 - 244.

[45] Farmer L.E. and Harris A.F., "Change of Datum of Dimensions on Engineering Drawings", Int. J. MTDR, Vol. 24, No 4, 1984, pp. 267 - 275.

[46] Goodrich L.J., "Adaptive Control-Theory and Application", Presented at SME's Cutting Tools and Materials and Techniques Conf., May 1976, Milling Methods and Machines, First Edition, SME, 1982, pp. 195 - 205.

[47] Technology of Machine Tools, M.T.T.F., Vol 5. Machine Tool Accuracy, Lawrence Livemore Laboratory, University of California, Livemore, California, UCRL-52960-5, 1980.

[48] McKeown P.A., "The Role of Precision Engineering in Manufacturing of the Future", Annals of the CIRP, Vol. 36/2/1987, pp. 495 - 501.

[49] Koval M.I. and Igonin G.A., "Comparative Analysis of Machining Error Components for a Heavy NC Machine Tool", Machine and Tooling, Vol. 50, No 9, 1979, pp. 9 - 13.

[50] Takeuchi Y., Sakamoto M., and Sata T., "Improvement in the Working Accuracy of an NC Lathe by Compensation for Thermal Expansion", Precision Engineering, Vol. 4 (1), 1982, pp 19 -24.

[51] Eman K.F., "A New Approach to Form Accuracy Control in Machining", Int. J. for Prod. Res., Vol. 24 (4), 1986, pp 825 - 838.

[52] Sata T.,Takeuchi Y. and Okubo N., "Improvement of Working Accuracy of a Machining Centre by Computer Control Compensation", Proc. 17th Int. MTDR Conf., 1977.

[53] Sata T., Takeuchi Y., Sakamoto M. and Wek M., "Improvement of Working Accuracy on NC Lathe by Compensation for the Thermal Expansion of Tool", Annals of the CIRP, Vol. 30/1/1981, pp. 445 - 449.

[54] Rahman M., "Factors Affecting the Machining Accuracy of a Chucked Workpiece", Precision Engineering, Vol. 8(1), January 1986, pp. 34 - 40.

[55] Rahman M., "Effect of Clamping Conditions on Chatter Stability and Machining Accuracy". Annals of the CIRP, Vol. 34/1/1985, pp. 339 - 342.

[56] Rahman M. and Narayan V., "Optimization of Error-of-Roundness in Turning Process", Annals of the CIRP, Vol. 35/1/1986, pp. 377 - 380.

[57] Nevelson M.S., "Factors Affecting Machining Accuracy and Selection of a Control Algorithm", Machines and Tooling, Vol. 44, No 3, 1973, pp. 25 - 28.

[58] Iwata K. and Sugimura N., "An Integrated CAD/CAPP System with "Know-hows" on Machining Accuracies of Parts", Trans. ASME, Vol. 109, May 1987, pp. 128 - 133.

[59] Petrov P., "Investigation into the Causes and Character of Variation of the Shape Accuracy During the Machining on NC Turning Machines", Mashinostroene, Vol. 34, No 10, 1985, pp. 443 - 446, (in Bulgarian).

[60] Bazrov B.M., "Investigating Machining Accuracy Using a Computer", Machines and Tooling, Vol. 47, No 8, 1976, pp. 15 - 20.

[61] Koval M.I. and Igonin G.A., "Certain Ways for Improving Machining Accuracy on NC Machine Tools", Machines and Tooling, Vol. 50, No 2, 1979, pp. 11 - 15.

[62] Koval M.I. et al, "Improving Machining Accuracy on Profiling Machines", Machines and Tooling, Vol. 45, No 10, 1974, pp. 11 - 15.

[63] Naumov V.V., "Increasing the Machining Accuracy of NC Lathes", Machines and Tooling, Vol.45, No 7, 1874, pp. 13 -14.

[64] Kadyrov Zh.N. et al, "Improving the Machining Accuracy of NC Lathes", Machines and Tooling, Vol. 51, No 4, 1980, pp. 12 - 13.

[65] Pronikov A.S., "Evaluating the Quality of Metal Cutting Machine Tools by Output Parameters", Machines and Tooling, Vol. 51, No 6, 1980, pp. 7 - 10.

[66] Wu S.M., and Ni J., "Precision Machining without Precise Machinery", Annals of the CIRP, Vol. 38/1/1989, pp. 533 - 536.

[67] Beadle B.R. and Bollinger J.G., "Computer Adaptive Control of a Machine Tool", Annals of CIRP, Vol. 19, 1971, pp. 61-65.

[68] El Gomyel, J.I. and Bregger, K.D., "On-line Tool Wear Sensing for Turning Operation", Trans. ASME, Vol 108, February 1986, pp. 44-47.

[69] Amitay G., Malkin S. and Koren Y., "Adaptive Control Optimization of Grinding", Trans. ASME, Vol. 103, February 1981, pp. 103-108.

[70] Bedini R., Lisini G.G. and Pinolli P.C., "Experiments on Adaptive Control of Milling Machine", Trans. ASME, Vol. 98(1), February 1976.

[71] Suzuki H. and Weinman K.J., "An On-line Tool Wear Sensor for Straight Turning Operations", Trans. ASME, Vol. 107, February 1985, pp. 397-399.

[72] Shiraishi, M., "Geometric Adaptive Control in NC Turning Operation", Trans. ASME, Vol. 106, February 1984, pp. 75-80.

[73] Koren Y., "Computer Control of Manufacturing Systems", McGraw-Hill International Book Company, 2nd Edition, 1985.

[74] Tlusty J. and Andrews G.C., "A Critical Review of Sensors for Unmanned Machining", Annals of the CIRP, Vol. 32/2/1983, pp. 563-572.

[75] Maithais R.A., "Adaptive Control for Machining Centres", Technical Paper, MS76-196, SME, 1976.

[76] Maithais R.A., "Adaptive Control for Eighties", Technical Paper, MS80-242, SME, 1980.

[77] Yamazaki K., Yamada A. and Sawai N., "A Study on Adaptive Control in an NC Milling Machine", Annals of the CIRP, Vol. 23/1/1974, pp. 153 - 154.

[78] Abdulov V.N., "Mechanical Adaptive Control Gives Improved Accuracy and Quality in Machining Operations", Soviet Engineering Research, Vol. 6, No.12, 1986, pp. 38-41.

[79] Yen D.W. and Wright P.K., "Adaptive Control in Machining - A New Approach Based on the Physical Constraints of Tool Wear Mechanisms", Trans. ASME, Vol. 105, February 1983, pp 31-38.

[80] Masory O., "Improving Contouring Accuracy of NC/CNC Systems With Additional Velocity Feed Forward Loop", Trans. ASME, Vol. 108, August 1986, pp. 227-230.

[81] Yamazaki K., Yamada A. and Sawai N., "A Study on Adaptive Control in an NC Milling Machine", Annals of the CIRP, Vol. 23/1/1974, pp. 153 - 154.

[82] Arsovski S.M., "Wear Sensors in the Adaptive Control Systems of Machine Tools", Int. J. Prod. Res., Vol. 21, No 3, 1983, pp. 347 - 456.

[83] Bedini R. and Pinotti P.C., "Experiments on Adaptive Constrained Control of a CNC Lathe", Trans. ASME, Vol. 104, May 1982, pp. 139 - 149.

[84] Liu M.Y. and Yang H.H., "An Adaptive Control Method for Machining Processes and a Digital Observer for Tool Wear Detection", Annals of the CIRP, Vol. 37/1/1988, pp., 469 - 472.

[85] De Filippi and Ippolito R., "Adaptive Control in Turning: Cutting Forces and Tool Wear Relationship for P 10, P 20 , P 30 Carbides", Annals of the CIRP, Vol. 17, 1969, pp. 377 - 385.

[86] Masory O and Koren Y., "Adaptive Control System for Turning", Annals of the CIRP, Vol. 29/1/1980, pp. 281 -284.

[87] Balakshin B.S., "Advantages of Equipping N.C. Machines with Adaptive Control Systems", Machines and Tooling, Vol. 44, No 3, 1973, pp. 8 - 10.

[88] Tlusty J. and Tarng Y.S., "Sensing Cutter Breakage in Milling", Annals of the CIRP, Vol. 37/1/1988, pp. 45 - 51.

[89] Inasaki I., Aida S. and Fukudas., "Monitoring System for Cutting Tool Failure Using an Acoustic Emission Sensor", JSME Int. J., Vol. 30, No 261, 1987, pp 523 - 526.

[90] Shirashi M., "In-Process Control of Workpiece Dimension in Turning", Annals of the CIRP, Vol. 28/1/1979, 333 - 337.

[91] Szafarczyk M.,"Automatic Measurement and Correction of Workpiece Diameter on NC Centre Lathe", Annals of the CIRP, Vol. 32/1/1983, pp. 305 - 308.

[92] Koren Y. and Masory O., "Adaptive Control with Process Estimation", Annals of the CIRP, Vol. 30/1/1981, pp. 373 - 376.

[93] Schultschik R., "Possibilities and Limits of Error Feedback in Automatic Machining", Annals of the CIRP, Vol. 30/1/1981, pp. 467 - 471.

[94] Tlusty J. and Elbestwai M.A.A., "Analysis of Transients in an Adaptive Control Servomechanism for milling with Constant Force", Trans. ASME, August 1977, pp. 766 - 772.

[95] Schaffer G., "Taking the Measure of CMMs", American Machinist, Special Report 749, October 1982, pp. 145-160.

[96] Sona C.M., "Three-Dimensional Interactive Co-ordinate Measuring Machines", CSIRO Division of Applied Physics, A Symposium on Trends in Dimensional Measurement, March 1984, pp. 1-12.

[97] McBain R.L., "Impact of Zesis UMM500, CNC 4-Axis-Co-ordinate Measuring Machine on Dimensional Metrology", CSIRO Division of Applied Physics, A Symposium on Trends in Dimensional Measurement, March 1984, pp. 13-44.

[98] Neve B., "Experience with an LK80 Computerized Numerical Control Coordinate Measuring Machine", CSIRO Division of Applied Physics, A Symposium on Trends in Dimensional Measurement, March 1984, pp. 45-56.

[99] Thwaite E.G., "Modern Coordinate Measuring Machines - Their Errors and Their Calibration", CSIRO Division of Applied Physics, A Symposium on Dimensional Measurement in Precision and Heavy Engineering, October 1986, pp. 53-69.

[100] Sona C.M., "Co-ordinate-Measuring-Machine (CMM) Software Performance", CSIRO Division of Applied Physics, A Symposium on Dimensional Measurement in Precision and Heavy Engineering, October 1986, pp. 71-85.

[101] McBain R.L., "Co-ordinate-Measuring-Machine (CMM) - The Awareness Factor", CSIRO Division of Applied Physics, A Symposium on Dimensional Measurement in Precision and Heavy Engineering, October 1986, pp. 87-101.

[102] Belforte G., et al, "Coordinate Measuring Machines and Machine Tools Selfcalibration and Error Correction", Annals of the CIRP, Vol 36/1/1987, pp. 359-364.

[103] Accuracy Specification for Coordinate Measuring Machines, Coordinate Measuring Machine Manufacturers Association, 1982.

[104] Nijs J.F.C. de et al, "Modelling for a Coordinate Measuring Machine for Analysis of Its Dynamic Behaviour", Annals of the CIRP, Vol 337/1/1988, pp. 507-510.

[105] Kunzmann H. and Waldele F., "Performance of CMMs", Keynote Paper, CIRP Conf., Tokyo, 1988, Annals of the CIRP, Vol. 37/2/1988, pp. 633 - 640.

[106] Zhang G., et al, "Error Compensation of Coordinate Measuring Machines", Annals of the CIRP, Vol 34/1/1985, pp. 445-448.

[107] British Standard BS6808, Co-ordinate Measuring Machines, Part 2. Methods for Verifying Performance, British Standards Institution, 1987 .

[108] ANSI/ASME Standard B89.1.12 - Method for Performance Evaluation of Co-ordinate Measuring Machines, 1986.

[109] CIRP Scientific Technical Committee on Dimensional Metrology and Quality Control Report, 1987, Annals of the CIRP, Vol. 36/2/1987, pp. 517-521.

[110] Hocken R. et al, "Three Dimensional Metrology", Annals of the CIRP, Vol. 26/2/1977, pp. 403 - 408.

[111] Oya M., Hokari H. and Tamura H., "A Study on Improvement of the Accuracy of a Three-co-ordinate Measuring Machine (A Method of Error Correction)", JSME Int. J., Vol 30, No.260, 1987, pp. 344-349.

[112] Peggs G.N., "Creating a standards Infrastructure for Co-Ordinate Technology in the U.K.", Annals of the CIRP, Vol. 38/1/1989, pp. 521 - 523.

[113] Osanna P.H. and Durakbasa N.M., "Comprehensive Analysis of Workpiece Geometry by Means of the Coordinate Measurement Technique", Int. Conf. on Metrology and Properties of Engineering Surfaces, Reprints, 1988, pp. 1 - 6.

[114] Yano H. and Nakamura T., "Simplified Method of Evaluating the Measurement Error of the Coordinate Measuring Machine", Annals of the CIRP, Vol. 25/1/1977, pp. 235 - 240.

[115] Draudin A.T., "A Method for Integrated Assessment of the Measurement Error on Co-ordinate Measuring Machines", Machines and Tooling, Vol. 50, No 8, 1979, pp. 34 - 37.

[116] Kunzmann H., "On Testing Coordinate Measuring Machines (CMM) with Kinematic Reference Standards (KRS)", Annals of the CIRP, Vol. 32/1/1988, pp. 465 - 468.

[117] Jony F., "Theoretical Modelisation and Experimental Identification of the Geometrical Parameters of Coordinate-Machines by Measuring a Multi-Directed Bar", Annals of the CIRP, Vol. 35/1/1986, pp. 393 - 396.

[118] Teeuwsen J.W.M.C., Soons J.A., and Schelleken P.H., "A General Method for Error Description of CMMs Using Polynomial Fittings Procedure", Annals of the CIRP, Vol. 38/1/1989, pp. 505 510.

[119] Trucks H.E., "Designing for Economical Production", Second Edition, SME, 1987.

[120] Rao P.K.R. and Shunmugam M.S., "Accuracy and Surface Finish in BTA Drilling", Int. J. Prod. Res., Vol. 25, 1987, pp. 31 - 44.

[121] Murthy T.S.R. and Rao Y.S., "A Simple Approach for Evaluation of Cylindrical Surfaces", Annals of the CIRP, Vol. 30/1/1981. pp. 441 - 444.

[122] Shunmugam M.S., "On Assessment of Geometric Errors", Int. J. Prod. Res., Vol 24, No 2, 1986, pp.413 - 425.

[123] Sona C.M. and Farmer L.E., "The Inspection of Holes with Co-ordinate Measuring Machines", 4th Int. Conf. on Manuf. Engg., Brisbane, 1988, pp.152 - 156.

[124] Bestrefield D.H., Quality Control, Second Edition, Prentice - Hall, 1986.

[125] Galloway D.F., "Some Experiments on the Influence of Various Factors on Drill Performance", Trans. ASME, Vol. 57, February 1957, pp. 191 - 231.

[126] Foster L.W., "Geometric Tolerancing", Manufacturing Engineering, October 1987, pp. 46 -48.

[127] Foster L.W., Geo - Metrics : The Metric Application of Geometric Tolerancing Techniques, Addison - Wesley Publ. Comp. Inc., 1986.

[128] Metals Handbook, Vol 3, Machining, 8th Edition, American Society for Metals, 1967.

[129] Programmers Manual ANCA 2000 Series CNC, Zenford Zeigler, 1984.

[130] Midgley R.P.J., "Commissioning of a Coordinate Measuring Machine", B.E. Thesis, University of Wollongong, November 1988.

[131] Tourret R., Performance of Metal Cutting Tools", Butterworths Scientific Publ., 1958.

[132] Armarego E.J.A. and Brown R.H., The Machining of Metals, Prentice - Hall Inc., 1969.

[133] Martellotti M.E., "An Analysis of the Milling Process", Trans. ASME, Vol. 63, November 1941, pp. 677 - 700.

[134] Fugelso M.A. and Wu S.M., "The Automated Measurement of Twist Drill Point Shape", VIII NAMRC Proc., May 1980, pp. 395 - 400.

[135] Tsai W.D. and Wu S.M.."Measurement and Control of the Drill point Grinding and Control of the Drill point Grinding Process", Int. J. of MTDR, Vol. 19, No 2, pp. 109 - 114.

[136] Malkiewicz H., "An Investigation of the Geometrical Variables Affecting the Drilling Process", M.Eng.Sc. Thesis, University of Melbourne, 1973.

[137] Wright J.D., "A Study of the Geometrical Variables of Manufactured Twist Drills", M.Eng.Sc. Thesis, University of Melbourne, 1975.

[138] Paramanik D.K., "The Influence of Geometrical Variables and Cutting Conditions on Twist Drill Performance", Ph.D. Thesis, University of Melbourne,1988.

[139] Appuswamy R., "Process Capability and Quality Improvement Studies of a Drill Blank Grinding Process", M.Eng.Sc. Thesis, University of Melbourne, 1988.

[140] Hayward A., Repeatability and Accuracy: An Introduction to the Subject and a Proposed Standard Procedure for Measuring the Repeatibility and Estimating the Accuracy of Industrial Measuring Instruments, London, 1977.

[141] Australian Standard AS 2438 - 81, Twist Drill: General Purpose, Standard Association of Australia, 1981.

[142] American National Standard ANSI B 94.11M - 1979, Twist Drills, ASME, 1979.

[143] International Standard ISO 235 - 1980, Parallel Shank Jobber and Stub Drills and Morse Taper Shank Drills, International Organization for Standardization, 1980.

[144] British Standard BS 122, Milling Cutters, Part 4, Screwed Shank End Mills and Slot Drills, British Standards Inst., 1980.

[145] German Standard (Deutsche Norman) DIN 1412 - 1966, Twist Drills, 1966.

[146] Tipnis V., "The Versatile End Mill", Reprinted from Modern Machine Shop, April 1980, Milling Methods and Machines, SME, 1982, pp. 68 - 73.

[147] Kline W.A. et al, "The Prediction of Surface Accuracy in End Milling", Trans. ASME, Vol. 104, August, 1982, pp 272 - 278.

[148] Devor R.E., "Control of Surface Error in End Milling", XI NAMRC Proc., 1983, pp. 356 - 362.

[149] Babin T.S. et al, "A Model for End Mill surface Topography", XIII NAMRC Proc., 1985, pp. 362 - 368.

[150] Machining Data handbook, 3rd Edition, Vol. 2, Metcut Research Associates Inc., 1980.

[151] Mannan M.A., "Performance for End Mills Made of Different Tool Materials with Regards to Tool Life and Stability", Annals of the CIRP, Vol. 35/1/1986, pp. 37 -40.

[152] Lee C.E., Chung S.C. and Kim J.S., "Geometric Adaptive Control System for the Peripheral End Milling Process", Int. J. of machine Tools and Manufacture, Vol. 27, No 4, 1987, pp. 417 - 430.

[153] Tlusty J. and MacNeil P., "Dynamics of Cutting Forces in End Milling", Annals of the CIRP, Vol. 24/1/1975, pp. 21 - 25.

[154] Yellowley I., "Observations on the Mean Values of Forces, Torque and Specific Power in the Peripheral Milling Process", Int. J. of MTDR, Vol. 25, No 4, 1985, pp.337 - 346.

[155] Ber A., Rotberg J. and Zombach S., "A Method for Cutting Force Evaluation of End Mills", Annals of the CIRP, Vol.37/1/1988, pp.37 - 40.

[156] Armarego E.J.A. and Whilfield R.C., "Computer Based Modelling of Popular Machining Operations for Force and Power Prediction", Annals of the CIRP, Vol. 34/1/1985, pp. 65 - 69.

[157] Armarego E.J.A. and Deshpande N.P., "Computerized Predictive Cutting Models for Forces in End-Milling Including Eccentricity Effects", Annals of the CIRP, Vol. 38/1/1989, pp. 45 - 49.

[158] Tlusty J. and Elbestawi M., "Constraints in Adaptive Control with Flexible End Mills", Annals of the CIRP, Vol. 28/1/1979, pp. 253 - 255.

[159] Gygax P.E., "Experimental Full Cut Milling Dynamics", Annals of the CIRP, Vol. 29/1/1980, pp. 61 - 66.

[160] Gygax P.E., "Dynamics of Single-Tooth Milling, Annals of the CIRP, Vol. 28/1/1979, pp. 65 - 70.

[161] Fujii Y. and Iwabe H., "Improvement of Profile Error by Dwell Function of Controller", Bull. Japan Soc. of Prec. Engg., Vol 18, No 4, December 1984, pp. 305 - 311.

[162] Martellotti M.E., "An Analysis of the Milling Process, Part II - Down Milling, Vol. 61, May 1945, pp. 233 - 251.

[163] Roth R. and Van Haeringen I.A., Australian Engineering Drawing Hand Book, Part 1, I.E.Aust., 1987.

[164] Australian Standard AS2536 - 1982, Surface Texture, The Standards Association of Australia, 1982.

[165] Nowicki B., "Multiparameter Representation of Surface Roughness", Wear, Vol. 102, 1985, pp. 161 - 176.

[166] Metals Handbook, Desk Edition, American Society of Metals, 1985.

[167] Milling Handbook of High-Efficiency Metal Cutting, Carboloy Inc., Michigan, 1980.

[168] Chisholm A.J., Conf. on Machinability, Proc. Inst. Mech. Engrs., Vol. 155, 1946, pp. 267 - 278.

[169] Arai N., Adachi K., Nishiguchi M. and Sugihara T., "A Study on Finished Accuracy in Low Frequency Vibratory Drilling", The Science and Engineering

Review of Doshisha University, Vol. 28, No 3 - 4, February 1988, pp. 52 - 62, (in Japanese).

[170] Shaw M.C. and Crowell J.A., "Finish Machining", Annals of The CIRP, Vol. XIII, 1965, pp. 5 -22.

[171] Nakamyama K., Shaw M.C. and Brewer R.C., "Relationship between Cutting Forces, Temperatures, Built - up Edge and Surface Finish", Annals of the CIRP, Vol. XIV, 1966, pp. 211 - 233.

[172] Selvam M.S. and Radhakrishnan V., "Influrnce on Side-Flow and Built-up Edge on the Roughness and Hardness of the Surface Machined with a Single Point Tool", Wear, Vol. 26, 1973, pp. 393 - 403.

[173] Gladman C.A., "Control of Quality in Production Engineering", Annals of the CIRP, Vol. XIV, 1966, pp. 161 - 175.

[174] Smith D., "Tips on How to Do a Better Job of Finish Milling", Part 1, Reprinted from the Cutting Edge, November 1970, Milling Methods and Machines, SME, 1982, pp. 96 - 99.

APPENDICES

Appendix A

Terms Used in GD & T

Extract from ANSI Y 14.5 - 1982 - Dimensioning and Tolerancing [11]

1.3 DEFINITIONS

The following terms are defined as their use applies in this standard.

1.3.1 Dimension. A numerical value expressed in appropriate units of measure and indicated on a drawing and in other documents along with lines, symbols, and notes define the size of geometric characteristic, or both, of a part or part feature.

1.3.2 Basic Dimension. A numerical value used to describe the theoretically exact size, profile, orientation,or location of a feature or datum target. It is the basis from which permissible variations are established by tolerances on the dimensions, in notes, or in feature control frames (see Fig. 78).

1.3.3 True Position. The theoretically exact location of a feature established by basic dimensions.

1.3.4 Reference Dimension. A dimension, usually without tolerance used for information purposes only. It is considered auxiliary information and does not govern production or inspection operations. A reference dimension is a repeat of dimension or is derived from other values shown on the drawing or on related drawings.

1.3.5 Datum. A theoretically exact point, axis, or plane divided from the true geometric counterpart of a specified datum feature. A datum is the origin from which the location or geometric characteristics of features of a part are established.

1.3.6 Datum Target. A specified point, line, or area on a part used to establish a datum.

1.3.7 Feature. The general term applied to a physical portion of a part, such as a surface, hole, or slot.

1.3.8 Feature of Size. One cylindrical or spherical surface, or a set of two plane parallel surfaces, each of which is associated with a size dimension.

1.3.9 Datum Feature. An actual feature of a part that is used to establish a datum.

1.3.10 Actual Size. The measured size.

1.3.11 Limits of Size. The specified maximum and minimum sizes.

1.3.12 Maximum Material Condition (MMC). The condition in which a feature of size contains the maximum amount of material within the stated limits of size - for example, minimum hole diameter, maximum shaft diameter.

1.3.13 Least Material Condition (LMC). The condition in which a feature contains the least amount of material within the stated limits of size - for example, maximum hole diameter, minimum shaft diameter.

1.3.14 Regardless of Feature Size (RFS). The term used to indicate that geometric tolerance or datum reference applies at any increment of size of the feature within its size tolerance.

1.3.15 Virtual Condition. The boundary generated by the collective effects of the specified MMC limit of size of a feature and any applicable geometric tolerances.

1.3.16 Tolerance. The total amount by which a specified dimension is permitted to vary. the tolerance is the difference between the maximum and minimum limits.

1.3.17 Unilateral Tolerance. A Tolerance in which variation is permitted in one direction from the specified dimension.

1.3.18 Bilateral Tolerance. A tolerance in which variation is permitted in both directions from the specified dimension.

1.3.19 Geometric Tolerance. The general term applied to the category of tolerances used to control from, profile, orientation, location, and runout.

1.3.20 Full Indicator Movement (FIM). The total movement of an indicator when appropriately applied to a surface to measure its variations.

1.4 FUNDAMENTAL RULES

Dimensioning and tolerancing shall clearly define engineering intent and shall confirm to the following.

(a) Each dimension shall have a tolerance, except for those dimensions specially identified as reference, maximum, minimum, or stock (commercial stock size). The tolerance may be applied directly to the dimension (or indirectly in the case of basic dimensions), indicated by a general note, or located in a supplementary block of the drawing format (see ANSI Y14.1).

(b) Dimensions for size, from, and location of features shall be complete to the extent that there is full understanding of the characteristics of each feature. Neither scaling (measuring the size of a feature directly from en engineering drawing) nor assumption of a distance or size is permitted.

NOTE: Undimensioned drawings - for example, loft, printed wiring, templates, master layouts, tooling layout - prepared on stable material are excluded, provided the necessary control dimensions are specified.

(c) Each necessary dimension of an end product shall be shown. No more dimensions than those necessary for complete definition shall be given. The use of reference dimensions on drawing should be minimizes.

(d) Dimensions shall be selected and arranged to suit the function and mating relationship of a part and shall not be subject to more than one interpretation.

(e) The drawing should define a part without specifying manufacturing methods. Thus, only the diameter of a hole is given without indicating whether it is to be drilled, reamed, punched, or made by any other operation. However, in those instances where manufacturing, processing, quality assurance, or environmental information is essential to the definition of engineering requirements, it shall be specified on the drawing.

(f) It is permissible to identify as nonmandatory certain processing dimensions that provide for finish allowance, shrink allowance, and other requirements, provided the final dimensions are given on the drawing. Nonmandatory processing dimensions shall be identified by an appropriate note, such as NONMANDATORY (MFG DATA).

(g) Dimensions should be arranged to provide required information for optimum readability. Dimensions should be shown in true profile views and refer to visible outlines.

(h) Wires, cables, sheets rods, and other materials manufactured to gage or code numbers shall be specified by linear dimensions indicating the diameter or thickness. Gage or code numbers may be shown in parentheses following the dimension.

(i) A 90° angle is implied where center lines and lines depicting features are shown on a drawing at right angles and no angle is specified (see 2.1.1.2)

(j) A 90° BASIC angle applies where centre lines of features in a pattern or surfaces shown at right angles on the drawing are located or defined by basic dimensions and no angle is specified.

(k) Unless otherwise specified, all dimensions are applicable at 20°C (68°F). Compensation may be made for measurements made at other temperature.

Appendix B

A Comparison of Symbols Used in GD & T by Different Standards

Extract fron AS 1100.201 - 1984, Technical Drawing, Mechanical Drawing [12]

TABLE A1
COMPARISON OF SYMBOLS

Characteristic	ISO	Australia AS 1100	U.S.A. Y14.5	U.K. BS 308	Canada B78.2
Decimal sign	,	• on line or mid-height	• (on line)	• (on line)	• (mid-height)
Cipher before decimal sign	Yes	Yes	No for inch units Yes for metric units	Yes	No
Diameter	Øx	Same	Same	Same	Same
Radius	Rx	Same	Same	Same	xR
Square	□x	Same	Same	—	—
Taper		Same	Same	Same	—
Slope		Same	Same	—	—
TP		Same	Same	Same	Same
Feature identification	A		—	A	—
Datum identification	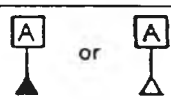	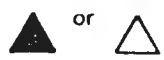	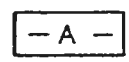	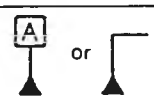	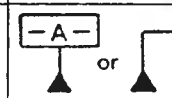
MMC		Same	Same	Same	Same
Envelope principle	See Note 1		—	—	—
Straightness		Same	Same	Same	Same
Flatness		Same	Same	Same	Same
Roundness		Same	Same	Same	Same
Cylindricity		Same	Same	Same	Same

Characteristic	ISO	Australia AS 1100	U.S.A. Y14.5	U.K. BS 308	Canada B78.2
Profile of a line		Same	Same	Same	Same
Profile of a surface		Same	Same	Same	Same
Parallelism		Same	Same	Same	Same
Squareness		Same	Same	Same	Same
Angularity		Same	Same	Same	Same
Position		Same	Same	Same	Same
Concentricity		Same	Same	Same	Same
Symmetry		Same	None	Same	Same
Run-out (Circular)		Same	Same	Same	Same
Total run-out		Same	 See Note 2	—	—
Regardless of feature size	—	—		—	—
Projected tolerance zone		Same	Same		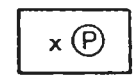 Adjacent to tolerance frame
Datum target	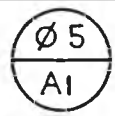	—	Same		Same
Part symmetry		Same	—	Similar with thick lines	—

LEGEND:
Same = same as in Column 2 (ISO)
— = none
x = a dimensional value
y = a number 1 to 6 identifying the datum target
A = an upper case letter

NOTES:
1. The symbol Ⓔ has been adopted by ISO/TC 10/SC 5 but not yet embodied in any standard.
2. 'TOTAL' specified under the tolerance frame (ANSI refer to this as the 'feature control symbol').
3. The symbol Ⓟx on a dimension line or adjacent to the tolerance frame has been adopted by ISO/TC 10/SC 5 but not yet embodied in any standard.

Appendix C

Programme for Test Component

```
(--------------------------
(TEST COMPONENT
(--------------------------
G90
G71
G17
G94
G51
G40
G52Z0
G00X-50.Y-50.D32
G50X-50.Y-50.Z000.D0
G52Z0
N1G52X-500.Y-150.
T3M6 (100 MM FACE MILLING CUTTER)
F100.S1000
G0X-60.Y37.5
G0Z0D3
M03M08
G01Z-1.0
X260.
G0Z10.
M5M9
G52Z0
N2G52X-500.Y-150.
T2M6 (16 MM END MILL)
F125.S2500
G00X-50.Y-50.
G00Z10.D2
M03M08
(-------------------------)
G00X-10.Y-20.
G0Z-12.
G41H2X7.Y7.I-20.
G01Y68.
```

```
X193.
Y7.
X14.
Y61.
X186.
Y14.
X15.
Y60.
X185.
Y15.
X-10.
G40
Y0.
Z-25.
G41H2X0.Y0.I-20.
Y75.
X200.
Y0.
X-10.
G0Z10.
G40
(------------------------)
M5M9
G52Z0
N3G52X-500.Y-150.
G95T4M6 (CENTRE DRILL)
F0.15S1000
G0Z5.D4
M03M08
G81X40.Y37.5R2.Z-11.
X70.
X100.
X130.
X160.
G0Z10.
M5M9
G52Z0
N4G52X-500.Y-150.
```

```
G95T5M6 (12 MM  DRILL)
F0.15S2000
G00Z03.D5
M03M08
(------------------------)
G83X40.Y37.5R3.Z-31.Q5.
X70.
X100.
X130.
X160.
M5M9
G52Z0
G52X-500.Y-150.
T0M6
G40
G51
G00X0.Y0.
G50X0Y0Z0D0
M02
```

Appendix D

Tool Path

Appendix D includes following figures:

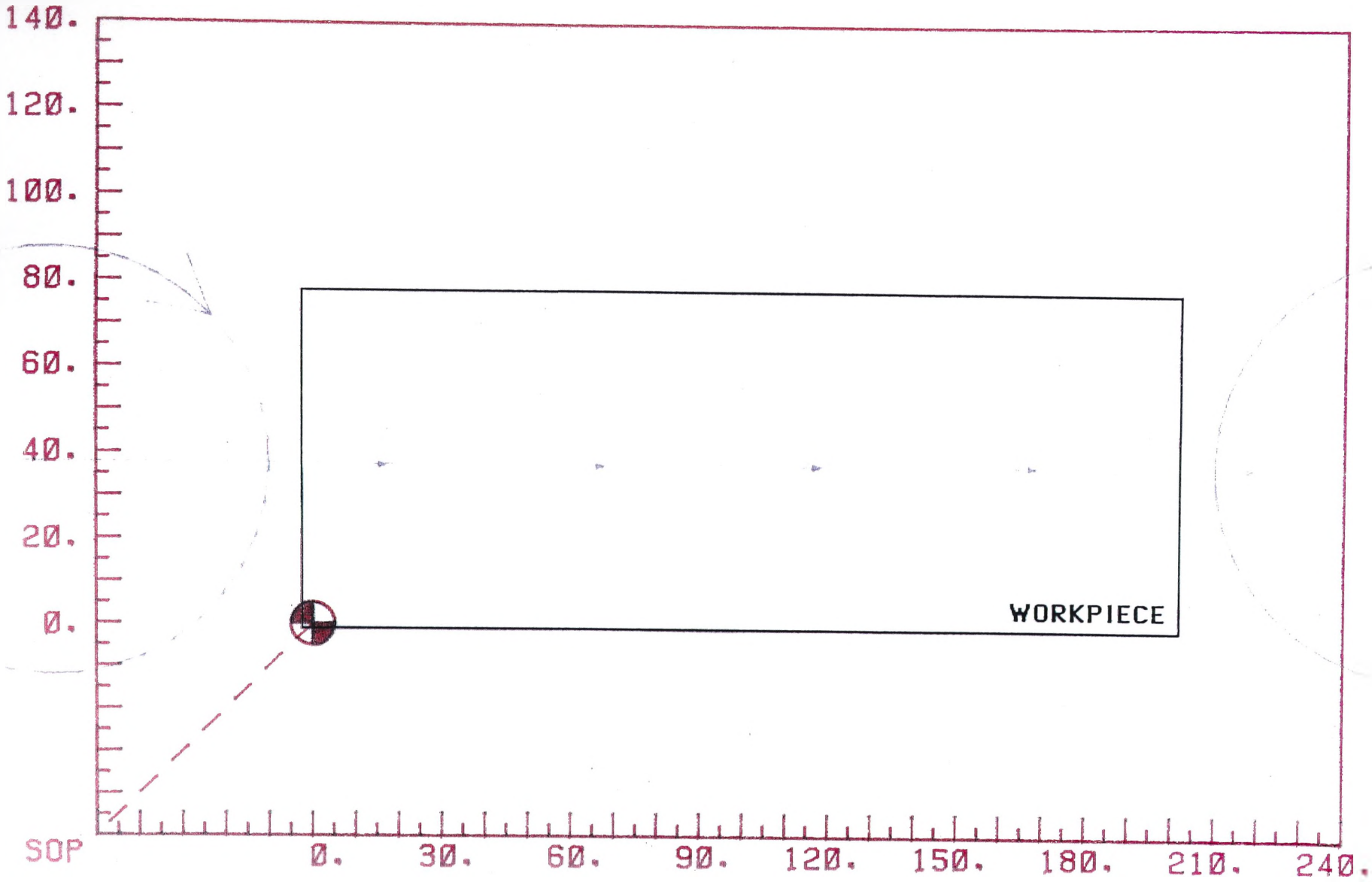

Figure D.1 Tool Path of ϕ 100 mm Face Cutter.

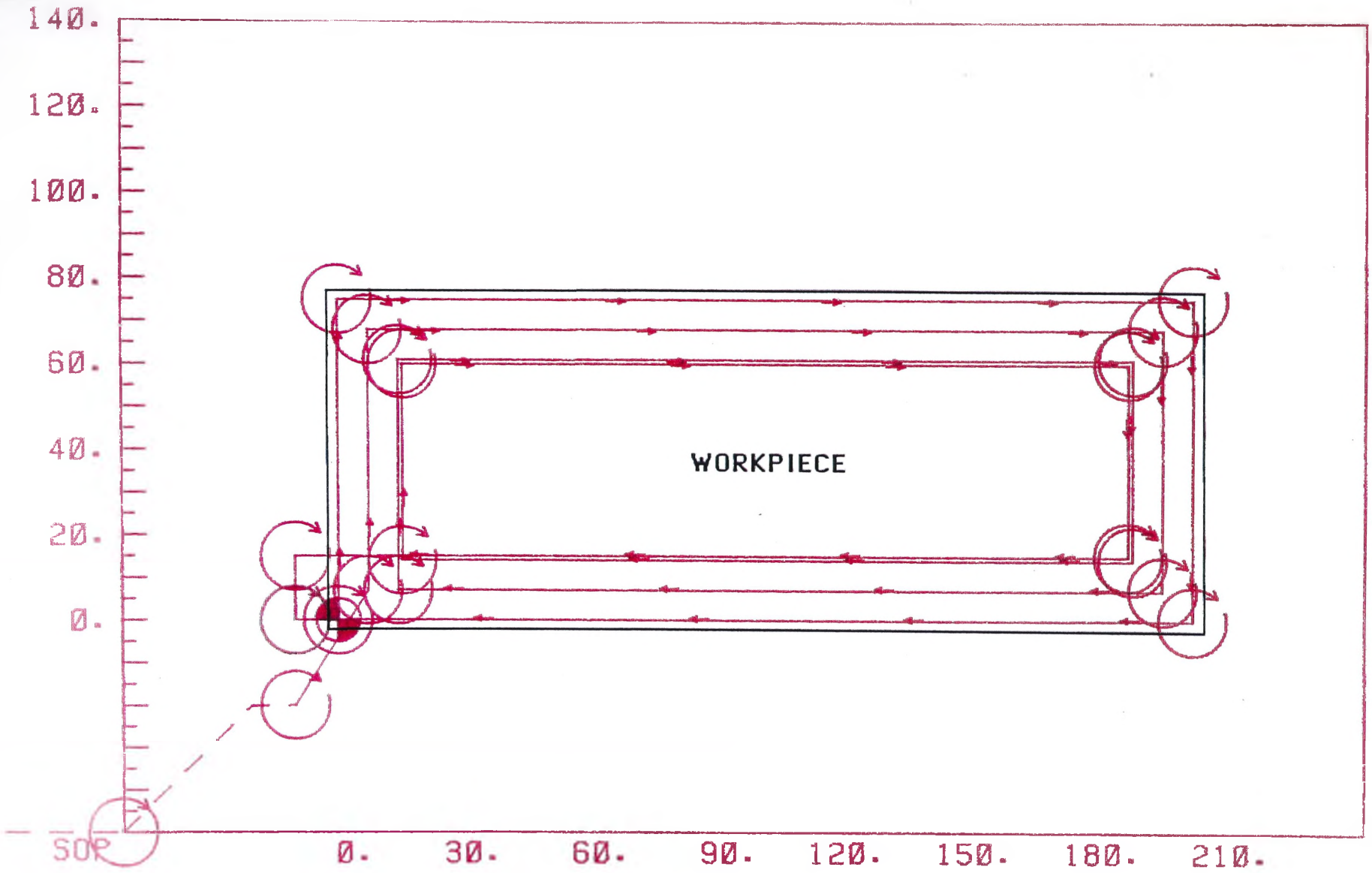

Figure D.2 Tool Path of ϕ 16 mm End Mill.

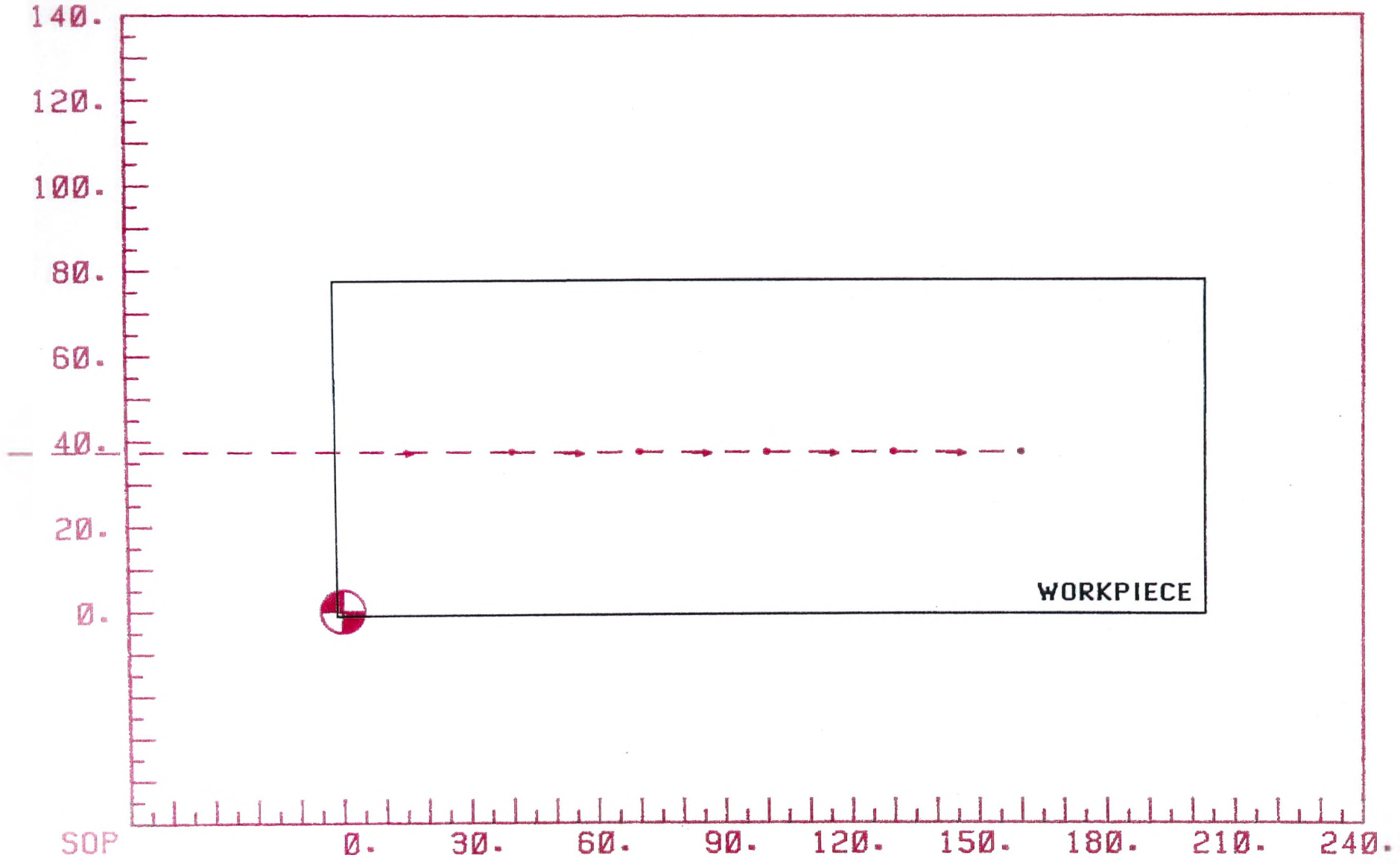

Figure D.3 Tool Path of Centre Drill.

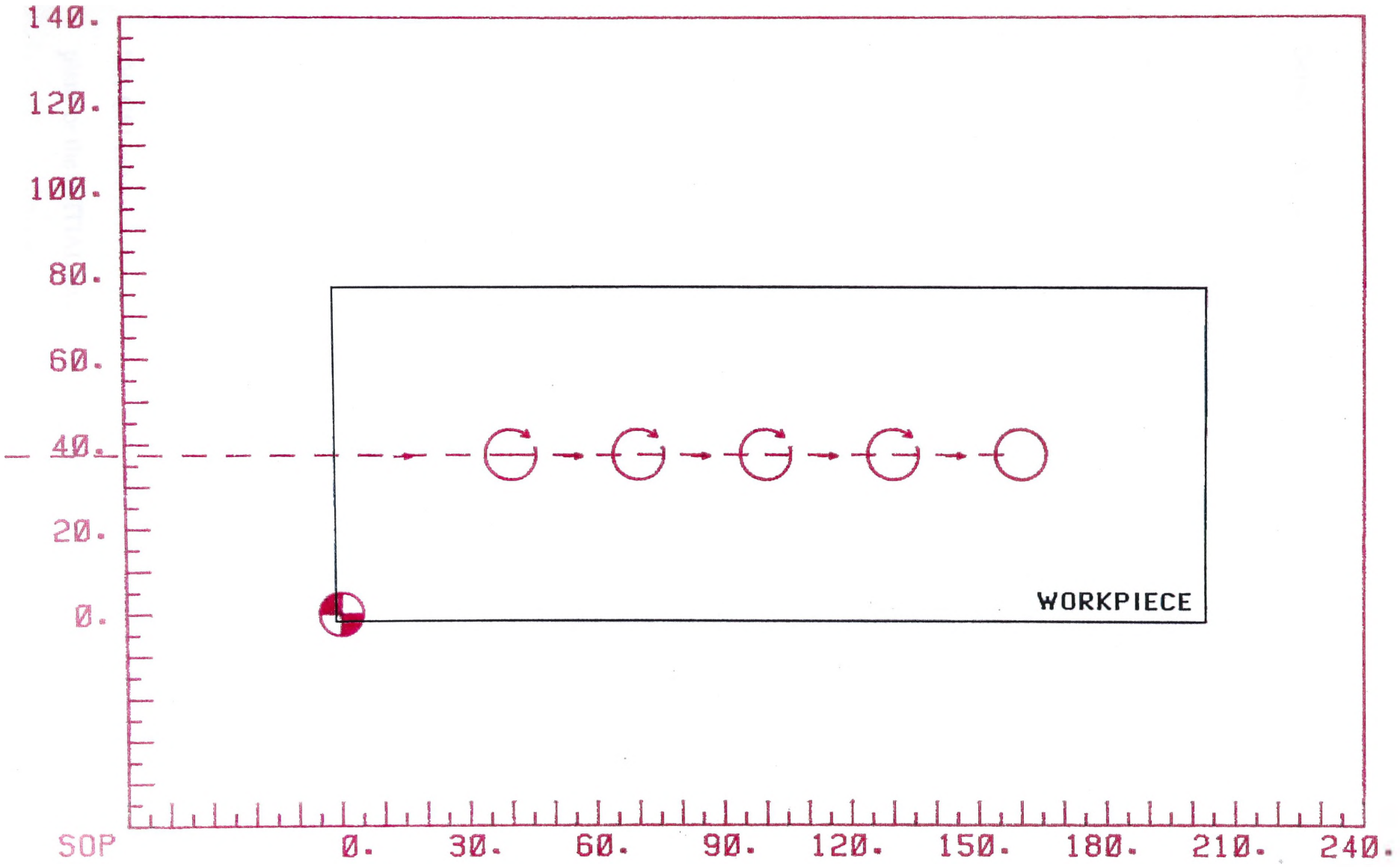

Figure D.4 Tool Path of ϕ 12 mm Drill.

Appendix E

Different Drilling Canned Cycles

Details of the three drilling canned cycles used (G73, G81 and G83) are given below [129]:

G73 Chip Break Canned Cycle

Example: G73 X10. Y215. Z-60. R2. Q6.

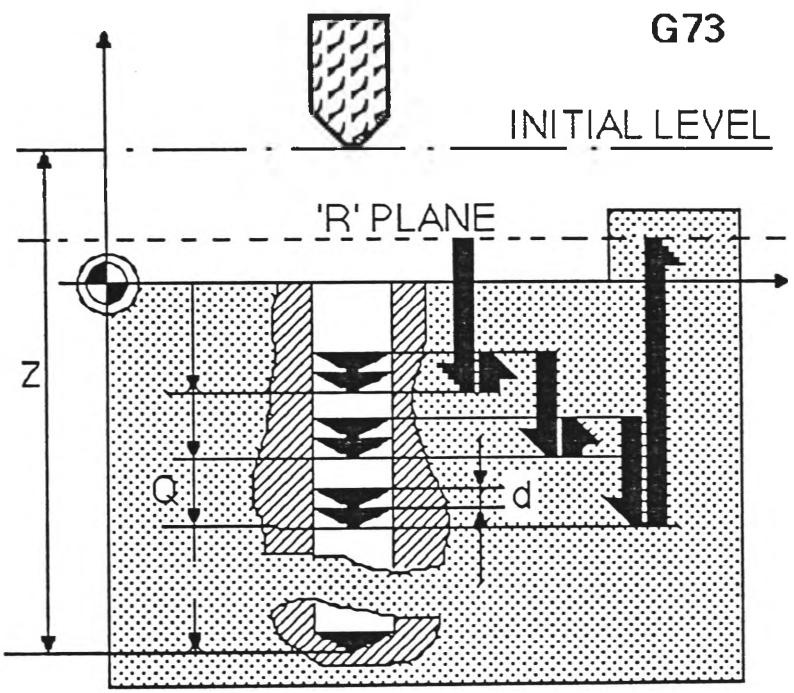

Figure E.1 Chip Break Canned Cycle (G73).

The G73 will initially rapid to the R plane + "d".

G81 Spot Drilling Canned Cycle

Example: G90 G81 X10. Y45. R2. Z-20.

The G81 canned cycle will rapid to the R plane, feed to the depth (z) and then out to the R plane or the INITIAL level depending on G99 or G98.

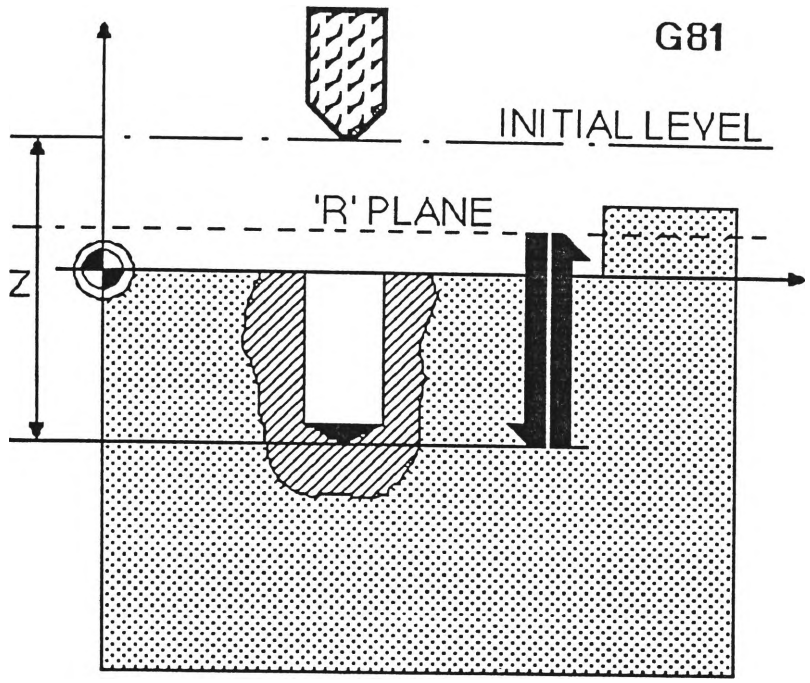

Figure E.2 Spot Drilling Canned Cycle (G81).

G83 **Deep Hole Drilling Canned Cycle**

Example: G83 X10. Y12. R2. Z-100. Q8.

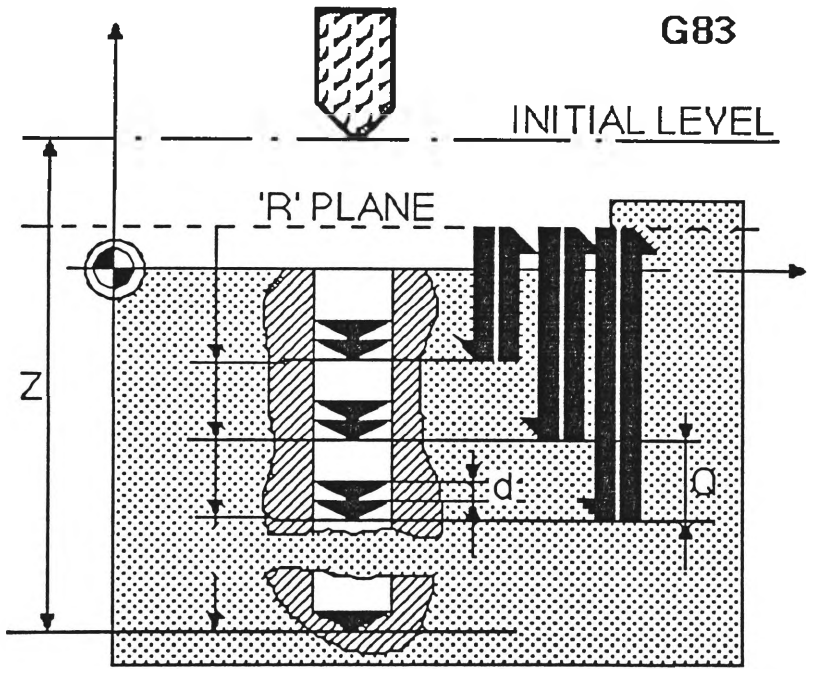

Figure E.3 Deep Hole Drilling Canned Cycle (G83).

The G83 canned cycle is a full withdrawal cycle where the tool is restricted at the completion of each infeed to the R plane. The tool is then rapidly back down to the previous depth less "d".

Appendix F

Linear Dimension Calculation Procedure

When some linear dimensions for a prismatic component(like our test piece) are placed in a drawing, it is assumed that the surfaces which define these dimensions are "perfect". (In that case the distance between two surfaces defines a dimension of the component.) But in reality, the surfaces obtained after machining are not perfect; thus it is difficult to identify the real actual dimensions. Unfortunately in the standards there is no definite guideline to solve this problem. In this thesis the following procedure was adopted to find the actual dimensions of a machined component.

First a number of points were probed on those surfaces which define a particular dimension.The mean values for each surface texture were calculated. The difference between the two mean values were taken as the actual dimension (see Figure F.1). The upper and lower limits of the dimensions are related to the half of the sum of the ranges. As the number of points are increased, in place of ranges plus minus three times standard deviations should be used.

It is also interesting to find the nature of frequency distribution of the points. Because to apply statistical rules the points should be normally distributed. A computer programme (STAT-PACK)* was used for this purpose. A copy of that programme and procedure for determining a dimension are attached. Findings showed that in most of the cases the points were normally distributed.

* The original programme is given in [124] . We have modified the programme to suite our needs.

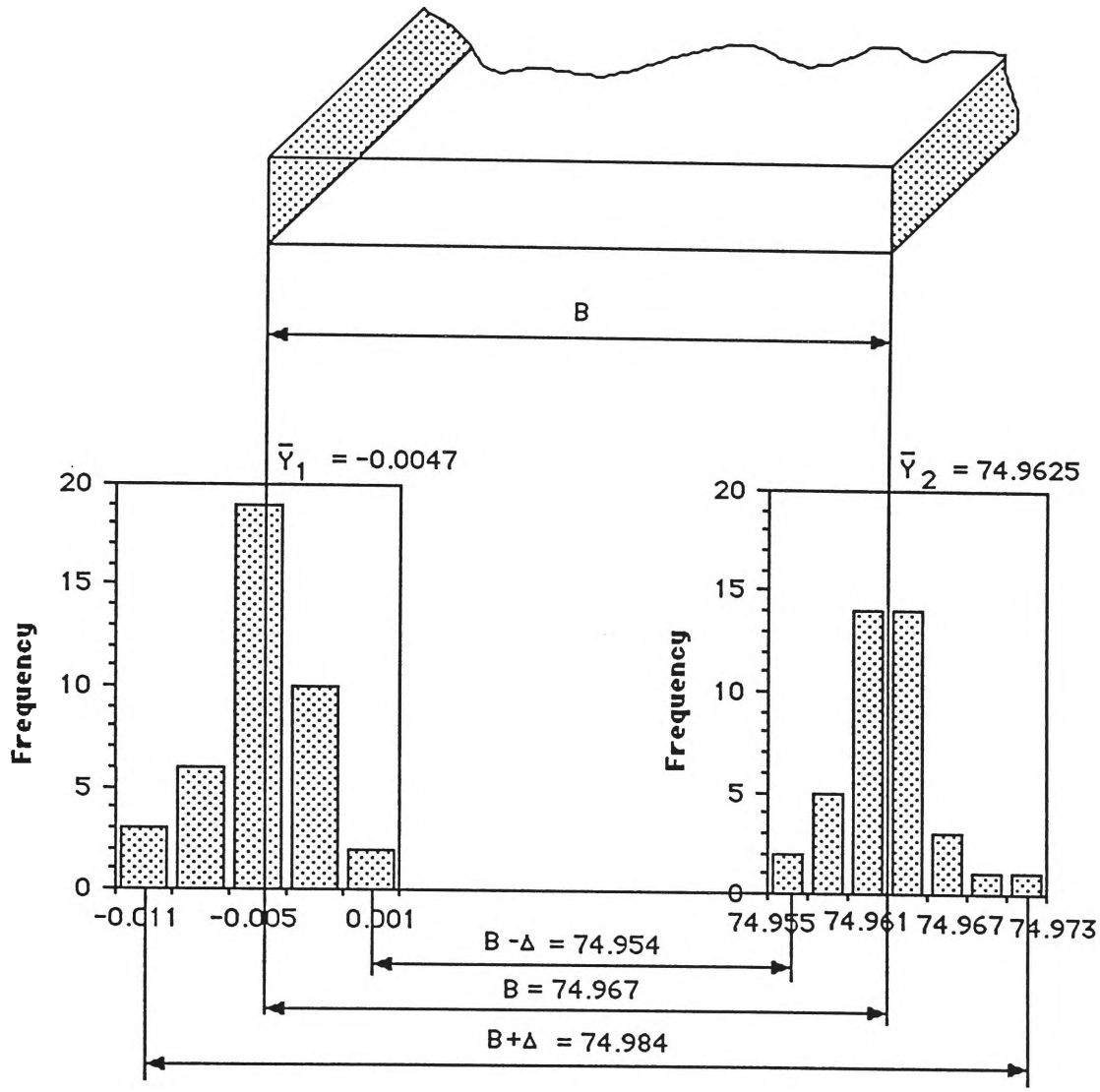

Figure F.1 Linear Dimension Determination.

```
10  REM                    STAT-PACK
20    R E M      ************************************
30  REM      Average, Median, Range, Standard Deviation
40  REM       Variance, Kurtosis, Skewness,
50  REM       Frequency Distribution
60    R E M      ************************************
70  DIM  X (600), MP (20), LB (20), UB (20), F (600)
80  PRINT  " Enter part number." :  INPUT A$
90  LPRINT   TAB (10); A$
100   LPRINT
110   PRINT    "Enter base value." :    INPUT B$
120   LPRINT   TAB (10); B$
130   LPRINT : LPRINT
140  LPRINT TAB(40); "DELTA IN MICRONS"
150   LPRINT
160   PRINT  " Enter number of data points." :  INPUT N
170   PRINT  "Enter data."
180        FOR I = 1 TO N
190        INPUT  X(I)
200        NEXT  I
210   REM          Average
220   SX  = 0
230        FOR  I = 1 TO N
240    LPRINT  X(I);TAB(12*I)
250        SX  =  SX  +  X(I)
260        NEXT  I
270   AVG  =  SX  /  N
280   LPRINT : LPRINT
290   LPRINT   TAB (10) ; "Average  =  "; AVG
300   REM                    Sample Standard Deviation, Variance,
310   REM                    Skewness, Kurtosis
320   S2  =  0 :  S3  =  0 :  S4  =  0
330        FOR  I  =  1  TO  N
340         D  =  X(I)  -  AVG
350        S2  =  S2  +  D^2
360        S3  =  S3  +  D^3
370        S4  =  S4  +  D^4
380             NEXT  I
390   SD  =  SQR (S2 / (N-1))
400   VA  =  SD^2
410   A3  =  S3 / N / SD^3
420   A4  =  S4 / N / SD^4
```

```
430  LPRINT  TAB (10) ; "Sample Standatd Deviation  =  "; SD
440  LPRINT  TAB (10) ; "Variance  =  "; VA
450  LPRINT  TAB (10) ; "Skewness  =  "; A3
460  LPRINT  TAB (10) ; "Kurtosis  =  "; A4
470  REM                Sort Routine
480       FOR J = 1 TO (N-1)
490       K = N - J
500       FOR I = 1 TO K
510       Q = I + 1
520       IF X (I) < X (Q) GOTO 560
530        A = X (I)
540        X (I) = X (Q)
550       X (Q) = A
560       NEXT I
570       NEXT J
580  REM           Range
590  R = X (N) - X (1)
600  LPRINT  TAB (10) ; "Range  =  "; R
610  REM             Median
620  J = (N + 1) / 2
630  K = (N + 1) / 2
640  MD = ( X (J) + X (K) ) /2
650  LPRINT  TAB (10) ; "Median  =  "; MD
660  REM              Frequency Distribution
670  PRINT " Enter Interval---odd value preferred."
680  INPUT IN
690  PRINT " Enter 1 if lowest cell midpoint is lowest X(I) value."
700  PRINT " Enter 0 if another lowest cell midpoint is desired."
710  INPUT M
720  IF M = 1 THEN MP(1) = X(1) : GOTO 750
730  PRINT " Enter midpoint value of lowest cell."
740  INPUT  MP (1)
750  LB (1) = MP (1) - IN /2
760  UB (1) = MP (1) + IN /2
770  MPS = MP (1) : LBS = LB(1) : UBS = UB(1)
780       FOR K = 2 TO 20
790       MPS = MPS + IN
800       MP (K) = MPS
810       LBS = LBS + IN
820       LB (K) = LBS
830       UBS = UBS + IN
840       UB (K) = UBS
850       IF UB (K) >= X(N) GOTO 910
```

```
860          NEXT K
870   IF UB (K -1) < X (N) GOTO 890
880   GOTO 910
890   PRINT "Cell interval too small select a larger one."
900   GOTO 670
910   H = K
920          FOR J = 1 TO H
930          FS = 0
940          FOR I = 1 TO N
950          IF X (I) < LB (J) GOTO 990
960          IF X (I) > UB (J) GOTO 990
970          FS = FS + 1
980          F (J) = FS
990          NEXT I
1000         NEXT J
1010   LPRINT : LPRINT
1020   LPRINT TAB (10) ; " BOUNDARIES";TAB (29) ; "MIDPOINT";
  TAB (45); "FREQUENCY";TAB (57);"FREQUENCY DISTRIBUTION"
1030         FOR J = 1 TO H
1040         FS = F(J)
1050         IF FS = 0 GOTO 2020
1060         LPRINT
1070         LPRINT TAB (10) ; LB (J) ; "/"; UB (J); TAB(31); MP(J);
        TAB (47); F(J);TAB(62);
1080         FOR I = 1 TO FS-1
1090         LPRINT "*";
2000         NEXT I
2010         LPRINT "*"
2020         NEXT J
2030   PRINT " if the frequency distribution is satsfacory, Enter 1."
2040   PRINT  " if the frequency distribution is unsatisfactory, Enter 0."
2050   PRINT  "   and select another interval and/or midpoint."
2060   INPUT M
2070   IF M = 1 GOTO 2090
2080   IF M = 0 GOTO 570
2090   END
```

PART NO TP 2

Y = 0000 + DELTA

DELTA IN MICRONS

-4	-4	-10	-11	-10	-4	-6	-3
-1	-1	-3	-1	-4	0	-6	-6
-4	-8	-6	-8	-9	-4	-1	-4
-8	-7	-4	-4	-2	-7	-6	-6
-4	-4	-4	-3	-5	-3	-2	0

Average = -4.675

Sample Standard Deviation = 2.767833

Variance = 7.660898

Skewness = -.3792648

Kurtosis = 2.480597

Range = 11

Median = -4

BOUNDARIES	MIDPOINT	FREQUENCY	FREQUENCY DISTRIBUTION
-12.5 / -9.5	-11	3	***
-9.5 / -6.5	-8	6	******
-6.5 / -3.5	-5	19	*******************
-3.5 / -.5	-2	10	**********
-.5 / 2.5	1	2	**

PART NO TP 2

Y = 74900 + DELTA

DELTA IN MICRONS

57	64	61	63	62	58	64	68
72	63	62	63	62	59	62	56
62	62	63	55	60	71	63	67
65	62	64	61	64	62	64	64
59	57	61	64	64	66	62	62

Average = 62.5

Sample Standard Deviation = 3.471467

Variance = 12.05108

Skewness = .3477955

Kurtosis = 3.867094

Range = 17

Median = 62

BOUNDARIES	MIDPOINT	FREQUENCY	FREQUENCY DISTRIBUTION
53.5 / 56.5	55	2	* *
56.5 / 59.5	58	5	* * * * *
59.5 / 62.5	61	14	* * * * * * * * * * * * * *
62.5 / 65.5	64	14	* * * * * * * * * * * * * *
65.5 / 68.5	67	3	* * *
68.5 / 71.5	70	1	*
71.5 / 74.5	73	1	*

Appendix G

Extracts from AS 2438 - 1981, Twist Drills (General Purpose) [141]

STANDARDS ASSOCIATION OF AUSTRALIA

Australian Standard
for
TWIST DRILLS (GENERAL PURPOSE)

1 SCOPE. This standard specifies the general requirements, terminology, dimensions and tolerances for the following types of drills:

(a) Morse taper (MT) shank twist drills.

(b) Parallel shank twist drills, Jobber series.

(c) Parallel shank twist drills, Stub series.

(d) Parallel shank twist drills, Long series.

The general dimensions of tangs are given in Appendix A, and Appendix B sets out the terminology used for describing the elements, linear dimensions and angles of twist drills. Ordering information is given in Appendix C.

2 DEFINITIONS. For the purpose of this standard, the following definitions apply:

2.1 'Shall' and 'should'—'shall' is taken to be mandatory, 'should' is taken to be advisory.

2.2 Twist drill—a rotary cutting tool having two helical flutes to provide cutting lips at the point of the drill and space for chip removal and admission of cutting fluid. At one end a point consisting of the lips, flanks, faces and chisel edge is formed for cutting the workpiece, while at the other end a parallel or Morse taper shank is formed for holding the drill.

2.3 Right-hand cutting—when viewed along the axis from the point end, the counter clockwise cutting rotation of the drill.

2.4 Left-hand cutting—when viewed along the axis from the point end, the clockwise cutting rotation of the drill.

3 NOMINAL SIZE. The nominal size of a drill shall be the nominal size of the drill diameter (see Appendix B, Paragraph B3.6).

4 SERIES. The series of a drill with parallel shank shall be determined by the length to diameter relationship and shall be expressed as jobber, stub or long.

5 DIMENSIONS AND TOLERANCES.

5.1 Dimensions (See Appendix B, Paragraphs B3.6 and B3.12 to B3.15). The nominal diameter d, the nominal flute length l_1 and the nominal drill length l shall conform to the dimensions shown in Fig. 1 and specified in Tables 1 to 8 for the particular type and series of drill.

5.2 Tolerances.

5.2.1 *Drill diameter* (See Appendix B, Paragraph B3.6). The tolerance on the drill diameter shall be h8 as specified in AS 1654.

5.2.2 *Lengths.* The tolerances on the nominal flute length and nominal drill length shall conform to the values specified in Table 9 for MT shank twist drills and in Table 10 for parallel shank jobber, stub and long series twist drills.

6 GENERAL REQUIREMENTS.

6.1 Twist Drill Point Geometry. The flutes and flanks of twist drills shall be capable of producing straight lips symmetrical about the drill axis with a point angle of about 118 degrees. The chisel edge shall be symmetrical about the drill axis and shall give an approximately straight line when projected onto a plane normal to the drill axis.

Positive lip clearance angle, lip circumferential clearance and body clearance shall be provided, and should be adequate.

6.2 Back Taper. The drill shall be provided with back taper conforming to the values specified in Table 11.

6.3 Hand of Cutting. Drills shall be right-hand cutting, unless otherwise specified.

6.4 Sharpening. Drills shall be sharpened ready for use.

6.5 Shank. The shank shall be parallel or Morse taper (MT); as appropriate.

7 MATERIAL AND HEAT TREATMENT. Drills shall be manufactured from suitable grade high-speed steel and shall be heat treated to a minimum hardness of 690HV (60HRC).

The hardness value shall be reported without conversion to any other scale.

NOTE: The Vickers method of test is to be used for the purpose of any referee tests (see AS 1817).

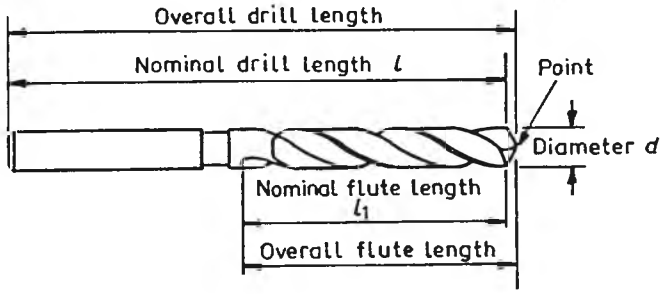

Fig. 1. GENERAL DETAILS—PARALLEL SHANK TWIST DRILL

TABLE 3
PARALLEL SHANK TWIST DRILLS, JOBBER SERIES

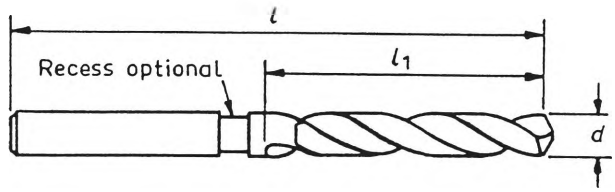

d (h8)*	l_1	l	d (h8)*	l_1	l	d (h8)*	l_1	l	d (h8)*	l_1	l	d (h8)*	l_1	l
0.20			1.35			3.60			7.70			11.60		
0.22	2		1.40			3.70	48	76	7.80	81	114	11.70	110	146
0.25			1.45	22	48	3.80			7.90			11.80		
0.28	3	19	1.50			3.90	51	79	8.00			11.90		
0.30			1.55			4.00			8.10			12.00		
0.32			1.60			4.10	54	83	8.20	84	117	12.10	111	150
0.35			1.65			4.20			8.30			12.20		
0.38			1.70			4.30			8.40			12.30		
0.40			1.75			4.40			8.50	87	121	12.40		
0.42	5		1.80	25	51	4.50	56	86	8.60			12.50		
0.45		22	1.85			4.60			8.70			12.60		
0.48			1.90			4.70	59	89	8.80			12.70	114	152
0.50			1.95			4.80			8.90	89	124	12.80		
0.52			2.00			4.90			9.00			12.90		
0.55	6	25	2.05			5.00	62	92	9.10			13.00		
0.58			2.10	29	54	5.10			9.20			13.10		
0.60			2.15			5.20			9.30	92	127	13.20		
0.62	8	29	2.20			5.30	64	95	9.40			13.30		
0.65			2.25			5.40			9.50			13.40		
0.68	10	32	2.30	32	57	5.50			9.60			13.50		
0.70			2.35			5.60			9.70			13.60	122	168
0.72			2.40			5.70	67	98	9.80	95	130	13.70		
0.75			2.45	35	60	5.80			9.90			13.80		
0.78	13	35	2.50			5.90			10.00			13.90		
0.80			2.55			6.00			10.10			14.00		
0.82			2.60	37	64	6.10	70	102	10.20			14.25		
0.85			2.65			6.20			10.30	98	133	14.50		
0.88			2.70			6.30			10.40			14.75		
0.90	16	38	2.75	38	67	6.40			10.50			15.00		
0.92			2.80			6.50			10.60	100	137	15.25		
0.95			2.85			6.60			10.70			15.50	132	181
0.98			2.90			6.70	73	105	10.80			15.75		
1.00	18	41	2.95	41	70	6.80			10.90	103	140	16.00		
1.05			3.00			6.90			11.00			16.25		
1.10	19	44	3.10			7.00			11.10			16.50		
1.15			3.20			7.10			11.20			16.75		
1.20			3.30			7.20	75	108	11.30	106		17.00	143	194
1.25	22	48	3.40	45	73	7.30			11.40			17.25		
1.30			3.50			7.40			11.50			17.50		
						7.50	78	111						
						7.60								

*See AS 1654.

NOTE: For tolerances on lengths l and l_1, see Table 10.

TABLE 4
PARALLEL SHANK TWIST DRILLS, JOBBER SERIES—GENERAL TABLE

millimetres

Diameter range (h8)*		Corresponding length	
Over	Up to and including	l_1	l
0.19	0.25	2	19
0.25	0.35	3	19
0.35	0.40	5	19
0.40	0.51	5	22
0.51	0.58	6	25
0.58	0.64	8	29
0.64	0.71	10	32
0.71	0.84	13	35
0.84	0.97	16	38
0.97	1.07	18	41
1.07	1.19	19	44
1.19	1.62	22	48
1.62	2.00	25	51
2.00	2.19	29	54
2.19	2.38	32	57
2.38	2.53	35	60
2.53	2.70	37	64
2.70	2.87	38	67
2.87	3.27	41	70
3.27	3.57	45	73
3.57	3.80	48	76
3.80	3.99	51	79
3.99	4.37	54	83
4.37	4.63	56	86
4.63	4.85	59	89
4.85	5.16	62	92
5.16	5.56	64	95
5.56	5.95	67	98
5.95	6.35	70	102
6.35	7.05	73	105
7.05	7.37	75	108
7.37	7.67	78	111
7.67	8.05	81	114
8.05	8.33	84	117
8.33	8.75	87	121
8.75	9.13	89	124
9.13	9.58	92	127
9.58	10.09	95	130
10.09	10.50	98	133
10.50	10.72	100	137
10.72	11.11	103	140
11.11	11.51	106	143
11.51	11.91	110	146
11.91	12.30	111	150
12.30	13.00	114	152
13.00	14.68	122	168
14.68	16.67	132	181
16.67	17.50	143	194

TABLE 9
TOLERANCES ON LENGTHS
(for MT shank twist drills)

millimetres

Diameter range		Tolerance
Over	Up to and including	Nominal drill length and Nominal flute length
2.65	3.75	±3.0
3.75	4.75	±4.0
4.75	6.00	±5.0
6.00	10.60	±6.0
10.60	14.00	±7.0
14.00	16.00	±6.0
16.00	100.00	±5.0

TABLE 10
TOLERANCES ON LENGTHS
(for parallel shank jobber, stub and long series twist drills)

millimetres

Diameter range		Tolerance	
Over	Up to and including	Nominal drill length	Nominal flute length
0	0.3	±0.8	±0.4
0.3	3.0	+3.0 −1.5	+3.0 −1.5
3.0	13.2	±3.0	±3.0
13.2	25.5	+6.5 −3.0	+6.5 −3.0
25.5	51.0	±6.5	±6.5
51.0	89.0	±9.5	±9.5

TABLE 11
BACK TAPER

millimetres

Diameter range		Back taper per millimetre length of drill
Over	Up to and including	
—	3.0	Nil
3.0	38.0	0.0005 to 0.001
38.0	—	0.0005 to 0.0015

APPENDIX B
TERMINOLOGY

B1 SCOPE. This Appendix sets out the terminology used for describing the elements, linear dimensions and angles of twist drills. An asterisk placed against a term signifies that it is illustrated in Fig. B1.

B2 ELEMENTS.

B2.1 Axis*—the longitudinal centreline of the drill.

B2.2 Body—the portion of the drill extending from the extreme cutting end to the commencement of the shank.

B2.3 Body clearance surface—the portion of the fluted lands reduced in diameter to provide diametral clearance.

B2.4 Chisel edge*—the edge formed by the intersection of the flanks at the point end.

B2.5 Chisel edge corner*—the corner formed by the intersection of a lip and the chisel edge at the point end.

B2.6 Drill point heel—the line (edge), containing the heel corner, formed by the intersection of the flute surface and the flank.

B2.7 Face*—that portion of the flute surface adjacent to the lip on which the chip impinges as it is cut from the workpiece.

B2.8 Flank*—the surface on the drill point bounded by the lip, fluted land, the following flute, and the chisel edge.

B2.9 Fluted land*—the surface at the periphery of the body consisting of the land and body clearance surface but excluding the flute surfaces.

B2.10 Flutes*—the helical or straight grooves in the body of the drill which intersect the corresponding flanks to provide the lips, permit the removal of chips, and allow cutting fluid to reach the lips.

B2.11 Heel*—the line (edge) formed by the intersection of the flute surface and the body clearance surface.

B2.12 Heel corner*—the corner formed by the intersection of the heel and flank.

B2.13 Land*—the conical or cylindrical surface at the periphery of the drill body. The land forms part of the fluted land.

B2.14 Leading edge of the land*—the line (edge) formed by the intersection of the land and flute surface.

B2.15 Lip (cutting edge)*—the edge formed by the intersection of the flank and face.

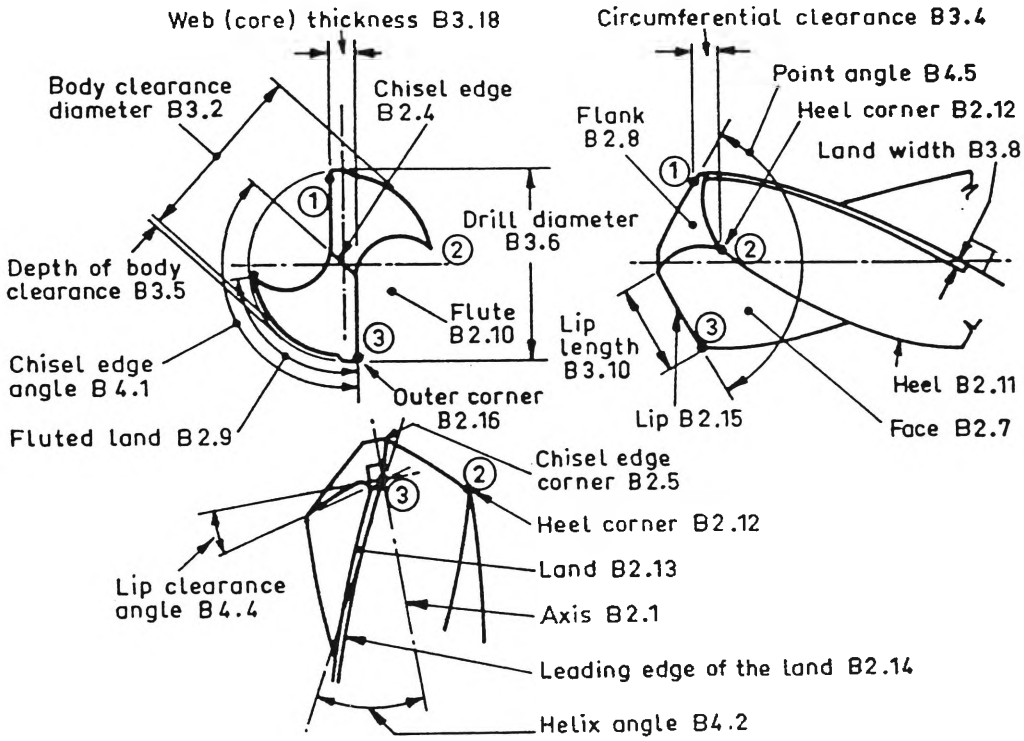

Fig. B1. TWIST DRILL POINT AND OTHER DETAILS (STRAIGHT SYMMETRICAL LIPS)

B2.16 Outer corner*—the corner formed by the intersection of the lip and the corresponding leading edge of the land.

B2.17 Point (cutting part)—the sharpened end of the drill, consisting of all that part of the drill which is shaped to produce lips, faces, flanks, and chisel edge.

B2.18 Shank—that portion of the drill by which it is held and driven.

B2.19 Web (core)—the central portion of the drill situated between the roots of the flutes and extending from the point end towards the shank. The chisel edge is formed at the web (or core) at the point end when the flanks are ground.

B3 LINEAR DIMENSIONS.

B3.1 Back taper (longitudinal clearance)—the reduction in diameter at the lands per unit length of drill from the point towards the shank.

B3.2 Body clearance diameter*—the diameter of the body clearance surface behind the lands.

B3.3 Chisel edge length—the distance between the projections of the chisel edge corners on a plane normal to the drill axis.

B3.4 Circumferential clearance*—the axial displacement between a point on the lip and a specified point on the flank at the same radial distance from the axis (the circumferential clearance when the heel corner is the specified point on the flanks is shown in Fig. B1).

B3.5 Depth of body clearance*—the radial distance between the land and the corresponding body clearance surface.

B3.6 Drill diameter*—the diameter measured across the lands at the outer corners of the drill.

B3.7 Fluted land width—the distance between a point on the leading edge of the land and a point on the corresponding heel in a plane normal to the leading edge of the land containing these two points.

B3.8 Land width*—the distance between a point on the leading edge of the land and a point on the trailing edge of the corresponding land in a plane normal to the leading edge of the land containing these two points.

B3.9 Lead of helix—the distance, measured parallel to the axis of the drill, between corresponding points on the leading edge of a land in one complete turn of the land.

B3.10 Lip length*—the minimun distance between the outer corner and the corresponding chisel edge corner (for a straight lip it is the true length of the lip as in Fig. B1).

B3.11 Lip spacing—the shortest distance through the drill axis between the projections of the straight lines joining the outer corners to the corresponding chisel edge corners on a plane normal to the drill axis (for drills with symmetrical lips it is equal to the web thickness, see Fig. B1).

B3.12 Nominal drill length—the distance between two planes normal to the drill axis, one containing the outer corners and the other touching the extreme end of the shank.

B3.13 Nominal flute length—the distance between two planes normal to the drill axis, one containing the outer corners and the other at the termination of the flutes at the shank end of the drill.

B3.14 Overall drill length—the distance between two planes normal to the drill axis at the extreme ends of the point and shank respectively.

B3.15 Overall flute length—the distance between two planes normal to the drill axis, one at the extreme end of the point and the other at the termination of the flutes at the shank end of the drill.

B3.16 Relative lip height—the axial displacement between corresponding points on the lips at the same radial distance from the drill axis. The relative lip height, caused by deviations from symmetry about the axis, is usually specified and measured at the outer corners of the drill.

B3.17 Web (core) taper—the increase in web or core thickness per unit length of drill from the point towards the shank end of the flute.

B3.18 Web (core) thickness*—the diameter of the circle through the roots of the flutes in a plane normal to the axis. The web thickness is usually specified and measured at the point end of the drill (for drills with straight symmetrical lips it is the distance between the projections of the lips on a plane normal to the axis as in Fig. B1).

B4 ANGLES.

B4.1 Chisel edge angle*—the obtuse angle between the tangent to the projection of the chisel edge, at the axis, and the projection of the line through either outer corner and the corresponding chisel edge corner on a plane normal to the drill axis. This angle lies in a plane normal to the drill axis.

B4.2 Helix angle*—the acute angle between the tangent to the helical leading edge of the flute at a point on this edge and a plane containing the (drill and helix) axis and the point in question. This angle lies in a plane normal to the radius at the point on the edge. The helix angle is usually measured at a point close to or coincident with the outer corner.

B4.2.1 *Normal spiral or helix angle*—a typical normal helix angle is 24 degrees to 30 degrees, approximately (see inset).

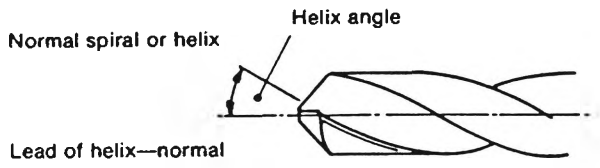

B4.2.2 *Quick helix angle*—a quick helix angle is one which is larger in angular value, i.e. number of degrees, than the normal helix angle, thereby shortening the lead of helix. A typical quick helix angle is 37 degrees to 43 degrees, approximately (see inset).

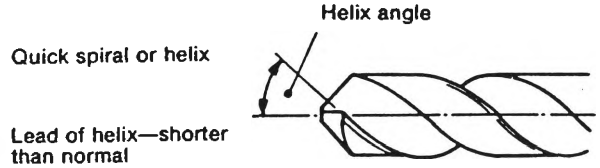

B4.2.3 *Slow helix angle*—a slow helix angle is one which is smaller in angular value, i.e. number of degrees, than the normal helix angle, thereby lengthening the lead of helix. A typical slow helix angle is 12 degrees to 18 degrees, approximately (see inset).

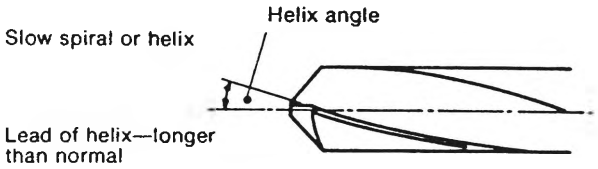

B4.3 Lip circumferential clearance angle—the acute angle whose tangent is equal to the circumferential clearance divided by the length of the minor circular arc between the projection of the two specified points at the lip and flank, on a plane normal to the drill axis. The circle containing the minor arc lies in this plane and has its centre on the drill axis.

B4.4 Lip clearance angle*—the acute angle between a plane normal to the (drill) axis and the tangent, at a point on the lip, to the drill flank in a plane normal to the radius at the point in question. This angle is usually specified and measured at the outer corner as shown in Fig. B1.

B4.5 Point angle*—the included angle between the projections of the lines joining the outer corners to the corresponding chisel edge corners on a plane parallel to one (or both) of these lines and the drill axis.

B4.6 Rake angle—the acute angle between the tangent to a helical line on the flute at a point on the lip and a plane containing the (drill and helix) axis and the point on the lip. This angle lies in a plane normal to the radius at the point in question. The rake angle at the outer corner is equal to the specified helix angle.

Appendix H

Extracts from BS 122: Part 4: 1980, Milling Cutter [144]

BS 122 : Part 4 : 1980

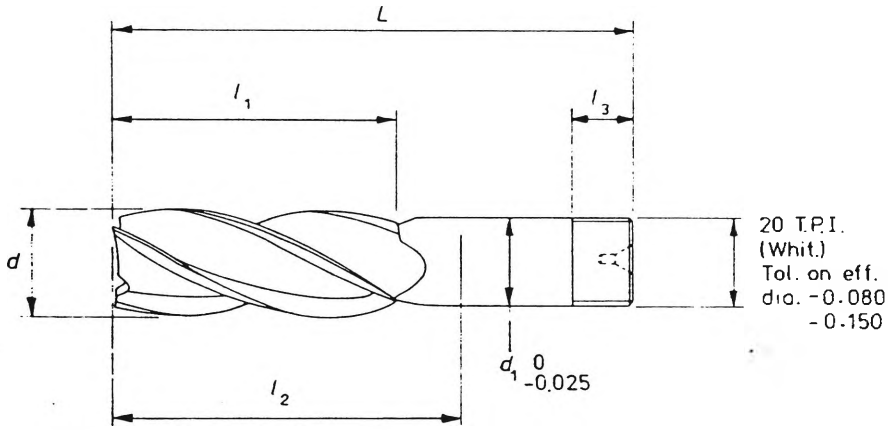

NOTE 1. Tolerances on *d*:
up to 38 mm +0.063
-0.013
over 38 mm +0.125
-0

Figure 2. Screwed shank end mill: normal series

Table 2. Dimensions of screwed shank end mills: normal series

All dimensions are in millimetres.

Cutter diameter *d*	Cut length l_1	Shank diameter d_1	Nominal length below chuck l_2	Overall length *L*	Thread length l_3
2.5	6.5	6	13.5	51	9.5
3	9.5	6	16.5	54	
3.5	12.5	6	19.5	57	
4					
4.5					
5	16	6	23	60.5	
5.5					
6					
6.5	16	10	22.5	60.5	
7	15				
7.5	18	10	25.5	63.5	
8					
8.5	21	10	28.5	66.5	
9					
9.5					
10					
10.5	19	12	28.5	66.5	
11					
11.5	22.5	12	32	70	
12	24.				
13	24.5				
14	28.5	12	35	73	
15	26.5	16	38	77	
16					
17	32	16	41	80	
18	35				
19	38	16	44.5	83.5	
20					

Cutter diameter *d*	Cut length l_1	Shank diameter d_1	Nominal length below chuck l_2	Overall length *L*	Thread length l_3
21	38	25	42.5	95	15
22	41.5	25	46	98.5	
23					
24					
25	44.5	25	49	101.5	
26	43				
28	46	25	52	104.5	
30					
32	49	25	55.5	108	
34					
35	52.5	25	58.5	111	
36					
38	55.5	25	62	114.5	
40	58.5	25	65	117.5	
42	60.5				
44	63.5	25	68	120.5	
45					
32	51	32	58.5	112.5	
33					
34					
35	54	32	62	116	
36					
38					
40	55.5	32	63.5	117.5	
42	54	32	62	116	
44	57	32	65	119	
45					
50	65	32	73	127	

Appendix I

Measurement Results for Twist Drills

Appendix I includes following tables:

Measurement	DRILL No									
No	1	2	3	4	5	6	7	8	9	10
1	11.994	11.964	11.998	11.990	11.979	11.996	11.996	11.993	11.983	11.996
2	11.990	11.960	11.996	11.985	11.987	11.999	11.993	11.995	11.971	11.998
3	11.997	11.966	11.990	11.998	11.982	11.998	11.990	11.996	11.976	11.997
4	11.997	11.964	11.992	11.988	11.980	11.989	11.990	11.993	11.976	11.987
5	11.987	11.963	11.995	11.991	11.983	12.006	11.997	11.997	11.968	12.002
6	11.998	11.963	11.991	11.970	11.979	12.001	11.996	11.994	11.970	11.989
7	11.977	11.960	11.992	11.997	11.981	11.997	11.999	11.998	11.976	11.998
8	11.994	11.962	11.992	11.994	11.979	11.994	11.990	11.993	11.976	11.997
9	11.991	11.960	11.989	11.988	11.980	11.996	11.996	11.996	11.970	12.000
10	11.994	11.966	11.989	11.988	11.972	11.990	11.989	11.90	11.976	11.997
11	11.988	11.960	11.992	11.992	11.979	11.996	11.987	11.996	11.976	11.999
12	11.991	11.964	11.988	11.999	11.982	12.000	11.992	11.990	11.974	11.998
13	11.994	11.957	11.991	11.998	11.982	11.998	11.984	11.991	11.975	11.995
14	11.990	11.961	11.997	11.975	11.985	11.994	11.990	11.993	11.974	11.990
15	11.995	11.964	11.998	11.978	11.985	12.001	11.992	12.000	11.980	11.996
16	11.994	11.963	11.988	11.999	11.980	11.995	11.990	11.989	11.973	11.991
17	11.987	11.964	11.990	11.992	11.977	11.996	11.989	11.999	11.973	11.993
18	11.993	11.960	11.998	11.978	11.984	11.995	11.993	11.995	11.978	11.996
19	11.990	11.965	11.997	11.992	11.983	11.996	11.95	11.988	11.973	12.009
20	11.987	11.957	11.998	11.980	11.980	11.998	11.990	11.987	11.970	11.995
Average	11.991	11.962	11.993	11.989	11.981	11.997	11.991	11.994	11.974	11.996
Std. Dev.	0.0048	0.0027	0.0037	0.0083	0.0033	0.0035	0.0039	0.0036	0.0036	0.0049
Repeatibility	0.0100	0.0056	0.0077	0.0178	0.0069	0.0073	0.0081	0.0075	0.0075	0.0102

* All measurements are in mm

Table I.1 Measurement Results of Drill Diameter of Nominally Similar 12 mm Diameter Drills.

Measurement	DRILL No									
No	1	2	3	4	5	6	7	8	9	10
1	2.054	2.219	1.995	2.074	1.739	2.065	1.543	2.193	1.834	1.989
2	2.087	2.293	2.016	2.081	1.819	1.985	1.635	1.989	1.991	2.110
3	2.063	2.085	1.952	1.996	1.756	2.148	1.655	2.049	1.995	1.980
4	1.993	2.098	2.168	1.917	1.737	2.021	1.680	2.005	1.784	2.100
5	1.952	1.996	1.968	1.973	1.880	2.061	1.545	1.995	1.864	1.995
6	2.090	2.005	1.882	2.616	1.690	1.965	1.556	2.061	1.953	1.829
7	2.051	2.081	1.986	2.149	1.761	2.006	1.692	2.053	1.751	1.949
8	2.105	2.084	1.905	1.979	1.905	2.109	1.693	2.089	1.904	1.980
9	2.056	2.290	1.968	1.954	1.732	1.903	1.709	2.046	1.763	1.907
10	2.095	2.196	2.019	2.053	1.663	2.096	1.540	1.985	1.841	2.005
11	2.009	1.986	2.114	2.005	1.809	2.203	1.681	2.063	1.932	2.109
12	1.998	2.185	1.969	2.182	1.815	1.876	1.661	2.054	1.922	1.919
13	2.095	2.260	2.058	1.989	1.791	1.905	1.595	1.986	1.754	1.981
14	2.091	2.165	1.980	1.921	1.908	1.974	1.551	1.995	1.835	2.110
15	2.082	2.280	1.981	1.979	1.669	1.917	1.519	1.980	1.781	2.008
16	2.085	2.285	1.992	2.031	1.809	2.139	1.588	2.058	1.773	2.115
17	2.092	2.180	1.985	2.140	1.813	1.922	1.563	2.031	1.853	2.015
18	2.062	2.197	2.115	2.083	1.795	2.016	1.593	2.006	1.861	2.018
19	2.048	2.279	1.990	1.982	1.788	1.834	1.664	2.027	1.882	2.019
20	1.993	2.289	1.876	1.868	1.761	1.962	1.566	2.034	1.751	2.098
Average	2.055	2.163	1.996	2.049	1.782	2.003	1.611	2.035	1.851	2.016
Std. Dev.	0.0336	0.1034	0.0737	0.1564	0.0681	0.0991	0.0628	0.0492	0.0794	0.0809
Repeatability	0.091	0.2161	0.1540	0.3269	0.1423	0.2071	0.1312	0.1028	0.1659	0.1691

* All measurements are in mm

Table I.2 Measurement Results of Web Thickness of Nominally Similar 12 mm Diameter Drills.

Measurement	DRILL No									
No	1	2	3	4	5	6	7	8	9	10
1	0.106	0.093	0.079	0.171	0.098	0.116	0.118	0.188	0.139	0.135
2	0.149	0.089	0.124	0.146	0.075	0.161	0.086	0.163	0.093	0.191
3	0.090	0.109	0.054	0.184	0.048	0.119	0.096	0.125	0.105	0.118
4	0.066	0.081	0.068	0.099	0.056	0.090	0.085	0.113	0.139	0.187
5	0.089	0.089	0.059	0.074	0.163	0.150	0.125	0.084	0.107	0.084
6	0.194	0.065	0.085	0.145	0.081	0.118	0.105	0.152	0.073	0.097
7	0.165	0.138	0.082	0.178	0.098	0.095	0.126	0.086	0.098	0.151
8	0.183	0.065	0.097	0.146	0.143	0.060	0.118	0.126	0.089	0.124
9	0.101	0.072	0.047	0.135	0.109	0.125	0.132	0.086	0.2136	0.182
10	0.075	0.080	0.077	0.189	0.136	0.087	0.116	0.118	0.166	0.116
11	0.118	0.108	0.086	0.087	0.115	0.072	0.128	0.098	0.172	0.159
12	0.086	0.068	0.073	0.076	0.139	0.125	0.089	0.125	0.095	0.131
13	0.051	0.091	0.116	0.152	0.159	0.118	0.081	0.103	0.076	0.088
14	0.153	0.124	0.081	0.186	0.146	0.109	0.115	0.095	0.083	0.075
15	0.085	0.185	0.084	0.163	0.082	0.088	0.106	0.182	0.108	0.160
16	0.106	0.076	0.126	0.171	0.088	0.071	0.112	0.186	0.093	0.152
17	0.069	0.128	0.066	0.101	0.078	0.082	0.106	0.165	0.124	0.183
18	0.081	0.061	0.123	0.118	0.095	0.109	0.120	0.086	0.065	0.103
19	0.057	0.111	0.081	0.069	0.068	0.093	0.151	0.091	0.153	0.123
20	o.o73	0.123	0.096	0.083	0.071	0.143	0.094	0.089	0.085	0.087
Average	0.105	0.098	0.085	0.134	0.102	0.102	0.112	0.122	0.110	0.132
Std. Dev.	0.0422	0.0314	0.0228	0.0417	0.0347	0.0337	0.0177	0.0373	0.0316	0.0367
Repeatability	0.0882	0.0656	0.0476	0.0872	0.0725	0.0704	0.0370	0.0780	0.0660	0.0767

* All measurements are in mm

Table I.3 Measurement Results of Relative Lip Height of Nominally Similar 12 mm Diameter Drills.

Measurement	DRILL No									
No	1	2	3	4	5	6	7	8	9	10
1	118.692	116.985	119.458	116.441	118.988	118.124	118.980	116.092	118.861	117.981
2	118.654	116.992	119.192	116.531	118.722	118.159	118.768	116.921	119.160	118.052
3	118.725	117.006	119.812	116.830	118.768	118.320	118.896	116.080	119.033	118.125
4	118.921	117.096	118.476	117.008	118.926	118.456	118.957	116.052	118.925	118.012
5	118.701	117.040	118.921	116.536	118.788	118.459	118.875	116.097	119.045	117.763
6	119.005	117.082	118.856	116.590	118.809	118.501	118.992	116.274	118.852	117.931
7	118.521	117.432	119.150	116.521	118.892	118.560	118.621	116.891	119.126	117.780
8	118.786	117.005	119.352	116.526	118.920	118.509	119.081	116.825	118.907	118.014
9	118.792	117.321	119.081	116.860	118.520	118.881	118.836	116.021	119.134	117.890
10	118.762	116.851	118.881	116.534	118.789	118.548	118.869	116.086	118.821	118.092
11	118.780	117.095	119.132	116.489	118.892	118.531	118.969	116.092	119.345	117.892
12	118.625	116.956	119.201	116.480	118.920	118.498	118.831	116.531	119.321	117.651
13	118.695	117.094	119.205	116.563	119.526	118.560	118.541	116.098	119.210	118.106
14	118.686	117.152	119.189	116.860	118.782	118.468	118.785	116.491	118.863	117.500
15	118.703	117.099	119.206	116.582	118.826	118.541	119.063	116.080	119.350	117.985
16	118.781	117.651	119.080	116.593	118.521	118.691	118.761	116.031	119.428	117.691
17	118.757	117.210	119.069	116.690	119.152	118.584	118.968	116.000	119.269	117.980
18	118.915	117.006	119.216	116.435	119.056	118.341	118.831	116.482	119.311	117.685
19	118.722	117.081	119.286	116.601	118.950	118.597	118.922	116.582	118.842	117.986
20	118.765	117.092	118.972	116.526	118.909	118.561	118.945	116.089	118.961	117.921
Average	118.749	117.162	119.137	116.609	118.883	118.494	118.875	116.291	119.088	117.902
Std. Dev.	0.1078	0.2340	0.2635	0.1582	0.2146	0.1676	0.1354	0.3137	0.2027	0.1705
Repeatability	0.2253	0.4891	0.5507	0.3306	0.4485	0.3503	0.2830	0.6556	0.4236	0.3563

* All measurements are in mm

Table I.4 Measurement Results of Point Angle of Nominally Similar 12 mm Diameter Drills.

Measurement	DRILL No									
No	1	2	3	4	5	6	7	8	9	10
1	138.891	133.01	134.819	132.950	134.891	137.014	138.081	138.954	133.914	137.280
2	137.320	133.043	135.281	133.081	133.350	136.951	137.964	137.481	133.650	136.891
3	136.667	132.954	134.679	132.062	135.201	135.811	137.680	136.524	133.694	135.465
4	135.477	134.084	134.084	132.054	133.459	135.712	135.964	138.663	133.688	134.982
5	136.591	133.911	135.285	133.114	132.821	135.809	138.951	136.081	132.891	135.861
6	138.726	133.591	133.219	133.624	132.628	136.981	135.806	136.184	133.791	135.840
7	138.694	133.890	135.811	133.188	133.561	136.891	137.981	138.649	134.564	136.411
8	139.005	133.681	133.241	132.988	132.819	136.114	135.512	137.584	132.744	136.560
9	136.695	132.871	135.624	131.169	132.966	136.094	135.128	136.654	136.891	134.893
10	136.080	132.911	136.093	132.082	133.579	134.861	136.004	136.244	133.694	135.595
11	136.869	132.980	135.340	134.526	133.828	134.914	137.951	137.561	135.591	136.081
12	136.548	134.891	135.087	131.294	133.526	135.814	134.814	135.594	134.963	136.818
13	137.983	136.911	135.641	134.621	133.679	137.181	134.660	136.284	134.884	135.585
14	137.309	136.892	134.268	133.695	133.768	133.881	135.664	137.620	134.981	134.919
15	137.629	133.640	134.890	134.938	133.790	134.089	132.819	138.821	134.981	134.863
16	136.956	136.685	135.214	134.592	133.762	134.184	133.394	138.814	135.782	135.691
17	137.081	133.114	135.000	132.061	134.394	137.194	134.082	133.411	136.059	134.971
18	137.891	135.118	136.090	132.865	136.891	134.282	136.362	137.614	132.921	135.621
19	137.622	135.106	136.185	131.862	133.669	137.519	137.592	135.140	132.847	136.782
20	137.590	134.582	136.921	131.519	136.089	138.811	133.814	135.850	132.606	135.894
Average	137.381	134.194	135.139	132.914	133.934	135.855	136.002	136.986	134.257	135.850
Std. Dev.	0.9568	1.3496	0.9366	1.1539	1.0874	1.3893	1.7649	1.4534	1.2277	0.7417
Repeatability	1.9997	2.8206	1.9575	2.4116	3.9167	2.9036	3.6886	3.0376	2.5659	1.5502

* All measurements are in mm

Table I.5 Measurement Results of Chisel Edge Angle of Nominally Similar 12 mm Diameter Drills.

Measurement	DRILL No									
No	1	2	3	4	5	6	7	8	9	10
1	11.936	11.901	11.941	11.947	11.906	11.944	11.939	11.937	11.910	11.941
2	11.939	11.903	11.937	11.953	11.909	11.935	11.945	11.934	11.916	11.939
3	11.938	11.904	11.942	11.949	11.901	11.933	11.942	11.935	11.910	11.940
4	11.931	11.902	11.932	11.947	11.904	11.934	11.942	11.944	11.918	11.940
5	11.935	11.902	11.935	11.947	11.904	11.941	11.941	11.941	11.912	11.946
6	11.941	11.902	11.935	11.948	11.906	11.936	11.943	11.943	11.914	11.940
7	11.933	11.904	11.944	11.946	11.908	11.942	11.942	11.943	11.914	11.938
8	11.939	11.903	11.936	11.947	11.903	11.934	11.939	11.940	11.912	11.940
9	11.932	11.901	11.935	11.946	11.905	11.940	11.942	11.938	11.910	11.939
10	11.938	11.908	11.936	11.945	11.904	11.938	11.948	11.940	11.916	11.939
11	11.938	11.902	11.938	11.949	11.909	11.942	11.943	11.941	11.914	11.936
12	11.938	11.900	11.942	11.953	11.911	11.940	11.938	11.932	11.916	11.933
13	11.939	11.900	11.940	11.953	11.906	11.942	11.943	11.933	11.915	11.946
14	11.935	11.906	11.934	11.950	11.907	11.938	11.945	11.939	11.917	11.939
15	11.940	11.908	11.938	11.949	11.905	11.944	11.940	11.940	11.911	11.940
16	11.936	11.903	11.940	11.946	11.906	11.934	11.944	11.935	11.918	11.942
17	11.940	11.905	11.943	11.951	11.904	11.939	11.948	11.943	11.907	11.938
18	11.938	11.901	11.939	11.944	11.906	11.943	11.950	11.934	11.908	11.930
19	11.936	11.903	11.938	11.949	11.903	11.945	11.941	11.936	11.918	11.936
20	11.936	11.906	11.934	11.948	11.904	11.939	11.943	11.937	11.915	11.940
Average	11.937	11.903	11.938	11.948	11.906	11.939	11.943	11.938	11.914	11.938
Std. Dev.	0.0024	0.0024	0.0033	0.0026	0.0024	0.0038	0.0031	0.0037	0.0034	0.0028
Repeatability	0.0050	0.0050	0.0069	0.0054	0.0050	0.0079	0.0065	0.0077	0.0071	0.0058

* All measurements are in mm

Table I.6 Measurement Results of Shank Diameter of Nominally Similar 12 mm Diameter Drills.

Measurement	DRILL No									
No	1	2	3	4	5	6	7	8	9	10
1	0.008	0.006	0.016	0.012	0.004	0.001	0.015	0.004	0.018	0.004
2	0.009	0.008	0.015	0.008	0.005	0.002	0.016	0.006	0.006	0.008
3	0.008	0.004	0.014	0.009	0.016	0.002	0.017	0.002	0.004	0.002
4	0.006	0.010	0.014	0.010	0.018	0.004	0.020	0.016	0.006	0.003
5	0.002	0.006	0.016	0.009	0.008	0.000	0.015	0.10	0.016	0.004
6	0.008	0.002	0.014	0.004	0.009	0.003	0.014	0.10	0.008	0.006
7	0.010	0.004	0.008	0.004	0.014	0.006	0.020	0.006	0.002	0.004
8	0.006	0.008	0.010	0.008	0.012	0.005	0.015	0.008	0.010	0.006
9	0.006	0.009	0.010	0.006	0.006	0.004	0.016	0.012	0.011	0.010
10	0.012	0.008	0.010	0.009	0.008	0.005	0.013	0.008	0.012	0.002
11	0.010	0.016	0.016	0.008	0.010	0.008	0.012	0.010	0.004	0.002
12	0.008	0.008	0.018	0.008	0.009	0.008	0.013	0.006	0.008	0.001
13	0.008	0.012	0.018	0.006	0.006	0.010	0.016	0.006	0.010	0.003
14	0.000	0.006	0.015	0.008	0.008	0.002	0.013	0.008	0.009	0.006
15	0.005	0.005	0.017	0.010	0.009	0.004	0.010	0.009	0.010	0.005
16	0.008	0.006	0.017	0.010	0.010	0.006	0.014	0.008	0.012	0.006
17	0.007	0.009	0.018	0.007	0.008	0.007	0.013	0.006	0.011	0.007
18	0.006	0.008	0.016	0.008	0.009	0.006	0.013	0.008	0.008	0.008
19	0.008	0.006	0.010	0.008	0.010	0.008	0.016	0.008	0.007	0.006
20	0.010	0.005	0.018	0.007	0.010	0.009	0.017	0.010	0.009	0.005
Average	0.007	0.007	0.014	0.008	0.009	0.005	0.015	0.008	0.009	0.005
Std. Dev.	0.0027	0.0031	0.0032	0.0020	0.0035	0.0028	0.0025	0.0030	0.0039	0.0023
Repeatability	0.0056	0.0065	0.0067	0.0042	0.0073	0.0059	0.0052	0.0063	0.0082	0.0048

* All measurements are in mm

Table I.7 Measurement Results of Shank Runout (Radial) of Nominally Similar 12 mm Diameter Drills.

Measurement	DRILL No									
No	1	2	3	4	5	6	7	8	9	10
1	151.913	152.057	152.099	151.589	150.860	152.165	151.196	152.018	151.878	151.517
2	151.955	152.040	152.047	151.564	150.910	152.168	151.215	152.012	151.881	151.553
3	151.961	152.083	152.071	151.560	150.940	152.172	151.190	152.036	151.880	151.553
4	151.958	152.046	152.053	151.581	150.918	152.052	151.206	152.052	151.863	151.556
5	151.947	152.050	152.089	151.567	150.908	152.170	151.234	152.054	151.864	151.560
6	151.950	152.012	152.072	151.561	150.825	152.159	151.208	152.036	151.888	151.536
7	151.923	152.041	152.076	151.549	150.915	152.201	151.231	152.060	151.841	151.560
8	151.945	152.063	152.076	151.572	150.891	152.018	151.211	152.018	151.891	151.530
9	151.943	152.045	152.071	151.560	150.888	152.109	151.209	152.041	151.878	151.554
10	151.971	152.050	152.078	151.548	150.904	152.198	151.198	152.048	151.889	151.503
11	151.950	152.047	152.073	151.565	150.921	152.147	151.183	152.046	151.870	151.566
12	151.945	152.042	152.051	151.573	150.935	152.177	151.175	152.024	151.888	151.510
13	151.946	152.051	152.071	151.569	150.865	152.221	151.216	152.031	151.901	151.554
14	151.945	152.042	152.063	151.579	150.901	152.150	151.224	152.066	151.861	151.520
15	151.951	152.083	152.098	151.549	150.908	152.169	151.214	152.056	151.912	151.525
16	151.930	152.029	152.053	151.563	150.851	152.177	151.208	152.037	151.905	151.558
17	151.958	152.051	152.090	151.561	150.889	152.190	151.198	152.041	151.789	151.567
18	151.943	152.033	152.091	151.569	150.893	152.211	151.211	152.037	151.880	151.528
19	151.951	152.029	152.048	151.546	150.905	152.150	151.195	152.024	151.863	151.540
20	151.948	152.061	152.061	151.548	150.907	152.169	151.203	152.014	151.884	151.533
Average	151.947	152.048	152.072	151.562	150.897	152.176	151.206	152.038	151.875	151.540
Std. Dev.	0.0130	0.0168	0.0162	0.0130	0.0282	0.0269	0.0148	0.0158	0.0263	0.0191
Repeatability	0.0272	0.0351	0.0339	0.0272	0.0590	0.0562	0.0309	0.0330	0.0550	0.0399

* All measurements are in mm

Table I.8 Measurement Results of Overall Length of Nominally Similar 12 mm Diameter Drills.

Measurement	DRILL No									
No	1	2	3	4	5	6	7	8	9	10
1	110.530	112.326	110.933	110.705	111.171	110.873	110.863	111.260	110.323	111.590
2	110.358	112.278	110.839	110.534	111.317	110.853	110.923	111.738	110.356	111.597
3	110.442	112.129	110.875	110.674	111.338	111.050	110.939	111.675	110.329	111.846
4	110.445	111.971	110.882	110.532	111.267	111.174	110.929	111.435	110.318	111.576
5	110.446	112.400	110.868	110.708	111.250	111.065	110.860	111.361	110.325	111.935
6	110.480	112.698	110.883	110.750	111.282	111.056	110.905	111.454	110.330	111.763
7	110.498	112.311	110.930	110.630	111.293	110.961	110.968	111.536	110.351	111.654
8	110.440	112.203	110.893	110.888	111.265	111.017	110.960	111.805	110.356	111.840
9	110.392	112.424	110.884	110.680	111.280	111.051	110.930	111.746	110.320	111.833
10	110.505	112.420	110.786	110.741	111.286	111.064	110.895	111.333	110.324	111.670
11	110.448	112.326	110.876	110.710	111.264	110.981	110.963	111.815	110.289	111.679
12	110.461	112.289	110.915	110.768	111.269	110.881	110.945	111.485	110.366	111.732
13	110.481	112.345	110.884	110.685	111.319	111.084	110.931	111.450	110.321	111.783
14	110.398	112.276	110.880	110.760	111.381	111.045	110.927	111.493	110.350	111.698
15	110.446	112.324	110.863	110.589	111.263	111.036	110.963	111.470	110.288	111.606
16	110.440	112.315	110.811	110.768	111.198	110.892	110.931	111.431	110.295	111.752
17	110.485	112.189	110.905	110.782	111.264	111.005	110.982	111.561	110.281	111.731
18	110.385	112.408	110.885	110.768	111.276	111.091	110.936	111.506	110.324	111.760
19	110.501	112.389	110.801	110.795	111.268	111.064	110.891	111.498	110.329	111.728
20	110.493	112.320	110.880	111.651	111.195	110.985	110.930	111.621	110.343	111.750
Average	110.454	112.317	110.874	111.706	111.269	111.012	110.929	111.534	110.326	11.726
Std. Dev.	0.0448	0.1409	0.0388	0.0885	0.0549	0.0827	0.0327	0.1550	0.0239	0.0954
Repeatability	0.0936	0.2945	0.0811	0.1850	0.1147	0.1728	0.0683	0.3239	0.0499	0.1993

* All measurements are in mm

Table I.9 Measurement Results of Flute Length of Nominally Similar 12 mm Diameter Drills.

ELEMENT	DRILL No									
	1	2	3	4	5	6	7	8	9	10
Drill Diameter (mm)	11.991	11.962	11.993	11.989	11.981	11.997	11.991	11.994	11.974	11.996
Shank Diameter (mm)	11.937	11.903	11.938	11.948	11.906	11.939	11.943	11.938	11.914	11.938
Flute Length (mm)	110.454	112.317	110.874	111.706	111.269	111.012	110.929	111.534	110.326	111.726
Back Taper (mm / mm) X 10^{-4}	4.89	5.25	4.96	3.67	6.74	5.22	4.33	5.02	5.44	5.19

Table I.10 Measurement Results of Back Taper of Nominally Similar 12 mm Diameter Drills.

Measurement	DRILL No									
No	1	2	3	4	5	6	7	8	9	10
1	12.022	12.024	11.999	12.037	12.036	12.041	12.038	12.056	12.025	12.041
2	12.030	12.011	12.019	12.040	12.030	12.038	12.039	12.068	12.014	12.045
3	12.039	12.023	12.039	12.039	12.028	12.039	12.025	12.052	12.024	12.049
4	12.022	12.032	12.026	12.052	12.032	12.038	12.044	12.042	12.025	12.027
5	12.032	12.013	12.023	12.036	12.033	12.040	12.033	12.034	12.027	12.047
6	12.027	12.033	12.029	12.033	12.031	12.043	12.030	12.40	12.021	12.048
7	12.032	12.029	12.031	12.035	12.034	12.044	12.041	12.050	12.019	12.045
8	12.027	12.028	12.025	12.036	12.030	12.041	12.035	12.038	12.032	12.049
9	12.041	12.034	12.034	12.044	12.023	12.037	12.022	12.080	12.022	12.045
10	12.041	12.003	12.029	12.048	12.027	12.040	12.034	12.060	12.020	12.043
11	12.031	12.014	12.021	12.043	12.023	12.041	12.038	12.047	12.020	12.041
12	12.030	12.011	12.024	12.041	12.025	12.043	12.032	12.058	12.025	12.044
13	12.031	12.008	12.021	12.039	12.020	12.046	12.027	12.068	12.035	12.052
14	12.023	12.007	12.031	12.042	12.024	12.036	12.027	12.038	12.029	12.043
15	12.039	12.000	12.021	12.028	12.026	12.044	12.022	12.076	12.028	12.038
16	12.042	12.011	12.025	12.034	12.024	12.035	12.029	12.049	12.025	12.039
17	12.038	11.988	12.020	12.044	12.023	12.040	12.026	12.061	12.022	12.050
18	12.031	11.983	12.018	12.037	12.026	12.040	12.021	12.071	12.028	12.050
19	12.037	12.001	12.016	12.038	12.035	12.036	12.027	12.053	12.024	12.051
20	12.038	11.996	12.033	12.039	12.024	12.042	12.030	12.065	12.021	12.049
Average	12.033	12.011	12.024	12.039	12.028	12.040	12.031	12.055	12.024	12.045
Std. Dev.	0.0064	0.0144	0.0079	0.0054	0.0046	0.0030	0.0066	0.0133	0.0048	0.0058
Repeatability	0.0134	0.0301	0.0165	0.0113	0.0096	0.0063	0.0138	0.0278	0.0100	0.0121

* All measurements are in mm

Table I.11 Measurement Results of Effective Diameter of Nominally Similar 12 mm Diameter Drills.

Appendix J

Measurement Results for End Mills

Appendix J includes following tables:

Measurement	END MILL No									
No	1	2	3	4	5	6	7	8	9	10
1	16.013	16.022	16.041	15.973	15.999	15.990	15.975	15.981	15.991	15.984
2	15.959	16.048	16.045	15.996	15.967	15.949	15.992	15.990	15.962	15.977
3	15.990	16.005	16.006	15.999	15.993	15.949	16.011	15.975	15.999	16.022
4	15.982	15.965	16.005	15.966	15.969	15.998	15.965	15.996	15.994	16.038
5	16.002	16.006	16.008	15.969	16.021	16.005	15.978	15.978	15.969	16.002
6	16.012	15.971	15.989	15.978	16.017	16.042	15.939	15.999	16.000	15.994
7	15.945	15.998	16.028	15.985	16.017	15.999	16.019	15.968	15.960	15.981
8	15.967	15.996	16.028	15.996	16.004	16.041	16.017	15.996	15.978	15.999
9	15.988	16.008	16.027	15.990	15.971	16.009	16.002	15.986	15.955	16.002
10	16.008	15.986	16.044	15.993	16.004	16.006	16.002	15.996	15.987	15.983
11	16.004	16.009	16.025	15.990	15.995	16.005	15.990	15.976	15.975	15.996
12	16.003	15.999	16.016	15.980	15.997	16.037	15.995	15.998	15.999	15.990
13	15.979	16.018	15.978	15.989	16.005	16.007	16.001	15.989	15.965	16.005
14	15.990	16.008	16.010	15.969	15.990	15.996	15.980	15.981	15.994	15.989
15	15.975	16.009	16.008	15.976	15.998	16.011	15.985	16.000	15.962	15.975
16	15.992	16.009	16.018	15.981	16.000	16.008	15.975	15.999	15.989	15.988
17	16.002	16.015	16.041	15.990	16.008	15.993	15.995	15.998	15.982	15.973
18	16.001	16.007	16.006	15.978	16.009	15.998	15.992	15.981	15.980	15.985
19	16.005	16.008	16.041	15.988	15.995	15.996	15.986	15.979	15.960	15.991
20	15.998	16.008	16.015	16.001	15.998	16.006	15.987	15.992	15.958	15.998
Average	15.991	16.004	16.019	15.984	15.995	16.005	15.990	15.988	15.978	15.993
Std. Dev.	0.0182	0.0174	0.0185	0.0107	0.0208	0.0263	0.0188	0.0099	0.0156	0.0155
Repeatability	0.0380	0.0364	0.0386	0.0224	0.0435	0.0549	0.0393	0.0207	0.0326	0.0324

* All measurements are in mm

Table J.1 Measurement Results of Cutter Diameter of Nominally Similar 16 mm Diameter End Mills.

Measurement	END MILL No									
No	1	2	3	4	5	6	7	8	9	10
1	15.989	15.984	15.985	15.988	15.991	15.985	15.982	15.987	15.988	15.983
2	15.988	15.982	15.982	15.986	15.989	15.983	15.990	15.984	15.990	15.991
3	15.988	15.988	15.987	15.987	15.984	15.985	15.987	15.983	15.983	15.981
4	15.983	15.984	15.983	15.988	15.983	15.981	15.989	15.988	15.988	15.981
5	15.987	15.985	15.986	15.991	15.986	15.986	15.985	15.990	15.982	15.982
6	15.990	15.985	15.983	15.991	15.980	15.981	15.990	15.983	15.980	15.987
7	15.991	15.987	15.986	15.990	15.985	15.981	15.987	15.991	15.986	15.978
8	15.986	15.981	15.988	15.989	15.989	15.989	15.986	15.982	15.985	15.980
9	15.984	15.987	15.980	15.991	15.986	15.984	15.986	15.986	15.981	15.983
10	15.986	15.984	15.983	15.991	15.985	15.984	15.990	15.983	15.986	15.984
11	15.988	15.991	15.984	15.994	15.986	15.985	15.987	15.986	15.985	15.980
12	15.987	15.984	15.985	15.991	15.982	15.980	15.986	15.986	15.990	15.984
13	15.986	15.985	15.979	15.990	15.987	15.980	15.983	15.989	15.986	15.983
14	15.989	15.988	15.989	15.989	15.986	15.980	15.988	15.986	15.981	15.982
15	15.984	15.982	15.985	15.990	15.989	15.983	15.981	15.988	15.982	15.990
16	15.985	15.985	15.988	15.990	15.987	15.984	15.988	15.990	15.983	15.980
17	15.985	15.988	15.989	15.986	15.990	15.980	15.990	15.983	15.982	15.986
18	15.988	15.985	15.987	15.988	15.982	15.980	15.986	15.988	15.988	15.984
19	15.987	15.984	15.986	15.991	15.990	15.980	15.991	15.989	15.992	15.990
20	15.988	15.990	15.984	15.990	15.984	15.980	15.986	15.986	15.985	15.987
Average	15.987	15.985	15.985	15.990	15.986	15.983	15.987	15.986	15.985	15.984
Std. Dev.	0.0021	0.0026	0.0028	0.0020	0.0030	0.0028	0.0028	0.0027	0.0034	0.0037
Repeatability	0.0044	0.0054	0.0058	0.0042	0.0063	0.0059	0.0059	0.0056	0.0071	0.0077

* All measurements are in mm

Table J.2 Measurement Results of Shank Diameter of Nominally Similar 16 mm Diameter End Mills.

Measurement	END MILL No									
No	1	2	3	4	5	6	7	8	9	10
1	0.004	0.009	0.003	0.007	0.009	0.014	0.009	0.008	0.021	0.010
2	0.003	0.008	0.009	0.006	0.010	0.020	0.009	0.009	0.025	0.013
3	0.005	0.009	0.005	0.014	0.005	0.012	0.005	0.007	0.015	0.004
4	0.006	0.009	0.003	0.006	0.003	0.010	0.000	0.009	0.018	0.012
5	0.008	0.011	0.002	0.007	0.006	0.007	0.009	0.012	0.018	0.020
6	0.003	0.005	0.005	0.008	0.010	0.009	0.006	0.012	0.009	0.013
7	0.009	0.015	0.009	0.008	0.003	0.010	0.009	0.015	0.021	0.009
8	0.005	0.003	0.005	0.006	0.003	0.016	0.001	0.014	0.018	0.013
9	0.005	0.014	0.006	0.007	0.004	0.015	0.003	0.015	0.022	0.011
10	0.008	0.009	0.004	0.012	0.009	0.006	0.008	0.013	0.013	0.009
11	0.002	0.008	0.005	0.012	0.005	0.007	0.007	0.016	0.015	0.014
12	0.007	0.010	0.007	0.010	0.008	0.009	0.009	0.020	0.016	0.013
13	0.005	0.011	0.004	0.011	0.008	0.012	0.010	0.020	0.017	0.010
14	0.008	0.009	0.006	0.007	0.006	0.012	0.012	0.014	0.015	0.010
15	0.008	0.012	0.003	0.008	0.010	0.013	0.008	0.018	0.016	0.014
16	0.009	0.008	0.006	0.009	0.012	0.013	0.009	0.018	0.018	0.013
17	0.004	0.009	0.005	0.012	0.008	0.008	0.010	0.009	0.009	0.009
18	0.006	0.010	0.006	0.014	0.009	0.008	0.006	0.010	0.015	0.008
19	0.005	0.015	0.004	0.008	0.006	0.015	0.005	0.015	0.020	0.009
20	0.008	0.010	0.006	0.009	0.006	0.010	0.009	0.016	0.021	0.008
Average	0.006	0.010	0.005	0.009	0.007	0.011	0.007	0.013	0.017	0.011
Std. Dev.	0.0021	0.0029	0.0018	0.0026	0.0027	0.0036	0.0031	0.0039	0.0040	0.0033
Repeatability	0.0044	0.0061	0.0038	0.0054	0.0056	0.0075	0.0065	0.0082	0.0084	0.0069

* All measurements are in mm

Table J.3 Measurement Results of Shank Runout of Nominally Similar 16 mm Diameter End Mills.

Measurement	END MILL No									
No	1	2	3	4	5	6	7	8	9	10
1	30.277	30.622	29.876	33.564	31.271	27.005	27.008	29.792	32.901	29.397
2	30.395	27.989	30.561	30.110	30.300	27.036	29.258	29.479	29.645	29.517
3	30.356	30.889	29.098	29.281	30.491	28.819	33.132	27.715	28.424	29.216
4	30.331	29.567	29.984	28.961	31.469	28.691	28.748	29.381	28.610	30.369
5	30.606	29.640	29.980	29.088	31.235	33.066	26.391	30.061	29.866	29.250
6	30.246	28.226	30.985	31.020	30.322	28.153	29.799	29.563	29.814	29.551
7	30.178	29.519	30.651	32.439	31.687	28.188	29.961	28.633	30.072	30.311
8	30.344	29.861	31.169	30.051	29.127	28.696	29.042	31.635	30.063	31.335
9	30.310	29.280	30.113	28.734	31.400	28.891	28.453	30.192	28.389	29.424
10	30.615	29.091	30.247	31.069	29.290	29.305	29.542	28.591	30.811	29.335
11	29.385	30.658	28.865	32.516	30.650	28.680	29.313	29.458	28.562	29.761
12	29.675	27.893	29.977	30.625	29.861	28.611	28.958	30.634	32.615	29.665
13	31.255	28.181	29.104	28.616	30.831	28.592	29.138	29.611	29.053	29.632
14	31.344	27.660	29.711	31.892	30.585	29.016	29.866	29.593	31.005	29.881
15	30.594	27.592	31.089	30.218	29.872	30.561	26.889	28.326	31.075	30.418
16	30.618	28.386	30.147	31.310	29.935	31.369	29.518	29.797	29.861	30.894
17	29.986	28.651	28.341	30.658	30.711	29.632	28.891	29.501	32.069	31.631
18	30.350	29.305	30.286	31.782	30.281	28.865	29.831	29.604	29.542	30.314
19	30.863	27.611	30.015	29.965	29.816	29.459	29.651	29.611	29.581	29.185
20	29.631	28.625	29.686	29.813	31.832	30.631	29.832	29.710	29.619	29.663
Average	30.368	28.962	29.994	30.586	30.548	29.163	29.161	29.544	30.079	29.937
Std. Dev.	0.4822	1.0439	0.7360	1.3697	0.7701	1.4002	1.3960	0.8279	1.3168	0.7077
Repeatability	1.0078	2.1818	1.5382	2.8627	1.6095	2.9264	2.9176	1.7303	2.7521	1.4791

* All measurements are in mm

Table J.4 Measurement Results of Helix Angle of Nominally Similar 16 mm Diameter End Mills.

Measurement	END MILL No									
No	1	2	3	4	5	6	7	8	9	10
1	6.189	6.019	6.592	7.989	8.963	6.721	5.806	5.858	6.219	7.910
2	6.397	5.391	6.817	8.341	9.010	6.835	5.799	5.680	6.209	7.839
3	6.580	5.121	6.800	7.880	8.868	6.839	5.780	5.671	6.398	7.790
4	6.810	5.292	6.321	7.898	8.591	6.921	5.600	5.891	6.959	7.891
5	5.988	5.621	6.680	8.109	8.626	6.711	5.921	5.685	6.015	8.010
6	6.321	5.832	6.080	8.005	8.722	6.134	5.415	5.621	6.920	7.925
7	6.115	5.824	6.920	8.185	8.633	6.891	5.521	6.005	6.818	7.859
8	6.321	5.869	6.594	7.909	9.080	6.921	5.682	5.861	6.219	8.198
9	6.817	5.968	6.414	8.006	8.623	6.506	5.934	5.807	6.810	8.004
10	5.973	5.559	6.920	7.928	8.984	6.341	5.276	6.009	6.181	8.114
11	6.992	5.992	5.981	8.010	8.728	6.518	5.692	6.008	6.825	7.924
12	6.109	6.089	5.996	8.005	8.960	6.243	5.576	5.989	6.215	8.112
13	6.314	6.132	6.807	8.129	8.119	6.824	5.919	5.724	7.016	7.864
14	6.084	5.684	6.995	7.986	8.971	6.114	5.511	5.893	6.212	7.860
15	6.180	5.885	6.561	8.093	8.780	6.510	5.920	5.119	6.892	7.914
16	6.086	5.924	6.546	7.995	8.893	6.541	5.925	5.993	6.895	7.809
17	6.618	6.005	5.821	7.986	8.992	6.637	5.421	5.114	6.792	7.981
18	5.834	6.110	5.985	7.990	8.639	6.691	5.334	5.832	6.890	7.820
19	5.994	6.184	6.092	7.925	8.792	6.694	5.635	5.620	6.778	7.624
20	6.120	6.189	6.166	8.109	8.891	6.821	5.274	5.714	6.321	7.391
Average	6.392	5.999	6.429	8.019	8.793	6.621	5.674	5.755	6.579	7.892
Std. Dev.	0.3617	0.7712	0.3797	0.1140	0.2212	0.2528	0.2267	0.2557	0.3435	0.1747
Repeatability	0.7559	1.6118	0.7936	0.2383	0.4623	0.5284	0.4738	0.5344	0.7179	0.3651

* All measurements are in mm

Table J.5 Measurement Results of Radial Rake Angle of Nominally Similar 16 mm Diameter End Mills.

Measurement	END MILL No									
No	1	2	3	4	5	6	7	8	9	10
1	16.028	16.004	16.048	16.012	16.016	16.012	16.058	16.046	16.018	16.040
2	16.044	16.010	16.042	16.000	16.020	16.012	16.064	16.042	16.034	16.044
3	16.026	16.000	16.042	16.000	16.018	16.018	16.062	16.028	16.022	16.048
4	16.018	16.002	16.038	16.004	16.024	16.008	16.048	16.044	16.018	16.050
5	16.036	16.014	16.038	16.002	16.014	16.012	16.040	16.040	16.026	16.050
6	16.016	16.010	16.032	16.014	16.016	16.020	16.046	16.056	16.016	16.040
7	16.026	16.004	16.028	16.002	16.012	16.014	16.056	16.034	16.034	16.046
8	16.030	16.006	16.030	16.008	16.016	16.008	16.052	16.048	16.020	16.048
9	16.030	16.010	16.028	16.006	16.024	16.016	16.060	16.052	16.030	16.058
10	16.026	16.014	16.042	16.002	16.016	16.014	16.060	16.048	16.044	16.006
11	16.030	16.018	16.040	16.010	16.018	16.010	16.052	16.046	16.032	16.004
12	16.032	16.012	16.038	16.002	16.030	16.012	16.056	16.070	16.030	16.038
13	16.030	16.002	16.032	16.000	16.030	16.002	16.052	16.040	16.042	16.040
14	16.028	16.010	16.038	16.012	16.012	16.004	16.006	16.044	16.030	16.060
15	16.032	16.006	16.044	16.000	16.018	16.008	16.036	16.040	16.030	16.066
16	16.030	16.008	16.042	16.022	16.018	16.014	16.034	16.040	16.024	16.058
17	16.032	16.006	16.038	16.028	16.010	16.014	16.046	16.054	16.032	16.038
18	16.030	16.006	16.028	15.992	16.018	16.012	16.050	16.044	16.024	16.052
19	16.030	16.016	16.044	16.000	16.004	16.014	16.032	16.056	16.030	16.048
20	16.030	126.014	16.040	16.012	16.010	16.010	16.050	16.050	16.026	16.056
Average	16.029	16.009	16.038	16.006	16.017	16.012	16.051	16.046	16.028	16.050
Std. Dev.	0.0057	0.0050	0.0060	0.0085	0.0064	0.0043	0.0098	0.0090	0.0075	0.0088
Repeatability	0.0119	0.0104	0.0125	0.0178	0.0134	0.0090	0.0205	0.0188	0.0157	0.0184

* All measurements are in mm

Table J.6 Measurement Results of Effective Diameter of Nominally Similar 16 mm Diameter End Mills.

Appendix K

Effect of End Mill Deflection on Profile of Machined Surfaces

Appendix K includes following figures:

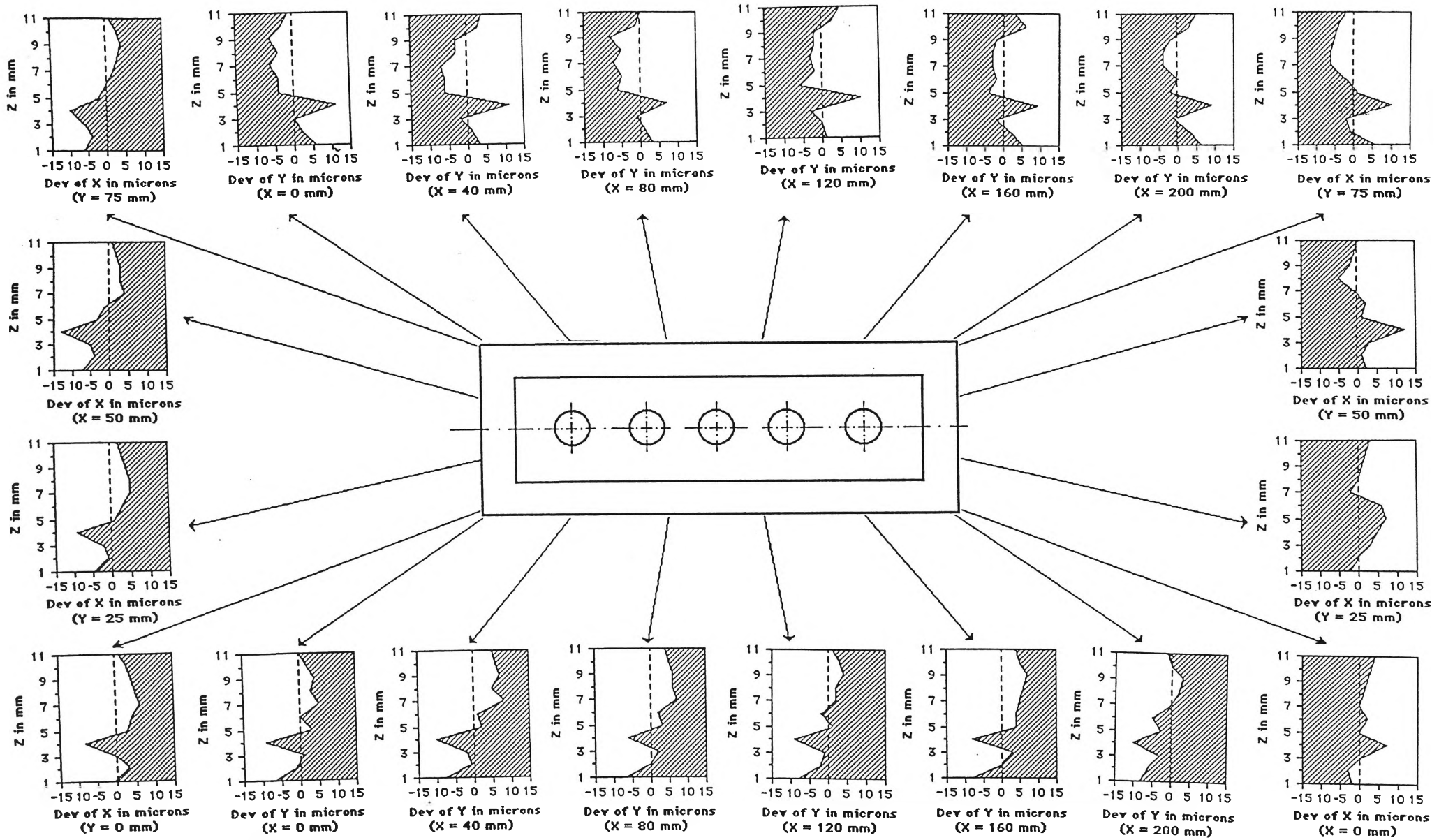

Legend	Part No	Type of Milling	Cutting Speed U (m/mm)	Feed rate S_m (mm/min)	Depth of Cut d (mm)
———	TP 6	Down	126	125	1.0

Figure K.1 Effect of End Mill Deflection on Profile of Workpiece in Down Milling.

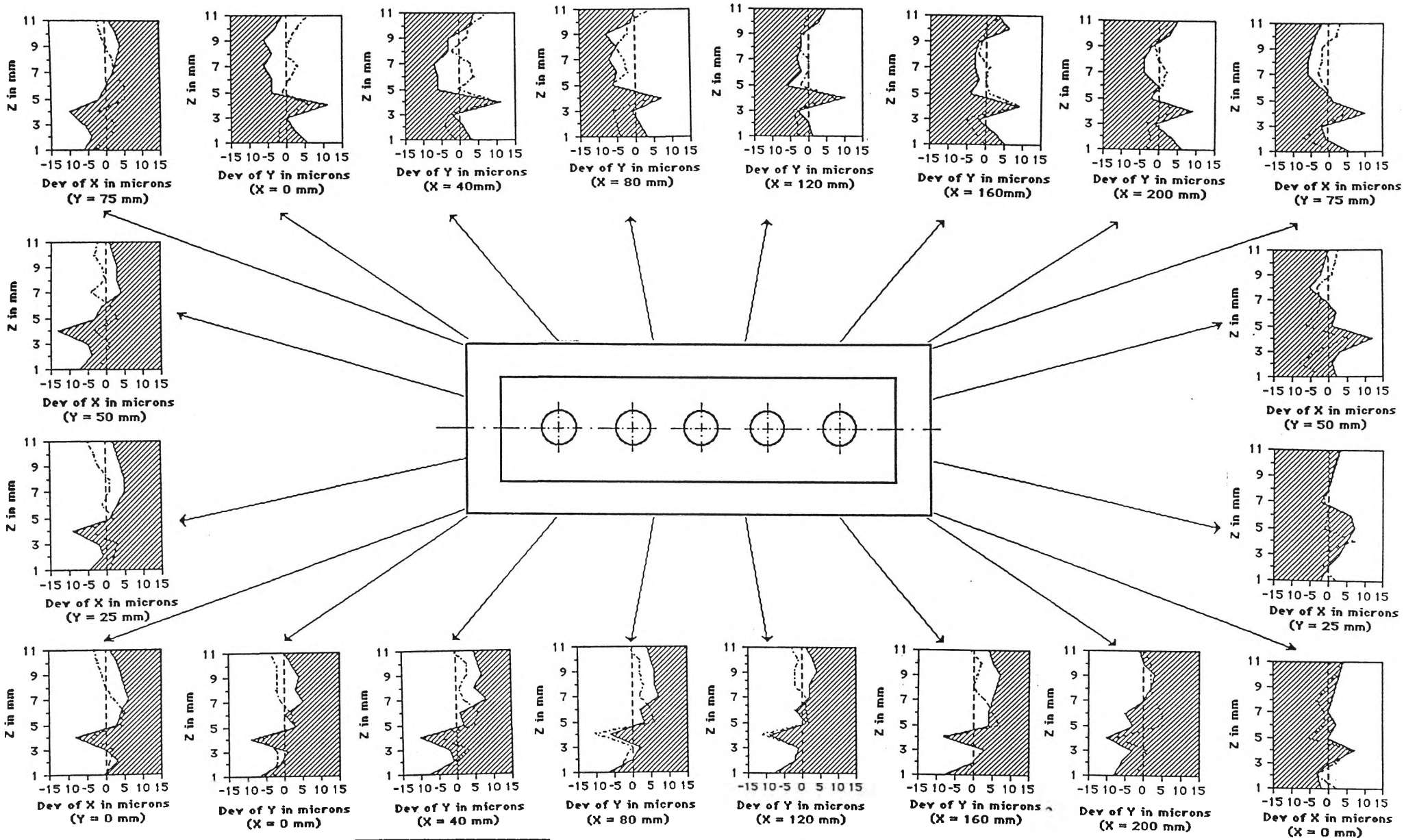

Legend	Part No	Type of Milling	Cutting Speed U (m/mm)	Feed rate S_m (mm/min)	Depth of Cut d (mm)
———	TP 6	Down	126	125	1.0
·-·-·-·-·	TP 11	Down	126	125	0.5

Figure K.2 Effect of Depth of Cut on End Mill Deflection in Down Milling.

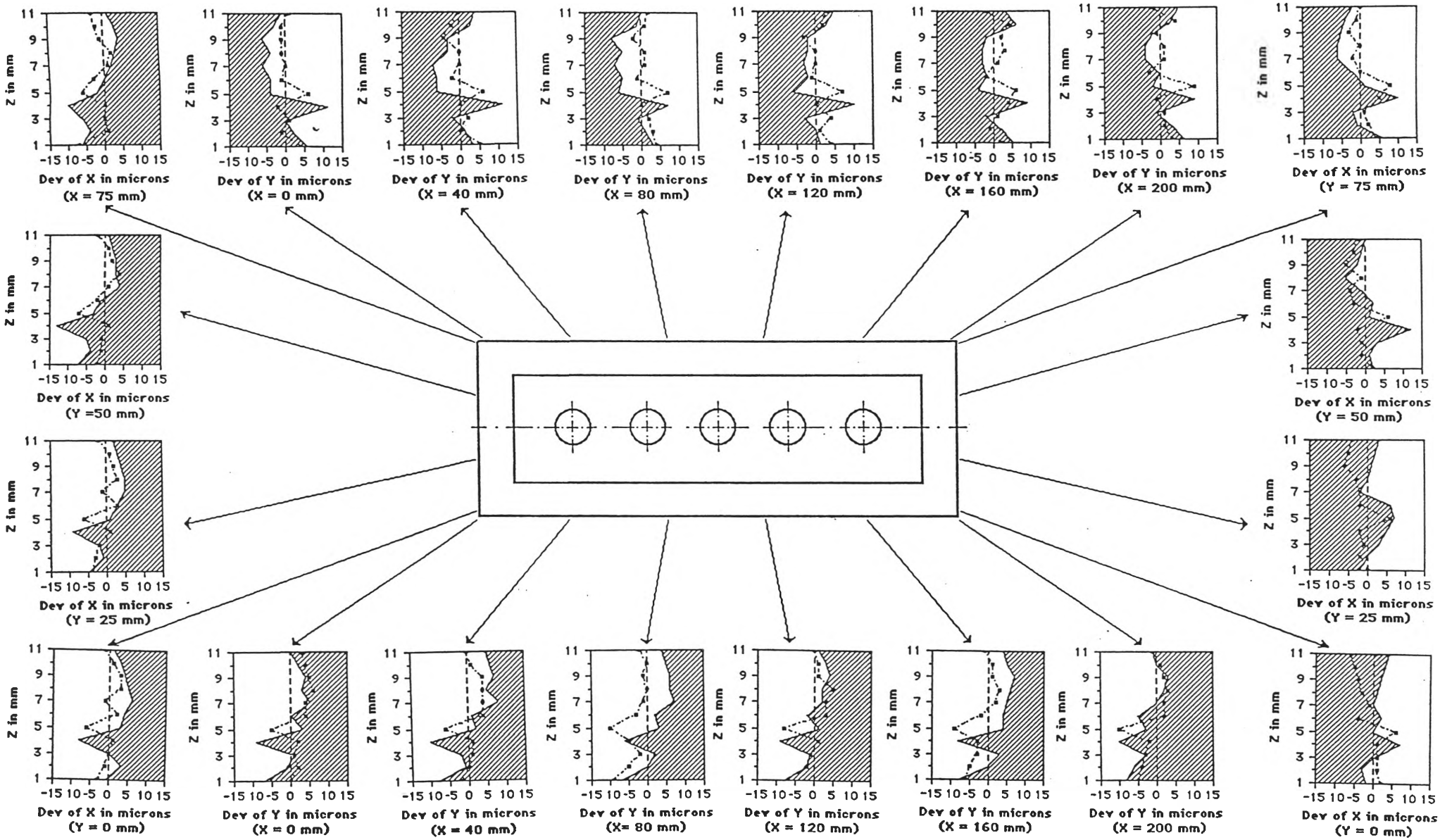

Legend	Part No	Type of Milling	Cutting Speed U (m/mm)	Feed rate S_m (mm/min)	Depth of Cut d (mm)
———	TP 6	Down	126	125	1.0
-·-·-·-	TP 21	Down	126	62.5	1.0

Figure K.3 Effect of Feed on End Mill Deflection in Down Milling.

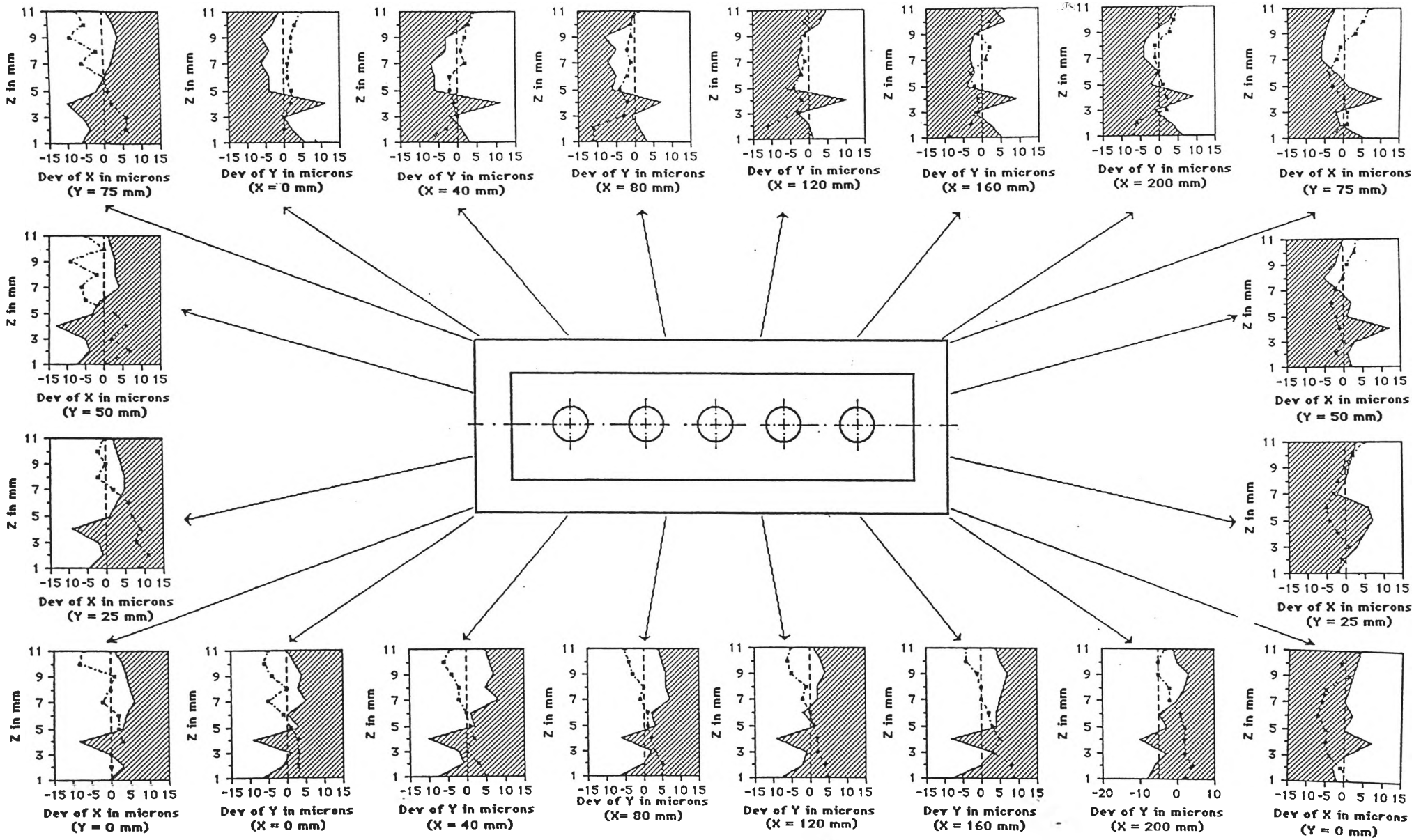

Legend	Part No	Type of Milling	Cutting Speed U (m/mm)	Feed rate S_m (mm/min)	Depth of Cut d (mm)
———	TP 6	Down	126	125	1.0
·-·-·-·	TP 22	Up	126	125	1.0

Figure K.4 Effect of Up and Down Milling on End Mill Deflection.

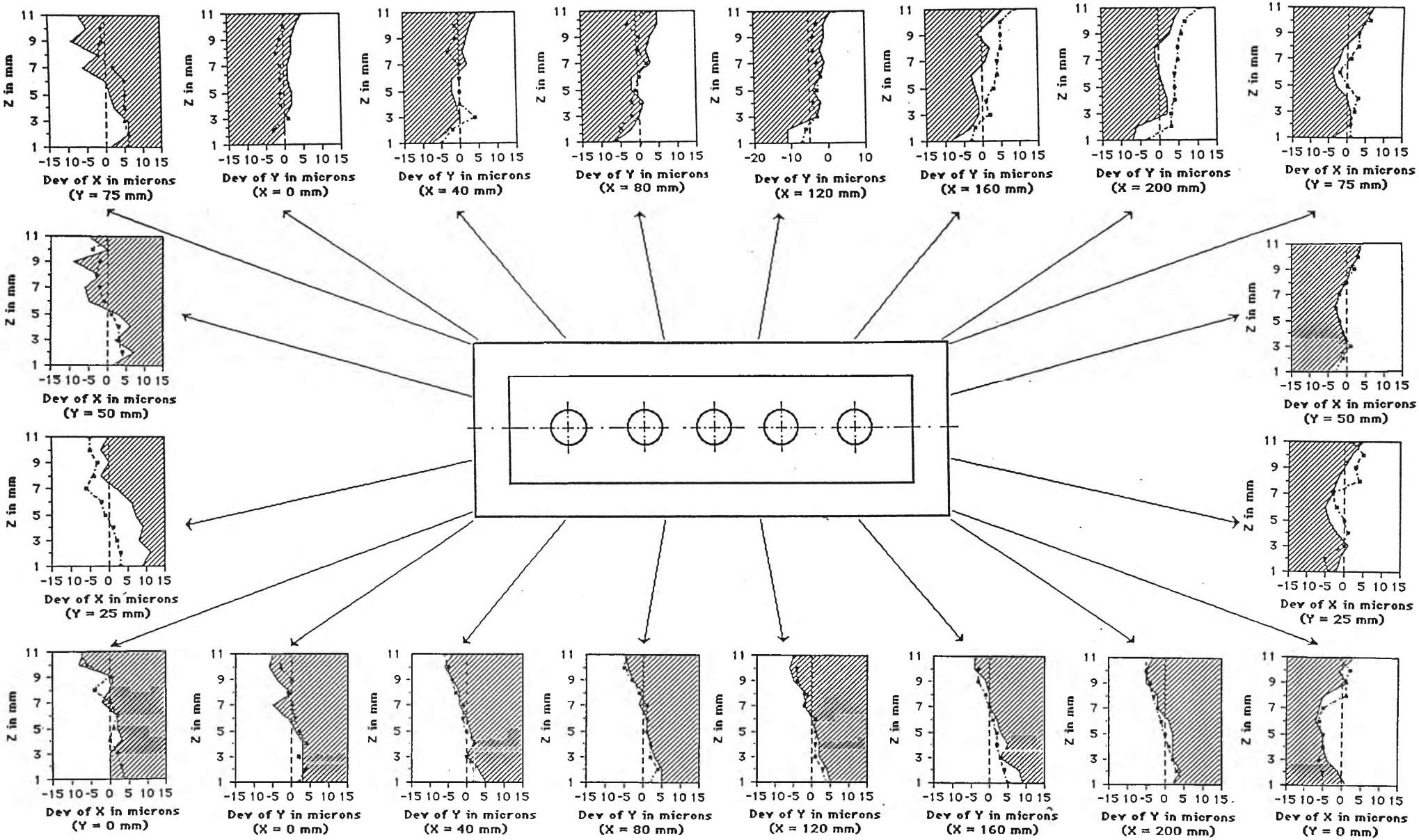

Legend	Part No	Type of Milling	Cutting Speed U (m/mm)	Feed rate S_m (mm/min)	Depth of Cut d (mm)
———	TP 22	Up	126	125	1.0
·—·—·	TP 23	Up	126	62.5	1.0

Figure K.5 Effect of Feed on End Mill Deflection in Up Milling.

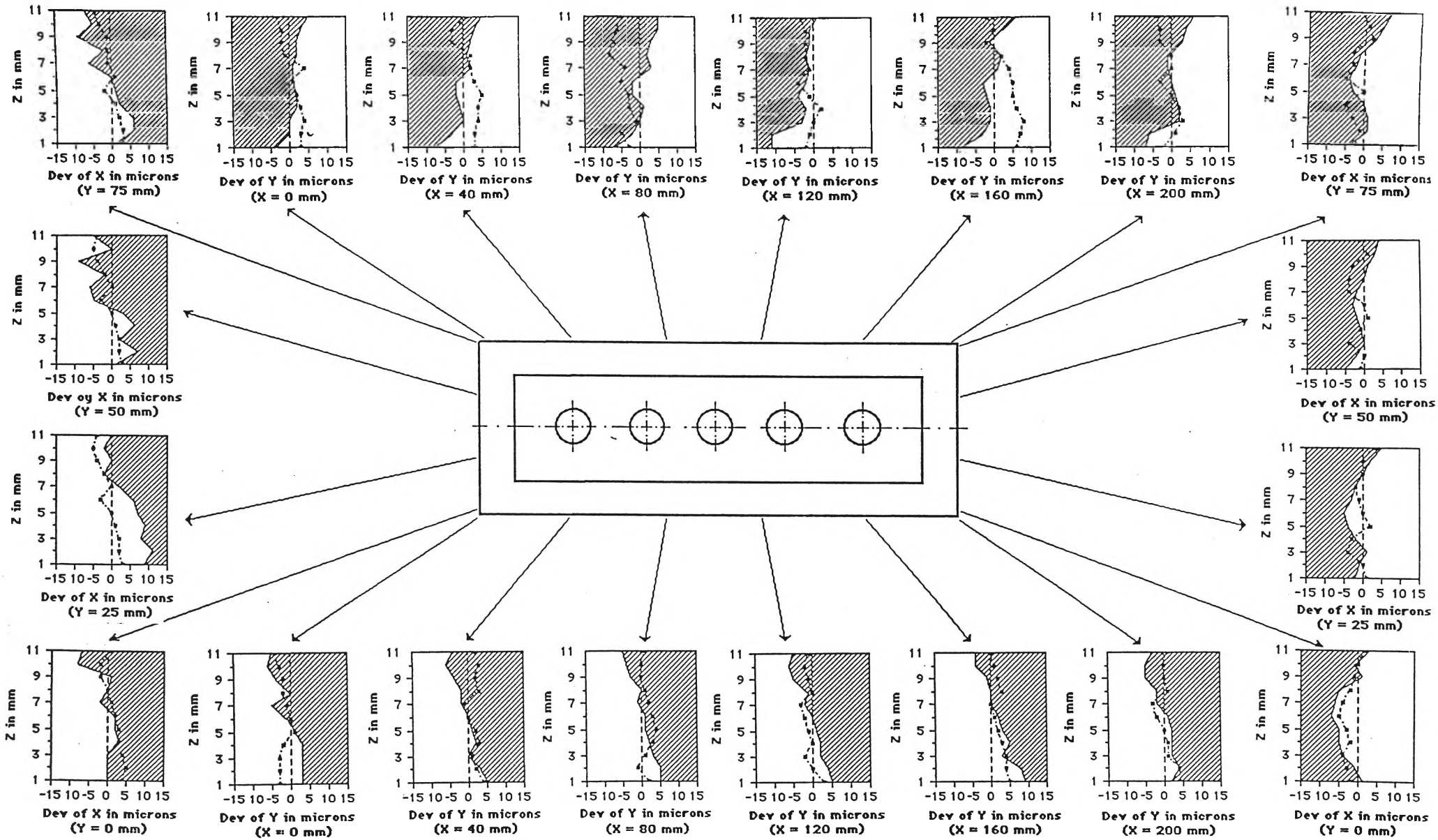

Legend	Part No	Type of Milling	Cutting Speed U (m/mm)	Feed rate S_m (mm/min)	Depth of Cut d (mm)
———	TP 22	Up	126	125	1.0
·-·-·-·	TP 24	Up	126	125	0.5

Figure K.6 Effect of Depth of Cut on End Mill Deflection in Up Milling.

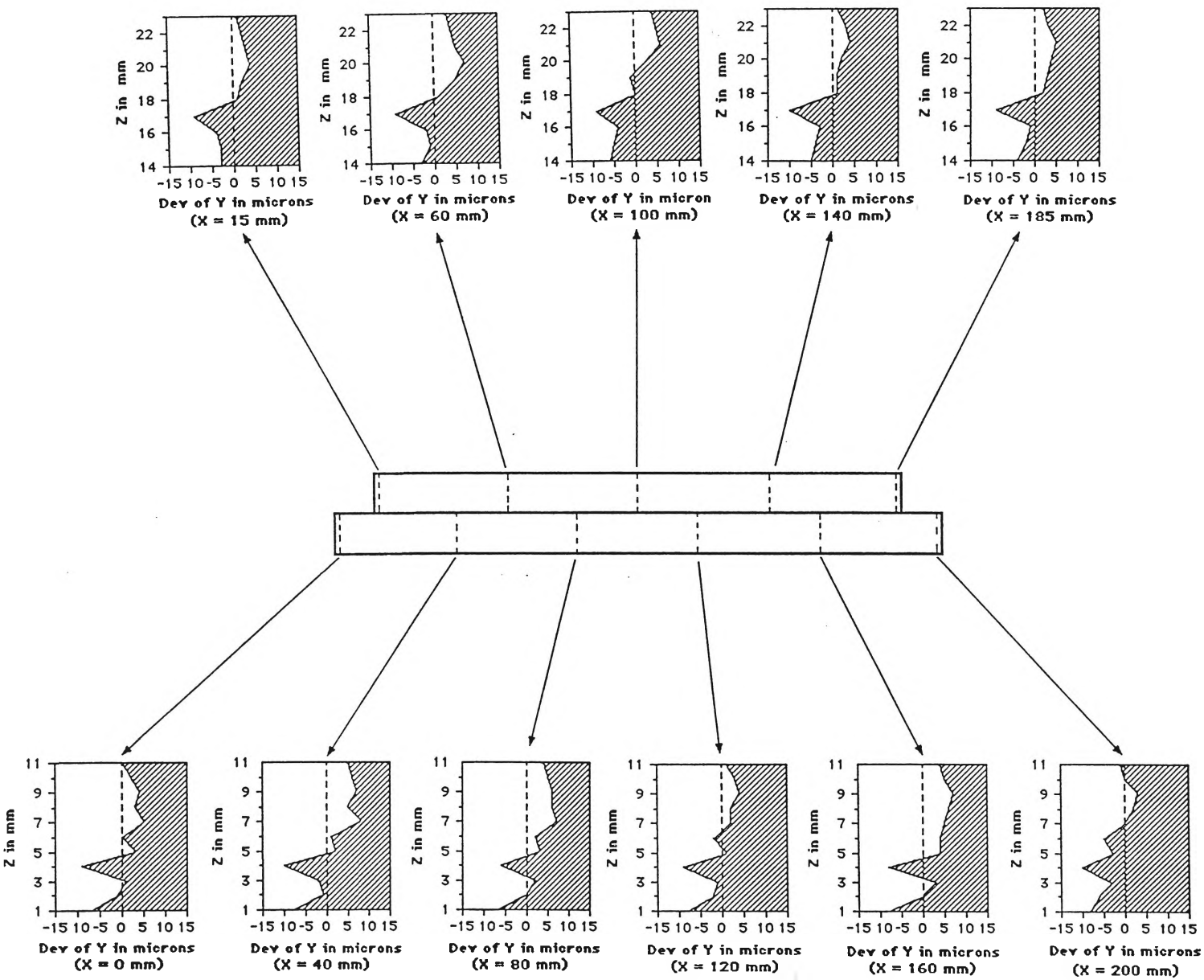

Legend	Part No	Type of Milling	Cutting Speed U (m/mm)	Feed rate S_m(mm/min)	Depth of Cut d (mm)
——	TP 6	Down	126	125	1.0

FigureK.7 Comparison of End Mill Deflection in Peripheral and Combined Milling.

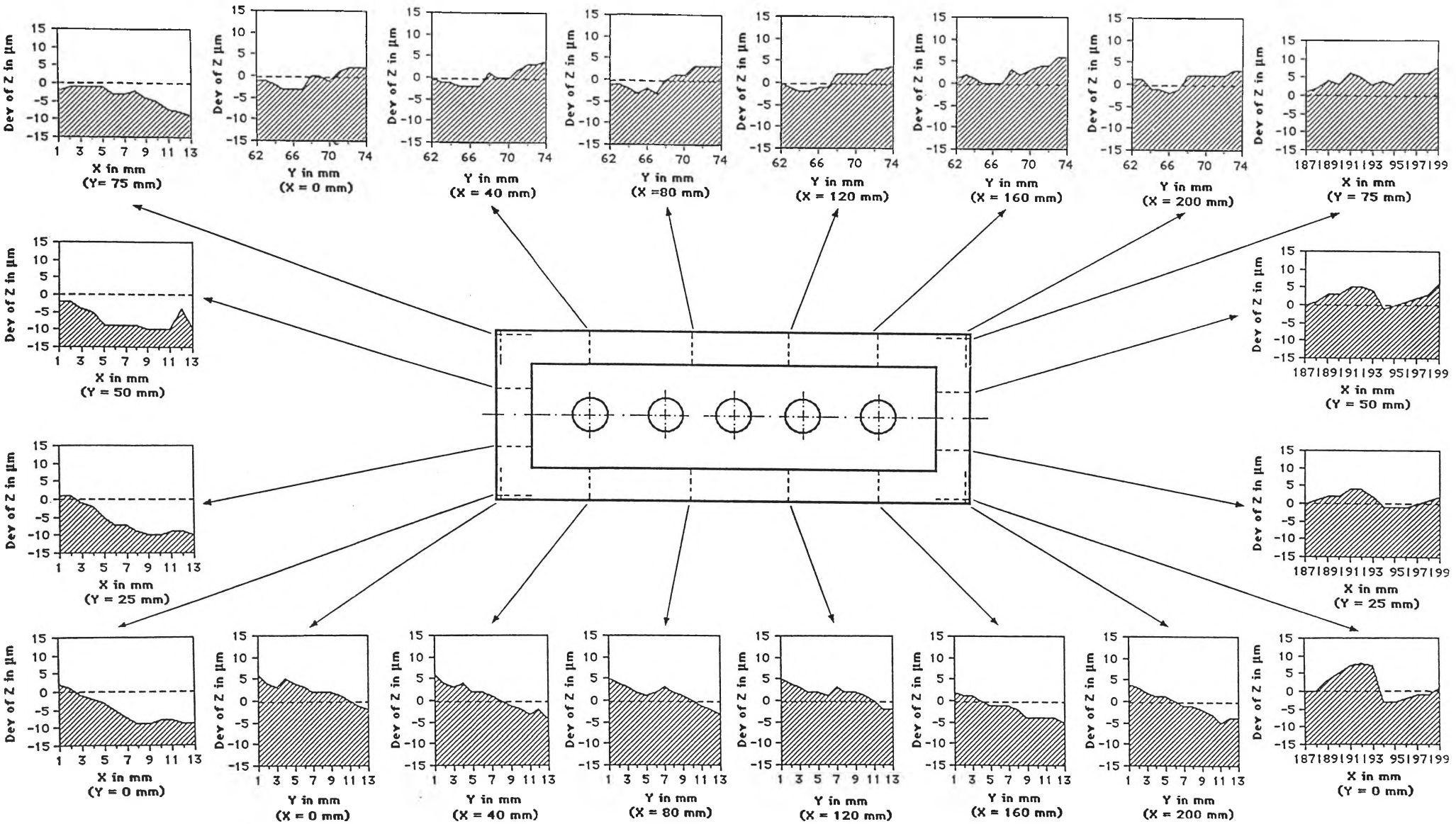

Legend	Part No	Type of Milling	Cutting Speed U (m/mm)	Feed rate S_m (mm/min)	Depth of Cut d (mm)
———	TP 6	Down	126	125	1.0

Figure K.8 Inclined Surface Generated by Combined (Face) Milling due End Mill Deflection in Down Milling.

TABLE 1

Parameters and functions of surface roughness

Item	*Fundamental designation*	*Equivalent designation*	*Definition*	*Graphical interpretation*
1	R_a	CLA; AA; k_m; h_m	Arithmetical mean deviation of the profile	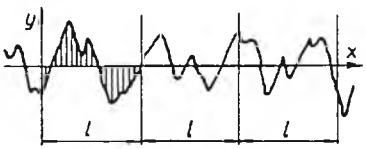
2	R_z	H_{sr}; R; H	Ten-point height of irregularities	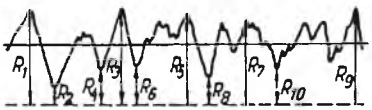
3	R_{max}	R_t; P_{max}	Maximum height of the profile	
4	R_q	H_{SK}; RMS	R.m.s. roughness	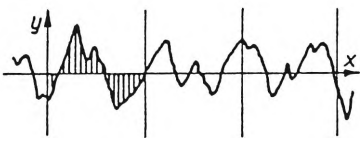

Parameters and Functions of Surface Roughness [165]

Formula	*Relationships with other parameters (functions)*
$R_a = \frac{1}{l}\int_0^l \lvert y(x)\rvert \, dx$	
$R_a = \frac{1}{n}\sum_1^n \lvert y_i\rvert$	
$R_z = \frac{1}{5}\{R_1 + R_3 + R_5 + R_7 + + R_9 - (R_2 + R_4 + R_6 + + R_8 + R_{10})\}$	$R_z = R_p + R_v$
	$R_{max} \approx 6R_a$
$R_q = \left[\frac{1}{L}\int_0^L \{y(x)\}^2 \, dx\right]^{1/2}$	$R_q \approx 1.25R_a$
$R_q = \left(\frac{1}{n}\sum_1^n y_i^2\right)^{1/2}$	

(continued)

TABLE 1 *(continued)*

Item	*Fundamental designation*	*Equivalent designation*	*Definition*	*Graphical interpretation*
5	R_p	R_u; R_e	Mean height of peaks	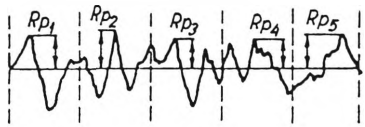
6	R_v	R_m	Mean depth of valleys	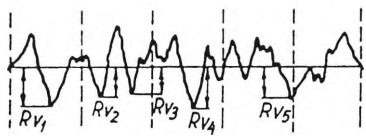
7	R		Peak-to-valley height	
8	R_{tm}		Mean of maximum height of profile	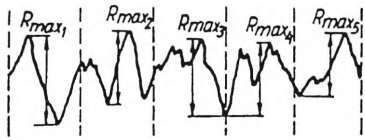
9	k		Profile solidity factor	

Formula	*Relationships with other parameters (functions)*
$R_p = \frac{1}{5}(R_{p_1} + R_{p_2} + \ldots + R_{p_5})$	
$R_v = \frac{1}{5}(R_{v_1} + R_{v_2} + \ldots + R_{v_5})$	
	$R_1 = R_{p_1} + R_{v_1}$
$R_{tm} = \frac{1}{5}(R_{max_1} + R_{max_2} + + \ldots + R_{max_5})$	
$k = R_v/R_{max}$	

(continued)

TABLE 1 *(continued)*

Item	*Fundamental designation*	*Equivalent designation*	*Definition*	*Graphical interpretation*
10	S_m	λ_a; λ_q; A_r; A_R	Mean spacing of the profile irregularities	
11	$n(0)$	N_c	Number of intersections of profile with mean line	
12	m	N_p	Number of peaks in profile	
13	g		Number of inflection points	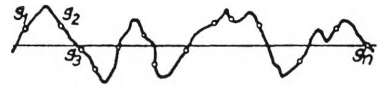
14	Δ_a		Mean slope of profile	

Formula	*Relationships with other parameters (functions)*
$\lambda_a = 2\pi \int_0^L \lvert y \rvert \, dx \Big/ \int_0^L \lvert y' \rvert \, dx$ $\approx 2\pi R_a / \Delta_a$	$\lambda_a \approx 0.9 S_m$ $n(0) = 2/S_m$
$n(0) = n_c/L$	$E\{n(0)\} = \frac{1}{\pi}\left\{-\frac{R_y''(0)}{R_y(0)}\right\}^{1/2}$
$m = n_m/L$	$E\{m\} = \frac{1}{2\pi}\left\{-\frac{R_y^{(4)}(0)}{R_y''(0)}\right\}^{1/2}$
$g = n_g/L$	$E\{s\} = \frac{1}{\pi}\left\{-\frac{R_y^{(6)}(0)}{R_y^{(4)}(0)}\right\}^{1/2}$
$\Delta_a = \frac{1}{L}\int_0^L \left\lvert \frac{dy}{dx} \right\rvert dx$	$\Delta_a \approx \pi n(0) R_a$
$\Delta_a = \frac{1}{n}\sum_1^n \left\lvert \frac{dy}{dx} \right\rvert_i$	

(continued)

TABLE 1 *(continued)*

Item	*Fundamental designation*	*Equivalent designation*	*Definition*	*Graphical interpretation*
15	γ, $\tan\gamma$	θ, $\tan\theta$	Profile slope at the mean line	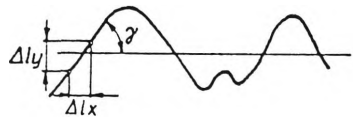
16	Δ_q		R.m.s. profile slope	
17	r	R_w, R, $r_\perp$, $r_\parallel$, r_{wz}	Radius of asperity	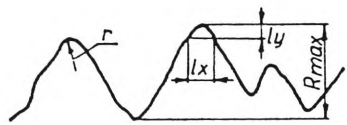
18	ρ	r_1	Curvature radius of profile	
19	l_0		Relative length of profile	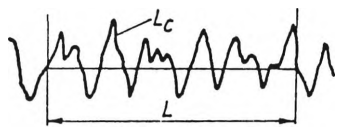

Formula	*Relationships with other parameters (functions)*
$\tan \gamma = \dfrac{\Delta l_y}{\Delta l_x}$	$E\{\tan \theta\} = 4E\{R_a\}E\{n(0)\}$
$\Delta_q = \left\{\dfrac{1}{L}\int_0^L \left(\dfrac{dy}{dx}\right)^2 dx\right\}^{1/2}$	
$r = \dfrac{l_x^2}{8l_y}$ valid for $l_y = 0.1R_{max}$, or $l_y \approx 0.05R_{max}$	$E\{r\} = \dfrac{1}{2\pi^2 E\{R_a\}E\{m\}E\{n(0)\}}$
$\rho = \dfrac{\{1 + (dy/dx)^2\}^{3/2}}{d^2y/dx^2}$	
$l_0 = L_c/L$	$l_0 \approx 1 + \frac{1}{2}\Delta_a^2$

(continued)

TABLE 1 *(continued)*

Item	*Fundamental designation*	*Equivalent designation*	*Definition*	*Graphical interpretation*
20	a	y, p	Approach	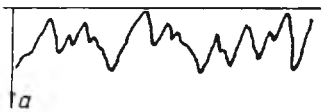
21	ϵ		Relative approach	
22	t_p	η, η_p, t_c, t_{op}, BAC(p)	Bearing length curve	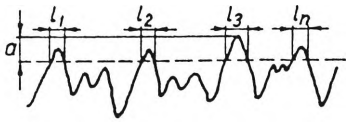
23	b, ν		Parameters of equation of bearing length curve $\eta = b(a/R_{max})^{\nu}$	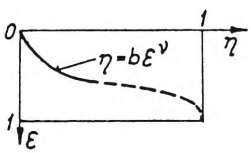
24	HSC	$m(h)$	High spot count	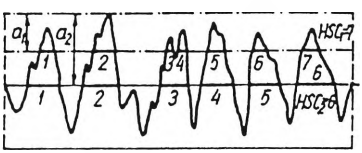

Formula	*Relationships with other parameters (functions)*
$\epsilon = a/R_{\max}$	
$\eta = \frac{1}{L}\sum_{1}^{n} l_i$	$\eta = b\epsilon^{\nu}$

(continued)

TABLE 1 *(continued)*

Item	*Fundamental designation*	*Equivalent designation*	*Definition*	*Graphical interpretation*
25	Δ'	Δ	Dimensionless complex roughness ratio	
26	$f_h(a)$	$f_h(y)$, $p(y)$, ADF, APDF	Amplitude density function	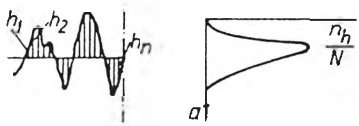
27	$f_m(a)$	$f_w(y)$	Asperity height distribution; density of peaks	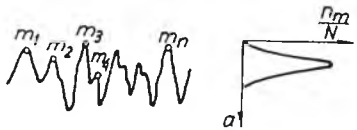
28	$R_y(\Delta x)$	$R_y(\Delta\tau)$, ACF, $A(\beta)$, $A(x)$	Autocorrelation function	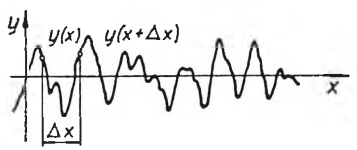
29	$G(f_0)$	$G(\omega)$, $P(\omega)$, $P(w)$, $S(\omega)$	Power spectral density	

Formula	*Relationships with other parameters (functions)*
$\Delta' = R_{\max}/rb^{1/\nu}$	$\Delta' \approx R_{\max}/r$
$R_y(\Delta x) = \frac{1}{L}\int_0^L y(x)y(x+\Delta x)\,dx$	
$G_y(f) = \lim_{\Delta f \to 0} \frac{1}{\Delta f} \times \left\{\frac{1}{L}\int_0^L y^2(x, f, \Delta f)\,dx\right\}$	$G_y(f) = 2\int_{-\infty}^{+\infty} R_y(\Delta x)\exp(-j2\pi fx)\,dx$

(continued)

TABLE 1 *(continued)*

Item	*Fundamental designation*	*Equivalent designation*	*Definition*	*Graphical interpretation*	*Formula*	*Relationships with other parameters (functions)*
30	S_K	R_{sk}, α, $\beta_1^{1/2}$, b_1	Skewness	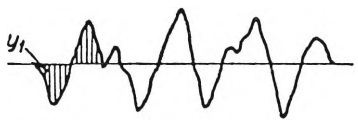	$S_K = \mu_3/\mu_2^{3/2}$	$\mu_2 = \frac{1}{N}\sum_1^N y_i^2$ $\mu_3 = \frac{1}{N}\sum_1^N y_i^3$
31	K	β, β_2, b_2	Kurtosis		$K = \mu_4/\mu_2^2$ $E_K = K - 3$	$\mu_4 = \frac{1}{N}\sum_1^N y_i^4$
32	γ		Randomness coefficient	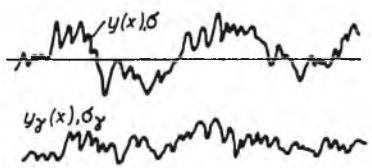	$\gamma = \sigma_\gamma/\sigma$	